Doctoral Thesis

Exploring the solution space for physical global energy system transformation using stochastic system dynamics modelling

Timothy John Harry Crownshaw

Department of Natural Resource Sciences

McGill University

Montréal, Québec

August 2021

A thesis submitted to McGill University in in partial fulfilment of the requirements of the degree of Doctor of Philosophy (Renewable Resources).

“Tug at any human use of energy and you will find its effects cascading throughout society, spilling into the environment and coming back to us. As we were building the edifice of the first high-energy society many things got unraveled in the process but one key reality made the task easier: during the twentieth century we were largely on a comfortable, and a fairly predictable, energy path of a mature fossil-fuel civilization. Things are different now: the world’s energy use is at the epochal crossroads. The new century cannot be an energetic replica of the old one and reshaping the old practices and putting in place new energy foundations is bound to redefine our connection to the universe.”

– Vaclav Smil [1]

TABLE OF CONTENTS

Abstract vii

English vii

Français viii

Acknowledgements x

List of illustrations xi

Figures xi

Tables xv

List of abbreviations xvi

List of mathematical symbols and operators xvii

Operators xvii

Variables and parameters xvii

Subscripts xix

Contribution to original knowledge xx

1 Introduction 1

1.1 The energy system and society: past and present 1

1.2 Competing future narratives 5

1.2.1 Returning to a solar civilization 9

1.2.2 The GES as a complex adaptive system 11

1.3 The path forward 16

1.3.1 The need for a moral foundation 17

1.3.2 Epistemic humility and pluralism 18

1.4 Research objectives 20

2 The global energy system 22

2.1 Primary energy resources 22

2.1.1 Primary energy quality 24

2.1.2 Resource variability and intermittency 34

2.2 Energy transformations 37

2.2.1 The efficiency paradox 37

2.2.2 Energy carriers 40

2.2.3 Energy services 42

2.3 Historical energy transitions 44

2.3.1 Technological diffusion, inertia, and lock-in 45

2.3.2 Lessons for future energy transitions 47

3 The conceptual landscape 49

3.1 The biophysical systems perspective 49

3.1.1 Complex adaptive systems ... 50
3.1.2 Implications for energy and society ... 53
3.1.3 Power, growth, and economic scale ... 59
3.1.4 Dynamic energy systems modelling ... 66
3.2 The current state of energy modelling ... 76
3.2.1 Conventional approaches to the study of energy transitions ... 76
3.2.2 The emerging biophysical systems view ... 91
3.3 Post-Normal Science ... 96
3.3.1 PNS modelling practices ... 98
3.3.2 Sensitivity and diagnostic analysis ... 99
3.4 The knowledge gap ... 101
4 Methodological approach ... 104
4.1 Pre-analytical framework ... 104
4.1.1 Conceptual orientation ... 104
4.1.2 Boundaries and scale of analysis ... 106
4.1.3 Epistemic uncertainty ... 108
4.2 Physical GES modelling principles ... 109
4.2.1 Energy flow schema ... 111
4.2.2 Power capacity ... 115
4.2.3 Flow routing ... 123
4.2.4 Dynamic energy cost modelling ... 126
4.2.5 Intermittency mitigation and impacts in electricity systems ... 137
4.2.6 Causal loop diagrams ... 141
4.2.7 Initialization ... 143
4.2.8 Exogenous interface modelling ... 145
4.2.9 Simulation of GES transformation pathways ... 147
5 The PRESS model ... 152
5.1 Selected array elements ... 153
5.2 System control ... 158
5.2.1 EC deficit projection ... 161
5.2.2 Investment shares ... 162
5.2.3 Investment magnitude ... 164
5.2.4 Intermittency mitigation ... 165
5.2.5 PC utilization control ... 165
5.3 Scenarios ... 167
5.4 Identified limitations ... 169
5.5 Results analysis ... 174
5.5.1 Sensitivity analysis ... 176

5.5.2 Diagnostic analysis *178*

6 Research findings 179

6.1 Base case 179

6.1.1 Sankey diagrams *179*

6.1.2 Supply/demand balance *181*

6.1.3 System stability *184*

6.1.4 Supply *184*

6.1.5 Demand *189*

6.1.6 Primary resources *192*

6.1.7 RE share of supply *195*

6.1.8 EROI *196*

6.1.9 Capacity factors *199*

6.1.10 Penetration *204*

6.1.11 Efficiencies *211*

6.1.12 GHG emissions *214*

6.1.13 Intermittency impacts in electricity systems *215*

6.1.14 GES metabolism *217*

6.2 Scenario analysis 218

6.2.1 Sankey diagrams *218*

6.2.2 System stability *222*

6.2.3 Supply *224*

6.2.4 Demand *225*

6.2.5 Primary resources *227*

6.2.6 RE share of supply *228*

6.2.7 EROI *229*

6.2.8 Penetration *231*

6.2.9 GHG emissions *237*

6.2.10 GES metabolism *240*

6.3 Sensitivity analysis 241

6.3.1 Non-decision input parameters *242*

6.3.2 Policy recommendations *244*

6.4 Diagnostic analysis 245

6.4.1 Stable time *246*

6.4.2 Cumulative GHG emissions *247*

7 Discussion 250

7.1 Proper interpretation of PRESS results 250

7.2 The solution space for GES transformation 251

7.2.1 The upstream sector *252*

7.2.2 The downstream sector ... 254
7.2.3 Efficiencies and PC utilization ... 255
7.2.4 Electricity systems ... 256
7.2.5 Socio-metabolic implications ... 257
7.2.6 System stability ... 259
7.2.7 GHG emissions ... 260
7.3 Sensitivity and leverage points ... 262
7.4 Epistemic risks ... 265
8 Summary and conclusions ... 266
8.1 Key findings ... 266
8.1.1 The centrality of primary energy and demand ... 267
8.1.2 The heat and liquid fuels problem ... 268
8.1.3 Limits to achievable pace of change ... 268
8.1.4 The prospects for demand-led versus supply-led transitions ... 268
8.1.5 Societal complexity and growth ... 269
8.1.6 Converging risks ... 269
8.1.7 Synergies and trade-offs ... 270
8.2 Realizing the solution space ... 271
8.3 Reframing GES transformation ... 272
8.4 What can be done with this information? ... 273
8.5 Avenues for future research ... 274
References ... 276
9 Appendix 1: PRESS model documentation ... 294
9.1 Version history ... 294
9.2 Feedback loop descriptions ... 294
9.3 Model sectors ... 297
9.3.1 Energy flow ... 299
9.3.2 Demand ... 308
9.3.3 PC and AI sectors ... 309
9.3.4 EROI ... 316
9.3.5 Energy cost of capital ... 320
9.3.6 System control ... 320
9.4 Model functions and parameters ... 324
9.4.1 Global parameters ... 324
9.4.2 Stochastic inputs ... 325
9.4.3 Stocks ... 338
9.4.4 Functions ... 344

9.4.5 Scripts ... *372*
9.4.6 Miscellaneous array label sets ... *374*
9.4.7 Input parameter correlations ... *374*
9.5 Input parameter calculations and assumptions ... 378
9.5.1 Data sources ... *378*
9.5.2 Preliminary data processing ... *380*
9.5.3 Initialization ... *383*
9.5.4 Primary resource ... *389*
9.5.5 Flow routing ... *393*
9.5.6 PC efficiencies ... *397*
9.5.7 Demand ... *407*
9.5.8 EROI ... *409*
9.5.9 Energy Cost of Capital ... *411*
9.5.10 Primary NRE sector ... *414*
9.5.11 Primary RE sector ... *415*
9.5.12 Secondary sector ... *417*
9.5.13 End-use sector ... *423*
9.5.14 System control ... *426*
9.5.15 Final input arrays ... *429*
9.6 Optimization and calibration ... 439
9.6.1 Global ensemble optimality check and manual adjustment ... *440*
9.6.2 Optimization and calibration results ... *441*
9.7 Scenario implementation ... 443
9.8 Pedigree assessment ... 445
10 Appendix 2: additional results ... 448
10.1 Penetration ... 448
10.1.1 Secondary ... *448*
10.1.2 End-use ... *450*
10.2 Efficiencies ... 451
10.3 ES demand ... 452
10.4 Intermittency impacts in electricity systems ... 454
10.5 Sensitivity analysis ... 455
10.6 Diagnostic analysis ... 457

ABSTRACT

ENGLISH

The urgent need to move away from fossil fuels is now unequivocal. Extensive academic and popular discourse in recent years has focussed on the prospects for transforming the global energy system (GES) from primarily non-renewable energy towards a renewable energy basis. However, conventional approaches to GES transformation typically sidestep irreducible uncertainties and neglect important physical constraints identified by recognizing the GES as a complex adaptive system. As such, they fail to conceptualize GES transformation as a *complex, physically bounded, path-dependent, socio-metabolic process* which will necessarily transform the basic configuration of modern, high-energy societies. They also overlook the 'net energy trap' phenomenon associated with the autocatalytic nature of energy production, in which net energy supply can become insufficient to provide vital energy services while maintaining the GES itself. Achieving a successful transformation of the GES requires identifying the 'solution space' of physically *feasible* and *viable* dynamic pathways, and by extension, ruling out those which are unlikely to succeed. New epistemic and methodological approaches are needed to navigate complexity, radical uncertainty, and conflicting socio-technical narratives.

This research project centres on developing a novel, exploratory approach to modelling dynamic GES transformation pathways under uncertainty, starting from a pre-analytical framework based in Post-Normal Science***.*** The resulting Probabilistic Renewable Energy Solution Space (PRESS) model is an attempt to map the GES transformation solution space and improve understanding of barriers, opportunities, trade-offs, and achievable outcomes.

Results reveal several unanticipated aspects of GES transformation. It is found that renewable energy is incapable of fully replacing non-renewable energy this century, even with drastic changes in predominant technologies and consumption patterns. Consequently, GHG emission budgets corresponding to 1.5°C and 2°C of warming will likely be exceeded before 2050 without large-scale deployment of negative emissions technology. The rising metabolic costs of GES autocatalysis are also likely to affect the wider human socio-ecological system adversely and unpredictably, including constraints on economic growth. Furthermore, the risk of a net energy trap outcome before 2100 is non-trivial and substantially worsened by policy interventions involving system 'forcing' toward preferred outcomes. While many of the factors affecting GES transformation outcomes are not within human control, those that are include targeted reductions in energy service demand, shifting to efficient mass transit, promoting greater electrification, and focussed technological improvements in process efficiency and lifecycle energy costs. Overall, these results portray the solution space for GES transformation as significantly more complex and challenging than is currently acknowledged.

FRANÇAIS

L'urgence de freiner notre dépendance aux énergies fossiles est désormais sans équivoque. Au cours des dernières années, un vaste discours universitaire et populaire s'est concentré sur les perspectives de transformation du système énergétique mondial (SEM) d'une énergie principalement non renouvelable vers une base d'énergie renouvelable. Cependant, les approches conventionnelles de la transformation du SEM contournent généralement les incertitudes irréductibles et négligent les contraintes physiques importantes identifiées en reconnaissant le SEM comme un système adaptatif complexe. En tant que telles, elles ne parviennent pas à conceptualiser la transformation du SEM comme un *processus socio-métabolique complexe, physiquement limité, dépendant de la trajectoire*, qui transformera nécessairement la configuration de base des sociétés modernes à haute énergie. Elles négligent également le phénomène de « piège énergétique net » associé à la nature autocatalytique de la production d'énergie, dans lequel l'approvisionnement énergétique net peut devenir insuffisant pour fournir des services énergétiques vitaux tout en maintenant le SEM lui-même. Réaliser une transformation réussie du SEM nécessite d'identifier « l'espace de solution » des voies dynamiques physiquement *réalisables* et *viables*, et par extension, d'exclure celles qui ont peu de chances de réussir. De nouvelles approches épistémiques et méthodologiques sont nécessaires pour naviguer dans la complexité, l'incertitude omniprésente, et les scénarios socio-techniques contradictoires.

Ce projet de recherche se concentre sur le développement d'une nouvelle approche exploratoire pour modéliser les voies de transformation dynamiques du SEM sous incertitude, à partir d'un cadre pré-analytique basé sur la Science Post-Normale. Le modèle PRESS (Probabilistic Renewable Energy Solution Space) qui en résulte est une tentative d'établir

l'espace de solution de transformation du SEM et d'améliorer la compréhension des obstacles, des opportunités, des compromis et des résultats réalisables.

Les résultats révèlent plusieurs aspects imprévus de la transformation du SEM. On constate qu'il est impossible de complètement remplacer l'énergie non-renouvelable avec l'énergie renouvelable ce siècle, même avec des changements radicaux dans les technologies prédominantes et les habitudes de consommation. Par conséquent, les quotas d'émission de GES correspondant à 1,5°C et 2°C de réchauffement seront probablement dépassés avant 2050 sans déploiement à grande échelle de technologie à émissions négatives. Les coûts métaboliques croissants de l'autocatalyse du SEM sont également susceptibles d'affecter de manière négative et imprévisible le système socio-écologique humain au sens large, y compris les contraintes sur la croissance économique. En outre, le risque d'un piège énergétique net avant 2100 n'est pas négligeable et considérablement aggravé par les interventions politiques impliquant le « forçage » du système vers des résultats préférés. Bien que de nombreux facteurs affectant les résultats de la transformation du SEM ne soient pas sous le contrôle des humains, ceux qui le sont incluent des réductions ciblées de la demande de services énergétiques, le passage à des transports en commun efficaces, la promotion d'une plus grande électrification et des améliorations technologiques ciblées de l'efficacité des processus et des coûts énergétiques du cycle de vie. Dans l'ensemble, ces résultats décrivent l'espace de solution pour la transformation du SEM comme beaucoup plus complexe et difficile qu'on ne le reconnaît actuellement.

ACKNOWLEDGEMENTS

I would like to thank my supervisor, Peter Brown, for his support, guidance, and encouragement during the completion of this work. None of this would have been possible without his singular vision and passion for bringing about a *mutually enhancing human-Earth relationship*.

I would also like to thank students and faculty in the *Economics for the Anthropocene (E4A)* and *Leadership for the Ecozoic (L4E)* research partnerships for providing an essential forum for conversations of this nature to take place. Special thanks to Dina Spigelski for her tireless efforts in solving problems and supporting all involved.

Thanks to Jim Fyles and Matthias Ruth for their guidance and advice as members of my supervisory committee.

Thank you to Brett Dolter, Mario Giampietro, and Iñigo Capellán-Pérez for the fascinating conversations and helpful input.

Thanks to Richard Heinberg and Rob Dietz for the interesting challenges they sent my way.

Thanks to Laura Gilbert for translation assistance.

Special thanks to my wife, Eunha Hwang, for her extreme patience, attention to detail, and profound care.

This research was made possible with partial funding from the *Social Sciences and Humanities Research Council of Canada (SSHRC)*.

The GoldSim simulation software (version 12.1.2) was used for development of the PRESS model and for general quantitative simulation, visualization, and analysis purposes.

Note: Only the author contributed materially to the collection of materials and data, the design and construction of methods, the performance of simulations, the analysis of results, and the preparation of the thesis.

LIST OF ILLUSTRATIONS

FIGURES

Figure 1: historical primary energy supply by resource, excluding traditional biomass (1900-2020; data from The Shift Project [43] and BP [40]) 4
Figure 2: historical total primary energy supply (1900-2020) with representative future projections . 6
Figure 3: biophysical view of the GES as a sub-system of the HSES and biosphere 12
Figure 4: energy systems language flow diagram for the GES 14
Figure 5: the resource quality pyramid (adapted from Heinberg [179]) 28
Figure 6: possible relationships between primary energy resource quality and production 29
Figure 7: energy conversion stages within the GES for the provision of energy services (adapted from Brockway et al. [206]) 37
Figure 8: the nested hierarchical organization, or 'holonic relations', of CAS (adapted from Eddy et al. [251]) 52
Figure 9: diagnostic analysis example diagram, with risk category regions 101
Figure 10: overview of the energy flow schema from primary energy resources to delivered energy services 111
Figure 11: functional schematic of power capacity 116
Figure 12: functional schematic of upstream power capacity 117
Figure 13: functional schematic of downstream power capacity 118
Figure 14: upstream conversion and reticulation efficiencies in relation to PC 122
Figure 15: downstream conversion and EU to ES efficiencies in relation to PC 122
Figure 16: upstream EROI and ECC in relation to PC and AI 127
Figure 17: downstream ECC in relation to PC and AI 128
Figure 18: energy flows over the capital lifecycle (adapted from [170]) 133
Figure 19: overview of the energy flow schema identifying the sum EC flows associated with the autocatalytic loop and capital hypercycle (the metabolic energy consumption of the GES) 136
Figure 20: causal loop diagram for demand, energy flows, and PC utilization 142
Figure 21: causal loop diagram for PC and AI investment and lifecycle 142
Figure 22: causal loop diagram for primary energy resources and EROI 143
Figure 23: logistic function examples, including approximate linear, exponential, and logarithmic curves 146
Figure 24: decision tree for the selection of probability distribution type for epistemically uncertain input parameters 150
Figure 25: causal loop diagram for system control 160
Figure 26: Sankey diagram for mean GES energy flows in 2015 179
Figure 27: Sankey diagram for mean GES energy flows in the base case in 2050 180
Figure 28: Sankey diagram for mean GES energy flows in the base case in 2100 181
Figure 29: examples of realization success (green) and failure (red) defined by EC deficit trends 182
Figure 30: mean EC deficit trends by EC component for successful and failed realization subgroups 183
Figure 31: EC deficit envelopes by EC component for successful realizations 183
Figure 32: cumulative probability distribution for stable time, including 90% confidence interval for failure rate 184
Figure 33: envelope for total primary energy supply (TPES) 185
Figure 34: mean primary energy supply by resource (NRE types in bold; adjusted for primary energy equivalence) 186
Figure 35: envelopes for primary NRE supply by resource 186
Figure 36: envelopes for primary RE supply by resource (major) 187
Figure 37: envelopes for primary RE supply by resource (minor) 188

Figure 38: envelopes for EC supply 188
Figure 39: envelopes for final (non-GES) EC demand 189
Figure 40: envelopes for GES metabolic EC demand, including autocatalytic loop and capital hypercycle shares 190
Figure 41: envelopes for ES demands (major) 191
Figure 42: envelopes for ES demands (moderate) 191
Figure 43: envelopes for ES demands (minor; semi-logarithmic) 192
Figure 44: envelopes for NRE depletion of primary resources, including EROI terminal limit (high depletion) 193
Figure 45: envelopes for NRE depletion of primary resources, including terminal EROI limit (low depletion) 193
Figure 46: envelopes for RE exhaustion of primary resources (low exhaustion) 194
Figure 47: envelopes for RE exhaustion of primary resources (high exhaustion) 195
Figure 48: envelopes for RE share of supply by EC type 195
Figure 49: envelope for RE share of TPES 196
Figure 50: envelopes for NRE PC mean EROI (high) 197
Figure 51: envelopes for NRE PC mean EROI (low) 197
Figure 52: envelopes for RE PC mean EROI (high) 198
Figure 53: envelopes for RE PC mean EROI (low) 198
Figure 54: envelopes for point-of-use EROI by EC type 199
Figure 55: primary and secondary PC median CFs for coal and nuclear 200
Figure 56: primary and secondary PC median CFs for oil and natural gas 201
Figure 57: primary and secondary PC median CFs for biomass and geothermal 201
Figure 58: primary and secondary PC median CFs for RE types excluding biomass and geothermal 202
Figure 59: EU PC median CFs for freight transportation 203
Figure 60: EU PC median CFs for passenger transportation 203
Figure 61: EU PC median CFs for EU PC types excluding transportation 204
Figure 62: mean secondary penetration by secondary PC type for electricity 205
Figure 63: mean secondary penetration by secondary PC type for LaG fuels 205
Figure 64: mean secondary penetration by secondary PC type for heat 206
Figure 65: mean EU penetration by EU PC type for regional passenger transportation 207
Figure 66: mean EU penetration by EU PC type for regional freight transportation 208
Figure 67: mean EU penetration by EU PC type for low temperature heating 209
Figure 68: envelopes for the aviation shares of IC passenger and freight transportation 210
Figure 69: envelopes for the electrified shares of static mechanical work and high temperature process heat 211
Figure 70: secondary PC mean efficiency trends and achievable maxima (markers at 5-year increments) 212
Figure 71: EU PC mean efficiency trends and achievable maxima (low conversion efficiency; markers at 5-year increments) 213
Figure 72: EU PC mean efficiency trends and achievable maxima (high conversion efficiency; markers at 5-year increments) 213
Figure 73: envelope for cumulative GHG emissions including emissions budget ranges 214
Figure 74: cumulative probability distributions for cumulative GHG emissions including emissions budget ranges 215
Figure 75: envelopes for intermittent penetration and diversity in electricity systems 216
Figure 76: envelopes for CF max. and reticulation efficiency multipliers in response to intermittent penetration 216
Figure 77: envelopes for built AI factor and intermittnet electricity AI in response to intermittent penetration 217
Figure 78: envelopes for ESMRs inclusing shaded curtailment region 218

Figure 79: Sankey diagram for mean GES energy flows in scenario 1 (Energy Breakthrough) in 2100 219
Figure 80: Sankey diagram for mean GES energy flows in scenario 2 (Relocalization) in 2100 219
Figure 81: Sankey diagram for mean GES energy flows in scenario 3 (RE Rapid Deployment) in 2100 220
Figure 82: Sankey diagram for mean GES energy flows in scenario 4 (Climate Constraints) in 2100 221
Figure 83: Sankey diagram for mean GES energy flows in scenario 5 (Delayed Consumer Response) in 2100 221
Figure 84: Sankey diagram for mean GES energy flows in scenario 6 (Policy Recommendations) in 2100 222
Figure 85: mean failure rate and stable time by scenario, including 90% confidence intervals 223
Figure 86: cumulative probability distributions for stable time by scenario, including 90% confidence intervals for failure rate 223
Figure 87: mean total primary energy supply (TPES) relative to the base case, by scenario 224
Figure 88: mean primary energy supply by resource, by scenario (NRE types in bold; adjusted for primary energy equivalence) 225
Figure 89: mean final (non-GES) electricity demand relative to the base case, by scenario 226
Figure 90: mean final (non-GES) LaG fuel demand relative to the base case, by scenario 226
Figure 91: mean final (non-GES) heat demand relative to the base case, by scenario 227
Figure 92: mean NRE depletion and RE exhaustion of primary energy resources in 2100 relative to the base case, by scenario 228
Figure 93: mean RE share of TPES in 2050 and 2100 by scenario, including 90% confidence intervals 229
Figure 94: mean PC mean EROI in 2100 relative to 2015 by scenario (low) 229
Figure 95: mean PC mean EROI and point-of-use EROI in 2100 relative to 2015 by scenario (high) . 230
Figure 96: mean secondary penetration by secondary PC type by scenario for electricity 231
Figure 97: mean secondary penetration by secondary PC type by scenario for LaG fuels 232
Figure 98: mean secondary penetration by secondary PC type by scenario for heat 233
Figure 99: mean EU penetration by EU PC type by scenario for regional passenger transportation 234
Figure 100: mean EU penetration by EU PC type by scenario for regional freight transportation 235
Figure 101: mean EU penetration by EU PC type by scenario for low temperature heating 235
Figure 102: mean aviation shares of IC passenger and freight transportation by scenario 236
Figure 103: mean electrified shares of static mechanical work and high temperature process heat by scenario 237
Figure 104: mean cumulative GHG emissions by scenario including emissions budget ranges, relative to the base case 238
Figure 105: cumulative probability distributions for cumulative GHG emissions in 2050 by scenario including emissions budget ranges 239
Figure 106: cumulative probability distributions for cumulative GHG emissions in 2100 by scenario including emissions budget upper limits 240
Figure 107: mean ESMRs by scenario relative to the base case 241
Figure 108: cumulative probability distributions for normalized sensitivity for selected results, including sensitivity thresholds 242
Figure 109: non-decision input parameters by sum normalized sensitivity across both selected results 243
Figure 110: decision input parameters grouped by policy action by sum normalized sensitivity across both selected results 245
Figure 111: diagnostic diagram for stable time (semi-logarithmic) 246
Figure 112: diagnostic diagram for cumulative GHG emissions (semi-logarithmic) 248
Figure 113: solution space visualization for the base case in 2050 and 2100 250
Figure 114: screenshot of the PRESS model within the GoldSim software UI 297

Figure 115: overview of the PRESS model and functional layers 298
Figure 116: screenshot of the energy flow sector within the GoldSim software UI..................... 299
Figure 117: screenshot of the initialization subsector within the GoldSim software UI 300
Figure 118: screenshot of the initial ES metabolism subsector within the GoldSim software UI 301
Figure 119: screenshot of the primary resource subsector within the GoldSim software UI 301
Figure 120: screenshot of the flow routing subsector within the GoldSim software UI 302
Figure 121: flow mappings between PC types at the primary, secondary, and EU stages, and ES demands..................... 303
Figure 122: screenshot of the new PC efficiencies subsector within the GoldSim software UI......... 304
Figure 123: screenshot of the mean stock efficiencies subsector within the GoldSim software UI .. 307
Figure 124: screenshot of the demand sector within the GoldSim software UI 308
Figure 125: screenshot of the primary NRE and RE sectors (identical) within the GoldSim software UI 310
Figure 126: screenshot of the secondary sector within the GoldSim software UI 311
Figure 127: mapping diagram from secondary PC types to required secondary AI types 312
Figure 128: screenshot of the electricity system subsector within the GoldSim software UI........... 312
Figure 129: screenshot of the end-use sector within the GoldSim software UI..................... 315
Figure 130: mapping diagram from EU PC types to required EU AI types..................... 316
Figure 131: screenshot of the EROI sector within the GoldSim software UI 317
Figure 132: screenshot of the new PC EROI subsector within the GoldSim software UI 319
Figure 133: screenshot of the energy cost of capital sector within the GoldSim software UI 320
Figure 134: screenshot of the system control sector within the GoldSim software UI..................... 320
Figure 135: screenshot of the EC committed subsector within the GoldSim software UI 321
Figure 136: screenshot of the investment share subsector within the GoldSim software UI............ 322
Figure 137: screenshot of the invest synchronization subsector within the GoldSim software UI.... 324
Figure 138: secondary penetration range magnitudes for secondary NRE PC..................... 449
Figure 139: secondary penetration range magnitudes for secondary RE PC 449
Figure 140: EU penetration range magnitudes for passenger transportation PC 450
Figure 141: EU penetration range magnitudes for freight transportation PC..................... 451
Figure 142: EU penetration range magnitudes for low temperature heating PC..................... 451
Figure 143: EU PC mean efficiency trend and achievable maxima for electric cooling (markers at 5-year increments) 452
Figure 144: scenario differences in mean ES demands (S2) 453
Figure 145: scenario differences in mean ES demands (S6; major)..................... 453
Figure 146: scenario differences in mean ES demands (S6; moderate and minor)..................... 454
Figure 147: mean electricity system intermittency mitigation variables relative to the base case in 2050 and 2100 455

TABLES

Table 1: comparison of selected aspects of the Cartesian-Newtonian and systems scientific paradigms 7
Table 2: selected global IAMs, energy transition studies, and meta-analyses with a significant energy focus 77
Table 3: exogenous interface functions using logistic modelling, including reference section for function equations 146
Table 4: selected array elements in the PRESS model with associated inflows and outflows 153
Table 5: selected ESs and predominant associated end-use sectors 156
Table 6: summary of scenarios implemented in the PRESS model 168
Table 7: summary of selected ensemble output variables for results analysis 174
Table 8: pedigree assessment scoring criteria 178
Table 9: high risk input parameters found via diagnostic analysis for stable time 247
Table 10: high risk input parameters found via diagnostic analysis for cumulative GHG emissions . 248
Table 11: descriptions and associated phenomena for balancing feedback loops 294
Table 12: descriptions and associated phenomena for reinforcing feedback loops 296
Table 13: summary of control parameters used in the PRESS model 439
Table 14: PRESS model optimization sequence results and finalized control parameter values 441
Table 15: implementation details for scenarios in the PRESS model 443
Table 16: pedigree assessment results and decision variable status by input array 445
Table 17: additional sensitivity results for non-decision input parameters above lower sensitivity thresholds 455
Table 18: additional sensitivity results for decision input parameters above lower sensitivity thresholds 456
Table 19: medium risk input parameters found via diagnostic analysis for stable time 457
Table 20: medium risk input parameters found via diagnostic analysis for cumulative GHG emissions 458

LIST OF ABBREVIATIONS

AI	Auxiliary infrastructure
CAS	Complex adaptive systems
CDF	Cumulative (probability) density function
CF	Capacity factor
CHP	Combined heat and power
E3	Energy–economy–environment (model)
EC	Energy carrier
ECC	Energy cost of capital
Eff.	Efficiency
EJ	Exajoules
Elec.	Electricity
EPBT	Energy payback time
$EROI_{st}$	Standard energy return on (energy) invested
$EROI_{pou}$	Point-of-use energy return on (energy) invested
$EROI_{ext}$	Extended energy return on (energy) invested
ES	Energy service
ESMR	Energy system metabolic ratio
EU	End-use
EV	Electric vehicle
GDP	Gross domestic product
GES	Global energy system
GHG	Greenhouse gas emissions
$GtCO_2e$	Giga tonnes carbon dioxide equivalent
HDI	Human Development Index
HSES	Human socio-ecological system
IAM	Integrated Assessment Model
IC	Intercontinental
ICE	Internal combustion engine
ICEV	Internal combustion engine vehicle
Intermit.	Intermittent
IPaC	Information processing and communication
kJ	kilojoules
LaG	Liquid and gaseous
OTEC	Ocean thermal energy conversion
NER	Net energy ratio
NRE	Non-renewable energy
PC	Power capacity
PDF	Probability density function
PNS	Post-Normal Science
PRESS	Probabilistic Renewable Energy Solution Space (model)
PV	Photovoltaic
RE	Renewable energy
Reg.	Regional
RHS	Right-hand side (of equation)
RURR	Remaining ultimately recoverable resource
Temp.	Temperature
TPES	Total primary energy supply
Trans.	Transportation
URR	Ultimately recoverable resource

List of mathematical symbols and operators

Operators

$\circ$	Hadamard (elementwise) multiplication
$\oslash$	Hadamard (elementwise) division
$x^{\circ y}$	Hadamard (elementwise) exponentiation

Variables and parameters

$\boldsymbol{0}$	Vector of zeros (dimensionless)
$\boldsymbol{\alpha}$	Logistic efficiency function lower asymptote vector (dimensionless)
β	Intermittent diversity (dimensionless)
$\boldsymbol{\gamma}$	Intermittency mitigation modification vector (dimensionless)
$\boldsymbol{\delta}$	Final demand EC proportion vector (dimensionless)
$\boldsymbol{\varepsilon}$	Primary energy equivalent factor vector (dimensionless)
ζ	Intermittency mitigation reduction factor coefficient (dimensionless)
$\boldsymbol{\eta}$	Penetration vector (dimensionless)
$\boldsymbol{\theta}$	NRE GHG emissions intensity vector (units: $GtCO_2e$/EJ)
$\boldsymbol{\kappa}$	Energy system metabolic ratio vector (dimensionless)
$\boldsymbol{\iota}$	PC initial growth rate vector (dimensionless)
$\boldsymbol{\lambda}$	Construction EC consumption vector (units: EJ/year)
μ	Sample mean
$\boldsymbol{\xi}$	Operational EC consumption vector (units: EJ/year)
$\boldsymbol{\pi}$	Decommissioning EC consumption vector (units: EJ/year)
ρ	Intermittent penetration generation response coefficient (dimensionless)
ς	GHG emissions rate (units: $GtCO_2e$/year)
σ	Population standard deviation
τ	Elapsed time (units: years)
υ	Logistic function upper asymptote (dimensionless)
$\boldsymbol{\upsilon}$	Logistic function upper asymptote vector (dimensionless)
$\boldsymbol{\varphi}$	Relative EC input energy cost proportion vector (dimensionless)
$\mathit{\Phi}$	Relative EC input energy cost proportion matrix (dimensionless)
χ	Electricity system multiplier (dimensionless)
ψ	Intermittency mitigation decision variable (dimensionless)
$\boldsymbol{\omega}$	Maximum cumulative NRE production vector (units: EJ)
a	Maximum EC deficit failure threshold (units: years)
$\boldsymbol{a}$	AI requirement vector (units: EJ/year)
b	Mean EC deficit failure threshold (units: years)
$\boldsymbol{b}$	Cumulative supply/demand balance vector (units: EJ)
Б	EC surplus limit (units: years)
c	Maximum EC deficit rate of change failure threshold (dimensionless)
$\boldsymbol{c}$	PC or AI stock vector (units: EJ/year)
ç	Intermittency mitigation EC cost vector (units: EJ/year)
C	Composite conversion matrix (dimensionless)
d	Mean EC deficit rate of change failure threshold (dimensionless)
$\boldsymbol{d}$	NRE depletion vector (dimensionless)
ɖ	Projected EC deficit vector at time horizon (units: EJ)
$\boldsymbol{e}$	PC stock mean efficiency vector (dimensionless)
ə	New PC efficiency vector (dimensionless)
$\boldsymbol{f}$	Capital fraction vector (dimensionless)

F	Relative flow proportion matrix (units: EJ/year)
g	Decommissioning fraction vector (dimensionless)
h	PC or AI addition rate vector (units: EJ/year^2)
$\hat{\boldsymbol{h}}$	PC or AI investment flow vector (units: EJ/year^2)
I	Identity matrix (dimensionless)
j	Vector of ones (dimensionless)
J	Matrix of ones (dimensionless)
k	PC stock mean EROI vector (dimensionless)
ʞ	New PC EROI vector (dimensionless)
l	Capital lifetime (units: years)
ƚ	ESMR limit (dimensionless)
L	Lower unitriangular matrix (dimensionless)
m	Intermittent penetration (dimensionless)
n	Technology age vector (units: years)
ɑ	Normalized cumulative power output from PC stock vector (units: EJ)
p	Energy flow vector (units: EJ/year)
P	Conversion factor matrix (dimensionless)
ƥ	Normalized cumulative power output vector (units: EJ)
q	Demand flexibility (dimensionless)
r	Combined intermittency mitigation reduction factor (dimensionless)
s	Normalized initial PC input proportion vector (dimensionless)
ş	Investment share curtailment vector (dimensionless)
S	EC input energy cost proportion matrix (dimensionless)
t	Time (units: years)
ƫ	Simulation base time period (units: years)
u	Capacity factor vector (dimensionless)
U	EC flow change projection matrix (units: EJ/year)
v	Peak factor vector (dimensionless)
w	PC or AI stock in construction vector (units: EJ/year)
W	Utility matrix (dimensionless)
x	RE exhaustion vector (dimensionless)
y	ECC vector (units: years)
Y	PC yield matrix (dimensionless)
z	Capital build time (units: years)
ɣ	System control parameter (units vary)

SUBSCRIPTS

β	Intermittent diversity
κ	Energy system metabolic consumption
a	Autocatalytic loop
b	Baseload generation
c	Capital hypercycle
ct	Curtailment threshold constant
d	ES demand
e	EU
ea	EU AI
eb	EU base
ei	EU input (EC to EU)
em	Maximum EU
eo	EU output (EU to ES)
es	Investment share
et	EU CF target
f	Intermittent electricity AI required
fh	Intermittent electricity AI investment
g	Intermittent electricity reticulation efficiency
h	Upstream CF maxima
i	EC inflow (upstream)
k	Primary electricity production
m	Intermittent generation
mc	Investment magnitude coefficient
n	NRE
ne	Non-energy
nm	Maximum NRE
nr	NRE mean annual utility reduction rate
ns	NRE secondary input to output (NRE primary to EC)
nsi	NRE secondary input (NRE primary to secondary)
o	EC outflow (downstream)
p	Peaking generation
q	Demand flexibility
r	RE
rh	Effective new PC EROI (including redevelopment)
rm	Maximum RE
rs	RE secondary input to output (RE primary to EC)
rsi	RE secondary input (RE primary to secondary)
s	Secondary
sa	Secondary AI
sb	Secondary base
sh	Investment share coefficient
si	Secondary input (primary to secondary)
sm	Maximum secondary
so	Secondary output (secondary to EC)
tc	Time increment constant
th	Time horizon
x, xy, y	Placeholder subscript

CONTRIBUTION TO ORIGINAL KNOWLEDGE

The research presented here represents a novel synthesis drawing from several distinct areas of scholarship, and associated qualitative and quantitative methods, including ecological and biophysical economics and 'thermoeconomics', complex systems theory, systems ecology, dynamic and probabilistic computational modelling, Post-Normal Science, control and optimization theory, electric power systems, energy transitions, and technological diffusion.

The core of this conceptual synthesis is established in the methodological approach presented in chapter 4 and the corresponding Probabilistic Renewable Energy Solution Space (PRESS) model, detailed in chapter 5. This synthesis features the following original aspects:

- Dynamic representation of the GES in terms of evolving, non-fungible power capacity stocks – i.e., the hypercyclic component of the GES associated with capital turnover and autocatalytic energy production.
- Integration of endogenous and dynamic energy return on investment (EROI), efficiency, and capital lifecycle into a dynamic energy cost model.
- Disaggregated representation of non-equivalent energy flows characterizing the dynamic, energetic metabolism of the GES, including the disaggregation of EROI and explicit global-scale energy carrier substitution processes.
- Representation of bounded co-evolution of supply and demand, including the identification of net energy trap outcomes, and the use of this information at the ensemble level as a metric of energy system stability.
- Disaggregated modelling of the end-use conversion stage and the dynamic provision of final energy services.
- Endogenous technological change driven by goal seeking energy investment allocation and technological learning effects based on cumulative output.
- Endogenous optimization of mitigation options for rising supply intermittency, based on energetic cost logic.
- Introduction and estimation of an energy cost of capital (ECC) metric.
- Representation of exogenous model interfaces via stochastically generated logistic functions.
- Model initialization achieved using parsimonious model inputs and initial flow reconciliation via a novel, non-linear iterative solver.

- Endogenous system control via a stability calibrated, feedback-driven heuristic, including treatment of supply and demand energy investment allocation options on an equivalent, functional, net energy basis.
- Comprehensive probabilistic representation of epistemically uncertain model inputs for use in Monte Carlo simulation of system behaviour.
- Implementation of a unique metric for multivariate sensitivity analysis capturing both the strength and slope of correlation, suitable for assessing non-linear relationships between model input parameters and selected output variables.

Subsequently, a distinct and substantive contribution to knowledge is achieved via the quantitative characterization of the GES transformation solution space found using the PRESS model, including:

1) the identification of system ‘leverage points’ and investigation of the potential use of these in forming useful system-cognizant policy recommendations, and
2) the application of diagnostic analysis for the identification of epistemic risks arising from imperfect knowledge associated with uncertain model input parameters.

1 INTRODUCTION

1.1 THE ENERGY SYSTEM AND SOCIETY: PAST AND PRESENT

> *"We can think thoughts wildly, but if we do not have the wherewithal to convert them into action, they will remain thoughts. […] History acts in unpredictable ways. Events in history, however, necessarily take on a structure or organization that must accord with their energetic components."*
>
> – Richard Adams [2]

Energy is the ability to effect change in the world. It is the motive force by which we create valuable goods from raw materials and transmute knowledge into useful services. Human societies require continuous supplies of energy for their essential functions, including food production, shelter, and transportation, and all other forms of social and economic activity [3]. Moreover, energy surpluses are central to the formation and development of societies, including their ultimate scale, and levels of technical and cultural complexity [4-12]. The energy systems providing these surpluses therefore represent essential interfaces between human societies and the natural world. While energy does not offer a complete explanation of the evolution of societies, or determine specific cultural or economic forms, energy availability imposes a firm limit on the set of physical possibilities [6, 13].

Until relatively recently in human history, accessible flows of exosomatic energy were modest and often unreliable. These consisted largely of biomass burned for heating and illumination, and used as fodder for draft animals, direct sunlight for heating and drying, and flows of wind and water powering transportation and simple mechanical processes, such as the milling of lumber and grain. This energetic basis firmly constrained the levels of aggregate economic activity and societal complexity that could be achieved and maintained, while subjecting humankind to the unpredictable fluctuations of natural energy flows.

Major transitions in patterns of energy provision and utilization have occurred only twice in human history: the shift from hunting and gathering to settled, agricultural societies, and the more recent, and still incomplete, shift from agrarian to an industrialized, globally interconnected economy [4, 5, 14-18]. Both energy transitions have expanded possibilities for livelihoods, modes of social organization, and socio-technical capacities by increasing the size and consistency of energy surpluses [6, 12, 15, 19, 20]. The industrial revolution, beginning with the discovery and widespread exploitation of the fossil fuels (first coal, later petroleum and natural gas), catalysed the mechanization of agriculture and industry, and the subsequent shift from physical labour to specialized, knowledge-based employment for large segments of the global population [12, 21]. This shift spurred mass urbanization alongside unprecedented increases in the scale and interconnectedness of the global economy, scientific and technological advances, and gains in material standards of living culminating in the emergence of high-energy modernity. The associated boom in global population and societal complexity is a unique and nonreplicable occurrence in human history [4, 22-24]. As noted by Tainter et al. [25], "The Industrial Revolution, as we experienced it, cannot be repeated, for we have used many of the most accessible, high-quality reserves that made it possible."

Stemming from the second energy transition, the pervasive use of technological capital for accessing and utilizing increasing flows of exosomatic energy has become a defining feature of industrial civilization [26, 27]. Consequently, the global energy system (GES)[1] has grown to become the largest, most technologically advanced collection of built capital and socio-technical capacities that has ever existed [26, 28]. The average North American consumer now depends on the energetic equivalent of the labour of approximately 90 'energy slaves' [29], a prodigious energy subsidy underpinning the modern way of life which is being swiftly replicated around the world. This pursuit of ever-greater levels of power has become self-perpetuating and the global economy now exhibits many of the characteristics of an energy-hungry superorganism [30-32].

Energy flows are derived from both renewable energy (RE) and non-renewable energy (NRE) resources. A useful functional definition is offered by Georgescu-Roegen [26]: *RE resources consist of natural flows which are not permanently depleted by their exploitation, while NRE resources consist of depletable terrestrial stocks*. In other words, the consumption of RE does not permanently change the boundary conditions of society, while the consumption of NRE does [21]. RE resources include solar energy reaching the surface of the earth and its

[1] Built capital constituting the GES can be described as stocks of 'power capacity', organized in sequential stages, for the conversion, transportation, and utilization of energy flows for the provision of final energy services, including all required supporting infrastructures.

derivative forms (including wind, hydropower, and biomass), plus geothermal and tidal energy. NRE resources are comprised of the fossil and nuclear fuels. While the totality of the primary energy resources available to humankind is colossal, it must be recognized that accessible magnitudes are subject to considerable uncertainties. For RE, 'sustainable' long-term potentials are highly contentious, particularly for energy derived from biomass [33-36], while for NRE, the proportions of total *in situ* resources to eventually become practically accessible are strongly dependent on geological, technical, and economic factors which cannot be predicted with certainty. Furthermore, both represent thermodynamic gradients characterized by heterogenous quality distributions[2], subject to declining aggregate quality under conditions of progressive resource exploitation [8, 37-39]. These thermodynamic gradients cannot be produced by humans, only extracted or harvested [21].

The extent and rapidity of the growth of the GES over the last several centuries highlights the extremely anomalous historical position of high-energy modernity. As shown in Figure 1, global total primary energy supply (TPES) was approximately 630 exajoules (EJ), 20 terawatts, or 15 billion tonnes of oil equivalent per year, as of 2020 according to BP data[3] [40]. This rate of energy consumption increased almost 20-fold during the 20th century alone [41], and continues to grow at a rate of around 1-3% per year [40]. NRE resources remain economically critical. As noted by Day et al. [42],

> *"Fossil fuels currently dominate energy use—providing over 80% of global primary energy supply and roughly 75% of energy end use—and power many critical economic activities related to transportation, chemicals and fertilizers, heavy machinery, heavy industry, and considerable domestic use."*

[2] Primary energy resource quality can be defined in terms of net energy production, with quality distributions describing net energy ratios as functions of either the energy production rate (for RE) or cumulative energy productions (for NRE). See section 2.1.1 for details.

[3] Primary energy data presented here follows BP's primary energy accounting approach, which uses the thermal energy equivalence method and excludes traditional biomass.

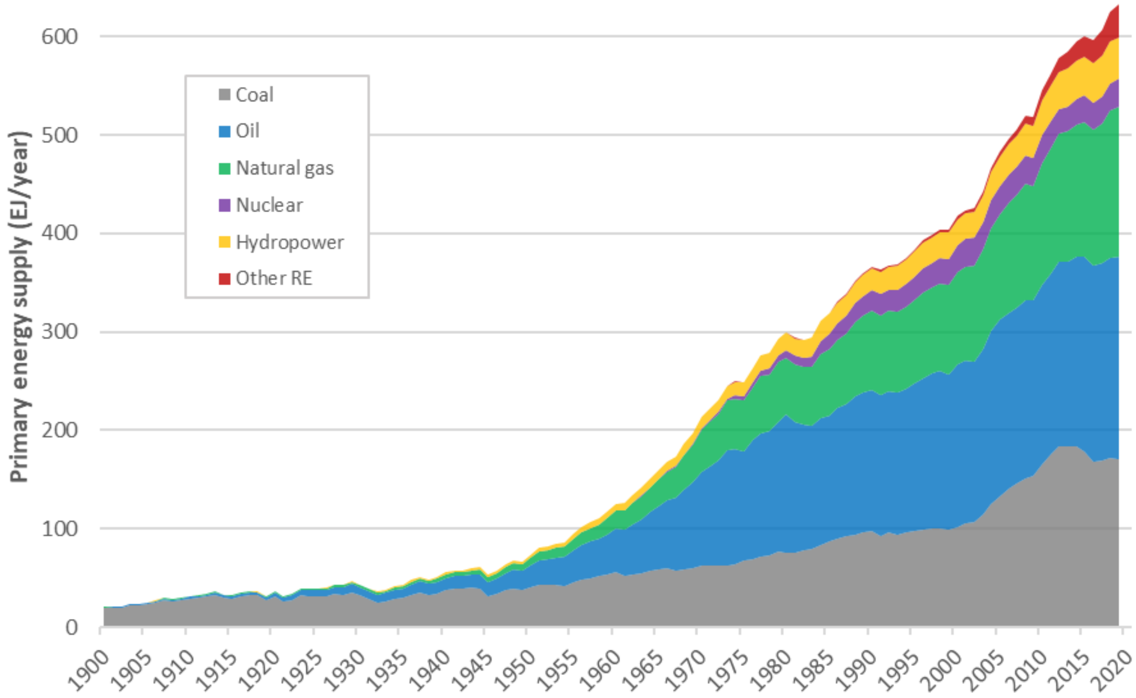

Figure 1: historical primary energy supply by resource, excluding traditional biomass (1900-2020; data from The Shift Project [43] and BP [40])

It is crucial to note that despite rapid growth in RE supply in recent years – widely reported in the popular media and described by Edenhofer et al. [44] and the Frankfurt School-UNEP Centre/BNEF [45], among many others – RE sources still account for only around 12% of the global TPES, or 5% excluding hydropower (the red segment in Figure 1) as of 2020 [40]. Smil [28] notes that RE growth rates are in fact significantly lower than peak rates observed for each of the fossil fuels, observing that "Global energy transition has been, so far, overwhelmingly a shift in electricity generation that has had only a small effect on the decarbonization of the overall primary energy supply." Projected RE growth rates required to meet climate targets far exceed those recently observed [42, 46]. Properly conceived, the third energy transition has only just begun; *ergo*, developments to date cannot be considered as indicative of the remaining challenges involved in a comprehensive shift to a RE basis.

Nevertheless, the global energy system (GES) is necessarily on the cusp of transformative change during the 21st century. Aside from the amelioration of significant local social and environmental impacts stemming from expansive energy infrastructures and extractive activities, the most significant global drivers affecting the evolution of the GES include:

- **Anthropogenic climate change** – the widely recognized threat of global climate destabilization requiring an urgent shift away from reliance on the fossil fuels representing the largest sources of anthropogenic greenhouse gas (GHG) emissions [47-49].

- **Resource depletion** – the progressive exploitation of NRE resources, affecting resource quality and ultimately primary energy availability, with significant socio-economic and environmental implications [14, 35, 50-56].
- **Alleviating energy poverty** – improving energy access and affordability to address crippling energy poverty globally, as 1.3 billion people still lack access to electricity and 2.7 billion continue to use biomass directly for cooking with significant impacts on respiratory health [49, 57, 58]. There remains an unequivocal positive relationship between energy access and affordability, and human wellbeing, as measured by the United Nations Human Development Index (HDI) [59, 60].

1.2 COMPETING FUTURE NARRATIVES

Planning effectively for the future requires identifying the full set of possibilities, or 'solution space', for transformation[4] of the GES and, by extension, the range of future possibilities for society. However, the study of GES transformation has not yet arrived at definitive methods, or even consensus on the appropriate socio-technical narratives framing the nature of the challenge [21]. Consequently, highly diverse perspectives exist regarding the future of the GES, including its ultimate scale and composition, and the achievable pace of transition. Considering projections for global TPES alone, expectations vary widely, typically ranging between 400 and 850 EJ/year by 2050 [61, 62]. Figure 2 illustrates a representative range of projections, from continued increases along linear or logistic trends, to steep declines described by annual percentage decreases. While most scenarios seek to restrict cumulative GHG emissions, projections tending towards the latter are generally more optimistic regarding carbon capture and storage (CCS) and other technological solutions to climate change than projections approximating the former, which often assume strong efficiency improvements and changes in consumption behaviours leading to decreases in aggregate primary energy consumption.

[4] The term 'transformation' is used to emphasise the aspects of complexity and interdependence involved in a fundamental reconstitution and reorganization of the GES, extending well beyond simple substitution processes.

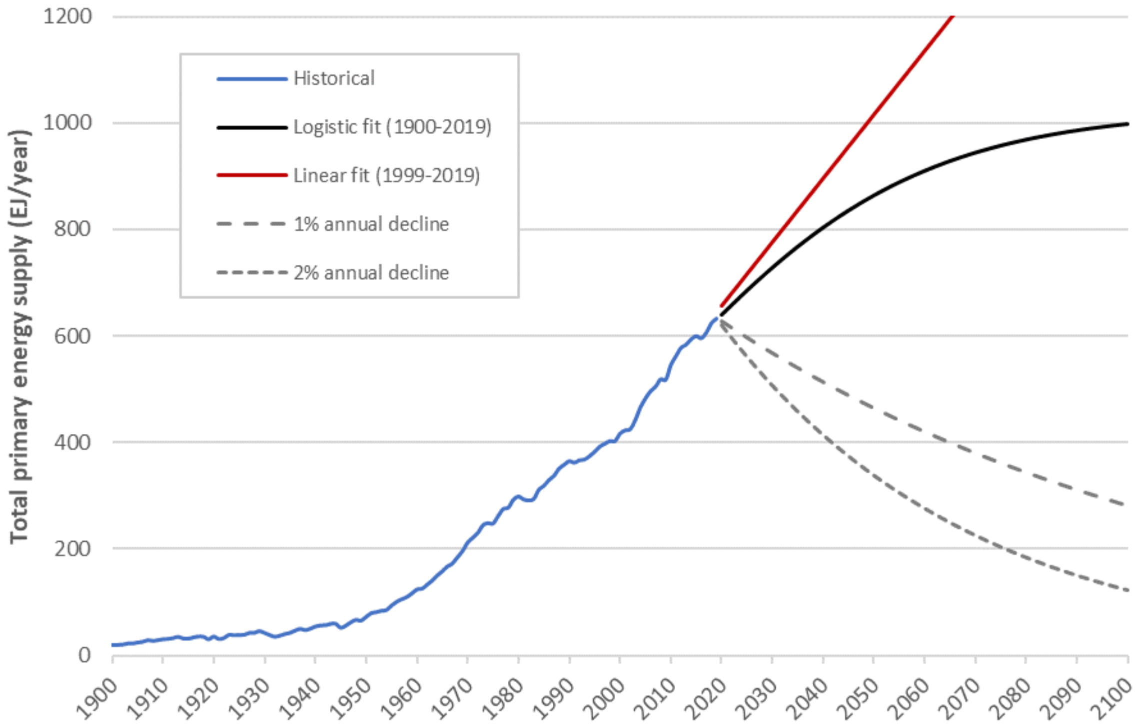

Figure 2: historical total primary energy supply (1900-2020) with representative future projections

The differences in GES transformation narratives are stark, raising questions regarding the origin of these discrepancies. While not always immediately apparent, competing narratives can stem from mutually incompatible presuppositions rooted in distinct scientific paradigms. As described by Thomas Kuhn in *The Structure of Scientific Revolutions* [63], scientific paradigms consisting of established ontological frameworks with associated terminology and methodologies periodically give way to new, incommensurate paradigms following the accumulation of anomalies which cannot be explained by the prior worldview. Such a paradigm shift may now be unfolding, affecting perspectives of GES transformation, among many other areas of scientific inquiry. As described by Prigogine and Stengers [3] and Capra and Luisi [64], the Cartesian-Newtonian worldview, dominant in Western thought since the scientific revolution of the 16th and 17th centuries, is increasingly unable to meaningfully address modern problems of energy, environment, and society characterized by complexity and interdependence. In its place, the 'systems' paradigm, originating in late 19th and early 20th century advances in mathematics and the life sciences, now offers an alternative scientific paradigm centred on an appreciation of the nature of complex systems. Table 1 compares pertinent aspects broadly aligned with and emphasized by these two scientific paradigms across the domains of ontology, terminology, and methodology.

Table 1: comparison of selected aspects of the Cartesian-Newtonian and systems scientific paradigms

Domain	Cartesian-Newtonian paradigm	Systems paradigm
Ontology	Ahistoricism	Historical path-dependence
	The whole as the sum of its parts	Emergent phenomena, synergy
	Linearity	Non-linearity, chaos, self-organization
	Technological fundamentalism	Biophysical limits
	Inexorable progress	Cyclical progress & regression
	Culture as intangible	Culture as embodied
	Logical positivism	Pragmatism, falsificationism
Terminology	Elements	Elements & relations
	Mechanistic causation	Feedback loops
	Static equilibria	Dynamic stability domains
	Costs & benefits	Socio-metabolic patterns
	Economistic language	Ecological & thermodynamic language
Methodology	Analytical reductionism	Synthetic holism
	Marginal analysis	Multi-scale, integrated analysis
	Design, prediction, & control	Exploration & leverage points
	Scientific consensus	Epistemic humility & pluralism
	Specialization of knowledge	Radical transdisciplinarity
	Optimization	Multi-criteria analysis & heuristic techniques

Paradigms are powerful – facilitating but also constraining thought. As noted by Cleveland and Ruth [65], "By definition, adherents to a paradigm believe that all relevant phenomena are best understood through the conceptual lens of that paradigm, and that all problems can be solved with the analytical tools used in that paradigm." Such perspective-dependent framing applies to contemporary narratives regarding relationships between energy and society, which can be separated into two broad categories as described by King [31]:

- *Technological optimism*, which focusses on human adaptability and problem-solving prowess via technological innovation, assuming a practically unlimited capacity for substitution.
- *Technological realism*, which emphasizes the evolving limits imposed on human societies by the laws of physics and fundamental dependencies on a finite biosphere.

Broadly speaking, technological optimism emerges from the Cartesian-Newtonian paradigm and tends to employ mechanistic conceptions of society within a linear, progress-centric view of history. In contrast, technological realism, aligned with the systems paradigm, seeks to uncover relationships and dependencies affecting complex societal problems, including understanding the biophysical foundations of the economic process. The former remains almost ubiquitous in perspectives of GES transformation, informing the majority of popular, institutional, and policy problem framings. Its psychological pull is self-evident; as observed by Georgescu-Roegen [26], "Naturally, the innovations in artefacts, being more impressive, have enslaved our imagination and, *ipso facto*, our thoughts of what we can achieve." Unfortunately, reductionist approaches to complex problems spanning multiple interconnected systems will often produce confused and counterproductive solutions [21, 66]. Smil [14] concurs, "Unfortunately, common expectations of energy futures – shared not only by poorly informed enthusiasts and careless politicians but, inexplicably, by too many uncritical professionals – have been, for decades, resembling more science fiction than unbiased engineering, economic and environmental appraisals." Consequently, a revolution in the understanding of what energy transition fundamentally is and what can be expected for the future, followed by the popularization of this knowledge, is increasingly instrumental.

Meanwhile, the need to implement appropriate policies to expedite the third energy transition is now unambiguous. The two narrative types described above typically arrive at highly disparate problem framings and associated policy positions, particularly regarding:

- the relative importance of technical innovation,
- the appropriate balance of individual, market, and state responses, and
- ultimately sustainable scales of the GES and the economic activity it can support.

It is true that remarkable technological progress has been achieved in recent years as the world has gained a greater awareness of emerging threats, particularly climate change, bolstering the optimistic case. However, as noted by Giampietro et al. [21] many remain unaware that the discontinuity in human development following the industrial revolution is a function of not only new energy converting technologies and social institutions, but also of cheap and abundant fossil fuels. Expectations of an imminent technological resolution to the major crises of the 21st century frequently suffer from 'Moore's curse': a categorical error mistaking rapid progress in some fields, such as computing and information technology, for a general exponential trend in technological innovation [28, 67]. Furthermore, it must be remarked that observations at one scale of analysis, often made at the technology or process level, cannot be applied to the behaviour of the system as a whole [68]. The systems perspective underscores the impossibility of identifying *a priori* the precise pathway GES transformation will ultimately take and its broader socio-economic implications. As explained in the following sections, properly contextualizing the challenge from a systems perspective is therefore crucial for improving the state of knowledge.

1.2.1 Returning to a solar civilization

> *"But there is always the sun, from which man has derived all of his energy, directly or indirectly, in the past. And it may well be that it will become, directly, our chief source of power in the future."*
>
> – Leslie White [5]

Energy flows in natural ecosystems are derived from and constrained by solar flux. Humans alone have devised the means to break free of this constraint by creating technological systems for provisioning vastly greater power from the fossil and nuclear fuels [13]. This technological capability underlies the progressive substitution of abundant but diffuse, rate-limited solar energy and its derivative forms by the energy-dense fossil fuels which can be used at desired rates [22, 26]. Consequently, modern, industrialized societies now rely overwhelmingly on depletable energy stocks, while inexhaustible energy flows have assumed a lesser importance. Smil [69] aptly describes the stark implications of this situation:

> *"Our current energy system is self-limiting: even on a historical time scale our high-energy civilization, exploiting the accumulated store of ancient radiation transformed into fuels, is just an interlude because even if the combustion of those fuels had no environmental impacts it could not, unlike its predecessors, based on harvesting near-instant solar energy flows, last for millennia."*

White [5], Georgescu-Roegen [26], Winter [70], and Odum and Odum [71] have also remarked on the likelihood of eventually returning to a flow-based, solar civilization, barring the discovery of new energy technologies of unparalleled potential. While direct solar irradiance reaching the surface of the Earth far surpasses current global primary energy consumption [14, 34, 72-74], the relevant bottleneck is not the total availability of primary energy but the dynamically evolving capacities of industrial societies to build the requisite capital to harvest and process this energy while subsisting on the energy flows produced [16, 54, 75]. As noted by Cottrell [12],

> *"[T]he amount of radiant energy is so far in excess of man's present ability to convert it that it cannot be considered to limit human behaviour. Energy-imposed limits stem from the particular means by which energy is converted into the particular forms desired by man at a particular time and place."*

The required reconstitution of the GES will not be a simple substitution and instead likely to be a protracted process, taking multiple decades to centuries to complete [14, 54]. This process is energetically disadvantageous, complicated by multiple factors, including:

- the low power density and uneven geographical distribution of solar and other RE primary energy gradients [4, 8, 53, 76-78] with implications for land utilization [14, 54, 79-81] and the spatial distribution of industrial capital [12],
- larger upfront energy investments required for RE capital compared to NRE [9, 75, 82],
- the reliance of RE production on limited and depletable mineral resources without the possibility of perfect recycling [39, 72, 83], and
- the need for many RE technologies to be paired with energy storage and supporting infrastructures, or backup generation capacity, in order to meet demand reliably given their variable and unpredictable power output [35, 84-86].

The ability of RE energy sources to sustain high-energy industrial societies remains unproven and can be called into question [4, 9, 14, 20, 27, 35, 42, 54, 55, 87, 88]. As noted by Odum [66], low-quality RE energy sources may cease to be viable at all without the high-quality energy subsidies provided by the fossil fuel economy. To date, RE sources have not meaningfully displaced fossil fuels [23, 89] and do not provide energy flows of similar versatility, energy density, transportability, or storage potential [15, 35, 42, 53, 82]. Additionally, this transition must unfold in the context of critical fuels being sourced from increasingly expensive and lower-quality NRE resources, a dynamic which tends to undermine economic growth [50, 52, 90, 91]. This runs counter to widespread but potentially implausible assumptions for deep decarbonization of the GES under conditions of continued economic growth and stability [92-94]. The long-term implications of this situation are difficult to anticipate but may impinge upon the current scale and dominant modes of energy consumption [25, 27, 54, 82] and will entail a profound restructuring of modern economies.

Assumptions for the continuation of high-energy modernity made possible by the currently unsustainable configuration of the GES are commonplace, as noted by Floyd et al. [54]. However, maintaining desirable aspects of societal complexity while shifting to a fundamentally different energy basis is an energetic experiment without historical precedent and cannot be presumed. Returning to a solar civilization represents the reverse direction of the historical process by which high-energy modernity came into existence, and as such will necessarily bring changes to the social and economic structures underpinning human societies [14, 25]. Institutions and forms of social organization predominant in high-energy societies today are, in part, products of their current energetic foundation and may be inseparable from it [12, 95, 96]. As such, the third energy transition will likely bring with it novel and unanticipated socio-political challenges [9, 21, 97, 98], the implications of which extend beyond the present discussion.

The scale and complexity of a comprehensive transformation of the GES are frequently underestimated, often overshadowed by narratives rooted in technological optimism lacking recognition of the novel challenges and irreducible uncertainties involved [54, 59, 69, 99-101]. Furthermore, it must be remembered that GES transformation alone is not a sufficient condition for ecological sustainability, as the return to a RE basis is just one facet of the retreat from the advanced stage of ecological overshoot and resource drawdown presently faced by industrial civilization described by Catton [102], Wackernagel et al. [103], and Meadows et al. [104]. The broader context described above will inevitably constrain pathways for GES transformation. Such constraints may manifest as failures to achieve prevailing expectations for future social, economic, and technological development, with unpredictable and far-reaching impacts in modern, high-energy societies [105].

1.2.2 The GES as a complex adaptive system

The biophysical perspective emerging from the systems paradigm reveals the GES as a nested sub-system of the wider human socio-ecological system (HSES), which is itself a sub-system of the Earth's biosphere, as depicted in Figure 3. All have been recognized as examples of complex adaptive systems (CAS): thermodynamically open, far-from-equilibrium, dissipative systems consisting of co-evolving networks of interactions between elements, exhibiting properties of non-linearity, self-organization across multiple scales, path-dependence and irreversibility, emergent and adaptive behaviours, and autopoiesis[5] [10, 16, 21, 64, 106-110]. As described by Court [16],

> *"[S]elf-organization driven by thermodynamic laws works in combination with the general algorithm of evolution (variation, selection, and replication) to*

[5] Autopoiesis is the capacity for system 'self-creation' through endogenous metabolic processes allowing the maintenance and regeneration of the system's constituent elements.

explain the emergent dynamics of complex adaptive systems such as living organisms, ecosystems, and even economic systems."

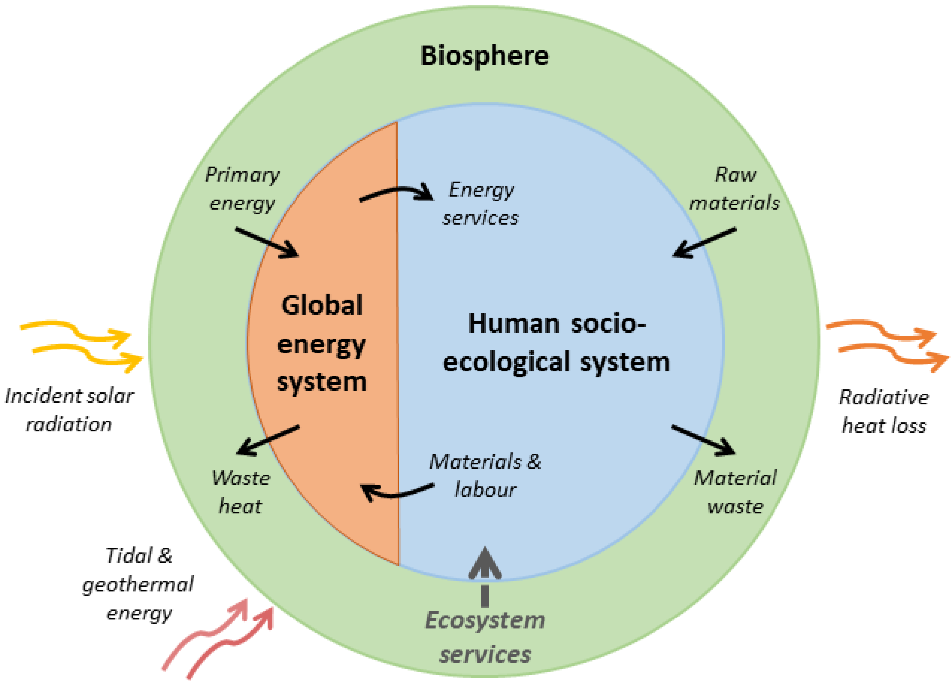

Figure 3: biophysical view of the GES as a sub-system of the HSES and biosphere

Consequently, Giampietro et al. [21] explain that energy systems analysis should properly be defined as "the systematic study of integrated sets of energy transformations that can be associated with the stability of self-organizing dissipative systems (metabolic systems)." As a CAS, mechanistic, linear descriptions cannot meaningfully describe or predict the behaviour or evolution of the GES [26, 110]. Instead, the interdisciplinary field of systems theory and associated modelling techniques are foundational to the exploration of interdependent GES and HSES futures [64, 68, 104, 110-113]. As noted by Levin et al. [110], ignoring the characteristics of CAS "can distort our picture of how these systems work, causing policies to be less effective or even counterproductive."

At the simplest level, CAS can be characterized by identifying 'leverage points', or system parameters amenable to human control which can produce significant effects on system behaviour, as described by Meadows [114]. Leverage points can facilitate the specification of effective interventions and policies for GES transformation. For example, leverage points can highlight relative system responsiveness to various intervention types, such as technological versus behavioural adaptation, or the likely future importance of specific technologies or primary energy resources.

Due to the CAS property of path-dependence, the study of GES transformations cannot reference the initial or final states alone, but instead must identify dynamic pathways[6] between these states. As outlined by Giampietro et al. [21], the exploration of such pathways in complex, autopoietic systems requires an irreducible dual analysis: the external perspective describing energy exchanges between the system and its environment for the maintenance of boundary conditions, and the internal perspective describing energetic processes between elements of the system for the production of useful power. These perspectives allow the specification of exogenous and endogenous system constraints, respectively, originating in intrinsic co-evolutionary processes occurring at multiple scales:

- Exogenous constraints are imposed by the availability of primary energy gradients, described in section 1.1, and co-evolution between the GES and the HSES, outlined by Sorman and Giampietro [27]. As shown in Figure 3, the latter directs resources towards the operation and renewal of the former, while the former provides final energy services[7] required for the expression of necessary societal functions. This continuous exchange prevents the transformation of either of system independently of the other.
- Endogenous constraints arise from the internal metabolic structure of the GES, the energetic aspect of which is outlined in Figure 4 using Odum's 'energy systems language'[8] [71, 115]. This diagram identifies RE and NRE resources as the ultimate sources of exosomatic energy flows with sequential primary, secondary, and end-use conversion stages required for the provision of final energy services. Structural change within the GES requires the co-evolution of its constituent elements, in terms of the magnitudes and composition of its capital stocks across all stages. The GES cannot be modified arbitrarily due to the requirement to maintain approximate internal coherence both between and within the stages [21].

[6] Each dynamic GES transformation pathway represents a unique trajectory corresponding to physical and organizational changes within the GES over the relevant time interval.
[7] See section 2.2.3 for the definition and enumeration of final energy services.
[8] Energy systems language (or 'Energese'), developed by systems ecologist H. T. Odum, uses symbols and circuit diagrams to describe energetic flows, transformations, and interactions within complex systems.

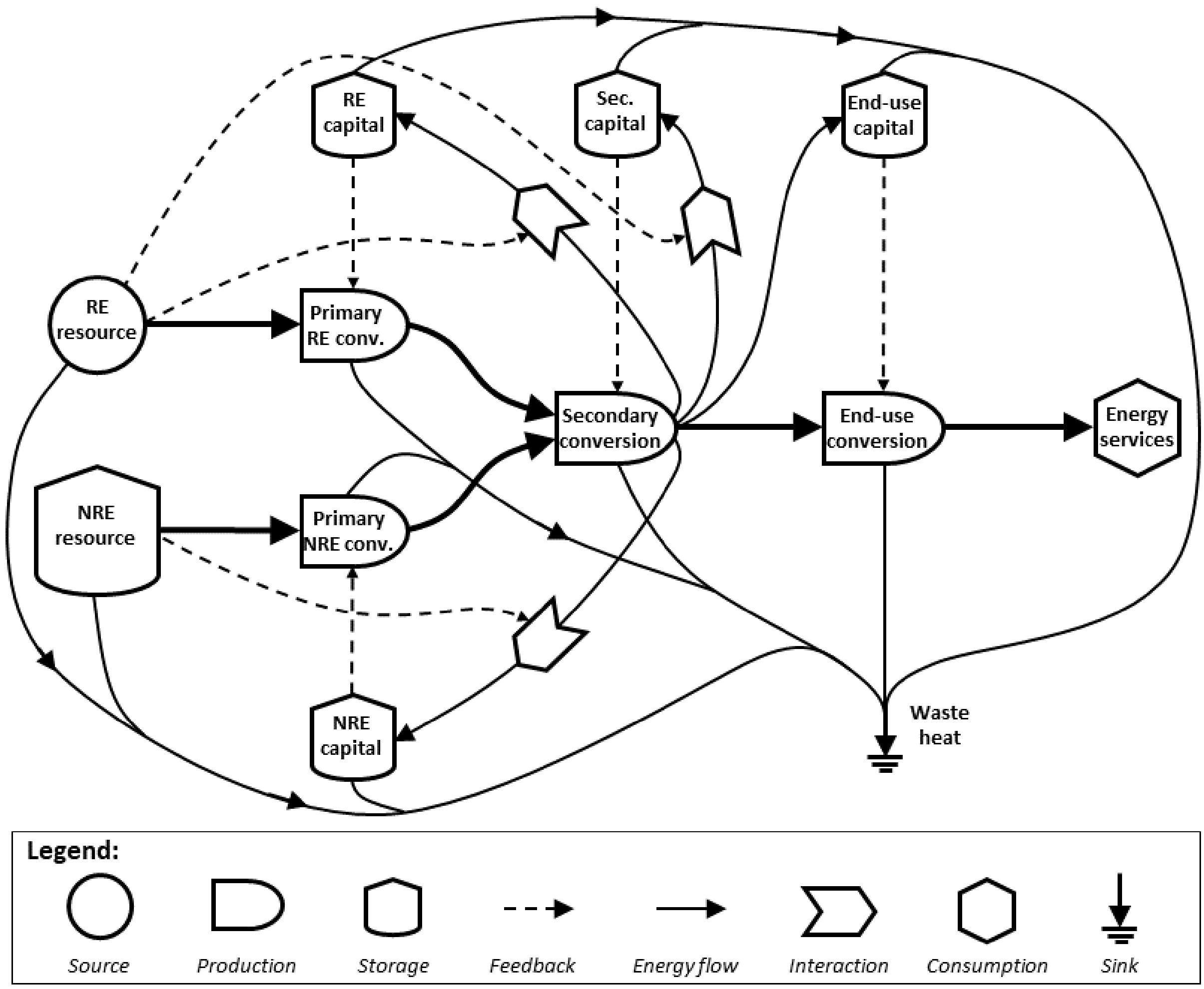

Figure 4: energy systems language flow diagram for the GES

GES transformation pathways can be characterized by reference to the above system constraints in terms of three descriptors, which can be assigned useful semantic definitions [116]:

- *Feasibility* relates to compatibility with exogenous constraints.
- *Viability* relates to compatibility with endogenous constraints.
- *Desirability* relates to compatibility with societal preferences and expectations.

The *desirability* descriptor, in the context of the present study, includes addressing climate change via decarbonization and the avoidance of conditions of energy poverty or scarcity (i.e., responding to the global drivers of GES evolution discussed in section 1.1). The GES transformation solution space is then defined by the full set of physically *feasible* and *viable* transformation pathways, with associated transformation outcomes described in terms of *desirability*.

The production of exosomatic energy is strongly autocatalytic, unlike the production of most other economic commodities [9, 12, 14, 21, 115]. Energetic autocatalysis, for the production of necessary system structures and energy reserves, is a basic property of CAS as noted by Odum [115]. Part of the output of secondary conversion (i.e., energy carriers, such as electricity, liquid transportation fuels, and heat fuels) is diverted for the creation and maintenance of capital stocks constituting the GES, as depicted in Figure 4. That is, a significant component of the output of the GES must be directed back into its own autopoietic processes. This conceptualization, while largely ignored within mainstream narratives and analyses, is becoming increasingly pertinent as the ongoing depletion of fossil fuels and associated declines in resource quality effectively reduce the efficacy of this autocatalytic process in a positive feedback loop [21].

Critically, this autocatalytic nature creates the potential for the 'net energy trap' phenomenon, in which a subset of GES transformation pathways can encounter insufficient net energy available to meet demand for final energy services required by the HSES while simultaneously maintaining the autopoietic processes of the GES itself [9, 39, 117, 118]. In a net energy trap, chronic energy scarcity can become inexorable, undermining the energetic foundation of the HSES. As such, energetic autocatalysis imparts a prominent bifurcation potential[9] for GES transformation pathways, with the net energy trap representing a highly undesirable transformation outcome.

The persistent misunderstandings present in common narratives and problem framings of energy transition have been described by Giampietro et al. [21] as a "clash of reductionism against the complexity of energy transformations". The systems perspective portrays GES transformation not simply as a complicated technical, political, or economic challenge, but as a *complex, physically bounded, path-dependent, socio-metabolic process*, which will necessarily transform the basic configuration of modern, high-energy societies. Furthermore, it is important to acknowledge that, due to path-dependence, uncertainty, and the presence of complex feedback loops, *the future configuration of the GES cannot be designed* in the ordinary sense. Ultimately, a post-transformation GES must provide sufficient energy surplus to support the societal complexity and economic activity necessary for its own autopoietic

[9] This bifurcation potential relates to a system phase change to a new basin of attraction associated with a different stable state, in this case metabolic collapse and a return towards thermodynamic equilibrium.

functions [84, 119], while remaining within long-term ecological limits locally, regionally, and globally [42]. This perspective informs the choice of appropriate theoretic and methodological approaches for the study of GES transformations.

Several relevant research questions can be formulated:

- *What is the set of physically feasible and viable pathways for GES transformation?*
- *To what degree are desirable transformation outcomes physically achievable, and how quickly can they occur?*
- *What are the factors which most strongly influence desirable GES transformation outcomes?*
- *What interventions and policies are best able to improve these outcomes (i.e., leverage points)?*
- *Conversely, what interventions and policies entail undesirable or unintended outcomes?*
- *What possible implications for broader changes within the HSES stem from the identified set of GES transformation pathways?*

1.3 The path forward

> *"Yet we cannot turn back; neither can we consolidate our gains and remain where we are. In fact, we have no choice but to proceed into a future which we may be assured will differ markedly from anything we have experienced thus far."*
>
> – M. King Hubbert [24]

If the GES remains on its current trajectory, it threatens the integrity and habitability of the biosphere itself [120]. Given the current 'full-world' global context characterized by manifold environmental and social crises, continuing a decentralized, market-based, profit-driven, and value-free approach to development of the GES is no longer defensible or pragmatic. Furthermore, conventional societal problem-solving frameworks lacking comprehensive treatment of uncertainty are increasingly inadequate in the face of catastrophic or even existential risks such as runaway climate change and the net energy trap. This underscores the need for an overarching epistemic and moral reorientation as a precondition for meaningfully evaluating pathways for GES transformation.

1.3.1 The need for a moral foundation

The nature of energy demand is an expression of societal values and goals, with changes in energy supply reshaping of those values over time, as described by Cottrell [12]. No widely-recognized normative principles underlying the satisfaction of these demands currently exist, and no ultimate purpose is defined for the GES other than to make available as much low-cost energy as possible in the service of aggregate consumptive and economic growth [121]. However, as argued by Healy et al. [122], efforts to undertake the third energy transition without an explicit, democratically produced axiological foundation amount to a continuation of the predominant patterns of extractive industrialism, neo-colonialism, social inequality, and profound environmental harms that have been the hallmarks of the fossil fuel age.

As an essential human-nature interface responsible for approximately three quarters of total anthropogenic GHG emissions [123], the GES cannot be properly contextualized without a moral dimension. The historical development, present utilization, and future evolution of the GES all have profound ethical implications, with distributional, intertemporal, and ecological aspects, briefly outlined below.

Energy transitions have strong repercussions for social equity [124, 125]. Access to energy services remains highly unequal globally [120, 126] and addressing energy poverty presents a key driver of GES evolution (as described in section 1.1), imposing clear upward pressure on energy demand. Given profligate energy consumption among some segments of the global population, it is appropriate to question the baseline energy needs of society. It is clearly possible to significantly reduce conspicuous consumption and energy waste with considerable environmental co-benefits [120]. The positive relationship between energy consumption and HDI only holds at low to moderate consumption levels, implying that excess energy consumption can be eliminated with little to no impact on wellbeing [60].

However, as noted by Dholakia et al. [127], in practice it is often difficult to separate discretionary and non-discretionary energy use as consumption patterns are strongly informed by social norms which typically fail to distinguish need from want. There are also limits to volitional reductions in energy consumption, for example, many crucial socio-technical capacities and modes of social organization are likely not viable at significantly lower levels of energy consumption [4, 14, 27, 95]. Currently, no countries in the world achieve sufficient provision of basic human needs for their populations with levels of energy and material consumption that can be maintained indefinitely [128, 129], indicating the presence of fundamental trade-offs. At a minimum, it is likely necessary to establish a basic principle of sufficiency, without which energy demand will continue to be inflated by growing affluence without satisfying basic needs for much of the world's population [120, 126, 130, 131].

Choices made regarding the composition and scale of the GES have acute intergenerational implications. Patterns of energy consumption can either be structured such that they favour current near-term affluence or the needs of future generations. Most notably, NRE resources used today are not available to meet the needs of future generations tomorrow. Questions of intergenerational allocation are inherently complex, characterized by deep uncertainties regarding future socio-economic trajectories, questions of appropriate moral principles, and the preponderance of 'wicked' collective action problems [132, 133].

Ultimately, modern societies need arrive at a mutually enhancing, or at least non-adversarial, relationship with the broader biosphere if they are to have an acceptable future [134, 135]. The GES exerts major impacts on the non-human world in via expansive infrastructures, climate change, waste heat and pollutants, and increasingly, direct harvesting of the biomass contained within living ecosystems [122, 136, 137]. This highlights the necessity for a general shift from anthropocentric problem framings towards greater ecocentrism in the consideration of pathways for GES transformation.

The above ethical dilemmas are politically contentious and, in many cases, intractable due to the presence of fundamental social and biophysical trade-offs. While this research project does not aim to provide a suitable moral framework for GES transformation, a better understanding of the solution space from a systems perspective can be highly instructive for such efforts. For example, normative propositions presupposing no conflict between the present depletion of NRE and the provision of sufficient energy services to future generations, or the adoption of high-energy lifestyles globally without widespread and environmentally destructive bioenergy production, may be revealed as biophysically untenable.

1.3.2 Epistemic humility and pluralism

As Henri Poincaré famously observed, the choice of relevant facts is a central problem for any science [138]. However, the myriad challenges of the third energy transition cannot be fully understood via singular, definitive problem framings as they are fundamentally complex, highly interconnected, urgent, and subject to numerous uncertainties and conflicting socio-technical narratives [25, 139, 140]. Acknowledgement of this epistemic context highlights the inadequacy of conventional, largely deterministic problem-solving frameworks. Floyd et al. [54] stress the need for 'knowledge humility' regarding energy transition futures, noting,

> *"The nature of the envisaged transition means that we are entering entirely unexplored territory, and the pathways that we walk into existence are subject to inherent, irreducible uncertainty. It is impossible to know up front just how these pathways will unfold, the full range of challenges that will be encountered along the way, and where the novel responses to them will take us."*

Limitations in the quality and availability of detailed data pertaining to energy production and consumption presents another challenge [37, 141]. This is complicated by inconsistencies in the semantic definitions of energy flows applied between major data sources, leading to conflicting characterizations of the current state of the GES and even the nature of emerging trends [21, 142, 143]. Consequently, decision making under uncertainty requires greater transparency and the explicit quantification of the 'strength of knowledge' representing the sum of factors such as the mode of information production, the quality of source data, the degree of peer consensus, and the robustness of assumptions employed [144].

Given the presence of irreducible uncertainties in the study of GES transformations, approaches centred on epistemic humility and pluralism of socio-technical perspectives are needed [26, 54]. No one quantitative approach can offer a complete of description of complex phenomena, rather a diversity of methods, perspectives, and assumptions is increasingly vital [145, 146]. Levin et al. [110] note that given the nature of risk and uncertainty facing CAS, a greater emphasis on precaution is also warranted. Convergence toward a clear scientific consensus cannot be expected. As such, methods lacking sufficient transparency or representation of alternative possibilities should be treated with scepticism and avoided.

Relevant research question:

Where is the characterization of GES transformation pathways most constrained by insufficient strength of knowledge?

1.4 RESEARCH OBJECTIVES

Rather than attempting to answer the epistemically dubious question *what will happen* in the third energy transition, this research project instead asks *what can happen*. As such, the research orientation embraced here, conceptually aligned with the emergent, self-organizing, and adaptive properties of complex systems, is essentially exploratory, not predictive.

The foundational understanding of the GES as a CAS outlined in this chapter (and explored further in chapter 3) can be summarized as a basic axiom framing the research project:

> Pathways for the coupled evolution of the GES and HSES are fundamentally constrained by the set of *feasible* and *viable* metabolic possibilities for the autocatalytic production of exosomatic energy.

This axiom can be demonstrated by analogy to biological organisms as a more intuitively familiar form of CAS: the continuation of their metabolic processes and adaptation to changing conditions is constrained by the basic requirement for sufficient net energy derived from available food sources. As noted by Brown et al. [10], “consider the analogy to biological metabolism: Gradually reducing an individual’s food supply leads initially to physiological adjustments, but then to death from starvation, well before all food supplies have been exhausted.”

In summary, the ultimate purpose of this research project is to develop a CAS-cognizant methodological approach and practical tool for improving knowledge of the solution space for GES transformation, including barriers, opportunities, trade-offs, and achievable outcomes. This approach:

- centres on system processes and constraints arising from the energetic, autocatalytic aspect of GES autopoiesis, rather than an exhaustive accounting of all metabolic processes, recognizing this as the most basic metabolic pattern giving rise to system bifurcation potential (i.e., the possibility of net energy trap outcomes, or metabolic collapse),
- identifies the physical *feasibility* and *viability* of GES transformation pathways, including quantification of multiple pertinent aspects of the *desirability* of

transformation outcomes (using the definitions of these descriptors introduced in section 1.2.2), and

- considers the central role of uncertainty and the strength of knowledge stemming from various input data, including implications for the characterization of GES transformation pathways.

The primary research objective can be stipulated as follows:

> To identify the solution space of energetically *feasible* and *viable* pathways for transformation of the GES from present NRE dependence towards a future RE basis, under uncertainty.

Note that the solution space defined here relates approximately to its broadest possible extent, as the consideration of non-energetic (i.e., social, political, and economic) factors can only diminish the set of energetic possibilities. Secondary research objectives are indicated by the research questions introduced in sections 1.2.2 and 1.3.2:

- *Identify the degree to which desirable transformation outcomes are physically achievable, including associated timeframes.*
- *Identify the factors which most strongly influence desirable GES transformation outcomes.*
- *Identify the interventions and policies that are best able to improve these outcomes (i.e., leverage points).*
- *Identify the interventions and policies which entail undesirable and unintended outcomes.*
- *Discuss possible implications for broader changes within the HSES which stem from the identified set of GES transformation pathways.*
- *Identify where characterization of GES transformation is most constrained by insufficient strength of knowledge.*

2 THE GLOBAL ENERGY SYSTEM

2.1 PRIMARY ENERGY RESOURCES

Energy is a universal quantity in all physical systems, widely understood as the capacity to perform physical work [13, 99]. The production of useful work, or thermal change, requires the presence of thermodynamic gradients representing natural concentrations of energy which can be brought into equilibrium with their surroundings via dissipative processes [3, 21]. Primary energy resources can be defined as the subset of thermodynamic gradients which are socio-technically accessible and economically useful to human societies. These energy resources are present in kinetic, thermal, chemical, nuclear, gravitational, and radiative forms [13].

Primary RE resources, including solar, wind, hydro, geothermal, biomass, tidal, and oceanic energy, exist as natural energy fluxes that cannot be permanently depleted but can be exploited up to practical flow rate limits, or 'technical potentials', determined by various physical, technical, and economic factors. While rates of replenishment and local exhaustion effects do constrain short-term availability for some primary RE resources, such as biomass, hydro, geothermal, and wind energy [14], theoretically, RE production below respective sustainable technical potentials can be continued indefinitely.

In contrast, primary NRE resources, such as oil, coal, natural gas, and the fissile fuels consist of geological stocks of chemical potential or nuclear energy which are progressively depleted until further production becomes impractical or uneconomic. The components of total NRE resources considered to technically and economically viable at a given time are termed 'reserves' [74]. The estimated quantity of an initial resource to eventually be converted to reserves is known as the ultimately recoverable resource (URR)[10]. The URR less cumulative extraction to date represents the remaining ultimately recoverable resource (RURR). Many primary energy resources can also be used for non-energy purposes, primarily as chemical feedstocks and for the manufacture of construction materials. Sousa et al. [147] note that

[10] URR estimates are defined probabilistically, including both discovered resources and projections for undiscovered resources specified at varying confidence levels.

non-energy uses of primary energy resources, currently equivalent to approximately 5% of TPES, are growing in relative importance.

The accessible magnitudes of all primary energy resources are fundamentally uncertain, as mentioned in section 1.1. The production of primary energy resources is technologically mediated, and consequently, technological advances can increase accessible reserves and technical potentials [6, 13, 38]. This process can be expected to continue, however, it is limited by the ultimately finite nature of the terrestrial resource base, constrained in all cases by either flow or stock limits. Smil [14] observes that economically and technically recoverable reserves, and accessible technical potentials, typically represent small shares of the respective *in situ* deposits or total energy fluxes. Hall et al. [53], Ayres et al. [148], and Benes et al. [149] caution that for primary NRE resources, the effect of geological depletion on reserves will inevitably overtake technological progress and may be doing so already in many cases. All primary energy resource magnitudes can be expected to asymptotically approach finite upper limits over time, subject to significant geographic diversity [14].

Resource estimates vary widely, particularly for RE resources as uncertainties regarding ultimate technical and economic limits are typically greater than for NRE [34, 150]. As such, assessments of primary RE resources cannot rely on their total physical availability (or energy content) alone. Floyd et al. [54] explain that "There are myriad socio-political, economic and engineering reasons why the practically realisable potential of renewables will remain a fraction only of even conservative estimates for technical potential." According to Moriarty and Honnery [35], the definition of 'sustainable' RE technical potential is highly contentious – estimates can range over several orders of magnitude, particularly for biomass and solar, due to conflicting estimation methodologies, and consideration of declining resource quality and competing land uses. A growing scientific consensus urges scepticism regarding significant expansions of biomass energy over concerns of economic feasibility, technological uncertainties, competition with food production, limitations facing water and nutrient inputs, soil erosion, biodiversity loss, and compatibility with existing GES infrastructures [14, 23, 28, 33, 35, 36, 78, 151]. Large-scale environmental impacts are also observed for hydroelectricity [35, 59], and wind energy [14, 152, 153], limiting their realizable potentials.

Giampietro et al. [21] note that adequate descriptions of primary energy resources must include two interrelated factors: their gross magnitudes and their quality distributions.

Resource quality is discussed next, in section 2.1.1. It is also necessary to consider qualitative differences in primary energy resources in terms of temporal availability and implications for their prospective integration into the GES, as detailed in section 2.1.2.

2.1.1 Primary energy quality

The capacity to produce useful work, or thermal change, depends not only on the *quantity* of energy available but also its *quality* [13, 66, 154, 155]. Various perspectives on the factors constituting energy quality exist. Cleveland et al. [156] note that primary energy quality refers to various attributes describing the ability of resources to support useful activities, including energy density, geographical accessibility, flexibility of use, requirements for conversion and processing, and associated end-use efficiencies. Giampietro et al. [21] suggest that energy quality can be seen as a measure of concentration along respective thermodynamic gradients. According to Hall et al. [13], the quality of energy resources varies primarily with the energy costs of obtaining them. While primary energy resource magnitudes are widely studied, resource quality distinctions receive considerably less mainstream attention [13, 21, 39, 53, 157].

Quality for any given natural resource is not homogeneous but rather can be described by a distribution. The specific quality distributions describing available primary energy resources are more important than, and in fact determine, their accessible magnitudes (reserves and technical potentials) due to the existence of thresholds below which production is uneconomic and energetically unfavourable (see Figure 5 below). Quality varies widely between primary energy resources, and between energy carriers[11]. Hall et al. [13] note that oil and gas are typically higher quality fuels than coal. Processed energy carriers are generally higher quality than the primary energy resources they are derived from, with electricity the highest quality among them representing a near equivalence to useful work, as described by Ayres and Warr [141].

Two prominent measures of energy quality are overviewed in this section: exergy and energy return on investment (EROI). Exergy is a thermodynamic attribute of all energy and material

[11] Energy carriers are finished, high-quality fuels used in end-use applications, such as electricity, heat, and liquid transportation fuels (discussed further in section 2.2.2).

flows, while EROI is defined for specific primary energy resources and energy production processes (up to the scale of society as a whole).

2.1.1.1 Exergy

The technical definition of exergy is *the maximum amount of useful work recoverable from a physical system as it approaches equilibrium with its environment reversibly* (i.e., infinitely slowly) [141, 154, 156, 158]. Exergy is a function of the organization and concentration of matter and energy and its corresponding distance from thermodynamic equilibrium, relative to a selected reference state. Exergy is similar to the standard heat of combustion, or enthalpy, and these two quantities are nearly identical for the fossil fuels [141, 156]. As described by Glucina and Mayumi [73],

> *"Simply put, exergy is the energy remaining after "nature's tax" has been subtracted during a transformation. In other words, exergy is the amount of energy in a system that is actually available to do work, and so is always less than or equal to the total energy of the same system."*

Exergy is now widely recognized as an important concept at multiple scales: at the process level for the identification of potential efficiency improvements and at the macroeconomic level as instrumental to growth (discussed further in section 3.1.3) [16, 20, 26, 73, 141, 148, 154, 156, 158-164]. While energy is conserved in all processes (the first law of thermodynamics), exergy is destroyed as useful work is extracted and equilibrium is approached [154, 158]. Ayres and Warr [141] and Romero and Linares [154] argue this fact makes exergy the more economically relevant measure. However, while exergy offers useful information and can be used to improve understanding of thermodynamic processes within the GES and HSES, the concept suffers from ambiguities preventing its use as a definitive measure of primary energy resource quality [21, 73, 154, 156, 158], including:

- sensitivity to chosen reference conditions,
- specification relative to idealised, reversible processes which are not practically achievable and, as such, are often not meaningful (discussed further in section 2.2.1),
- 'one-dimensionality', excluding non-thermodynamic aspects of economic usefulness, such as transportability, cleanliness, cost of conversion, etc., and
- confusions associated with arbitrary and anthropocentric definitions of useful work.

2.1.1.2 EROI

Energy surpluses available to society can be analysed as gross energy flows but are more appropriately specified in terms of the net provision of energy to society, calculated as gross output less sum energy inputs to the production process. There is now a comprehensive literature outlining the biophysical and economic importance of net energy supplies for human societies [12, 13, 42, 51, 53, 66, 165-167]. Distinct supply contributions can also be considered on a net energy basis using a variety of related metrics, including EROI, the net energy ratio (NER), and energy payback time (EPBT), often calculated via similar techniques [168, 169]. EROI is one of the conceptually simplest and most useful measures, defined as *the ratio of gross energy returned from an energy producing process to energy expended in the process over its lifetime* [13, 37, 170]:

$$\mathrm{EROI} = \frac{Lifetime\ energy\ output\ from\ a\ process}{Lifetime\ energy\ input\ required\ to\ carry\ out\ the\ process}$$

The EROI concept has origins in the work of Lotka, Boulding, Georgescu-Roegen, and Odum [26, 171-173], and was later developed further and standardized by Cleveland, Hall, Murphy, and others [13, 37, 39, 174]. Many estimates now exist for the of EROI for NRE and RE resources, both historically and currently, using a diversity of methods. EROI is typically calculated via the *cumulative energy demand method* or similar techniques: summing the energy inputs required over the capital lifecycle, considering both the direct and the indirect contributions along its production chain where possible [39, 117]. The primary energy resource flow itself is not counted as an energy input – only finished energy carriers diverted from other possible uses are included [175]. Alternative approaches are required to model EROI dynamically, with diverse methods developed by D'Alessandro et al. [91], Capellán-Pérez et al. [39], and Brandt [51].

Quality corrections are required where distinct energy inputs must be aggregated to a common basis. Multiple aggregation methods exist, including the use of thermal equivalents, economic price-based techniques such as the 'Divisia Index', and exergy analysis [156, 170]. Cleveland et al. [156] argue that economic methods are preferable, as prices give more comprehensive information about quality distinctions extending beyond thermodynamic factors which do not fully capture the practical value of different fuels. Murphy et al. [170]

propose both price and exergy quality adjustments, noting that “At a minimum, electricity should be multiplied by a factor of 2.6 to represent mean thermal requirements.”

EROI can be defined at various stages within energy systems, subject to varying boundary definitions for the specification of energy inputs (i.e., the denominator) [39, 53, 170, 176]:

- *Standard EROI* ($EROI_{st}$) corresponds to the sum lifecycle energy requirements for the production of primary energy flows (onsite and offsite), including exploration activities, prior to processing and transportation (i.e., at the site boundary).
- *Point of Use EROI* ($EROI_{pou}$) corresponds to the sum energy requirements for the production and delivery of energy to the point of end-use (as finished energy carriers), including the lifecycle energy requirements of processing, transportation, and distribution.
- *Extended EROI* ($EROI_{ext}$) corresponds to the sum energy requirements for effective provision of useful energy services, including energy carrier production and delivery, and the lifecycle energy requirements of requisite end-use capital.

As boundaries specifying the inclusion of energy inputs expand, reported EROI values decrease, i.e., $EROI_{st} < EROI_{pou} < EROI_{ext}$ [39, 86]. EROI can also be specified for entire countries or regions, termed ‘societal EROI’, by aggregating over all useful fuels. Estimation of societal EROI is technically challenging and remains a nascent field, but several attempts have been made [42, 166, 176-178].

Hall et al. [13] observe that EROI varies with resource exploitation, tending toward lower values over time with the successive utilization of lower quality resources. This phenomenon is a direct consequence of heterogenous quality distributions, depicted using the ‘resource pyramid’ shown in Figure 5. When ordered by quality, the highest quality and most economically valuable resources occupy the apex of the pyramid, while the much more abundant base of the pyramid consists of lower quality, less valuable resources. Three crucial observations can be made:

1) Most cumulative production to date has come from the ‘conventional’ high-quality, low-cost end of the pyramid (erroneously informing expectations of future resource quality in many cases).
2) While technically and economically recoverable reserves tend to increase over time as prices rise and technology improves, a significant proportion of the

'unconventional' resource will remain inaccessible due to technical and economic limits, as described by Smil [14].

3) Accessible resources are constrained by an energetic boundary below which no net energy is returned (EROI < 1), a limit which is largely unresponsive to technological improvements (discussed further in section 2.1.1.3).

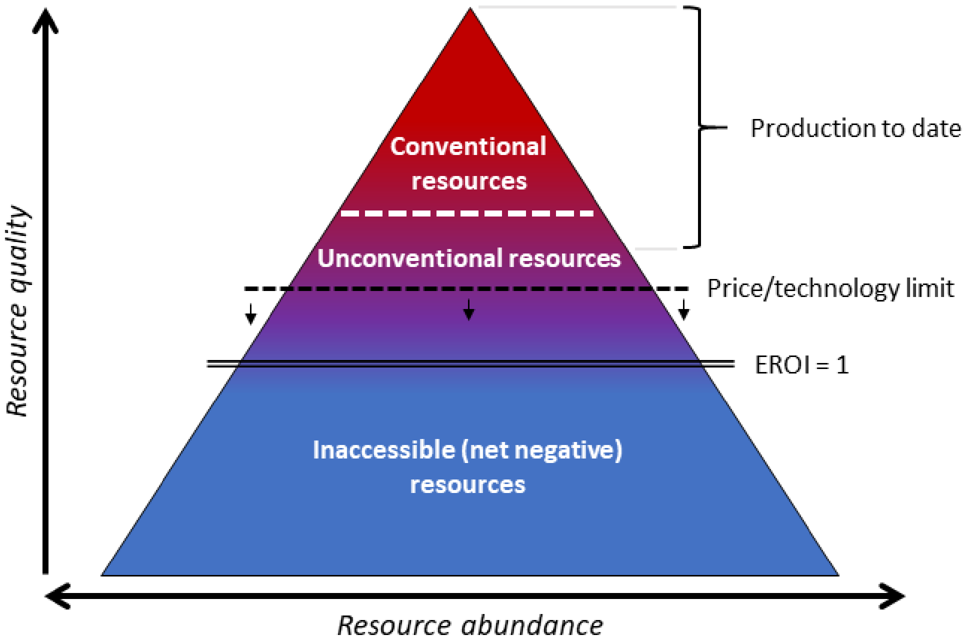

Figure 5: the resource quality pyramid (adapted from Heinberg [179])

For most significant primary energy resources and fuels, EROI has been declining steadily over recent decades [37, 53, 56, 180]. Taylor and Tainter [4] note that "The energy return on investment (EROI) of fossil fuels has been historically high, but is now decreasing." According to Court and Fizaine [181], the EROI of global oil and gas production reached their maximum values in the early 20th century, respectively around 50 and 150, and have subsequently declined, while the EROI of global coal production may not have yet reached its maximum value. RE resources tend to exhibit relatively low EROI compared to those previously seen for the fossil fuels, with the notable exception of hydropower [53, 88, 182]. In particular, the very low EROI of biomass-derived fuels is now widely recognized [36, 42, 53-55, 78].

Note that this research project employs EROI as the functional metric for primary energy resource quality due to its simplicity and extensive literature. Exergy, while conceptually important, is primarily useful for the aggregation of non-equivalent energy flows to a common unit of measurement and as such is not used (discussed further in section 3.1.2).

2.1.1.3 The physical basis of declining quality

The main causal factor explaining declining EROI is an economically driven process of selecting and exploiting primary energy resources sequentially, in approximate order of quality, in terms of energy density, ease of exploitation, and geographical accessibility [9, 75, 82, 183]. Hall and Klitgaard [184] note that while the underlying mechanisms are different for NRE and RE, as RE resource sites are simply occupied rather than depleted, the resulting EROI decline is similar. The economic drivers of EROI declines are most obvious in the NRE resources, demonstrated by the rising extraction costs of marginal reserves as the highest quality resources are progressively depleted [42, 52, 181, 183]. Dale et al. [75] describe this process, noting,

> *"In general, those resources that offer the best returns (whether financial or energetic) will be exploited first. Attention will then turn to resources offering lower returns as production continues. The result is that the accessibility of the resource declines as a function of production."*

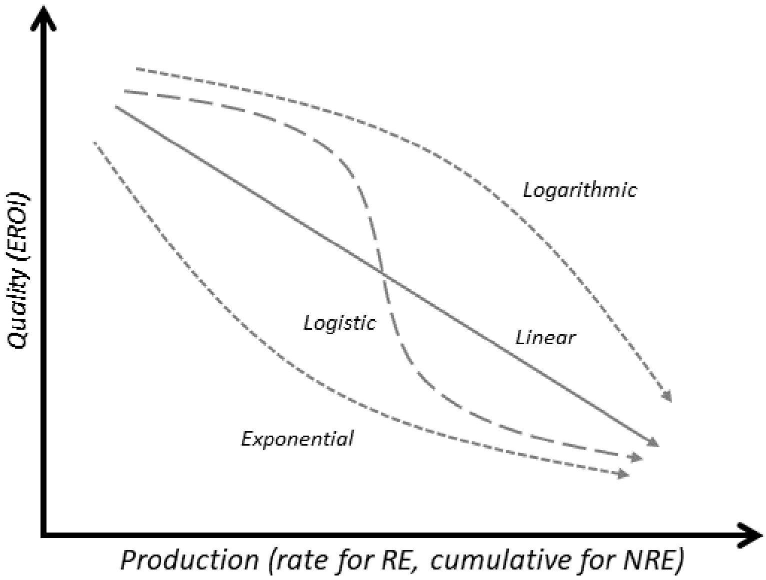

Figure 6: possible relationships between primary energy resource quality and production

A variety of possible negative relationships between quality and production are depicted in Figure 6, ranging exponential to logarithmic. Note that the specific form of the relationship, reflecting the underlying resource quality distribution, is not well known for most primary energy resources due to limited data and the presence of complex interactions between supply, demand, prices, and technology that cannot be predicted with reasonable certainty.

The energetic implications of technological change for primary energy resource quality must also be considered. Technological learning effects typically decrease energy costs markedly in the early development phase, during prototyping and early diffusion, raising EROI [4, 38, 39, 181]. However, as described by Hall [183], technological advances eventually approach practical limits and cease to keep up with depletion, causing EROI to begin to fall. Murphy et al. [170] agree that declining EROI indicates depletion is overwhelming technological change. According to Brand-Correa et al. [176],

> *"In the case of fossil fuels, it is argued that the depletion of easily recoverable fossil fuel reserves is outpacing technological advancements for the improvement of fossil fuel extraction, leading to decreasing values of EROI for these fossil energy sources."*

Ongoing technological advances can allow the exploitation of lower quality energy resources but do not necessarily compensate for their declining quality or quantity. Verbruggen and Al Marchohi [185] note that in many cases, such as the application of enhanced recovery techniques in oil extraction, increases in recoverable reserves come directly at the expense of lower EROI. For mature primary energy technologies, improvements typically have a minimal effect on EROI, instead raising or maintaining power output, allowing for the conversion of additional NRE resources to reserves, or lowering production costs [13, 38, 39, 84, 149, 184-186]. Odum [66] argues that while technological innovations often increase process level efficiencies, lifecycle net energy return is not typically improved due to the need for more advanced and energy-intensive manufacturing methods.

In effect, more advanced technology is not always energetically favourable when seen from a lifecycle perspective. As such, Hall [56] argues that assumptions that technology can mitigate resource depletion and declining EROI should be treated with caution. EROI for mature energy technologies is instead primarily affected by physical, geological, and geographic factors impacting resource quality [38, 39, 42, 84], including:

- decreasing energy and power densities of the primary energy gradient (e.g., lower grade hydrocarbons, lower wind speeds, lower insolation, lower land productivity),

- increased technical and infrastructural requirements for accessing more geologically challenging resources (e.g., deeper deposits, lower reservoir permeability, deep water drilling and production, secondary energy requirements for primary processing),
- increased infrastructural and transportation requirements for accessing and integrating more geographically remote primary energy resources (e.g., electricity transmission for isolated RE resource sites, pipelines for distant oil and gas basins),
- declining quality and rising energy intensity of required material inputs, particularly for critical metal ores, and
- various other factors relating to operating under less ideal, more unstable, more complex, and more costly socio-technical conditions.

Changes in resource predominance can be expected to have an impact at the level of overall system EROI. For example, Murphy [165] notes that declining production from conventional oil resources has initiated a global transition to unconventional oil, with lower EROI. The unfolding shift towards RE is also critically important in this regard. Murphy and Hall [52] caution that the lower EROI of most RE resources compared to NRE implies a significant reduction in aggregate EROI as the world transitions away from the carbon-intensive fossil fuels. However, plausible declines in system EROI are bounded; the RE resources with very large technical potentials, namely solar and wind, will likely vary only minimally with foreseeable production rates, suggesting forthcoming EROI declines at the system level will be asymptotic [53]. Hall [183] notes that, considering historical EROI trends, it is highly likely that EROI declines will continue.

2.1.1.4 Implications of declining EROI

As a measure of the thermodynamic quality of energy resources and their ability to yield necessary energetic surpluses, EROI is a critical indicator of the sustainability and long-term prospects of human societies [8, 14, 37, 53, 56, 180]. As such, declining EROI presents serious societal challenges and will strongly influence GES transformation pathways. Cottrell [12] argues that while earlier, pre-industrial societies quickly detected and rectified energetic deficits, modern societies frequently fail to do this leaving them to be resolved instead by crisis or system change. Greater awareness of primary energy resource quality declines and visibility of the causal pathways involved are now central to improved decision-making.

Primary energy resources cannot be considered in isolation, as all require the broader GES to enable their use. No individual resource has the necessary characteristics or abundance to act as the sole energy source for society. Odum [66] notes that from the system perspective, poorer quality energy sources are dependent on effective energy subsidies from higher quality energy sources (i.e., higher grade energy must be expended to develop the lower grade) and can fail to be viable without them. Hall and Klitgaard [184] argue that this cross-subsidisation of energy sources is occurring in current RE production, which remains heavily reliant on the petroleum-driven economy and associated infrastructures. According to Hall et al. [180], this dependency is particularly acute for energy sources with EROI values less than 10, including biofuels and possibly solar photovoltaics (solar PV). Consequently, the true EROI, and even viability, of low quality RE resources is still highly uncertain independent of the fossil fuel economy and cannot be assumed, as noted by Day et al. [42].

A common response to the challenges of falling EROI is that any decline in the net energy ratio can simply be compensated by an increase in the absolute scale of energy production activities. This kind of energy sector 'ramp up' would be equivalent to increasing both the EROI denominator and numerator until the required quantity of net energy is provided. However, in practice, this supply-side response is subject to limitations in both critical resources and the factors of production[12], and diverts these away from the non-energy sectors of the economy. This EROI-driven reallocation of both energy and money implies a relative reduction in discretionary consumption and investment, and an increase in intermediate consumption [165, 184, 186]. Energy prices will also be affected as they tend to rise in inverse proportion to declining EROI, with the potential for highly non-linear effects as EROI falls below 10 [148, 165]. Brandt [51] constructs a four-sector input-output model showing that not only does falling EROI cause direct increases in material and energy use within the energy sector, but also indirect increases due to rising intermediate consumption of output from the non-energy sectors. These direct and indirect effects are also reported by Fagnart and Germain [167], who note that declining EROI increases the capital requirements of the economy while decreasing the average productivity of capital. EROI-driven

[12] Conventionally, the factors of economic production include capital and labour, although the inclusion of exergy and/or useful work is now well-supported, as discussed in section 3.1.3.

macroeconomic reallocation effects will likely be exacerbated by climate policy promoting a rapid shift towards RE, as described by Day et al. [42],

> *"Rapidly transforming the energy system to lower EROI renewables to meet climate targets will mean that society must allocate substantially more GDP to investing in renewable energy plants, electric grids, energy storage, and liquid fuel substitutes. These compete with other economic drivers."*

Constrained investment in the non-energy sectors of the economy and reductions in discretionary output have serious implications for sustainable economic scale and societal complexity. Economic growth rates will likely be adversely impacted by declining EROI [157, 167, 184]. Murphy [165] argue that supply-side solutions will not be sufficient to offset these growing headwinds to long-term economic growth. Hall et al. [53] concur, concluding that an eventual cessation of economic growth is possible, or even likely. The macroeconomic implications of declining energy quality and EROI are discussed further in section 3.1.3.

As described by Lambert et al. [166], net energy has a close association with the generation of societal benefits. Similarly, Day et al. [42] find a clear positive relationship between societal EROI and prosperity. Rye and Jackson [157] suggest that declining EROI is likely to cause reductions in material prosperity in the 21st century. These associations have led to a growing research interest in the possibility of a minimum level for societal EROI, below which modern, high-energy societies would become untenable. Using a variety of conceptual approaches, studies have estimated this minimum EROI to be as low as 3 and potentially as high as 11 [178, 184]. Hall et al. [180] caution that estimates towards the lower end of this range would likely not include the provision of sufficient surplus for essential social services, such as education and healthcare. This threshold raises concerns regarding the ability of the scalable RE sources, solar and wind, to maintain the current configuration of the HSES, purely on net energy grounds.

2.1.1.5 EROI limitations

EROI is subject to several valid conceptual and methodological criticisms which must be adequately considered and addressed, particularly where EROI is used in a dynamic framework. Diesendorf and Wiedmann [175] observe that "The calculation of EROIs of technologies and systems has inherent uncertainties that require subjective judgements". It is widely appreciated that EROI depends strongly on the process boundaries applied in the analysis, which can produce large variances in reported values between studies using inconsistent boundaries [42, 184, 186]. Giampietro et al. [21] explain the determination of energy quality, in general, requires arbitrary criteria and is necessarily context-dependent, noting specific problems for the use of the EROI concept:

- Aggregation of inputs requires criteria of equivalence to be specified, which arbitrarily references chosen ideal conversion processes.
- No universally accepted aggregation methods exist, and the choice of method strongly affects the results of EROI analyses.
- The EROI index fails to capture critical information, including:
    - the system levels at which various energy forms are defined,
    - heterogeneous requirements for non-energy inputs,
    - the absolute extent of associated primary energy gradients, and
    - the relevant spatial and temporal scales (including power level).
- Low EROI estimates (< 2.5) are particularly sensitive to assumptions.
- EROI as a measure of resource quality is meaningful only where inputs and outputs are defined within the same autocatalytic loop.

Consequently, Giampietro et al. [21] conclude it is not possible to calculate a comprehensive net energy index over a complex set of energy transformations. Instead, EROI should only be used in conjunction with additional information regarding constraints facing the utilization of primary energy resources.

2.1.2 Resource variability and intermittency

Primary energy resources differ in their patterns of temporal availability. NRE resources are available almost continuously, while the natural energy fluxes constituting RE resources typically exhibit a combination of predictable temporal patterns and weather-related aleatory variability (with the notable exceptions of geothermal energy and large-scale hydropower). As such, most RE technologies, which primarily produce electricity, suffer from issues that become increasingly problematic during large-scale deployment stemming from both short-term and seasonal variability (i.e., ‘intermittency’) across highly heterogenous spatial distributions [35, 85, 88, 99, 187]. Notably, this is true of solar PV and wind, the RE technologies with the greatest scalability [54, 81, 188]. As described by Odum [66], the economic utilization of these intermittent resources requires the use of various means to buffer their inherent fluctuations.

Electricity differs from other energy carriers as it is not a physical substance that can be easily stored for later use during times of excess supply. Consequently, electricity supply and demand must be matched on very short timescales to maintain stable, functioning transmission and distribution networks with acceptable standards of reliability (i.e., 'security of supply') [15, 59, 85]. Aggregate electricity demand is largely stochastic although subject to predictable diurnal and seasonal patterns, and typically some degree of responsiveness to supply availability. Consequently, supply is conventionally 'dispatched'[13] to meet expected demand.

With the growing prevalence of intermittent, non-dispatchable RE supply in electricity systems, more frequent and larger imbalances between supply and demand will manifest across multiple timescales: milliseconds to seconds, minutes to hours, days to weeks, inter-seasonal, and multiannual [189-191]. Established, low-cost methods for matching supply and demand already exist for shorter timescales and are widely used in electric power system operations, including scheduling, frequency regulation, reserve generation capacity, and short-term demand response (i.e., dispatchable demand). However, longer timescale imbalances will require more extensive solutions with significant associated energetic and monetary costs, subject to various physical and socio-technical limitations [84, 86, 192, 193]. Electricity systems can integrate more intermittent, non-dispatchable generation capacity while maintaining security of supply via multiple mitigation options [35, 54, 81, 85, 193-201]:

1) Building additional infrastructures to manage imbalances over larger spatial and temporal scales, including bulk electricity storage and additional transmission capacity to improve the connectivity of electricity networks over large distances.[14] This infrastructural expansion requires various associated equipment for voltage and frequency regulation, distributed control, protection, and switching in both transmission (high-voltage) and distribution (low-voltage) networks.

[13] Dispatchable generation capacity can be separated into two functional sub-categories: baseload (relatively inflexible and slow-responding) and peaking (flexible and fast-responding).

[14] Storage includes the use of electrochemical, hydrological, pneumatic, thermal, and kinetic means. Enhancing long distance transmission capacity often relies on high-voltage direct current (HVDC) transmission technology.

2) Building greater quantities of intermittent electricity generation capacity than required (in terms of average power production) to raise the associated stochastic electricity supply profile, alongside the installation of backup dispatchable peaking generation capacity to cover supply shortfalls. This approach effectively lowers the average utilization of both intermittent and baseload generators, as it involves curtailing slow-responding and non-dispatchable output when supply exceeds demand, while simultaneously raising the average utilization of fast-responding peaking generation capacity.
3) Improving the level of aggregate demand responsiveness to intermittent supply via various behavioural and technological means.
4) Raising the technological and geographical diversity of intermittent generation to lower the stochasticity of the associated supply profile.[15]

Electricity systems can typically tolerate low to moderate intermittent, non-dispatchable supply contributions (or RE 'penetration level') with minor operational adjustments only, depending on widely-varying degrees of flexibility across different systems, as noted by Heptonstall et al. [85] and Denholm and Hand [194]. However, the requirement for intermittency mitigation measures will rise approximately exponentially with increasing RE penetration levels in electricity systems if acceptable levels of security of supply are to be preserved [81, 193, 197, 198, 201-204]. Jenkins and Thernstrom [81] stress the importance of technological diversity and dispatchable generation capacity as the foundation for the successful integration of intermittent RE in electricity systems.

The need for intermittency mitigation will negatively affect EROI at both the system level and for intermittent primary energy resources. The already low EROI for most RE resources is further reduced when the energy costs of intermittency mitigation are included [39, 86, 184]. This effect is influenced by the low exergy density of electrical storage devices where infrastructural mitigation is used [14, 82, 205]. Day et al. [42] find the inclusion of storage reduces EROI for wind and solar by 40-75%, but note that demand response can lessen this effect. Trainer [88] argues that if energy systems are pushed toward 100% RE, the energetic

[15] Temporal electricity output correlation is generally lower over longer distances and between distinct intermittent resources (and associated RE technologies).

costs of the required storage capacity may reduce system EROI below the level required to support high-energy societies.

2.2 Energy transformations

The provision of final energy services from primary energy resources requires multiple sequential conversion stages, as depicted in Figure 7. Cottrell [12] explains that input and output flows at each stage are qualitatively different, with the output typically being of greater practical value. Proportional losses at each stage can be quantified using the concept of efficiency: the ratio of output to input for any given conversion (at the process level, or in aggregate). Implementing efficiency improvements is a primary avenue for the promotion of desirable GES transformation outcomes. However, the dynamics of efficiency change are complex, and must be properly characterized to understand realistic prospects, as discussed in section 2.2.1. The production and use of energy carriers are detailed in section 2.2.2. Energy services and related efficiency considerations are then overviewed in section 2.2.3.

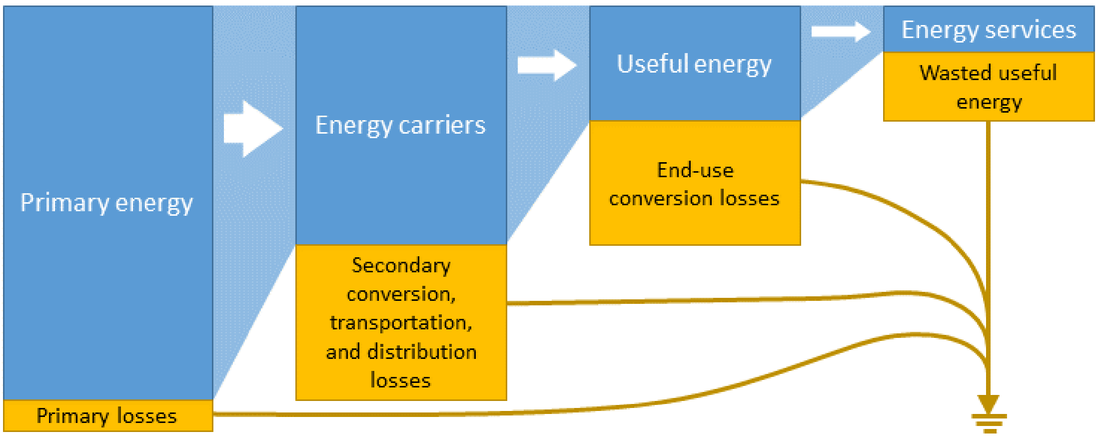

Figure 7: energy conversion stages within the GES for the provision of energy services (adapted from Brockway et al. [206])

2.2.1 The efficiency paradox

> *"Civilisation […] is the economy of power, and our power is coal. It is the very economy of the use of coal that makes our industry what it is; and the more we render it efficient and economical, the more our industry will thrive, and our works of civilisation grow"*
>
> – William Stanley Jevons [207]

Significant components of the losses evident at each conversion stage depicted in Figure 7 are unavoidable due to the irreversible and asymmetrical nature of energy transformations [14, 21, 65, 71]. The entropy law (the second law of thermodynamics) places calculable theoretical efficiency limits on any energy conversion process [11, 16, 208-210]. Glucina and Mayumi [73] note that technological advances can approach but not exceed these limits, as they are functions of the extant thermodynamic gradients. For example, the maximum theoretical efficiency for heat engines depends on the available temperature differential only, known as the 'Carnot efficiency' [14, 65]. Conversion efficiencies can be specified relative to theoretical maxima using 'second law efficiency' (or 'exergy efficiency'): the ratio of the theoretical minimum exergy to actual exergy consumed [141, 154]. It is important to note that thermodynamic efficiency measures and theoretical limits are not directly applicable beyond specific, well-defined processes, i.e., to sectoral or societal scales, as described by Giampietro et al. [21] and Ruzzenenti and Basosi [211] (discussed further in section 3.1.3.1).

Theoretical efficiency limits correspond to reversible processes, which occur infinitely slowly [16, 73, 154, 208]. As such, a distinction must be made between 'infinite time' and 'finite time' thermodynamic efficiency limits. This distinction recognizes the role of time as a relevant resource, as moving further away from theoretical efficiency maxima and increasing the degree of irreversibility allows power output (energy per unit time) to increase [21, 68, 171, 212]. According to Glucina and Mayumi [73],

> *"[I]t has long been known that in real world production, there is a tradeoff between the speed of a process and its energy efficiency. This tradeoff is closely linked to the second law's implication that maximally efficient (reversible) processes necessarily require infinite time. Real processes entail energy dissipative effects, which is what makes them irreversible; the dissipated heat can not be retrieved."*

Court [16] explains that real-world systems strongly tend towards the greatest possible efficiency at the maximum attainable power level, which is substantially less efficient than the theoretical limit. Ruzzenenti and Basosi [211] note that sub-optimal efficiency levels result from the typically greater opportunity cost of time relative to the cost of energy inputs, observing that "consumers and producers can substitute energy for time by speeding up the process or the service provided or used." Consequently, thermodynamic efficiencies across many natural and human systems are typically observed close to the power maximizing efficiency level, which occurs at approximately half the theoretical efficiency maxima, and rarely exceeds 60% [141, 211, 212].

Thermodynamic conversion efficiencies for most energy technologies started from very low historical levels; order-of-magnitude improvements to the values seen today are common, as noted by Smil [6]. For many common energy conversion devices, process-level efficiency gains are now largely exhausted. Ayres and Warr [141] find little to no improvement in engine efficiencies since the 1970s. Similarly, Smil [14] notes only very minor efficiency gains in wind turbines and steam turbines (providing most of the world's electricity) over the same timeframe. Ayres and Warr [141] argue that practically achievable efficiency gains are increasingly limited by the properties of materials used in energy device manufacture. However, further design improvements are still achievable, and significant process-level efficiency gains for many energy technologies will continue for the foreseeable future driven by technological learning effects [14, 28, 212-215]. Aside from thermodynamic conversion efficiencies, substantial efficiency gains are also realizable in the transformation of output power to useful energy services (discussed further in section 2.2.3).

It is important to note that efficiency gains are not exogenous or automatic. Capital heterogeneity implies that improving efficiencies at the system level depends on the slow and costly process of replacing capital stocks [26, 216]. Furthermore, technological improvements associated with increased process-level efficiency typically require greater technological and organizational complexity, advanced materials and manufacturing methods, longer supply chains, and consequently, greater capital energy costs [28, 73, 141, 217]. As such, energy efficiency gains manifesting at the system level, associated with lifecycle energy efficiencies, are often more modest than expected.

Another key consideration is the existence of rebound effects (also known as 'Jevon's paradox'): the tendency for improved efficiencies to result in increased demand, partially counteracting expected energy savings [141, 211, 218-221]. Rebound effects are, in part, a consequence of the power maximization of thermodynamic processes, described above. Ayres and Warr [141] note that while energy efficiencies are often analysed at the engineering design level, rebound effects at the system level are pervasive. Efficiency gains emerging from technology improvements are typically applied to scale increases, to produce greater quantities of useful output, rather than input reductions [220, 221]. Brockway et al. [219] estimate that rebound effects may erode more than half of future expected energy savings from improved energy efficiency.

Rebound effects are also associated with macroeconomic processes related to economic growth. Brockway et al. [219] argue that larger than commonly assumed system-level rebound effects may explain the close historical relationship between energy consumption and economic output. Ruzzenenti and Basosi [211] note that labour productivity is strongly enhanced by rising energy efficiency, suggesting that "energy efficiency may stimulate a process of factors substitution for industries or prompt marginal consumers who previously could not afford some energy services, to enter the market", causing energy demand to grow in response. Ayres and Warr [141] and Sakai et al. [222] go further, suggesting that thermodynamic efficiency gains and the resulting increases in exergy and useful work production are, in fact, the primary engine of economic growth.

This connection to growth has implications for the mitigation of rebound effects, as described by Glucina and Mayumi [73],

> *"In general, promoting energy efficiency means promoting "slowness" of process. This result would seem to add weight to the thesis that economic growth fueled by continuously more efficient use of energy, in the absence of imposed limits, is not possible."*

The mitigation of rebound effects, although challenging, appears necessary to realize the full benefits of voluntary reductions in energy consumption and the promotion of energy efficiency via market interventions, such as carbon pricing [14, 148, 178]. This may require counteracting the role of the time scarcity in the consistent selection of power over efficiency. Explicit decisions will need to be made regarding the appropriate balance between economic growth and efficiency-driven downsizing of the GES to achieve desired outcomes. The relationship between efficiency and growth is discussed further in section 3.1.3.

2.2.2 Energy carriers

Energy carriers are high quality, energy dense, fungible, and transportable fuels or energy flows including (at the highest level of functional aggregation), electricity, liquid and gaseous fuels, and heat [21]. Energy carriers are:

- produced from primary energy flows via various secondary conversions and consumed by end-use devices to provide useful energy services (see Figure 7),
- functionally distinct, exhibiting different physical characteristics, transportation and distribution systems, temporal flow constraints, and storage potential (as discussed for electricity in section 2.1.2), and
- generally non-substitutable without corresponding changes in end-use devices.

Giampietro et al. [21] notes that the production of energy carriers requires primary energy gradients and profiles of input energy carriers (i.e., autocatalysis), in addition to the necessary capital, labour, land, and material inputs. The GES now exhibits intractable dependencies on high-EROI, energy dense, transportable fuels [21]. Notably, liquid transportation fuels are of critical importance for the global economy as they enable complex, long-distance logistics networks and the international trade that these networks support [82, 205].

Limits to substitution within the GES arise, in large part, due to the non-equivalence of energy carriers. As discussed in section 2.1.2, most RE technologies produce electricity, underscoring the need for an overall electrification of various end-uses to facilitate the growth of RE and decarbonization of the GES [81, 223]. This presents a challenge, as electricity currently occupies only a minor share of global total final energy consumption despite its very high exergy and utility [21, 83, 86]. While some end-uses are easy to electrify, such as space heating and short-distance passenger transportation, others are much more challenging owing to technical, economic, and behavioural barriers, such as aviation, long-distance freight, and many high-temperature industrial processes [14, 42, 59, 82, 205]. According to Smil [14], "Refined liquid fuels that are used to energize all modern transportation (electric trains being the only notable exception) cannot be easily and rapidly replaced by alternatives." Smil [28] notes that, "Replacing thermal electricity generation by new renewables is much easier than displacing liquid fossil fuels in transportation". Similarly, Ayres and Warr [141] conclude that the transportation and construction sectors have little scope for large-scale electrification.

The non-equivalence of the energy carriers can also explain why some primary production processes are carried out with very low, or even negative, net energy output. Giampietro et al. [21] note that such processes can represent an 'upgrading' of energy flows, producing an output flow of greater utility than the input flows (e.g., biofuel production).

The above underscores the need for explicit consideration of distinct energy carriers within GES transformation pathways and the processes of substitution between them. The functional non-equivalence of energy flow categories and associated capital stocks is discussed further in section 3.1.2.4.

2.2.3 Energy services

Societies and individuals alike do not require energy consumption *per se* but rather useful services corresponding to changes in the physical, spatial, visual, thermal, or informational states of matter. According to Fell [224], “energy services are those functions performed using energy which are means to obtain or facilitate desired end services or states.” Brand-Correa and Steinberger [11] describe energy services as “satisfiers” of human needs, delivered as the product of the energy transformation processes performed by end-use devices, which can vary in both nature (e.g., transport via motorbike vs. commercial airliner) and level (e.g., travelling more, heating to higher temperatures). They note that, in practice, service levels are more challenging to improve as they are limited by slowly changing systemic factors, such as available infrastructure and population density. ‘Final’ energy services refer to those delivered to the HSES, rather than used internally within the GES. The ultimate purpose of the GES can be seen as the provision of reliable flows of high-quality final energy services supporting the autopoietic processes of the HSES, as noted by Giampietro et al. [21] and discussed in section 1.2.2 (shown in Figure 3).

Various classification schemata for energy services exist, based on chosen functional and technological distinctions, and levels of aggregation. As described by Spreng [74],

> *“The effect each Joule of useful energy has when turning to waste heat or to embodied energy is different. The time, the place, and the purpose are different. In essence, energy performs a virtually infinite number of tasks for us. To speak about these tasks, then, requires that they be aggregated into a manageable number of classifications of energy services.”*

Brand-Correa and Steinberger [11] note that the aggregation of energy services can be challenging owing to the wide variety of possible units and representations, suggesting the basic categories of heat (at defined temperature levels), mechanical drive, light, electricity for appliances, and food. Fell [224] notes a diverse array of energy service categories considered in the literature, with the most common being heating (including space, process, and water heating subcategories), space cooling, refrigeration, cooking, lighting, and motive power. Spreng [74] includes drying, mobile equipment, transport services, and chemical feedstocks. In contrast, Cullen and Allwood [225] use an energy service classification schema based on ultimate desired purposes, including transport (passenger and freight), structure, sustenance, hygiene, thermal comfort, communication, and illumination categories. The choice of energy service aggregations must, at a minimum, preserve functional distinctions while being aligned with the goals of the analysis.

The study of energy systems has historically focussed on final energy consumption (of energy carriers) at the point of end-use [212]. However, this neglects 1) the conversion of energy carriers to useful energy, or end-use device output power, and 2) the application of this power for the provision of energy services (see Figure 7). Cullen et al. [212] note a critical distinction: the former step occurs within conversion devices and is well-understood, while the latter step is more ambiguous and is mediated by 'passive systems'. As described by Court [16], "energy services (transport of passengers and goods, space heating, and illumination) are the outcomes of the interaction of useful energies (mechanical drive, heat, and light) with passive devices/infrastructures." Cullen and Allwood [225] group passive systems into vehicles, factories, and buildings, noting the important role these systems play in the production of energy services from useful energy. Efficient passive systems reduce losses of useful energy and 'trap' energy more effectively as useful energy services, for example, well-insulated homes, aerodynamic vehicles, and brightly painted rooms [212]. Remaining realizable efficiency gains within the GES are largely associated with passive system design. According to Lovins [226],

> *"Increasing energy end-use efficiency—technologically providing more desired service per unit of delivered energy consumed—is generally the largest, least expensive, most benign, most quickly deployable, least visible, least understood, and most neglected way to provide energy services."*

Nakićenović and Grübler [216] concur, noting "energy services appear to be the least efficient and perhaps the weakest link in the efficiency of the whole energy system." Consequently, greater attention must be given to the realistic, holistic design prospects for providing energy services with much lower energy inputs [227]. However, as cautioned by Nakićenović and

Grübler [216], improvements in passive system efficiency can be difficult to achieve due to the behavioural changes typically required.

2.3 HISTORICAL ENERGY TRANSITIONS

> *"The history of the development of industrial society has been a history of plowing surplus energy back into more energy converters."*
>
> – Earl Cook [228]

To better understand the factors affecting GES transformation processes, it is instructive to examine the nature of historical energy transitions, including driving forces, dynamic processes, and constraints. Smil [14] notes that energy transitions are invariably socio-economically disruptive and transformative, changing the form and structure of economic activities and compelling slow and costly infrastructural changes. These processes are fundamentally multi-dimensional, as described by Sovacool and Geels [124], occurring across four tangible 'layers': extractive industries, systems of conversion and supply, prime movers, and delivery infrastructures. They note associated changes are generally required across a broad set of institutions, markets, and political systems.

As depicted in Figure 1, the addition of new energy sources has not historically displaced prior sources, but rather added to the total [6, 23, 89]. For example, while coal dropped from around 95% to less than 30% of TPES between 1900 and 2020 (excluding traditional biomass), consumption rose almost 10-fold over the same period [40, 43]. As described by Sgouridis and Csala [9],

> *"[W]hile it is commonly perceived that the fossil fuel era has supplanted the use of biomass, traditional biomass remains a significant primary energy resource exceeding nuclear primary energy on a global scale. The same is true for the transitions from coal to petroleum and natural gas."*

Overall, changes observed in the GES over the 20th and early 21st centuries demonstrate unambiguous trends towards greater absolute power and power density of both energy sources and uses, as outlined by Smil [14]. A significant share of energy surplus was historically reinvested back into the autocatalytic production of energy [9], expanding overall supply and reducing costs in a positive feedback loop. These changes were technology-enabled but demand-led, driven by the falling costs and the increasing quality of energy services. Fouquet [229] notes the price of energy services, including price shocks, played a crucial role in creating the necessary incentives for energy transitions. Even where the costs of final energy services may initially be higher, new technologies can offer enhanced services levels and related amenities which spur their rapid uptake [229]. It should be noted that while the degree of technological progress enabling energy transitions has been remarkable, future advances cannot be predicted and are ultimately subject to both physical limits and declining returns on innovation [14, 188, 230].

Processes of technological change within energy transitions and associated time constraints are reviewed in section 2.3.1. Relevant learnings for future energy transitions are then summarized in section 2.3.2.

2.3.1 Technological diffusion, inertia, and lock-in

Ayres and Warr [141] explain that energy transitions are shaped by the diffusion of new technologies through a process of discontinuous, 'Schumpeterian' creative destruction. This process is subject to the ubiquitous logistic or 'S-curve'[16] diffusion of novel innovations: a slow formative experimentation phase, the emergence of better designs and declining costs through standardization, accelerating uptake aided by emulation and efficiencies of scale, and eventually, technological maturity and saturation [28, 215, 231, 232]. As explained by Smil [6], "New energy sources or techniques become dominant only after long periods of gradual diffusion." The overall pace of change is primarily influenced by the extent and technological complexity of the required changes. According to Grübler et al. [231],

> *"Adoption of technologies using existing infrastructures happens fast (a decade), upgrading existing infrastructures takes longer (up to three decades), and building entire new infrastructures (technological systems) involves transition times of four to 5 decades. Lastly, "systems of systems", the ensemble of what constitutes our modern transport infrastructures (our waterways, railways, roads, and airways and associated communication networks) takes yet longer"*

[16] 'S-curve' typically refers to the logistic curve, but technological diffusion can also be described by Gompertz, Weibull, or hyperlogistic functions.

As such, energy transitions cannot be predicted by developments at the technology or industry level and are constrained by dynamic, systemic factors which can significantly extend the transition process, including [215, 229, 231]:

- the number of related technological, organizational, and institutional systems which must simultaneously change,
- the need to replace long-lived and highly networked system components,
- the necessity for investments in costly, large-scale infrastructures with a high adoption effort, with only long-term or non-market benefits,
- greater technological novelty and the need for first movers to initiate the transition without the benefit of learning externalities and best practices,
- the spatial scale of the transition (e.g., local, national, regional, or international), and
- the presence of unfavourable technical, organizational, socio-political, or economic circumstances, including resistance from incumbent industries.

Consequently, major energy transitions are typically slow, taking multiple decades or centuries to see substantial changes at the global level [9, 14, 28, 231, 232]. In contrast, energy transitions characterized by smaller scales, partial substitutions, technological modularity and maturity, and the existence of established precedents in other regions, can happen much more quickly [124, 231, 232].

An important phenomenon in energy transitions is known as technological or infrastructural 'lock-in': a resistance to change frequently observed in embedded technological systems, and associated patterns of resource consumption, even where preferable alternatives are available [42, 232, 233]. Technological lock-in results from the logic of sunk investment, socio-technical change reticence, and the overwhelming predominance of earlier technologies, as described by Cottrell [12]. Grübler et al. [231] notes that lock-in of 'techno-institutional complexes' is highly relevant to energy transitions, and typically forestalls subsequent transition processes, particularly for first movers or core markets. Jenkins and Thernstrom [81] argue that technological lock-in can frustrate decarbonization of the GES, as short-sighted policies can result in suboptimal resource portfolios becoming embedded, with significant environmental costs.

Taken together, the processes of technological diffusion and lock-in manifest at the system level as a marked inertia evident in energy systems, greatly increasing the time, cost, and complexity of change. This phenomenon underscores the degree of path-dependence to be expected in the evolution of the GES.

2.3.2 Lessons for future energy transitions

The future of energy systems will not look like the past, or the present, as noted by Grübler et al. [215] and Sovacool and Geels [124]. However, lacking strong evidence of forthcoming socio-technical discontinuities, it is parsimonious to expect that fundamental patterns and relationships will continue to hold. As described in section 1.2, appeals to exponential technological progress in narrow domains are likely to be misleading when considering the macroscale evolution of the GES.

From the brief discussion presented in this section, several tentative lessons can be drawn regarding the prospects for the forthcoming third energy transition:

1) Energy transitions are shaped not only by techno-economic factors, but also by socio-institutional contexts.
2) The historical tendency for new energy sources to add to, rather than displace, prior energy sources implies that the growth of RE cannot be expected to reduce NRE use and related GHG emissions, absent other changes.
3) The global transition will be slower than commonly expected, on the scale of at least a comprehensive change of technological systems, as defined by Grübler et al. [231], implying a corresponding timeframe of a half century or more.
4) However, fast transitions are possible within smaller regions in the global periphery following the example set by first movers, especially where political support exists and where changes involve fewer technological elements characterized by modularity and clear economic benefits or improvements in the nature of energy services provided.
5) Past energy transitions have been driven by demand and rapid technological change, shifting to progressively more energetically advantageous primary sources and technologies unlocking enhanced energy service levels at lower per unit costs. The forthcoming transition to RE does not appear capable of replicating this process. As cautioned by Sovacool and Geels [124], "While past transitions may have been rooted in abundance, future ones may involve scarcity."

However, the future is unknown. As Fouquet [229] optimistically observes, “Crucially, energy transitions are non-deterministic. That is, energy transitions are not inevitable; instead, they depend on a series of actors and forces creating a new path.” This emerging future can only be properly understood via a broad survey of the theoretical foundations of energy transition, starting with the essential recognition of the GES as an example of a CAS.

3 THE CONCEPTUAL LANDSCAPE

3.1 THE BIOPHYSICAL SYSTEMS PERSPECTIVE

> *"Our inability to comprehend the behavior of complex and interdependent wholes […] makes any specific (and now so commonly proffered) scenarios of distant futures mere speculation. In contrast, outlining the extremes is easy, as the visions of future range from dismal to ecstatic."*
>
> – Vaclav Smil [69]

Biophysical, systems-oriented perspectives of the relationships between energy, society, and the environment began to gain prominence in the early 1970s with the publication of the *Limits to Growth* report commissioned by the Club of Rome [104, 234, 235] and the rise of 'systems ecology' spearheaded by Howard T. Odum [71, 171]. Both built on a new complex systems synthesis emerging from earlier work in the fields of cybernetics [236, 237], general systems theory [111, 238, 239], non-equilibrium thermodynamics [3, 240], biophysical economics [26, 241-243], biology and ecology [173, 244], and the mathematics of non-linear and dynamical systems [245, 246].

Complex systems theory is now an essential but under-appreciated conceptual backdrop for virtually all major problems facing the modern world. Chief among these is the transformation of high-energy, industrialized societies from NRE dependence towards RE. As discussed in section 1.2, approaches to investigating GES transformations must begin from an ontological foundation that recognizes two basic points:

1) the GES is an example of a CAS, co-evolving with, and nested within, the broader HSES (depicted in Figure 3), and therefore,
2) GES transformation is a *complex, physically bounded, path-dependent, socio-metabolic process*.

Consequently, employing a biophysical, complex systems perspective is essential to the formulation of meaningful problem framings and effective interventions for GES transformation. The essential characteristics of CAS are overviewed in section 3.1.1, followed by implications for energy and society in section 3.1.2. Relationships between power, economic growth, and sustainable scale are then reviewed in section 3.1.3. Finally, energy systems modelling principles and techniques are outlined in section 3.1.4.

3.1.1 Complex adaptive systems

CAS consist of networks of dynamically interacting elements, or agents, possessing collective capacities to adapt and learn in response to changes in their environments [110, 247]. As described by Levin et al. [110], the individual agents constituting CAS follow relative simple rules and can be described as 'boundedly-rational'. These agents possess distinct functional roles and heterogeneous rulesets (i.e., agendas), leading to varying patterns of competition, co-operation, resource exploitation, and parasitism. The macroscopic properties of CAS, distinct from the properties of the agents, emerge from such lower-level interactions [110].

King [31] notes that CAS are "goal-seeking, self-preserving, and self-organizing". As discussed in section 1.2.2, CAS exhibit properties of path-dependence, self-organization and emergent behaviour, autopoiesis, feedback loops, and non-linearity. Positive feedback is responsible for growth, decline, and system phase shifts, while negative feedback is responsible for adaptive responses and system homeostasis [145]. CAS are characterized by path dependency (or 'hysteresis') and are subject to irreversible evolutionary processes [21, 26, 110]. Court [16] notes that, "While strong tendencies can exist, system evolution is not deterministically extremal, but rather historically determined, context-specific and highly contingent." Local changes in CAS have the effect of generating readjustments within the rest of the system while changes in boundary conditions extending beyond the relevant 'stability domain' can bring instability, phase shifts, or termination of the system.

The degree of complexity exhibited by CAS refers to the number and variety of their constituent elements, and the density of interactions between these elements. Chaisson [248] notes that, across a variety of systems, complexity is closely related to energy and mass density. This implies that complexity is energetically expensive. As explained by Hall et al. [13], while complex systems cannot be reduced to energetic representations, energy (or more precisely, exergy) is an essential and limiting resource for the growth and maintenance of complex systems as the provision of any other necessary resource entails energy expenditure. Additionally, CAS are self-referential, or 'impredicative', defining for themselves what constitutes energy sources, useful work, and waste [21, 68].

CAS arise via evolutionary processes and are universally dissipative structures, as noted by Prigogine and Stengers [3]. CAS maintain themselves far from thermodynamic equilibrium and increase their own internal order and power[17] by accelerating the degradation of natural energy gradients [3, 16, 21, 64, 109, 110]. According to Giampietro et al. [21], in addition to a purely dissipative component (analogous to consumption), CAS also possess a hypercyclic component responsible for the autocatalytic production of energy inputs as well as processes of system growth and maintenance. They explain that the relative size of the dissipative component competes with the operation of the hypercycle, and in turn, the development of complexity.

Growth patterns in CAS are adaptive to exogenous constraints. Given competition between dissipative and hypercyclic system components, CAS face fundamental trade-offs between short-term consumption and long-term development [21]. In all physical systems, growth eventually reaches limits (due to the finiteness of primary energy gradients in any given environment) and the system either enters a mature, conservation phase or collapses. According to Odum [66], when faced with little or no energetic surplus, systems grow selectively, investing energy in high diversity, high quality structures. In isolation, without energy inputs, all complex systems will quickly degrade, depleting their stored energy before ceasing to function [26]. As described by Court [16], “As thermodynamic constraints are applied to a system, maximum entropy production turns to minimum specific (per unit mass) energy dissipation – rapid growth turns to conservation, e.g. transition to a mature ecosystem.”

CAS are typically arranged in nested hierarchies, both contained within and containing other CAS which operate over different spatial and temporal scales [21, 115, 247, 249]. For example, a population of organisms is comprised of individuals but is itself contained within an ecosystem. Similarly, the HSES contains the GES but is itself contained by the biosphere. As such, CAS are subject to both top-down and bottom-up causation. As noted by Giampietro et al. [21], there exist “multiple non-equivalent identities for the same system when it is observed at different scales”. This can be explained using Arthur Koestler’s concept of the

[17] Power maximization is, in fact, a primary characteristic of organisms favoured by natural selection, as described in section 3.1.3.

‘Holon’, depicted in Figure 8, describing the fundamentally dual nature of complex systems [21, 250-252]:

- Each holon is simultaneously a whole and a part – parts express functions which are useful within the whole, while the whole provides functional meaning to the parts. For example, a firm is comprised of specific workers, offices, intellectual property, and capital equipment, while it also forms part of its wider industry.
- The same functional role has diverse structural realizations which can change over time while the whole remains intact; system evolution and emergence occur as functional-structural mappings change. For example, traditional media outlets give way to social media companies, both fulfilling the functional role of information dissemination within society, giving rise to new patterns of social organization.
- Holons exhibit both self-assertive and integrative tendencies within their hierarchy. Destroyed holons cause higher level holons to cease functioning, but holons on the same or lower levels can survive and reorganize.
- The scale used to describe the function of the holon is higher than the scale used to describe its structure. Multi-scale analysis is required to fully capture the interactions involved.

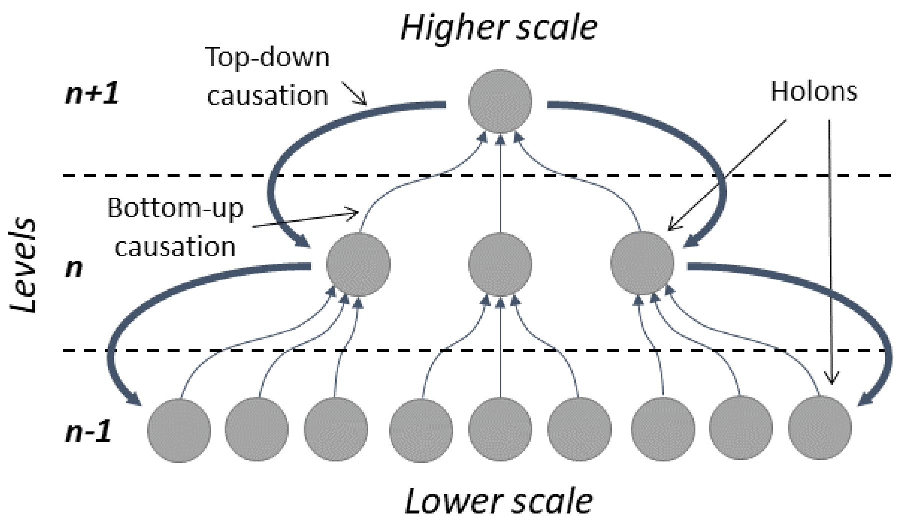

Figure 8: the nested hierarchical organization, or ‘holonic relations’, of CAS (adapted from Eddy et al. [251])

As described by Giampietro et al. [21], “the term holon underlines that what is special about the organization of living systems is the systemic coupling of a functional (the role) and a structural (realization of an organized structure) type in relation to higher and lower levels of organization.” The expression of structures and functions within complex systems characterizing internal and external relations, respectively, arises from self-organization within dissipative systems [3, 27, 171].

3.1.2 Implications for energy and society

> *"Energy flow and sociopolitical organization are opposite sides of an equation. Neither can exist, in a human group, without the other, nor can either undergo substantial change without altering both the opposite member and the balance of the equation. Energy flow and sociopolitical organization must evolve in harmony."*
>
> – Joseph Tainter [253]

Economic scale and complexity in human societies are ultimately constrained by their energy resource base [12, 13, 19, 42]. This basic fact will inevitably influence societal development, regardless of any social, technological, or political adaptions which seek to obviate limits. Societies compete for economic survival, growing rapidly via the autocatalytic acceleration of energy consumption in the presence of an energetic surplus to promote their own economic vitality, even at the expense of significant waste [13, 66]. According to Giampietro et al. [21], the hypercycle within society is shaped by choices regarding the use of energy surplus and, when surplus is sufficient, drives the development of societal complexity over time. Tainter [19] notes that this tendency towards greater complexity is central to the resolution of societal problems, implying voluntary reductions in energy consumption are unlikely.

Energy and society follow a reflexive coevolution informed by their holonic relations. Notably, the dynamic capacity of the HSES to facilitate the transformation of the GES depends on the scale and composition of energy surplus, which is itself a function of the GES transformation pathway taken. Ayres and Warr [141] point out that this co-evolution is fundamentally path-dependent, not optimal, in large part due to the technological lock-in phenomenon discussed in section 2.3.1. As outlined in section 1.2.2, two classes of constraints can limit the evolution of society and its ability to express desired functions: external, relating to the availability of sources and sinks (discussed further in section 3.1.2.3), and internal, relating to the ability to maintain the necessary internal structures required to control energy flows [21].

Sgouridis and Csala [9] describe tight coupling between energy systems and economic systems subject to delays and pronounced non-linearities, noting "The global energy-economy system is complex, exhibiting strong feedback mechanisms." As such, intervention in socio-ecological systems is difficult; changes will often yield unanticipated results and sufficiently large changes can lead to chaotic behaviour and system reorganization (invalidating *ex-ante* conceptual models and assumptions). Ruth [249] argues that policy interventions and investment decisions in complex systems need to be "cognizant of the temporal and spatial lags among decisions and outcomes" and "operating within constraints imposed by processes at higher and lower levels of the system hierarchy".

The existence of a hypercycle within the GES implies that TPES is not a sufficient measure of the energy available to society. Sgouridis and Csala [9] note that gross energy supply "is not fully available to society as a portion must be reinvested in further energy recovery". This hypercyclic component of society can be expected to grow over time with the declining quality and falling EROI of primary energy production (described in section 2.1.1), forcing a relative decline in the dissipative, discretionary consumption-oriented component of society with potentially far-reaching consequences. This dynamic corresponds closely to the concept of energy gain described by Tainter et al. [8], which "constrains resource use, social organization, and landscape organization in human and other living systems" and informs likely changes engendered by the transition to RE-based, post-industrial societies.

3.1.2.1 Socio-metabolic patterns

According to Giampietro et al. [21], the term 'societal metabolism' can be used to describe patterns of exosomatic energy conversions under human control encompassing the production and consumption of energy carriers for the expression of useful functions within society. As described by Brown et al. [10], "Just as a body has a metabolism that burns food energy to survive and grow, a city or national economy has a metabolism that must burn fuel in order to sustain itself and grow." Hall et al. [13] concur, noting that both human and natural systems rely on energy to acquire the necessary inputs for their internal metabolic processes.

Sorman and Giampietro [27] note that socio-metabolic patterns can be defined, describing both societal scale and the complexity of structural and functional organization. Socio-metabolic patterns of human energy and material use have historically fallen into distinct 'socio-metabolic regimes': hunter-gatherer, agrarian, and industrial [17, 18]. According to Haberl et al. [18], global problems of sustainability relate strongly to these regimes and transitions between them, noting "Transitions between these regimes fundamentally change socio-ecological interactions, whereas changes and variations within each regime are gradual." Krausmann et al. [17] note that the successive socio-metabolic regimes can differ in their per capita energy and material use by up to an order of magnitude, producing profoundly different impacts on the natural world. According to Sorman and Giampietro [27],

> *"Modern societies have had the possibility to become complex over time because of the progressive use of technologies and the benefit from high quality and easily accessible energy sources. The industrial civilization has been around for more than one century now, enough to establish a well-rooted and robust metabolic pattern. Changing such a pattern will not be easy."*

The implications of socio-metabolic patterns extend beyond the physical, affecting the predominance and viability of various social, political, institutional, and cultural forms throughout society. Capra and Luisi [64] suggest that "The biological structure of an organism corresponds to the material infrastructure of a society, which embodies the society's culture". The close association between energy supplies and socio-cultural development was described by anthropologist Leslie White and is known as *White's law* [5]: "Other things being equal, the degree of cultural development varies directly as the amount of energy per capita per year harnessed and put to work." This basic observation gave rise to the anthropological theory of *cultural materialism*, proposed by Harris [7, 254], which stresses generalizable dependencies of the evolution of culture on material conditions, or 'infrastructure'. This more general notion of the evolution and structure of societies is echoed by Smil [6], who cautions against using energy as a singular explanation of society and emphasizes that there are many other relevant aspects to consider.

3.1.2.2 Power and capital

The GES does not consist of energy flows alone, but also capital equipment and infrastructures required for the production, transformation, transportation, and utilization of theses flows. This relates to the observation by Giampietro et al. [21] that power levels must be explicitly considered within complex systems as time is a relevant dimension. The term 'power capacity'[18], identifies technological capital capable of transforming a given exosomatic

[18] Power capacity is also known by the term 'energy converters'.

input energy flow to produce a useful output flow [12, 26, 255]. Power capacity is quantified by its maximum long-term output flow rate (often equivalent to 'nameplate capacity'), which is greater than its average utilization rate given by its temporal utilization profile. The definition of both energy carriers and primary energy resources depends on the functional characteristics of the associated power capacity type [12, 21].

The operation of the GES exhibits intrinsic structural dependencies on the production and maintenance of sufficient power capacity stocks, operating at all stages of the GES depicted in Figure 7 [21]. Various infrastructures are also required which are not directly involved in transforming energy flows but facilitate the operation of power capacity, such are roads, airports, electricity transmission networks, and various supporting industries. Georgescu-Roegen [26] notes that the production and maintenance of these capital stocks depends on almost all economic sectors, either directly or indirectly. As Giampietro et al. [21] explain, the production and utilization of exosomatic energy flows require not only autocatalytic energy inputs and power capacity, but also human labour for control purposes. These distinct inputs cannot be assigned relative importance as they are fundamentally complementary.

Ayres and Warr [141] note that capital involved in energy transformations can be measured in terms of its power capacity as well as its embodied energy. As all capital requires input energy to produce, the power capacity concept directly links energy flows with the hypercyclic component of the GES (as depicted in Figure 4). Odum [66] notes that technology improvements and associated efficiency gains represent diversions of high-quality energy into system structures. As such, evolution of the GES can be seen in terms of changes in the underlying power capacity and supporting infrastructure stocks, and in their patterns of utilization. Explicit consideration of changing profiles of power capacity, including dynamic metabolic implications and viability, is crucial but under-utilized in the study of GES transformations. As described by Diaz-Maurin [255],

> *"The inclusion of power capacity in sustainability assessment would be very beneficial to the discussion over the energy and societal transitions as it makes it possible to consider the long-term effects of external constraints over the metabolism of human societies. […] Reconstructing patterns of use of power capacity across societal scales would be very beneficial for the study of the role*

this factor played in the development of human societies and for facing the external constraints ahead."

Power capacity, defined as an aggregate quantity, is diffuse and does not exhibit one-to-one correspondence with tangible capital (devices) as most types represent composite power capacities. For example, passenger vehicles provide the energy service of transportation, but can also provide heating, cooling, information processing, and communication. Additionally, multiple conversion stages (as outlined in Figure 7) and associated power capacities can be contained within the same physical device, such as a blast furnace using coal (a primary energy flow) to provide high temperature process heat (an energy service).

3.1.2.3 Scarcity and boundary conditions

Energy scarcity can profoundly affect the viability and feasibility of CAS, including the coupled GES and HSES, via both internal and external constraints as discussed in section 3.1.2 and section 1.2.2. The former corresponds to energy transformations comprising socio-metabolic patterns and the dynamic provision of power capacity (outlined in sections 2.2, 3.1.2.1, and 3.1.2.2, respectively). Notably, scarcity can arise endogenously from the failure of the hypercycle. This occurs when the production of energy carriers becomes insufficient for autocatalytic energy production and other metabolic demands of the GES while simultaneously providing energy services required by the HSES, posing a system bifurcation potential (i.e., the net energy trap). However, scarcity can also arise from exogenous factors representing a system's boundary conditions, both in terms of both sources and sinks.

On the source side, Giampietro et al. [21] note that socio-metabolic patterns and the autopoietic processes of the HSES are ultimately constrained by the magnitude and quality of primary energy sources (i.e., extant thermodynamic gradients described in section 2.1) available to the GES. In turn, GES autopoiesis is constrained by the dynamic capacity of the HSES to provide the necessary labour and resources. Both Hall et al. [13] and Ayres and Warr [141] stress the importance and necessity of considering primary energy resource scarcity, and implications for societal stability and evolution. While metabolic requirements beyond energy must also be considered, exergy can only be used once to drive a useful process and is thereby destroyed, while most materials can be reused and recycled with sufficient exergy inputs. Also, as Georgescu-Roegen [26] cautions, the irreversibility of thermodynamic processes implies that material waste generation within economies is unavoidable, with no possibility of perfect circularity.

Regarding sinks, the most prominent scarcity relates to anthropogenic climate change, although sink limits can manifest at various spatial and temporal scales across ecosystems, including acute local impacts [14, 23, 33, 78-80, 103, 151, 256, 257]. The scale of these challenges is now immense, testing the ability of societies to grasp their true extent and possible ramifications, let alone proffer effective solutions. As noted by Smil [6], "there is no doubt that high-energy civilization has been engaged in an unprecedented geophysical experiment on a planetary scale." Levin et al. [110] note that negative changes in socio-ecological environments tend to accumulate imperceptibly slowly, and can be effectively ignored where societal decision making occurs at different system levels to the primary effects of these environmental feedbacks.

The property of sustainability refers to the nature of relationship between a CAS and its environment. Giampietro et al. [21] define sustainability as maintaining the stability of the boundary conditions affecting a particular system. As such, boundary condition instability indicates unsustainable and transitory system behaviour and consequently, inevitable system re-organization (without exogenous restoration of boundary conditions).

3.1.2.4 Functional differentiation and non-equivalence

Primary energy resources and the fuels derived from them are not interchangeable with respect to all end-uses; they exist in qualitatively distinct, non-fungible forms [21, 42, 68, 158]. Similarly, the various power capacity types responsible for energy transformations at each conversion stage within the GES are functionally non-equivalent. Energy carriers, as defined in section 2.2.2, are an obvious case. For example, electricity cannot be used to operate an internal combustion engine while the application of heat serves no useful purpose to a personal computer. At the system level, this characteristic imposes non-trivial limits to substitution between distinct primary energy resources, energy carriers, and capital stocks for the provision of final energy services, as noted by Cleveland et al. [156].

However, any tractable representation of energy systems must allow for sensible aggregations, which will necessarily overlook some degree of non-equivalence and non-fungibility. As discussed in section 2.1.1, multiple aggregation methods exist for energy flows, including the use of thermal equivalents, prices, or exergy. These common techniques are often applied in a conceptually invalid way. According to Giampietro et al. [21], energy flows "can only be defined and measured after having selected a narrative about a well-defined and finite set of energy conversions requiring the adoption of a pertinent scale of analysis." The aggregation of distinct energy flows requires semantic definitions based on selected equivalence classes, or 'typologies', which reference specific means of conversion and environmental conditions, and are only meaningful over the same semantic category (even where quantities are denoted in the same physical unit). As such, it is necessary to avoid "nonsensical aggregation of energy forms defined within non-equivalent narratives about energy transformations" [21]. Similarly, Santos et al. [163] note that heterogenous capital stocks with dissimilar functional characteristics cannot be meaningfully aggregated.

3.1.3 Power, growth, and economic scale

> *"The flow of energy should the primary concern of economics"*
>
> – Frederick Soddy [241]

Georgescu-Roegen [26] observed that the economic history of humanity is best described as an "entropic struggle", subject to both physical and social laws. Energy conversions are indispensable in all forms of economic production [20, 158, 160, 164]. As such, the energy perspective is paramount in understanding the economic process, as claimed by Hall et al. [13]. Social development, supported by economic prosperity, can also be seen as intimately tied with energy consumption [10, 71, 107]. Without sufficient, reliable energy inputs, there can be no functioning economy and no society. Despite this, as noted by Capellán-Pérez et al. [50], there remains a "lack of consensus in the literature about the quantification of the impact of energy scarcity on the future economic growth."

The discussion in this section reveals the global economy as fundamentally demand-driven but also physically bounded and supply-constrained. This view broadly aligns with heterodox economic theory, particularly *post-Keynesian ecological theory* as outlined by Kronenberg [258] and Fontana and Sawyer [259].

3.1.3.1 Economic development and growth

There are clear historical correlations between energy consumption and the growth of economies [53, 71, 73, 141, 156]. According to Brown et al. [10], "Empirically, the central role of energy in modern human economies is demonstrated by the positive relationship between energy use and economic growth". King [31] notes that changes in energy technologies and corresponding increases in resource access enable profound changes in the size and structure of economies. Since the beginning of the industrial era, growth has been driven by the rapidly expanding exploitation and declining real costs of the fossil fuels – coal, oil and natural gas – allowing the progressive substitution of human labour with energy-consuming machines and the rise of mass production and consumption [21, 148, 260]. Equally important were the technological breakthroughs delivering vast increases in the efficiency of turning these energy sources in useful work and energy services [20, 26, 148, 163].

Markets and prices play a key role in the energy-growth dynamic. Ayres and Warr [141] suggest that economic growth is driven by a positive feedback between falling prices attributable to economies of scale and technological learning effects, demand growth, increased investment, and increased supply. Fizaine and Court [178] note that energy expenditures relative to gross domestic product (GDP) are inversely correlated with economic growth rates. This ratio reflects the balance between saving rates and consumption and is related to the tension between hypercyclic and dissipative system components, influencing long-term economic trajectories. As in biological systems, growth competes with consumption [12, 26].

The laws of thermodynamics constrain both the economic process and the application of new technologies, as they determine what is physically possible [26, 141, 261]. As described by Glucina and Mayumi [73],

> *"Where economics is concerned with production and consumption, thermodynamics is relevant. This is because production and consumption of material goods are essentially transformations of matter-energy, and as such are governed by the laws of thermodynamics."*

The second law (entropy law) is particularly pertinent, as noted by Ayres and Nair [261] and Giampietro et al. [21], due to the incontrovertible limits it places on energy transformations, such as their fundamental asymmetry and irreversibility. Irreversibility also manifests at the system level, as the evolutionary path-dependence evident in economies [13, 210, 262].

Fizaine and Court [178] and King [31] suggest that the laws of thermodynamics prevent economic growth ever becoming completely independent of energy consumption.

As discussed in sections 2.1.1.1 and 2.2.1, exergy is instrumental to growth at the macroeconomic level. Georgescu-Roegen [26] argues that this can be explained by conceptualizing the economic process as a dissipative structure. Court [16] agrees, noting that economic development can only be understood through a "thermo-evolutionary" perspective centred on "energy conversion and exergy degradation set by physical constraints that determine the growth of production and income."

However, while exergy is necessary, it is insufficient to explain economic production and value [26]. Giampietro et al. [21] cautions that classical thermodynamics cannot be applied to complex, far-from-equilibrium systems as the first law provides trivial information only while the second law is not directly relevant to macroscopic energy analysis (it relates to specific thermodynamic cycles only). Glucina and Mayumi [73] echo this critical perspective on the applicability of thermodynamic analysis at the macroeconomic level, noting that thermodynamic considerations do not directly govern value. According to Baumgärtner [263],

> *"[T]hermodynamics is necessary to identify which options and scenarios of resource use, economic production, and waste generation are feasible and which are not. However, it neither includes nor allows value statements, and as such, cannot provide answers to the normative questions imposed by sustainability."*

3.1.3.2 Energy as a factor of production

A growing body of empirical evidence supports the existence of a causative relationship from energy consumption to aggregate economic output (i.e., GDP), and not in the reverse direction as mainstream economic theory assumes [141, 148, 156, 159-163, 178]. This identifies energy as a relevant factor of economic production. As explained by Fizaine and Court [178], "energy is crucial for economic growth, which tends to reinforce the conclusion drawn by the biophysical movement and weakens the mainstream position which sees energy as a common (if not minor) factor of production."

The importance of energy has historically been downplayed due to its relatively low 'cost share': the ratio of (monetary) energy expenditures to GDP. However, output elasticities for energy reveal a much greater importance than cost shares would indicate when calculated under non-equilibrium conditions [148, 163, 264]. According to Ayres and Warr [141], the relative importance of energy exceeds its cost share by up to an order of magnitude.

There remains some disagreement regarding the most appropriate measure to represent energy as a factor of production, with various candidates including exergy, quality-adjusted energy, useful work, work mediated by information processing, and efficiency growth rates [73, 141, 148, 156, 159, 163, 264]. However, there is strong agreement that energy can account for a large part of 'total factor productivity', the component of economic growth not explained by changes in capital and labour (i.e., the conventional factors of production), typically attributed to technological progress and rising labour productivity [141, 159, 264]. Warr and Ayres [161] find that while technology does influence growth alongside energy, technological innovations affecting energy productivity have the most pronounced effects. As described by Cleveland et al. [156],

> *"This runs counter to much of the conventional wisdom that technical improvements and structural change have decoupled energy use from economic performance. To a large degree, technical change and substitution has increased the use of higher quality energy and reduced use of lower quality energy."*

Adequate consideration of the quality dimension is vital. For example, as noted by Smil [6], electrification had a significantly greater impact on economic growth than the rise of coal. Glucina and Mayumi [73] suggest that this shift toward higher-quality fuels may have been more impactful overall than improvements in energy efficiency. According to Cleveland et al. [156], properly accounting for energy quality yields important information than may remain obscured otherwise, including the declining energy surplus from fossil fuel extraction and the lack of decoupling between GDP and aggregate energy use, contrary to common perceptions.

Importantly, energy cannot be perfectly substituted by other factors due to strong complementarity, i.e., the productivity of both capital and labour is supported by energy [12, 26, 141, 163]. Hall et al. [13] note that exergy is consumed in the productive process while capital and labour are not, implying it is ultimately the scarcer input. Ayres et al. [148] observe weak substitutability only between energy and capital. These relationships are typically highly non-linear, as noted by Ayres and Voudouris [260]. Furthermore, as the degree of substitutability between factors is likely significantly lower than is generally assumed, economic growth may be more vulnerable to conditions of potential energy scarcity than is currently considered in common energy transition narratives.

While uncertainties and analytical issue persist, economic growth can be seen as closely connected with absolute energy supply, moderated by both changes in efficiencies and the relative size of the societal hypercycle (indicated by net energy metrics, such as EROI).

3.1.3.3 Power maximization and metabolic scaling

As discussed in section 2.2.1, dissipative processes tend towards the maximization of power, both at the process-level due to the power/efficiency trade-off and through macroscale rebound effects. Economic and societal development represents a continuation of organismic evolution in energy consumption, scale, and complexity, a process which generally follows the *maximum power principle* [3, 16, 32, 115, 211, 265]. This principle describes the acquired evolutionary propensity of complex systems to maximize their utilization rate (power) of available energy gradients, first observed by Alfred Lotka [173].

Ruzzenenti and Basosi [211] explain that this power maximization occurs via two paths originating on different hierarchical levels within the system – by increasing efficiency (under conditions of energy scarcity) or by increasing energy intake (under conditions of energy abundance). The opportunity cost, or scarcity, of time also plays a key role and can change the effective balance of power and efficiency, as outlined in in section 2.2.1. Smil [6] notes that maximizing short-term energy throughput, while evolutionarily adaptive, is often highly counterproductive in the modern context and can be considered the root cause of many serious social and environmental issues.

The relationship between metabolic power and scale is non-linear, shaped by *Kleiber's law* which observes that for biological organisms, basal metabolic rate (power consumption) scales with mass sublinearly, with an exponent of 3/4 (or 2/3 for some species) [31, 266]. Various explanations have been offered for this relationship, including trade-offs between structure and mass, heat radiation, network efficiency in nutrient distribution, and energy conservation during rest. Brown et al. [10] observes that a similar relationship exists within societal metabolism:

"The exponent for the scaling of energy use as a function of GDP, 0.76, is reminiscent of the three-quarter-power scaling of metabolic rate with body mass in animals […] The energy and other resources that sustain these systems are supplied by hierarchically branching networks, such as the blood vessels and lungs of mammals and the oil pipelines, power grids, and transportation networks of nations."

The above suggests that voluntary reductions in societal power for the promotion of desirable long-term outcomes may be more limited in scope than is commonly acknowledged. Efficiencies of metabolic scaling explain the relative (but not absolute) decoupling of economic growth and energy consumption noted by Brand-Correa and Steinberger [11], Csereklyei and Stern [267], and UNEP [268]. However, any decline in metabolic scale may incur a loss of such efficiencies, causing energy throughput to fall more slowly than aggregate economic output.

3.1.3.4 Future trends and sustainable scale

"Only widespread scientific illiteracy and innumeracy […] prevents most people from dismissing the idea of sustainable growth at healthy rates as an oxymoronic stupidity whose pursuit is, unfortunately, infinitely more tragic than comedic."

– Vaclav Smil [1]

In the context of NRE depletion, falling primary energy quality, and a socio-metabolically demanding and energetically disadvantageous transformation to RE, future economic growth will be adversely affected and will likely reach eventual limits [54, 65, 148, 163, 169, 269]. This has broadly negative implications for material standards of living and sustainable levels of societal complexity [19, 50-52, 56, 141, 166, 270]. According to Bardi et al. [271], an eventual decline in societal complexity and scale will be driven primarily by diminishing returns in the exploitation of a wide range of natural resources, including energy. Responses to this situation are hampered by the limits to substitution facing energy as an essential factor of production. As cautioned by Odum [66], under conditions of a diminishing energy surplus, growth-promoting policies and economic structures can quickly become an energy liability, exacerbating societal difficulties and raising the spectre of collapse.

Ayres and Warr [141] and Ayres and Voudouris [260] argue that future economic growth will depend on some combination of declines in the cost of primary energy and a trend towards increasing exergy-to-work efficiency. Efficiency gains have been declining since the 1970s and appear to be waning as a driver of growth [148, 159]. On the other hand, maintaining sufficient low-cost energy supplies required for economic growth may be untenable given falling primary energy quality and rising costs of exploitation. Heun and de Wit [55] posit that the energy cost share will likely rise over time causing declines in disposable income and growing recessionary pressures, eventually leading to falling energy demand, prices, and supply. Ayres et al. [148] note that continued economic growth appears doubtful given the trend towards higher energy prices, suggesting instead policies to accelerate increases in exergy efficiency while actively controlling for the rebound effect. Court [16] agrees, emphasizing a redoubled pursuit of greater efficiency as one of the few remaining avenues to materially improve economic prospects for human societies. However, as noted by Romero and Linares [154], the presence of significant rebound effects implies that efficiency improvements cannot be relied on to achieve sustainability.

The importance of trends in energy quality for future growth is central and often overlooked. As discussed in section 2.1.1.4, declining EROI is associated with falling discretionary output, increased capital and energy requirements within the GES, and likely adverse impacts on economic growth. Furthermore, Ayres et al. [148] note that limits may have been reached in the shift from lower quality to higher quality energy carriers, constraining future growth. Sorman and Giampietro [27] remark on the seeming unavoidability of economic 'degrowth' in response, implying a reduction and simplification of socio-metabolic patterns:

> *"[S]ocieties will be obliged to divert a very large share of hours of paid work, energy, technological capital, from the various sectors of the economy to be invested in the operation of the energy sector itself. […] the internal organization of the society and its structural and functional characteristics will be severely affected by this forced withdrawal of resources"*

In light of these converging constraints, Brown et al. [10] question the continued plausibility of trajectories seen over recent decades in population, resource extraction, technological progress, and material standards of living. They warn that "the nonlinear, complex nature of the global economy raises the possibility that energy shortages might trigger massive socioeconomic disruption" while also suggesting major technological, socio-economic, demographic, and behavioural adaptations are still possible. Giampietro et al. [21] argue there is a "standard pattern of structural and functional change in the metabolic pattern of modern societies, associated with economic growth" and, as such, a trend towards less abundant and more costly energy "implies that the viability domain of the metabolic pattern of modern society is gradually contracting as both external and internal constraints tighten."

3.1.4 Dynamic energy systems modelling

> *"Since all models are wrong the scientist cannot obtain a "correct" one by excessive elaboration. On the contrary following William of Occam he should seek an economical description of natural phenomena."*
>
> – George Box [272]

Quantitative models are useful tools, allowing the mathematical representation of phenomena of interest for both predictive and elucidative purposes. This capacity is instrumental in in research, pedagogy, and policy making alike – as observed by Bernstein [273], "The ability to define what may happen in the future and to choose among alternatives lies at the heart of contemporary societies." Building such models is a particularly challenging task for complex systems, requiring a pre-analytic assessment of the nature of models as epistemic devices including their limitations.

The GES can be considered a 'hyperobject' as defined by Morton [274] – objects massively distributed in time and space, ecologically entangled, and existing beyond human comprehension as their totality cannot be perceived via any local manifestation. Narrative simplifications are required to render hyperobjects in forms amenable to investigation. This is the proper role of modelling, to create useful abstractions while losing as little important information as possible. Critically, what is lost in this process must be carefully considered and the modeller should avoid overconfidence in their model [21, 145, 275].

As remarked by Alfred Korzybski, *"the map is not the territory"*, implying that any given abstract representation must not be confused with reality. This maxim is reinforced by Gödel's *incompleteness theorem* [276], which, as described by Odum [115], effective rules out perfect understanding of a system from within, as the representation would be more complex than the system itself. Models are appropriate for the identification of implausibility but cannot demonstrate objective truth (i.e., falsification over verification) and as such, are epistemically aligned with the *post-positivist* approach to science, as expounded by Karl Popper [277] and Thomas Kuhn [63]. Any knowledge derived from modelling must therefore be considered both contingent and imperfect, subject to a finite descriptive domain.

All models require specific, subjective choices regarding the elements and relationships to represent. According to Floyd et al. [54], "What is assumed to be relevant for a particular model is a function, in part, of the modeller's worldview, and worldviews give rise to perspectives that are unavoidably partial." Modelling necessarily entails the exclusion of certain system aspects. As described in section 3.1.2.4, tractable representations of energy systems must allow for aggregation based on an appropriate selection of semantic categories corresponding to meaningful narratives about energy transformations. Giampietro et al. [21] note that these narratives must be suitable for the objectives of the analysis, and caution that improper aggregation can result in a "loss of grip on the physical side of the energy transformations." In general, the validity of semantics must take precedence over calculation rigour to yield meaningful results.

In principle, aggregations should be chosen to maximize the representation of distinct functional roles while minimizing the total number of included elements. Consequently, high-level models focussing on the behaviour of a selected holon must prioritise functional representation, typically at the expense of exhaustive representation of structural details contained within lower level holons. This will inevitably disregard some constraints and feedbacks influencing the holon of interest via bottom-up causation (see Figure 8). As noted by Ruth and Hannon [145], models should be as simple as possible and will therefore not reproduce all aspects of the real-world system they represent. Similarly, Levin et al. [110] note that models do not need to incorporate every possible detail, "indeed, the art of modelling is to incorporate the essential details, and no more." According to Forrester [275],

> *"There is no way to prove validity of a theory that purports to represent behavior in the real world. One can achieve only a degree of confidence in a model that is a compromise between adequacy and the time and cost of further improvement."*

Models also require the specification of boundaries of analysis, requiring the exclusion of certain interactions between the system and its environment. According to Giampietro et al. [21], "in energy analysis, quantification forces us to choose and adopt a pre-analytical definition of boundaries both in space and in time for the set of energy transformations of interest." Ruth and Hannon [145] explain that chosen analytical boundaries effectively impose *ceteris paribus* assumptions, some of which may be justified while others are not. As described by Floyd et al. [54],

> *"All models are conceived and implemented within superordinate, encompassing and exogenous contexts that are necessarily external to the model itself. These contexts are by definition fixed for the purpose of the modelling exercise – the model cannot respond to or influence them. There is a boundary beyond which the model cannot 'see', because those aspects of the real world are not endogenized. In the real world though, these superordinate contexts are always subject to potential change, possibly under the influence of changes originating from processes that are included in the model itself."*

Aggregations and boundaries suitable for chosen objectives can be encapsulated in a task-dependent 'energy grammar', as described by Giampietro et al. [21]: an energy grammar consists of a pre-analytically defined set of semantic categories (i.e., equivalence classes) and an associated set of formal categories (i.e., quantification protocols, or units). Explicitly specifying an energy grammar helps to avoid confusion and increase transparency regarding model development and the resulting valid descriptive domain.

3.1.4.1 Systems-cognizant energy modelling approaches

> *"Most misbehavior of corporate, social, and governmental systems arises from […] dependence on erroneous intuitive solutions to complex behavior."*
>
> – Jay Forrester [275]

Complex systems require vastly different methodologies than those applied to simple, deterministic phenomena. Levin et al. [110] suggest that the characteristic features of complex system pose significant challenges for modelling, making general analytical solutions impossible. Additional difficulties relate to the current 'full world' context faced by the nested socio-metabolic systems comprising the HSES, described by Ruth [249], Daly [278], and Klitgaard and Krall [279]. However, modelling complex systems remains highly worthwhile and offers vital capabilities, as described by Motesharrei et al. [23]:

> *"The ability of dynamic models to capture various interactions of complex systems, their potential to adapt and evolve as the real system changes and/or the level of the modelers' understanding of the real system improves, their ability to model coupled processes of different temporal and spatial resolutions and scales, and their flexibility to incorporate and/or couple to models based on other approaches (such as agent-based modeling, stochastic modeling, etc.) render them as a versatile and efficient tool to model coupled Earth–Human Systems."*

Rigorous quantitative methodologies are essential to understand the range of future potentialities, as intuition and linear thinking are fundamentally inadequate for evaluating the behaviour of complex systems [26, 275]. There is no universally valid protocol for energetic analysis of GES transformations, as noted by Giampietro et al. [21], and as such, prior attempts and established precedents offer little guidance, particularly where modelling approaches are not adequately oriented towards complexity.

A useful complex system model must encompass the holons of interest in their entirety, with all internal elements and relationships endogenized (albeit in necessarily aggregated form), while interactions with other holons and the general environment are treated as exogenous. For example, socio-metabolic systems modelled at sub-global scales, such as at the national or regional level, will require arbitrary boundaries and the specification of complex exchanges with the rest of the global system (e.g., trade flows, migrations), and will fail to capture system-level emergent behaviours as significant feedbacks are be rendered static and exogenous. However, as described by Capellán-Pérez et al. [39], models designed for the global level often produce results applicable to sub-global scales due to high levels of technological and organizational similarity, and the presence of common challenges.

Complex systems modelling must begin with a conceptually appropriate technique. The 'system dynamics' modelling approach is well suited for quantitative analysis of complex systems characterized by non-linear behaviour arising from dynamic interactions across multiple feedback loops [50, 275, 280]. System dynamics is based on the quantitative simulation of changing stock and flow elements using a system of equations updated via discrete, iterative calculation, or 'time-stepping', over a chosen simulation period [145]. According to Levin et al. [110],

> *"Complexity entails substantial modelling challenges, but simple models can incorporate some elements of complexity to provide novel insights. […] At the core of all the recent advances are models of dynamic systems, represented by systems of differential equations."*

Clear advantages are apparent in the system dynamics modelling approach, including consistency of the stock and flow basis with fundamental physical processes in complex systems [156] and the inclusion of non-linear feedbacks via the mutual dependence of variables [141]. As described by Forrester [275], "In system dynamics, description leads to equations of a model, simulation to understand dynamic behavior, evaluation of alternative policies, education and choice of a better policy, and implementation."

Formulating system dynamics models begins with causal loop mapping, which involves identifying causal relationships between system variables including their direction, polarity, and the presence of any time delays. Any resulting loops exhibiting a continuous sequence of influences can then be classified as either positive (reinforcing) or negative (balancing) and are largely responsible for observed system behaviour, as described in section 3.1.1. As noted by Forrester [275], this process provides useful information but is insufficient to understand system behaviour and must be followed by a process of iterative development to produce a model capable of achieving the stated research objectives. As noted by Ruth and Hannon [145], while models of complex systems focus on causal relationships between elements, they also typically incorporate control logic which requires auxiliary techniques extending beyond the conventional system dynamics approach.

According to Giampietro et al. [21] complex energy systems analysis must include adequate functional representation of the following aspects contributing to non-linearity, stock and flow non-equivalence, and critical power thresholds within the metabolic pattern of society:

- Necessary distinctions between gross and net energy carrier flows, and between throughput efficiencies and the lifecycle energy costs of capital, to properly characterize the autocatalytic loop describing system-level energy production (i.e., this rules out linear, reductionist representations).

- Specific, dynamic profiles of distinct energy carriers invested into non-equivalent power capacities across various hierarchical levels, both for the provision of final energy services via end-use capital and consumed within the autocatalytic loop.
- The need for dynamic equilibrium between energy carrier supply and demand via a co-evolutionary process (i.e., this rules out the representation of either supply or demand in isolation).
- The provision of final energy services required by the HSES to express necessary functions for its own autopoietic processes (thereby supporting the GES).

Several additional considerations pertinent to modelling of GES transformation can be identified in the literature:

- Soddy [241] advocates the use of biophysical flows rather than monetary flows as more fundamental to economic change. Monetary indicators have a limited correspondence, at best, to physical phenomena, within a narrow set of market conditions only (i.e., equilibrium) and cannot be used to reliably describe processes involved in major system transformations.
- Levin et al. [110] note that most models ignore spatial heterogeneity due to the considerable analytical and computational difficulties this introduces, instead representing relevant spatial dynamics in the time domain via feedback delays.
- Georgescu-Roegen [26] stresses the importance of representing dynamic qualitative change, alongside quantitative change, in both stocks and flows.
- Grübler et al. [215] suggests endogenizing technological change processes requires the explicit representation of technological choice and allocation (i.e., goal seeking).
- Ruth [249] and Ayres and Warr [141] describe the lack of mono-dimensional optimality within complex systems, noting that real-world behaviour is instead based on 'satisficing' multiple criteria.

3.1.4.2 Prediction versus exploration

> *"And the record is also unequivocal as far as the notion of any mechanistically preordained primary energy transitions is concerned: As in so many other*

> *cases, complex and nuanced reality does not fit any simplistic deterministic models that are supposed to capture the past and reveal the future."*
>
> – Vaclav Smil [14]

It is widely understood among expert modellers that models are of very limited usefulness for the direct prediction and management of complex systems, as described by Sorman and Giampietro [27] and Ravetz [281]. Georgescu-Roegen [26] explains that models serve multiple purposes, including facilitating arguments, clarifying results, and the correction of faulty reasoning, but have no meaning without dialectic reasoning and therefore do not predict. Ruth [249], Sterman [280], and Meadows [114] agree, noting the purpose of system dynamics modelling is rather to better understand system behaviour, particularly regarding possible system responses to interventions, i.e., the identification of system leverage points, as described in section 1.2.2.

According to Giampietro et al. [21], the prediction of autopoietic systems is, in fact, not possible; models can only improve comprehension of available pathways while excluding those that are metabolically infeasible. As such, complex system models can be understood to have a fundamentally exploratory epistemic orientation. They are useful to present a plausible range of system potentialities and uncover behavioural tendencies not accessible via intuition or reductionism but should not be relied on as singular guides to the future.

A common approach drawing on the exploratory strengths of modelling is scenario analysis, the implementation of selected sets of inputs designed to test model behaviour under specific narratives of interest. According to Grübler et al. [215],

> *"Because uncertainties abound at the macro scale, almost every model-based analysis employs scenarios. Scenarios bound possible futures, and they make it possible to focus attention on analytically tractable issues, such as how the adjustment of one or more "policy'' variables causes changes in emissions from a baseline scenario."*

Scenarios also offer a partial approach to uncertainty, allowing selected uncertain input parameters or model structures to be varied over a typically small but representative set of discrete alternatives. Notably, system dynamics models are highly amenable to scenario analysis, as described by Capellán-Pérez et al. [50],

> *"Scenario methodology offers an approach to deal with the limited knowledge, uncertainty and complexity of natural and social sciences and, applied to System Dynamics models, can be used to group the variations of policies into coherent and meaningful scenarios. Each scenario (or storyline) represents an archetypal and coherent vision of the future"*

Scenario construction is subjective and results are often highly sensitive to the chosen implementation within the limits of a model [50, 145]. For this reason, scenarios should be used carefully, analysed primarily in reference to a default state or 'base case' of the model.

It is important to note that while models can represent aspects of complexity, they are not truly complex themselves. Exogenous stressors can impact a complex system sufficiently to push it out of its domain of stability and towards a phase change characterized by system re-organization. Levin et al. [110] note that complex system models necessarily assume the system will remain within its current basin of attraction, described by a corresponding system of equations, outside of which unanticipated behaviours will occur. As noted by Georgescu-Roegen [26], "the strongest limitation to our power to predict comes from entropic indeterminateness, and especially from the emergence of novelty by combination." Consequently, models cannot capture emergent behaviour or evolutionary processes occurring in response to novel conditions. As described by Ruth and Hannon [145],

> *"By enclosing a selected number of system components in the model and determining the model–system's behavior over time solely in response to the forces inside the model, the model becomes closed. Real systems, in contrast, are not closed but open, allowing for new, even unprecedented development in response to highly infrequent but dramatic changes in their environment."*

As in all quantitative modelling, real-world events have the potential to invalidate complex system models. This does not render these models incorrect, only incomplete with repect to novel circumstances [145]. This observation is in alignment with the nature of models, discussed in section 3.1.4 – useful abstractions designed to represent only the subset of real-world behaviours pertinent to the goal of the analysis.

3.1.4.3 Probabilistic approaches

> *"Our knowledge of the way things work, in society or in nature, comes trailing clouds of vagueness. Vast ills have followed a belief in certainty."*
>
> – Kenneth Arrow [282]

Modelling of the complex social-ecological systems implicated in major contemporary environmental and sustainability issues is subject to partial knowledge and irreducible uncertainty [27, 54, 113, 251]. As discussed in section 1.3.2, approaches to complex problems must acknowledge the presence of epistemic uncertainty and adequately address this via quantification of the strength of knowledge and fostering pluralism of socio-technical perspectives. Therefore, uncertainty must not be ancillary, but rather central to the practice of complex systems modelling. Scenario analysis, discussed in section 3.1.4.2, is a step towards this but is insufficient where uncertainty is pervasive. As noted Retortillo et al. [283],

> *"A handful of simulation runs do not give much information when one faces large models with many stock variables, nonlinear dynamics and a high degree of uncertainty in the parameters, and the tools for analyzing large scale models are not very developed."*

Attempts to quantify complex systems suffer from both aleatory uncertainties, or inherent temporal randomness, and epistemic uncertainties associated with the limits of knowledge pertaining to system structures, parameters, and boundary conditions. While epistemic uncertainty can be partially reduced through greater empirical efforts, at least for known uncertainties, aleatory uncertainty cannot. Saltelli et al. [284] warn of the possibility of an "uncertainty cascade" given excessive complexity – this must be recognized and averted where necessary.

Epistemic uncertainty can originate not only from the strength of knowledge (associated with data quality), but also from indeterminacy in the selected semantic definitions of modelled functional elements, lacking structural specificity (as discussed in section 3.1.4). That is, valid alternate boundaries of modelled functional elements necessarily exist, as each is an aggregate across diverse structural types. While these boundaries have operative implications for modelled behaviour, 'correct' boundary definitions cannot be determined analytically. Consequently, an overriding pursuit of precision and specificity is often misplaced in high-level complex systems models. One answer to this indeterminacy is found in Georgescu-Roegen's concept of *dialectical penumbras*: semantic definitions and associated boundaries which intentionally avoid definitive and inflexible specification, instead admitting multiple valid interpretations [26].

Comprehensive probabilistic modelling goes beyond the limitations of scenario analysis to test model uncertainty from all identifiable sources concurrently. Monte Carlo simulation achieves this by replacing estimates for all epistemically uncertain input parameter values with probability distributions, followed by repeated sampling of these distributions and simulation of the corresponding deterministic models (each referred to as a 'realization' of the model) [285-288]. This allows the creation of an arbitrarily large, representative set of modelled realizations, referred to as an 'ensemble'. The value of this approach to modelling uncertainty within complex system models is emphasized by Motesharrei et al. [23]:

> *"Uncertainty is another important challenge in producing future behavior and scenarios with models. This problem has been addressed successfully in meteorology by using, instead of a single forecast, an ensemble of typically 20–200 model forecasts created by adding perturbations in their initial conditions and in the parameters used in the models. […] A similar approach, i.e., running ensembles of model projections with perturbed parameters, could be used with coupled Earth–Human System models to provide policymakers with an indicator of uncertainty in regional or global projections of sustainability associated with different policies and measures."*

As noted by Harrison [289], a principal advantage of Monte Carlo simulation is the detection of consistent model tendencies at the ensemble level, given the sum effect of uncertainties across many input dimensions. Effectively, this achieves a system-level filtering of bias (e.g., optimism or pessimism in framing narratives) via the semi-independent variation of inputs. This is significant given that narratives regarding the future of the GES rooted in technological optimism, outlined in section 1.2, frequently presuppose a coincidence of favourable parameter values across many epistemically uncertain system attributes. With probabilistic modelling, such optimistic coincidences can be revealed as highly improbable and the corresponding socio-technical narratives are implicitly de-emphasized or refuted outright.

Monte Carlo methods also enable multivariate sensitivity analysis, noted as critical for complex systems modelling by Ayres and Warr [141] (discussed further in section 3.3.2).

3.2 THE CURRENT STATE OF ENERGY MODELLING

Energy modelling is employed extensively in both research and policy, for various purposes and across widely varying spatial and temporal scales ranging from local infrastructure planning to analysis of global GHG emission trajectories. Many of these disparate approaches are increasingly being oriented towards studying the prospects for a large-scale shift towards RE, but often remain entrenched in methodologies which conceptualize energy systems simplistically and reductively via a limited set of largely techno-economic problem framings.

Notable shortcomings identified in the literature affecting major energy transition models and studies in widespread use are summarized in section 3.2.1. Recent developments in the emerging field of biophysical energy systems modelling are then outlined in section 3.2.2.

3.2.1 Conventional approaches to the study of energy transitions

Despite the significant diversity observed over the range of publicly available energy transition models and studies – in research scope, stated objectives, quantitative methods, and levels of detail – substantial conceptual similarities exist. Loftus et al. [223] classify four general approaches:

- *Top-down back-casting* extrapolates deployment of preselected technology portfolios to achieve proposed target states.
- *Top-down Integrated Assessment Models* (IAMs) use linked sub-models of energy, climate, and economic systems to determine minimum cost technology deployment strategies subject to a selected constraint (typically decarbonization targets).
- *Bottom-up energy systems modelling* uses highly detailed and data-intensive regional and global energy system representations to construct scenarios consistent with selected goals.
- *Bottom-up techno-economic assessments* assess technology options in reference to specified criteria then construct scenarios based on preferential deployment of the highest-ranking technologies.

IAMs, or energy–economy–environment (E3) models, are of particular interest given their central role in informing and framing high-level governance, including international climate negotiations including those organized under the United Nations Framework Convention on Climate Change [146, 188, 290]. DeCarolis et al. [291] observes there has been a recent proliferation of E3 models, offering detailed quantitative simulations, support for decision making under uncertainty, and useful pedagogic tools. However, these models often exhibit a notable lack of transparency regarding modelling choices and assumptions, adversely affecting their robustness and credibility [146, 188, 291]. As such, many E3 models are effectively black boxes, making them difficult to compare and validate.

Table 2 lists selected IAMs, global energy transition studies (many of which employ IAMs), and related meta-analyses which include an explicit focus on energy. Among these studies, energy system representations range from simple, linear economic optimization models to detailed, multi-scale, regionally disaggregated models.

Table 2: selected global IAMs, energy transition studies, and meta-analyses with a significant energy focus

IAMs	Global energy transition studies		Meta-analyses
IMAGE [292] $\text{MESSAGE}_{\text{ix}}$ [293] AIM/GCE [294] GCAM [295] REMIND-MAgPIE [296] MARKAL/TIMES [297] WEM [298] En-ROADS [299] E3ME [300]	Pacala and Socolow [301] Barker and Scrieciu [302] Jacobson and Delucchi [303, 304] Randers and Gilding [305] Deep Decarbonization Pathways Project [306] van Vuuren et al. [307, 308] Edenhofer et al. [309] Worldwatch Institute [310] World Wildlife Fund [311]	IPCC [312] Teske et al. [313] Singer et al. [314] IRENA [61] IRENA [315] Ram et al. [316] IEA [317] GEA [49] Magne et al. [318] Willson et al. [319]	Söderholm et al. [320] Wilson et al. [321] Wiseman et al. [322] Loftus et al. [223] Kempener et al. [323] Stammer et al. [324] Eggler [325]

The study of future energy transitions remains an immature field, limited by conceptual weaknesses in the available quantitative techniques (detailed in subsequent sections), clear motivated reasoning, and a historical dearth of prior examples of a similar degree of scale and complexity to the forthcoming third energy transition (as discussed in chapter 1 and section 2.3). Giampietro et al. [21] observe that current energy transition scenarios, plans, and associated commentary are generally not conceptually robust. Substantial advances are necessary, as described by Loftus et al. [223],

> *"To be reliable guides for policymaking, these types of scenarios clearly need to be supplemented by more detailed analyses addressing the key constraints*

on energy system transformation, including technological readiness, economic costs, infrastructure and operational issues, and societal acceptability with respect to each of the relevant technology pathways."

It is not feasible here to carry out an exhaustive evaluation of the variety of quantitative energy transition models in widespread use today due to their extremely diverse modelling philosophies, quantitative methods, and underlying assumptions. However, a diversity of critical analyses from the literature are summarized in the following sections into four broad themes describing common issues: fundamental oversights regarding economic principles (section 3.2.1.1), ignorance of the complex systems basis of energy transition (section 3.2.1.2), biases towards technological optimism (section 3.2.1.3), and unsubstantiated projections of key variables (section 3.2.1.4).

3.2.1.1 Economic foundations

Most energy modelling, as with other forms of techno-economic analysis, is heavily influenced by the prevailing corpus of mainstream, neoclassical economic theory [264, 326, 327]. Consequently, energy modelling, and IAMs in particular, exhibit a distinct lack of plurality in economic perspectives, as noted by Capellán-Pérez et al. [188]. Georgescu-Roegen [26] describes neoclassical theory as fundamentally mechanistic, portraying the economic process as isolated and ahistorical, constrained by reliance on static marginalist analytical techniques and excessive mathematical abstraction. This theoretical basis is now a significant handicap in energy modelling, preventing the necessary conceptual reorientation suggested by a growing critical literature.

Neoclassical theory largely fails to identify the biophysical basis of the economic process and associated constraints [13, 328]. This failure, and in particular the neglect of dependence on natural resources, can be seen as largely a result of historical circumstances of relative resource abundance [9, 13, 20]. As described by Hall et al. [13],

"Since most modern economic theory was derived during times of expanding availability of high-grade energy resources, much of that theory could ignore the fundamental constraints imposed ultimately by the depletion of high-quality energy and other resources."

This oversight results in basic incompatibilities with thermodynamics. Most notably, the irreversibility of energy transformations, the role of power, and the unavoidability of waste generation are generally not considered within mainstream economics [31, 73, 222]. This strongly undermines the applicability of neoclassical theory to real-world economies comprised of biophysical processes. As noted by Glucina and Mayumi [73], "any model or method of analysis concerned with production and consumption, which is inconsistent with the laws of thermodynamics, should be viewed as highly questionable."

Overreliance on monetary quantification (discussed in section 3.1.4.1) is another clear weakness in E3 models. Cost and price, as mono-dimensional indicators, convey insufficient information to fully characterize economic systems, particularly regarding scarcity and dynamic change [21, 148, 188]. As remarked by Giampietro et al. [21], "Given the crucial importance of the issue of scale in the analysis of the metabolic pattern of society, using prices to study structural changes of the economy is like using a microscope to study the ecology of elephants." This limitation is most apparent in studies that reduce complex processes of energy transition to the simple maximization of net benefits and consider interventions only via subsidies, carbon pricing, and other market instruments. Sgouridis et al. [46] note that all IAMs use such benefit maximization, or cost minimization, techniques introducing ambiguities regarding long-term price forecasts and the obfuscation of important physical processes. Technological allocation in energy modelling suffers from a reliance on cost minimization approaches rather than a wider consideration of biophysical criteria (such as EROI or mineral resource availability), as noted by Capellán-Pérez et al. [39] and Jenkins and Thernstrom [81]. Monetary aggregation of highly heterogeneous, non-fungible capital stocks is also inappropriate, often to the point of meaningless abstraction [12, 26, 141]. This is further exacerbated by practices common in E3 models that arbitrarily distort the time dimension, such as the use of high discount rates giving preferential consideration to near-term costs and benefits at the expense of future needs, as described by Fiddaman [329].

Most IAMs inherit a predominantly static economic framework from neoclassical theory, favouring optimality (i.e., perfect markets) and general or partial equilibrium assumptions, largely for mathematical convenience [20, 31, 141, 188, 329]. This, and related concepts such as marginal productivity, are misleading and inapplicable to real-world economies which do not operate in equilibrium [26, 73]. As described by Ayres and Warr [141] and Ayres and

Voudouris [260], static equilibria are incompatible with growth, evolution, incentives, innovation, and structural change. Equilibrium conditions also serve to obfuscate the true importance of energy in economic production, as discussed in section 3.1.3.2. Some recent progress has been made – the E3ME IAM [300] and Barker and Scrieciu [302] (using E3ME) avoid general equilibrium and instead allow non-optimality.

As discussed in section 3.1.3, the economic process is fundamentally dissipative, revealing energy (or exergy) as necessary but not sufficient for economic production. However, there is a relative lack of appreciation of energy as a factor of production in neoclassical theory [9, 16, 73, 163, 261]. Cottrell [12] argues that the standard assumptions regarding the centrality of labour and capital in production break down upon introduction of energy converters driven by exosomatic energy. As described by Sgouridis and Csala [9], "the perceived abundance of fossil fuels that has allowed energy to be considered a necessary economic factor of production but in sufficient reserve quantities, that, like oxygen, can be accessed as necessary." This omission effectively downplays the potential impacts of energy transition on economic output while overestimating the potential for absolute decoupling of energy and economy, as outlined by Brockway et al. [219]. Even where the aggregate role of energy in production is properly identified this is often not sufficient, for two reasons:

1) Common assumptions of perfect factor substitutability fail to capture strong complementarity between capital, labour, and energy (described in section 3.1.3.2) [9, 73, 148, 163, 188, 327].
2) Sectoral economic structure, while critical due to sector interdependence and induced effects, is missed by common aggregate production functions [20, 188, 327].

Mainstream, neoclassical economic theory assumes economic growth and energy are independent, typically treating energy consumption simply as a consequence of growth [141, 148, 327]. This has implications on both the source and sink sides of the economic system; potential limits to growth arising from energy resource shortages are typically dismissed [10, 327] while it is assumed that energy-related GHG emissions can be reduced arbitrarily without materially affecting growth [148]. Consequently, E3 models often presuppose greater future prosperity relative to the present without confirming the energetic feasibility of this assertion, as described by Ayres et al. [148].

Floyd et al. [54] notes that assumptions of continued economic growth are almost universal in E3 model formulations. This is typically implemented in the form of exogenous economic growth projections [23, 329], often based on Solow-type economic growth models which ignore the role of energy (MESSAGE$_{ix}$ [293] and GEA [49] are prominent examples) [141]. According to Ayres et al. [148], this is attributable to overestimation of the role of technology in driving economic growth and consequent expectations of inexorable growth into the future (i.e., "manna from heaven" as described by Solow [330]). Explicit and endogenous modelling of the macroeconomic role of energy is required in E3 models, particularly considering changes in the profile of energy carriers (of varying energy quality) available to the economy and associated economic constraints [141, 156, 169]. Foxon [20] and Ayres and Warr [141] argue that representations of endogenous growth also need to be closely linked to wider processes of structural change and co-evolution within economies.

3.2.1.2 Complex systems blindness

Most approaches to the current crises of energy, climate, and sustainability remain conceptually bound within the Cartesian-Newtonian scientific paradigm, lacking an appreciation of the biophysical, complex systems perspective, as described by Seibert and Rees [83]. As such, they are characteristically simplistic, deterministic, and mechanistic. Critically, almost all energy modelling approaches and associated energy transition studies fail to recognize the GES and HSES as CAS (described in sections 1.2.2 and 3.1) [21, 23, 42, 75, 110, 327].

Nieto et al. [327] argue that this omission explains a lack of integration in E3 models between the representations of the economic system and the manifold biophysical systems that ultimately support it. Giampietro et al. [21] describe this more generally as a failure of reductionist analysis to capture complex adaptive behaviour, noting "it is impossible to deal with complex phenomena by adopting simplistic analytical tools based on reductionism." This incompatibility between reductionist methods and complex systems is fundamental, as described by Dale et al. [75], "Dynamic systems are characterised by their complex nature, with many interacting causal and feedback loops that must be analysed at the systems level; they cannot be decomposed into simpler independent elements or processes." Levin et al. [110] emphasize the negative consequences that can stem from ignorance of the characteristics of CAS, noting,

> *"[E]mpirical observations suggest that simple linear and reductionist dynamics give a misleading representation of how social-ecological systems work. Moreover, important features of complex adaptive systems must be studied and understood in an integrated way, because they all matter for the outcome of any management and policy intervention."*

Giampietro et al. [21] note additional common methodological issues stemming from a lack of "complex perception and representation of the metabolic pattern of societies", including:

- failures to effectively consider multi-level system organization, and
- the 'truncation problem', pertaining to the loss of information associated with chosen narrative simplifications and resulting representations (as discussed in section 3.1.4).

Day et al. [42] conclude that "developing future energy policy requires a systems approach with global boundaries and new levels of appreciation of the complex mix of interrelated factors involved." New, systems-cognizant methodologies are needed, including:

- external constraints (boundary conditions) other than climate change, including finite NRE resources, heterogenous and declining primary energy resource qualities, and the evolving requirements of the HSES for the provision of energy services,
- internal constraints associated with power capacities and the production of useful power, including the hypercyclic component of the GES and energy autocatalysis,
- feedback loops and associated non-linear behaviour,
- path-dependence stemming from dynamic co-evolutionary processes,
- non-equivalence among energy carriers and other energy flows, and
- the role of uncertainty and transparency regarding modelling limitations.

As discussed in section 3.1.2.3, the sustainability of CAS is effectively indicated by the maintenance of the relevant boundary conditions, with failure to do so signalling transitory behaviour. While mitigation of climate change receives significant attention in E3 models and often represents their ostensible purpose, source constraints related to the availability and quality of primary energy and other resources are typically downplayed [21, 42, 188, 327].

Capellán-Pérez et al. [50] observe that few models recognize NRE resource limits and possible implications for energy transition, noting, "Most of the current Economy-Energy-Environment models tend to use (very) large resource estimates that are subject to high uncertainties and are strongly biased towards overestimation." For example, GEA [49] does not acknowledge issues of NRE depletion. This lack of supply-side biophysical limits explains the consistent underestimation of the challenge presented by energy transition built into most IAMs, typically seeing it simply as a demand-driven change in the supply mix constrained only by available monetary investments [188, 327]. As noted by Day et al. [42] "relatively few studies discuss the thermodynamic and biophysical implications of switching from fossil fuels to a renewable energy system." Other biophysical factors subject to significant uncertainties, including supply intermittency, and mineral and land requirements, also receive cursory treatment at best [39, 42, 81, 188]. Ayres and Voudouris [260] caution that "energy policies need to continuously explore the existence of plausible signs of collision between increasing consumption of useful energy and the finite energy resources of the planet."

Explicit representations of heterogenous primary energy resource quality distributions, and associated declining quality trends via EROI or alternative metrics (discussed in section 2.1.1), are rare in E3 models [42, 157]. Capellán-Pérez et al. [188] note that this effectively disregards the implications of the rising energy investment flows required to achieve a transition to RE and the need to limit these by maintaining favourable EROI. According to Giampietro et al. [21] energy modelling lacks suitable methods even to assess the relative merits of energy sources based on a broad accounting of criteria, including biophysical factors.

Fiddaman [329] notes that most energy transition modelling approaches include no representation of environmental impacts beyond climate change. However, various sink constraints are highly pertinent to energy transition, including general environmental degradation and biodiversity loss associated with the expansion of land-intensive RE sources such as biomass and hydropower [14, 35, 42, 54, 59, 79, 80]. Day et al. [42] concludes that "a disconnect exists between discussion of renewable energy development and the biophysical limits constraining that development." Even regarding climate change, few modelling approaches adequately capture the potentially catastrophic or even existential nature of risks which cannot meaningfully be represented using calculable costs; an oversight seen in, for example, Edenhofer et al. [44], van Vuuren et al. [307], and Pacala and Socolow [301].

The ultimate purpose (or holonic functional role) of the GES can be seen as the provision of energy services required by the HSES for the expression of vital societal functions supporting its autopoiesis (as described in sections 2.2.3 and 3.1.2.1). However, Brand-Correa and

Steinberger [11] note that accounting frameworks used in energy modelling often report only final energy (i.e., energy carriers) delivered to consumers and omit the final conversion stages to useful energy and energy services. As such, E3 models fail to consider the scope for dynamic changes in energy service provisioning systems (including vastly more efficient integrated supply) as well as the nature and levels of energy services provided [11, 226]. Moriarty and Honnery [35] and Seibert and Rees [83] argue that absolute reductions in energy service consumption may be required, particularly among high consumers in developed countries, and should be explicitly considered. Currently, the possibility of such reductions is not included in most energy transition studies, as noted by Floyd et al. [54].

A comprehensive shift towards RE will be constrained by the rising energetic costs stemming from the hypercyclic component of the GES (as discussed in section 3.1.2). Such constraints arise endogenously, associated with autocatalytic energy production and the co-evolution of power capacities for the production of useful power via shifting metabolic patterns [21]. The dynamic profile of energy flows reinvested back into the GES must be accounted for as substantial increases are likely [54, 190, 331, 332]. Sgouridis and Csala [9] note that the predominant focus of energy transition research on the environmental impacts of fossil fuels has tended to overshadow the dynamic energy costs of the transition. For example, both WEM [298] and GEA [49] fail to take a critical perspective on the internal viability of their respective energy transition scenarios by considering the necessary reinvestment of energy. Giampietro et al. [21] note that the power capacity concept is typically neglected altogether in energy analysis due to insufficient attention given to time as a relevant dimension, resulting in significant ambiguities between power levels and energy flows.

Non-linear behaviour arising from the interaction of multiple feedback loops is an essential aspect of CAS, as detailed in sections 3.1.1 and 3.1.2. As noted by Motesharrei et al. [23], interactions between the GES, HSES, and biosphere are crucial to understanding system behaviour, however, these are largely ignored by IAMs which instead rely heavily on exogenous projections of key variables. Arvesen et al. [221] explain that over-simplification or exclusion of these relationships, and second-order effects, leads to excessive optimism regarding technological solutions. The relative lack of feedback in IAMs can be largely attributed to their historical development from separate modules which were often not originally designed to be interlinked, as described by Capellán-Pérez et al. [188].

Fiddaman [329] observes that most E3 models include no positive feedback mechanisms other than capital accumulation. This is a major conceptual deficit given that positive feedback loops play a vital role in processes of growth, change, and transformation in CAS. Giampietro et al. [21] agree, noting that simple, linear representations of energy systems cannot adequately capture feedback and its role in the evolution of metabolic patterns. There are important consequent implications for how these models and their quantitative results should be interpreted and used, as described by Motesharrei et al. [23]:

> *"Nonlinear systems often feature important dynamics which would be missed if bidirectional interactions between subsystems are not modeled. These models also may call for very different measures and policy interventions for sustainable development than those suggested by models based on exogenous forecasts of key variables."*

A special case of system feedback with particular importance for near-term policy formulation is the rebound effect, described in section 2.2.1. Brockway et al. [219] explain that the basic mechanisms driving rebound effects are typically absent in E3 models:

> *"[T]he current generation of energy-economy models lacks the capacity to capture these rebound effects effectively. The inclusion of broader, economy-wide rebound effects within energy and IAM models are vital if we are to have confidence in global energy scenarios, and if policymakers are to effectively anticipate and address the possibility of large rebounds."*

The presence of feedback loops and system constraints (both exogenous and endogenous), together with a consideration of the time dimension, underscores the importance of path-dependence arising from dynamic co-evolutionary processes, as described in sections 1.2.2 and 3.1.1. In all analytical approaches employed in energy transition studies introduced in section 3.2.1 (described by Loftus et al. [223]), with the exception of *bottom-up techno-economic assessments*, the end goal or target system state is predetermined via normative criteria, with subsequent analysis then populating a series of changes expected to achieve this target. Wiseman et al. [322] notes that most large-scale studies of energy transition do not adequately explain their pathways, particularly where rapid societal change is assumed. This is inconsistent with the path-dependent and non-linear behaviour of CAS, raising serious questions about the validity of mainstream energy transition scenarios. Capellán-Pérez et al. [39] explain that modelling path-dependence must include dynamic representations of both resource quality and energy investment lifecycles to accurate apportion energy costs and outputs over time, particularly given non-equilibrium, energy transition contexts.

Another important consideration is the non-equivalence of distinct energy carriers and other energy flows, described in section 3.1.2.4. Explicit modelling of substitution processes involved in changing patterns of flows at the system level is necessary due to the non-fungibility of associated power capacities and the dynamic metabolic costs associated with capital turnover. Modelling of non-equivalence is lacking in most E3 models, which often use dubious aggregation methods, as noted by Giampietro et al. [21]: "it is rare to find a systemic consideration, in the pre-analytical phase, of the epistemological nature of qualitative differences among non-equivalent energy forms".

Finally, the role of uncertainty and transparency regarding modelling limitations are both central to an appropriate contextualization of quantitative energy transition scenarios and their proper interpretations, not as predictions but as explorations of possible futures (as discussed in sections 3.1.4.2 and 3.1.4.3). However, adequate treatment of uncertainty, disclosure of contestable and often internally inconsistent assumptions, presentation of plausible alternatives, and comprehensive sensitivity analysis are uncommon in conventional E3 models and energy transition studies [54, 333]. Even where uncertainty is acknowledged, few studies attempt to materially address it, for example, Edenhofer et al. [44]. Furthermore, an implicit positivist orientation is common in energy modelling, resulting in a lack of distinction between models and the systems they represent. This is inadequate, as described by Floyd et al. [54]:

> *"[E]nergy transition modelling exercises are necessarily based on myriad complex and often controversial assumptions that necessitate the interpretation of their findings strictly in relation to the model as an abstract representation of a real world as understood by the modeler. Any conclusions drawn from such studies should be presented and applied with due acknowledgement of the deep uncertainties and limitations inherent therein."*

These gaps are in urgent need of rectification before energy modelling can offer useful and meaningful descriptions of energy transition pathways and appropriate policy guidance.

3.2.1.3 Technological optimism

Conventional energy transition studies typically exhibit strong optimistic biases regarding ongoing technological innovation, infrastructural change, mitigation of impacts arising from supply intermittency, and socio-economic contexts affecting technological development. These biases both reflect and reinforce common socio-technical narratives of energy transition across a broad array of institutional settings.

Mainstream perspectives on energy transition often prominently feature technologies which remain speculative and unproven at scale, despite significant uncertainties regarding their eventual availability [65, 81, 223]. As described by Grübler et al. [231], there is a "pro-innovation bias of the literature, i.e. mostly successful diffusion or transition cases are studied and described, with failures remaining largely undocumented." This is readily apparent among major studies – for example, GEA [49] exhibits significant optimism regarding new and unproven technologies with little consideration of potential downsides, leading to heavy emphasis placed on carbon capture and storage (CCS), next-generation nuclear energy, and geo-engineering. In many cases, a general lack of technical limitations at the system level is simply asserted (e.g., by Edenhofer et al. [44]), often by appeal to the very large magnitudes of many primary RE resources without considering possible constraints at other scales of analysis. As cautioned by Clack et al. [334], a complete energy transition to 100% RE would be extremely difficult with currently available technologies, particularly where technological portfolios are limited *a priori* to a narrow range of options. Jenkins and Thernstrom [81] also stress the importance of technological diversity, ruling out overwhelming reliance on selected energy sources, such as solar PV and wind.

Even among existing technologies, the possibility for diminishing returns on innovation (discussed in section 2.2) is not widely acknowledged in energy transition studies and technological progress is assumed to either continue at a steady pace or accelerate, particularly regarding energy efficiency. Fiddaman [329] notes that most E3 models assume substantial, exogenously defined efficiency improvements and carbon intensity reductions. For example, GEA [49] assumes "very strong efforts in energy efficiency improvement for buildings, industry and transportation, offering much-needed flexibility to the energy supply system" resulting in projected 60—75% declines in energy consumption between 2005 and 2050 for developed regions in the 'state of the art' scenario. These assumptions are unsupported and are likely inconsistent with realistic efficiency gains emerging from power maximization under finite-time theoretical efficiency limits (as discussed in section 2.2.1).

Many energy transition studies take relatively simplistic approaches to infrastructural change which fail to capture the degrees of complexity, interdependence, and cost involved. Smil [14] notes that this is particularly true of plans presupposing rapid, policy-led energy transitions. Loftus et al. [223] examine 17 decarbonization scenarios, finding "all of the studies present comparatively little detail on strategies to decarbonize the industrial and transportation sectors, and most give superficial treatment to relevant constraints on energy system transformations." Electrification of transportation, heating, and industrial end-uses will play a central role in energy transition, facilitating the uptake of electricity-producing RE sources, however, associated infrastructural challenges, and the long lead times required, receive relatively little attention in major studies [81, 223]. Expectations for the electrification of industry and transportation are highest in the most optimistic transition studies, including as Jacobson and Delucchi [303, 304], Teske et al. [313], Worldwatch Institute [310], and World Wildlife Fund [311], and may be unrealizable, as noted by Loftus et al. [223]:

> *"With multiple low-carbon electricity generation options and the possibility of wider electrification, the power sector will invariably be central to global decarbonization efforts. Nevertheless, reducing industrial and transportation sector emissions will not be accomplished through electrification alone, and decarbonization scenarios should focus greater attention on the challenges associated with these sectors."*

Jenkins and Thernstrom [81] review 30 decarbonization studies, identifying critical weaknesses which require additional consideration and effective long-term planning, including the presence of sectors which are significantly more challenging to transform (e.g., aviation, shipping, heavy transport, and agriculture), costly and unproven technology portfolios required for deep decarbonization, and the implied necessity of large-scale CCS for full decarbonization. Edenhofer et al. [44] concede that IAMs do not adequately represent the electrification of the transport and heating sectors, and include insufficient temporal and geographical resolution. Loftus et al. [223] concludes that "To be reliable guides for policymaking, scenarios such as these need to be supplemented by more detailed analyses realistically addressing the key constraints on energy system transformation."

Most E3 models project significant increases in the contribution of RE sources to TPES, but typically underrepresent or ignore the need for mitigation of resource intermittency, particularly at high penetration levels (as described in section 2.1.2) [44, 54, 59, 81, 223]. According to Day et al. [42], "most studies do not fully consider the complexities of multiple factors including production intermittency, storage, the need to replace a massive infrastructure network, and lack of fungibility of different energy sources." Heard et al. [59] review 24 studies proposing the feasibility of 100% RE, finding none convincingly demonstrate the capacity to match supply and demand reliably across all required timescales.

Loftus et al. [223] observe that most energy transition studies suggest a common portfolio of technological solutions including 'smart grids', demand response, high-voltage transmission expansion, and energy storage, but fail to adequately consider associated costs and integration issues. Notably, the provision of 'ancillary services' required for the stable operation of electricity networks, such as frequency regulation and reserve generation, are not typically considered in high RE penetration scenarios [59, 223]. Furthermore, key technological elements of proposed intermittency mitigation strategies are often speculative or unproven at scale, such as the production of hydrogen via electrolysis and other forms of medium- and long-term electricity storage [59, 81, 82, 223]. Consequently, aggressive energy transition scenarios claiming the feasibility of 100% RE without detailed assessments of intermittency mitigation tend to be overly optimistic and are highly questionable [39, 54, 59].

Finally, energy transition studies frequently disregard the myriad socio-economic dependencies of technological change, instead focussing solely on techno-economic factors. As described by Floyd et al. [54], "the management of 'energy systems' and their transitions is better understood not as a technological or even techno-economic challenge, but as a complex of interacting challenges that are essentially socio-technical in character." Energy transition will necessarily affect societies in profound and transformative ways, as described in sections 1.2.2 and 3.1.2. Gambhir et al. [146] note that one of the main criticisms of IAMs centres on inadequate representation of real-world policies and processes involved in implied behavioural adaptations. Stammer et al. [324] conclude that many widely popularized energy transition and climate scenarios are revealed as implausible when considered from both social and techno-economic perspectives.

3.2.1.4 Unfounded projections

E3 models and energy transition studies frequently invoke unsubstantiated projections of key variables, out of step with historical trends:

- Brockway et al. [219] note that many global scenarios assume structural breaks in both efficiency growth trends and the historically close relationship between energy consumption and economic output (described in sections 3.1.3.1 and 3.2.1.1), despite little or no empirical evidence to support these assumptions. Loftus et al. [223] also identify historically unprecedented and likely implausible implied rates of change in the energy intensity of GDP across many studies, declining at approximately double the most rapid rates observed over recent decades.
- The deployment rates of RE technologies are frequently assumed to increase discontinuously in the near future, up to 15-fold over historical rates – a buildout not likely to be practically achievable in real-world settings [14, 223]. To justify this, many studies make tenuous comparisons to prior, partial energy transitions which occurred under more energetically favourable conditions (as discussed in section 2.3). For example, GEA [49] compares the forthcoming transition to RE to the transition from coal to oil during the 20th century, drawing highly optimistic conclusions.
- As noted by Loftus et al. [223], energy transition studies often assume very high rates of final energy demand reduction arising from efficiency gains. However, mechanisms to achieve such reductions and corresponding effects on the provision of energy services and economic output are typically ignored. These assumptions conflict with absolute increases in energy demand stemming from larger than expected rebound effects and demand growth needed for the amelioration of energy poverty worldwide, described by Brockway et al. [219].

The prevalence of such discontinuities in key variables, without sufficient empirical or theoretical justification, is strongly indicative of the presence of motivated reasoning in energy transition scenario development. Moreover, it highlights the epistemic weaknesses apparent in the normative, pre-analytical specification of energy transition end goals or target states in many analyses.

3.2.2 The emerging biophysical systems view

The mounting critique of conventional approaches to the study of energy transition, summarized in section 3.2.1, has motivated several attempts to construct models with an explicit biophysical, complex systems orientation (described in chapter 3). This emerging field of energy modelling is briefly outlined in this section.

Biophysical energy systems modelling approaches typically exhibit a greater focus on supply-side constraints (i.e., primary energy and other resource limits) rather than the predominant climate change focus seen in most mainstream energy transition studies. To a lesser degree, these models have also included aspects of complex system behaviour, primarily non-linearity and path-dependence represented via feedback-rich system dynamics formulations. Formative attempts to create systems-based models incorporating biophysical factors include the World3 model used in the original *Limits to Growth* study [234], the STER model developed by Hounam [335] and later iterations including the ECCO model [336], Sterman [337], Bodger and Baines [338], and the FREE model [329, 339]. These models typically seek to either explore various plausible scenarios or maximize economic growth (or stability) subject to resource constraints. They all feature representations the productivity of primary energy production (including reinvested energy), avoid intertemporal optimization, and often include disequilibrium conditions, feedback delays, and endogenous technological change.

Encouragingly, a significant increase in research in general biophysical systems modelling has begun in recent years, which, while still largely absent in major institutional and governmental settings, is gaining wider recognition within the modelling community. As noted by Sherwood et al. [328],

> *"Within the last 10 years, a wide variety of research papers have been published that include some biophysical aspects in a model of the economy. These papers all have one thing in common: the model of the economy includes physical and/or energetic exchanges, as well as monetary exchange."*

Hafner et al. [340] reviews 11 recent ecological macroeconomic energy models featuring representation of complexity, non-equilibrium, and uncertainty, concluding "the reviewed models are policy relevant, especially in the context of the complexity and urgency of rapid energy transitions, where increasingly policymakers require economic models able to capture real-world characteristics.” Several recent examples relevant to energy transition are outlined in section 3.2.2.1 followed by a summary of their findings in section 3.2.2.2.

3.2.2.1 Notable recent examples

D’Alessandro et al. [91] create a stylized dynamic macroeconomic model to examine the effects of energy scarcity on economic growth during the transition to RE, tracking investment and stocks of capital, RE capacity, and fossil fuels. The EETRAP model, developed by Victor & Sers [341], uses a similar but expanded approach to simulate macroeconomic pathways for RE investments required to avoid exceeding selected GHG emissions targets, including consideration of EROI declines implied by the shift from NRE to RE. While energy is considered as a factor of production in both studies, several methodological issues are apparent, including their highly aggregated formulations (ignoring issues of functional stock and flow non-equivalence and non-fungibility), a lack of realistic capital lifecycle dynamics (with corresponding feedback delays), and little to no representation of intermittency mitigation – likely unsuitable for modelling high RE penetration levels.

The GEMBA model developed by Dale [342] and Dale et al. [75, 343] goes beyond these limitations, using a top-down, globally aggregated, and empirically calibrated formulation to determine the sufficiency of RE resources to meet projected demand, the likelihood of energy descent, and wider physical system effects resulting from a transition to RE. GEMBA includes a detailed representation of the energy system and directly simulates processes behind declining EROI during the energy transition using biophysical criteria to represent primary energy resource quality rather than price-based methods (in contrast to conventional IAMs). However, GEMBA uses a relatively simplistic economy model (although based on ecological economics principles) and includes no environmental aspects aside from primary energy supply. The model does not consider stock and flow non-equivalence, effectively disregarding the implications of changing metabolic patterns, as conceded by Dale [342], “Energy sources are assumed to be perfectly substitutable, i.e. demand within the model is not specific to a particular energy source but rather just for energy, regardless of source or carrier.” Furthermore, capital outside of the supply sector is highly aggregated, implying underestimation of the energy costs of infrastructural change (i.e., capital turnover) required for energy carrier substitution. Uncertainty is considered via Monte Carlo simulation (1,000 realizations) but is carried out with only three probabilistic model parameters.

The NETSET model developed by Sgouridis et al. [46] (based on earlier work by Sgouridis and Csala [9]) offers a unique approach among biophysical models, working backwards from selected GHG emissions budgets to determine a range of energy transition pathways that meet specified minimum per capita energy requirements (conceptually similar to *top-down back casting*, described in section 3.2.1). NETSET is globally aggregated and incorporates energy resource availability (using EROI), delayed price feedbacks (affecting demand, stock retirement, and reinvestment), and both energetic and economic dynamic processes to examine "basic energy metabolism relations" characterizing energy transition pathways. NETSET is primarily a physical model, without detailed macroeconomic representation, and is based on a demand-driven, supply constrained view of the energy system (i.e., consistent with the post-Keynesian ecological approach described in section 3.1.3). NETSET includes qualitative technological change, with efficiencies varying over time as functions of investment.

Owing to its high-level approach designed to allow analytical solutions, NETSET does not feature significant technological detail, instead using aggregated RE and fossil fuel capital stocks. As acknowledged by Sgouridis and Csala [9], "Modeling and calibrating the dynamic relationship between energy prices, equipment turnover, technology development and utilization is a complex undertaking." Several key variables are exogenously defined, including population, available energy efficiency improvements, per capita energy demand, and the energy intensity of GDP. NETSET does not consider stock and flow non-equivalence, likely underestimating energy carrier substitution costs, and disregards declining RE resource quality (justified by appeal to large RE resource magnitudes). NETSET is optimistic regarding intermittency mitigation at high RE penetration levels, assuming sufficient storage and demand side management. Notably, NETSET uses pre-determined energy consumption targets ranging between 0.7 and 6 kW per capita (a '2 kW society' baseline is used by Sgouridis and Csala [9]) – the lower end of this range implies drastic reductions in final energy consumption relative to levels currently seen in developed countries.

Perhaps the most detailed and fully realized biophysical energy model currently available is the open-source MEDEAS framework [188, 193]. MEDEAS was developed from the earlier WoLim model [50, 344], employs both bottom-up and top-down aspects, and is designed to test congruence between resource limitations (including minerals, land, and water) and expected economic growth trajectories. MEDEAS exhibits a high level of detail in primary energy production and includes the use of production rate constraints as functions of RURR, representing physical depletion processes. Energy carrier non-fungibility is addressed, with dynamic substitution processes driven by scarcity. MEDEAS incorporates a hybrid post-Keynesian ecological approach for macroeconomic representation including explicit sectoral economic structure, with production constraints imposed under conditions of energy scarcity. Inland transport and household energy demand are modelled in detail, via bottom-up methods. Feedbacks are modelled between climate emissions and economic growth, ranging from negligible at low levels to non-linear and potentially catastrophic at high levels. Additionally, MEDEAS endogenously calculates:

- technological portfolios for intermittency mitigation, in response to RE penetration,
- rising energy efficiencies considering thermodynamic efficiency limits and substitution processes between energy carriers,
- dynamic EROI for intermittent RE sources, including mineral depletion effects, and
- energy demand, via sectoral energy intensities (including induced effects).

MEDEAS also includes comprehensive treatment of uncertainty. As noted by Capellán-Pérez et al. [188], "MEDEAS takes as reference the precautionary principle, which is the most robust approach in uncertainty contexts such as the one characterizing climate change and the sustainability crisis". Consequently, unproven, speculative technologies such as CCS, hydrogen as an energy carrier, and next-generation nuclear are not included. MEDEAS includes uncertainty, sensitivity, robustness, and stability analyses using Monte Carlo simulation (1,000 realizations) with 72 probabilistic model parameters.

However, MEDEAS exhibits several notable weaknesses. Transition pathways are driven by exogeneous GDP, population, and income distribution projections. The sectoral approach to demand modelling, while effective for capturing economic interdependencies, rules out explicit representation of end-use capital and energy service provision (aside from the inland transport and household sectors). As maximum improvements in sectoral energy intensities are based on statistical analysis of historical data, the potential for transformative change in end-use capital is not considered. Consequently, the hypercyclic component of the GES in MEDEAS is somewhat underdeveloped. MEDEAS does not include endogenous goal seeking behaviour (other than scarcity-induced adaptation), such as technology allocation or fuel switching based on biophysical indicators, as noted by Capellán-Pérez et al. [39]. Various other path-dependent and feedback phenomena are not represented, such as the net energy trap (or equivalent) and rebound effects.

Assumed URR values for NRE resources in MEDEAS are biased towards the upper end of the range of estimates in the literature. Critically, $EROI_{st}$ values for NRE and non-intermittent RE sources are assumed to be constant and MEDEAS approaches resource constraints using production rate limits instead. This approach to primary energy resource modelling is artificial and may not correspond closely to underlying physical processes – it is both pessimistic regarding the flexibility of production rates in response to changing economic and technological factors while being highly optimistic regarding dynamic net energy production over the duration of the energy transition. As Capellán-Pérez et al. [188] admit, "this approach does not capture the metabolic implications of the drop of the EROI of the system to very low levels". Different temperature levels for heat are not considered, disregarding non-trivial technological limits to substitution, particularly for high-temperature industrial processes. MEDEAS is also relatively pessimistic regarding near-term climate damages, assuming these to begin to exceed incremental GDP additions at 1.75°C warming. Finally, MEDEAS includes a relatively low level of detail regarding feedback between the social and environmental systems, an area the authors note requires further attention.

3.2.2.2 Indicated challenges

Studies starting from a biophysical systems perspective typically find that achieving a successful global energy transition will be considerably more difficult than anticipated by conventional analyses, requiring comprehensive adaptations including profound behaviour change and reductions in energy service consumption [9, 35, 345]. For example, the NETSET model [46] identifies biophysically possible energy transition pathways, but only with drastic increases in RE investment rates (up to 100-fold) alongside large reductions in per capita final energy consumption. These modelled outcomes in NETSET are also strongly influenced by assumptions regarding delays before initiating a rapid transition, appropriate GHG emissions targets, and NRE EROI values. This transformation is likely to be highly socially and behaviourally challenging, as the authors warn, "The upfront energy invested in constructing a RE infrastructure subtracts from the net energy available for societal energy needs".

D'Alessandro et al. [91], Victor & Sers [341], GEMBA [75, 342, 343], and MEDEAS [188, 193] all identify significant redirections of available investment and resource flows into the required RE infrastructures causing economic growth to decline, or even reverse (as described in sections 2.1.1.4 and 3.1.3.4). GEMBA model results indicate the capital requirements of the GES will likely increase during the energy transition, to approximately half the total capital of the global economy. D'Alessandro et al. [91] note a trade-off between higher growth rates and the accelerated depletion of NRE resources, risking energy scarcity, and conclude lower growth rates are preferable to facilitate the energy transition. Likewise, MEDEAS suggests low (or no) growth rates may be required for achievable energy transition scenarios. Victor & Sers [341] suggest that the pursuit of steady economic growth during the energy transition is not advisable and may not be biophysically possible. The advantageous nature of reductions in economic growth for the energy transition is echoed by Keyßer and Lenzen [346]:

> *"[D]egrowth scenarios minimize many key risks for feasibility and sustainability compared to technology-driven pathways, such as the reliance on high energy-GDP decoupling, large-scale carbon dioxide removal and large-scale and high-speed renewable energy transformation. However, substantial challenges remain regarding political feasibility. Nevertheless, degrowth pathways should be thoroughly considered."*

MEDEAS results suggest current consumption growth trajectories worldwide are highly unsustainable regarding both resource limitations and the prospect of avoiding dangerous levels of climate change. GEMBA and MEDEAS both highlight the likelihood of a mid-21st century decline in net energy availability, with far-reaching economic consequences.

3.3 Post-Normal Science

Post-Normal Science (PNS) is a new approach to complex scientific problems characterized by uncertainty, urgency, conflicting perspectives, insufficient data, and a high degree of public interest, developed by Silvio Funtowicz and Jerome Ravetz in the early 1990s [25, 54, 139, 347-349]. The term is defined in reference to Thomas Kuhn's notion of 'normal science' and identifies the period preceding a revolution in science in which established ontological and methodological frameworks increasingly struggle to address mounting anomalies [63, 348].

PNS starts from a basic stance of epistemic humility (as discussed in section 1.3.2), acknowledging the inability of singular problem framings to capture the complex nature of many modern, socio-ecological problems. As explained by Floyd et al. [54],

> *"A disposition of knowledge humility entails reflexivity with respect to the epistemological foundations and commitments that inform transition-oriented decision making and action. Here the response to the dilemma of uncertainty and ignorance is not to deny it or seek to eliminate it, but to learn to live with it through reflexive governance."*

The lack of singular, definitive problem framings demands a much greater degree of interdisciplinarity in complex problem solving than is typical presently, as described by Levin et al. [110] and Sherwood et al. [328]. Ravetz [350] notes that PNS advocates for a shift towards 'extended peer communities' and away from expert monopolies on knowledge, which often suffer from reductionism and conceptual rigidity. A PNS perspective fundamentally reorients the researcher, as described by Kay et al. [351],

> *"In the post-normal paradigm, a scientist's role in decision making shifts from inferring what will happen, that is, making predictions which are the basis of decisions, to providing decision makers and the community with an appreciation, through narrative descriptions, of how the future might unfold."*

This scientific approach is highly applicable to the study of complex socio-ecological systems, including the forthcoming third energy transition, as noted by Tainter et al. [25]. According to Floyd et al. [54], "there is much insight to be gained by locating the investigation of energy-society futures squarely within the domain of post-normal science". Consideration of a wide range of plausible futures is now crucial. However, as described in section 3.2.1.2, many conventional energy transition models and studies do not explore a sufficient range alternative possibilities and fail to adequately acknowledge and address uncertainty. Charting a path forward requires consideration of modelling practices consistent with PNS (outlined in section 3.3.1) and the use of analytical techniques for the management of uncertainty and risk in complex energy systems modelling (section 3.3.2).

3.3.1 PNS modelling practices

In addition to the overview of principles for biophysical systems modelling presented in section 3.1.4, several supplementary modelling practices originating from PNS can be introduced. At the most basic level, the limits of any quantitative method must be recognized and clearly communicated to allow the proper interpretation of results [21, 54, 284]. Funtowicz and Ravetz [348] suggest that computer models are essentially untestable and are subject to the 'garbage in, garbage out' (GIGO) principle. They note, "a GIGO science is one where the uncertainties in the inputs must be suppressed, lest the outputs become completely indeterminate."

The characteristic PNS response to limitations inherent to any given modelling approach is to embrace greater pluralism of perspectives in modelling. For example, Gambhir et al. [146] suggest that conventional IAMs "should increasingly be supplemented with other models and analytical approaches". Ruth and Hannon [145] note that plurality and competition among models is needed to improve knowledge of the behaviour of real-world systems. As demonstrated by the current state of conventional energy transition analysis, outlined in section 3.2.1, uncritical emulation of prevailing modelling practices can become a major impediment to necessary advances.

The formation of extended peer communities can also help in energy modelling, as no single researcher can claim definitive expertise – complex systems are inherently multi-scale and resist simplification. Ravetz [281] suggests a participatory approach to mathematical modelling, with less emphasis on prediction and control and more on understanding narrative framings and exploration of areas of ignorance. Although stakeholder policy design and extended peer communities can play a vital role in building better models, Ruth [249] notes that success can be limited by the availability of real-world data and sufficient understandings of the system, without which the process can result in "negotiated nonsense". This stresses the need for a careful balance between valuing expertise and fostering broader participation.

Socio-technical narratives and associated problem framings play a central role in quantitative analyses, but often go unrecognized due to their ubiquity and implicit portrayal as 'common sense'. In fact, appropriate problem framings are often more important than technical or methodological aspects [21, 284, 352]. Saltelli et al. [326] argue that quantitative techniques cannot be considered neutral, but rather influence, and are influenced, by prevailing narratives. Saltelli et al. [284] warn that “Mathematical models are a great way to explore questions. They are also a dangerous way to assert answers” and suggest that a high degree of transparency regarding normative values, researcher bias, potential consequences, and unknowns is required to ensure the productive use of models within society.

Giampietro et al. [21] describe an epistemological impasse facing the quantitative analysis of complex energy systems, requiring comprehensive pre-analytical framing regarding:

- the choice of methodology,
- research objectives,
- boundary conditions, and spatial and temporal scales of analysis,
- semantic choices regarding relevant energy forms (i.e., an appropriate energy grammar, as described in section 3.1.4),
- the intended approach to uncertainty and data quality,
- choices regarding relevant indicators and their respective descriptive domains, and
- interpretation of the usefulness of results.

3.3.2 Sensitivity and diagnostic analysis

The PNS perspective emphasizes the need to evaluate the implications of uncertainty in quantitative models via comprehensive ‘sensitivity audits’ [284, 326, 333, 353]. As described in section 3.1.4.3, uncertainty in models stems from both imperfect data quality and semantic indeterminacy resulting from the chosen modelling formulation. Sensitivity analyses are rare in conventional energy transition studies (as discussed in section 3.2.1.2), representing a major deficit. Even where they are performed, methodological flaws are common – in particular, the lack of simultaneous variation of inputs leaving most of the input space unexplored – as noted by Van Der Sluijs et al. [333].

Saltelli [354] defines sensitivity analysis as “the study of how the uncertainty in the output of a model (numerical or otherwise) can be apportioned to different sources of uncertainty in the model input”. Sensitivity values therefore provide an indication of the *potential impacts of estimation errors* in each uncertain model input with respect to a given model output. Monte Carlo simulation, by surpassing the limitations of deterministic models, is well-suited to the PNS perspective and can effectively facilitate multivariate sensitivity analysis via the creation of result ensembles. Even so, epistemic limits facing of quantification of uncertainty are apparent and must be acknowledged. As described by Van Der Sluijs et al. [352],

> *"Mainstream uncertainty methods such as Monte Carlo analysis, or Bayesian updating alone are not suitable for this class of problems because the main problem characteristic is that unquantifiable uncertainties dominate the quantifiable ones. Unquantifiable uncertainties include those associated with problem framings, model structures, assumptions, system boundaries, indeterminacies, and value ladenness."*

Crucially, sensitivity analysis is necessary but often insufficient as is does not characterize the absolute risk of modelling errors. To determine absolute risk associated with each input, it is necessary to consider both the *potential impacts of estimation errors* (sensitivity) and the *likelihood of estimation error* (i.e., *risk = impact × likelihood*). This process of input risk identification can be performed using diagnostic analysis, described by Van Der Sluijs et al. [352] and Berner and Flage [144]. The primary purpose of diagnostic analysis is to identify inputs which must be treated with greater caution and critical scrutiny, and consequently, to highlight where further data gathering efforts would be most advantageous.

The likelihood of input estimation error is related to the strength of knowledge attributable to the data sources and methods used to estimate the relevant probability distributions. Quantifying strength of knowledge is necessarily subjective and requires expert elicitation [352], but can be systematized. 'Pedigree' assessment is useful for this purpose, employing an ordinal scale to rate each uncertain input across distinct aspects of strength of knowledge, such as the mode of production, degree of peer acceptance, and realism of assumptions (see Berner and Flage [144]). The average of the component scores can be taken as the overall pedigree score representing the strength of knowledge for each input. Risk is then assessed as a function of sensitivity and pedigree scores for each uncertain input and can be categorized into risk levels defined by chosen thresholds, as illustrated in Figure 9.

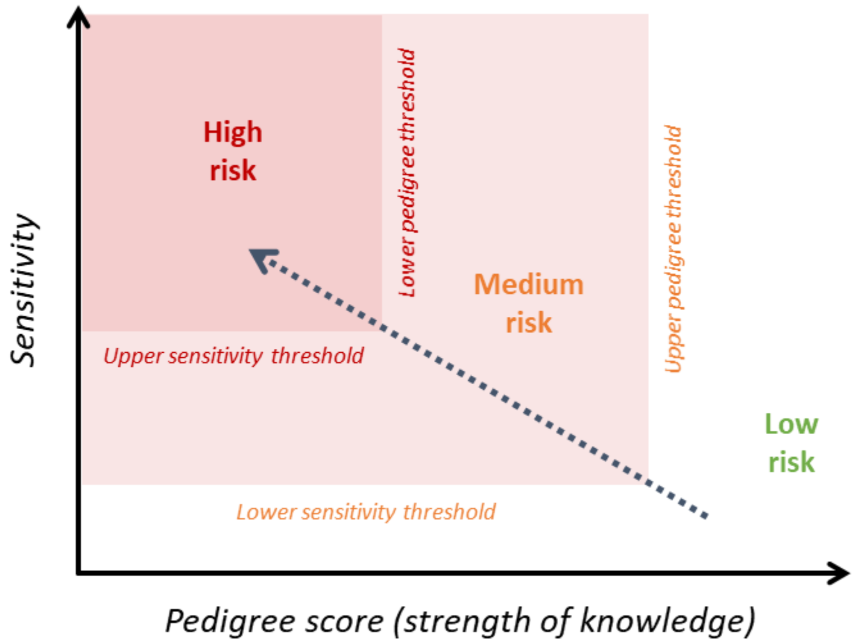

Figure 9: diagnostic analysis example diagram, with risk category regions

Risk category thresholds are arbitrary but are chosen to separate values along each axis into distinct, meaningful groups as effectively as possible.

3.4 The knowledge gap

The study of future global energy transitions remains an immature and contested field of research, as discussed in section 3.2.1. Despite the pervasiveness and wide variety of energy-economy-society forecasts, most are limited by a basic reductionist, techno-economic, and positivist orientation. In the author's estimation, no conceptually valid best-practice methodologies for dynamic complex energy systems modelling have yet been developed. As introduced in section 3.1, any valid conceptual approach to the study of GES transformations must recognize the GES is an example of a CAS and understand energy transition as a *complex, physically-bounded, path-dependent, socio-metabolic process.* There is a lack of such systems-cognizant GES models incorporating adequate treatment of irreducible uncertainty and necessary acknowledgement of the epistemic limitations of the implied approach. This deficit presents a clear gap in the literature.

The model, and subsequent analysis of results, must be consistent with the conceptual synthesis presented in this chapter, including principles of dynamic systems modelling and modelling practices consistent with PNS, discussed in sections 3.1.4 and 3.3, respectively.

Note that it is not practical or appropriate to attempt to address all identified shortcomings of existing modelling approaches (discussed in section 3.2) in this research project – this can only address priority concerns while contributing to a growing plurality of models and perspectives.

As described in section 1.4, the chosen primary research objective centres on exploratory modelling of the solution space of energetically feasible and viable pathways for GES transformation towards RE, under uncertainty. As a primarily physical approach, detailed representation of the global macroeconomy and feedback between the HSES and biosphere (including, for example, climate impacts on the HSES) are not within scope. This relates to selection of the GES as the holon of interest for modelling purposes (as described in section 3.1.4). However, the following aspects are addressed (relevant sections indicated):

- The implications of finite primary energy resources, heterogeneous resource quality distributions, and declining EROI for net energy production (section 2.1).
- Endogenous technological change driven by goal seeking technology allocation (section 3.1.4.1) and technological learning effects (sections 2.1.1.3 and 2.2.1).
- Distinctions between energy and power levels, including structural dependence on distinct, non-fungible capital stocks (section 3.1.2 and 3.1.2.2).
- Representation of the hypercyclic component of the GES associated with the production of necessary capital (section 3.1.2.2), including energy costs of autocatalytic energy production (section 3.1.4.1) and constraints arising from the capacity of the HSES to provide the necessary labour and resources (section 3.1.2.3).
- Disaggregated representation of non-equivalent energy flows to properly characterize the energetic metabolism of the GES (sections 3.1.2.4 and 3.1.4.1.
- Representation of substitution processes between non-equivalent energy carriers via capital turnover, driven by technology allocation (sections 2.2.2 and 3.1.2.4).
- Explicit modelling of the end-use conversion stage and the dynamic provision of energy services (sections 2.2.3 and 3.1.4.1).
- Realistic time dynamics and delays, particularly for capital lifecycles (section 3.2.1.2).
- Inclusion of supply intermittency impacts and required mitigation (section 2.1.2).
- Representation of technological lock-in effects (sections 2.3.1 and 3.1.2).

- Avoidance of monetary quantification and time discounting in the model formulation (sections 3.1.4.1 and 3.2.1.1).
- Representation of the bounded co-evolution of supply and demand (section 3.1.4.1), including rebound effects (sections 2.2.1 and 3.2.1.2) and the identification of net energy trap outcomes following terminal supply/demand divergence (section 3.1.2.3).
- Characterization of high-level ecological impacts associated with GES transformation via the calculation of cumulative GHG emissions (section 3.1.2.3).

Implementation of these aspects into a synthetic methodological approach to studying transformation pathways of the GES towards RE, starting with a pre-analytical framework aligned with PNS, is detailed in chapter 4.

4 METHODOLOGICAL APPROACH

Equations presented in this thesis are simplified for brevity and clarity. Excluded details primarily concern recursive loop and error handling, corrections for initialization and boundary conditions, and interpolation functions. While expressions are presented as continuous, the systems dynamics modelling approach uses iterative calculation at discrete time steps due to variable interdependence in the form of feedback loops (as described in section 3.1.4.1). See section 9.4 for full calculation details.

Vectors are denoted by bold, italicized, lower case letters and have units of power (EJ/year) unless otherwise stated. Matrices are denoted by italicized, upper case letters and are dimensionless unless otherwise stated. Hadamard, or elementwise, operations of multiplication, division, and exponentiation are denoted by the symbols $\circ$, $\oslash$, and $x^{\circ y}$, respectively. Vectors of zeros and ones are denoted $\boldsymbol{0}$ and $\boldsymbol{j}$, respectively, with lengths inferred from the relevant linear algebraic operations. All vectors are treated as column vectors.

4.1 PRE-ANALYTICAL FRAMEWORK

The purpose of the pre-analytical framework described in this section is to define the ontological and epistemological foundations of the methodological approach developed to achieve the research objectives stated in section 1.4. Such foundations are crucial, as the transformation of the GES towards a RE basis represents an unprecedented, urgent, highly complex, and multi-scale challenge subject to conflicting socio-technical narratives, and as such, falls under the aegis of Post-Normal Science (PNS), as discussed in section 3.3.

4.1.1 Conceptual orientation

As described in section 3.1.4, CAS can be modelled using systems of equations developed via the system dynamics method. As discussed, system dynamics models are well suited for the quantitative simulation of non-linear behaviour arising from multiple, interacting feedback loops, but are not truly complex themselves and are unable to capture emergent behaviours under novel conditions outside of the system's assumed domain of stability. This reinforces a fundamentally exploratory modelling orientation bound by a limited descriptive domain. The goal is not to produce a predictive model capable of forecasting real-world behaviour as this is considered unattainable given the nature of CAS, and is inconsistent with the PNS perspective, as discussed in sections 3.1.4.2 and 3.3.

GES transformation is considered primarily from a biophysical, complex systems perspective, focussing on *feasibility* and *viability* associated with the energetic, autocatalytic aspect of GES metabolism, as outlined in chapter 1. In contrast, comprehensive characterization of *desirability* requires detailed consideration of socio-economic factors that extends beyond the stated research objectives. *Desirability* is treated as indicative only, represented via goal seeking towards preferred states (detailed in section 5.2) and the quantification of high-level GES transformation outcomes (detailed in section 4.2.9.3).

The general modelling approach to uncertainties in system interactions and boundary conditions is to use the least constraining defensible representations. This creates a pervasive but inevitable optimism – as noted by Capellán-Pérez et al. [50], "The omission of restrictions when solving a system can only lead to optimistic results." Consequently, hypothesized GES transformation outcomes reflecting greater degrees of desirability than indicated by the modelled solution space across multiple dimensions can be identified as either physically implausible or predicated on the existence of one or more of the following:

1) significant (beneficial) feedbacks that are not modelled,
2) model input parameters representing boundary conditions different from that modelled, biased towards greater optimism,
3) novel technologies permitting functional roles different from those modelled, or
4) decision making capable of performing better than that modelled.

All of the above are considered improbable due to 1) the use of least constraining assumptions regarding the internal structure of the GES, 2) the very low statistical probability associated with the manifestation of consistent optimism across multiple key model parameters, 3) the rarity and slow diffusion of technological breakthroughs allowing new functional relations (as opposed to structural iterations, as discussed in sections 2.3.1 and 3.1.1), and 4) the real-world ubiquity of social, political, and economic factors affecting decision making, with generally adverse implications for high-level transition outcomes relative to outcomes found via physical modelling (discussed further in section 5.2).

Necessarily, the identification of physical implausibility here is dependent on the range of socio-technical narratives implied by the full set of possible model configurations considered within the probabilistic formulation. By employing a highly inclusive set of initial states and boundary conditions and thereby maximizing the model's descriptive domain, implausibility takes on a more reliable and unambiguous meaning.

4.1.2 Boundaries and scale of analysis

As discussed in section 3.1.4, designing an appropriate methodological approach requires the selection of a suitable scale of analysis, including levels of aggregation and analytical boundaries. Modelling GES transformation pathways while maintaining tractability necessitates a high-level approach involving substantial simplification and aggregation. The relative paucity of high-quality input data for quantification of the GES further supports the use of a simple, conceptual model, as greater model complexity is often overshadowed by irreducible uncertainties. However, the model must be complex enough to represent pertinent system behaviours that may influence and constrain GES transformation pathways.

The chosen modelling approach is global and spatially aggregated, optimistically assuming no substantive geographic or geopolitical barriers regarding the distribution of GES infrastructures or movement of flows. However, it is disaggregated with respect to functionally non-equivalent energy flows and capital (see section 3.1.2.4). As discussed in section 3.1.4, high-level models must focus on functional representation of the system's components at the expense of fully enumerating structural details and will therefore tend to overlook constraints that manifest at lower scales of analysis. Included energy flow and capital elements are chosen such that the modelling formulation is manageable while maintaining as much functional differentiation as possible. Given that globally aggregated capital stocks will necessarily encompass broad technological and operational diversity, modelled parameters refer to the functional averages applicable to these stocks. The selected temporal scale is from years to decades, covering the remainder of the 21st century.

Social, political, and economic (i.e., non-energy) factors will not be directly considered in the modelling approach beyond a simple representation of feedback between the HSES and GES (described in section 4.2.4.5). While comprehensive a biophysical macroeconomic representation would be advantageous, as described in sections 3.1.3 and 3.2.1.1, this would introduce vastly greater uncertainties and ambiguities, and is a considerable research endeavour in its own right, and is therefore not considered practical or within scope. However, macroeconomic implications for the broader HSES are discussed qualitatively in sections 7.2.5 and 8.1.5.

As discussed in section 3.1.4, an explicit energy grammar must be defined prior to any meaningful quantification of the GES. Semantic categories constituting the energy grammar for the methodological approach outlined in this chapter can be summarized as follows:

- The set of energy quantities, flows, and transformations under consideration is limited to anthropogenic, exosomatic, technologically mediated energy production, conversion, and end-use processes. This excludes the production and utilization of non-scalable or economically extraneous energy flows, for example,
    - food production and mechanical work performed using endosomatic energy (human or animal muscle power),
    - obsolete technologies such as sailing ships and steam locomotives, and
    - natural energy flows associated with the provision of ecosystem services.
- Primary energy resources considered consist of natural energy fluxes and geological stocks of chemical potential or nuclear energy available for the production of the above energy flows, at scale.
- As described above, energy flows and corresponding capital stocks are aggregated into equivalence classes to maximize functional differentiation within a manageable number of elements (arrays defining selected equivalence classes are presented in section 5.1).

The formal category in all cases is power (EJ/year), quantified in terms of basic calorific content (heating values) or work, except for delivered energy services which require the application of semantic definitions based on ideal provision 'reference modes' (detailed in sections 4.2.1.3 and 4.2.2.5).

The selected modelling approach is generally optimistic regarding ongoing improvements in technologies fulfilling existing functional roles, reflected in increasing process efficiencies, but does not include new functional roles corresponding to technologies that have not yet demonstrated commercial viability and scalability. The inclusion of speculative or unproven technologies is epistemically unjustified as no meaningful estimates can be made regarding the likelihood or timing of their eventual availability. As such, the criteria applied for inclusion of technologies are as follows:

- the technology must have advanced beyond the prototyping and pilot stages,
- established technological standards and means of system integration must exist,
- the technology must be commercially viable (without major subsidies), and
- associated supply chains and secondary industries must exist at scale.

In consideration of the above, the identified solution space is properly interpreted as *a high-level set of best-case GES transformation pathways and associated outcomes, generated from a biophysical, complex systems perspective, under uncertainty and excluding the possible impacts of speculative technologies*. Additional scenarios are constructed to explore socio-technical narratives of interest and query weaknesses evident in the chosen methodological approach (see section 5.3). As described in section 3.1.4.2, real-world events have the potential to invalidate the model, particularly where they correspond to a phase change to a novel system state.

4.1.3 Epistemic uncertainty

As discussed in sections 1.3.2, 3.1.4.3, and 3.3, analysis of GES transformation pathways requires acknowledgement of the high degree of irreducible uncertainty involved. Note that aleatory uncertainties are largely irrelevant at the spatial and temporal scales adopted for the methodological approach described here and can be disregarded.[19]

In response to uncertainty arising from indeterminacy in high-level semantic definitions applied to CAS, discussed in section 3.1.4.2, a basic principle of *semantic openness* is adopted (analogous to Georgescu-Rogen's *dialectical penumbras* discussed in section 3.1.4.3). This principle treats modelled elements and analytical boundaries (e.g., between the GES and wider HSES) as open to varying implicit definitions, without the possibility of a definitive standard. As such, modelling flexibility is given preference over precision.

The GES transformation solution space is explored via Monte Carlo simulation of transformation pathways, under uncertainty. As discussed in section 3.3, the PNS perspective emphasizes the necessity of comprehensive sensitivity audits. Monte Carlo simulation offers

[19] This excludes the temporal variability of RE resources and corresponding effects manifesting at the system level, described in section 4.2.5.

an ideal approach to facilitate these audits by generating ensembles of GES transformation pathways and allowing comprehensive multivariate sensitivity and diagnostic analyses, outlined in sections 5.5.1 and 5.5.2, respectively. All input parameters subject to epistemic uncertainty are modelled probabilistically to capture the strength of knowledge and corresponding implications for GES transformation at the ensemble level. Uncertainty is represented to the degree possible given practical modelling limitations:

- Uncertainty regarding model input parameter values is comprehensively represented via probability distributions (section 4.2.9.2).
- Uncertainty regarding model structures and feedback loops is less well represented, as representation of the very large number plausible of alternatives is analytically prohibitive. However, this is partially addressed via scenario analysis and the exploration of specific socio-technical narratives (see section 5.3), and also aligns with conceptualizing the present modelling effort as part of a growing plurality of perspectives, not as a definitive approach (as discussed in section 3.3.1).

4.2 Physical GES modelling principles

As in the recent examples of biophysical energy systems models overviewed in section 3.2.2.1, GES evolution is assumed to be driven by exogenous energy demand, and as such, the simulated solution space effectively identifies feasible and infeasible demand projections. However, unlike these studies, demand is represented at the level of final energy services (outlined in section 4.2.1.3), allowing explicit representation of dynamic substitution processes between distinct energy carriers (adaptation in end-use capital; see section 4.2.2.2). The modelling approach also incorporates the aspects listed in section 3.4:

- Structural representation of the GES via distinct power capacity stocks (section 4.2.2).
- Modelling of end-use conversion and the provision of energy services (section 4.2.2.2).
- Endogenous changes in power capacity efficiencies driven by technological learning effects and capital turnover, bounded by maximum theoretical efficiencies, including delayed feedbacks associated with the technological lock-in effect (section 4.2.2.5).
- Heterogeneous primary energy resource quality distributions determining the energy costs of autocatalytic energy production, including terminal depletion thresholds for NRE resource production (section 4.2.4.1).

- Disaggregation of the metabolic energy costs of the GES to specific, dynamic energy carrier profiles (section 4.2.4.3).
- Realistic time dynamics for energy infrastructure lifecycles, with representation of differences between distinct capital types (section 4.2.4.4).
- Representation of the hypercyclic component of the GES subject to constraints arising from the limited capacity of the HSES to provide labour and resources (section 4.2.4.5).
- Representation of intermittency impacts and corresponding mitigation options within electricity systems (section 4.2.5).
- Co-evolution of the supply and demand sectors with explicit modelling of changes in both over time and energy carrier substitution in response to signals of energy carrier scarcity, including partial representation of rebound effects (section 4.2.9.1).
- Metrics relating to the implications of GES transformation pathways for climate change (cumulative energy related GHG emissions) and the identification of net energy trap outcomes following critical divergence between supply and demand (section 4.2.9.3).

Note that goal seeking technology allocation (in terms of power capacity investment) drives system evolution, as discussed in section 4.2.9.1. This is an aspect of system control logic applied in the specific implementation of the modelling principles presented in this chapter, outlined in section 5.2.

The high-level, spatially aggregated modelling approach described here can be considered 'semi-stylized', particularly regarding model aspects subject to a relative lack of high-quality data or simplifying assumptions, particularly:

- reconciliation of upstream and downstream model sectors using a cumulative supply/demand balance function (section 4.2.1.2),
- representation of auxiliary infrastructures required by the GES (section 4.2.2.4),
- estimation of the energy costs of secondary and end-use capital (section 4.2.4.2),
- representation of exogenous model interfaces using stochastically generated logistic functions (section 4.2.8),
- the specific heuristic method used for system control purposes (section 5.2), and
- the wide probabilistic ranges for exogenous energy service demand (section 4.2.1.3).

Despite the semi-stylized nature of the modelling approach, inputs and model structures are intended to correspond to the real-world GES as closely as possible. Identified model limitations are listed in section 5.4.

4.2.1 Energy flow schema

The energy flow schema depicted in Figure 10 spans primary energy resources to energy carriers (EC) to delivered energy services (ES). Primary, secondary, and end-use power capacity (PC) stocks are involved in the production of primary flows, conversion of primary energy flows to ECs, and conversion of ECs to ESs, respectively. Note that energy losses are evident at all stages. This schema is spatially aggregated so is robust to varying degrees of infrastructural centralization.

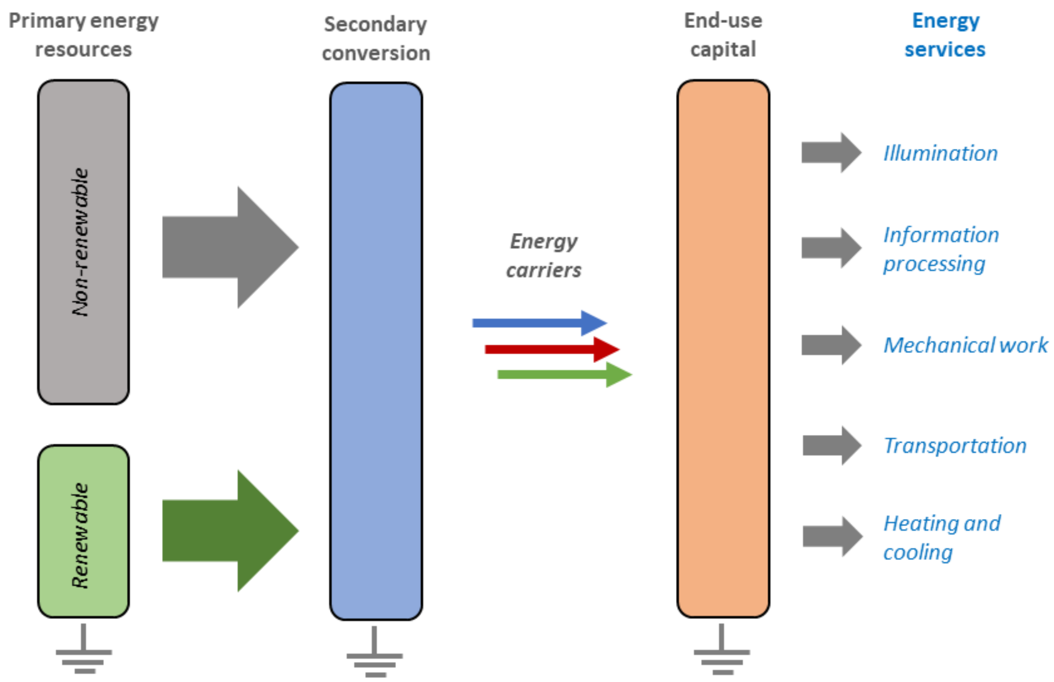

Figure 10: overview of the energy flow schema from primary energy resources to delivered energy services

Note that all PC, EC, and ES types are disaggregated into distinct functional types, as specified in section 5.1.

4.2.1.1 Primary energy resources

Primary energy resources provide a series of primary RE and NRE flows to the secondary conversion stage, which can be described by vectors (specified in terms of flow rates) evolving as functions of time as the production of energy changes:

$$\boldsymbol{p_r} = \boldsymbol{f}(t) \text{ and } \boldsymbol{p_n} = \boldsymbol{f}(t)$$

Where $\boldsymbol{p_r}$ consists of flows derived from all functionally distinct, renewable, primary energy resources available to the GES, and similarly, $\boldsymbol{p_n}$ consists of flows from all distinct non-renewable primary energy resources. These flows are limited by the physical availability of respective resources:

$$\boldsymbol{p_r} \leq \boldsymbol{p_{rm}} \text{ and } \int_{t=0}^{\infty} (\boldsymbol{p_n} + \boldsymbol{p_{ne}}) < \boldsymbol{\omega_{nm}}$$

Where, $\boldsymbol{p_{rm}}$ is the vector of maximum RE flow rates, or technical potentials,

$\boldsymbol{\omega_{nm}}$ (units of EJ) is the vector of maximum ultimate cumulative NRE production, and

$\boldsymbol{p_{ne}}$ is the vector of direct (non-energy) use of NRE resources, as primary energy equivalent.

That is, RE production is flow limited while NRE production is stock limited, by definition. Note, the direct use of primary energy resources without conversion to ECs is considered outside the boundary of the GES and is modelled as resource outflows only. For NRE, this is modelled as a vector of outward flows from NRE resource stocks, $\boldsymbol{p_{ne}}$ (expression given in section 4.2.1.3). For RE, non-energy use is ignored as RE technical potentials as modelled are those components of total resources assumed to be available for energy purposes.

As discussed in section 2.1.1, the quality of primary energy resources quality is non-homogeneous and can be described by quality distributions as functions of production relative to the above absolute limits. Production can be specified relative to respective limits using normalized vectors: exhaustion, $\boldsymbol{x}$, for RE and depletion, $\boldsymbol{d}$, for NRE (both dimensionless):

$$\boldsymbol{x}(t) = \left(\boldsymbol{p_r} - \boldsymbol{p_r}(0)\right) \oslash \left(\boldsymbol{p_{rm}} - \boldsymbol{p_r}(0)\right)$$

$$\boldsymbol{d}(t = \tau) = \int_0^{\tau} (\boldsymbol{p_n} + \boldsymbol{p_{ne}})\, dt \oslash \boldsymbol{\omega}$$

Where, $\boldsymbol{p_r}(0)$ is the vector of RE production rates at the beginning of the study period, and

$\boldsymbol{\omega}$ (units of EJ) is the vector of NRE technically recoverable resources available with EROI values above specified terminal values (RURR at the beginning for the study period).

Both $\boldsymbol{p_{rm}}$ and $\boldsymbol{\omega}$ are defined as primary resource quantities accessible above specified terminal EROI values, after which production is assumed to be impractical and uneconomic. These accessible primary resource quantities and associated primary flows, $\boldsymbol{p_r}$ and $\boldsymbol{p_n}$, are both defined net of losses for simplicity (making explicit modelling of primary losses unnecessary).

Note that it is possible for RE production to fall below its initial rate, in which case exhaustion becomes negative. In contrast, depletion of NRE resources can only increase. However, NRE depletion values can exceed one if cumulative production exceeds $\boldsymbol{\omega}$, after which EROI falls below terminal values (see section 4.2.4.1). In effect, the economic and technical limits to production determining technical potentials and RURR are treated as coincident with specified terminal EROI values. As a full treatment of economic factors involved in resource exploitation is out of scope for this study, primary energy resources, $\boldsymbol{p_{rm}}$ and $\boldsymbol{\omega}$, are modelled probabilistically to account for epistemic uncertainty (see section 4.2.9.2). Additionally, intermittency related feedbacks affect the production of primary energy resources, as described in section 4.2.4.

4.2.1.2 Energy carriers

As discussed in section 2.2.2, the non-equivalence of distinct ECs must be considered explicitly. Therefore, disaggregation of EC supply/demand imbalances and consequent implications for investment requirements and substitution are paramount. The dynamic supply and demand of ECs represents an operative interface, indicating relative scarcity or abundance due to dynamic changes or constraints affecting the production or consumption of ECs. EC supply and demand flows can be described by vectors, $\boldsymbol{p_i}$ and $\boldsymbol{p_o}$, respectively, evolving as functions of time as the production and consumption of energy changes:

$$\boldsymbol{p_i} = \boldsymbol{f}(t) \text{ and } \boldsymbol{p_o} = \boldsymbol{f}(t)$$

Where both vectors consist of all functionally distinct ECs produced and consumed within the GES. Differences between the inflow and outflow of ECs over time can be tracked using a cumulative supply/demand balance vector, $\boldsymbol{b}$ (in units of EJ):

$$\boldsymbol{b}(t = \tau) = \int_0^\tau (\boldsymbol{p_i} - \boldsymbol{p_o})\, dt \qquad (1)$$

Note that while supply/demand imbalances over time are represented mathematically as integral functions, this does not necessarily correspond to commensurate physical quantities. Instead, the $\boldsymbol{b}$ vector can be seen as a price proxy and signal of scarcity or abundance motivating dynamic changes in investment and consumption, as discussed in section 4.2.9.1.

4.2.1.3 Energy services

As discussed in section 2.2.3, the purpose of the GES is the provision of ESs required by the HSES. While final energy consumption is conventionally defined in terms of the outflow of ECs (or 'final energy demand'), $\boldsymbol{p_o}$, it is advantageous to extend the model boundary to include end-use (EU) PC and the dynamic provision of ESs. This conceptual expansion allows the dynamic, explicit representation of EC substitution processes, including investment flows and time required for capital turn-over.

It is generally not possible to precisely delineate the component of energy delivered to end-users comprising 'useful' services from that which is not useful. Therefore, flows of ESs can only be quantified with reference to chosen benchmarks. Thermodynamic energy input minima exist for any physical process (corresponding to maximum second law efficiency), such as the specific heat capacity for heating substances or the kinetic energy of motion. However, while relevant at the local process level, these minima are not applicable to definitions of useful energy at the global aggregate level due to the complexity and heterogeneity of real-world ES delivery systems and processes. As such, useful energy in the form of ESs requires semantic definitions; the corollary to the definition of efficiencies for the delivery of ESs, as discussed further in section 4.2.2.5. Delivered ES flows can be described by a vector evolving as a function of time as the consumption of energy changes:

$$\boldsymbol{p_d} = \boldsymbol{f}(t)$$

Where $\boldsymbol{p_d}$ consists of all functionally distinct ESs demanded by the HSES; the main set of independent variables driving GES evolution, as described in section 4.2. Owing to significant epistemic uncertainty regarding future ES demands, $\boldsymbol{p_d}$ is modelled probabilistically (as described in section 4.2.9.2). ES demands as modelled exclude intermediate services used directly or indirectly for the construction, operation, and decommissioning of capital comprising the GES itself (modelling of this internal component of end-use energy consumption is detailed in section 4.2.4).

The discretionary and non-discretionary components of ES demand are not differentiated. Discretionary demand can be expected to respond more strongly to signals of scarcity or abundance than non-discretionary demand (due to higher price elasticity of demand).

However, modelling of this distinction is out of scope, as it would require additional feedback loops and behavioural assumptions that extend beyond a physical representation of the GES.

Aggregate ES demand can also be characterized by the metric 'demand flexibility', q (dimensionless scalar), to describe the normalized degree of demand responsiveness to temporal patterns in infrastructure utilization and the availability of supply. At the extremes, a value of zero implies no demand response while a value of one implies perfect correlation between demand and infrastructure capacity limitations and intermittent supply. Demand flexibility is assumed to increase over time as improved consumer responsiveness via behavioural and technological changes causes demand patterns to become more sensitive to, and synchronized with, primary energy availability and capacity constraints.

$$q = f(t) \text{ where } 0 \leq q \leq 1$$

See section 4.2.8 for details of functions for ES demand and demand flexibility (equations given in section 9.3.2).

For simplicity, it is assumed that direct, non-energy NRE use, $\boldsymbol{p_{ne}}$, is subject to similar underlying economic drivers to those affecting ES demands and, therefore, non-energy use scales with the mean of delivered ES demands relative to their initial levels, $\boldsymbol{p_d}(0)$:

$$\boldsymbol{p_{ne}} = \frac{\boldsymbol{p_{ne}}(0)}{n} \sum_{i=1}^{n} \left(\boldsymbol{p_d} \oslash \boldsymbol{p_d}(0)\right)_{\boldsymbol{i}}$$

Where n is the length of ES demand type vectors. While the embodied energy in chemical feedstocks and other non-energy NRE uses could be considered among ESs, these flows are taken directly from the primary energy resource and do not traverse the energy flow schema shown in Figure 10.

4.2.2 Power capacity

As discussed in section 3.1.2, PC consists of technological capital capable of transforming exosomatic energy flows. Each PC stock is modelled as a homogenous and continuous quantity specified by maximum aggregate output flow rate. Note that the retrofitting of capital is consistent with this representation, via incremental additions of PC. Losses inevitably occur in any energy conversion, distribution, or utilization process, such that output power flows from PC are always less than the associated input flows, as depicted in Figure 11.

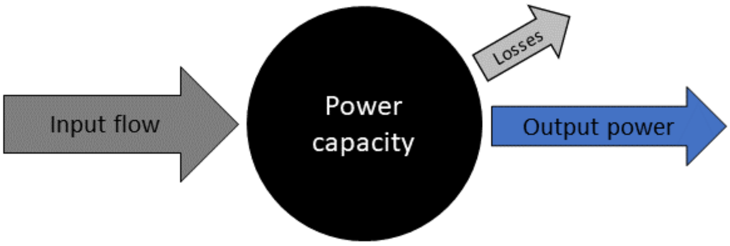

Figure 11: functional schematic of power capacity

Changes in the production and consumption of ECs, $\boldsymbol{p_i}$ and $\boldsymbol{p_o}$, can be represented via evolving profiles of power capacities comprising the supply and demand sectors, respectively. These profiles are affected by additions of new PC, decommissioning of end-of-life PC, changes in utilization, and improvements in process efficiencies (ratios of input to output flows).

PC stocks can be described by vectors, $\boldsymbol{c_x}$, calculated as integral functions starting from initial PC stocks, $\boldsymbol{c_x}(0)$, PC addition flows, $\boldsymbol{h_x}$ (units of EJ/year^2), less decommissioning flows:

$$\boldsymbol{c}_{\boldsymbol{x}}(t=\tau) = \boldsymbol{c}_{\boldsymbol{x}}(0) + \int_{\boldsymbol{0}}^{\boldsymbol{l}_{\boldsymbol{x}}} (\boldsymbol{h}_{\boldsymbol{x}} - \boldsymbol{c}_{\boldsymbol{x}}(0) \oslash \boldsymbol{l}_{\boldsymbol{x}})\, dt + \int_{\boldsymbol{l}_{\boldsymbol{x}}}^{\tau \boldsymbol{j}} \big(\boldsymbol{h}_{\boldsymbol{x}} - \boldsymbol{h}_{\boldsymbol{x}}(\tau \boldsymbol{j} - \boldsymbol{l}_{\boldsymbol{x}})\big)\, dt$$

The subscript $\boldsymbol{x}$ is replaced with $\boldsymbol{r}$, $\boldsymbol{n}$, $\boldsymbol{s}$, and $\boldsymbol{e}$ to denote primary RE, primary NRE, secondary, and EU PC, respectively. The output power flows these sets of PC stocks produce are then described by vectors $\boldsymbol{p_r}$, $\boldsymbol{p_n}$, $\boldsymbol{p_s}$, and $\boldsymbol{p_e}$, respectively. Note that decommissioning flows are represented by delayed PC addition flows, $\boldsymbol{h_x}(\tau\boldsymbol{j} - \boldsymbol{l_x})$, where $\boldsymbol{l_x}$ is the vector of the operating lifetimes of PC (in units of years). As the delayed PC addition flow function for PC decommissioning is only defined after time $\boldsymbol{l_x}$ has elapsed, decommissioning flows are represented by a uniform depletion of the initial PC stocks prior to this time.

Additional PC quantities are not added immediately to operating PC stocks after investment decisions are made (in terms of PC additions, not monetary investment). Instead, these investment decision flows, $\boldsymbol{\hat{h}_x}$ (units of EJ/year^2), are first added to stocks of PC in the construction phase, $\boldsymbol{w_x}$ (in units of EJ/year):

$$\boldsymbol{w}_{\boldsymbol{x}}(t=\tau) = \boldsymbol{w}_{\boldsymbol{x}}(0) + \int_{\boldsymbol{0}}^{\boldsymbol{z}_{\boldsymbol{x}}} \big(\widehat{\boldsymbol{h}}_{\boldsymbol{x}} - \boldsymbol{w}_{\boldsymbol{x}}(0) \oslash \boldsymbol{z}_{\boldsymbol{x}}\big)\, dt + \int_{\boldsymbol{z}_{\boldsymbol{x}}}^{\tau \boldsymbol{j}} \Big(\widehat{\boldsymbol{h}}_{\boldsymbol{x}} - \widehat{\boldsymbol{h}}_{\boldsymbol{x}}(\tau \boldsymbol{j} - \boldsymbol{z}_{\boldsymbol{x}})\Big)\, dt$$

Where $\boldsymbol{z_x}$ is the vector of build times for new PC (in units of years). PC addition flows, $\boldsymbol{h_x}$, are then given by outflows from the stock of PC in the construction phase:

$$\boldsymbol{h}_x = \begin{cases} \boldsymbol{w}_x(0) \oslash \boldsymbol{z}_x \; for \; t\boldsymbol{j} \; < \; \boldsymbol{z}_x \\ \widehat{\boldsymbol{h}}_x(t\boldsymbol{j} - \boldsymbol{z}_x) \; for \; t\boldsymbol{j} \; \geq \; \boldsymbol{z}_x \end{cases}$$

4.2.2.1 Upstream sector

All PC affecting the supply of ECs, $\boldsymbol{p}_i$, can be termed the upstream sector. As depicted in Figure 12, upstream PC can be separated into three stages (with losses modelled at the latter two stages only):

1) production of primary RE or NRE flows ($\boldsymbol{p}_r$, $\boldsymbol{p}_n$),
2) conversion of primary RE or NRE flows to output ECs ($\boldsymbol{p}_r$, $\boldsymbol{p}_n \rightarrow \boldsymbol{p}_s$), and
3) transportation and distribution of output ECs to the point of end-use ($\boldsymbol{p}_s \rightarrow \boldsymbol{p}_i$).

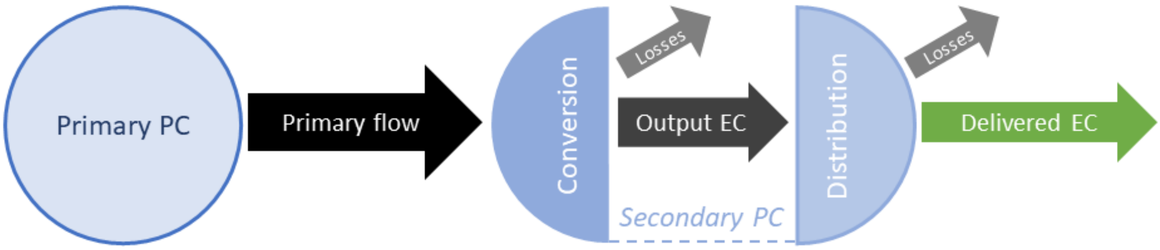

Figure 12: functional schematic of upstream power capacity

Secondary conversion involves the production of ECs through various processes, including combustion, fuel refining, and electricity generation. Output ECs are then delivered to the point of end-use via transportation and distribution networks, such as electricity transmission networks, fuel tankers and pipelines, and steam systems for transmitting heat. Note that these networks and associated infrastructures are required for the delivery of ECs but are not included in the definition of secondary PC (see section 4.2.2.4).

Secondary conversion can be nominal where ECs are produced at the primary stage (e.g., solar PV and hydroelectricity). Where this occurs, secondary PC is still typically needed for system integration (e.g., transformers and electrical equipment). Therefore, EC flows are considered delivered and available to the GES only after having traversed the secondary conversion stage.

Note that the extant quantities of primary and secondary PC are mutually dependent, i.e., primary PC to produce primary flows and secondary PC to process these flows must be approximately equal over time, with unused capacity indicating sub-optimal investment. The practical handling of upstream synchronization of PC additions is detailed in section 5.2.5.2.

4.2.2.2 Downstream sector

All PC affecting the final, non-energy system demand for ECs (a subset of $\boldsymbol{p_o}$) can be termed the downstream sector. As depicted in Figure 13, downstream PC can be separated into two stages (with losses modelled at both stages):

1) conversion of input EC flows to output power ($\boldsymbol{p_o} \rightarrow \boldsymbol{p_e}$), and
2) provision of ESs using output power via passive systems ($\boldsymbol{p_e} \rightarrow \boldsymbol{p_d}$)

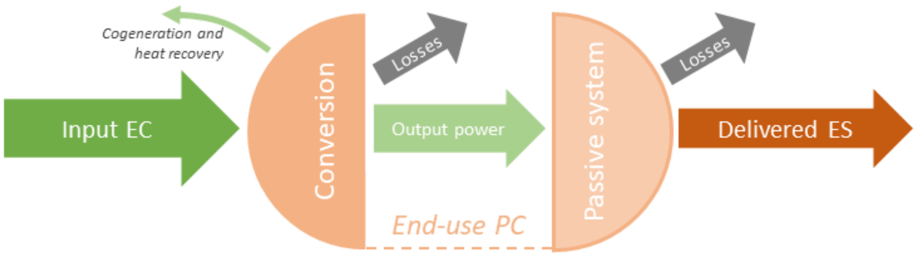

Figure 13: functional schematic of downstream power capacity

EU conversion involves the production of useful output power by various means, including internal combustion engines, electric motors, and heating elements. Output power is then delivered as final ESs via various passive systems, such as passenger vehicles, driven systems, or furnaces [212, 225]. Note that passive systems are typically, but not always, included in the definition of EU PC (see section 4.2.2.4).

Changing the profile of final EC consumption needed to meet ES demands, $\boldsymbol{p_d}$, requires PC addition flows, $\boldsymbol{h_e}$, to change the composition of downstream PC stocks. While major changes in EU PC composition have historically required extensive reorganizations of infrastructure, production, trade, and population densities [6, 14], detailed modelling of these processes is out of scope. The energy costs of such spatial reorganization processes are assumed to:

- be represented implicitly in exogenous ES demands and explicitly in the turnover of modelled auxiliary infrastructures (defined in section 4.2.2.4), and
- pose no constraints to GES transformation beyond those modelled.

Note that cogeneration and heat recovery (depicted in in Figure 13) allows for a partial return of ECs where large waste heat flows are generated (primarily from high temperature industrial processes). See sections 4.2.3 and 9.5.5.5 for modelling details.

4.2.2.3 Capacity utilization

While PC is quantified with reference to a technical maximum (or 'nameplate') capacity to produce output power, aggregate PC is not used at full utilization due to various technical, operational, and economic factors, including the temporal heterogeneity of demand, typical use behaviours, and the need for downtime to maintain PC in working order. The average ratio between the actual output rate and maximum output rate can be used as a measure of PC utilization and is termed 'capacity factor' (CF). CFs for each category of PC stocks can be described over time by a vector, $\boldsymbol{u}$ (dimensionless):

$$\boldsymbol{u} = \boldsymbol{p} \oslash \boldsymbol{c} \text{ where } \boldsymbol{c} > \boldsymbol{p} \text{ such that } 0 < \boldsymbol{u} < 1$$

For upstream PC, capacity factors can increase up to defined limits:

$$\boldsymbol{c_x} \circ \boldsymbol{u_x} = \boldsymbol{p_x} \text{ where } \boldsymbol{u_x} \leq \boldsymbol{\gamma_x} \circ \boldsymbol{u_{xm}}$$

The subscript $\boldsymbol{x}$ is replaced with $\boldsymbol{r}$, $\boldsymbol{n}$, and $\boldsymbol{s}$, to denote primary RE, primary NRE, and secondary PC, respectively. CF maxima are given by the vectors $\boldsymbol{u_{rm}}$, $\boldsymbol{u_{nm}}$, and $\boldsymbol{u_{sm}}$. Note that CFs drop when capacity is unneeded. Effective upper limits can change due to dynamic interactions within electricity systems in response to intermittency mitigation, represented by the normalized vectors $\boldsymbol{\gamma_r}$, $\boldsymbol{\gamma_n}$, and $\boldsymbol{\gamma_s}$, as described in section 4.2.5. Maximum secondary CFs can also fall due to active curtailment by system control to avoid destabilizing levels of EC surplus (see section 5.2.5.3 for details):

$$\boldsymbol{u_{sm}} = \boldsymbol{f}(\boldsymbol{b})$$

For downstream PC, 'target' CFs described by the vector $\boldsymbol{u_{et}}$ change over time, as described in section 4.2.8 (equation given in section 9.3.1.3.1). Target CFs are optimistically assumed to rise as behavioural and technological changes lead to more efficient utilization of EU PC. CFs fall below target levels when more EU PC is present than needed to meet ES demands.

$$\boldsymbol{u_{et}} = \boldsymbol{f}(t)$$

$$\boldsymbol{c_e} \circ \boldsymbol{u_e} = \boldsymbol{p_e}$$

Unlike primary and secondary CF maxima, target CFs do not represent hard limits but rather, when exceeded, act as a trigger for investment in the relevant EU PC type to bring $\boldsymbol{u_e}$ back to $\boldsymbol{u_{et}}$ or below. This CF driven investment is described in section 5.2.5.1.

4.2.2.4 Auxiliary infrastructure

Auxiliary infrastructure (AI) is defined here as the various capital stocks not directly involved in converting or transforming energy flows but required for the operation of PC:

- In the upstream sector, supply infrastructures are required for the processing and transportation of primary RE and NRE flows, and for the delivery of ECs to the point of end-use (i.e., upstream AI supports the transformation of $\boldsymbol{p_r}$ and $\boldsymbol{p_n}$ to $\boldsymbol{p_o}$). This includes capital required for the mitigation of supply intermittency in electricity systems, such as storage and additional transmission capacity, as detailed in section 4.2.5.
- In the downstream sector, passive systems using applied power to deliver ESs often require extensive infrastructures for their operation, such as road and rail networks, ports, and airports (i.e., downstream AI supports the transformation of $\boldsymbol{p_e}$ to $\boldsymbol{p_d}$).
- For both upstream and downstream sectors, various direct and indirect requirements for socio-technical capacities can be considered part of aggregate AI, including institutions, organizational capacity, personnel training, and supporting industries.

While EU passive systems are typically considered part of PC, not AI, separations between passive systems and associated AI are relatively ambiguous for some EU PC types, e.g., rail carriages and railways, and illuminated, heated, and cooled spaces. This implies a considerable degree of epistemic uncertainty, handled via probabilistic modelling as described in section 4.2.9.2.

Like PC, AI is measured in terms of maximum power rate, however, AI must be sized to accommodate the maximum output level observed over the relevant temporal demand profile. As such, AI quantities required are determined by the ratios of peak to average utilization, or 'peak factors'. Lower peak factors imply less temporal variability of AI utilization and *vice versa*. Peak factors can be described by the vectors $\boldsymbol{v_{sa}}$ and $\boldsymbol{v_{ea}}$ (dimensionless), for secondary and EU AI, respectively, and can optimistically be expected to decline over time as demand flexibility, q, increases. As such, peak factors are assumed to decline linearly as functions of demand flexibility, with lower limits of one:

$$\boldsymbol{v_{sa}} = (1-q)(\boldsymbol{v_{sb}} - \boldsymbol{j}) + \boldsymbol{j} \quad \text{and} \quad \boldsymbol{v_{ea}} = (1-q)(\boldsymbol{v_{eb}} - \boldsymbol{j}) + \boldsymbol{j}$$

Where $\boldsymbol{v}_{sb}$ and $\boldsymbol{v}_{eb}$ are the base peak factor vectors defined at zero demand flexibility. As each AI type is associated with specific groupings of PC, required AI is specified via identity matrices, I_{sa} and I_{ea}:

$$(I_{sa}, I_{ea})_{ij} = \begin{cases} 1 \; where\ PC\ type\ i\ requires\ AI\ type\ j \\ 0 \; otherwise \end{cases}$$

Secondary and EU AI requirement vectors, $\boldsymbol{a}_{sa}$ and $\boldsymbol{a}_{ea}$, respectively, can then be calculated from average output power flows, $\boldsymbol{p}_s$ and $\boldsymbol{p}_e$:

$$\boldsymbol{a}_{sa} = \boldsymbol{\gamma}_{f} \circ (\boldsymbol{p}_s^{\boldsymbol{T}} I_{sa})^{\boldsymbol{T}} \circ \boldsymbol{v}_{sa} \text{ and } \boldsymbol{a}_{ea} = (\boldsymbol{p}_e^{\boldsymbol{T}} I_{ea})^{\boldsymbol{T}} \circ \boldsymbol{v}_{ea}$$

Where the vector $\boldsymbol{\gamma}_f$ represents dynamic interactions within electricity systems in response to intermittency mitigation affecting secondary AI required, as described in section 4.2.5.

Vectors of AI stocks in operation, $\boldsymbol{c}_{sa}$ and $\boldsymbol{c}_{ea}$ for secondary and EU AI, respectively, are modelled analogously to PC stocks (as integral functions, with $\boldsymbol{w}_{sa}$ and $\boldsymbol{w}_{ea}$ representing stocks in construction) but do not have directly associated output power flows. Investments into AI can, for simplicity, be considered a direct consequence of the requirement vectors, $\boldsymbol{a}_{sa}$ and $\boldsymbol{a}_{ea}$, with investment, $\hat{\boldsymbol{h}}_{sa}$ and $\hat{\boldsymbol{h}}_{ea}$, occurring in proportion to any deficit of AI in operation relative to the AI requirement:

$$\hat{\boldsymbol{h}}_{sa} = \boldsymbol{\gamma}_{fh} \circ max(\boldsymbol{0},\ (\boldsymbol{a}_{sa} - \boldsymbol{c}_{sa}) \oslash \boldsymbol{z}_{sa}) \text{ and } \hat{\boldsymbol{h}}_{ea} = max(\boldsymbol{0},\ (\boldsymbol{a}_{ea} - \boldsymbol{c}_{ea}) \oslash \boldsymbol{z}_{ea})$$

Where the vector $\boldsymbol{\gamma}_{fh}$ represents dynamic interactions within electricity systems in response to intermittency mitigation affecting AI investment flows, as described in section 4.2.5. As such, AI availability is not considered a hard limit for ES provision but will expand or shrink to accommodate changes in PC output power over time. This simplification is justified on the grounds that AI can be used, with some operational adjustments, to accommodate increased flows (overcapacity) but must ultimately be expanded to relieve pressure. This allows the energetic costs of AI to be dynamically included in GES transformation pathways without the use of complex logic for associated investment functions.

4.2.2.5 Efficiencies

Modelled energy losses occur within the GES at the primary, secondary, and end-use stages (with corresponding efficiencies) as depicted in Figure 14 and Figure 15. As discussed in section 2.2.1, process-level efficiencies are expected to continue to increase over time due to technological learning effects, causing proportional energy losses to decrease, but are ultimately limited by achievable maxima stemming from technical limitations and practical design considerations including the power/efficiency trade-off. See sections 9.3.1.4.1 and 9.5.6 for details of achievable efficiency maxima modelling and assumptions.

Distinct efficiencies can be identified for both upstream and downstream PC. For the upstream sector (depicted in Figure 14):

- Conversion efficiency is given by the ratio of the primary input flow to the output EC flow (at the physical PC boundary).
- Reticulation efficiency is given by the ratio of the output EC flow to the flow of EC delivered to the point of end-use via distribution networks.
- Note that there is no need for efficiencies to be explicitly modelled at the primary stage, as primary resource quantities, $\boldsymbol{\omega}$ and $\boldsymbol{p}_{rm}$, and associated primary flows, $\boldsymbol{p}_r$ and $\boldsymbol{p}_n$, are both defined net of losses, as noted in section 4.2.1.1.

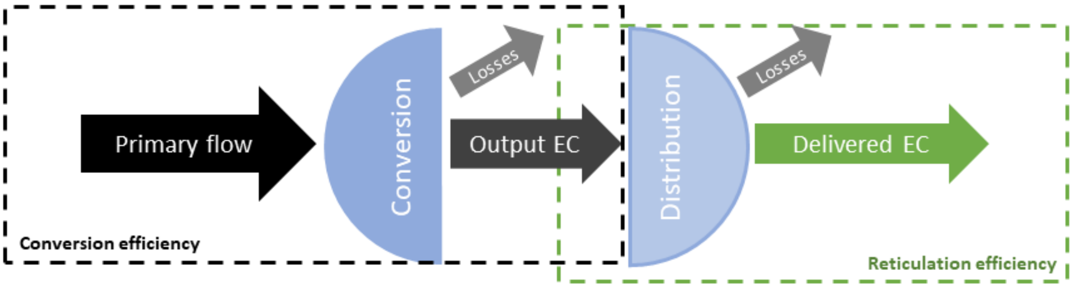

Figure 14: upstream conversion and reticulation efficiencies in relation to PC

For downstream PC (depicted in Figure 15):

- Conversion efficiency is given by the ratio of the input EC flow to the output power flow (at the physical PC boundary).
- EU to ES efficiency is given by the ratio of output power flow to the flow of useful ESs delivered via EU passive systems.

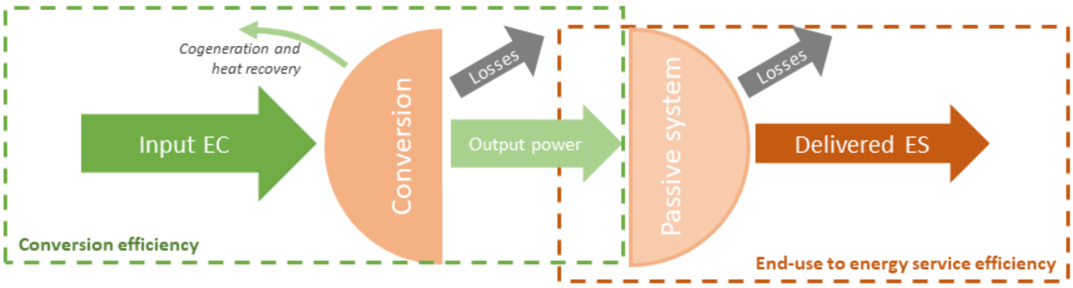

Figure 15: downstream conversion and EU to ES efficiencies in relation to PC

As described in section 4.2.1.3, EU to ES efficiencies must be defined in relation to chosen semantic definitions of delivered ESs. The convention used here is to quantify output power relative to 'reference modes' selected such that the greatest identified practically attainable efficiencies for delivering each given ES (i.e., the highest achievable efficiency maxima across all relevant PC types) are determined to have EU to ES efficiency values of one. These reference modes correspond to the lowest possible EU PC output power flow per unit of delivered ES, representing ideal ES provision from an efficiency point of view. Other EU to ES efficiencies for each ES demand type are then specified relative to this reference mode efficiency. See sections 5.1 and 9.5.6.5 for details.

Effective efficiencies for new PC, given by the vector ***ə***, can be modelled as functions of time, as cumulative PC power output increases and technological learning effects accumulate. Subsequently, mean PC efficiencies of the aggregate stock, ***e***, evolve as functions of investment as the composition of the PC stocks change:

$$\boldsymbol{e_{xy}} = \boldsymbol{f}\left(ə_{\boldsymbol{xy}}\left(\int \boldsymbol{p_x} dt\right), \boldsymbol{h_x}\right)$$

Where the subscript ***x*** is replaced by ***s*** and ***e*** to denote secondary and EU, respectively, and ***y*** is replaced by ***i*** and ***o*** to denote conversion (PC input) and reticulation or EU to ES (PC output) efficiencies, respectively. See section 4.2.8 for details (equations given in sections 9.3.1.4.1 and 9.3.1.5.1).

Effectively, the propagation of new PC to mean PC stock efficiencies represents path-dependence associated with the technological lock-in phenomena discussed in section 2.3. Higher efficiency PC options will tend to get preferential investment, leading to more cumulative output and higher efficiency in a positive feedback loop. However, this effect will tend to diminish over time as learning effects and efficiency gains continue, with investment eventually shifting towards PC options with greater efficiency potential.

4.2.3 Flow routing

One-to-many and *many-to-one* mappings exist between linked PC types at sequential stages within the GES as vectors describing each PC category have different dimensions. To manage flow routing and required aggregations, a sequence of identity matrices must be constructed:

- I_{rsi} for mapping primary RE PC types to secondary PC types,

- I_{nsi} for mapping primary NRE PC types to secondary PC types,
- I_{so} for mapping secondary PC types to EC types,
- I_{ei} for mapping EC types to EU PC types, and
- I_{eo} for mapping EU PC types to ES types.

Firstly, where all mappings are unitary,

$$(I_{rsi}, I_{nsi}, I_{eo})_{ij} = \begin{cases} 1 \; where \; a \; flow \; exists \; between \; PC \; type \; i \; and \; PC \; or \; ES \; type \; j \\ 0 \; otherwise \end{cases}$$

Special cases require non-unitary mappings. For I_{so}, this is due to multiple EC outputs for combined heat and power (CHP) PC types, which produce both electricity and heat (rows must represent actual output proportions and sum to one). For I_{ei}, cogeneration and waste heat recovery return a fraction of input energy as electricity and heat, respectively, for high temperature processes, reducing input factors for both ECs:

$$(I_{so})_{ij} = \begin{cases} 1 \; where \; a \; single \; flow \; exists \; from \; PC \; type \; i, to \; EC \; type \; j \\ < 1 \; where \; the \; flow \; from \; PC \; type \; i \; to \; EC \; type \; j \; is \; partial \; (row \; sums \; to \; 1) \\ 0 \; otherwise \end{cases}$$

$$(I_{ei})_{ij} = \begin{cases} 1 \; where \; a \; single \; flow \; exists \; from \; EC \; type \; i, to \; PC \; type \; j \\ < 1 \; where \; the \; net \; flow \; from \; EC \; type \; i \; to \; PC \; type \; j \; is \; reduced \; due \; to \; EC \; recovery \\ 0 \; otherwise \end{cases}$$

As primary energy flows from a given primary PC type can flow to multiple secondary PC types, an allocation principle is required. For simplicity, it is assumed that secondary PC types receive shares of primary flows in proportion to their respective input capacities to process these flows. These input capacities are given by extant secondary PC quantities multiplied by maximum CF (maximum aggregate output capacities), divided by secondary conversion efficiency to shift from outputs to the corresponding input flows. Therefore, matrices of relative proportional mappings for primary RE and NRE flows to secondary PC output power, F_{rsi} and F_{nsi} (units of EJ/year), are given by,

$$F_{rsi} = I_{rsi} \circ (\boldsymbol{c_s} \circ \boldsymbol{\gamma_s} \circ \boldsymbol{u_{sm}} \oslash \boldsymbol{e_{si}})^{\boldsymbol{T}} \text{ and } F_{nsi} = I_{nsi} \circ (\boldsymbol{c_s} \circ \boldsymbol{\gamma_s} \circ \boldsymbol{u_{sm}} \oslash \boldsymbol{e_{si}})^{\boldsymbol{T}}$$

First, note that primary energy flows, $\boldsymbol{p_r}$ and $\boldsymbol{p_n}$, are limited not only by primary PC maximum CFs but also by the above secondary maximum input capacities, aggregated by primary input type. Primary flows will maximize to the lower of these limits:

$$\boldsymbol{p_r} = max[\boldsymbol{c_r} \circ \boldsymbol{\gamma_r} \circ \boldsymbol{u_{rm}} \quad F_{rsi}\boldsymbol{j}]_j \text{ and } \boldsymbol{p_n} = max[\boldsymbol{c_n} \circ \boldsymbol{\gamma_n} \circ \boldsymbol{u_{nm}} \quad F_{nsi}\boldsymbol{j}]_j$$

The relative proportion matrices, F_{rsi} and F_{nsi}, must be normalized over each primary input type and multiplied by secondary conversion efficiencies to give actual flow conversion factors. Therefore, matrices of conversion factor mappings for primary RE and NRE flows to secondary PC output power, P_{rsi} and P_{nsi}, are given by,

$$P_{rsi} = \boldsymbol{e}_{\boldsymbol{si}}^{\boldsymbol{T}} \circ F_{rsi} \oslash F_{rsi}\boldsymbol{j} \text{ and } P_{nsi} = \boldsymbol{e}_{\boldsymbol{si}}^{\boldsymbol{T}} \circ F_{nsi} \oslash F_{nsi}\boldsymbol{j}$$

The matrix of conversion factor mappings for secondary PC output power to delivered EC, P_{so}, is given by,

$$P_{so} = \boldsymbol{\gamma}_{\boldsymbol{so}} \circ \boldsymbol{e}_{\boldsymbol{so}} \circ I_{so}$$

Where the vector $\boldsymbol{\gamma}_{\boldsymbol{so}}$ represents dynamic interactions within electricity systems in response to intermittency mitigation affecting secondary reticulation efficiencies, as described in section 4.2.5. Composite matrices for the conversion of primary RE and NRE flows to delivered ECs, C_{rs} and C_{ns}, are then given by,

$$C_{rs} = P_{rsi}P_{so} \text{ and } C_{ns} = P_{nsi}P_{so}$$

The supply of ECs can be described by the following equation:

$$\therefore \boldsymbol{p}_{\boldsymbol{i}} = (\boldsymbol{p}_{\boldsymbol{r}}^{\boldsymbol{T}}C_{rs} + \boldsymbol{p}_{\boldsymbol{n}}^{\boldsymbol{T}}C_{ns})^{\boldsymbol{T}} \qquad (2)$$

Similarly, ES demands can typically be met by multiple EU PC types, necessitating an allocation principle. As such, it is assumed that each ES demand is satisfied by EU PC types in proportion to their capacities to provide that ES at their respective target CFs. Downstream mappings must be characterized in the reverse direction, as exogenous ES demands propagate to aggregate EC inputs. ES provision capacities are given by extant EU PC quantities multiplied by EU target CFs (target aggregate output capacities), multiplied by EU to ES efficiencies to shift from output power to delivered ES flows. Therefore, the matrix of relative proportional mappings for ES demands satisfied by EU PC output power, F_{eo} (units of EJ/year), is given by,

$$F_{eo} = I_{eo} \circ \boldsymbol{c}_{\boldsymbol{e}} \circ \boldsymbol{u}_{\boldsymbol{et}} \circ \boldsymbol{e}_{\boldsymbol{eo}}$$

These relative proportions must be normalized over each ES type and divided by EU to ES efficiencies to give actual flow conversion factors. Therefore, the matrix of conversion factor mappings for ES demands to EU PC output power, P_{eo}, is given by,

$$P_{eo} = (F_{eo} \oslash \boldsymbol{j}^{\boldsymbol{T}}F_{eo}) \oslash \boldsymbol{e}_{\boldsymbol{eo}}$$

The matrix of conversion factors for EU PC output power to input ECs, P_{ei}, is given by,

$$P_{ei} = I_{ei} \oslash \boldsymbol{e}_{\boldsymbol{ei}}^{\boldsymbol{T}}$$

The composite matrix for the conversion of ES demands to input ECs (propagation in the reverse direction to actual energy flow), C_e, is then given by,

$$C_e = P_{eo}^T P_{ei}^T$$

EC demand can be described by the following equation:

$$\therefore \boldsymbol{p_o} = \left(\boldsymbol{p}_{\boldsymbol{d}}^{\boldsymbol{T}} C_e\right)^{\boldsymbol{T}} + \boldsymbol{p_a} + \boldsymbol{p_c} \qquad (3)$$

Where $\boldsymbol{p_a}$ and $\boldsymbol{p_c}$ are vectors representing intermediate, energy system related consumption of ECs (the autocatalytic loop and capital hypercycle, respectively, described in section 4.2.4).

Finally, secondary penetration, or the vector of shares of total EC production capacity in both operation and construction phases by secondary PC type, $\boldsymbol{\eta_s}$ (dimensionless), can be calculated as,

$$\boldsymbol{\eta_s} = max\left((\boldsymbol{c_s} + \boldsymbol{w_s}) \circ \boldsymbol{\gamma_s} \circ \boldsymbol{u_{sm}} \circ P_{so} \oslash \left((\boldsymbol{c_s} + \boldsymbol{w_s}) \circ \boldsymbol{\gamma_s} \circ \boldsymbol{u_{sm}}\right)^{\boldsymbol{T}} P_{so}\right)_i$$

For CHP PC types, the value returned is the higher of the respective heat and electricity penetration values. Similarly, EU penetration, or the vector of shares of total ES provision capacity in both operation and construction phases by EU PC type, $\boldsymbol{\eta_e}$ (dimensionless), can be calculated as,

$$\boldsymbol{\eta_e} = \left((\boldsymbol{c_e} + \boldsymbol{w_e}) \circ \boldsymbol{u_e} \circ \boldsymbol{e_{eo}} \circ I_{eo} \oslash \left((\boldsymbol{c_e} + \boldsymbol{w_e}) \circ \boldsymbol{u_e} \circ \boldsymbol{e_{eo}}\right)^{\boldsymbol{T}} I_{eo}\right) \boldsymbol{j}$$

Note that some PC types are subject to penetration limits due to technical, operational, and economic factors that manifest as a proportion of total EC production, or ES provision, that cannot practiacally be met by a given PC type. These limits can be specified using the vectors $\boldsymbol{\eta_{sm}}$ and $\boldsymbol{\eta_{em}}$:

$$\boldsymbol{\eta_s} \leq \boldsymbol{\eta_{sm}} \text{ and } \boldsymbol{\eta_e} \leq \boldsymbol{\eta_{em}}$$

4.2.4 Dynamic energy cost modelling

The energy system related consumption of ECs (given by the sum of $\boldsymbol{p_a}$ and $\boldsymbol{p_c}$) is a dynamic, delayed, path-dependent function of investment flows, $\boldsymbol{\hat{h}_x}$, via PC and AI stocks in construction and operation phases, $\boldsymbol{c_x}$ and $\boldsymbol{w_x}$, and the energy costs associated with these stocks:

- For primary PC, energy costs are modelled using EROI (detailed in section 4.2.4.1).
- For secondary and EU PC and AI, energy costs are represented by the Energy Cost of Capital (ECC) metric, defined as the total energy input per unit of PC or AI (detailed in section 4.2.4.2).

Note that energy costs above refer to EC flows required for the construction, operation, and ultimate decommissioning of PC or AI, but not energy throughput in the form of primary flows to secondary PC or input ECs to EU PC. As aggregation of non-equivalent energy flows is implied by the EROI and ECC metrics, energy quantities used in the calculation of both are expressed in terms of primary energy equivalent.

Flows of delivered ECs are necessarily diverted into the expansion, operation, and replacement of capital stocks comprising the GES (i.e., the hypercyclic component). The upstream production of ECs is supported by EC flows towards primary RE and NRE PC, and secondary PC and AI, collectively termed the 'autocatalytic loop', $\boldsymbol{p_a}$ (see Figure 16).

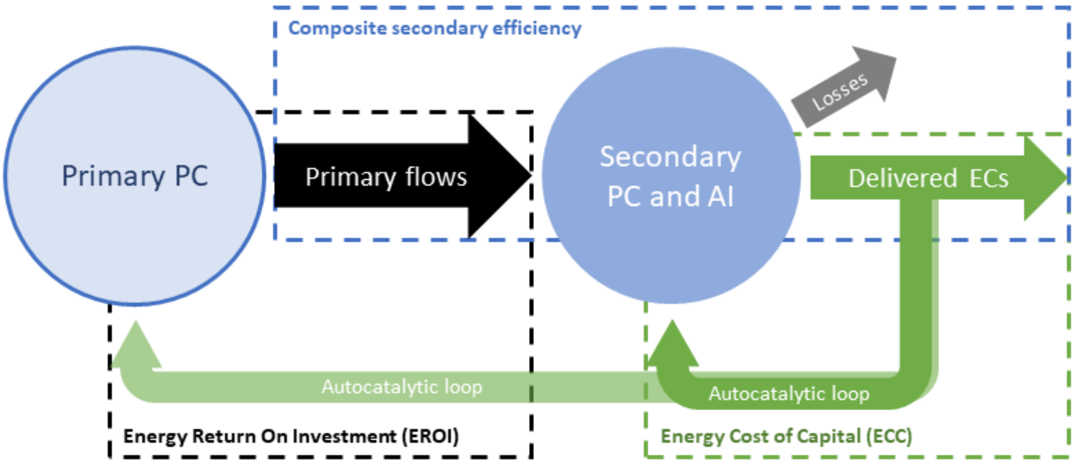

Figure 16: upstream EROI and ECC in relation to PC and AI

Similarly, the downstream provision of final ESs is supported by EC flows towards EU PC and AI, collectively termed the 'capital hypercycle', $\boldsymbol{p_c}$ (see Figure 17).

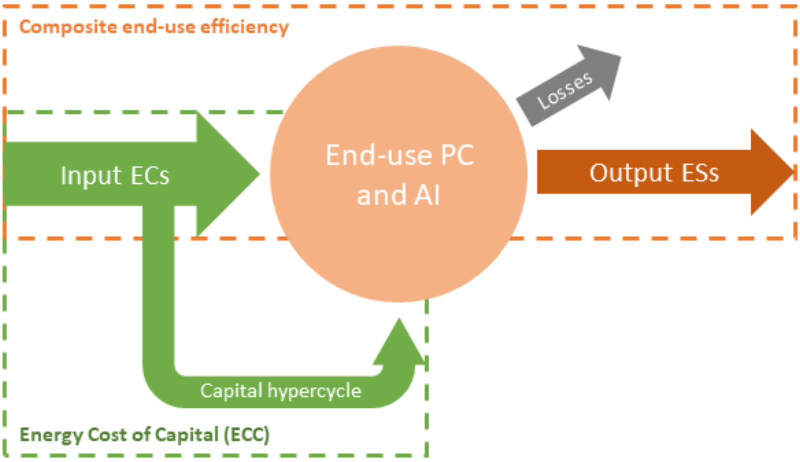

Figure 17: downstream ECC in relation to PC and AI

EROI and ECC are assumed to reflect total n^{th}-order effects, i.e., the EC costs of industrial capacity needed to build new PC and AI, training needed to properly operate it, administrative support, et cetera. In other words, EROI and ECC are assumed to correspond to the full induced energy consumption attributable to the lifetime processes of respective capital within the GES. As most EROI and associated ECC estimates will be calculated via more limited system boundaries than full, n^{th}-order accounting, the scale of energy system related consumption of ECs is represented conservatively. EROI and ECC are both modelled probabilistically to account for epistemic uncertainty (see section 4.2.9.2).

Technological complexity can be expected to continue increasing for energy technologies alongside the learning effects and efficiency improvements discussed in section 4.2.2.5. However, as detailed in section 2.1.1.3, beyond the early development phase, ongoing technological improvements typically have a minimal effect on EROI and physical, geological, and geographic factors affecting resource quality dominate. In contrast, ECC is unaffected by resource quality, but is affected by a balance of technological and scale factors (discussed in section 4.2.4.2). Consequently, and considering immature and speculative technologies are excluded *a priori* (see section 4.1), it is assumed greater technological complexity does not affect either EROI or ECC.

4.2.4.1 EROI

As discussed in section 2.1.1.2, EROI can be defined at various stages within energy systems corresponding to different boundary definitions. The main modelled input for calculating energy costs associated with the production of primary flows, $\boldsymbol{p_r}$ and $\boldsymbol{p_n}$, is standard EROI ($EROI_{st}$). Point of Use EROI ($EROI_{pou}$) can also be calculated for informational purposes by including all necessary upstream energy costs ($\boldsymbol{p_a}$), and similarly, extended EROI ($EROI_{ext}$) can be calculated by including all necessary upstream and downstream energy costs ($\boldsymbol{p_a}$ and $\boldsymbol{p_c}$). See section 4.2.9.3 for details.

NRE and RE EROI can be expected to decrease as functions of primary energy resource depletion, $\boldsymbol{d}$, and exhaustion, $\boldsymbol{x}$, respectively. This is because, as discussed in section 2.1.1.3, the highest quality resources tend to be produced first leaving lower quality resources for subsequent production. Therefore, incremental additions of primary PC at the aggregate level will generally fall progressively further down respective resource quality distributions, directly affecting net energy return for this PC increment over its lifetime. Investment in new PC can be expected to cease after terminal EROI values are reached, indicating that further expansions in production are considered impractical or uneconomic.

The EROI of new PC (additions to PC stocks) can be described by the vectors $\boldsymbol{\text{ʞ}_r}$ and $\boldsymbol{\text{ʞ}_n}$ (dimensionless) for RE and NRE, respectively. Subsequently, the mean EROI of the aggregate primary PC stocks, given by the vectors $\boldsymbol{k_r}$ and $\boldsymbol{k_n}$ (dimensionless), evolve as functions of investment as the composition of the PC stocks change:

$$\boldsymbol{k_n} = \boldsymbol{f}(\text{ʞ}_{\boldsymbol{n}}(\boldsymbol{d}), \boldsymbol{h_n}) \text{ and } \boldsymbol{k_r} = \boldsymbol{f}(\text{ʞ}_{\boldsymbol{r}}(\boldsymbol{x}), \boldsymbol{h_r})$$

NRE EROI decreases with cumulative NRE production while RE EROI changes in response to the RE production rate, therefore $\boldsymbol{k_r}$ can increase if aggregate production rates fall whereas declines in $\boldsymbol{k_n}$ are inexorable. RE resources are not depleted as energy flows are exploited and RE resources can be redeveloped after PC reaches its end of life. Consequently, it is possible for mean EROI to rise following PC decommissioning exceeding additions (see section 9.3.4.1). As RE exhaustion is defined relative to RE potential remaining at beginning of the study period, $\boldsymbol{x}$ can take negative values causing new PC RE EROI values to rise above their initial values. It is assumed here that primary energy resources can be adequately described by quality distributions in terms of EROI, ranging from currently observed values to terminal values (as $\boldsymbol{d}$, $\boldsymbol{x} \rightarrow \boldsymbol{j}$) via uncertain but declining paths (see section 4.2.8).

For both RE and NRE, investment decision flows for new PC, $\boldsymbol{\hat{h}_r}$ and $\boldsymbol{\hat{h}_n}$, cease after primary resources are fully exploited ($\boldsymbol{x}$, $\boldsymbol{d} > \boldsymbol{j}$). However, for NRE, EROI can continue to fall below terminal values as existing PC continues operation and non-energy use, $\boldsymbol{p_{ne}}$, persists (assumed to be unaffected by EROI). See section 4.2.8 for details (equations given in sections 9.3.4.1 and 9.3.4.2.1).

4.2.4.2 Energy cost of capital

ECC is used to represent the energy intensity of non-primary capital involved in the transformation of energy flows: secondary and EU PC and AI, represented by vectors $\boldsymbol{y_s}$, $\boldsymbol{y_e}$, $\boldsymbol{y_{sa}}$, and $\boldsymbol{y_{ea}}$ (units of years), respectively. ECC is defined as the total energy input per unit of installed PC or AI capacity, yielding the intuitive unit of years. This metric is similar to EPBT but is specified per unit maximum technical capacity rather than per unit power output. As such, ECC is independent of capacity utilization assumptions. For simplicity, ECC is optimistically modelled as static, given the likelihood of increasing capital energy costs due to rising socio-technical and organizational complexity associated with increased process-level efficiencies, as discussed in section 2.2.1).

ECC can be estimated where EROI data defined at both the primary stage ($EROI_{st}$) and the secondary stage ($EROI_{pou}$) are available, with other ECC values established by reference to these estimates (via technology cost tiers; see section 9.5.9 for details). The energy intensity of secondary PC is not modelled using $EROI_{pou}$ directly, as secondary conversion processes are not directly influenced by resource quality factors underlying EROI modelling described in section 4.2.4.1. Where EROI data at the primary and secondary stages are available, these are converted to ECC values as follows:

$$(\boldsymbol{y_s})_i = (\boldsymbol{u_{sm}})_i(\boldsymbol{l_s})_i\left(\frac{(\boldsymbol{\varepsilon_s})_i}{(\boldsymbol{k_s})_i} - \frac{1}{(\boldsymbol{e_{si}})_i\left(\boldsymbol{j^T}(\boldsymbol{k_r} \circ I_{rsi}) + \boldsymbol{j^T}(\boldsymbol{k_n} \circ I_{nsi})\right)_i^{\boldsymbol{T}}}\right)$$

Where, $\boldsymbol{\varepsilon_s}$ is a vector expressing conversion factors from secondary output type to primary energy equivalent (dimensionless; all entries 1, except for electricity output, where is 2.6 is used), and $\boldsymbol{k_s}$ is the vector of EROI values defined at the secondary stage ($EROI_{pou}$).

As a derived metric with no independent estimates in the literature, ECC is subject to a high degree of epistemic uncertainty and must be modelled probabilistically (see section 4.2.9.2). Notably, ECC is modelled using log-normal distributions as plausible estimates can be expected to vary by orders of magnitude.

4.2.4.3 EC disaggregation

Distinct ECs are generally non-equivalent and non-substitutable, as discussed in sections 2.2.2 and 3.1.2.4. While the operative energy throughput flows associated with PC and AI are homogeneous and can be explicitly identified (primary flows, output ECs, input ECs, and EU output power) input energy cost flows associated with the autocatalytic loop or the capital hypercycle will consist of a profile of ECs. EC input proportions will vary by PC type based on physical capital characteristics and will change over time as the dominant modes for ES provision change.

The energy cost metrics EROI and ECC are scalar ratios of aggregated energy input and output quantities (in terms of primary energy equivalent, with or without additional price- or exergy-based quality adjustments). Therefore, input energy cost flows indicated by these metrics must be disaggregated to allow for correct dynamic representation of the energy system related consumption of ECs. Firstly, the EC proportions of final demand normalized by the sum primary energy equivalent can be characterized by the vector, $\boldsymbol{\delta}$:

$$\boldsymbol{\delta} = \frac{\left(\boldsymbol{p}_{\boldsymbol{d}}^{\boldsymbol{T}} C_e\right)^{\boldsymbol{T}}}{\left(\boldsymbol{\varepsilon} \circ \left(\boldsymbol{p}_{\boldsymbol{d}}^{\boldsymbol{T}} C_e\right)^{\boldsymbol{T}}\right) \cdot \boldsymbol{j}}$$

Where $\boldsymbol{\varepsilon}$ is a vector expressing conversion factors from EC type to primary energy equivalent (dimensionless; all entries 1, except for electricity output, where is 2.6 is used). The $\boldsymbol{\delta}$ vector can act as a reference for the input energy cost EC proportions associated with PC and AI types. This effectively assumes the composition of PC implicitly represented within the autocatalytic loop and the capital hypercycle approximately mirrors that of modelled EU PC (providing final ES demands). However, it is necessarily to allow for specified EC input energy cost proportions for given PC types relative to the EC proportions of final demand, due to identifiable differentiating physical capital characteristics. Assuming a persistent structural reliance of the hypercyclic component of the GES on specific ECs is justified on the basis that:

- PC and AI comprising the GES are often highly geographically dispersed and resist centralization as they must link distant primary energy resources and demand centres. As such, persistent liquid transportation fuel inputs to PC and AI will tend to vary with the degree of geographical dispersion or remoteness, as transportation and logistics supporting more remote capital is difficult to electrify.

- Similarly, PC and AI comprising the GES often require heavy industry for their manufacture and contain significant embodied energy, as these infrastructures and devices typically must withstand near constant use and a wide variety of operating environments. As such, persistent heat inputs to PC and AI will tend to vary with the degree of heavy manufacturing required.
- Consequently, electricity will tend to represent a lesser proportion of EC input energy costs for many PC and AI types relative to the electricity proportion of final demand.
- Note that specific EC input energy cost proportions for PC and AI will still converge to zero if the corresponding EC proportions of final demand do.

Vectors representing static EC input energy cost proportions for PC and AI relative to the EC proportions of final demand can be specified. These vectors can be denoted $\boldsymbol{\varphi_{xy}}$ (dimensionless) for the y^{th} EC type (up to n) where the subscript $\boldsymbol{x}$ is replaced with $\boldsymbol{r}$, $\boldsymbol{n}$, $\boldsymbol{s}$, $\boldsymbol{sa}$, $\boldsymbol{e}$, and $\boldsymbol{ea}$ to denote primary RE PC, primary NRE PC, secondary PC, secondary AI, EU PC, and EU AI respectively. Next, these vectors can be combined to form matrices of relative EC input energy cost proportions by PC or AI type, Φ_x:

$$\Phi_x = [\boldsymbol{\varphi_{x1}} \quad \cdots \quad \boldsymbol{\varphi_{xn}}]$$

Matrices of initial input EC proportions by PC or AI type, re-normalized with respect to sum primary energy equivalent across EC types, $S_x(0)$, can then be expressed as,

$$S_x(0) = \boldsymbol{\delta}(0)^{\boldsymbol{T}} \circ \Phi_x \oslash \left(\left(\boldsymbol{\varepsilon} \circ \boldsymbol{\delta}(0)\right)^{\boldsymbol{T}} \circ \Phi_x\right) \boldsymbol{j}$$

Note that the vector for initial EC proportions of final demand, $\boldsymbol{\delta}(0)$, is not directly calculable and is approximated, as described in section 4.2.7. Matrices of dynamic EC input energy cost proportions by PC or AI type, S_x, are then given by,

$$S_x = \left(\boldsymbol{\delta} \oslash \boldsymbol{\delta}(0)\right)^{\boldsymbol{T}} \circ S_x(0) \oslash \left(\left(\boldsymbol{\varepsilon} \circ \boldsymbol{\delta} \oslash \boldsymbol{\delta}(0)\right)^{\boldsymbol{T}} \circ S_x(0)\right) \boldsymbol{j}$$

Note that this vector is again re-normalized with respect to sum primary energy equivalent across EC types as $\boldsymbol{\delta}$ changes.

Representation of price and exergy quality adjustments in disaggregated EC components is not attempted above, due to the diversity of such adjustments between EROI data sources sampled (complete alignment not practicable; see section 9.5.8 for details), and the high degree of analytical ambiguity introduced by such adjustments.

4.2.4.4 Lifecycle representation

The input energy costs for PC and AI, and the energy output of PC, do not occur instantaneously or synchronously. Rather, to accurately capture GES dynamics, a given increment of capital must be described by a sequence of distinct states over time: construction, operational lifetime, and decommissioning [170, 355], as depicted in Figure 18.

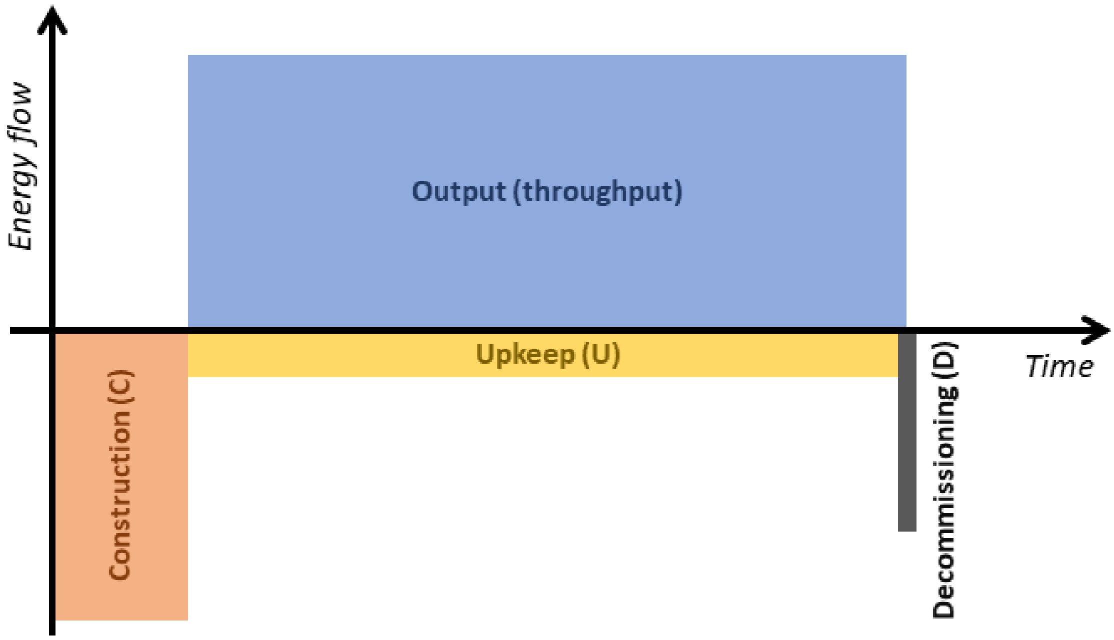

Figure 18: energy flows over the capital lifecycle (adapted from [170])

Two additional vectors can be used to describe the distribution of energy costs between capital lifecycle phases for all PC and AI types:

- The capital fraction vector, denoted $\boldsymbol{f_x}$ (dimensionless), specifies the shares of total primary equivalent input energy used for capital purposes (construction and decommissioning), or *(C+D)/ (C+U+D)* in Figure 18.
- The decommissioning fraction vector, denoted $\boldsymbol{g_x}$ (dimensionless), specifies the shares of capital energy used for decommissioning purposes, or *D/C* in Figure 18.

Where the subscripts ***x*** are replaced with ***r***, ***n***, ***s***, ***sa***, ***e***, and ***ea*** to denote primary RE PC, primary NRE PC, secondary PC, secondary AI, EU PC, and EU AI respectively. For simplicity, PC and AI lifetimes are modelled (probabilistically) as constant, regardless of the utilization of capacity, and the decommissioning phase is modelled as an instantaneous pulse.

Aggregate EC input energy costs constituting the autocatalytic loop and capital hypercycle, as indicated by the energy cost metrics, EROI and ECC, can be represented with appropriate EC proportions given by S_x correctly distributed over time with reference to the capital lifecycle. Separate components of EC input energy cost flows can be represented by vectors for construction, $\boldsymbol{\lambda_x}$, operation, $\boldsymbol{\xi_x}$, and decommissioning, $\boldsymbol{\pi_x}$. For primary PC,

$$\boldsymbol{\lambda_r} = \left(\left(\boldsymbol{\varepsilon_r} \circ \boldsymbol{f_r} \circ (\boldsymbol{j} - \boldsymbol{g_r}) \circ \boldsymbol{l_r} \circ \boldsymbol{w_r} \circ \boldsymbol{u_{rm}} \oslash (\boldsymbol{z_r} \circ \boldsymbol{\gamma_{rh}})\right)^{\boldsymbol{T}} S_r\right)^{\boldsymbol{T}}$$

$$\boldsymbol{\xi_r} = ((\boldsymbol{\varepsilon_r} \circ (\boldsymbol{j} - \boldsymbol{f_r}) \circ \boldsymbol{c_r} \circ \boldsymbol{u_r} \oslash \boldsymbol{k_r})^{\boldsymbol{T}} S_r)^{\boldsymbol{T}}$$

$$\boldsymbol{\pi_r} = \left(\left(\boldsymbol{\varepsilon_r} \circ \boldsymbol{f_r} \circ \boldsymbol{g_r} \circ \boldsymbol{l_r} \circ \boldsymbol{h_r}(t\boldsymbol{j} - \boldsymbol{l_r}) \circ \boldsymbol{u_{rm}} \oslash \boldsymbol{\gamma_{rh}}\big(\boldsymbol{x}(t\boldsymbol{j} - \boldsymbol{l_r})\big)\right)^{\boldsymbol{T}} S_r\right)^{\boldsymbol{T}}$$

and

$$\boldsymbol{\lambda_n} = \left(\left(\boldsymbol{\varepsilon_n} \circ \boldsymbol{f_n} \circ (\boldsymbol{j} - \boldsymbol{g_n}) \circ \boldsymbol{l_n} \circ \boldsymbol{w_n} \circ \boldsymbol{u_{nm}} \oslash (\boldsymbol{z_n} \circ \boldsymbol{\gamma_n})\right)^{\boldsymbol{T}} S_n\right)^{\boldsymbol{T}}$$

$$\boldsymbol{\xi_n} = ((\boldsymbol{\varepsilon_n} \circ (\boldsymbol{j} - \boldsymbol{f_n}) \circ \boldsymbol{c_n} \circ \boldsymbol{u_n} \oslash \boldsymbol{k_n})^{\boldsymbol{T}} S_n)^{\boldsymbol{T}}$$

$$\boldsymbol{\pi_n} = \left(\left(\boldsymbol{\varepsilon_n} \circ \boldsymbol{f_n} \circ \boldsymbol{g_n} \circ \boldsymbol{l_n} \circ \boldsymbol{h_n}(t\boldsymbol{j} - \boldsymbol{l_n}) \circ \boldsymbol{u_{nm}} \oslash \boldsymbol{\gamma_n}\big(\boldsymbol{d}(t\boldsymbol{j} - \boldsymbol{l_n})\big)\right)^{\boldsymbol{T}} S_n\right)^{\boldsymbol{T}}$$

Where $\boldsymbol{\varepsilon_r}$ and $\boldsymbol{\varepsilon_n}$ are vectors expressing conversion factors from primary flow type to primary energy equivalent (dimensionless; all entries 1, except for electricity output, where is 2.6 is used). Note that operational EC consumption for PC is assumed to scale linearly with CF, as lower utilization will require less maintenance related EC input, and *vice versa*.

The vectors $\boldsymbol{\gamma_{rh}(x(tj - l_r))}$ and $\boldsymbol{\gamma_n(d(tj - l_n))}$ refer to the effective EROI of PC stock removals, for RE and NRE, respectively, given by new PC EROI vectors delayed by PC lifetimes (see section 9.3.4.1):

$$\boldsymbol{x}(t\boldsymbol{j} - \boldsymbol{l_r}) \approx \boldsymbol{p_r}(0) \circ (t\boldsymbol{j} - \boldsymbol{l_r}) \oslash \left(\boldsymbol{n_r} \circ \left(\boldsymbol{p_{rm}} - \boldsymbol{p_r}(0)\right)\right) \text{ for } t\boldsymbol{j} < \boldsymbol{l_r}$$

and

$$\boldsymbol{d}(t\boldsymbol{j} - \boldsymbol{l_n}) \approx \boldsymbol{p_n} \circ (t\boldsymbol{j} - \boldsymbol{l_n}) \circ (\boldsymbol{j} + (t\boldsymbol{j} - \boldsymbol{l_n}) \oslash 2\boldsymbol{n_n}) \oslash \boldsymbol{\omega} \text{ for } t\boldsymbol{j} < \boldsymbol{l_n}$$

Where $\boldsymbol{n_r}$ and $\boldsymbol{n_n}$ are vectors of technology ages for RE and NRE PC, respectively (from technology inception to the start of the study period, in units of years). Note that for the calculation of these vectors for $\boldsymbol{0} < t\boldsymbol{j} < \boldsymbol{l_x}$, power output is assumed to take an approximately linear trend from technology inception to the start of the study period. That is, prior to a single elapsed PC operational lifetime, $\boldsymbol{y}_{rh}(\boldsymbol{x}(\boldsymbol{tj} - \boldsymbol{l}_r))$ uses exhaustion, $\boldsymbol{x}$, calculated at the RE output power rate at time $\boldsymbol{tj} - \boldsymbol{l}_r$, while $\boldsymbol{y}_n(\boldsymbol{d}(\boldsymbol{tj} - \boldsymbol{l}_n))$ uses depletion, $\boldsymbol{d}$, calculated via the time integral of NRE power output between $\boldsymbol{tj} - \boldsymbol{l}_n$ and $\boldsymbol{0}$.

For secondary and EU PC and AI, replacing subscript $\boldsymbol{x}$ with $\boldsymbol{s}$, $\boldsymbol{sa}$, $\boldsymbol{e}$, and $\boldsymbol{ea}$, respectively,

$$\boldsymbol{\lambda_x} = ((\boldsymbol{f_x} \circ (\boldsymbol{j} - \boldsymbol{g_x}) \circ \boldsymbol{w_x} \circ \boldsymbol{y_x} \oslash \boldsymbol{z_x})^{\boldsymbol{T}} S_x)^{\boldsymbol{T}}$$

$$\boldsymbol{\pi_x} = ((\boldsymbol{f_x} \circ \boldsymbol{g_x} \circ \boldsymbol{h_x}(\boldsymbol{tj} - \boldsymbol{l_x}) \circ \boldsymbol{y_x})^{\boldsymbol{T}} S_x)^{\boldsymbol{T}}$$

For secondary PC, operational EC consumption scales linearly with actual CF relative to maximum CF:

$$\boldsymbol{\xi_s} = \left(\left((\boldsymbol{j} - \boldsymbol{f_s}) \circ \boldsymbol{c_s} \circ \boldsymbol{u_s} \circ \boldsymbol{y_s} \oslash (\boldsymbol{l_s} \circ \boldsymbol{u_{sm}})\right)^{\boldsymbol{T}} S_s\right)^{\boldsymbol{T}}$$

For EU PC, operational EC consumption scales linearly with actual CF relative to target CF (i.e., operational EC consumption will rise above that indicated by ECC when $\boldsymbol{u_e} > \boldsymbol{u_{et}}$ and fall when $\boldsymbol{u_e} < \boldsymbol{u_{et}}$):

$$\boldsymbol{\xi_e} = \left(\left((\boldsymbol{j} - \boldsymbol{f_e}) \circ \boldsymbol{c_e} \circ \boldsymbol{u_e} \circ \boldsymbol{y_e} \oslash (\boldsymbol{l_e} \circ \boldsymbol{u_{et}})\right)^{\boldsymbol{T}} S_e\right)^{\boldsymbol{T}}$$

For secondary and EU AI, replacing subscript $\boldsymbol{x}$ with $\boldsymbol{sa}$ and $\boldsymbol{ea}$, respectively, CF is not defined so operational EC consumption becomes,

$$\boldsymbol{\xi_x} = \left(\left((\boldsymbol{j} - \boldsymbol{f_x}) \circ \boldsymbol{c_x} \circ \boldsymbol{y_x} \oslash \boldsymbol{l_x}\right)^{\boldsymbol{T}} S_x\right)^{\boldsymbol{T}}$$

4.2.4.5 Energy system metabolism

The autocatalytic loop, $\boldsymbol{p_a}$, is comprised of the sum of upstream energy cost flows:

$$\boldsymbol{p_a} = \sum \boldsymbol{\lambda_r}, \boldsymbol{\xi_r}, \boldsymbol{\pi_r}, \boldsymbol{\lambda_n}, \boldsymbol{\xi_n}, \boldsymbol{\pi_n}$$

Similarly, the capital hypercycle, $\boldsymbol{p_c}$, is comprised of the sum of downstream energy cost flows:

$$\boldsymbol{p_c} = \sum \boldsymbol{\lambda_s}, \boldsymbol{\xi_s}, \boldsymbol{\pi_s}, \boldsymbol{\lambda_{sa}}, \boldsymbol{\xi_{sa}}, \boldsymbol{\pi_{sa}}, \boldsymbol{\lambda_e}, \boldsymbol{\xi_e}, \boldsymbol{\pi_e}, \boldsymbol{\lambda_{ea}}, \boldsymbol{\xi_{ea}}, \boldsymbol{\pi_{ea}}$$

The sum of the autocatalytic loop and capital hypercycle ($\boldsymbol{p_a} + \boldsymbol{p_c}$; depicted in Figure 19) can be described as the metabolic energy consumption of the GES, referring to the sum energetic, autopoietic processes required for the functioning and evolution of the GES over time (i.e. the GES hypercyclic component, as discussed in section 3.1.1).

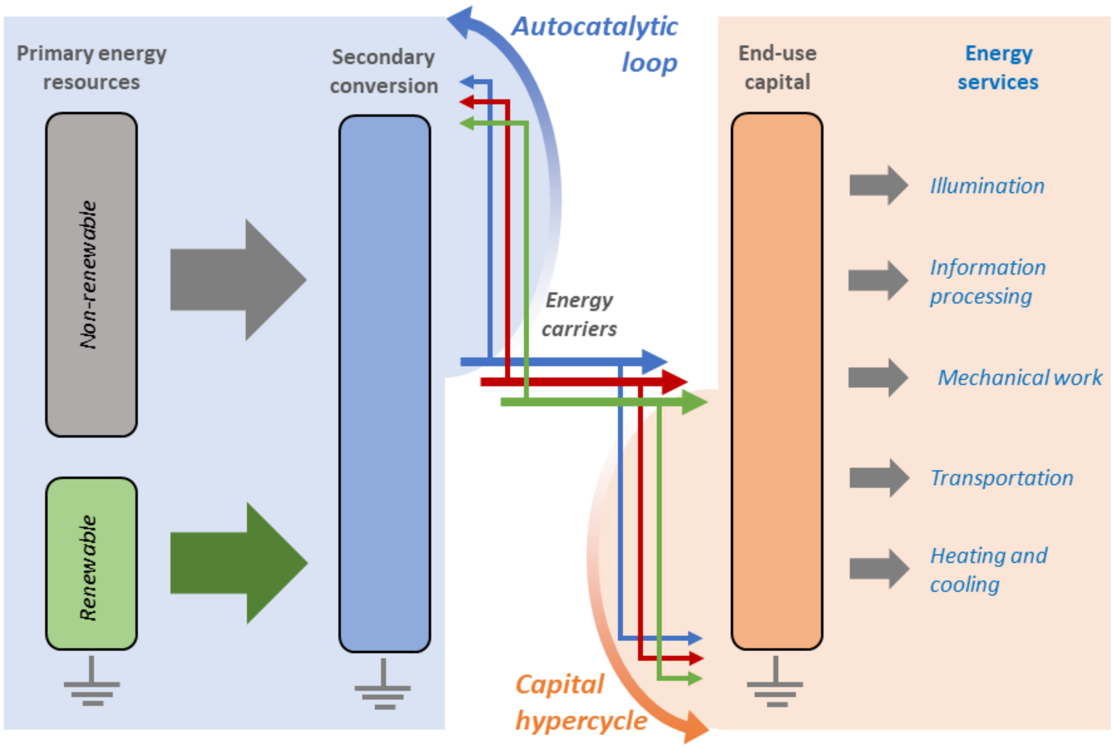

Figure 19: overview of the energy flow schema identifying the sum EC flows associated with the autocatalytic loop and capital hypercycle (the metabolic energy consumption of the GES)

As discussed in chapter 1, the GES is nested within the HSES, providing essential energy services but also intrinsically dependent on its parent system. However, a comprehensive enumeration of these interactions is extremely complex, uncertain, and includes factors that extend far beyond a physical system representation. As such, the exogeneous interface between the GES and the HSES must be represented in simple, physical, high-level terms.

The relative burden exerted by the GES on the HSES can be represented by GES metabolic energy consumption relative to total EC supply by EC type, or 'energy system metabolic ratios' (ESMRs), given by the vector $\boldsymbol{\kappa}$ (dimensionless):

$$\boldsymbol{\kappa} = (\boldsymbol{p_a} + \boldsymbol{p_c}) \oslash \boldsymbol{p_i} \quad \text{where} \quad \boldsymbol{\kappa} \ll \boldsymbol{j}$$

Giampietro et al. [21] note that these ratios, between the gross supply of ECs and the consumption of ECs within the GES, is a vital indicator of the quality of primary energy. There will necessarily be a negative relationship between this set of ratios and investment flows, $\boldsymbol{\hat{h}_x}$. That is, it will generally not be socio-metabolically feasible to devote arbitrarily high proportions of EC supply to the maintenance of the GES and away from final consumption purposes. In fact, the long-term proportion of EC supply directed towards the GES will be practically limited far below 100% due to limits facing the provision of the necessary processed materials, labour, and socio-technical capacities by the HSES. However, this broad relationship is subject to a very high degree of epistemic uncertainty, particularly considering such limits have not been seriously tested at the global scale in the context of modern industrial society, and therefore must be modelled probabilistically (see section 4.2.9.2). The nature of this feedback is determined as part of system control implementation, detailed in section 5.2.3.

ESMRs are corrected for active curtailment of secondary CFs maxima, $\boldsymbol{u_{sm}}$, due to excessive EC surplus (see section 5.2.5). Note that as ESMRs relate upstream and downstream energy costs to EC supply, and therefore correspond to the inverse of $EROI_{ext}$, disaggregated by EC component.

4.2.5 Intermittency mitigation and impacts in electricity systems

As discussed in section 2.1.2, non-linear dynamic relationships within electricity systems can be expected between the rising predominance of electricity generation from intermittent sources and both changes in the utilization of PC and associated AI requirements stemming from intermittency mitigation efforts. These interactions must be explicitly modelled to accurately capture high-level dynamic system processes involved in transformation of the GES towards RE, particularly given the need for greater electrification of ES provision. The intermittency mitigation options can be summarized as follows:

1) Building additional AI associated with intermittent PC.
2) Adding greater quantities of intermittent PC, lowering utilization.
3) Improving the responsivity of consumers to the temporal availability of supply (i.e., demand flexibility, *q*, as discussed in section 4.2.1.3)
4) Improving the technological and geographical diversity of intermittent generation.

Options 1 and 2 are referred to here as *AI mitigation* and *PC overbuild mitigation*, respectively, and represent explicit alternative intermittency mitigation strategies. Options 3 and 4 are treated as implicit factors affecting the sum requirement for intermittency mitigation.

To model intermittency impacts and the dynamic effects of mitigation strategies, identity vectors (dimensionless) are defined to specify secondary PC types belonging to intermittent, baseload, and peaking categories:

$$I_m = \begin{cases} 1 \text{ where PC type } i \text{ is considered intermittent electricity generation} \\ 0 \text{ otherwise} \end{cases}$$

$$I_b = \begin{cases} 1 \text{ where PC type } i \text{ is considered baseload electricity generation} \\ 0 \text{ otherwise} \end{cases}$$

$$I_p = \begin{cases} 1 \text{ where PC type } i \text{ is considered peaking electricity generation} \\ 0 \text{ otherwise} \end{cases}$$

An additional category identifies nominal secondary conversion (due to electricity generation at the primary stage):

$$I_k = \begin{cases} 1 \text{ where PC type } i \text{ is associated with electricity generation at the primary stage} \\ 0 \text{ otherwise} \end{cases}$$

Intermittent penetration, *m* (dimensionless scalar), the proportion of the total extant capacity to generate electrical output power consisting of intermittent generation, can then be calculated as,

$$m = \frac{(\boldsymbol{c_s} \circ \boldsymbol{u_{sm}}) \cdot I_m}{\sum_{i=1}^{n} (\boldsymbol{c_s} \circ \boldsymbol{u_{sm}} \circ I_{so})_{ic}}$$

Where electricity represents the c^{th} element in EC type vectors and secondary PC type vectors are of length *n*. Intermittent generation can also be characterized by the metric 'intermittent diversity', β (dimensionless scalar), to describe the distribution of intermittent generating capacity between various generation types. At the extremes, 0 implies power output from only one intermittent generation type while 1 implies perfect equality between all intermittent generation types.

$$\beta = \frac{(\boldsymbol{c_s} \circ \boldsymbol{u_{sm}}) \cdot I_m}{max(\boldsymbol{c_s} \circ \boldsymbol{u_{sm}} \circ I_m)_i (I_m \cdot \boldsymbol{j} - 1)} - \frac{1}{I_m \cdot \boldsymbol{j}}$$

That is, intermittent diversity is given by the mean of intermittent generation capacity divided by the maximum, adjusted to bring the lower end of the range towards 0. Note that the actual range for β is not precisely 0 to 1 but converges to this range as the number of intermittent generation types represented increases. Greater intermittent diversity is assumed to reduce the need for intermittency mitigation, as temporal supply profiles for different intermittent generation types will not be correlated, reducing the potential scale of aggregate supply/demand imbalances over shorter timescales. Greater demand flexibility, q, is also assumed to reduce the need for mitigation responses as demand will respond to align with the temporal profile of intermittent supply to a greater extent. A combined intermittency mitigation reduction factor, r (dimensionless scalar), can then be expressed as a linear function of β and q assuming the intermittent diversity and demand flexibility effects are independent and therefore multiplicative:

$$r = (1 - \beta\zeta_\beta)(1 - q\zeta_q)$$

Where ζ_β and ζ_q (dimensionless scalars) are coefficients specified for intermittent diversity and demand flexibility, respectively, representing the total fractional reduction in intermittency mitigation required should either input be equal to one. Functions can be defined to characterize the dynamic modification of various electricity system parameters via the PC overbuild and AI mitigation options:

$$\chi_f, \chi_g, \chi_h = rf(m)$$

Where χ_f, χ_g, and χ_h (dimensionless scalars) refer to fractional modification of intermittent electricity AI required, intermittent electricity reticulation efficiencies, and upstream CF maxima, respectively (equations given in section 9.3.3.2.1.1). Note that the functions are scaled linearly by the combined intermittency mitigation reduction factor, r. As the two mitigation options are alternative strategies, the functions are defined assuming the associated mitigation option is fully selected. Actual parameter modification is then assigned based on a decision variable, ψ (dimensionless scalar), representing the selected balance between the two options. ψ takes a value of zero when PC overbuild mitigation is fully selected and conversely, a value of one when the AI mitigation is fully selected. ψ is optimized dynamically within system control implementation as detailed in section 5.2.4.

To represent changes in the quantity of intermittent electricity AI required and the selected mitigation balance, the AI requirement and AI investment vectors, $\boldsymbol{a_{sa}}$ and $\boldsymbol{\hat{h}_{as}}$ (see section 4.2.2.4), are modified dynamically using modification vectors, $\boldsymbol{\gamma_f}$ and $\boldsymbol{\gamma_{fh}}$ (dimensionless), defined as,

$$(\boldsymbol{\gamma_f})_i = \begin{cases} \chi_f \text{ where element } i \text{ corresponds to intermittent electricity AI} \\ 1 \text{ otherwise} \end{cases}$$

$$(\boldsymbol{\gamma_{fh}})_i = \begin{cases} \psi \text{ where element } i \text{ corresponds to intermittent electricity AI} \\ 1 \text{ otherwise} \end{cases}$$

This implies that the full requirement for intermittent electricity AI grows as intermittent penetration increases, but the corresponding investment only takes place to the extent that the AI mitigation option is selected. AI mitigation has the side-effect of decreasing secondary reticulation efficiencies for intermittent generation from a combination of greater transmission distances and increased charge-discharge cycle losses associated with storage [193, 198, 201]. This modification of secondary reticulation efficiencies is represented via dynamic modification of the matrix of conversion factors for secondary PC output power to delivered EC, P_{so} (see section 4.2.3), using the modification vector, $\boldsymbol{\gamma_{so}}$ (dimensionless), where intermittent electricity AI represents the d^{th} element in secondary AI type vectors:

$$\boldsymbol{\gamma_{so}} = \boldsymbol{j} + \chi_g \frac{(\boldsymbol{c_{sa}})_d}{(\boldsymbol{a_{sa}})_d} I_m$$

Note that the ratio $(\boldsymbol{c_{sa}})_d/(\boldsymbol{a_{sa}})_d$, termed the built AI factor, represents the degree to which built intermittent electricity AI meets requirement for full AI mitigation.

At high intermittent penetration levels and without the requisite AI, intermittent generation and baseload generation are curtailed and peaking generation must cover more frequent supply shortfalls due to electricity system balancing dynamics [190, 356]. Therefore, changes in upstream CF maxima associated with the PC overbuild mitigation option can be expected to affect the various categories of electricity generating PC differently:

- Intermittent generation CF maxima will be suppressed by increasing intermittent penetration, as greater quantities of electricity output will need to be curtailed during more frequent instances of aggregate supply exceeding demand.
- Baseload generation CF maxima will also be suppressed by increasing intermittent penetration; however, the magnitude of this effect may be greater or less than the effect on intermittent generation depending on specific electricity system balancing dynamics, including temporal demand profiles and the system system requirement for the baseload generation role. As such, the effect magnitude relative to intermittent generation is specified by dimensionless coefficient $\rho_b > 0$.
- Peaking generation CF maxima will be increased by increasing intermittent penetration, as there will be a greater need for dispatchable, flexible generation during more frequent instances of aggregate demand exceeding supply. As such, the

effect magnitude relative to intermittent generation specified by dimensionless coefficient $\rho_p < 0$.

Changes in upstream CF maxima at the primary and secondary stages are represented via dynamic modification of the primary RE and secondary maximum CF vectors, $\boldsymbol{u_{rm}}$ and $\boldsymbol{u_{sm}}$ (see section 4.2.2.3), using the modification vectors, $\boldsymbol{\gamma_r}$ and $\boldsymbol{\gamma_s}$ (dimensionless), defined as,

$$\boldsymbol{\gamma_r} = \boldsymbol{j} + \chi_h \left(1 - \frac{(\boldsymbol{c_{sa}})_d}{(\boldsymbol{a_{sa}})_d}\right) I_{rsi}(I_k \circ I_m)$$

and

$$\boldsymbol{\gamma_s} = \boldsymbol{j} + \chi_h \left(1 - \frac{(\boldsymbol{c_{sa}})_d}{(\boldsymbol{a_{sa}})_d}\right) \left((\boldsymbol{j} - I_k) \circ I_m + \rho_b I_b + \rho_p I_p\right)$$

Note that no primary NRE PC types produce electricity at the primary stage, and therefore, $\boldsymbol{\gamma_n} = \boldsymbol{j}$. All parameters involved in intermittency mitigation modelling are subject to a high degree of epistemic uncertainty and must be modelled probabilistically (see section 4.2.9.2).

4.2.6 Causal loop diagrams

The physical GES modelling approach described in previous sections can be depicted via causal loop diagrams relating key model variables and interactions; demand, energy flows, and PC utilization in Figure 20, PC and AI investment and lifecycle in Figure 21, and primary energy resources and EROI in Figure 22. Note that the causal loops associated with system control are given in Figure *25* (in section 5.2). Descriptions of feedback loops and associated phenomena are provided in section 9.2. Diagrams use the following conventions:

- Bold elements are stocks, italic elements appear in more than one diagram.
- Lines with a double bar are subject to a time delay.
- Pluses (+) indicate causal influence in the same direction and minuses (-) in the opposite direction (arrows without either can influence in both directions).
- Feedback loops are numbered, circled with an arrow indicating loop direction, and labelled with an R for reinforcing (positive) loops or a B for balancing (negative) loops.
- Dotted lines indicate relationships that are simplified for clarity (fully detailed in a different diagram).

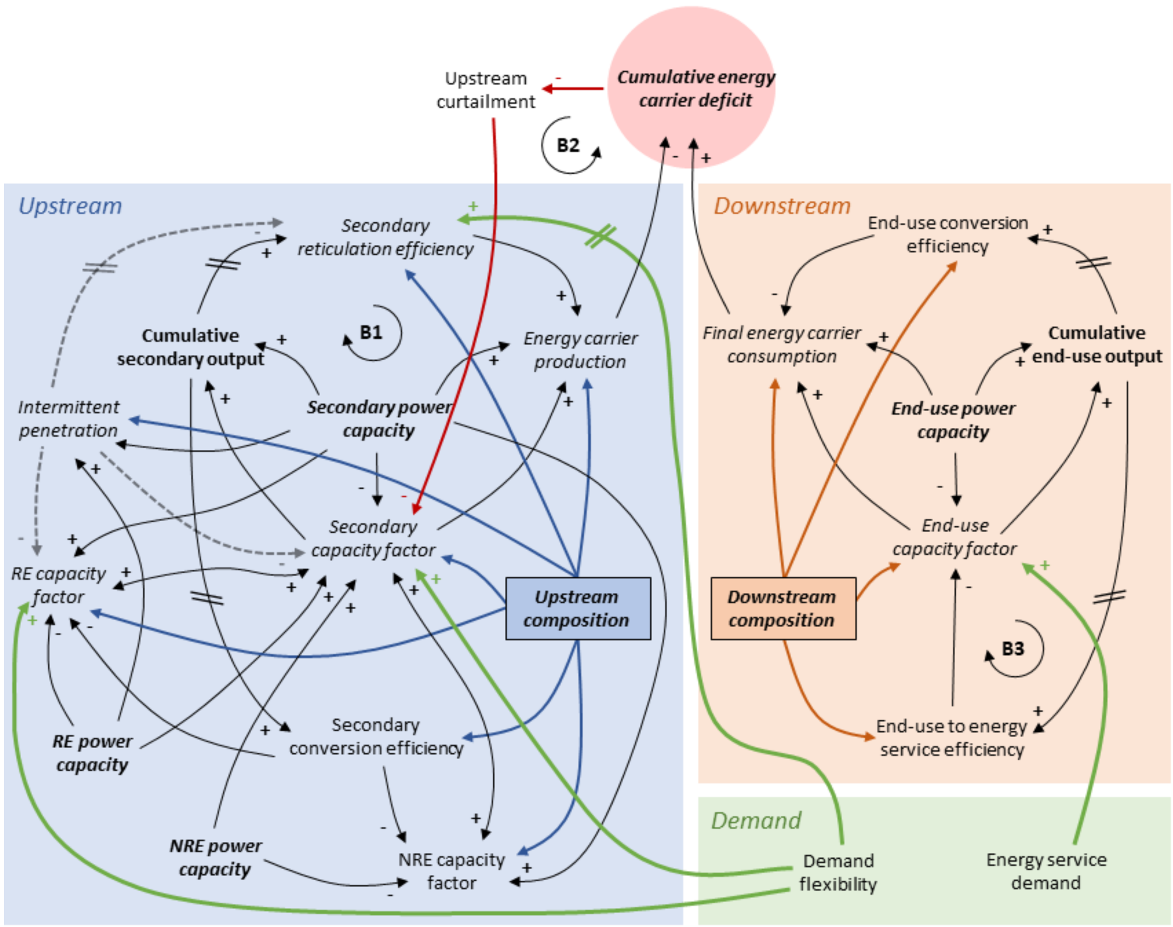

Figure 20: causal loop diagram for demand, energy flows, and PC utilization

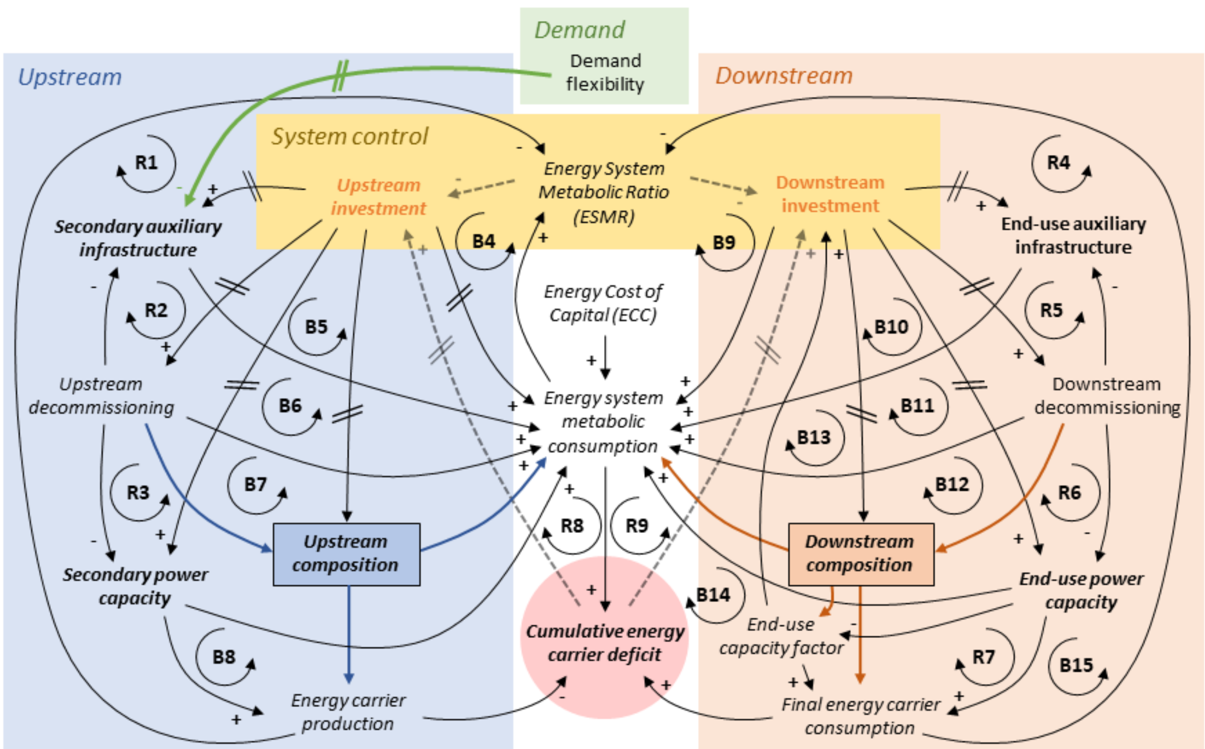

Figure 21: causal loop diagram for PC and AI investment and lifecycle

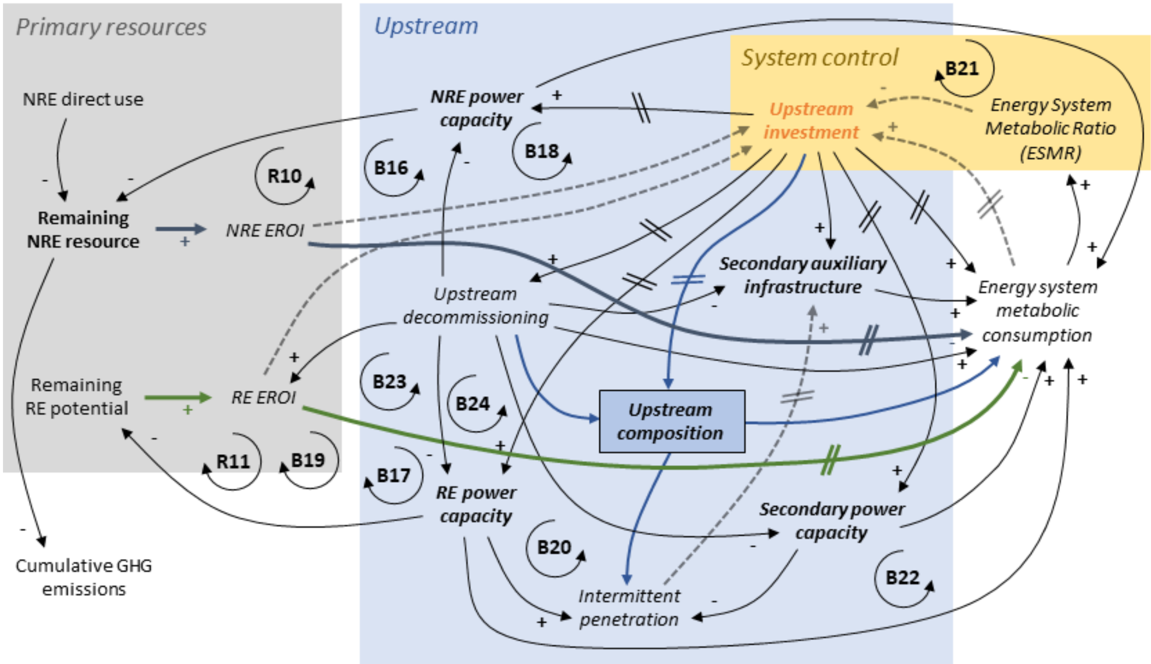

Figure 22: causal loop diagram for primary energy resources and EROI

4.2.7 Initialization

The initialization procedure is designed to establish initial values for all model variables using the simplest possible set of input information. As data to populate initial PC and AI stocks, $\boldsymbol{c_x}(0)$ as defined in section 4.2.2, are not directly available these quantities instead must be calculated from known inputs. This can be achieved via an initial static energy flow calculation, mirroring the dynamic formulation using known initial variable values. Data to populate initial ES demands, $\boldsymbol{p_d}(0)$ as defined in section 4.2.1.3, are also unavailable but are calculable via the static energy flow calculation.

Initial primary flows, $\boldsymbol{p_r}(0)$ and $\boldsymbol{p_n}(0)$, CF maxima, $\boldsymbol{u_{rm}}$, $\boldsymbol{u_{nm}}$, $\boldsymbol{u_{sm}}$, and initial target CFs, $\boldsymbol{u_{et}}(0)$, are well known and represent the main inputs to the initial static energy flow calculation. Initial primary RE and NRE PC stocks, $\boldsymbol{c_r}(0)$ and $\boldsymbol{c_n}(0)$, can be calculated assuming CFs are initially at their long-term maxima and no modifications of CF maxima due to intermittency mitigation are applied ($\boldsymbol{\gamma_r} = \boldsymbol{j}$):

$$\boldsymbol{c_r}(0) = \boldsymbol{p_r}(0) \oslash \boldsymbol{u_{rm}} \text{ and } \boldsymbol{c_n}(0) = \boldsymbol{p_n}(0) \oslash \boldsymbol{u_{nm}}$$

Calculation of initial secondary and EU PC stocks, $\boldsymbol{c_s}(0)$ and $\boldsymbol{c_e}(0)$, requires the definition of vectors for the initial input proportions of primary energy flows to secondary PC, and EC flows to EU PC, normalized across each flow type, $\boldsymbol{s_s}$ and $\boldsymbol{s_e}$ (dimensionless), respectively. Secondary PC and AI stocks, $\boldsymbol{c_s}$ and $\boldsymbol{c_{sa}}$, can be calculated directly:

$$\boldsymbol{p_s}(0) = \boldsymbol{e_{si}}(\mathbf{0}) \circ (\boldsymbol{p_r}(0)^{\boldsymbol{T}} I_{rsi} + \boldsymbol{p_n}(0)^{\boldsymbol{T}} I_{nsi})^{\boldsymbol{T}} \circ \boldsymbol{s_s}$$

$$\rightarrow \boldsymbol{c_s}(0) = \boldsymbol{p_s}(0) \oslash \boldsymbol{u_{sm}}$$

$$\rightarrow \boldsymbol{c_{sa}}(0) = (\boldsymbol{p_s}(0)^{\boldsymbol{T}} I_{sa})^{\boldsymbol{T}} \circ \boldsymbol{v_{sa}}(0)$$

Initial EC supply, $\boldsymbol{p_i}(0)$, and initial autocatalytic loop consumption, $\boldsymbol{p_a}(0)$, are then given by,

$$\boldsymbol{p_i}(0) = \left(\left(\boldsymbol{e_{so}}(\mathbf{0}) \circ \boldsymbol{p_s}(0)\right)^{\boldsymbol{T}} I_{so}\right)^{\boldsymbol{T}}$$

$$\boldsymbol{p_a}(0) = \sum \boldsymbol{\lambda_r}(0), \boldsymbol{\xi_r}(0), \boldsymbol{\pi_r}(0), \boldsymbol{\lambda_n}(0), \boldsymbol{\xi_n}(0), \boldsymbol{\pi_n}(0)$$

Where all the components of $\boldsymbol{p_a}(0)$ on the RHS are calculated as per the dynamic equivalents given in sections 4.2.4.3 and 4.2.4.4 (see section 9.3.4.1 for details of initial mean PC EROI calculations) using initial input values and the following approximation:

$$\boldsymbol{\delta}(0) \approx \frac{\boldsymbol{p_i}(0)}{\left(\boldsymbol{\varepsilon} \circ \boldsymbol{p_i}(0)\right) \cdot \boldsymbol{j}}$$

That is, the initial EC proportions of final demand are assumed to be equivalent to the initial EC proportions of EC supply. This approximation is required as initial flow calculations of metabolic energy consumption of the GES and final EC demand require $\boldsymbol{\delta}(0)$ as an input (which is itself a function of the metabolic energy consumption of the GES). Also, for all PC and AI stocks, $\boldsymbol{c_x}(0)$, associated stocks in construction, $\boldsymbol{w_x}(0)$, are calculated based on specified initial growth rates given by the vector $\boldsymbol{\iota_x}$:

$$\boldsymbol{w_x}(0) = (\boldsymbol{j} + \boldsymbol{\iota_x}) \circ \boldsymbol{c_x}(0) \circ \boldsymbol{z_x} \oslash \boldsymbol{l_x}$$

To complete the initial flow calculations, it is also assumed that initial EC supply, $\boldsymbol{p_i}$, and initial EC demand, $\boldsymbol{p_o}$, are approximately equal (i.e., no initial supply/demand imbalance):

$$\frac{d\boldsymbol{b}(0)}{dt} \approx \mathbf{0}$$

$$\therefore \boldsymbol{p_e}(0) = \boldsymbol{e_{ei}}(\mathbf{0}) \circ \left(\left(\boldsymbol{p_i}(0) - \boldsymbol{p_a}(0) - \boldsymbol{p_c}(0)\right)^{\boldsymbol{T}} I_{ei}\right)^{\boldsymbol{T}} \circ \boldsymbol{s_e}$$

The above expression cannot be solved analytically, as initial capital hypercycle consumption, $\boldsymbol{p_c}(0)$, is unknown and is a function of initial EU output power and corresponding PC. As such, a numerical solution is required. This is achieved by iteratively estimating EU PC, $\boldsymbol{c_e}(0)$, and calculating the resulting capital hypercycle consumption until the above relation holds within an acceptable margin of error (mean square error < 0.001 EJ^2/yr^2; see the initial capital hypercycle non-linear iterative solver script in section 9.4.5.2). After a numerical solution for $\boldsymbol{p_e}(0)$ is found, EU PC and AI stocks, $\boldsymbol{c_e}(0)$ and $\boldsymbol{c_{ea}}(0)$, can be calculated:

$$\rightarrow \boldsymbol{c_e}(0) = \boldsymbol{p_e}(0) \oslash \boldsymbol{u_{et}}$$

$$\rightarrow \boldsymbol{c_{ea}}(0) = (\boldsymbol{p_e}(0)^{\boldsymbol{T}} I_{ea})^{\boldsymbol{T}} \circ \boldsymbol{v_{ea}}(0)$$

Finally, initial ES demands, $\boldsymbol{p_d}(0)$, can be calculated from initial EU output power and initial EU to ES efficiencies:

$$\boldsymbol{p_d}(0) = \left(\left(\boldsymbol{p_e}(0) \circ \boldsymbol{e_{eo}}(\mathbf{0})\right)^{\boldsymbol{T}} I_{eo}\right)^{\boldsymbol{T}}$$

4.2.8 Exogenous interface modelling

The modelling approach described in previous sections involves instances where bounded relationships between two variables, representing factors exogenous to the modelling formulation, must be defined. Logistic (or sigmoid) functions are chosen to model these interfaces for specified dependent and independent variables. The general form of the logistic function used is,

$$f(x) = \frac{L - c}{1 + e^{-k(x - x_m)}} + c$$

Where, L and c are the upper and lower function asymptotes, respectively,
k is the logistic growth rate (determining the steepness of the curve), and
x_m is the x-value of the curve inflection point.

Logistic curves are commonly observed in physical systems, arising from growth and saturation effects within constraints. Using this general function, a wide variety of curve shapes between two arbitrary points can be generated depending on the input parameters selected, including curves which are approximately linear, exponential, and logarithmic, as shown in Figure 23 (parameters displayed in the format *(L, c, k, x_m)*).

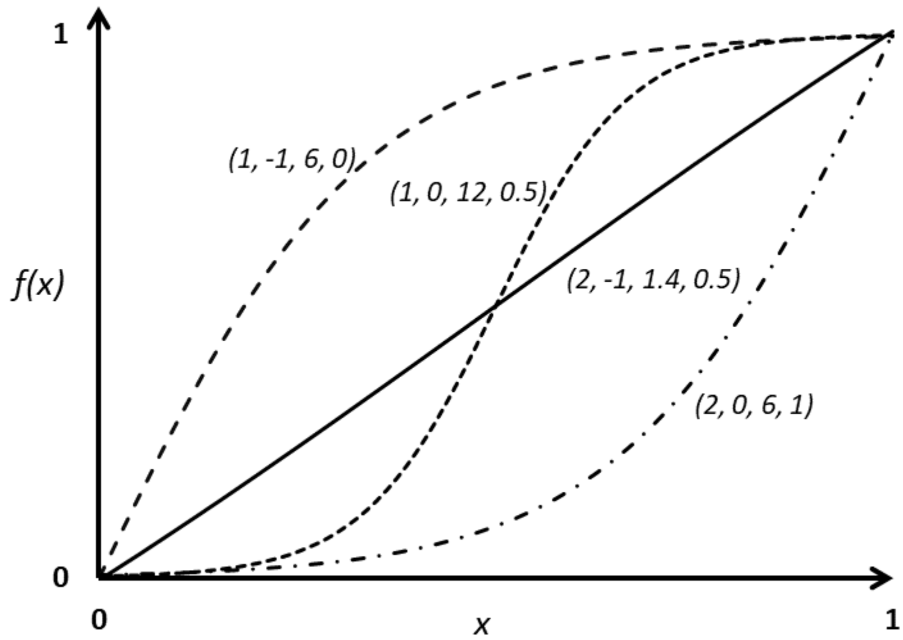

Figure 23: logistic function examples, including approximate linear, exponential, and logarithmic curves

Logistic modelling is used for the exogenous interface functions listed in Table 3, with probabilistically generated input parameters representing epistemic uncertainty (see section 4.2.9.2). Note that logistic modelling is not applied to the ESMR interface described in section 4.2.4.5 (see section 5.2.3 for details).

Table 3: exogenous interface functions using logistic modelling, including reference section for function equations

Dependent variable	Independent variable	Exogenous interface factor	Section
New PC EROI ($\boldsymbol{\chi}_r$, $\boldsymbol{\chi}_n$)	RE exhaustion, NRE depletion ($\boldsymbol{x}$, $\boldsymbol{d}$)	*Primary energy resource quality distributions*	9.3.4.2.1
New PC efficiency ($\boldsymbol{\partial}_{si}$, $\boldsymbol{\partial}_{so}$, $\boldsymbol{\partial}_{ei}$, $\boldsymbol{\partial}_{ei}$)	Cumulative secondary, EU power output ($\int \boldsymbol{p}_s dt$, $\int \boldsymbol{p}_e dt$)	*Technological learning effects on PC efficiencies*	9.3.1.4.1
EU CF target ($\boldsymbol{u}_{et}$)	Time (t)	*Achievable levels of EU PC utilization*	9.3.1.3.1
ES demand ($\boldsymbol{p}_d$)		*Final demand for delivered ESs*	9.3.2.1
Demand flexibility (q)		*Responsiveness of demand to the temporal availability of AI capacity and intermittent supply*	9.3.2.2
Intermittent electricity AI multiplier (χ_f)	Intermittent penetration (m)	*Electricity system AI dynamics for intermittency mitigation*	9.3.3.2.1.1
Reticulation efficiency multiplier (χ_g)		*Electricity system reticulation efficiency impacts associated with AI mitigation*	

Dependent variable	Independent variable	Exogenous interface factor	Section
Maximum CF multiplier (χ_h)		*Electricity system CF impacts associated with PC overbuild mitigation*	

4.2.9 Simulation of GES transformation pathways

4.2.9.1 GES evolution

The physical GES modelling approach described in this chapter centres on the reinvestment of energy required to support and transform the energy system over time while meeting society's needs for ESs. Using equation 1 from section 4.2.1.2 and equations 2 and 3 from section 4.2.3, the cumulative supply/demand balance vector, $\boldsymbol{b}$, can be rewritten as,

$$\boldsymbol{b}(t=\tau)=\int_0^{\tau}\left(\left(\boldsymbol{p}_{\boldsymbol{r}}^{\boldsymbol{T}}C_{rs}+\boldsymbol{p}_{\boldsymbol{n}}^{\boldsymbol{T}}C_{ns}-\boldsymbol{p}_{\boldsymbol{d}}^{\boldsymbol{T}}C_e\right)^{\boldsymbol{T}}-\boldsymbol{p}_{\boldsymbol{a}}-\boldsymbol{p}_{\boldsymbol{c}}\right)dt$$

Note that all terms on the RHS are functions of PC and AI stocks in various lifecycle stages within the GES, except for the vector of ES final demands, $\boldsymbol{p_d}$, which is exogenously (and probabilistically) defined and drives system evolution over time. This relation is central to the dynamic transformation of the GES. The relative scarcity or abundance of ECs acts as a bridge between the upstream and downstream sectors, allowing for a bounded co-evolution of supply and demand. Supply and demand are not forced into equality, but instead, imbalances provide signals for investment via upstream and/or downstream responses:

- Adding upstream PC, boosting the supply of scarce ECs.
- Shifting downstream PC composition towards modes of ES provision using more abundant ECs, conserving scarce ECs.
- These responses are determined via system control, as detailed in section 5.2.

As primary flows, $\boldsymbol{p_r}$ and $\boldsymbol{p_n}$, are flow and stock limited, respectively, due to finite primary energy resources, the overall GES transformation process can be seen as demand-driven but supply-constrained (i.e., consistent with the post-Keynesian ecological perspective; see section 3.1.3). Primary energy resource constraints impose inevitable increases in the autocatalytic loop over time as primary energy resource quality declines, requiring more energy to be redirected into primary energy production processes.

Any given sequence of PC investment flows, $\boldsymbol{\hat{h}_x}$, will have subsequent, delayed impacts on energy flows, PC and AI stocks, capacity utilization, efficiency improvements, RE and NRE

EROI, and the autocatalytic loop and capital hypercycle. As such, investment flows at any given time will reflexively determine possibilities for future investment flows, as the potential to redirect a proportion of gross EC supply towards investment within the GES is dynamically limited via ESMR feedback (as discussed in section 4.2.4.5). The resulting path-dependent evolutionary trajectory of the GES represents a single, unique transformation pathway.

Note that real-world ES demand destruction or stimulation in response to the cumulative EC supply/demand balance, $\boldsymbol{b}$ (as a price proxy), will act to flatten supply/demand imbalances and return $\boldsymbol{b}$ towards $\boldsymbol{0}$. While this is not explicitly modelled via the modification of $\boldsymbol{p_d}$, it is functionally consistent with the chosen representation of $\boldsymbol{b}$ as an integral function and the gradual elimination of cumulative EC imbalances via both upstream and downstream responses. That is, $\boldsymbol{b}$ will tend to be serially autocorrelated representing delayed price-consumption feedback, as periods where demand exceeds supply (signalling higher prices) will necessarily be followed by periods where supply exceeds demand (signalling lower prices), and *vice versa*. Also, adaptation to EC scarcity or abundance is achieved via changes in downstream investment flows, $\boldsymbol{\hat{h}_e}$, following changes in $\boldsymbol{b}$, decreasing the consumption of scarce ECs and increasing the consumption of more abundant ECs. Where EC surplus (suggesting lower prices) accrues due to efficiency improvements, this fuel switching effect represents a partial endogenization of the rebound effect (as discussed in section 2.2.1).

The internal viability of a given transformation pathway is defined by successfully avoiding a net energy trap (see section 3.1.2.3), indicated by the $\boldsymbol{b}$ vector returning towards $\mathbf{0}$ following deviations, while staying within acceptable bounds (see section 4.2.9.3). This outcome is contingent upon the specific sequence of $\boldsymbol{\hat{h}_x}$ as determined by system control, guided by chosen investment logic and normative goals for the GES transformation process (discussed in section 5.2). Conversely, failure of a given pathway (i.e., encountering a net energy trap) is indicated by an inexorable negative trend in at least one component of the $\boldsymbol{b}$ vector, implying insufficient EC supply to meet ES demands while supplying the metabolic energy consumption of the GES. This is a valid result only where the outcome is invariant to changes in the specific system control implementation and related parameters (detailed in section 5.2.3)

4.2.9.2 Probabilistic formulation

The implications of epistemic uncertainty for the GES transformation solution space can be investigated via probabilistic modelling (as outlined in section 4.1.3). As discussed in section 3.1.4.3, Monte Carlo methods can be applied to the repeated simulation of GES transformation pathways (each a model 'realization') to produce an ensemble representing the set of system possibilities given epistemic uncertainty in input parameters. This allows the detection of consistent system tendencies at the ensemble level (with implicit ensemble-level filtering of optimism or pessimism bias) and the identification of the potential impacts of estimation errors (i.e., sensitivity analysis; see section 5.5.1). Note that the initialization procedure, described in section 4.2.7, is carried out for each realization individually, after the sampling of probabilistic input distributions.

Some input parameters are not expected to vary independently, as higher values in one will tend to occur alongside higher (or lower) values in others, and *vice versa*. This can occur due to exogenous factors and causal relationships affecting specific parameter categories, or the need to align implicit assumptions and semantic definitions (applying the principle of semantic openness) for the generation of input parameter value sets. As such, correlations between sampled values for specific parameter categories should be modelled where required (see section 9.4.7 for details). Input correlation offers a useful refinement of the input space given the high number of dimensions involved, limiting input parameter value sets to those considered to be more plausible.

Selecting appropriate probability distribution types for input parameters is necessarily subjective, requiring expert elicitation. Note that it is not generally possible to perform valid statistical tests to determine distributions of best fit, as few relevant independent data sources exist for the estimation of most model input parameters (see section 9.5.1). The decision tree depicted in Figure 24 is used for the selection of appropriate distribution types (see sections 9.4.2 and 9.5 for distribution details) based on a preference hierarchy:

- Normal and log-normal distributions are used where a sufficient number of independent parameter data sources exist to estimate population standard deviation, σ (typically six or more). This is preferable as the effects of low probability values of input parameters on model behaviour corresponding to the distribution tails are incorporated.

- For log-normal distributions, the logarithm of the input parameter is normally distributed, resulting in sampled values varying by orders of magnitude.
- Truncated distributions are used where parameters have upper or lower limits.

- Where available data sources are insufficient to estimate σ:
    - Triangular distributions are used where probability density function (PDF) maxima can be identified.
    - Uniform distributions are used where no clear PDF maxima can be identified. These simple distribution types suffer from PDF discontinuities at the distribution extremes, so are avoided where possible.
- Pareto distributions are used solely where logistic function shape is controlled via specification of an upper asymptote, as explained in section 9.4.2.1.

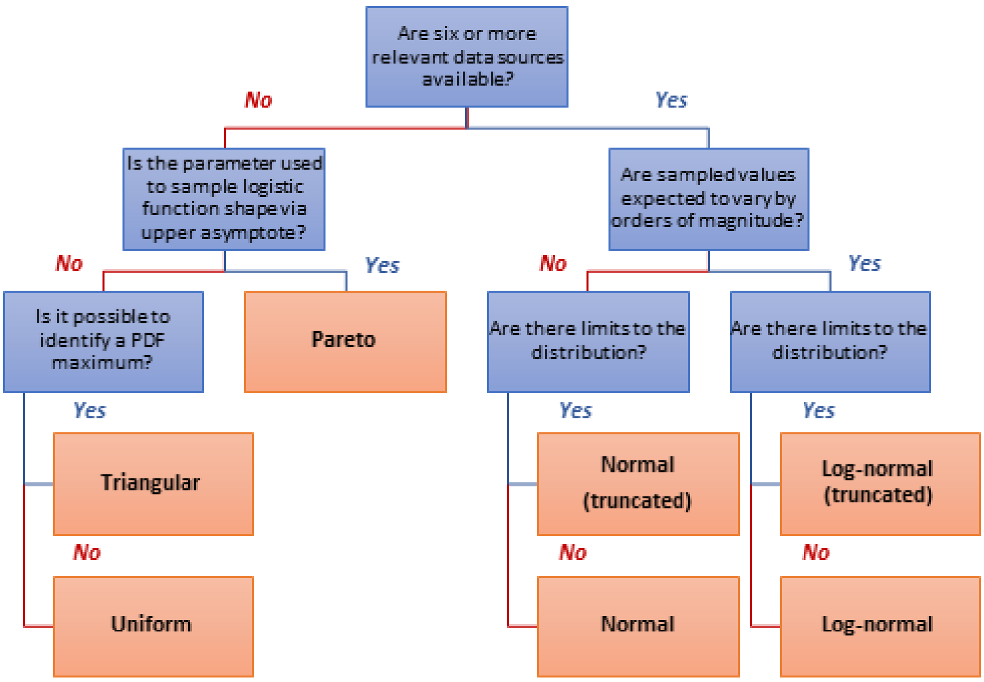

Figure 24: decision tree for the selection of probability distribution type for epistemically uncertain input parameters

Failed GES transformation pathways (exhibiting a net energy trap outcome, as discussed in section 4.2.9.1) can be expected occur in a subset of realizations within any ensemble. Failure at the realization level can be generalized to the ensemble level as the metric 'system stability', defined as the failure incidence rate.

4.2.9.3 Informational output metrics

A series of informational output metrics external to feedback loops determining model behaviour can be constructed to track pertinent aspects of GES evolution. The following metrics are used to characterize changes in the contribution of RE relative to NRE, net energy return at the point of end-use, climate implications of GES transformation, and the incidence of net energy trap outcomes.

Total primary energy supply (TPES) in terms of primary energy equivalent is given by,

$$\boldsymbol{p_n} \cdot \boldsymbol{j} + (\boldsymbol{\varepsilon_r} \circ \boldsymbol{p_r}) \cdot \boldsymbol{j}$$

The share of EC supply derived from RE sources by EC type is given by,

$$\boldsymbol{p_r^T} C_{rs} \oslash (\boldsymbol{p_r^T} C_{rs} + \boldsymbol{p_n^T} C_{ns})$$

The corresponding RE share of TPES, in terms of primary energy equivalent, is given by,

$$\left(\boldsymbol{\varepsilon^T} \circ \boldsymbol{p_r^T} C_{rs} \oslash \left(\boldsymbol{\varepsilon^T} \circ (\boldsymbol{p_r^T} C_{rs} + \boldsymbol{p_n^T} C_{ns})\right) \cdot \boldsymbol{j}\right) \cdot \boldsymbol{j}$$

Point of Use EROI ($EROI_{pou}$) calculated at the system-level and disaggregated by EC type is given by,

$$(\boldsymbol{p_r^T} C_{rs} + \boldsymbol{p_n^T} C_{ns}) \oslash \boldsymbol{p_a^T}$$

The global GHG emissions rate can be calculated using a vector of GHG emissions intensities by NRE type, $\boldsymbol{\theta}$ (units of $GtCO_2e/EJ$), and the non-energy GHG emissions rate, ς:

$$\left(\boldsymbol{\theta} \circ (\boldsymbol{p_n} + \boldsymbol{p_{ne}})\right)^{\boldsymbol{T}} \cdot \boldsymbol{j} + \varsigma$$

This metric assumes the GHG content of all NRE quantities produced ultimately reach the atmosphere, i.e., no CCS or other negative emissions technologies are represented. The corresponding cumulative global GHG emissions from the beginning of the study period at elapsed time τ, assuming a constant non-energy GHG emissions rate, is then given by,

$$\left(\boldsymbol{\theta} \circ \int_{t=0}^{\tau} (\boldsymbol{p_n} + \boldsymbol{p_{ne}}) dt\right)^{\boldsymbol{T}} \cdot \boldsymbol{j} + \varsigma\tau$$

Finally, failure of a given GES transformation pathway (implying a net energy trap outcome, as discussed in section 4.2.9.1) can be identified when the EC deficit (defined as negative cumulative supply/demand balance relative to total EC demand, by EC type) exceeds defined thresholds, either for individual ECs or as a mean across all ECs:

$$max(-\boldsymbol{b} \oslash \boldsymbol{p_o})_i > a \text{ or } \frac{-(\boldsymbol{b} \oslash \boldsymbol{p_o}) \cdot \boldsymbol{j}}{n} > b$$

Where EC type vectors are of length *n*. Failure can also be specified with reference to a supply/demand balance rate of change threshold:

$$max\left(\frac{-d(\boldsymbol{b} \oslash \boldsymbol{p_o})}{dt}\right)_i > c \text{ or } \frac{-d(\boldsymbol{b} \oslash \boldsymbol{p_o})}{dt} \cdot \frac{\boldsymbol{j}}{n} > d$$

Thresholds *a, b, c,* and *d* are arbitrary but should be selected such that they separate those realizations where recovery (***b*** vector returning towards **0**) is possible from those where EC deficits grow inexorably, as effectively as possible. That is, thresholds should correspond to GES bifurcation potential. As a corollary metric, stable time can be defined as the elapsed simulation time before failure thresholds are reached. A shorter stable time suggests greater inherent instability of the relevant pathway, and *vice versa*.

5 THE PRESS MODEL

The Probabilistic Renewable Energy Solution Space, or PRESS, model (v1.3) is an exploratory system dynamics computer model created to investigate the solution space for GES transformation from NRE to RE during the remainder of the 21st century, under uncertainty. This is an implementation of the physical GES modelling approach described in chapter 4.

PRESS was built using the GoldSim simulation platform (version 12.1.2). This software is designed for the Monte Carlo simulation of complex systems using an extended system dynamics syntax. This platform is ideal for the physical GES modelling approach as it is methodologically aligned with a biophysical, complex systems perspective incorporating a high degree of epistemic uncertainty.

GES evolution within transformation pathways generated by the PRESS model is endogenously directed during the simulation period via a control system, detailed in section 5.2. The selected study period is from 2015 to 2100:

- The study period begins at 2015 as this year approximately aligns with the majority of available data for the estimation of GES input parameters (without extrapolations requiring additional time series data).
- The study period ends at 2100 as simulation of GES transformation pathways beyond this point is less policy-relevant and is subject to excessive uncertainties.

- Hence, results generated using the PRESS model correspond to GES transformation pathways begun in the year 2015 (i.e., results are optimistic regarding GES transformation potentialities relative to currently achievable outcomes).

The PRESS model features 3,639 scalar input parameters, and 14,218 scalar and time series outputs. The model uses a simulation timestep of 6 weeks, resulting in 823 scheduled model time steps for each realization. Version history for the PRESS model is given in section 9.1. The calculation of input parameters, including data sources, data processing and assumptions, and final input parameter arrays are detailed in section 9.5.

5.1 SELECTED ARRAY ELEMENTS

The general arrays introduced in section 4.2 must be explicated by selecting specific elements comprising all vector types. These arrays simultaneously define chosen levels of aggregation and selected functional-structural mappings for high-level modelling of the GES (i.e., elements represent structural realizations with respect to the functional role defined by their characteristic inflow and outflow types). As established in the pre-analytical framework discussed in section 4.1, elements are chosen such that the simplified, high-level representation of the GES maintains as much functional differentiation as possible, while avoiding speculative and unproven technologies. Array elements are listed in Table 4.

Table 4: selected array elements in the PRESS model with associated inflows and outflows

Element set	Index	Label	Inflow	Outflow
RE types	1	Solar PV		Electricity
	2	Solar thermal		Solar thermal
	3	Wind		Electricity
	4	Biomass		Biomass
	5	Hydropower		Electricity
	6	Geothermal		Geothermal
	7	Other RE		Electricity
NRE types	1	Oil		Oil
	2	Natural gas		Natural gas
	3	Coal		Coal
	4	Nuclear fuels		Nuclear fuels
Secondary PC types	1	Oil generation	Oil	Electricity
	2	Refining		LaG fuels
	3	Oil heat		Heat
	4	Gas generation	Natural gas	Electricity
	5	Gas to LaG		LaG fuels
	6	Gas heat		Heat

Element set	Index	Label	Inflow	Outflow
	7	Gas CHP		Electricity and heat
	8	Coal generation	Coal	Electricity
	9	Coal to LaG		LaG fuels
	10	Coal heat		Heat
	11	Coal CHP		Electricity and heat
	12	Nuclear generation	Nuclear fuels	Electricity
	13	Solar PV generation	Electricity	
	14	Solar thermal generation	Solar thermal	
	15	Solar thermal heat		Heat
	16	Wind generation	Electricity	Electricity
	17	Biomass generation	Biomass	
	18	Biofuels		LaG fuels
	19	Biomass heat		Heat
	20	Biomass CHP		Electricity and heat
	21	Hydropower generation	Electricity	Electricity
	22	Geothermal generation	Geothermal	
	23	Geothermal heat		Heat
	24	Other RE generation	Electricity	Electricity
Secondary AI types	1	Electricity AI		
	2	Intermittent electricity AI		
	3	LaG fuels AI		
	4	Heat AI		
EC types	1	Electricity		
	2	LaG fuels		
	3	Heat		
EU PC types	1	Electric lighting	Electricity	Illumination
	2	IPaC devices		IPaC
	3	Electric mechanical		Static mechanical
	4	LaG fuel mechanical	LaG fuels	
	5	ICEV light		Transport passenger regional
	6	ICEV heavy passenger		
	7	ICE rail passenger		
	8	Electric vehicles	Electricity	
	9	Electric rail passenger		
	10	Aviation passenger regional	LaG fuels	
	11	Shipping passenger regional		
	12	Aviation passenger IC		Transport passenger IC
	13	Shipping passenger IC		
	14	ICEV heavy freight		Transport freight regional
	15	ICE rail freight		
	16	Electric rail freight	Electricity	
	17	Aviation freight regional	LaG fuels	
	18	Shipping freight regional		
	19	Aviation freight IC		Transport freight IC
	20	Shipping freight IC		
	21	Electric cooling	Electricity	Cooling
	22	LaG fuel heating low temp.	LaG fuels	Low temp. heating

Element set	Index	Label	Inflow	Outflow
	23	Electric heating low temp.	Electricity	
	24	Heat heating low temp.	Heat	
	25	Electric heating high temp.	Electricity	High temp. process heat
	26	Heat heating high temp.	Heat	
EU AI types	1	Electrical AI		
	2	IPaC AI		
	3	LaG fuels AI		
	4	Roading AI		
	5	Electric vehicles AI		
	6	Rail AI		
	7	Rail electrification AI		
	8	Aviation AI		
	9	Shipping AI		
	10	Heating AI		
ES types	1	Illumination		
	2	IPaC		
	3	Static mechanical		
	4	Transport passenger regional		
	5	Transport passenger IC		
	6	Transport freight regional		
	7	Transport freight IC		
	8	Cooling		
	9	Low temp. heating		
	10	High temp. process heat		

Primary energy resources consist of the fossil fuels (oil, coal, and natural gas) and nuclear fuels. Only fissile fuels used in current generation nuclear reactors are included (i.e., no experimental or speculative fuel types). Nuclear electricity generation is modelled at the secondary stage. Conventional and unconventional NRE resources are grouped together, as these categories can be defined within the same EROI quality distributions. For solar thermal, biomass, and geothermal primary RE resources, conversion to multiple ECs is possible and is modelled at the secondary stage. 'Other RE' includes all minor RE resources not otherwise specified, primarily ocean-based technologies such as tidal and wave power.

Selected ECs are electricity, liquid and gaseous (LaG) fuels, and heat as these categories are approximately exhaustive and exhibit distinct functional characteristics:

- Electricity is highly versatile and is the primary fuel for EU applications involving electric motors, electronic circuits, resistive heating and lighting, and electrochemical and semiconductor devices.

- Liquid and gaseous fuels (LaG fuels) are energy dense and portable combustible fuels, typically composed of various hydrocarbons (but can also include hydrogen and ammonia), primarily used in transportation and for mobile equipment.
- Heat is generated from solid and gaseous combustible fuels, and from solar thermal and geothermal sources, and can be applied to both high temperature (> 500 K) process heat and low temperature (< 500 K) heating applications.
- Note that limits to substitution exist within the LaG fuel and heat EC categories, as defined above. This is discussed further in section 5.4.

Selected ES categories are based on Fell [224], modified to correspond to exhaustive and functionally distinct roles within the GES. Transportation is separated by passenger and freight, and by approximate geographical range, as functional distinctions are apparent between these groups (i.e, mutual substitutability is minimal). These selected ESs are listed in Table 5 along with predominant associated end-use sectors.

Table 5: selected ESs and predominant associated end-use sectors

Energy service	End-use sector
Illumination	***Residential and commercial***
Information processing and communication (IPaC)	
Cooling	
Low temperature heating	
Static mechanical work	***Industrial***
High temperature process heat	
Regional passenger transportation	***Transportation of people***
Intercontinental passenger transportation	
Regional freight transportation	***Transportation of goods***
Intercontinental freight transportation	

IPaC refers to all forms of communication, entertainment, computing, and information storage (including end user devices and the PC comprising IPaC networks). Cooling refers to refrigeration and space cooling. Static mechanical work consists of all mechanical work performed by PC for purposes other than transportation or cooling. Passenger and freight transportation are each split into two categories based on distance and geographical factors:

- Regional transportation is typically land-based but can also utilize regional waterways and short- to medium-distance aviation.

- Intercontinental (IC) transportation is typically long-distance, transiting major geographical barriers such as oceans and territories lacking land-based transport infrastructure, and is practically limited to shipping and aviation.
- Non-trivial functional differences are apparent between PC serving these two transportation categories, in terms of PC utilization and conversion efficiencies.

Based on the selection of secondary PC types listed in Table 4, selected intermittent electricity generation PC types are solar PV, solar thermal generation, wind, and other RE. Selected baseload PC types are coal, nuclear, biomass, and geothermal generation. Selected peaking PC types are oil and gas generation (note, this includes both open-cycle and closed-cycle plant). Hydropower is not included in either baseload or peaking categories, as generating equipment is generally fast-responding but plant output is often constrained by local hydrology (particularly for smaller 'run-of-river' plant).

The use of light internal combustion engine (ICE) vehicles (or ICEVs) for freight transportation is not included due small payloads carried in such applications which can be considered part of passenger transportation. Electric vehicles are assumed to include all functionally equivalent vehicle types using electricity as an input, including battery and hydrogen fuel cell vehicles. Note that based on the selection of EU PC types listed in Table 4, the corresponding reference modes representing eventual ideal ES provision (as discussed in section 4.2.2.5) are:

- *Electric mechanical* for static mechanical work
- *Light vehicles (ICE and electric)* for regional passenger transportation (highest plausible achievable EU to ES efficiency maxima of 52 kJ per passenger-km)
- *Passenger aviation* for IC passenger transportation (256 kJ per passenger-km)
- *Freight rail (ICE and electric)* for regional freight transportation (38 kJ per tonne-km)
- *Freight shipping* for IC freight transportation (64 kJ per tonne-km)
- See section 9.5.6.5 for calculation details.

Secondary AI types are selected corresponding to each EC type, plus an additional category associated with the integration of intermittent generation into electricity systems (as discussed in section 4.2.5). EU AI types are selected corresponding to broad, overlapping infrastructural requirements:

- Infrastructure is required by all EU PC types for handling the associated EC input: electrical, LaG fuels, and heating.
- Basic transportation infrastructure is required for all EU PC types providing transportation ESs: roading, rail, aviation (airports), and shipping (ports).
- Supplemental infrastructure is required for specific EU PC types: IPaC (supplemental to electrical AI), electric vehicles (supplemental to roading AI), and rail electrification (supplemental to rail AI).

Note that applying the criteria for technology inclusion introduced in section 4.1.2 excludes several notable technologies, specifically the production of hydrogen via electrolysis and all subsequent 'power-to-X' conversions, and niche applications such as illumination and absorption refrigeration using combustible fuels.

For the specification of EC input energy cost proportions for PC and AI relative to the EC proportions of final demand, it is assumed electricity proportions are adjusted via normalization to account for specified relative proportions for LaG fuels and heat (i.e., $\boldsymbol{\varphi_{x1}} = \boldsymbol{j}$; refer to section 4.2.4.3).

5.2 SYSTEM CONTROL

The purpose of system control is to determine time-dependent PC investment decision flow and intermittency mitigation decision variables, $\boldsymbol{\hat{h}_r}$, $\boldsymbol{\hat{h}_n}$, $\boldsymbol{\hat{h}_s}$, $\boldsymbol{\hat{h}_e}$, and ψ, in such a way that minimizes sum supply/demand imbalances relative to total EC consumption over the duration of the study period (in units of years[2]). This must be executed subject to primary energy resource and penetration limits while satisfying various secondary objectives:

1) encouraging system-level energy efficiency by minimizing sum EC consumption,
2) facilitating decarbonization of the GES by minimizing energy related cumulative GHG emissions, and
3) maintaining high utilization of upstream PC by minimizing capacity imbalances between the primary and secondary stages.

That is,

$$Minimize \ \sum_{i=1}^{n} \left(\int |\boldsymbol{b} \oslash \boldsymbol{p_o}| dt \right)_i$$

Subject to,

$$\boldsymbol{p_r} \leq \boldsymbol{p_{rm}} \qquad \int_{t=0}^{\infty}(\boldsymbol{p_n} + \boldsymbol{p_{ne}}) < \boldsymbol{\omega_{nm}} \qquad\qquad \boldsymbol{\eta_s} \leq \boldsymbol{\eta_{sm}} \qquad \boldsymbol{\eta_e} \leq \boldsymbol{\eta_{em}}$$

While achieving secondary objectives:

1) $Minimize\ \ \boldsymbol{p_o} \cdot \boldsymbol{j}$
2) $Minimize\ \ (\boldsymbol{\theta} \circ \int \boldsymbol{p_n} dt) \cdot \boldsymbol{j}$
3) $Minimize\ \ \sum_{i=1}^{n} |(\boldsymbol{c_r} \circ \boldsymbol{\gamma_r} \circ \boldsymbol{u_{rm}} - F_{rsi}\boldsymbol{j})_i| + \sum_{i=1}^{m} |(\boldsymbol{c_n} \circ \boldsymbol{\gamma_n} \circ \boldsymbol{u_{nm}} - F_{nsi}\boldsymbol{j})_i|$

Minimization of sum supply/demand imbalances, across time and all EC types, is chosen as the objective function as this is the paramount requirement for the GES as it is fundamental to efficient operation and avoidance of destabilizing deviations between supply and demand (including net energy trap outcomes). However, the presence of secondary objectives necessarily detracts from achieving optimality in the primary objective.

The above system control specification can be accomplished via exhaustive simulation and optimization, but this approach is computationally prohibitive due to the number of simulation timesteps involved, each requiring specification of more than 4,000 independent decision variable values. Instead, a system control heuristic is used to dynamically regulate decision variables in response to the evolving state of the GES. This heuristic represents the collective decision-making capabilities of the HSES to control the reinvestment of energy into the GES, and:

- assumes investment decisions are based on physical optimality in terms of net energy return, without being constrained by social, political, or economic barriers (thus yields an optimistic solution space for GES transformation, as discussed in section 4.1.1),
- is simulated concurrently with GES transformation processes using a forward projection of the objective function, implying imperfect foresight,
- is feedback-driven, analogous to real world decision-making processes and likely to be less prone to arriving at local optima than other non-linear optimization methods,
- is similar in design to a *proportional-integral-derivative* control loop, widely used in engineering and operations research as described by Wang et al. [357], and
- can be considered a satisficing method (i.e., 'fast and frugal' heuristic) due to the presence of multiple objectives [358-360].

To maximize the efficacy of the control system, and manage suboptimality and trade-offs associated with the multi-objective approach, the system control heuristic is calibrated via specified control parameters at the ensemble level (see section 9.6 for details). Note that computational cost and software limitations prevents realization-level optimization and calibration (different optimized control parameter sets for each model realization). Note also that widely employed methods for the for calibration of computer models, including 'hindcasting', are not suitable for the PRESS model as it is exploratory in design rather than predictive, and as such is not designed to replicate past system behaviour. Historical conditions shaping the evolution of the GES are not expected to represent future conditions, primarily due to:

- a rising impetus to decarbonize the GES by accelerating the transition towards RE, resulting in discontinuities in both upstream and downstream investments, and
- growth in the autocatalytic loop over time as primary energy resource quality declines.

Causal loops associated with system control are depicted in Figure *25*:

- Minor inputs to the investment share calculation are omitted for clarity.
- Blue feedback symbols identify feedback loops introduced in section 4.2.6.
- Descriptions of feedback loops and associated phenomena are given in section 9.2.

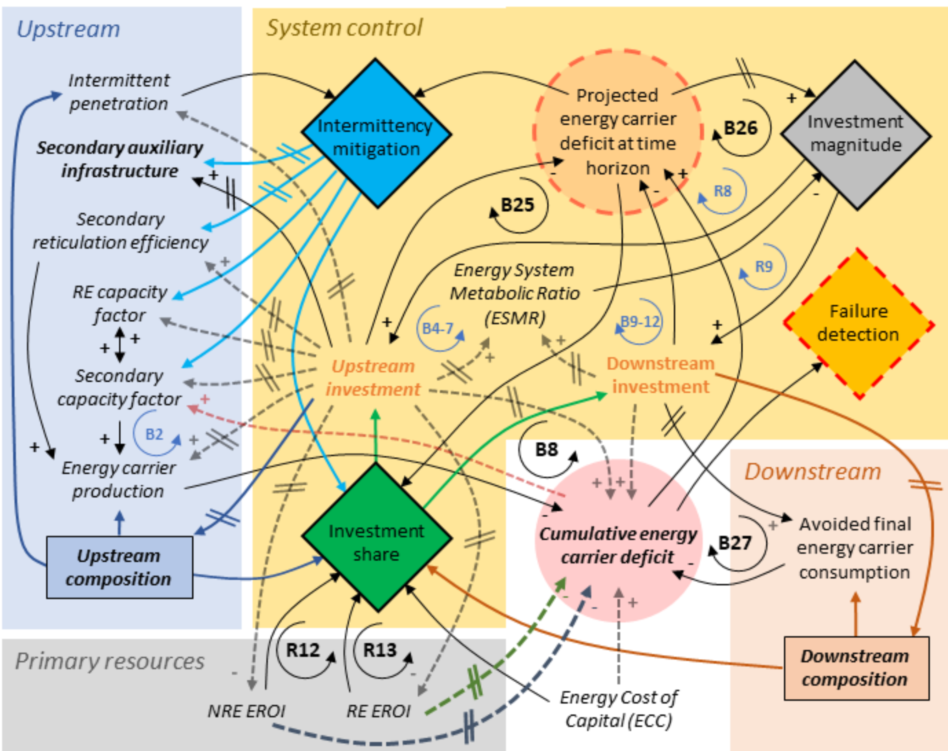

Figure 25: causal loop diagram for system control

Details of the components of the heuristic method are given in subsequent sections (5.2.1 to 5.2.5.3), simplified for brevity and clarity. Refer to section 9.4.4 for full function details.

5.2.1 EC deficit projection

System control requires an approximate future projection of the main input to the objective function, the cumulative supply/demand balance vector, $\boldsymbol{b}$, such that changes in the investment decision variables, $\hat{\boldsymbol{h}}_{\boldsymbol{x}}$, and subsequent expected changes in $\boldsymbol{b}$ can form a feedback loop. Using equation 1 from section 4.2.1.2 and equation 3 from section 4.2.3,

$$\boldsymbol{b}(t=\tau) = \int_0^{\tau} \left(\boldsymbol{p_i} - \left(\boldsymbol{p}_{\boldsymbol{d}}^{\boldsymbol{T}} C_e\right)^{\boldsymbol{T}} - \boldsymbol{p_a} - \boldsymbol{p_c}\right) dt$$

This process is based on linear projection of the main components affecting $\boldsymbol{b}$:

- The current supply/demand balance flow rate, $\boldsymbol{p_i} - \boldsymbol{p_o}$.
- Expected changes in EC production, $\boldsymbol{p_i}$, due to changes in upstream PC.
- Expected changes in EC final consumption, $(\boldsymbol{p}^{\boldsymbol{T}}{}_{\boldsymbol{d}} C_e)^{\boldsymbol{T}}$, due to changes in downstream PC.
- Expected changes the metabolic energy consumption of the GES, $\boldsymbol{p_a} + \boldsymbol{p_c}$, due to changes in upstream and downstream PC.

Expected net changes in PC are given by additions less decommissioning, where additions are represented the PC stocks in construction, $\boldsymbol{w_x}$, and decommissioning within the construction period is indicated by the vector of PC additions delayed by PC lifetime minus build time, $\boldsymbol{h_x}(tj + \boldsymbol{z_x} - \boldsymbol{l_x})$. Matrices, U_i, U_o, and U_K (units of EJ/year), are constructed to represent projected changes in inflow and outflow rates for each EC (j^{th} column) over a specified number of time increments (i^{th} row) included in the investment planning timeframe:

- U_i specifies future EC production rates associated with upstream PC in construction, minus expected decommissioning, phased in over the relevant PC build times.
- U_o specifies future changes to EC consumption rates associated with downstream PC in construction, minus expected decommissioning, phased in over the relevant PC build times.
- U_K specifies future EC consumption rates associated with the construction of new PC, phased out over the relevant PC build times, and new PC operation.

A vector representing EC deficit by EC type, $\boldsymbol{d}$ (in units of EJ), projected at a specified time horizon is then given by,

$$\boldsymbol{d} = -\left(J \circ \boldsymbol{b}^{\boldsymbol{T}} + \Upsilon_{tc} L (J \circ (\boldsymbol{p_i} - \boldsymbol{p_o})^{\boldsymbol{T}} + U_i + U_o + U_\kappa)\right)_j^{\boldsymbol{T}}$$

Where, J is a matrix of ones (dimensionless),

Υ_{tc} is a time increment constant indicating the time period represented by each matrix row (in units of years), and

L is a lower unitriangular matrix (dimensionless).

L is used for the summation of cumulative totals by timestep. The j^{th} column is taken to give $\boldsymbol{d}$, specified at time horizon Υ_{th} (in units of years) where $j = \Upsilon_{th} / \Upsilon_{tc}$.

5.2.2 Investment shares

The determination of investment flows requires a prioritization mechanism, identifying investment options best able to minimize the objective function while promoting secondary objectives. To achieve this, matrices are constructed to represent 'yield' by PC type, Y_i and Y_o (dimensionless), to allow the comparison of upstream and downstream investment options, respectively, on a consistent net energy basis. Yield is defined in terms of the energy return per energy invested into each PC type (i^{th} row) for each EC (j^{th} column):

- Y_i represents upstream EC production and is calculated from new PC EROI and secondary ECC ($\boldsymbol{\gamma_r}$, $\boldsymbol{\gamma_n}$, $\boldsymbol{y_s}$, and $\boldsymbol{y_{sa}}$) disaggregated by EC type, CF maxima for upstream PC ($\boldsymbol{u_{rm}}$, $\boldsymbol{u_{nm}}$, and $\boldsymbol{u_{sm}}$), and new PC efficiencies ($\boldsymbol{\partial_{si}}$ and $\boldsymbol{\partial_{so}}$).
- Y_o represents downstream avoided final EC consumption and is calculated from EU ECC ($\boldsymbol{y_e}$ and $\boldsymbol{y_{ea}}$) disaggregated by EC type, CFs for EU PC ($\boldsymbol{u_e}$), and new PC efficiencies ($\boldsymbol{\partial_{ei}}$ and $\boldsymbol{\partial_{eo}}$). Downstream yield uses actual CFs as these can diverge widely from CF target, strongly affecting yield calculations.
- Note that these matrices include the energy costs of associated AI for both upstream and downstream yield, and energy costs of associated primary PC for upstream yield.

Investment flows must respond to upstream and downstream penetration limits, $\boldsymbol{\eta_{sm}}$ and $\boldsymbol{\eta_{em}}$. For this purpose, stepwise curtailment function vectors, $\boldsymbol{\varsigma_i}$ and $\boldsymbol{\varsigma_o}$, for upstream and downstream, respectively, can be defined:

$$ȿ_x = \begin{cases} \boldsymbol{j} \ where \ \boldsymbol{\eta_x} \leq (1 - ɤ_{ct})\boldsymbol{\eta_{xm}} \\ \frac{1}{ɤ_{ct}}\left(\boldsymbol{j} - (\boldsymbol{\eta_x} \oslash \boldsymbol{\eta_{xm}})\right) \ where \ (1 - ɤ_{ct})\boldsymbol{\eta_{xm}} < \boldsymbol{\eta_x} < \boldsymbol{\eta_{xm}} \\ \boldsymbol{0} \ where \ \boldsymbol{\eta_x} \geq \boldsymbol{\eta_{xm}} \end{cases}$$

Where $ɤ_{ct}$ (dimensionless) is a curtailment threshold constant specifying the fraction of the input variable range over which output is linearly curtailed towards zero (also used in the investment magnitude function as detailed in section 5.2.3 below).

Next, matrices of utility values by PC type and EC type, W_i and W_o for upstream and downstream, respectively, can be calculated to compare the relative merits of each investment option to address the projected EC deficit, ***d***. For downstream investment options,

$$W_o = ɤ_{sh}(ɖ^{\boldsymbol{T}} \circ Y_o)$$

Where $ɤ_{sh}$ (units of 1/EJ) is an investment share coefficient scaling the magnitude of W_x matrices. Note that indices are rendered dimensionless by removing the unit of time. For upstream investment options,

$$W_i = ɤ_{sh}\left(ɖ^{\boldsymbol{T}} \circ Y_i \circ \left(\boldsymbol{j^T} I_{rsi} + \boldsymbol{j^T}\left(I_{nsi} \circ \left(\boldsymbol{j} - \frac{n ɤ_{nr}\boldsymbol{\theta}}{\sum_{i=1}^{n}\boldsymbol{\theta_i}}\right)^{\circ t\boldsymbol{j}}\right)\right)^{\boldsymbol{T}}\right)$$

Where n is the vector length for NRE type vectors and $ɤ_{nr}$ (dimensionless) is a selected mean NRE annual utility reduction rate. NRE utility reduction is implemented to decrease investment flows into upstream EC production from NRE sources over time representing the rising impetus to decarbonize the GES and associated policy efforts. The mean annual utility reduction rate is applied in proportion to the GHG emissions intensity of each NRE type relative to the mean GHG emissions intensity across all NRE types, hence higher emissions investment options will be phased out more rapidly. Note that NRE utility reduction is a forcing function rather than a hard constraint, progressively disincentivizing NRE production over time but still allowing investment flows towards NRE production where utility values are high enough. The value of $ɤ_{nr}$ is selected to allow sufficient forcing without adverse impacts to system stability (see section 9.6 for details).

Investment flow proportions directed towards each investment option (investment shares) are then calculated using logit choice functions, such that the value selected for $ɤ_{sh}$ controls the degree of concentration of investment flows into higher utility investment options (lower γ_{sh} values will spread investment flows more evenly between investment options):

$$\hat{\boldsymbol{h}}_{\boldsymbol{s}} \propto \frac{\S_{\boldsymbol{i}} \circ (e\boldsymbol{j})^{\circ W_i \boldsymbol{j}}}{\boldsymbol{j} \cdot (e\boldsymbol{j})^{\circ W_i \boldsymbol{j}} + \boldsymbol{j} \cdot (e\boldsymbol{j})^{\circ W_o \boldsymbol{j}}}$$

and

$$\hat{\boldsymbol{h}}_{\boldsymbol{es}} \propto \frac{\S_{\boldsymbol{o}} \circ (e\boldsymbol{j})^{\circ W_o \boldsymbol{j}}}{\boldsymbol{j} \cdot (e\boldsymbol{j})^{\circ W_i \boldsymbol{j}} + \boldsymbol{j} \cdot (e\boldsymbol{j})^{\circ W_o \boldsymbol{j}}}$$

Where the index vectors $W_x\boldsymbol{j}$ give the sum of utility values across all EC types, summarizing the relative merit each investment option. Note that the above relations are indicated in terms of proportionalities as investment shares must be corrected for the variable EC costs per unit of PC for each investment option. The calculation of primary PC investment flows associated with upstream investment options, $\hat{\boldsymbol{h}}_{\boldsymbol{r}}$ and $\hat{\boldsymbol{h}}_{\boldsymbol{n}}$, are detailed in section 0. The vector $\hat{\boldsymbol{h}}_{\boldsymbol{es}}$ indicates downstream investment flows originating from the above investment share calculation, as opposed to investment flows required to maintain EU PC utilization below target CFs, $\hat{\boldsymbol{h}}_{\boldsymbol{et}}$ (detailed in section 5.2.5.1).

The above investment allocation logic promotes energy efficiency at the system level by prioritizing investment options with higher yields, to the extent they address the projected EC deficit, $\boldsymbol{d}$. This minimizes sum EC consumption over time (secondary objective 1):

$$Minimize\ \ \boldsymbol{p_o} \cdot \boldsymbol{j}$$

In addition, the use of NRE utility reduction minimizes energy related cumulative GHG emissions to the extent possible within dynamic system constraints, by disincentivizing primary energy production from high GHG emissions intensity sources (secondary objective 2):

$$Minimize\ \ \left(\boldsymbol{\theta} \circ \int \boldsymbol{p_n} dt\right) \cdot \boldsymbol{j}$$

5.2.3 Investment magnitude

A feedback loop between projected sum EC deficit and the total investment flow magnitude is needed as greater deficits will require greater total investment to rectify, and *vice versa*. However, as discussed in section 4.2.4.5, the reinvestment of energy back into the GES is necessarily limited by HSES constraints, as indicated by the ESMR vector, $\boldsymbol{\kappa}$. To represent this limitation, investment magnitude is defined as a stepwise function with curtailment based on the maximum ESMR relative to a specified ESMR limit, ƚ (dimensionless):

$$\sum \boldsymbol{\hat{h}_r}, \boldsymbol{\hat{h}_n}, \boldsymbol{\hat{h}_s}, \boldsymbol{\hat{h}_{es}} \propto \begin{cases} \text{ɤ}_{mc}\text{ɖ} \cdot \boldsymbol{j} \ \ where \ \ max(\boldsymbol{\kappa})_{\boldsymbol{i}} \leq \text{ƚ}(1 - \text{ɤ}_{ct}) \\ \dfrac{\text{ɤ}_{mc}}{\text{ɤ}_{ct}}(\text{ƚ} - max(\boldsymbol{\kappa})_{\boldsymbol{i}})\text{ɖ} \cdot \boldsymbol{j} \ \ where \ \ \text{ƚ}(1 - \text{ɤ}_{ct}) < max(\boldsymbol{\kappa})_{\boldsymbol{i}} < \text{ƚ} \\ \boldsymbol{0} \ \ where \ \ max(\boldsymbol{\kappa})_{\boldsymbol{i}} \geq \text{ƚ} \end{cases}$$

Where ɤ_{mc} (units of 1/year^2) is an investment magnitude coefficient, controlling the strength of the investment response. PC investment flow decision variables, $\boldsymbol{\hat{h}_r}$, $\boldsymbol{\hat{h}_n}$, $\boldsymbol{\hat{h}_s}$, and $\boldsymbol{\hat{h}_e}$, are then determined by the total investment magnitude split between upstream and downstream investment options based on investment shares described in section 5.2.2.

5.2.4 Intermittency mitigation

The optimal balance between the intermittency mitigation options, represented by ψ, will change depending on the relative scarcity of ECs as indicated by projected EC deficit, $\boldsymbol{d}$. Firstly, EC costs associated with the two intermittency mitigation options are calculated:

- For AI mitigation, EC costs arise from the increased metabolic energy consumption of the GES associated with additional intermittent electricity AI, and lost EC due to the reduction of secondary reticulation efficiencies.
- For PC overbuild mitigation, EC costs arise from lost EC production due to the reduction of primary and secondary CFs.

Optimal ψ is then determined via an average of the lowest cost intermittency mitigation options for each EC type (indicated by one where AI mitigation is lower cost, zero otherwise), weighted by the normalized components of $\boldsymbol{d}$. This dynamically selects the balance of mitigation options best able to address the projected EC deficit. ψ is calculated using a script element in GoldSim (see section 9.4.5.1 for script details).

5.2.5 PC utilization control

5.2.5.1 EU CF regulation

EU PC investment flows driven by EU PC utilization, denoted $\boldsymbol{\hat{h}_{et}}$, are required for the upkeep of sufficient EU PC stocks (regardless of flows determined via the investment share and magnitude calculations, $\boldsymbol{\hat{h}_{es}}$). These flows are required to alleviate over-utilization of PC indicated by EU CFs, $\boldsymbol{u_e}$, relative to target CFs, $\boldsymbol{u_{et}}$. Investment quantities are given by the difference between ES demands and the ES flows EU PC (operating and in construction) can deliver if operating at target CFs, spread over the relevant PC build times, $\boldsymbol{z_e}$:

$$\widehat{\boldsymbol{h}}_{\boldsymbol{et}} = \begin{cases} \left(\left(\boldsymbol{p}_{\boldsymbol{d}}^{\boldsymbol{T}} - \left((\boldsymbol{c_e} \circ \boldsymbol{e_{eo}} + \boldsymbol{w_e} \circ \text{ə}_{\boldsymbol{eo}}) \circ \boldsymbol{u_{et}}\right)^{\boldsymbol{T}} I_{eo}\right)\left(\text{ʂ}_{\boldsymbol{o}} \circ F_{eo} \oslash \boldsymbol{j}^{\boldsymbol{T}}(\text{ʂ}_{\boldsymbol{o}} \circ F_{eo})\right)^{\boldsymbol{T}}\right)^{\boldsymbol{T}} \oslash (\boldsymbol{u_{et}} \circ \text{ə}_{\boldsymbol{eo}} \circ \boldsymbol{z_e}) \ where \ \boldsymbol{u_e} > \boldsymbol{u_{et}} \\ \boldsymbol{0} \ where \ \boldsymbol{u_e} \leq \boldsymbol{u_{et}} \end{cases}$$

The sum investment flow vector for EU PC, $\widehat{\boldsymbol{h}}_{\boldsymbol{e}}$, is then given by,

$$\widehat{\boldsymbol{h}}_{\boldsymbol{e}} = \widehat{\boldsymbol{h}}_{\boldsymbol{es}} + \widehat{\boldsymbol{h}}_{\boldsymbol{et}}$$

5.2.5.2 Synchronization of upstream PC additions

For upstream investment, primary PC investment flows, $\widehat{\boldsymbol{h}}_{\boldsymbol{r}}$ and $\widehat{\boldsymbol{h}}_{\boldsymbol{n}}$, commensurate with secondary PC investment flows, $\widehat{\boldsymbol{h}}_{\boldsymbol{s}}$, are required:

$$\widehat{\boldsymbol{h}}_{\boldsymbol{r}} = \left(I_{rsi} \circ \left(\widehat{\boldsymbol{h}}_{\boldsymbol{s}} \circ \boldsymbol{\gamma_s} \circ \boldsymbol{u_{sm}} \oslash \boldsymbol{e_{si}}\right)^{\boldsymbol{T}}\right)\boldsymbol{j} \oslash (\boldsymbol{\gamma_r} \circ \boldsymbol{u_{rm}})$$

$$\widehat{\boldsymbol{h}}_{\boldsymbol{n}} = \left(I_{nsi} \circ \left(\widehat{\boldsymbol{h}}_{\boldsymbol{s}} \circ \boldsymbol{\gamma_s} \circ \boldsymbol{u_{sm}} \oslash \boldsymbol{e_{si}}\right)^{\boldsymbol{T}}\right)\boldsymbol{j} \oslash (\boldsymbol{\gamma_n} \circ \boldsymbol{u_{nm}})$$

However, corresponding primary and secondary PC types have non-equivalent PC lifetimes, $\boldsymbol{l_x}$, and build times, $\boldsymbol{z_x}$. As such, total stocks of primary and secondary PC tend to desynchronize over time. Delay functions for upstream investment flows are used to maintain approximate synchronization. These functions use default delay times equal to the difference between the corresponding primary and secondary build times applied to the PC quantities with the shorter build times (i.e., no delay for the PC with the longer build times). This allows corresponding primary and secondary PC to be brought into operation simultaneously. These delay times are dynamically modified where primary PC exceeds corresponding secondary PC, or *vice versa*. Delay times are shortened to expedite the addition of PC in deficit, promoting the minimization of unused upstream PC (secondary objective 3):

$$Minimize \ \sum_{i=1}^{n} |(\boldsymbol{c_r} \circ \boldsymbol{\gamma_r} \circ \boldsymbol{u_{rm}} - F_{rsi}\boldsymbol{j})_i| + \sum_{i=1}^{m} |(\boldsymbol{c_n} \circ \boldsymbol{\gamma_n} \circ \boldsymbol{u_{nm}} - F_{nsi}\boldsymbol{j})_i|$$

5.2.5.3 Upstream CF curtailment

Excessive accumulation of ECs ($\boldsymbol{b} \gg \boldsymbol{0}$) can cause destabilization of the GES transformation pathway due to prolonged underinvestment and consequent large swings in the supply/demand balance flow rate, $\boldsymbol{p_i} - \boldsymbol{p_o}$. To promote system stability, active curtailment of upstream CFs is required, representing falling utilization of PC due to oversupply. This curtailment can be achieved via a stepwise function to linearly curtail the production of ECs in surplus:

$$\boldsymbol{u_{sm}} = \begin{cases} \boldsymbol{u_{sm}}(0) \ \ where \ \ \boldsymbol{b} \oslash \boldsymbol{p_o} \leq \boldsymbol{0} \\ \boldsymbol{u_{sm}}(0) \circ I_{so}\left(\boldsymbol{j} - \dfrac{\boldsymbol{b} \oslash \boldsymbol{p_o}}{\text{Б}}\right) \ \ where \ \ \boldsymbol{0} < \boldsymbol{b} \oslash \boldsymbol{p_o} < \text{Б}\boldsymbol{j} \\ \boldsymbol{0} \ \ where \ \ \boldsymbol{b} \oslash \boldsymbol{p_o} \geq \text{Б}\boldsymbol{j} \end{cases}$$

Where $\boldsymbol{u_{sm}}(0)$ is the initial maximum secondary CF, prior to any curtailment effect, and *Б* (units of years) is the specified EC surplus limit. This limit increases linearly as a function of time as greater cumulative surplus is allowable without adversely impacting system stability as elapsed simulation time increases.

5.3 SCENARIOS

The effects of various exogenous factors, trends, and circumstances on GES transformation pathways can be tested using scenario analysis. This, in effect, represents a reduction of the full range of socio-technical narratives implicitly considered in the standard ‘base case’ of the model to more specific ranges of interest. Scenario results can be used to infer optimal strategies, system leverage points, and policy implications for GES transformation. The simulation of diverse scenarios also serves to stress-test and further validate the model, particularly regarding weaknesses and limitations in the chosen methodological approach discussed in sections 4.1 and 5.4.

Scenarios are subjectively defined, representing a range of narratives present in the literature and popular commentary on the forthcoming energy transition (i.e., scenarios are not based on a formal survey or quantification of such narratives, but are instead based on the author’s interpretation). It should be noted that as scenarios are sensitive to their specific implementation, they should be considered primarily in reference to the model base case, as described in section 3.1.4.2. The selected scenarios are summarized in Table 6.

Table 6: summary of scenarios implemented in the PRESS model

Scenario	Name	Description
1	*Energy Breakthrough*	A new high-EROI, dispatchable, scalable technology for electricity production is available from the beginning of the study period. This scenario approximates the immediate availability of next generation nuclear (treated as functionally renewable), ocean thermal energy conversion (OTEC), or a similar breakthrough technology. To represent this, the 'Other RE' primary energy category is modified to be dispatchable, have an initial EROI of 50, and be effectively inexhaustible.
2	*Relocalization*	A general trend towards greater economic and social relocalization eventuates, reflected in aggregate ES demands. Demand for the transportation declines over the simulated period. Transportation of goods declines strongly while the transportation of people declines moderately, and greater declines are observed for IC transportation. To represent this, mean reductions of 25%, 50%, 60%, and 75% from 2015 levels are modelled for regional and IC passenger transportation, and regional and IC freight transportation, respectively.
3	*RE Rapid Deployment*	An expedited phase out of NRE investment is attempted. This represents a pronounced shift in subsidies away from NRE and towards RE, or similar policy mechanisms. To represent this, the mean NRE annual utility reduction rate, γ_{nr}, is quadrupled, from 2.5% to 10% per year.
4	*Climate Constraints*	Strong emissions regulations are introduced, such as absolute emissions caps or aggressive carbon taxes, aimed at secondary and end-use technologies with high GHG emissions intensities. In particular, the conversion of gas and coal to LaG fuels, electricity generation from fossil fuels, light internal combustion engine vehicles (ICEVs), and aviation are severely limed in this scenario. To represent this, penetration limits, $\boldsymbol{\eta}_{sm}$ and $\boldsymbol{\eta}_{em}$, for affected PC types are reduced to values between 50% and 5% (lower limits for less critical and/or higher GHG emissions intensity technologies).
5	*Delayed Consumer Response*	A significant delay occurs in the willingness of consumers to shift consumption behaviours towards ES provision using more efficient EU PC types. Consequently, downstream investment determined by the control system (based on physical optimality) is suspended for a period of 35 years. To represent this, no downstream investment flows originating from the investment share and magnitude calculations, $\hat{\boldsymbol{h}}_{es}$, occur before 2050. During this period, downstream investment is driven by EU PC utilization only ($\hat{\boldsymbol{h}}_{et}$).
6	*Policy Recommendation s*	Changes in model parameters corresponding to policy recommendations found via sensitivity analysis (i.e., leverage points) are implemented to the degree considered plausible (see section 5.5.1 and section 6.3.2). As such, this scenario can be seen as a highly optimistic best-case narrative, assuming planning foresight based on an understanding of the solution space for physical GES transformation. To represent this: • modelled ES demands are reduced, strongly for static mechanical work and high temperature process heat (at least 25% reductions from 2015 levels), moderately for IPaC, low temperature heating, and all

Scenario	Name	Description
		transportation ESs excluding IC passenger transportation (no increases from 2015 levels, reductions still possible), • penetration limits for electricity generation from coal and IC freight aviation are reduced to 10%, and • mean and SD ECC values are reduced by 50% for secondary PC associated with coal (except coal heat), biofuels, and geothermal generation, and for secondary AI for intermittent electricity mitigation.

These scenarios are implemented through the introduction of specific sets of model parameter values and additional functions affecting model interactions. See section 9.7 for scenario implementation details.

5.4 IDENTIFIED LIMITATIONS

As discussed in sections 4.1 and 4.2, the PRESS model and associated physical GES modelling approach are considered semi-stylized due to the high-level, spatially aggregated perspective, simplifying assumptions, and data limitations for the estimation of input parameter probability distributions. Consequently, potential limitations associated with the methodology presented in this chapter have been identified:

- Differences in the qualitative preferences for specific modes of ES provision are not modelled. In effect, this assumes indifference of the end-user to various aspects of ES provision, such as speed, convenience, privacy, and cost. Accounting for behavioural factors and preferences affecting mode choice for ES provision, expressed dynamically and globally over time, is considered out of scope. However, scenario 5 (Delayed Consumer Response) explores the implications of behavioural change reticence.
- Explicit modelling of the introduction of CCS for the abatement of GHG emissions in the upstream sector, and associated energetic costs, is not attempted. While cumulative GHG emissions as modelled could theoretically be reduced via these measures, this would come at the expense of a larger autocatalytic loop with unknown implications for GES transformation pathways.
- The model lacks the adverse impacts of rising global mean surface temperatures due to climate change, and reductions in mean utilization of PC due rising intermittent

penetration (PC overbuild mitigation), on thermal conversion efficiencies at the secondary stage.

- Thermal electricity generating PC types modelled at the secondary stage are aggregates of open-cycle and closed-cycle plant, which are subject to different mean utilization levels (CF maxima) and generator types (peaking or baseload). This effectively assumes that the composition of such PC types remains similar over time.
- The increasing energy costs of non-renewable, non-energy resource extraction (e.g., minerals) required for the GES due to decreasing resource quality are not modelled. While this can be expected to increase EROI for specific energy technologies, this effect is less relevant for a high-level, aggregated modelling approach and is represented only exogenously via probabilistic ES demand trends.
- Pre-simulation power output estimates, used in new PC efficiency and EROI functions, are based on assumed linear production trends (from technology inception to the start of the study period). This is less accurate than using actual historical time series power output data, but required given a relative paucity of such data for all PC types.
- The time-dependent effects of energy production efficiencies on primary energy resource magnitudes (affecting solar PV and wind resources, in particular) are not modelled. Instead, resource quantities, $\boldsymbol{p_{rm}}$ and $\boldsymbol{\omega}$, are defined as the energy resources which are ultimately accessible for simplicity.
- For RE PC, lower EROI values will, in reality, manifest partially as reduced capacity utilization due to poorer quality resources (weaker, more intermittent natural energy fluxes). For simplicity, this is represented via reduced EROI alone without resource quality affecting CF maxima.
- The model lacks explicit representation of feedbacks between EC scarcity or abundance (represented by $\boldsymbol{b}$, as a price proxy) and ES demands, $\boldsymbol{p_d}$. However, this is mitigated by probabilistic modelling of $\boldsymbol{p_d}$ and the representation of $\boldsymbol{b}$ as an integral function, with the downstream consumption of ECs changing in response to $\boldsymbol{b}$ (including fuel switching, as discussed in section 4.2.9.1). This is functionally consistent with rebound effects stemming from behavioural adaptation to price, although not necessarily in alignment with real-world rebound effect magnitudes.

- Price- and exergy-based quality adjustments for EROI are not represented in disaggregated EC components, due to the complexities and ambiguities this introduces to the disaggregated EC formulation. Instead, adjustment for primary energy equivalents (a factor of 2.6 applied to electricity) is considered sufficient.
- Downstream PC stocks involved in GES metabolic consumption (the autocatalytic loop and capital hypercycle) are not explicitly modelled but rather represented by the energy costs metrics, EROI and ECC (with required EC expenditures are taken directly from $\boldsymbol{b}$). This is optimistic as it effectively disregards capacity constraints and lifecycle-related delays associated with these PC stocks. It also assumes EROI and ECC values are comprehensive and include n^{th}-order requirements (as discussed in section 4.2.4).
- The estimation of ECC, as a derived metric with no available independent estimates, is subject to a high degree of epistemic uncertainty and estimates can be expected to vary by orders of magnitude (as discussed in section 4.2.4.2). Furthermore, the use of technology cost tiers for establishing ECC estimates by comparison (see section 9.5.9) is speculative. However, this is mitigated by the general probabilistic formulation, the use of input correlations (see section 9.4.7.3), and multiple lines of reasoning to establish appropriate probability distributions for these input parameters.
- The model is initialized using the initial EC proportions of EC supply as an approximation of the initial EC proportions of final EC demand, $\boldsymbol{\delta}(0)$ (as discussed in section 4.2.7). This effectively assumes that implicitly modelled downstream PC stocks involved in GES metabolic consumption have a similar initial composition to the explicitly modelled downstream PC stocks involved in final consumption. This is not strictly accurate due to the existence of $\boldsymbol{\varphi}$ vectors; however, approximation is necessary as a full numerical solution would require a more complex iterative solver, increasing computational cost and the risk of associated errors.
- For model initialization, it is assumed that the distribution of PC and AI ages along their respective lifecycles is uniform. This is a limitation of the material delay element in the GoldSim software used to represent stocks of PC and AI in the construction and operation lifecycle stages. While this is likely to be appropriate for most mature PC types, it may overestimate decommissioning in the early study period for emerging PC types (e.g., solar PV and wind) and underestimate decommissioning for PC types being

phased out (e.g., coal generation). Note that this error diminishes later in the study period, until it is gone by $t > max(\boldsymbol{l_x})_{x,i}$, but some residual influence of the error remains due to path-dependency.

- As all forms of heat production at the secondary stage are treated as interchangeable, industrial processes that have a direct reliance on specific primary energy flows may not be represented adequately. For example, steel production requires coke derived from coal, both to provide high temperature process heat (the ES) and as a chemical reactant in blast furnaces. Such processes are not generally amenable to substitution in heat production. While substitution limits are partially represented using probabilistic EU penetration limits, $\boldsymbol{\eta_{em}}$, detailed representation of the industrial sector is considered out of scope and is not attempted.
- Similarly, LaG fuels are treated as homogenous and interchangeable, which is not strictly accurate at the process or industry level. However, as PC types using different LaG fuels are generally functionally similar, and refining methods exist to adjust the chemical composition of fuels, it is optimistically assumed that the supply of specific LaG fuel components does not represent a significant constraint at the system level.
- For EU PC providing heating ESs, passive systems are assumed to be similar and have homogeneous EU to ES efficiency parameters. This is likely appropriate for low temperature heating, but less certain for high temperature process heat where there is a greater technological diversity of passive systems. As the representation of diverse industrial processes is out of scope, the related uncertainty is addressed by the general probabilistic formulation.
- New PC efficiencies are modelled as functions of cumulative power output, representing technological learning effects (see section 4.2.2.5) but can also be expected to respond to EC scarcity or abundance (represented by $\boldsymbol{b}$), i.e., increasing faster to address EC deficits or more slowly during period of surplus. However, this effect is behavioural in origin and is therefore considered out of scope.
- Due to the complexity and variety of methods and terminology involved in EROI calculation among the sources sampled (see section 9.5.8), collected values are not strictly harmonized. EROI methods are often relatively opaque and therefore exhaustive harmonization is not possible without introducing ad hoc assumptions.

Where possible, selected EROI estimates correspond to $EROI_{st}$ or $EROI_{1,lab}$ as defined by Murphy et al. [170]. Note that this approach is consistent with the principle of semantic openness discussed in section 4.1.

- The EC proportions of the metabolic energy consumption of the GES, $\boldsymbol{p_a}$ + $\boldsymbol{p_c}$, are assumed to follow the EC proportions of final demand, $\boldsymbol{\delta}$ (with constant specified relative differences via the $\boldsymbol{\varphi}$ vectors). This is appropriate for most PC and AI types as these are aggregates of technologically diverse capital, but may be less suitable in cases where PC types are comprised of relatively homogeneous technologies (structural types) with distinct EC requirements (e.g., solar PV and nuclear generation).
- The direct use of NRE resources for non-energy purposes, $\boldsymbol{p_{ne}}$, is assumed to scale with the mean of delivered ES demands relative to their initial levels. However, elements of $\boldsymbol{p_{ne}}$ can be expected to correlate much more strongly with some ES demands than others (e.g, the use of NRE resources as chemical feedstocks will be primarily correlated with the industrial ES demands). A detailed representation of these correlations is not attempted.
- Competing uses of NRE and RE resources for non-energy purposes are not represented. For example, growing demands on biomass to replace NRE resources for chemical feedstocks in a wide range of sectors, from manufacturing to pharmaceuticals [28], is not explicitly considered. This relates to the definition of probabilistically modelled RE resources given in section 4.2.1.1: RE technical potentials, $\boldsymbol{p_{rm}}$, refer to the components of total resources available for energy purposes (after consideration of competing uses).
- As discussed in sections 4.2.4.5 and 5.2.3, the reinvestment of energy into the GES is limited by the ESMR vector, $\boldsymbol{\kappa}$. The exogeneous interface between the GES and the HSES is extremely complex and is subject to highly non-linear behaviour and causal influences (particularly regarding the discretionary components of ES demands, $\boldsymbol{p_d}$). Characterizing the nature of these relationships is not practicable within a high-level physical representation of the GES. The intent is only to represent the ineluctability of such feedback and the corresponding risk of encountering a net energy trap outcome.

5.5 RESULTS ANALYSIS

Results analysis requires the generation of ensembles of GES transformation pathways via Monte Carlo simulation (as discussed in section 4.2.9.2), using the GoldSim platform. Latin Hypercube sampling is used to divide the probability distribution for each input parameter into equally likely 'strata', one for each realization, which are then placed in a random sequence and assigned to realizations to be simulated in the ensemble (using strata mid-points). This method ensures uniform sampling of the input parameter space. Ensembles of 1,000 model realizations are then simulated for the base case and for each scenario. Sampling sequences are repeated to allow direct comparison of realizations where required. Refer to Appendix B in GoldSim Technology Group [361] for probabilistic simulation details.

Graphical analysis is performed on selected output variable time series representing pertinent aspects of GES evolution, summarized in Table 7. Output variables are assessed at the ensemble level as probabilistic 'envelopes' defined by specified output variable percentiles over time. Central tendencies are indicated by envelope means and medians, while the practical limits are given by percentile extrema (the 5th and 95th percentiles). The analysis of the base case is comprehensive, including both central tendencies and practical limits over time, whereas scenario analysis generally focusses on differences in central tendencies relative to the base case. Note that failed realizations are included for the analysis of cumulative EC supply/demand balance and system stability but excluded elsewhere to depict envelopes representing only feasible and viable GES transformation pathways.

Table 7: summary of selected ensemble output variables for results analysis

GES aspect	Selected output variables	Failures	Notes
Supply/demand balance	• EC deficit ($-\boldsymbol{b} \oslash \boldsymbol{p}_o$) • Mean EC deficit	Included	*Omitted for scenario analysis*
System stability	• Failure rate • Failure rate confidence intervals • Stable time distributions		
Supply	• TPES • Primary energy flows ($\boldsymbol{p}_r$ and $\boldsymbol{p}_n$) • EC supply ($\boldsymbol{p}_i$)	Excluded	*Primary energy flows adjusted for primary energy equivalence for scenario analysis*
Demand	• Final EC consumption ($\boldsymbol{p}_o - \boldsymbol{p}_a - \boldsymbol{p}_c$) • GES metabolic EC consumption ($\boldsymbol{p}_a + \boldsymbol{p}_c$) • Mean autocatalytic loop and capital hypercycle consumption • ES demands ($\boldsymbol{p}_d$)		• *GES metabolism details omitted for scenario analysis* • *ES demands for scenarios given in section 10.3*

GES aspect	Selected output variables	Failures	Notes
Primary resources	• NRE depletion ($\boldsymbol{d}$) • RE exhaustion ($\boldsymbol{x}$)		
RE share of supply	• RE shares of EC supply • RE share of TPES		
EROI	• PC mean EROI ($\boldsymbol{k_r}$ and $\boldsymbol{k_n}$) • EC point-of-use EROI		
Upstream capacity factors	• Median primary CFs ($\boldsymbol{u_r}$ and $\boldsymbol{u_n}$) • Median secondary CFs ($\boldsymbol{u_s}$)		• *Medians used due to distribution skew* • *Omitted for scenario analysis*
Downstream capacity factors	• Median EU CFs ($\boldsymbol{u_e}$) • EU CF targets ($\boldsymbol{u_{et}}$)		
Secondary penetration	Mean secondary penetration by EC type ($\boldsymbol{\eta_s}$)		*Range (95th percentile minus 5th) results given in section 10.1.2*
End-use penetration	Mean EU penetration by ES type ($\boldsymbol{\eta_e}$)		
Secondary efficiencies	• PC mean secondary conversion efficiencies ($\boldsymbol{e_{si}}$) • PC mean secondary reticulation efficiencies ($\boldsymbol{e_{so}}$)		• *Results for electric cooling given in section 10.2* • *Omitted for scenario analysis*
End-use efficiencies	• PC mean EU conversion efficiencies ($\boldsymbol{e_{ei}}$) • PC mean EU to ES efficiencies ($\boldsymbol{e_{eo}}$)		
GHG emissions	• Cumulative GHG emissions • Cumulative GHG emissions distributions		
Intermittency impact in electricity systems	• Intermittent penetration (m) • Intermittent diversity (q) • Intermittent CF multiplier (χ_h) • Intermittent reticulation efficiency multiplier (χ_g) • Built AI factor • Intermittent electricity AI ($(\boldsymbol{c_{sa}})_d$)		• *Scenario results given in section 10.5* • *Omitted for scenario analysis*
GES metabolism	ESMRs ($\boldsymbol{\kappa}$)		

The combination of probabilistic envelopes across all relevant model output variables then represents the 'leading edge' (i.e., physically best-case outcomes, probabilistically defined) of the solution space for GES transformation identified by the PRESS model.

In addition, Sankey diagrams are created from ensemble mean energy flows across all GES stages for specified snapshots: 2015, 2050, and 2100 for the base case and 2100 for each scenario. These diagrams allow the direct visualization of the central tendency of GES evolution, including primary energy sources, the composition of ECs, efficiencies and associated waste energy flows, GES metabolic consumption, and final delivered ESs. Note, flows depicted in Sankey diagrams are not adjusted for primarily energy equivalence as no aggregation of non-equivalent flow types is involved.

Finally, comprehensive sensitivity and diagnostic analyses, described in the following sections, are performed for the base case to better understand:

- the strength and direction of relationships between input parameter values and the final values of selected output variables representing high-level GES transformation outcomes, and
- the levels of risk associated with input parameters considering both the above and the strength of knowledge arising from the data sources and estimation methods used.

5.5.1 Sensitivity analysis

Monte Carlo simulation enables assessment of the potential impacts of estimation errors for each probabilistic input parameter (as discussed in section 3.1.4.3). The determination of input parameter sensitivity is based on multivariate analysis applied to an expanded ensemble of 10,000 model realizations (to improve the quality of calculated statistics). Sensitivity must be defined relative to a chosen realization-level result, *Y*. Two results are selected with strong high-level implications for the desirability of GES transformation outcomes: stable time and cumulative GHG emissions. Both selected results correspond to serious threats that must be avoided to achieve a successful GES transformation.

To properly quantify potential impacts of input parameter estimation errors in the PRESS model, the definition of sensitivity must:

- capture both the statistical significance (correlation coefficients) and the slope (regression coefficients) of monotonic relationships between input parameter values X_i and selected results Y to indicate overall relationship strength,
- detect both linear and non-linear correlations,
- allow direct comparison of sensitivity between the two selected results Y, and
- account for specified input parameter correlations (as described in section 4.2.9.2).

To satisfy the above criteria, a normalized sensitivity metric is proposed, given by,

$$\mathcal{z}_{y,i} = \frac{|SRC_{y,i}| \cdot max(|p_{y,i,value}|, |p_{y,i,rank}|)}{max\left(|SRC_{y,i}| \cdot max(|p_{y,i,value}|, |p_{y,i,rank}|)\right)_i}$$

Where, $\mathcal{z}_{y,i}$ is the sensitivity metric value for selected result Y and input parameter values X_i,

$SRC_{y,i}$ is the standardized regression coefficient of result Y with respect to input parameter values X_i,

$p_{y,i,value}$ is the partial correlation of result Y to input parameter values X_i, and

$p_{y,i,rank}$ is the rank partial correlation of result Y to input parameter values X_i.

Partial correlation coefficients are used to emphasize the unique contributions of input parameters and remove the effect of specified input parameter correlations. The maximum of rank and value correlation coefficients is taken to admit either linear or non-linear monotonic relationships. Note that $z_{y,i}$ is a measure of relative relationship strength and therefore, the sign of $SRC_{y,i}$ must be referenced to determine the direction of the relationship. See Appendix B in [361] for details of the statistical inputs used above. Normalized sensitivity values of particular importance can be identified using selected lower and upper thresholds, $\mu_y + 2\sigma_y$ and $\mu_y + 2\sigma_y$, respectively (where μ_y is the mean and σ_y is the standard deviation of normalized sensitivity values for result *Y* across all input parameters *X*).

Normalized sensitivity values for both selected results, stable time and cumulative GHG emissions, can be summed to provide an indication of the sensitivity of GES transformation desirability, broadly conceived, to each input parameter (treating both selected results *Y* as approximately equally important). Signs are applied to sensitivity values (based on the sign of $SRC_{y,i}$) to distinguish between desirable and undesirable effects. The resulting sum sensitivity values are then ordered to identify input parameters for which estimation errors have the greatest potential impacts. This is carried out separately for input parameters categorized as decision and non-decision parameters:

- Decision parameters correspond to aspects of the GES over which human control can be exerted and are at least partially amenable to active modification via policy, such as efficiencies, ES demands, and penetration limits.
- Non-decision parameters correspond to factors that are not subject to control, including primary energy resources, the initial state of the GES, and the nature of intermittency mitigation options within electricity systems.
- Note, this is not to be confused with system control decision variables (see section 5.2).
- See section 9.8 for decision and non-decision parameter designations by input array.

The analysis of sum sensitivity for decision parameters uses additional aggregations based on notional policy recommendations (i.e., sum sensitivity values for input parameters approximately aligned with the same policy action are aggregated). Note, this allows sum sensitivity values for a given policy recommendation to exceed one. These policy recommendations are analogous to system leverage points, described in section 1.2.2. The results of this analysis are used in the design of the policy recommendations scenario (S6) described in section 5.3.

5.5.2 Diagnostic analysis

As outlined in section 3.3.2, the absolute risk associated with each input parameter can be identified via diagnostic analysis, considering both the potential impact of input parameter estimation error (normalized sensitivity, as defined in section 5.5.1) and the likelihood of error. For PRESS model input parameters, pedigree assessment is carried out using the ordinal five-point grading scale shown in Table 8 (based on Van Der Sluijs et al. [352]). The three distinct aspects representing strength of knowledge are chosen to be relevant to the data gathering and parameter estimation process used for the PRESS model (see section 9.5). Note that pedigree assessment for the PRESS model is performed at the level of input arrays (results given in section 9.8).

Table 8: pedigree assessment scoring criteria

Score	Number of data sources	Limiting quality of data sources	Strength of assumptions
5	5+	Meta-study	No assumptions required
4	4	Comprehensive report	Very strong
3	3	Broad empirical study	Strong
2	2	Limited empirical study	Moderate
1	1	Simple calculation/estimate	Weak
0	0 (own estimate)	Informal/speculative	Very weak

Diagnostic analysis is performed separately for each selected GES transformation result: stable time and cumulative GHG emissions. Based on the pedigree assessment results, selected upper and lower pedigree thresholds are 3 and 1, respectively. As outlined in section 3.3.2, the primary purpose of diagnostic analysis is to identify input parameters which require greater critical attention and to direct further data gathering and processing efforts. Particular attention must be given to input parameters categorized as high risk for both selected results.

6 RESEARCH FINDINGS

Ensemble results for the base case (1,000 realizations) are summarized in section 6.1, regarding both central tendencies and outer limits of variable envelopes, where possible. Scenarios results are presented in section 6.2, primarily regarding differences in ensemble central tendencies relative to the base case. Result of sensitivity and diagnostic analyses are then presented in sections 6.3 and 6.4, respectively.

6.1 BASE CASE

Penetration ranges, and end-use efficiencies for electric cooling are given in sections 10.1 and 10.2, respectively. Refer to section 5.5 for details of the approach to results analysis.

6.1.1 Sankey diagrams

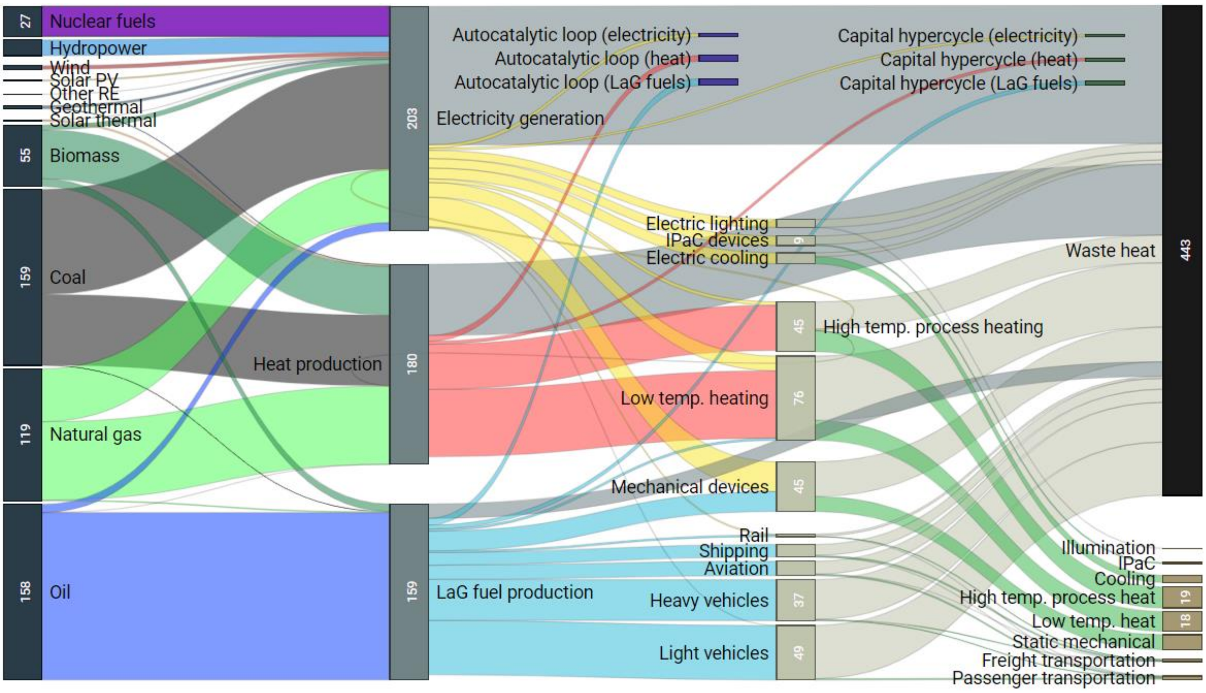

Figure 26: Sankey diagram for mean GES energy flows in 2015

Mean ensemble energy flows across all GES stages (failed realizations excluded) at specified years are depicted below: 2015 in Figure 26, 2050 in Figure 27, and 2100 in Figure 28. Note that Figure 26 also represents the mean initial state of the GES for all scenarios (scenario Sankey diagrams for 2100 presented in section 6.2.1). As these diagrams depict ensemble mean values, input and output totals at each node do not necessarily equal. Note that the Sankey diagrams use aggregated subsets of EU PC types and ES types for display purposes.

Figure 27 depicts marked shifts in energy flows in 2050 relative to 2015. At the primary stage, the production of fossil fuels is significantly reduced, both in absolute terms and as a share of TPES. Notably, the mean production of oil declines by 63%. Production of primary flows from nuclear fuels and all RE types increase strongly, particularly geothermal and solar thermal (by approximately 700% and 1600%, respectively). The combined contribution from wind and solar PV is around 13 EJ/year by this time (a 200% increase from 2015). Despite a 30% reduction in total demand for LaG fuels, the conversion of biomass, natural gas, and coal to LaG fuels increases strongly, by 3200% and 5800%, respectively. A pronounced shift in ECs towards electricity occurs. This is reflected in EC consumption at the EU stage, particularly in high temperature process heating, rail, and light vehicles. The composition of metabolic GES energy consumption changes significantly, with a reduction in the capital hypercycle and a strong increase in the autocatalytic loop. This indicates greater capital efficiency at the EU stage but a higher energy cost of primary energy production. There is a pronounced increase in the provision of all ESs. Waste heat flows are reduced in both absolute and relative terms, particularly those originating from the EU stage, reflecting higher efficiencies.

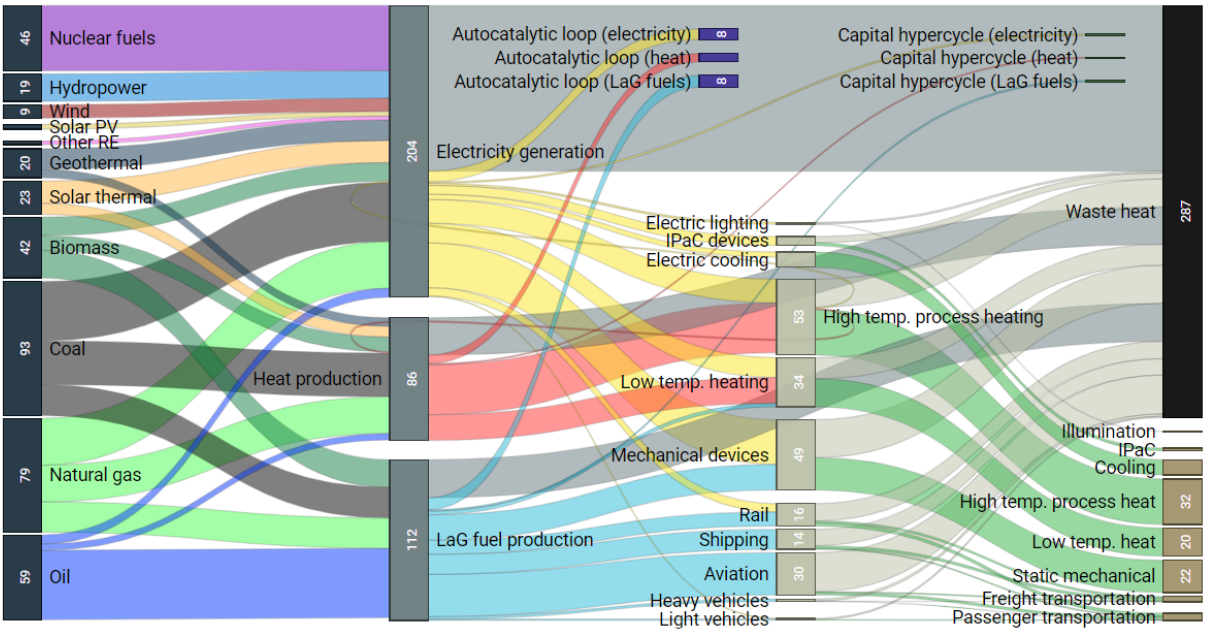

Figure 27: Sankey diagram for mean GES energy flows in the base case in 2050

Figure 28 depicts a continuation of several trends observed between 2015 and 2050. Mean oil production continues to decline, to 4% of TPES by 2100. RE production continues to grow in both relative and absolute terms, however, this growth is more balanced between the various RE types than prior to 2050. Mean solar PV and wind output amounts to 41 EJ/year by 2100, still a minor share of TPES. Growth in the conversion of biomass, natural gas, and coal to LaG fuels, continues albeit at a slower rate. Growth in the autocatalytic loop accelerates, as the energy cost of primary energy production continues to increase, partially due to the advanced depletion of most NRE resources by this time. Delivered ES flows continue to increase at a slower rate.

Several trends observed early in the GES transformation appear to stall after 2050, including the decline in natural gas production, the decline in the capital hypercycle, the shift in ECs towards electricity, and the decline in total waste heat flows. Notably, two key trends reverse direction:

- the production of nuclear fuels begins to decline due to primary resource depletion, and
- coal production rises 42% from 2050, approaching 2015 levels, driven primarily by residual demand for heat and LaG fuels.

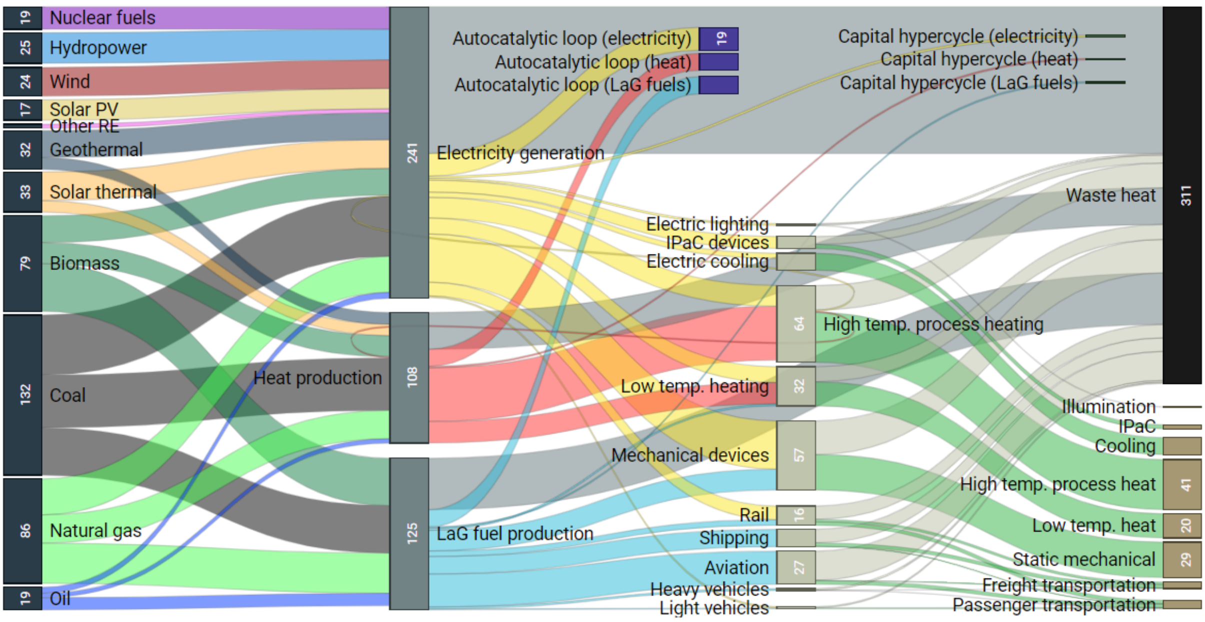

Figure 28: Sankey diagram for mean GES energy flows in the base case in 2100

6.1.2 Supply/demand balance

As described in section 4.2.9.1, failed realizations corresponding to a net energy trap outcome can be identified by thresholds applied to EC deficit, defined as negative cumulative supply/demand balance relative to demand, by EC type ($-\boldsymbol{b} \oslash \boldsymbol{p}_o$). For the analysis of PRESS model, thresholds are chosen to separate possible recovery from terminal deficit, as effectively as possible. To define realization failure, any of the following criteria must be true at some point during the simulated period:

- any individual EC deficit component must exceed 5 years,
- the mean EC deficit across all components must exceed 3 years, or
- the mean rate of change of EC deficit across all components must exceed one.

This is depicted in Figure 29; six realizations are selected from an ensemble for 10,000 realizations for illustration purposes, three failed and three successful (labelled with realization number). Note that the highlighted lines show the LaG fuels component of EC deficit for each realization, with other components displayed using transparent lines. Stable times (elapsed simulation time prior to failure criteria being met) are indicated for failed realizations. The rate of change limit refers to a failure threshold defined by (mean) gradient.

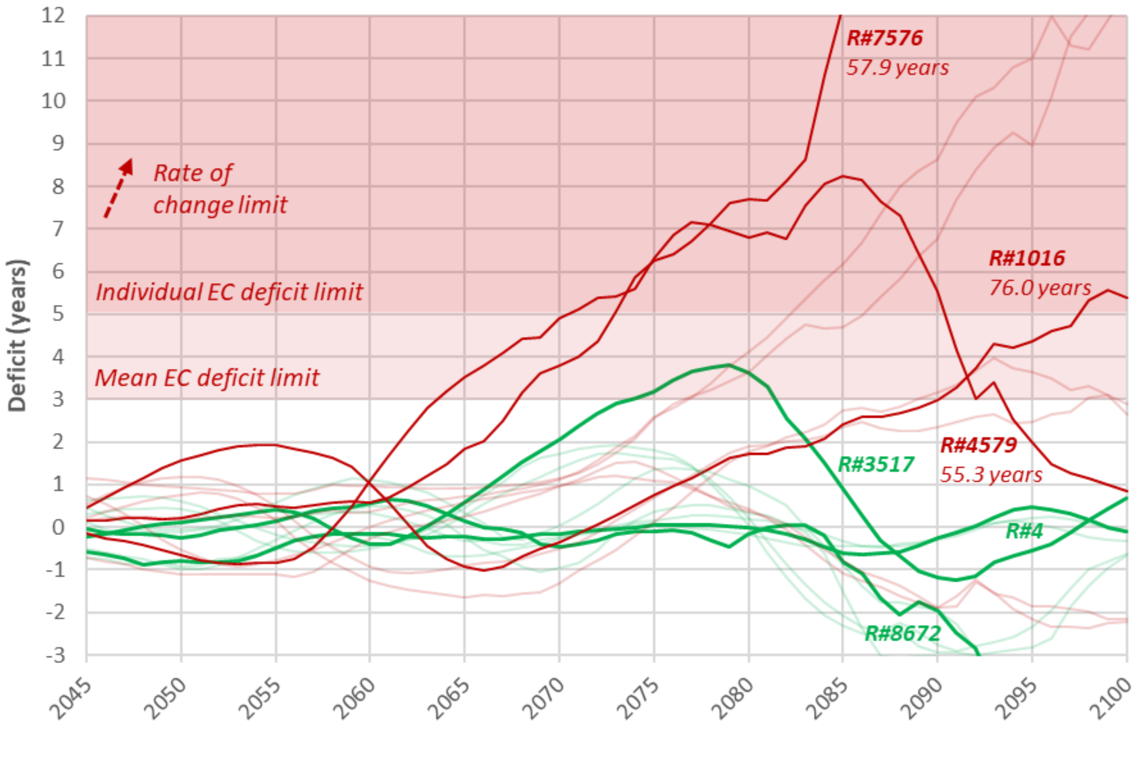

Figure 29: examples of realization success (green) and failure (red) defined by EC deficit trends

Figure 30 shows mean EC deficit trends by EC component for the successful and failed realization subgroups. The failed subgroup exhibits a clear divergence towards greater deficit, indicating inexorable EC shortages characteristic of net energy trap outcomes. Conversely, the successful subgroup maintains a tendency to self-correct towards ***0***. In both subgroups, maintaining sufficient supplies of LaG fuels appears to be more challenging than for other ECs, especially in the late simulation period.

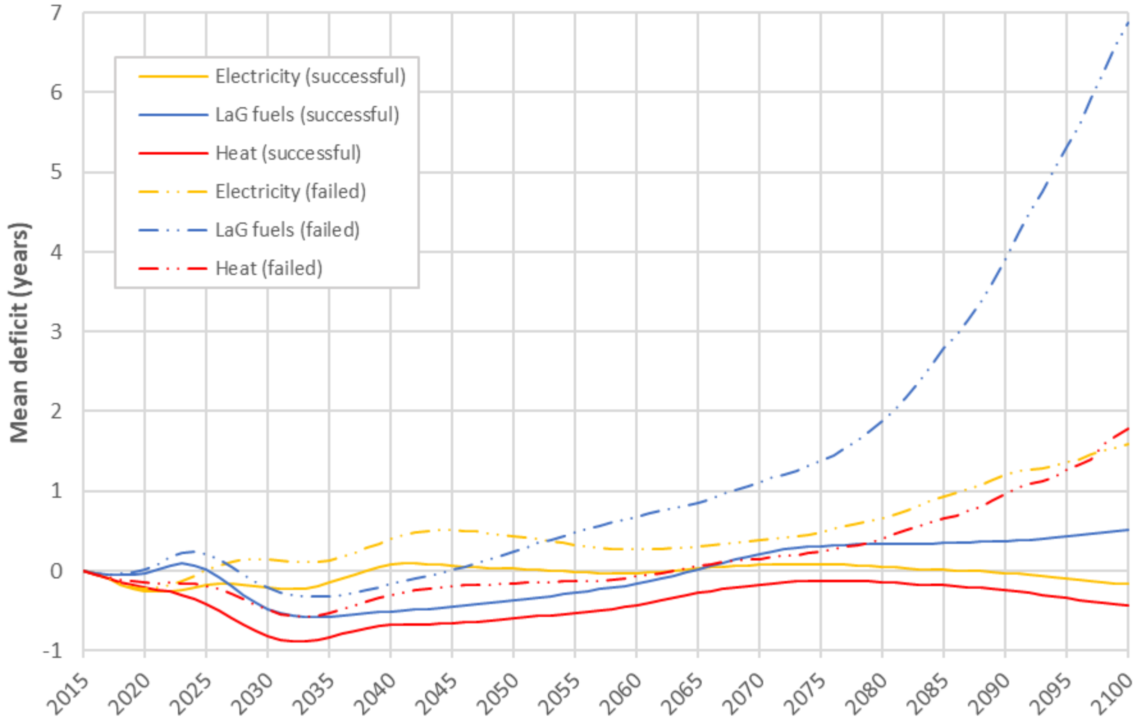

Figure 30: mean EC deficit trends by EC component for successful and failed realization subgroups

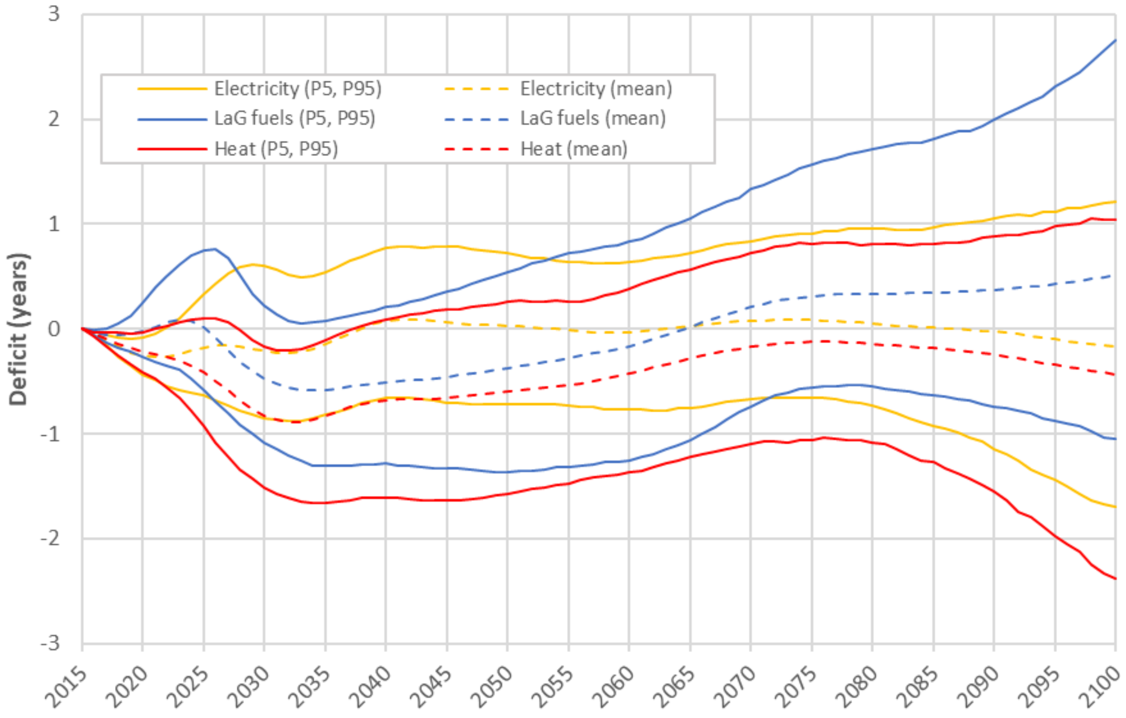

Figure 31: EC deficit envelopes by EC component for successful realizations

Probabilistic envelopes for EC deficit by EC component for the successful realization subgroup are shown in Figure 31. The supply of heat and LaG fuels consistently exceeds demand early in the simulation period. LaG fuel deficits become more common in the late simulation period. Supply and demand of electricity remain approximately balanced over the simulation period.

6.1.3 System stability

Figure 32 shows the cumulative probability distribution for stable time. Note that failed realizations are included here, by necessity, and stable time is equal to the full simulation period of 85 years for successful realizations. Mean stable time is 84.5 years. 99% of realizations have stable times exceeding 68 years (i.e., no realization failure prior to 2083), with the risk of failure rising sharply after this time. The final failure rate in the base case is 5% (indicated by the intercept of the trend line with the vertical axis) implying a small but non-trivial risk of a net energy trap outcome. The blue bars show the 90% confidence interval for the failure rate (4.7% to 5.4%).

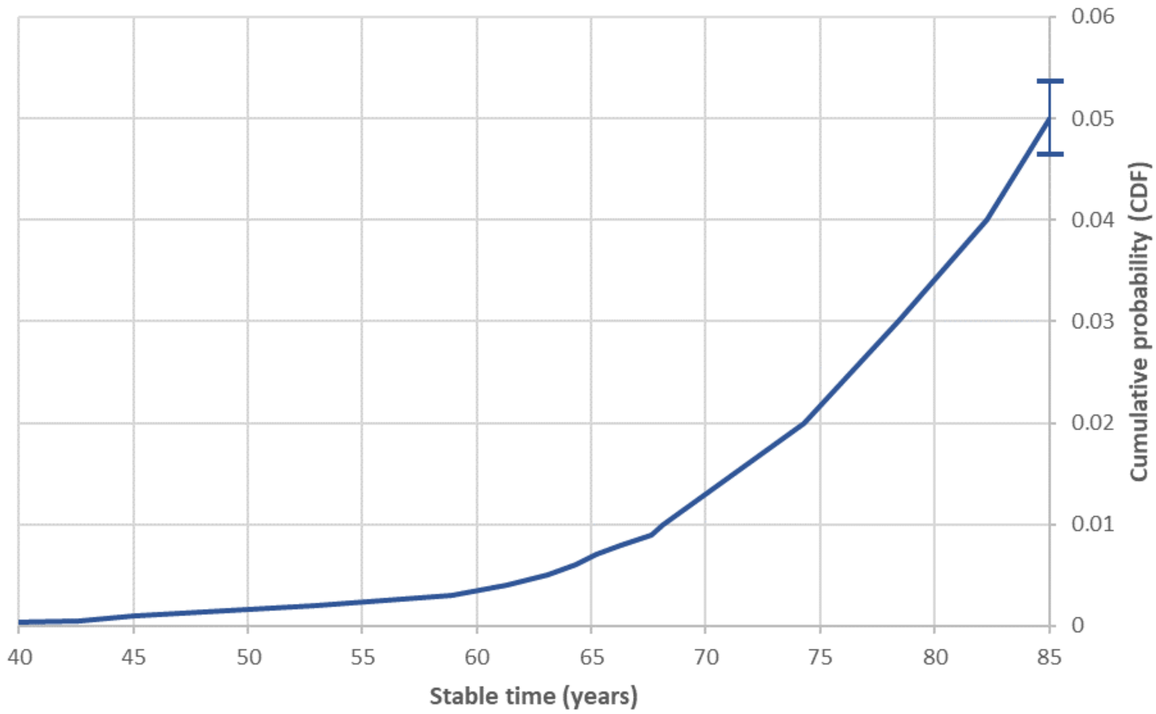

Figure 32: cumulative probability distribution for stable time, including 90% confidence interval for failure rate

6.1.4 Supply

The probabilistic envelope for total primary energy supply (TPES) for successful realizations is depicted in Figure 33. TPES declines markedly from the beginning of the simulation period to around 2035. After this time, TPES stays relatively constant or increases. By 2100, mean and median TPES has returned to its initial level. The 95th percentile for TPES in 2100 exceeds the initial level by approximately 75%, while the 5th percentile represents a reduction of 53% from the initial level. Note that contributions to TPES are adjusted for primary energy equivalence.

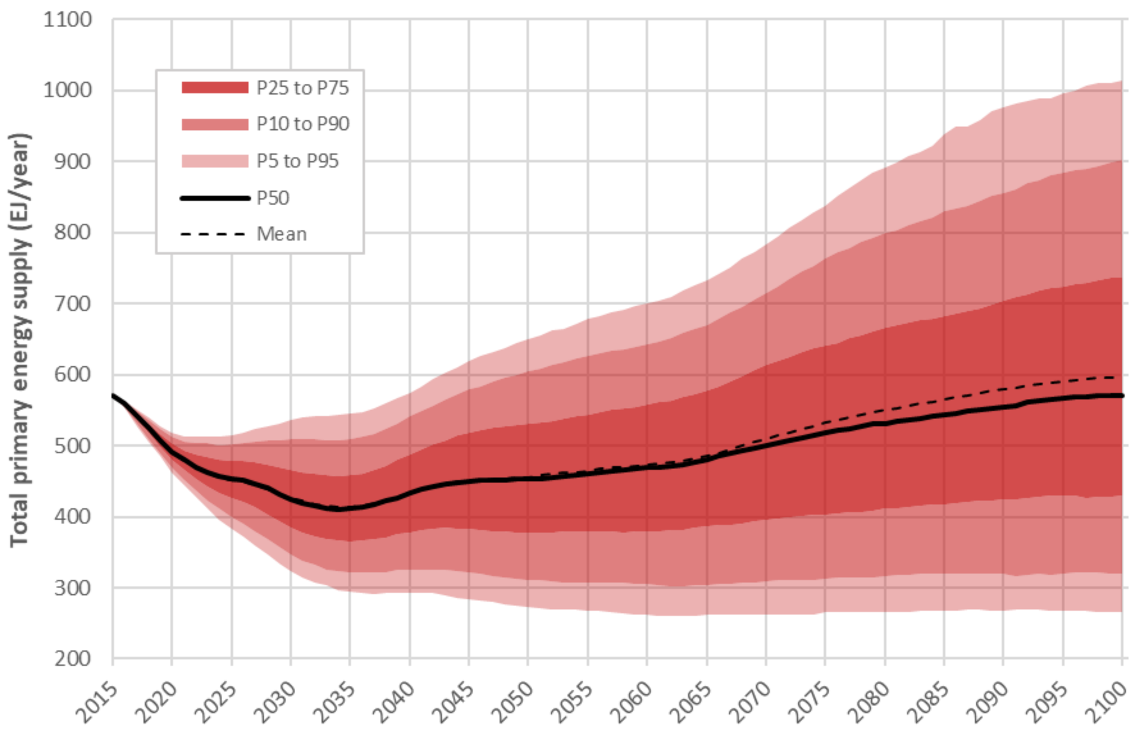

Figure 33: envelope for total primary energy supply (TPES)

Figure 34 shows mean primary energy supply by resource, adjusted for primary energy equivalence. NRE supply declines rapidly from the start of the simulation period until approximately 2050, after which coal and natural gas partially recover while oil continues to decline, to 12% of its initial level. Nuclear fuel supply grows to a peak approximately twice its initial level by 2060 before declining to less than its initial level by 2100. Supply from all RE sources grows over the simulation period, most strongly for geothermal, solar thermal, wind, solar PV, and other RE. However, biomass and hydropower are still the largest RE sources by 2100, closely followed by wind.

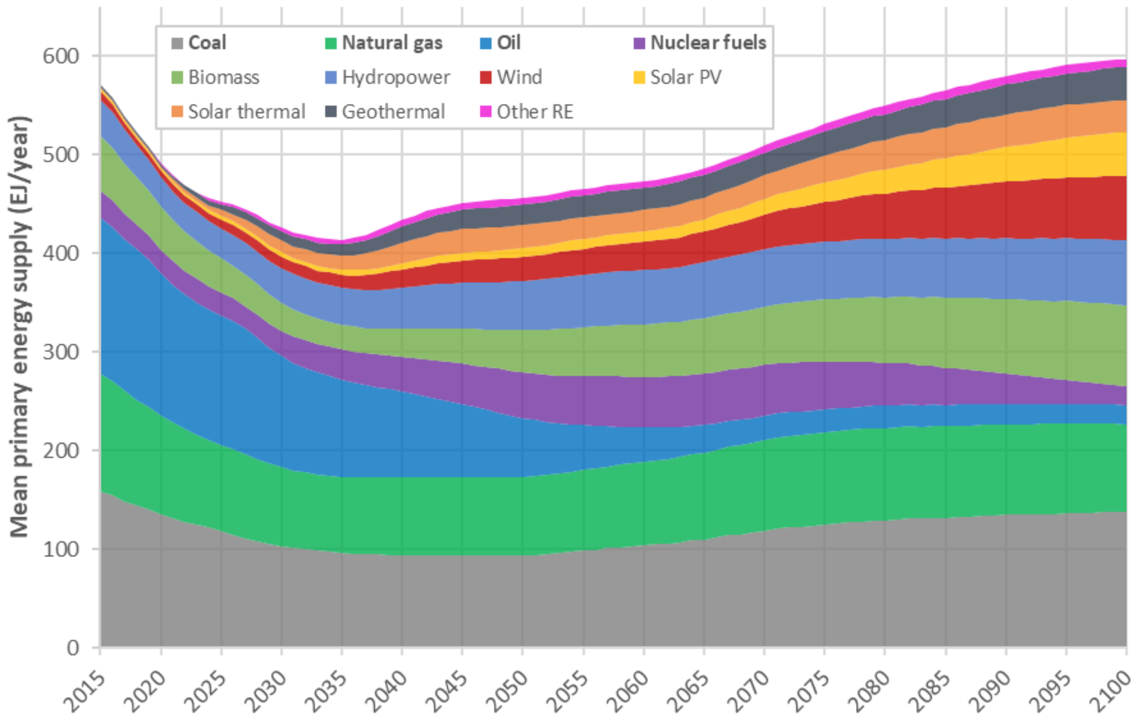

Figure 34: mean primary energy supply by resource (NRE types in bold; adjusted for primary energy equivalence)

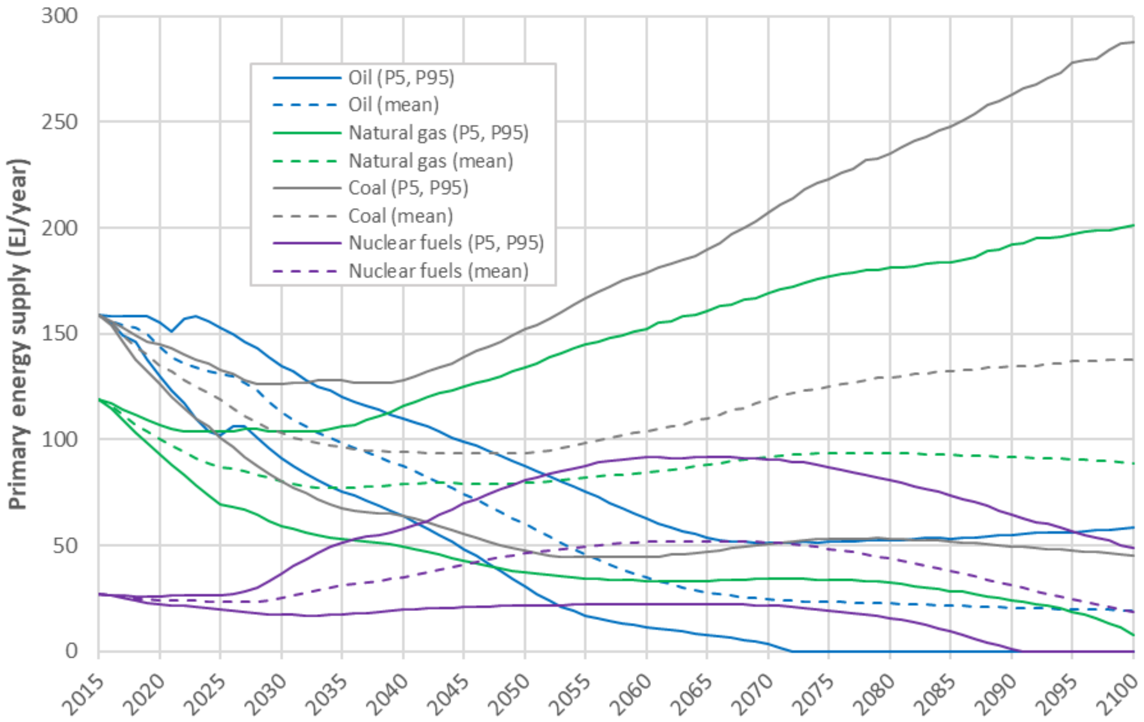

Figure 35: envelopes for primary NRE supply by resource

Envelopes for NRE supply by resource, shown in Figure 35, show far wider distributions for coal and natural gas than for oil and nuclear fuels from 2035 onwards, implying greater uncertainties. While it is possible for coal and natural gas to reach stable minima and continue to decline, respectively (indicated by the 5th percentiles), it is also possible to see strong growth in supply from both resources after 2035, reaching 69% and 81% above their initial levels, respectively (indicated by the 95th percentiles). Oil exhibits monotonous declines while nuclear fuels peaks around 2060 before declining in essentially all realizations. It is possible for oil and nuclear fuels supply to reach zero by 2072 and 2091, respectively.

Envelopes for the major resources constituting RE supply, shown in Figure 36, exhibit significant growth over the simulated period. All have very wide and expanding distributions, solar PV and wind in particular, implying considerable uncertainties. Biomass and hydropower production declines until around 2035 and 2025, respectively, after which they resume growth. It is possible for solar PV and wind to remain minor contributors to overall supply, as indicated by the 5th percentiles.

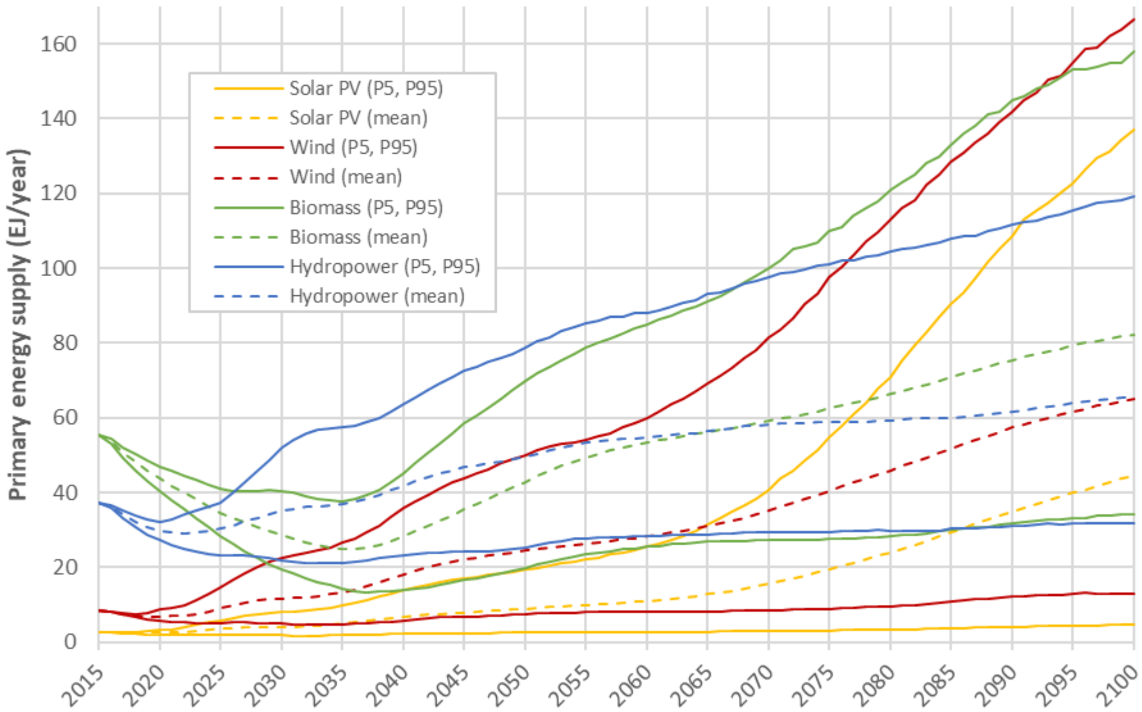

Figure 36: envelopes for primary RE supply by resource (major)

Envelopes for the minor contributions to RE supply, shown in Figure 37, exhibit strong initial growth. However, this growth is weaker and less consistent in the later simulation period, after 2045. Solar thermal and geothermal have very wide and expanding distributions, implying high uncertainties.

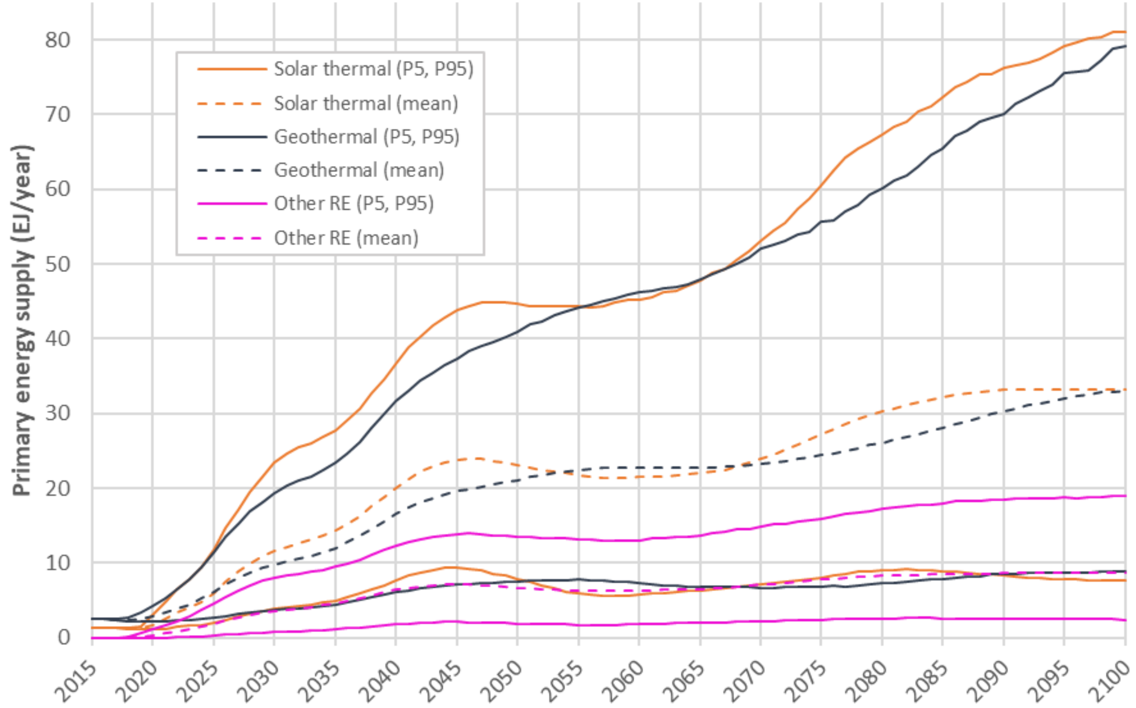

Figure 37: envelopes for primary RE supply by resource (minor)

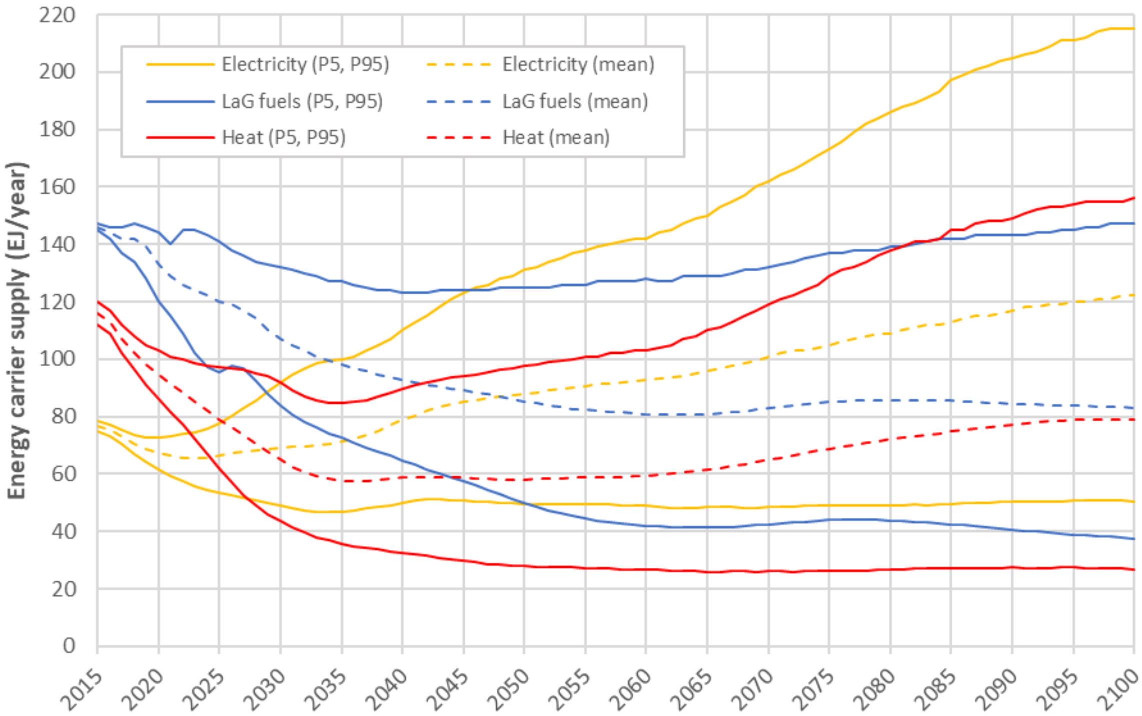

Figure 38: envelopes for EC supply

Figure 38 shows envelopes for EC supply. LaG fuel and heat supply decline markedly until around 2035. Electricity shows consistent growth from this time while LaG fuel and heat stay relatively constant. This is consistent with a general trend towards greater electrification despite uncertainties indicated by widening distributions. However, limits are apparent in reducing the shares of LaG fuel and heat in total EC supply, and in no realizations do these components converge towards zero.

6.1.5 Demand

Envelopes for final, non-energy related EC demand, shown in Figure 39, follow similar profiles to EC supply (in Figure 38) with initial rapid declines flowed by growth or gradual decline. Shares of LaG fuel and heat in final EC demand are slightly reduced relative to supply from around 2060. Note that initial uncertainties in final EC demand are greater than corresponding uncertainties in supply.

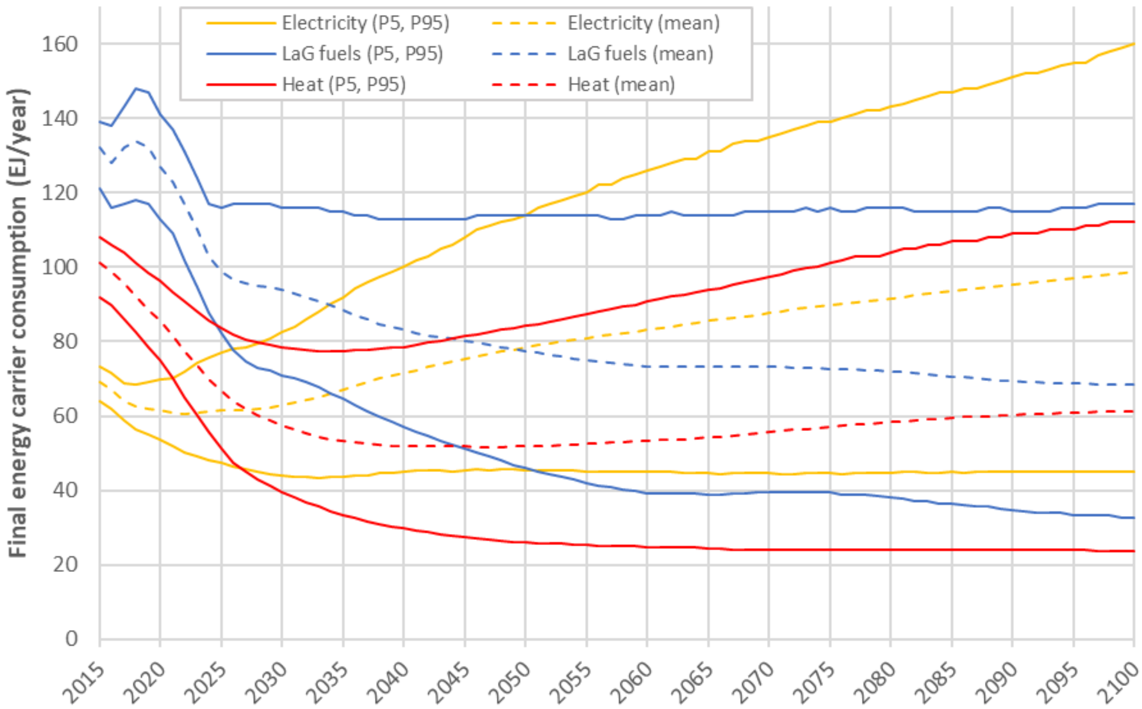

Figure 39: envelopes for final (non-GES) EC demand

Figure 40 shows envelopes for GES metabolic EC demand. These exhibit instabilities early in the simulated period followed by generally stable trends, in central tendencies and envelope extrema, to approximately 2055. After this time, GES metabolic demand for all ECs increases consistently towards 2100 with widening uncertainties. Note that while unlikely, the lower limits of the distributions (5th percentiles) allow for approximately constant GES metabolic demand over the simulated period. The mean composition of this GES metabolic demand shifts rapidly from a roughly equal split between the autocatalytic loop and capital hypercycle initially to predominantly autocatalytic loop consumption by around 2030, followed by slower increases in the share allocated to the autocatalytic loop.

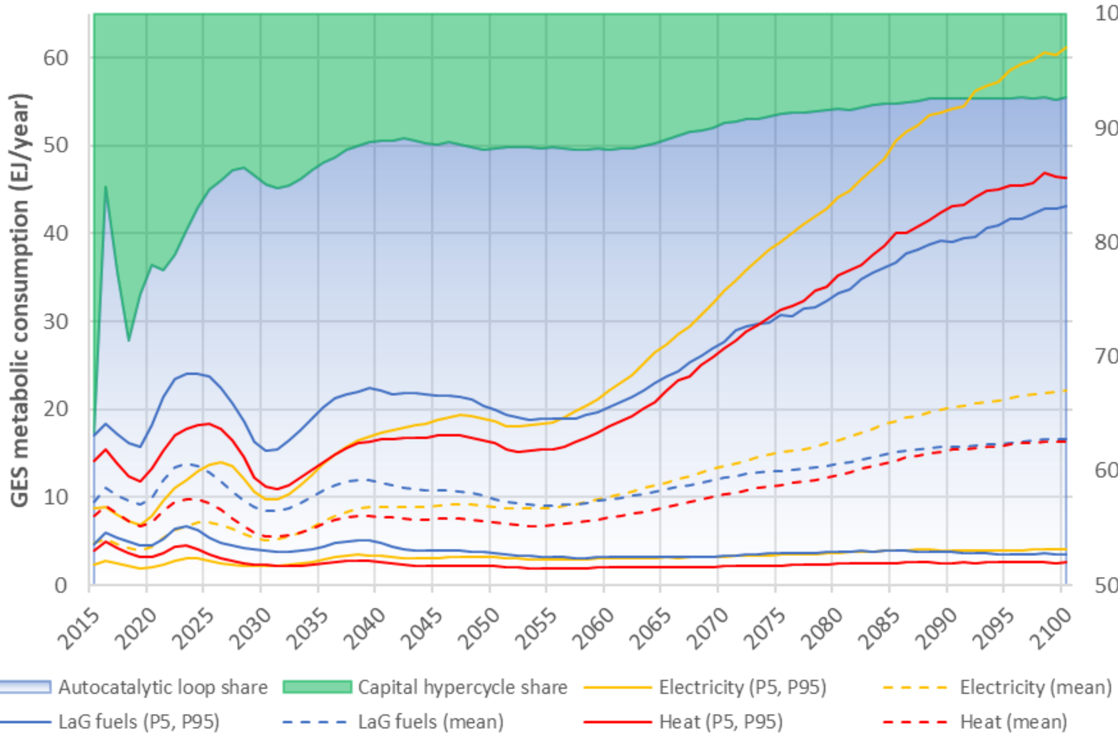

Figure 40: envelopes for GES metabolic EC demand, including autocatalytic loop and capital hypercycle shares

Figure 41, Figure 42, and Figure 43 show envelopes for the major, moderate, and minor ES demand components, respectively, in terms of absolute delivered ES flows defined via reference modes introduced in section 4.1.2. These delivered ES flows span three orders of magnitude. For all ES demands, slight declines are possible, but growth is more likely. Note that Figure 43 is presented with a logarithmic vertical axis.

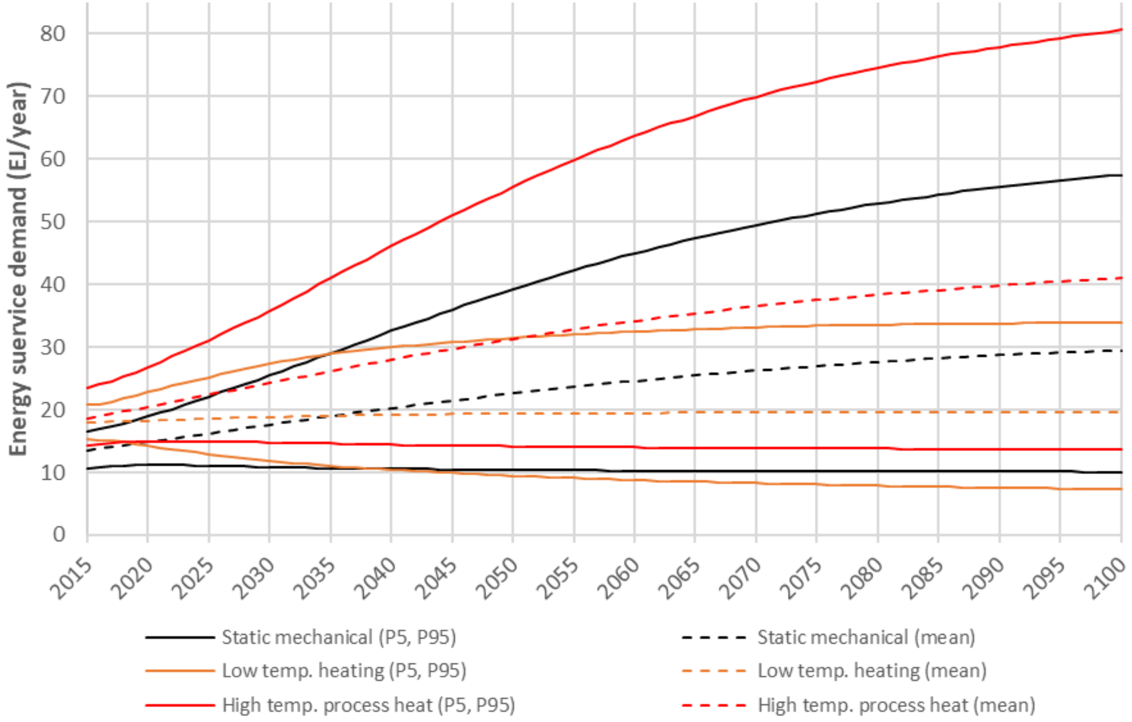

Figure 41: envelopes for ES demands (major)

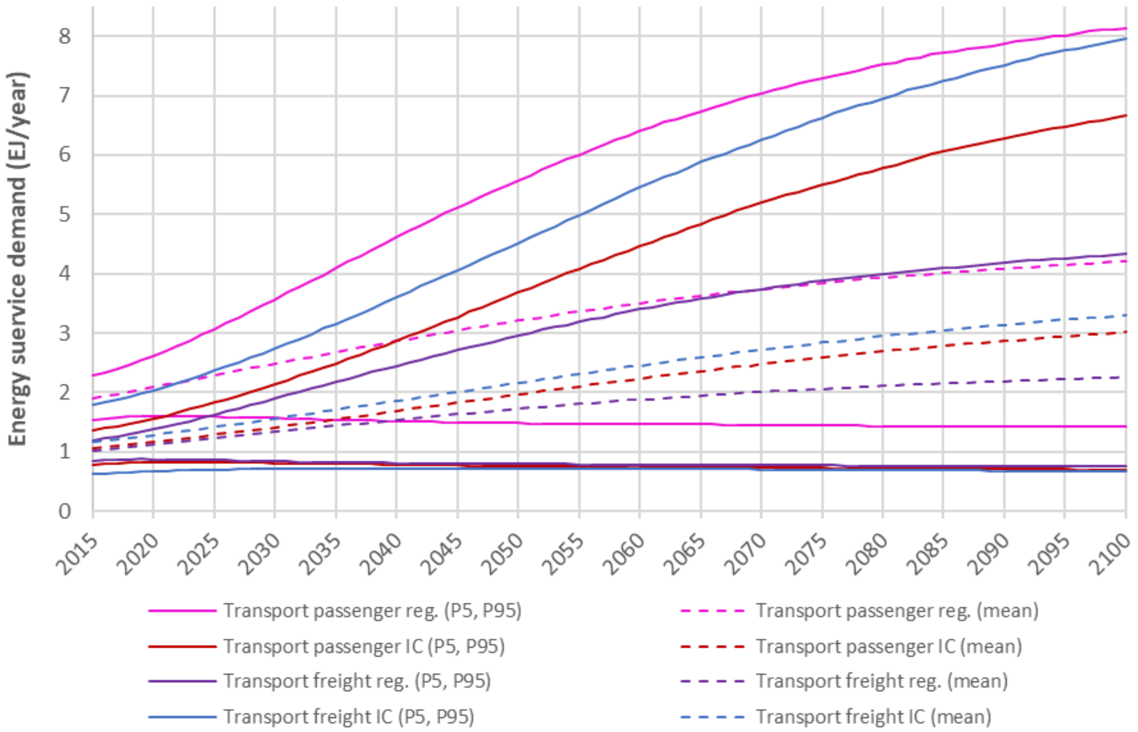

Figure 42: envelopes for ES demands (moderate)

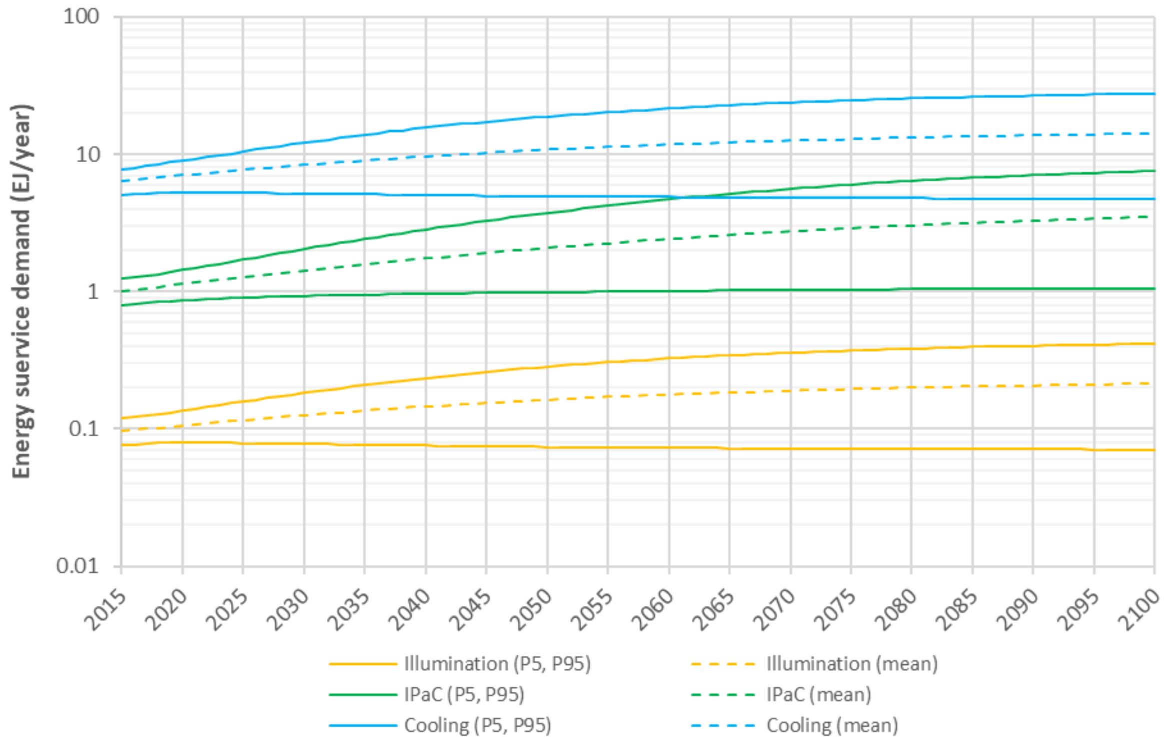

Figure 43: envelopes for ES demands (minor; semi-logarithmic)

6.1.6 Primary resources

Envelopes for NRE depletion, ***d***, shown in Figure 44 and Figure 45, depict earlier and more aggressive depletion for nuclear fuels and oil than for natural gas and coal. For all resources, it is possible to reach a value of one by 2100, at which point production may continue (below specified terminal EROI values) but further investment in PC ceases. This highly likely for current generation nuclear fuels and moderately likely for oil, but relatively unlikely for coal and natural gas. For the fossil fuels, depletion gradients in both the means and envelope extrema quickly fall below their initial levels but remain relatively constant in the later part of the simulation period. For nuclear fuels, depletion accelerates from 2030 before reaching an inflection point between 2060 and 2070. For all NRE resources, distributions progressively widen, indicating significant uncertainties.

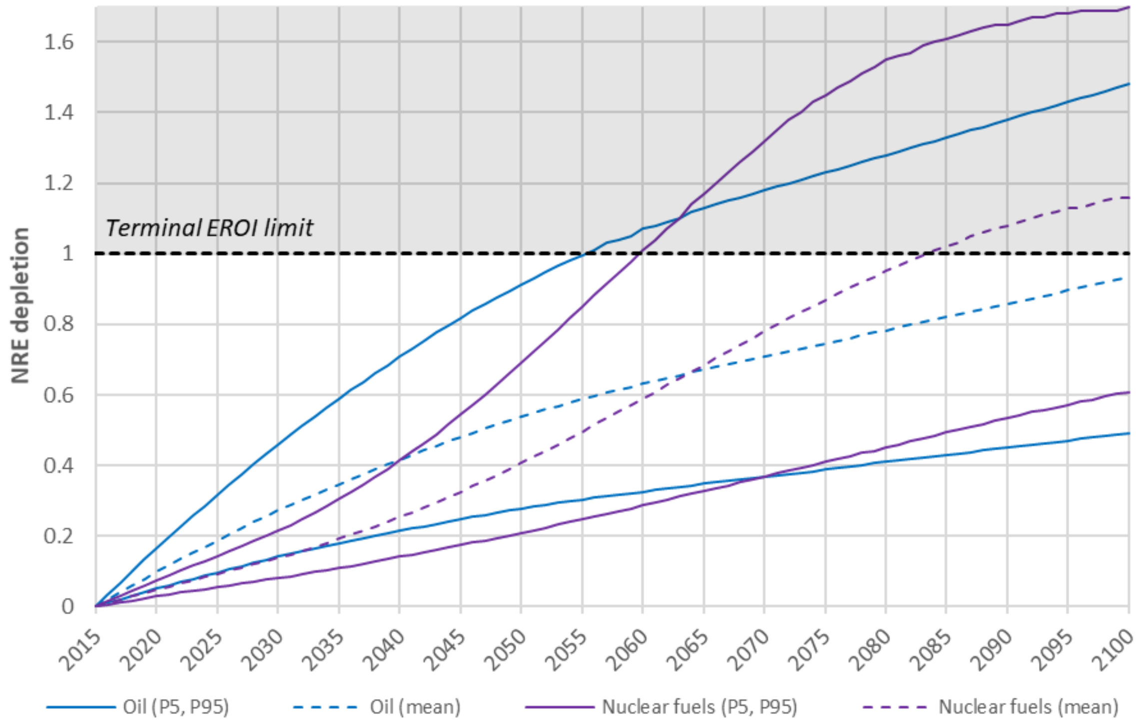

Figure 44: envelopes for NRE depletion of primary resources, including EROI terminal limit (high depletion)

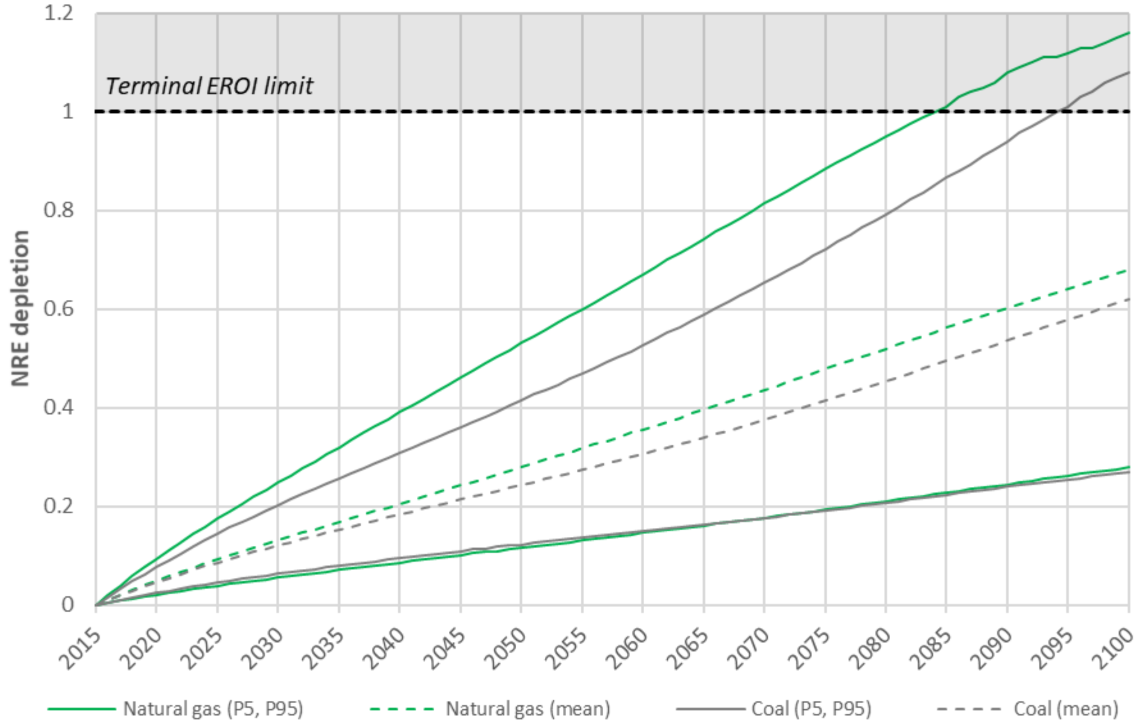

Figure 45: envelopes for NRE depletion of primary resources, including terminal EROI limit (low depletion)

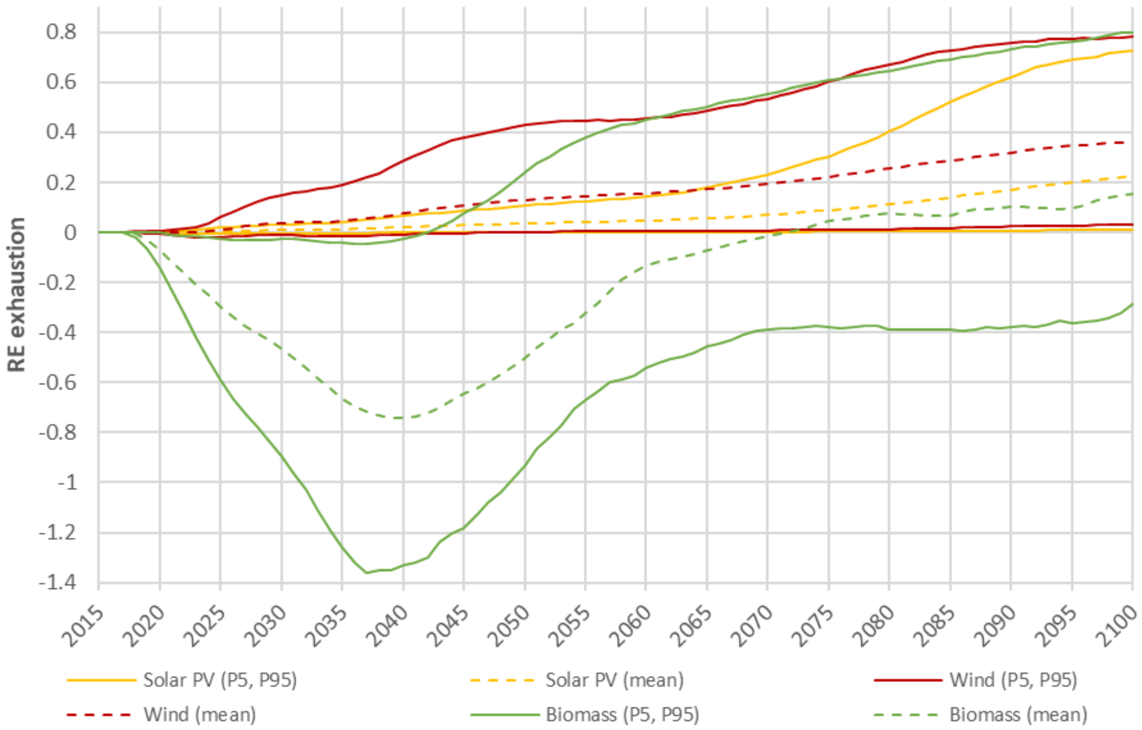

Figure 46: envelopes for RE exhaustion of primary resources (low exhaustion)

Envelopes for RE exhaustion, $\boldsymbol{x}$, shown in Figure 46, depict slow increases in resource utilization with significant ranges of possible outcomes. Mean exhaustion values by 2100 are less than 40% and upper limits are less than 80%, implying total available resources will not be fully utilized. In contrast, the RE resources in Figure 47 can reach near total exhaustion at the upper envelope limits, while means converge towards 50-60% exhaustion. Both biomass and hydropower can enter negative exhaustion in the early part of the simulated period, implying production rates below their initial levels. Uncertainty in solar PC exhaustion is relatively low until around 2070. Biomass exhaustion is subject to particularly high uncertainties over the entire simulated period.

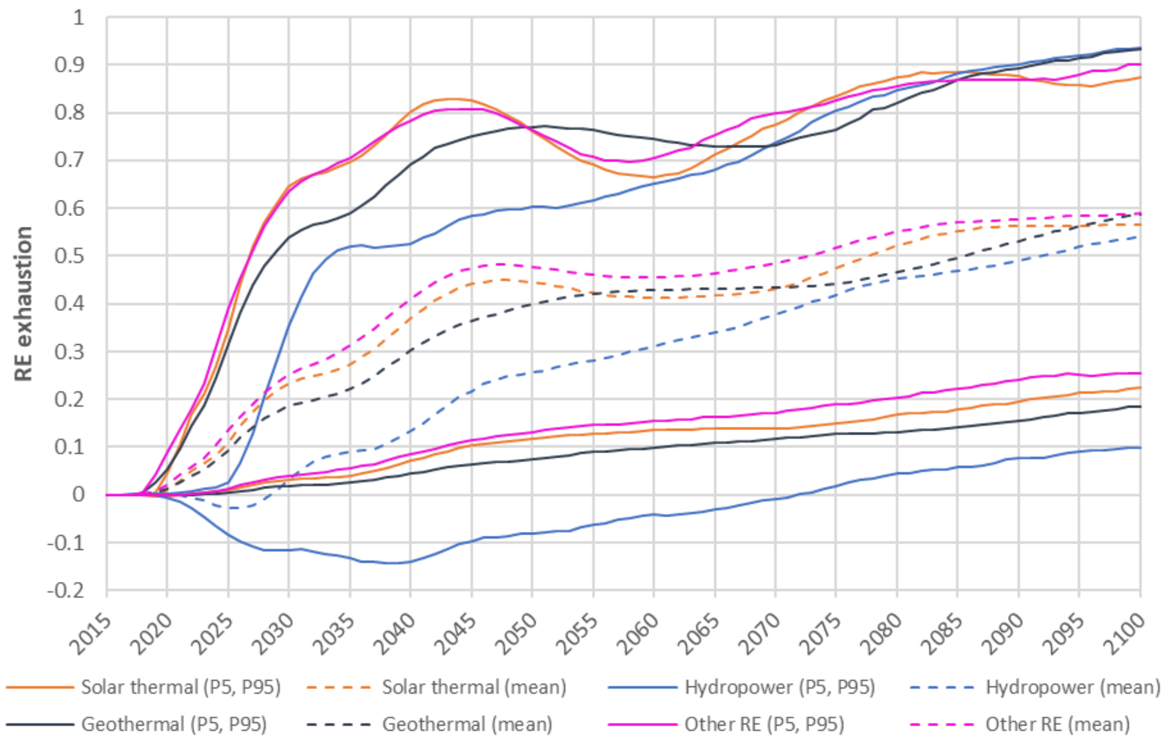

Figure 47: envelopes for RE exhaustion of primary resources (high exhaustion)

6.1.7 RE share of supply

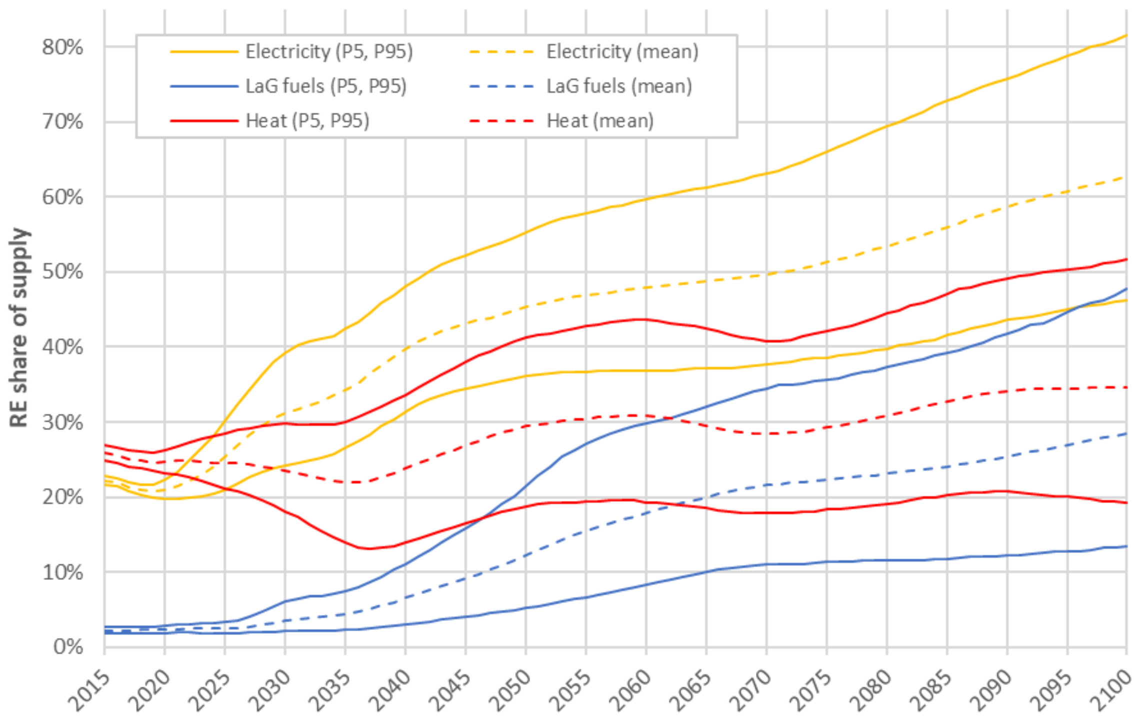

Figure 48: envelopes for RE share of supply by EC type

As shown in Figure 48, the shares of electricity and heat production coming from RE resources start at similar levels, but the share for electricity is able to increase more consistently and to a higher level. The RE share of electricity production is likely to be well over 50% by 2100. The RE share of heat production is likely to remain below 50%. The share for LaG fuels starts at a very low level but can increase substantially, to at least 15% and up to 45% by 2100. None approach 100% RE shares before 2100. All exhibit widening distributions implying significant uncertainties.

The RE share of TPES, shown in Figure 49, increases strongly after a brief initial decline. The mean and median increase to approximately 35% by 2050 and 50% by 2100. At the most optimistic limit, the RE share of TPES increases to around 43% by 2050 and 70% by 2100.

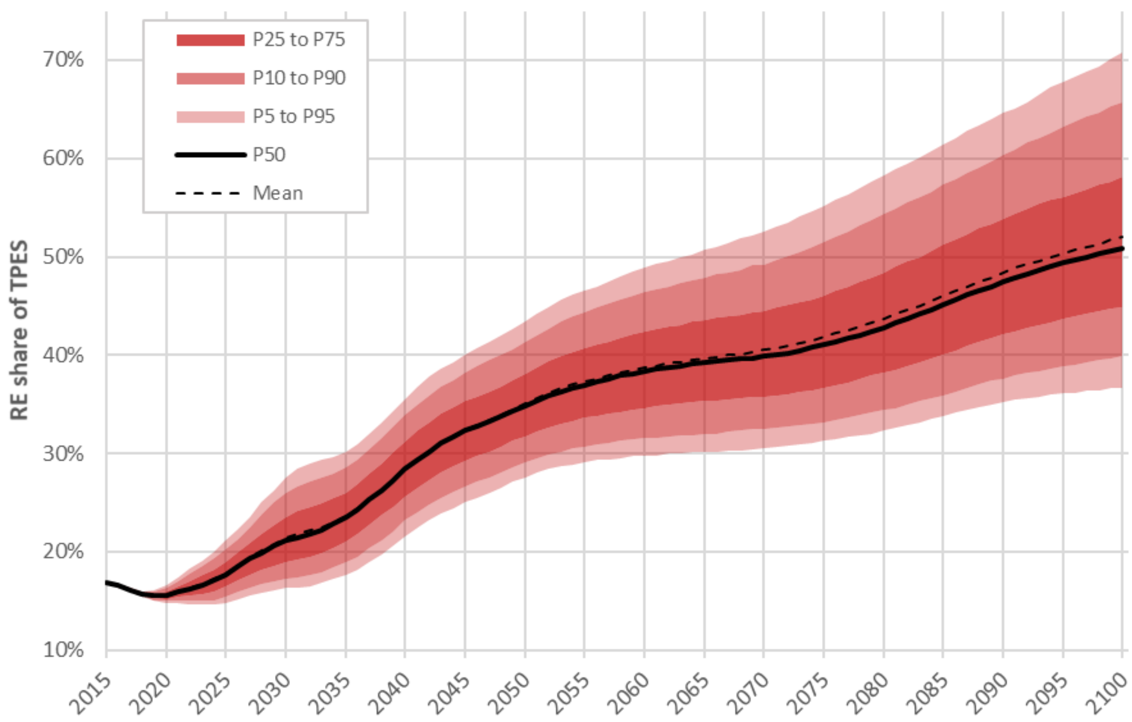

Figure 49: envelope for RE share of TPES

6.1.8 EROI

Envelopes for PC mean NRE EROI, shown in Figure 50 and Figure 51, show strongly declining trends despite considerable initial uncertainties. PC mean NRE EROI values remain in the same order as their initial values during the simulated period, except for nuclear fuels, which is likely to fall below coal EROI before 2100. Notably, EROI distributions for all NRE sources narrow over time, indicating convergence to ultimate EROI values. By 2100, the upper distribution limits for PC mean EROI for all NRE sources is below 40. It is possible for all NRE PC mean EROI values to fall below 10 by this time.

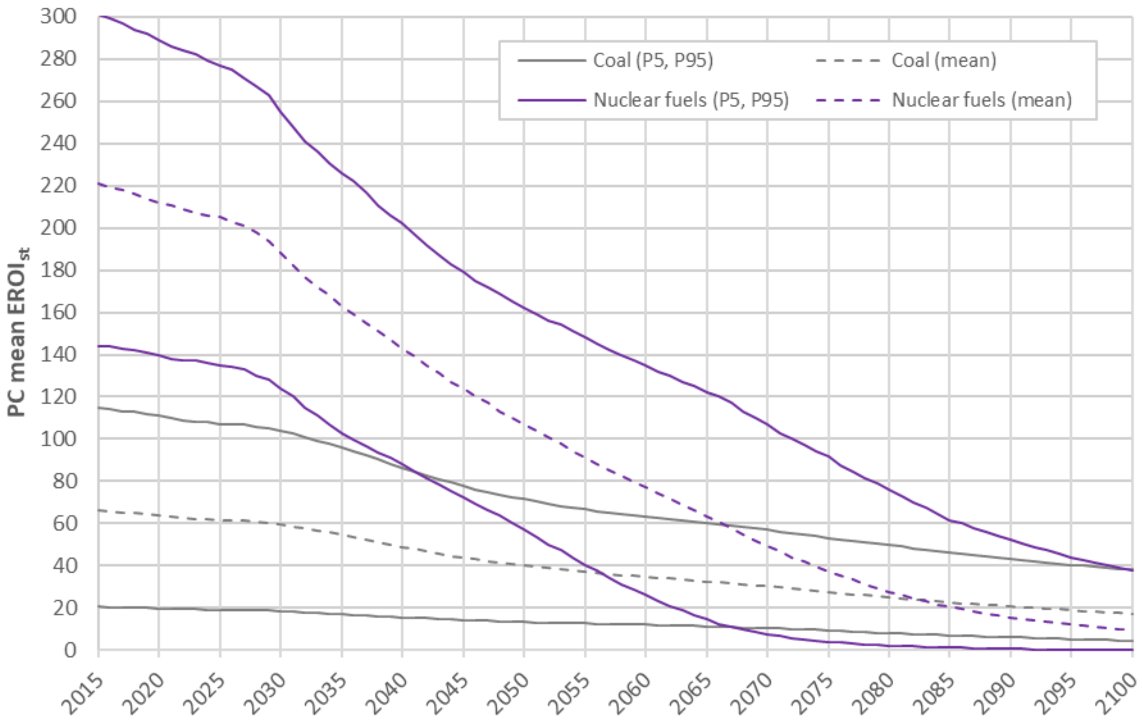

Figure 50: envelopes for NRE PC mean EROI (high)

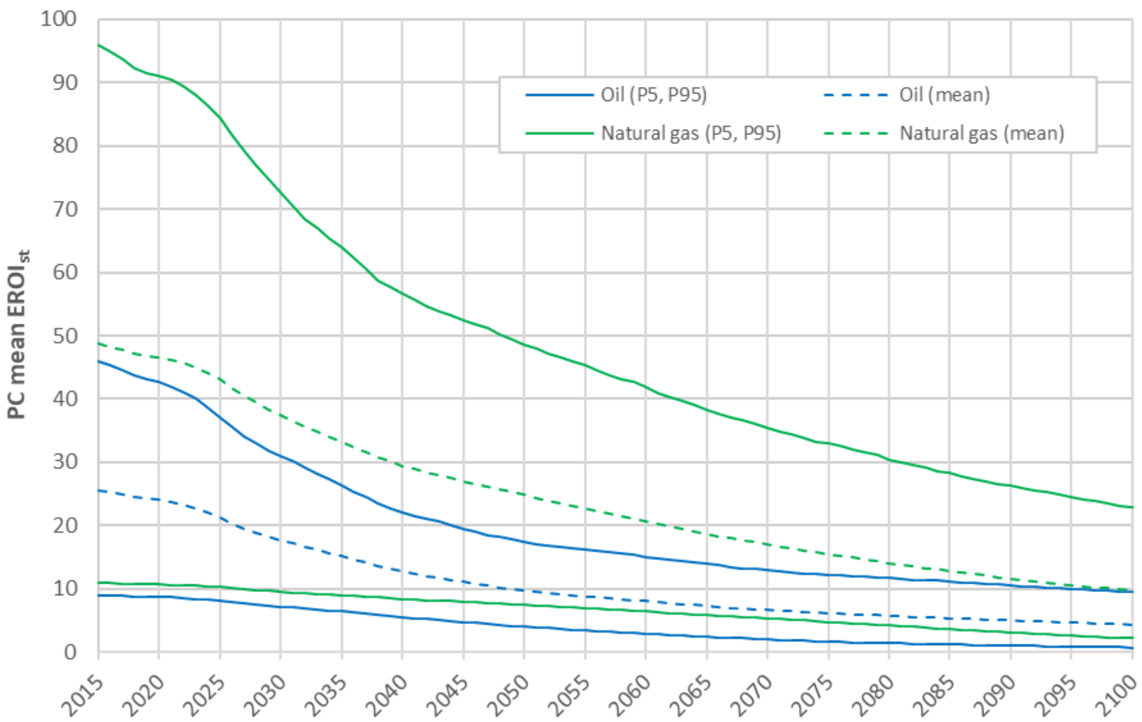

Figure 51: envelopes for NRE PC mean EROI (low)

Envelopes for PC mean RE EROI, shown in Figure 52 and Figure 53, exhibit generally declining trends. However, EROI declines are relatively muted for solar PV and wind, with means falling by only 6% and 22%, respectively. Biomass is unique as it is subject to increasing EROI after 2035 before declining again after 2055 (observed both in the distribution mean and extrema).

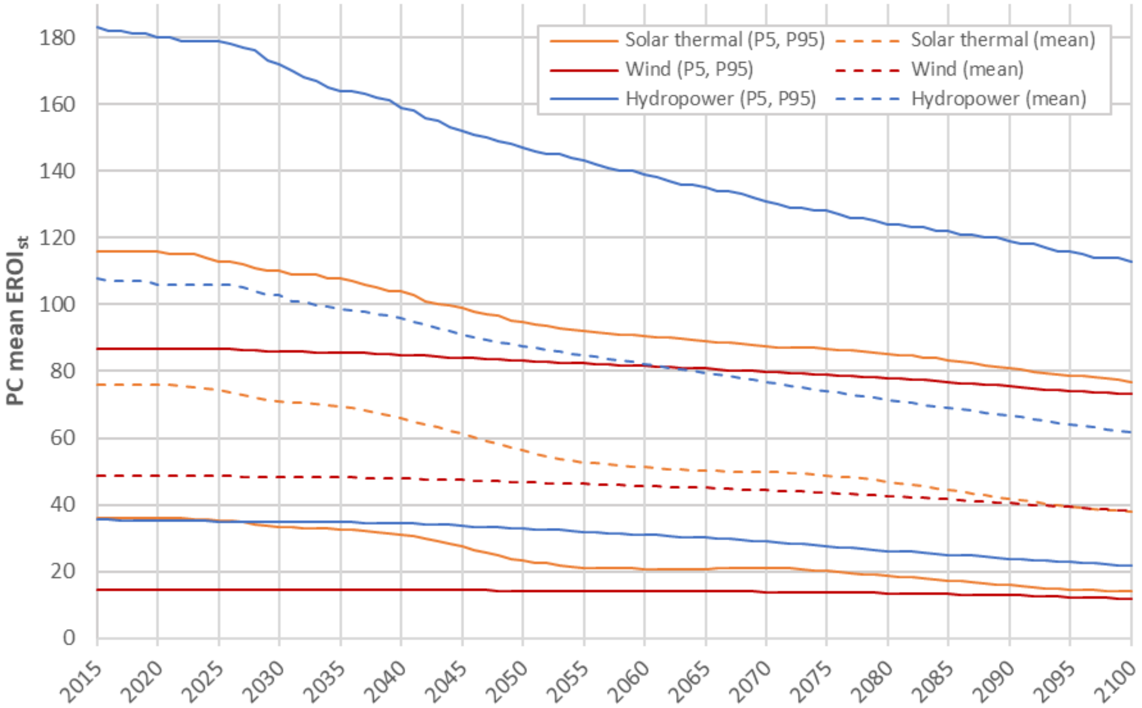

Figure 52: envelopes for RE PC mean EROI (high)

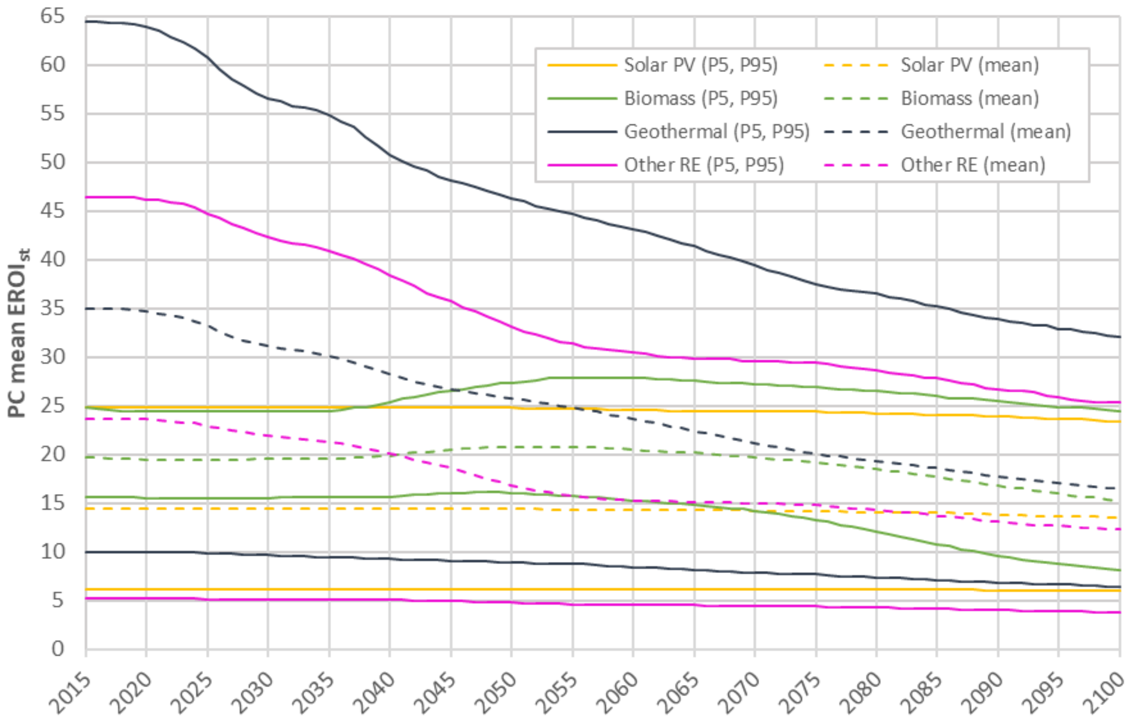

Figure 53: envelopes for RE PC mean EROI (low)

As with NRE EROI, distributions for RE sources narrow over time, indicating convergence to ultimate EROI values, with the exception of biomass which is subject to increasing uncertainty. By 2100, mean EROI values for all RE sources still exceed 10. However, lower distribution limits begin or fall below 10 for solar PV, biomass, geothermal, and other RE.

Figure 54 depicts envelopes for point-of-use EROI trends for ECs. These envelopes exhibit declines over the simulated period, with pronounced instabilities prior to 2055 in central tendencies and envelope extrema, particularly at the upper distribution limits (95th percentiles). Mean point-of-use EROI values decline between 44% and 47% from their initial values by 2100, to below 10 for all ECs. Electricity EROI remains consistently higher than heat and LaG fuel EROI during the simulated period. It is possible for point-of-use EROI for all ECs to drop below 3 by 2100.

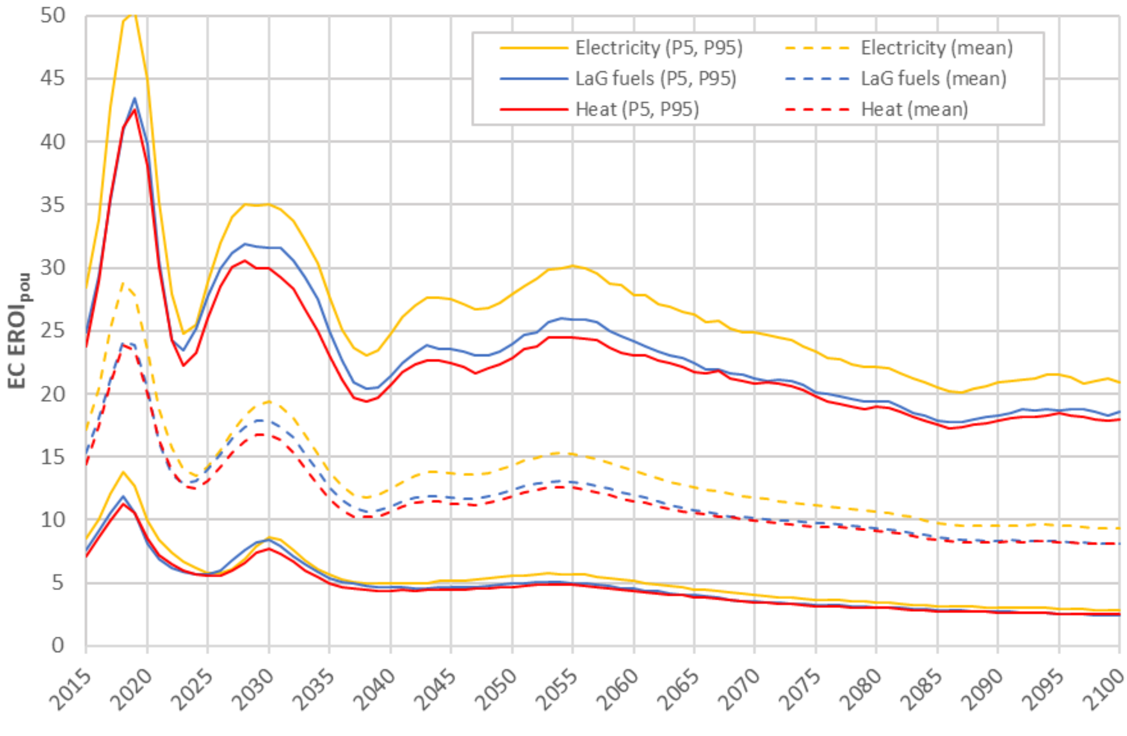

Figure 54: envelopes for point-of-use EROI by EC type

6.1.9 Capacity factors

PC utilization trends, driven by relative EC surplus or abundance, are indicated by median CFs. Medians are used to indicate central tendencies due to the presence of highly skewed CF distributions.

6.1.9.1 Upstream

As described in section 4.2.2.3, initial CFs for primary and secondary PC are assumed to coincide with their long-term maxima.

Median CFs for primary and secondary NRE PC are shown in Figure 55 and Figure 56. Early CF declines occur for all PC types, most notably for secondary heat production prior to 2030. Median CFs for secondary PC then typically increase slowly towards their respective CF maxima, reaching or approaching these between 2035 and 2070. Median CFs for primary PC generally oscillate between 70% and 100% of CF maxima following initial declines. Nuclear primary and secondary PC median CFs exhibit marked declines after 2070 due to advanced primary resource depletion.

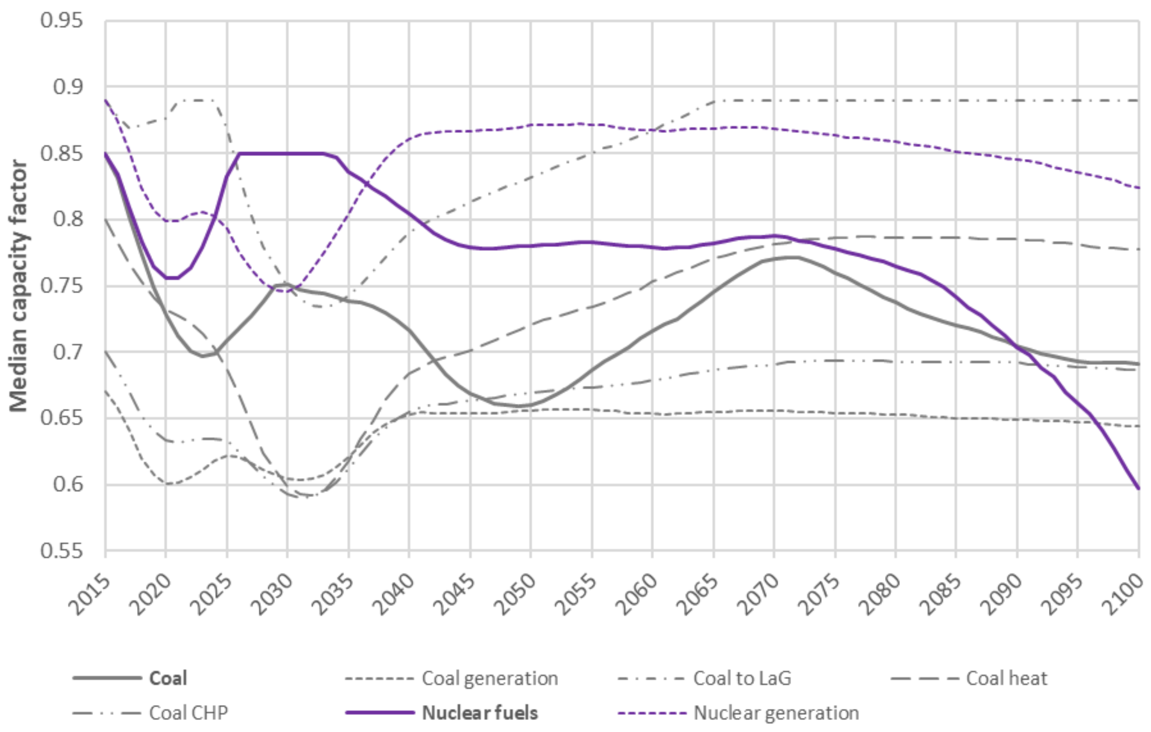

Figure 55: primary and secondary PC median CFs for coal and nuclear

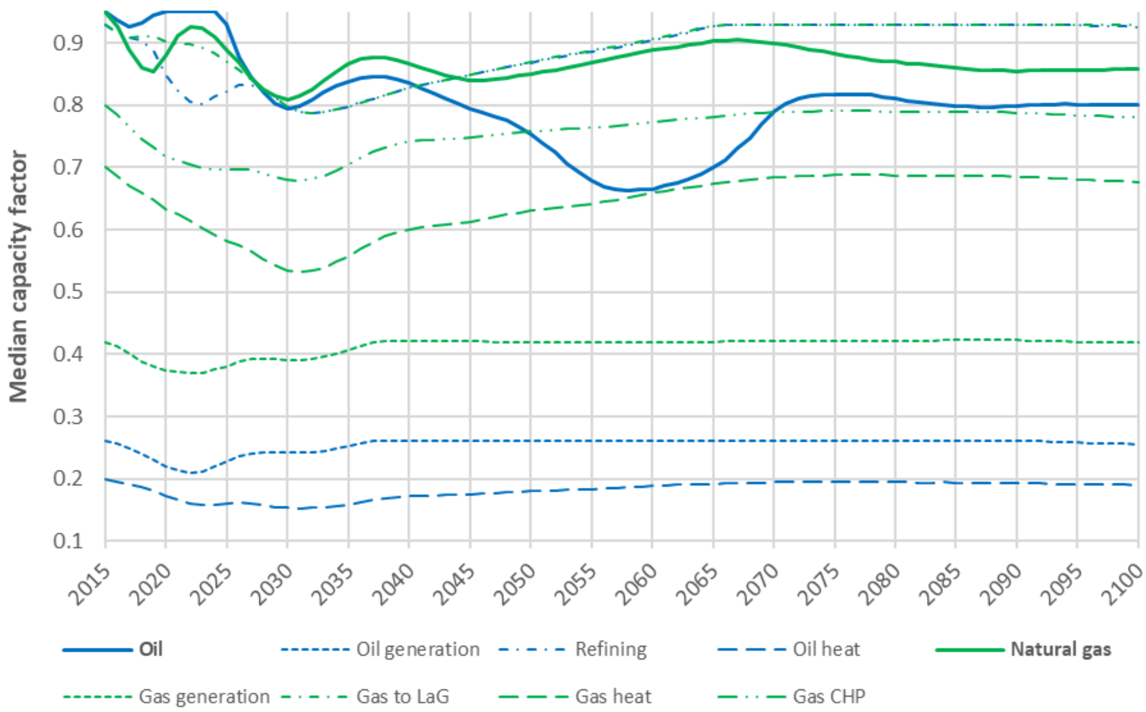

Figure 56: primary and secondary PC median CFs for oil and natural gas

Median CFs for primary and secondary RE PC are shown in Figure 57 and Figure 58. Again, early CF declines occur for all PC types, most notably for biomass and secondary heat production prior to 2030 (median declines of up to 32% from CF maxima).

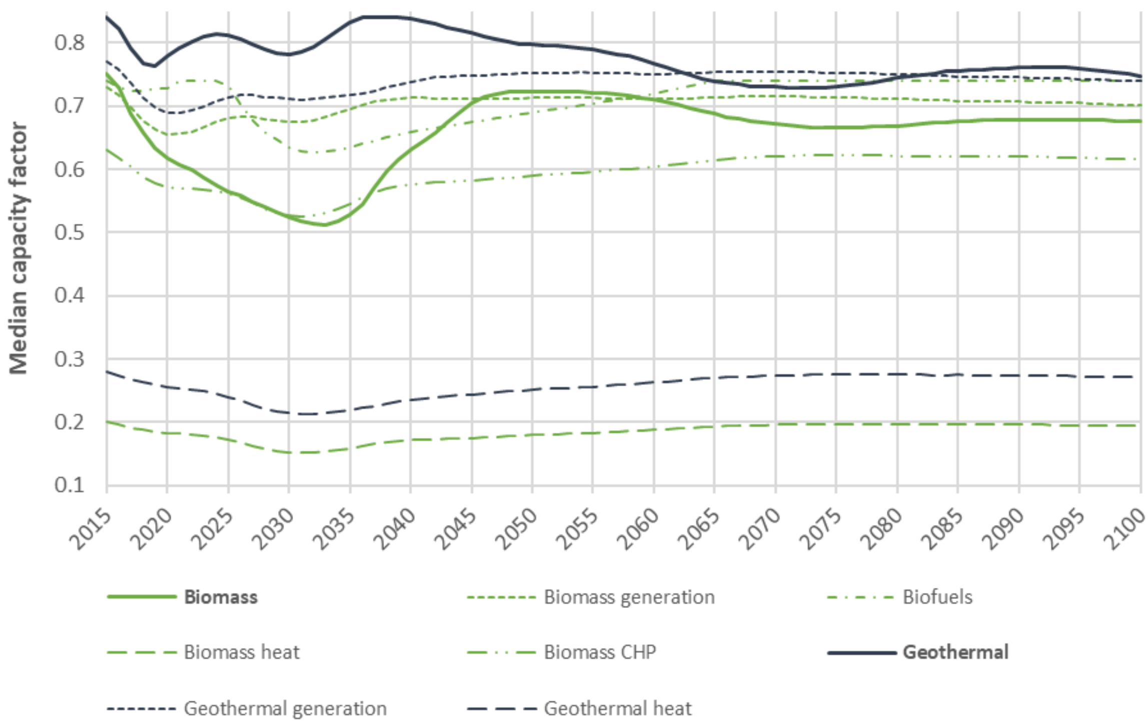

Figure 57: primary and secondary PC median CFs for biomass and geothermal

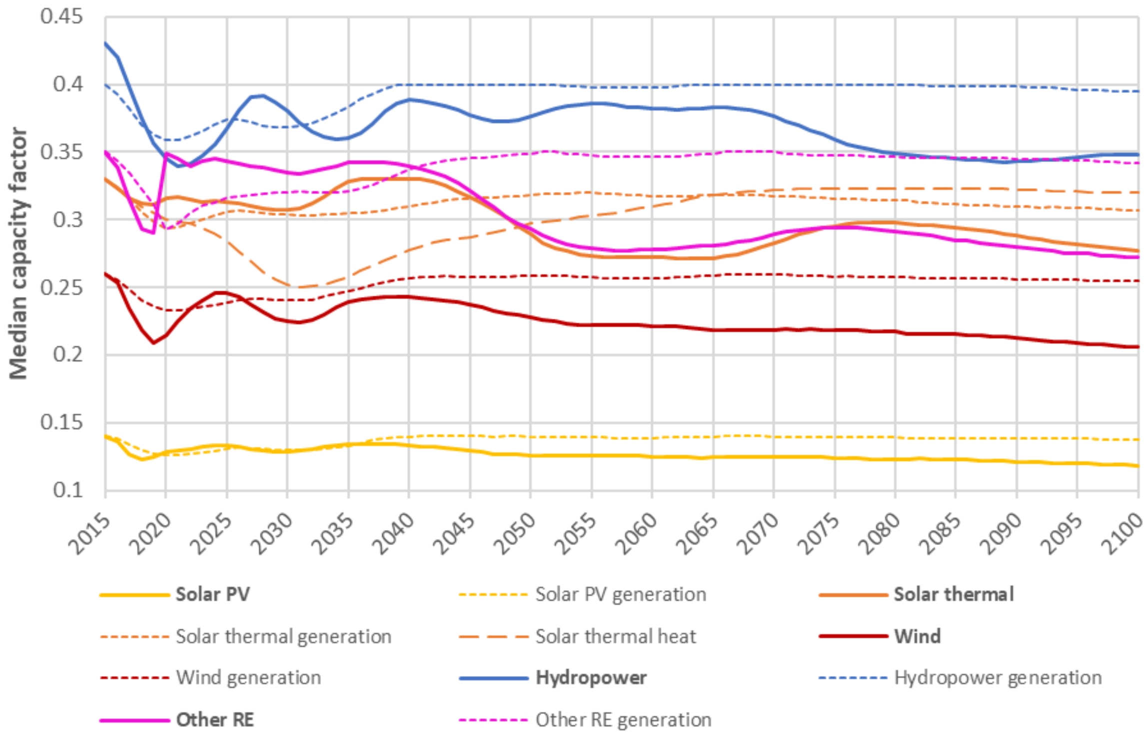

Figure 58: primary and secondary PC median CFs for RE types excluding biomass and geothermal

As with NRE, secondary PC median CFs recover from these declines between 2035 and 2070 while primary PC median CFs generally oscillate between 70% and 100% of CF maxima.

6.1.9.2 Downstream

Dotted lines in Figure 59, Figure 60, and Figure 61 represent target CFs, indicating the levels at which investment flows are triggered to bring CFs back below target levels, as described in section 4.2.2.3.

Median CFs for transportation related EU PC are shown in Figure 59 and Figure 60. All PC types exhibit significant early CF declines, with median declines between 54% and 69% from initial CF targets by 2030 due to rapid changes in transportation penetration. Following initial declines, most median CFs remain suppressed, partially recovering by mid-century before declining moderately again over the late simulation period. This implies transportation related EU PC tends towards significant oversupply (approximately double the aggregate amount required for transportation ES provision), despite ongoing behaviourally driven increases in target CFs. Note that CF (actual and target) trends overlap for rail (ICE and electric) and regional aviation in Figure 59, and for light vehicles (ICE and electric), rail (ICE and electric), and regional aviation and shipping in Figure 60.

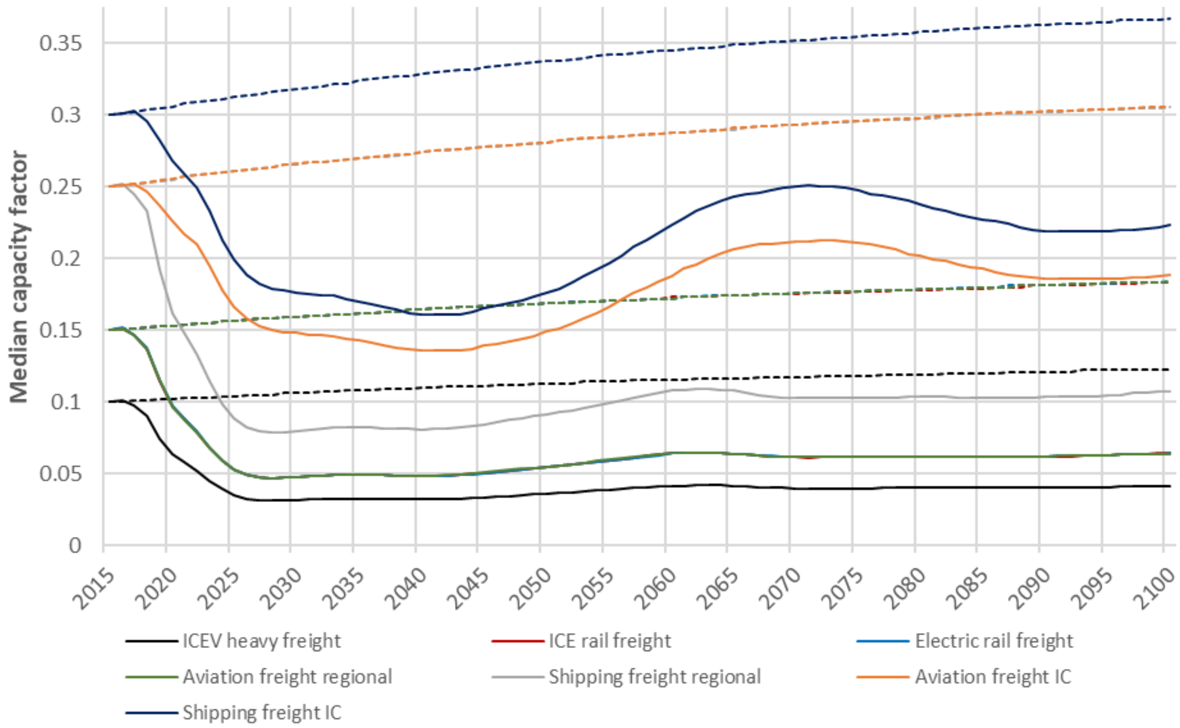

Figure 59: EU PC median CFs for freight transportation

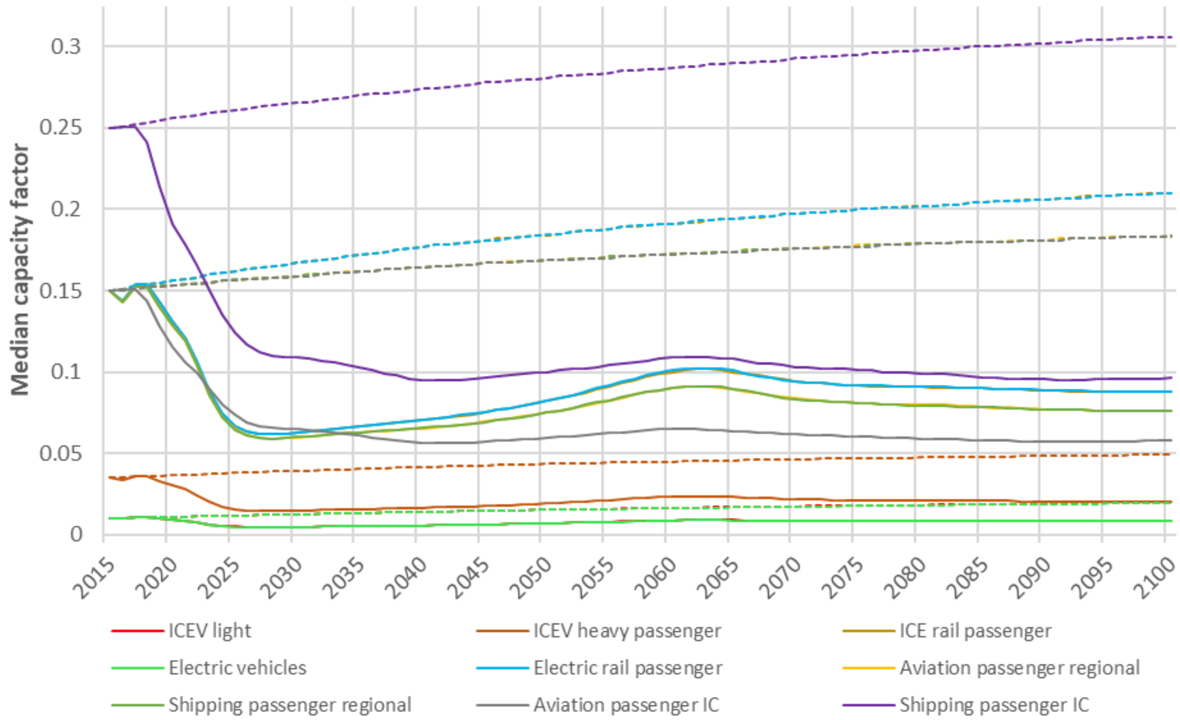

Figure 60: EU PC median CFs for passenger transportation

Median CFs for EU PC excluding transportation are shown in Figure 61. All PC types shows CF declines between two and six years after the beginning of the simulated period, with median declines between 9% and 59% from initial CF targets. Two groups are apparent, with the first recovering towards CF targets by mid to late century (IPaC devices, electric lighting, and electric cooling) and the second experiencing continual declines toward the end of the simulation period (all other). The former group consists of PC types with one-to-one mappings with ES demands (i.e., where no alternative PC exists). Within the latter group, electric and heat high temperature process heating experience the greatest median CF declines from initial CF targets by 2100 (50%), followed by LaG fuel, electric, and heat low temperature heating (31%). Note that CF trends and targets overlap for electric and heat high temperature process heating, and LaG fuel, electric, and heat low temperature heating.

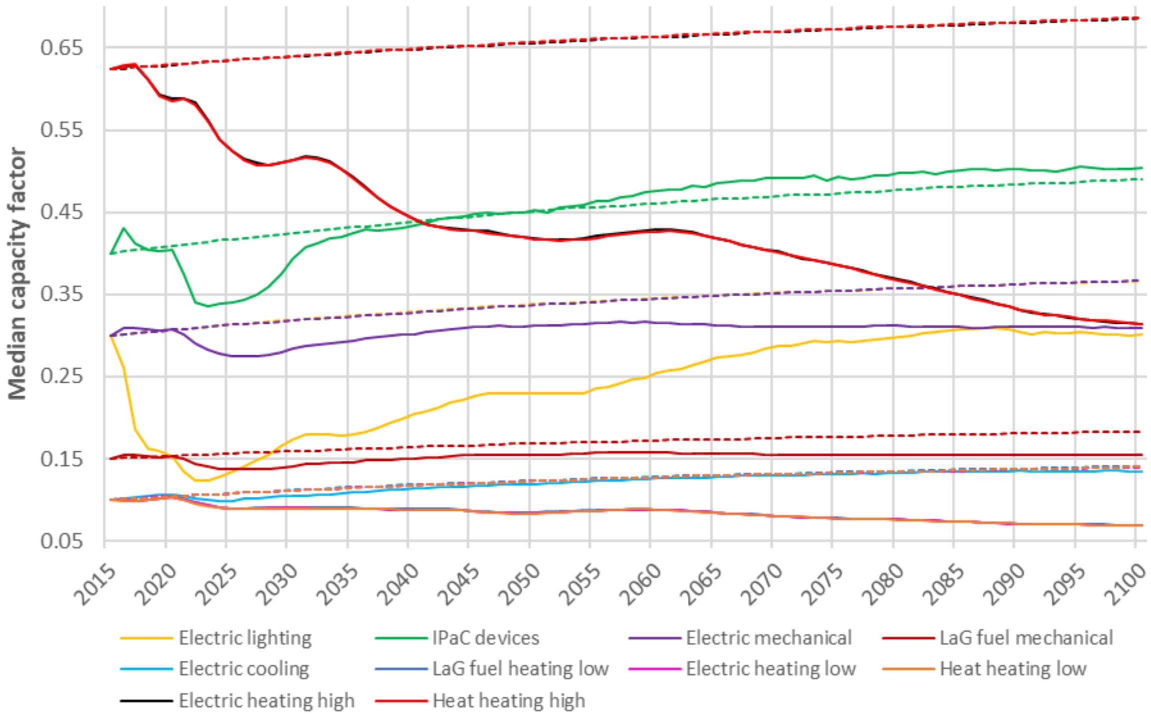

Figure 61: EU PC median CFs for EU PC types excluding transportation

6.1.10 Penetration

6.1.10.1 Secondary

Figure 62, showing mean secondary penetration by secondary PC type for the production of electricity, depicts a strong decline in combined fossil fuel penetration from 2020 to 2060 with an approximately static trend after this time. Nuclear penetration grows significantly by mid-century before declining to less that its initial level. Penetration for all RE sources grows, most strongly for wind, solar PV, and hydropower. However, hydropower penetration ceases growing after 2065 and remains stable. Electricity production from biomass CHP grows alongside and is approximately equal to direct biomass generation. In contrast, penetration for natural gas and coal CHP remains minor relative to direct natural gas and coal generation.

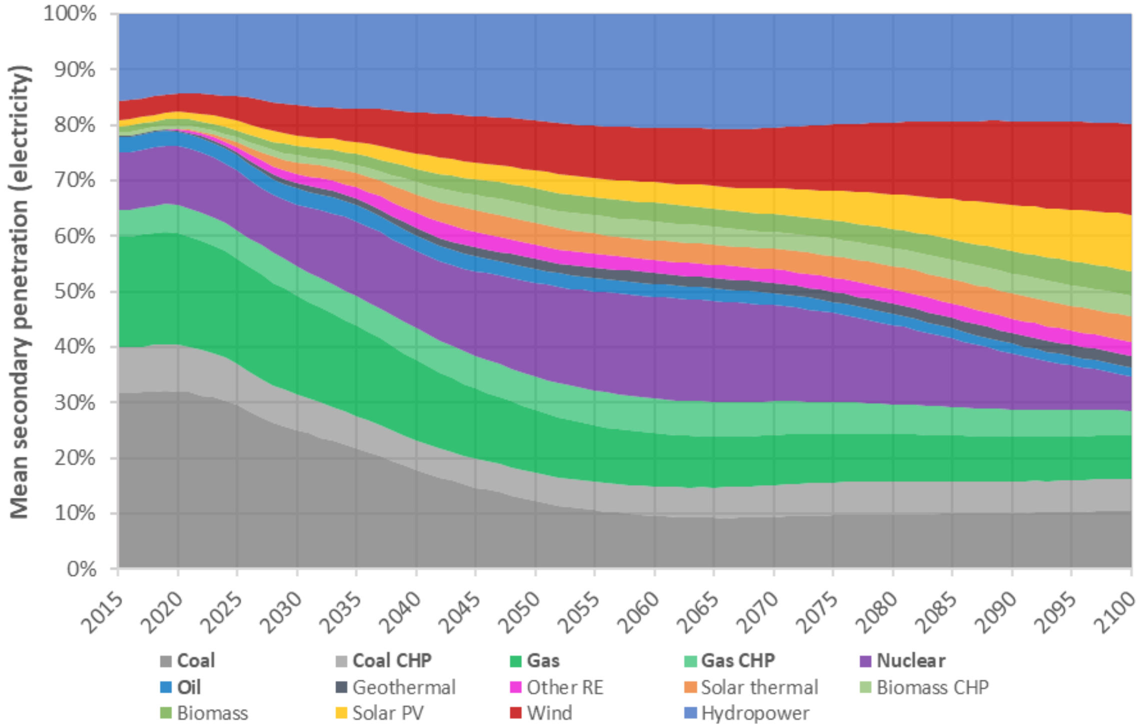

Figure 62: mean secondary penetration by secondary PC type for electricity

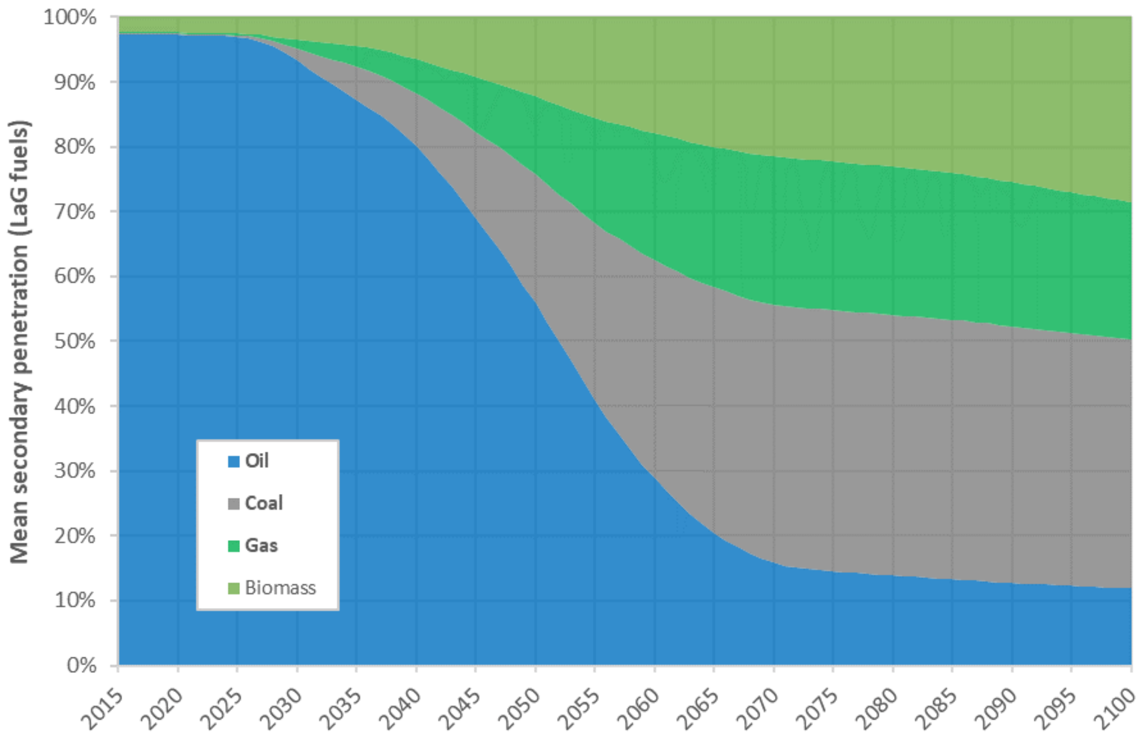

Figure 63: mean secondary penetration by secondary PC type for LaG fuels

Figure 63, showing mean secondary penetration by secondary PC type for the production of LaG fuel, depicts a strong shift away from the predominance of oil refining from 2025, declining to around 15% of supply by 2070 and continuing to fall slowly after this time. The gap is filled by continued growth in biofuel production, rising to almost 30% by 2100, and strong growth in the conversion of natural gas and coal to LaG fuels from currently negligible levels to approximately 20% and 40%, respectively.

Figure 64, showing mean secondary penetration by secondary PC type for the production of heat, depicts a marked persistence of fossil fuels, declining from a combined penetration level of approximately 75% to 65% by 2100. This fossil fuel component changes in composition during the simulated period, with strong declines in natural gas after 2035, increases in oil and natural gas CHP from 2025, and increases in coal from 2055. The RE component of heat production shifts from primarily biomass to greater shares from solar thermal, geothermal, and biomass CHP during the early part of the simulation period.

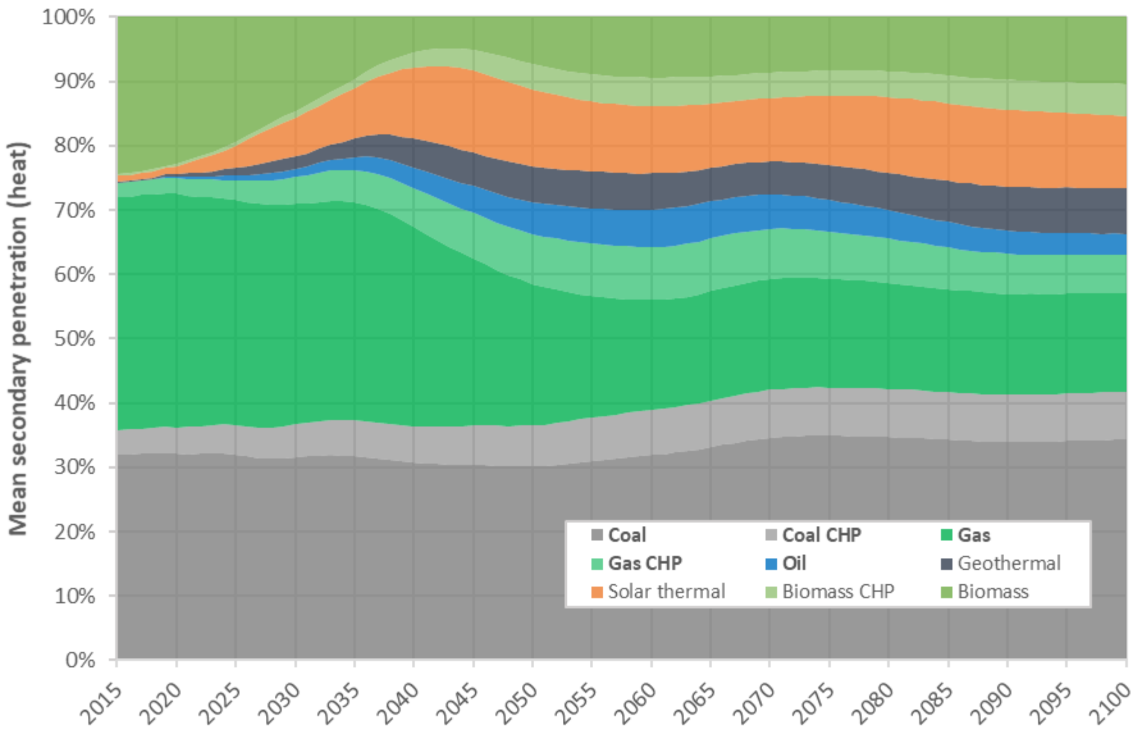

Figure 64: mean secondary penetration by secondary PC type for heat

A summary of secondary penetration variations is given in section 10.1.1.

6.1.10.2 End-use

Figure 65, showing mean EU penetration by EU PC type for the provision of regional passenger transportation, depicts an immediate and rapid shift away from light ICE vehicles largely towards passenger rail. After 2040, light ICE vehicles account for less than 5% of regional passenger transportation. The increase in rail is split between ICE and electric until around 2045, after which electric continues to grow to almost 60% by 2100 and ICE declines towards 10%. The penetration of heavy ICE vehicles declines more slowly, from more than 20% to less than 5% during the simulated period. Aviation provides an approximately constant share of regional passenger transportation, between 5% and 10%, until declining to less than 5% after 2060. Passenger shipping increases from less than 5% initially to almost 15% by 2045 before declining back towards 5% by 2100. Overall, these trends represent a general shift from private to mass transit. Electric vehicles increase very slowly until 2045, then somewhat faster after this time, reaching approximately 15% by 2100.

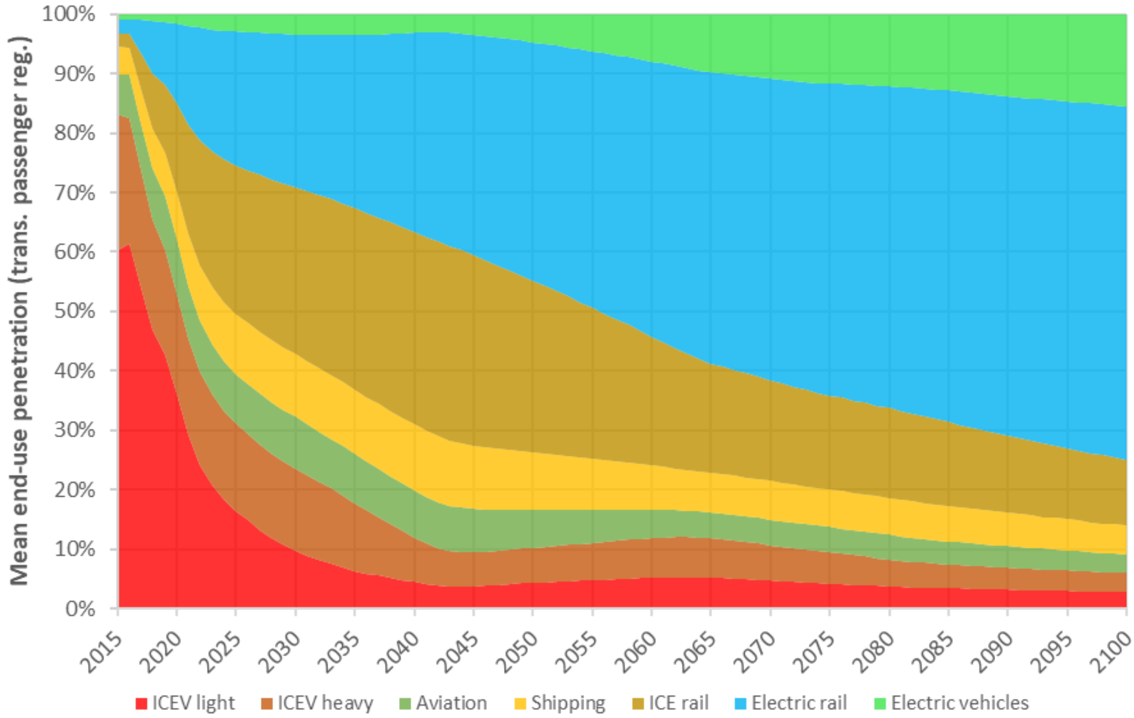

Figure 65: mean EU penetration by EU PC type for regional passenger transportation

Figure 66, showing mean EU penetration by EU PC type for the provision of regional freight transportation, depicts a rapid shift away from heavy ICE vehicles (which reaches negligible levels around 2045). Freight rail (ICE and electric) and aviation initially increase rapidly, however, aviation soon reaches a maximum level less than 10% before declining slowly to negligible levels while rail continues to grow. The increase in rail is split between ICE and electric until around 2040, after which electric continues to grow to almost 70% by 2100 and ICE declines to around 25%. Freight shipping stays constant at around 15% until mid-century, after which it declines slowly to less than 10%.

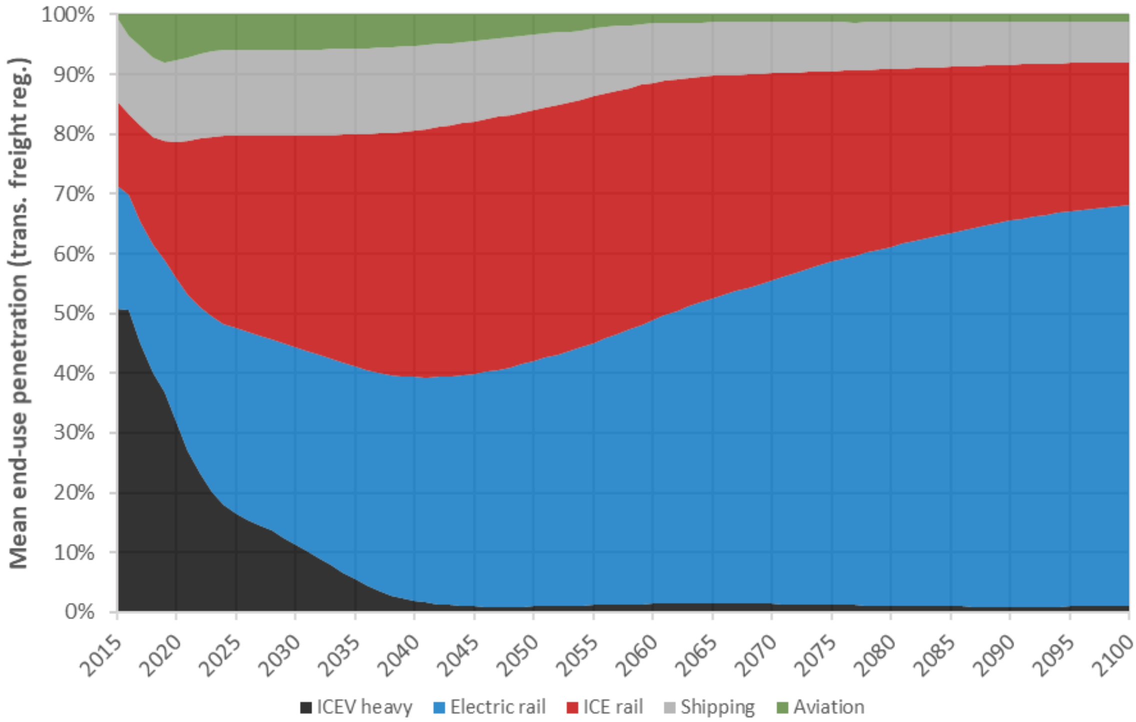

Figure 66: mean EU penetration by EU PC type for regional freight transportation

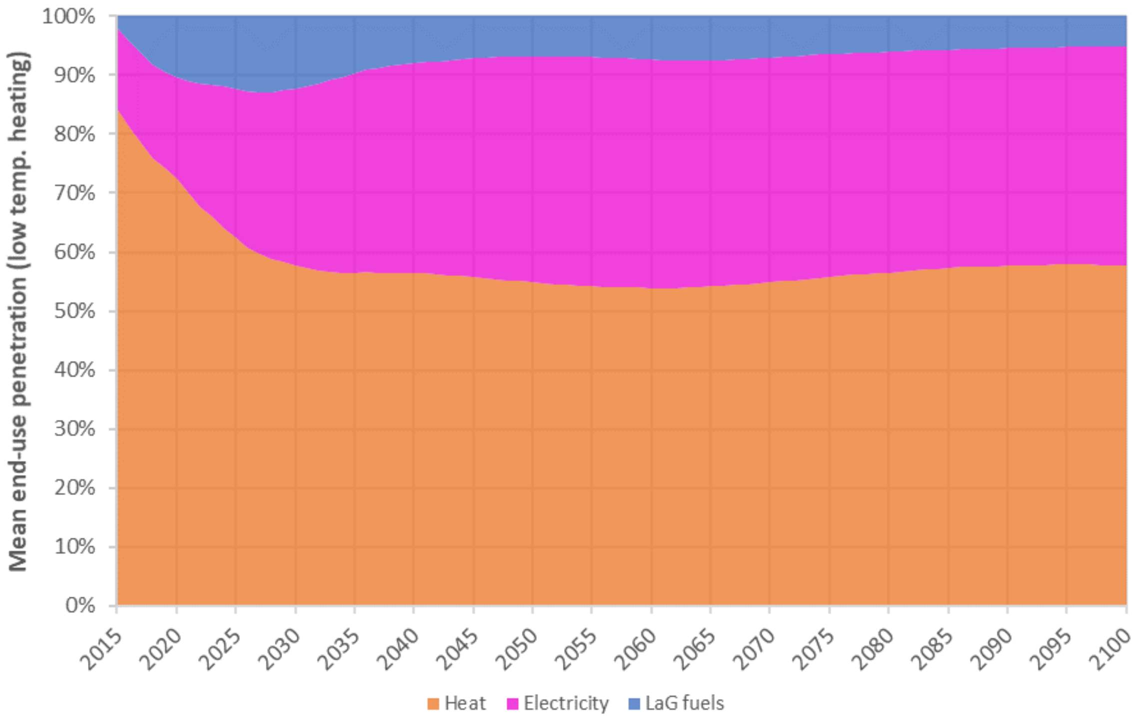

Figure 67: mean EU penetration by EU PC type for low temperature heating

Figure 67, showing mean EU penetration by EU PC type for the provision of low temperature heating, depicts direct use of heat offset by increases in electric and LaG fuel heating I the early simulated period. LaG heating penetration peaks around 2030 at less than 15% before declining to around 5% by 2100. Electric heating penetration continues to grow, reaching around 35% by 2100. The penetration of the direct use of heat stays relatively constant after 2030, around 55%.

A summary of EU penetration variations for the above ES types is given in section 10.1.2.

Envelopes for the shares of IC passenger and freight transportation provided by aviation (as opposed to shipping), shown in Figure 68, exhibit initially rapid changes. IC passenger transportation shifts from almost entirely based on aviation to between 15% and 50% shipping by 2030. After this, the mean aviation share increases again towards 90% by 2100. However, the lower distribution limit (5th percentile) continues to decline indicating that it is possible (but unlikely) for shipping to provide a progressively greater share of IC passenger transportation, up to 75% by 2100. For IC freight transportation, the share provided by aviation increases strongly to between 20% and 55% by 2030, after which a slow decline occurs, to between 5% and 35% by 2100. IC passenger transportation exhibits a widening distribution over time implying greater uncertainties while for freight, uncertainty peaks early in the simulated period before declining moderately.

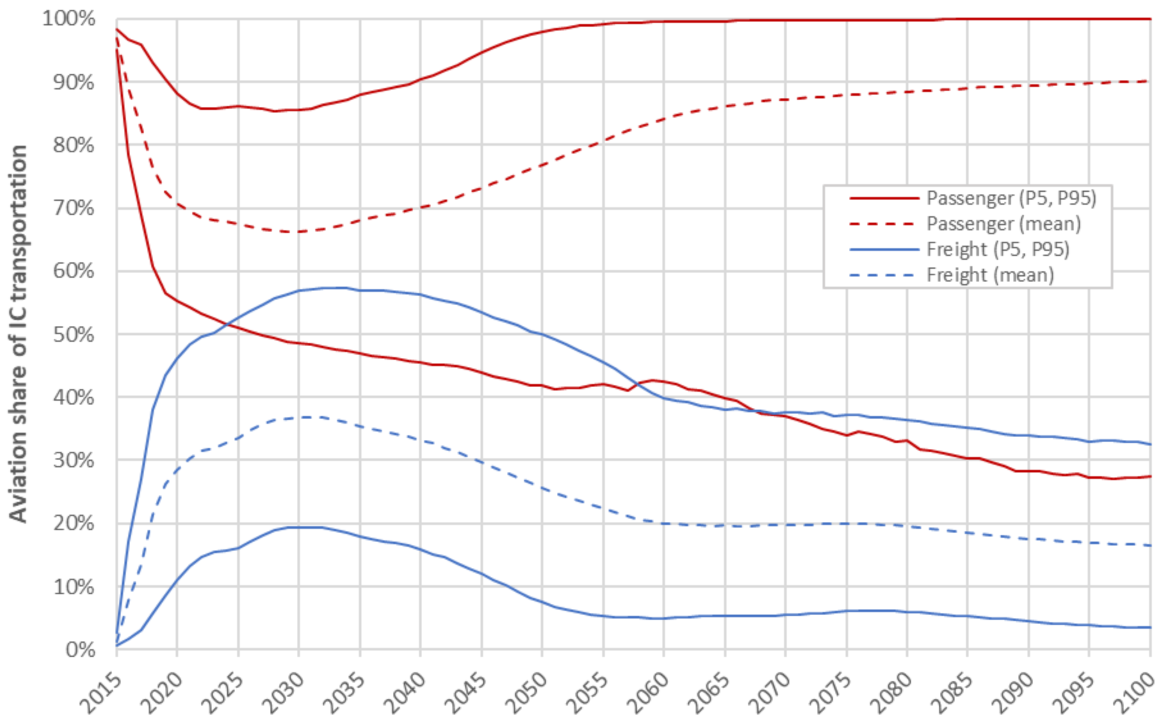

Figure 68: envelopes for the aviation shares of IC passenger and freight transportation

Envelopes for the shares of static mechanical work and high temperature process heat provided using electricity (as opposed to LaG fuels and heat, respectively), shown in Figure 69, depict a general trend towards greater electrification over the simulated period. The electrified share for static mechanical work exhibits an initial decline of 5% to 20% before increasing modestly from 2030. By 2100, between 70% and 95% of static mechanical work is provided using electricity. The electrified share for high temperature process heat initially increases strongly, from around 5% to between 10% and 45% by 2045, after which it stays approximately constant (although subject to high uncertainty).

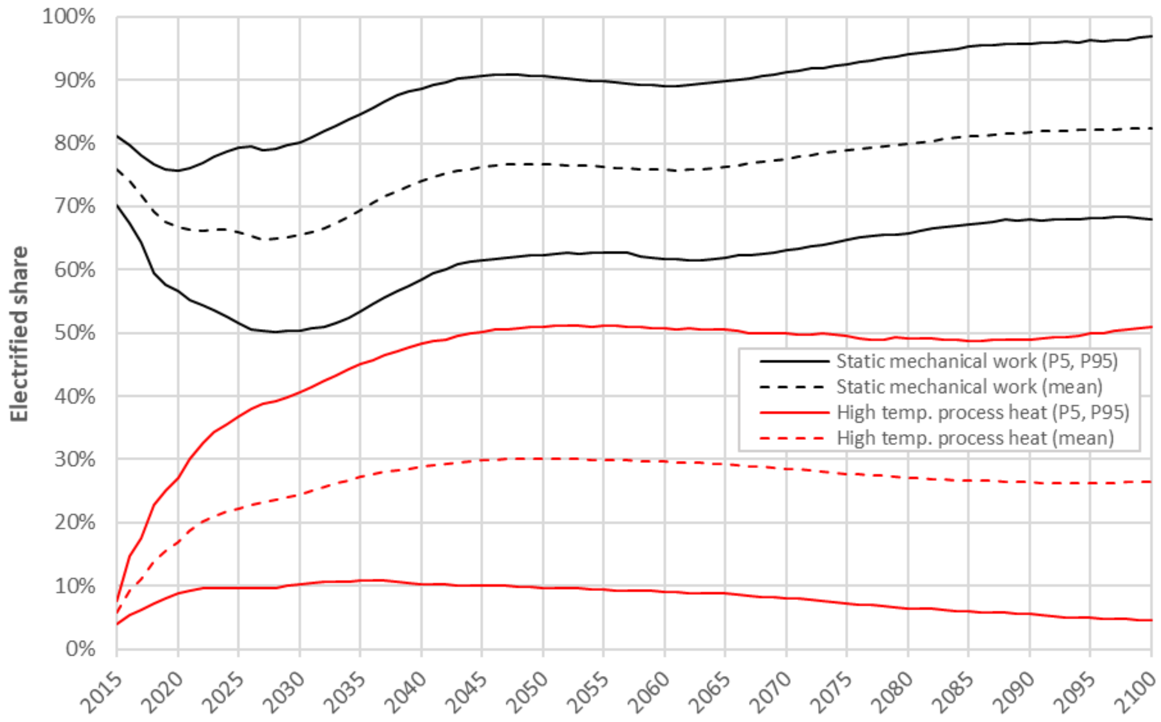

Figure 69: envelopes for the electrified shares of static mechanical work and high temperature process heat

6.1.11 Efficiencies

6.1.11.1 Secondary

Figure 70 shows the progression in secondary conversion and reticulation efficiencies (indicated by 5-year increment markers linked by lines), by secondary PC type, towards their respective achievable maxima (indicated by bold markers). Secondary efficiency improvements are typically minor (< 0.1) and trends generally approach but do not converge to their achievable maxima. Note that LaG fuel production is modelled with perfect reticulation efficiencies (losses modelled at the EU stage) and where ECs are produced at the primary stage, corresponding secondary conversion efficiencies are modelled as perfect (nominal secondary conversion).

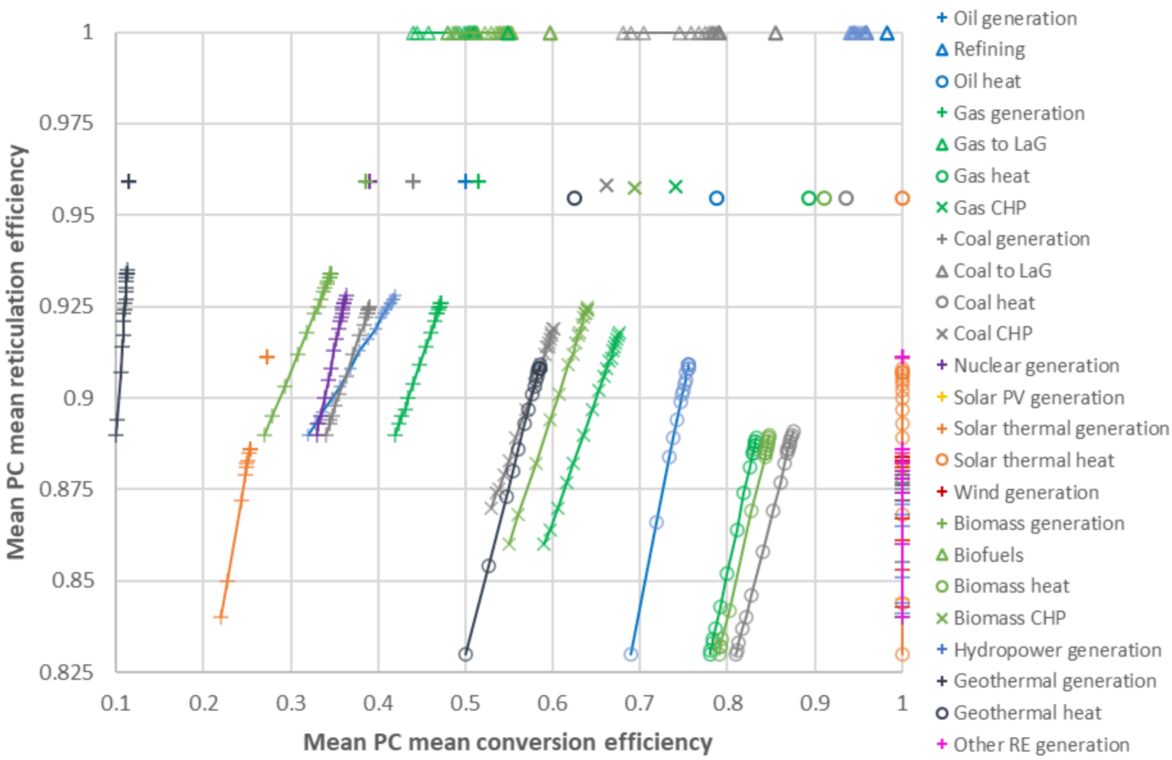

Figure 70: secondary PC mean efficiency trends and achievable maxima (markers at 5-year increments)

6.1.11.2 End-use

Figure 71 and Figure 72 show the progression in EU conversion and EU to ES efficiencies (indicated by 5-year increment markers linked by lines), by EU PC type, towards their respective achievable maxima (indicated by bold markers). EU conversion efficiency improvements are typically minor (< 0.1) except for electric lighting, IPaC devices, and low temperature heating (electric and LaG fuels). However, substantial EU to ES efficiency improvements are seen for many EU PC types. IPaC devices are the only PC type to exhibit mean conversion efficiency gains exceeding EU to ES efficiency gains. As with secondary efficiencies, trends generally approach but do not converge to their achievable maxima. Note that heat consumption is modelled with perfect conversion efficiencies (conversion modelled at the secondary stage).

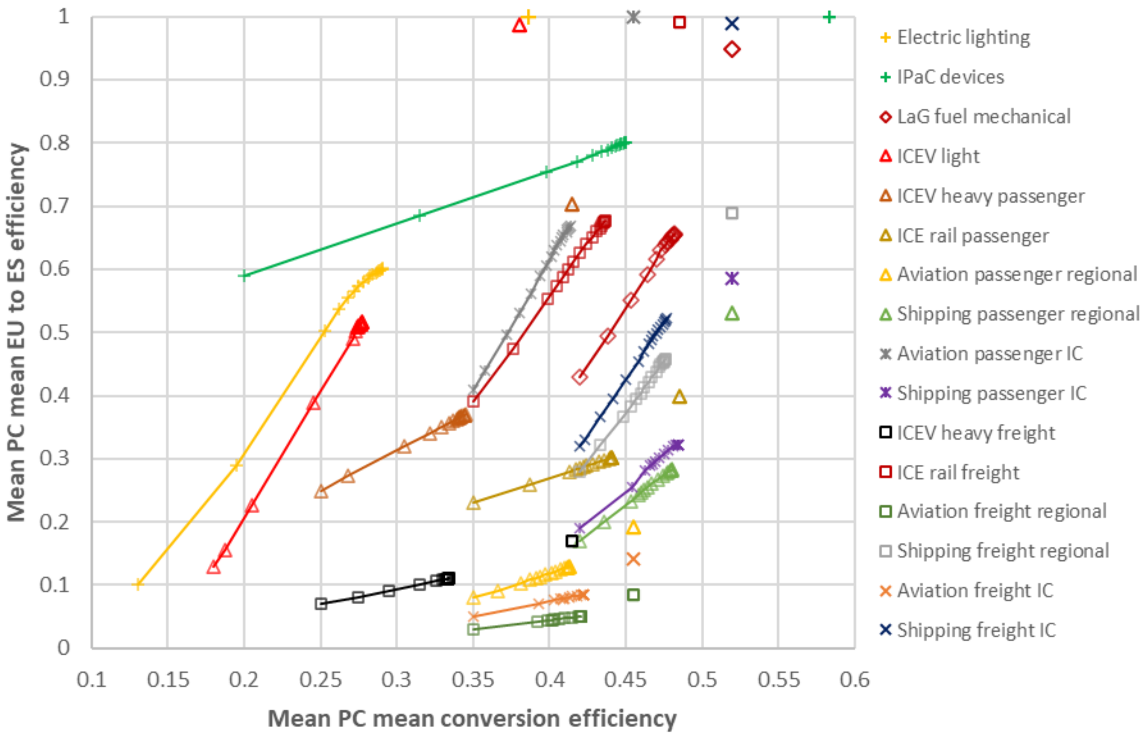

Figure 71: EU PC mean efficiency trends and achievable maxima (low conversion efficiency; markers at 5-year increments)

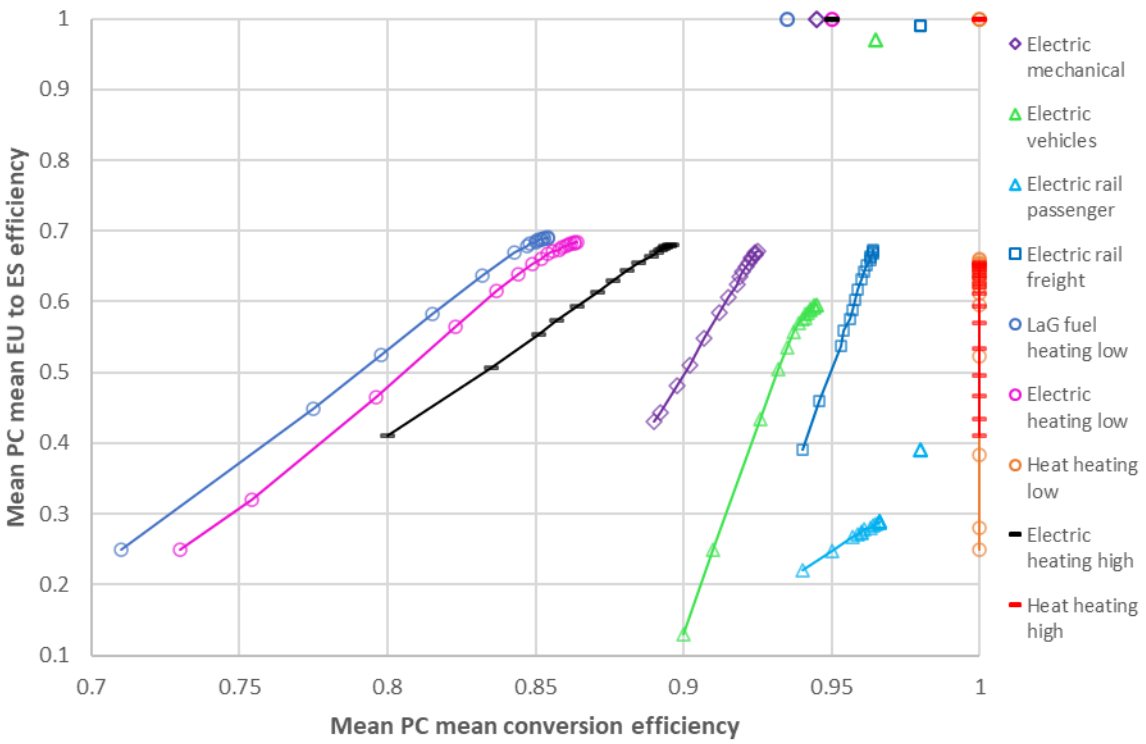

Figure 72: EU PC mean efficiency trends and achievable maxima (high conversion efficiency; markers at 5-year increments)

End-use efficiencies for electric cooling are given in section 10.2 (conversion efficiencies for this PC type are substantially above one).

6.1.12 GHG emissions

Cumulative GHG emissions results can be compared with emissions budgets for a 66% chance of remaining below warming thresholds of 1.5°C and 2°C above pre-industrial levels, sourced from Millar et al. [362] and Friedlingstein et al. [363], respectively. Note that these emissions budgets are subject to considerable uncertainty, and as such exhibit significant overlap. As described in section 4.2.9.3, calculated emissions assume no CCS and a constant rate for non-energy emissions.

As shown in Figure 73, while the mean and lower distribution limit exhibit marked decreases in the total GHG emission rate (indicated by trend gradient), the upper distribution limit remains on an approximately linear trend over the simulated period. 1.5°C and 2°C emissions budget range extrema are displayed with dotted lines in the diagram. Considering uncertainty in both emissions budget ranges and the envelope for cumulative GHG emissions, the 1.5°C budget is depleted by 2036 at the earliest and 2071 at the latest, while the 2°C budget is depleted by 2038 at the earliest and 2077 at the latest. Mean cumulative GHG emissions by 2050 are approximately equal to the budget range midpoints (slightly above for 1.5°C and slightly below for 2°C). Cumulative GHG emissions by 2100 are between 66% and 190% above the 2°C budget range midpoint (mean of 123%).

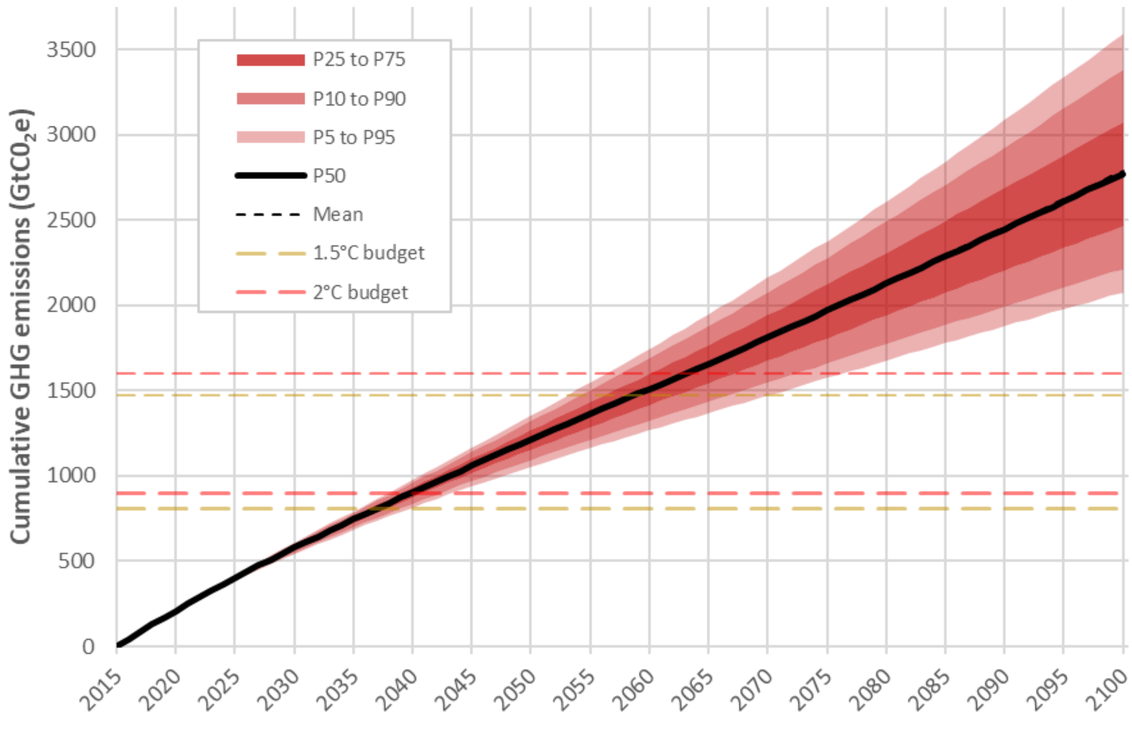

Figure 73: envelope for cumulative GHG emissions including emissions budget ranges

Cumulative probability distributions for cumulative GHG emissions in 2025, 2050, 2075, and 2100, shown in Figure 74, exhibit a clear progression in emissions over the simulated period with steadily widening distributions indicating growing uncertainty. While the 2025 distribution is well below the 1.5°C and 2°C emissions budget ranges, the entire 2050 distribution is situated within these ranges, implying that cumulative emissions by this time will risk more than 1.5°C and 2°C of warming. By 2075, it is approximately 95% likely that the 2°C budget range upper limit has been exceeded. By 2100, cumulative emissions are well past both the 1.5°C and 2°C budgets (by almost 1200 $GtCO_2e$ at the median).

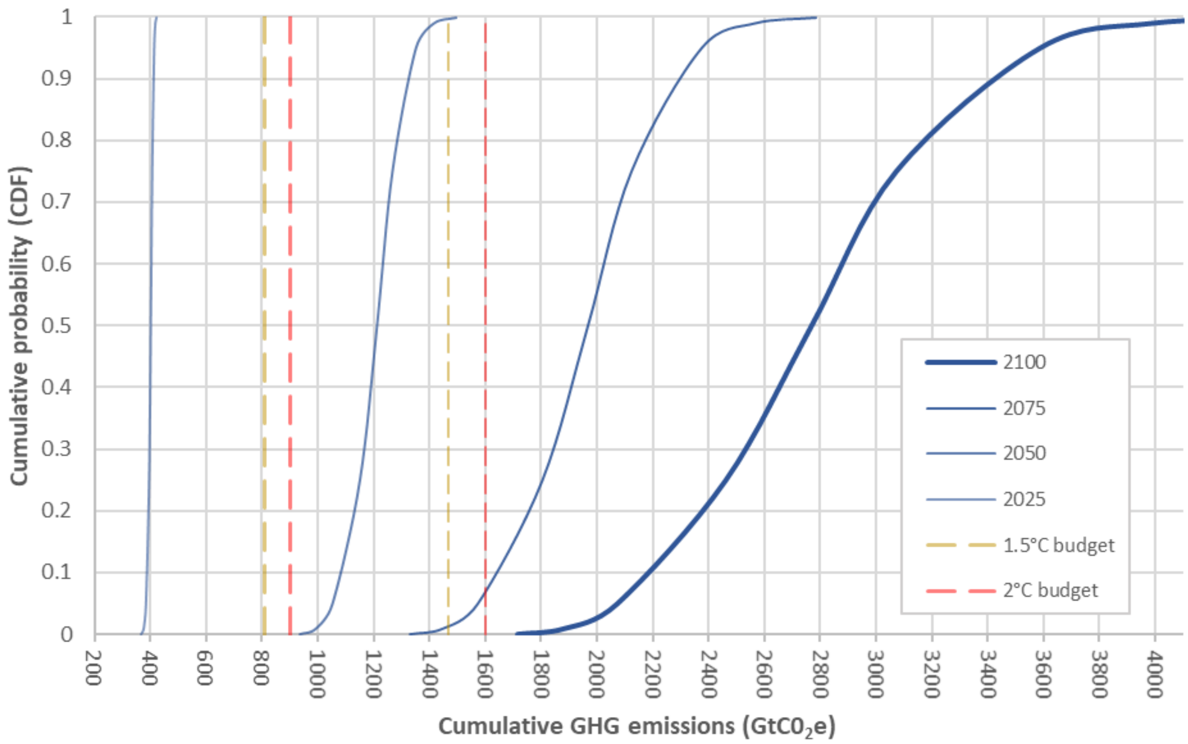

Figure 74: cumulative probability distributions for cumulative GHG emissions including emissions budget ranges

6.1.13 Intermittency impacts in electricity systems

All variables describing intermittency impacts and mitigation in electricity systems are defined in section 4.2.5. Scenario results relative to the base case are given in section 10.4.

Envelopes for intermittent penetration and diversity metrics are presented in Figure 75. Intermittent penetration rises steadily over the simulated period with a widening distribution, from less than 5% initially to between 19% and 53% by 2100 (mean of 33%). Meanwhile, intermittent diversity rises strongly from 20% initially to between 30% and 78% by 2040 (mean of 51%) with a widening distribution, before declining slowly to between 21% and 66% by 2100 (mean of 41%) with a relatively constant distribution.

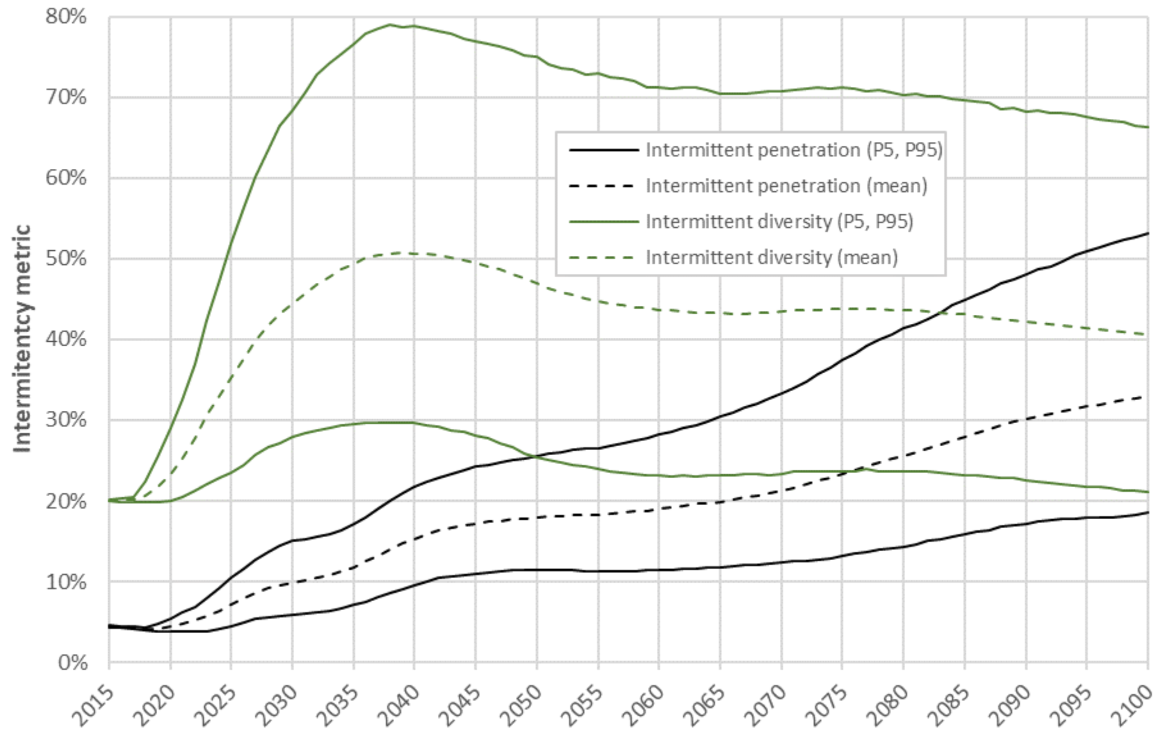

Figure 75: envelopes for intermittent penetration and diversity in electricity systems

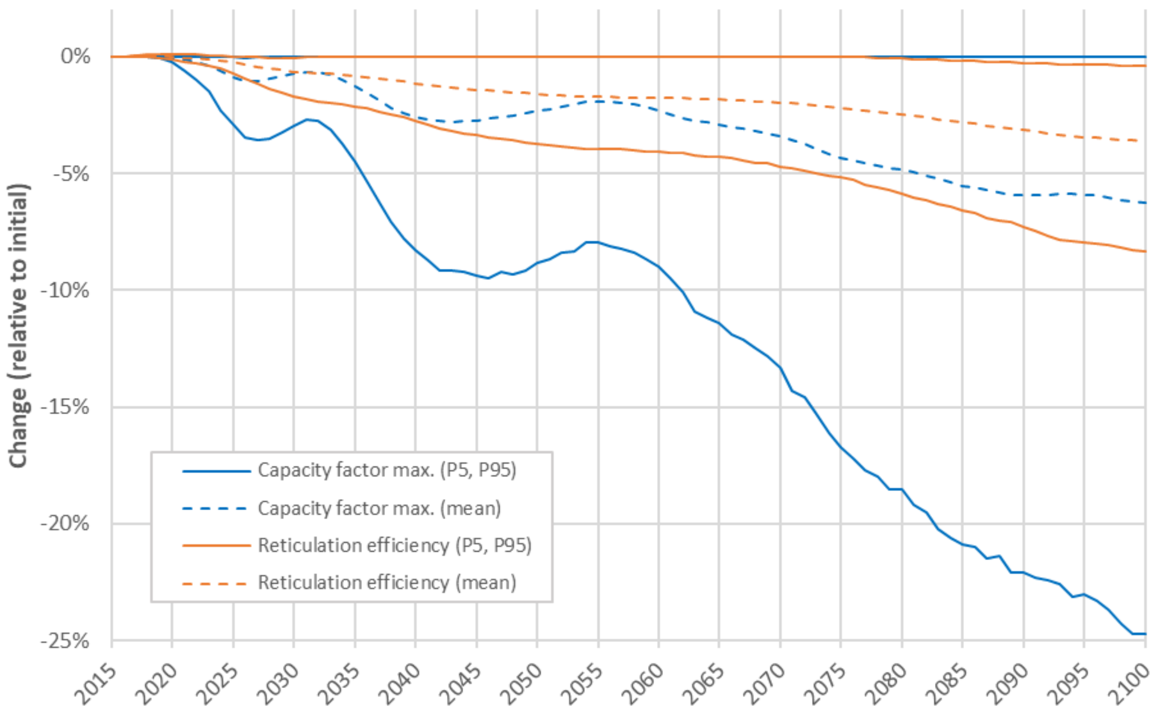

Figure 76: envelopes for CF max. and reticulation efficiency multipliers in response to intermittent penetration

Envelopes for intermittent CF maximum and reticulation efficiency multipliers are presented in Figure 76. The mean and distribution lower limit for intermittent CF maximum multiplier decreases over the simulated period but exhibits oscillations prior to 2060. This multiplier can range from 0% to almost -25% by 2100 (mean of -6%). The intermittent reticulation efficiency also decreases but more steadily and is subject to significantly less uncertainty, ranging between 1% and -8% by 2100 (mean of -4%).

Envelopes for built AI factor and intermittent electricity AI are presented in Figure 77. Built AI factor quickly occupies the full possible range, from 2035, with a mean between 60% and 80%. The lower distribution limit (5th percentile) rises after 2075 to around 30%, implying PC overbuild mitigation alone is not sufficient in the late simulation period. Installed intermittent electricity AI increases strongly from very minor levels initally to up to 4000 EJ/year by 2100 (mean of 1000 EJ/year) but is subject to very high uncertainty, particularly after 2070.

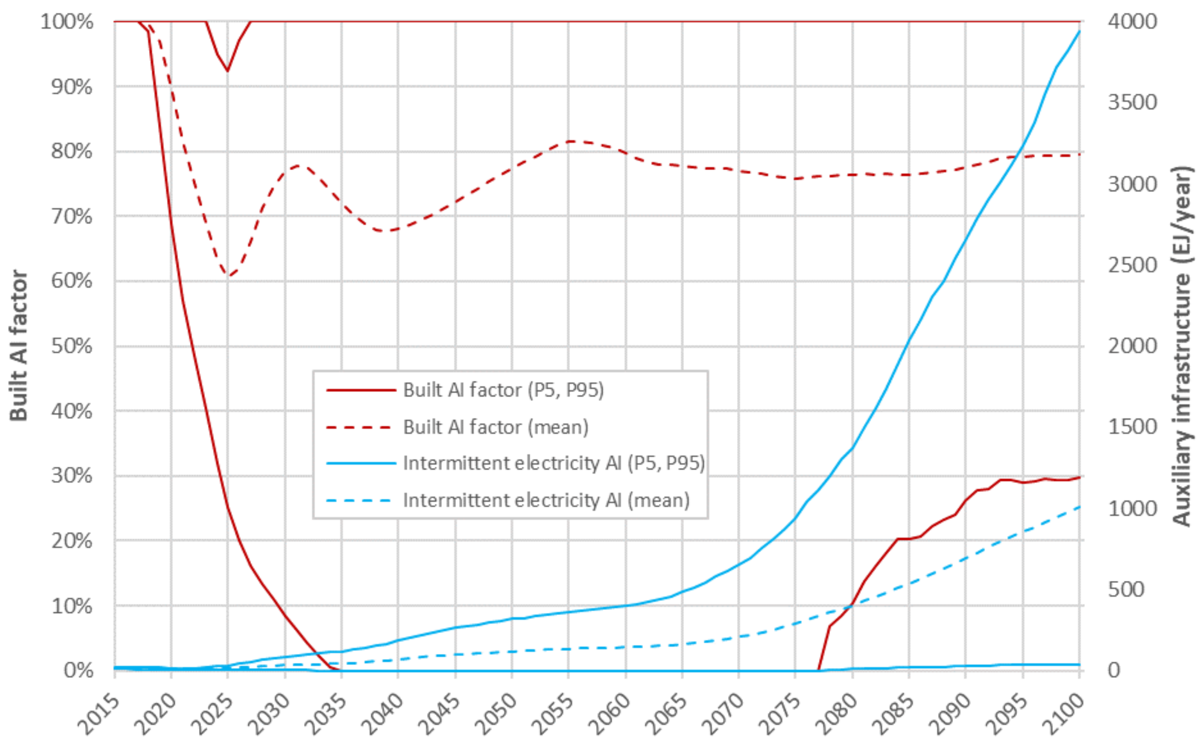

Figure 77: envelopes for built AI factor and intermittnet electricity AI in response to intermittent penetration

6.1.14 GES metabolism

The potential relative size of GES metabolism can be inferred from envelopes for ESMRs, shown in Figure 78. As discussed in section 4.2.4.5, these results indicate relative burdens imposed on the wider global socio-economic system by the GES. Distinct positive trends are observed, with oscillations early in the simulated period, prior to 2040. ESMRS range between 3% and 12% initially (means ranging from 6% and 7%), rising to between 5% and 44% by 2100 (means ranging from 16% to 19%). After 2050, the ESMR for electricity is consistently lower than ESMRs for heat and LaG fuels, in both the mean and distribution extrema. Note that with the selected curtailment threshold (0.8), the investment magnitude curtailment range starts between 10% and 20%, depending on the ESMR limit, with complete curtailment possible at 50%. The above ESMR values correspond approximately to ranges for $EROI_{ext}$ of 33 to 8.3 (mean of 15) initially and 20 to 2.3 (mean of 5.7) by 2100.

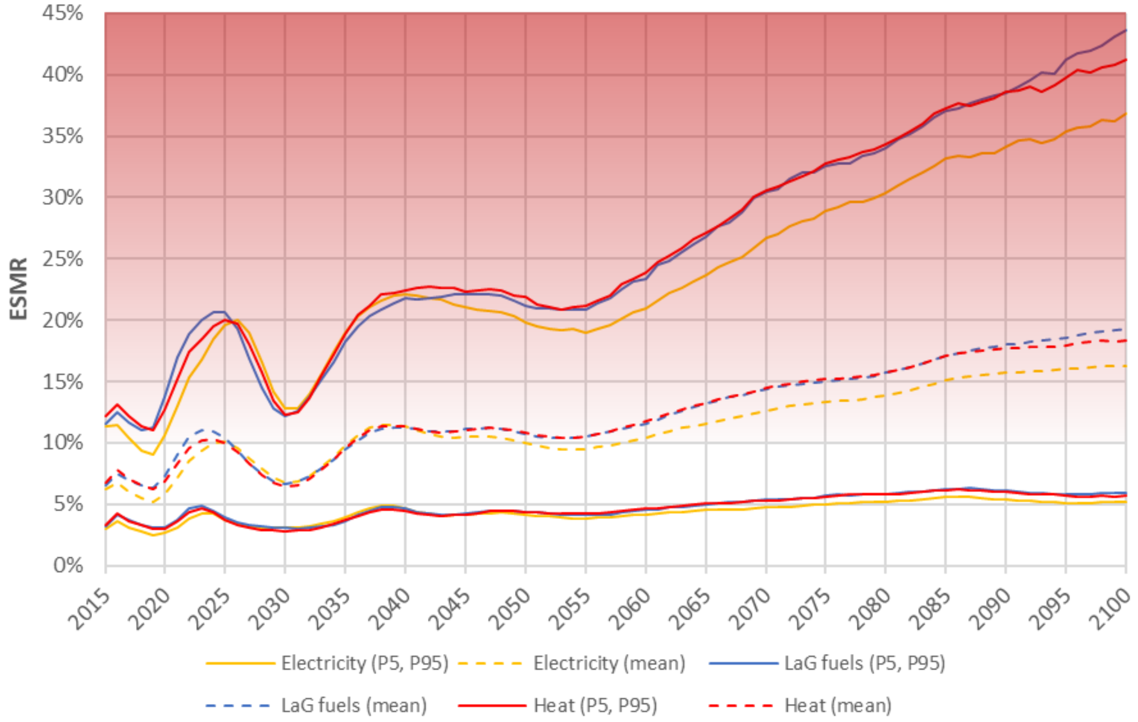

Figure 78: envelopes for ESMRs inclusing shaded curtailment region

6.2 Scenario Analysis

Results for scenario specific ES demands and intermittency impacts in electricity systems are given in sections 10.3 and 10.4, respectively. Refer to section 5.3 for scenario descriptions and to section 9.7 for scenario implementation details.

6.2.1 Sankey diagrams

The scenario Sankey diagrams below can be compared to Figure 26 depicting the mean state of the GES in 2015 to indicate change over time, and to Figure 28 depicting the mean state of the GES in 2100 in the base case to indicate scenario impacts.

The Energy Breakthrough scenario (Figure 79) exhibits a contribution to primary energy supply from 'Other RE' 1300% higher than in the base case by 2100 ('Other RE' is modelled as an effectively inexhaustible, dispatchable, high EROI source of electricity in this scenario). This expanded contribution largely displaces primary energy flows from coal, natural gas, and solar

PV. Other aspects of the GES are slightly improved relative to the base case: a reduced autocatalytic loop, reduced waste heat flows, and greater electrification (primarily for high temperature process heating and low temperature heating, reducing heat demand).

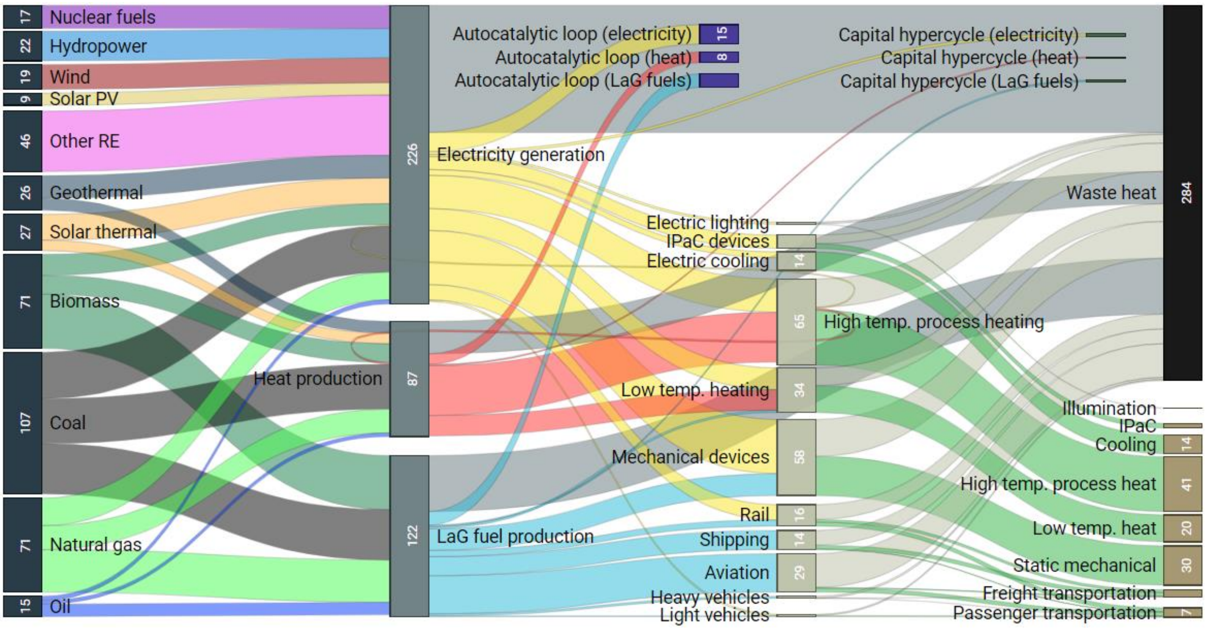

Figure 79: Sankey diagram for mean GES energy flows in scenario 1 (Energy Breakthrough) in 2100

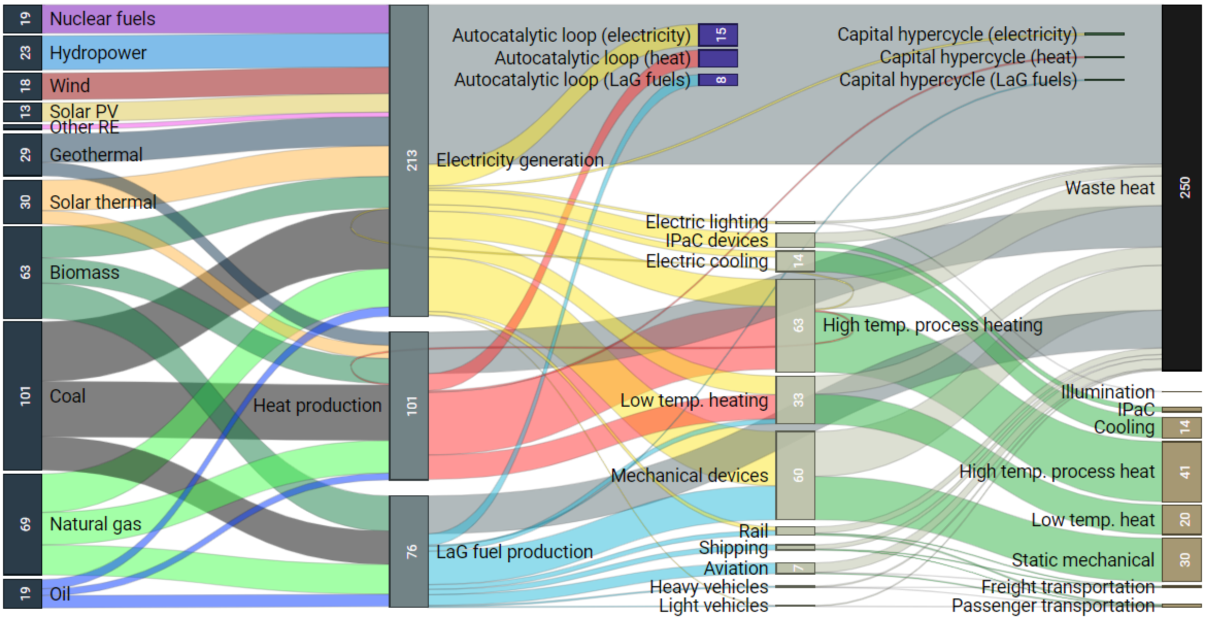

Figure 80: Sankey diagram for mean GES energy flows in scenario 2 (Relocalization) in 2100

The Relocalization scenario (Figure 80) exhibits reductions in all primary energy flows relative to the base case by 2100, with the greatest reductions coming from biomass, natural gas, and coal. All transportation EU types see substantial reductions in EC consumption (mostly LaG fuels), resulting from lower transportation ES demands. There are also minor reductions in the autocatalytic loop and waste heat flows. However, there are slight increases in LaG fuel consumption by mechanical devices and low temperature heating.

The RE Rapid Deployment scenario (Figure 81) exhibits little change relative to the base case by 2100. Most measures are very slightly higher (< 1%), notably coal and natural gas production, EC production, and autocatalytic loop consumption. Nuclear fuel production and high temperature process heating see minor reductions.

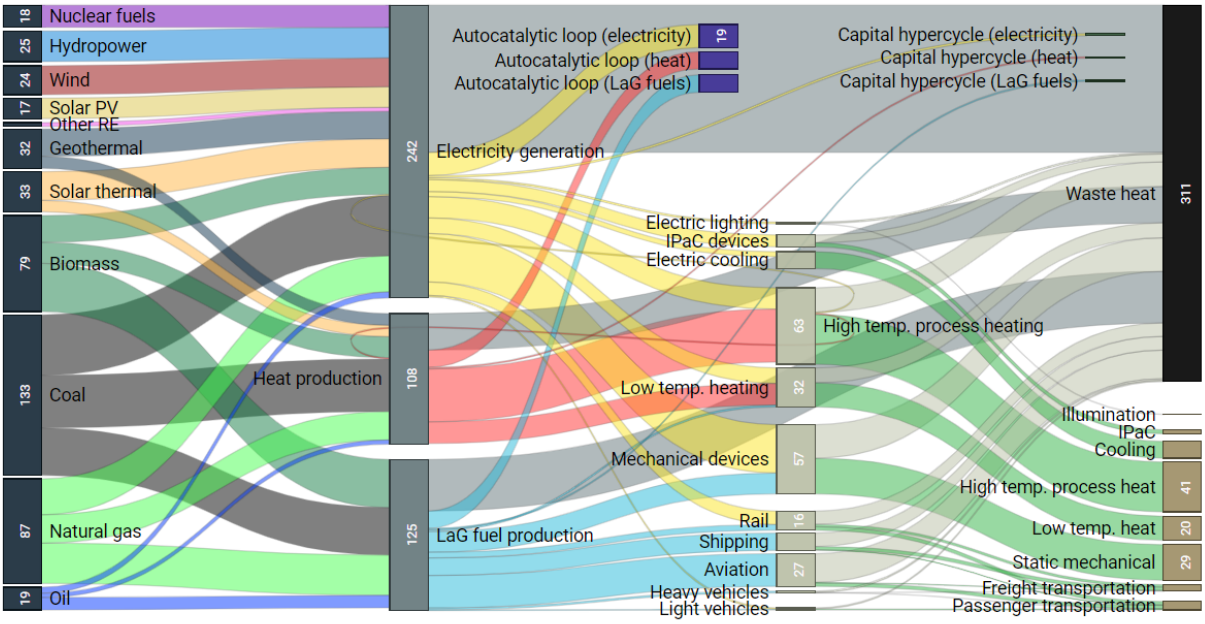

Figure 81: Sankey diagram for mean GES energy flows in scenario 3 (RE Rapid Deployment) in 2100

The Climate Constraints scenario (Figure 82) exhibits substantial changes relative to the base case by 2100. Primary energy flows from coal production are reduced by 33% relative to the base case at the same time and by 45% relative to 2015 levels. However, this comes at the expense of higher TPES and increases in primary energy flows from biomass, natural gas, and oil (14%, 9%, and 165% higher than the base case in 2100, respectively). A greater trend towards electrification is observed than in the base case, primarily for high temperature process heating and low temperature heating, reducing heat demand. Total waste heat flows are increased by around 5%.

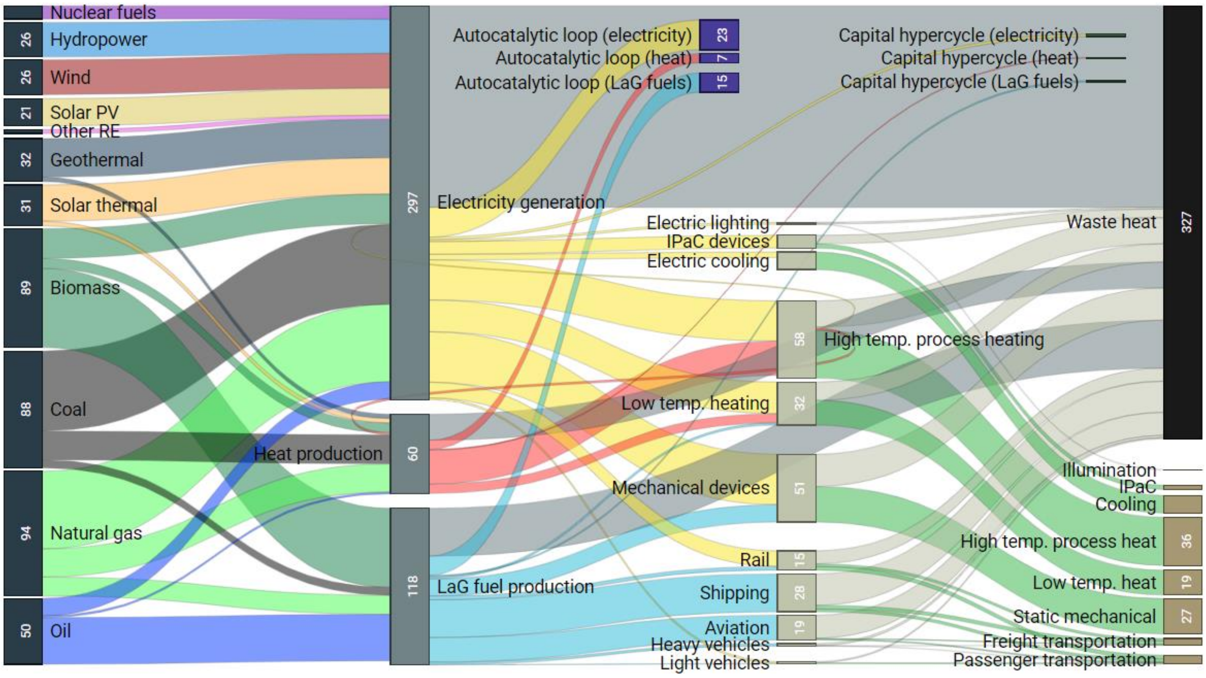

Figure 82: Sankey diagram for mean GES energy flows in scenario 4 (Climate Constraints) in 2100

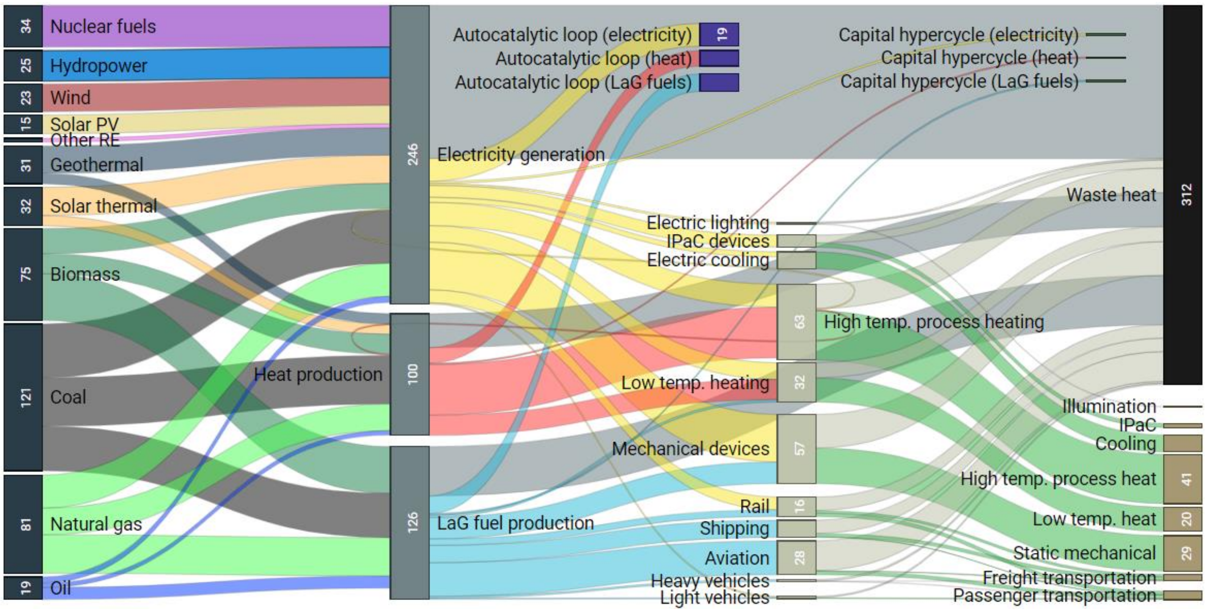

Figure 83: Sankey diagram for mean GES energy flows in scenario 5 (Delayed Consumer Response) in 2100

The Delayed Consumer Response scenario (Figure 83) exhibits significant differences in the composition of primary energy flows relative to the base case by 2100. Production rates of biomass, coal, and natural gas are reduced by 5%, 8%, and 6%, respectively. This gap is filled primarily by the production of nuclear fuels, which is 80% higher than the base case. Few other measures are substantially different.

The Policy Recommendations scenario (Figure 84) exhibits the most significant mean changes relative to the base case by 2100. All primary energy flows are reduced, most notably coal, natural gas, oil, and solar PV, by 67%, 61%, 54%, and 84%, respectively. Total EC supply is significantly lower, and demand is reduced in all EU types, with increased electrification of low temperature heating, but lower electrification of high temperature process heating, mechanical devices, and rail. Sum autocatalytic loop consumption, representing the energy cost of primary energy production, is 76% lower than the base case at the same time and by 22% lower than 2015. Total waste heat flows are reduced by 55%.

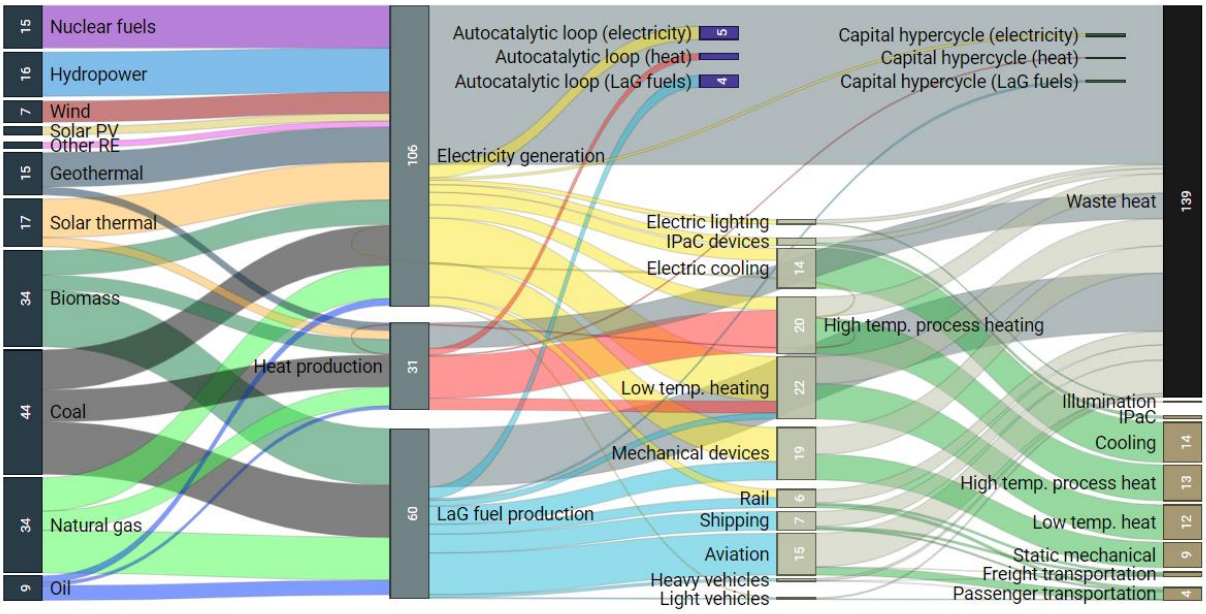

Figure 84: Sankey diagram for mean GES energy flows in scenario 6 (Policy Recommendations) in 2100

6.2.2 System stability

Figure 85 summarizes system stability across all scenarios, in terms of the failure rate and mean stable time. Scenarios 1, 2, and 6 have positive impacts on system stability relative to the base case, decreasing the failure rate below 2% (0% for scenario 6), and increasing mean stable time above 84.8 years. 90% confidence intervals for scenario 3 and the base case overlap for both failure rate and mean stable time, indicating no statistically significant differences except higher variances for scenario 3. Scenario 5 has modest negative impacts on system stability, increasing the failure rate to 10% and decreasing mean stable time to 83.9 years. Scenario 4 has a strongly detrimental impact on system stability, with a failure rate of 29% and a mean stable time of 80.3 years.

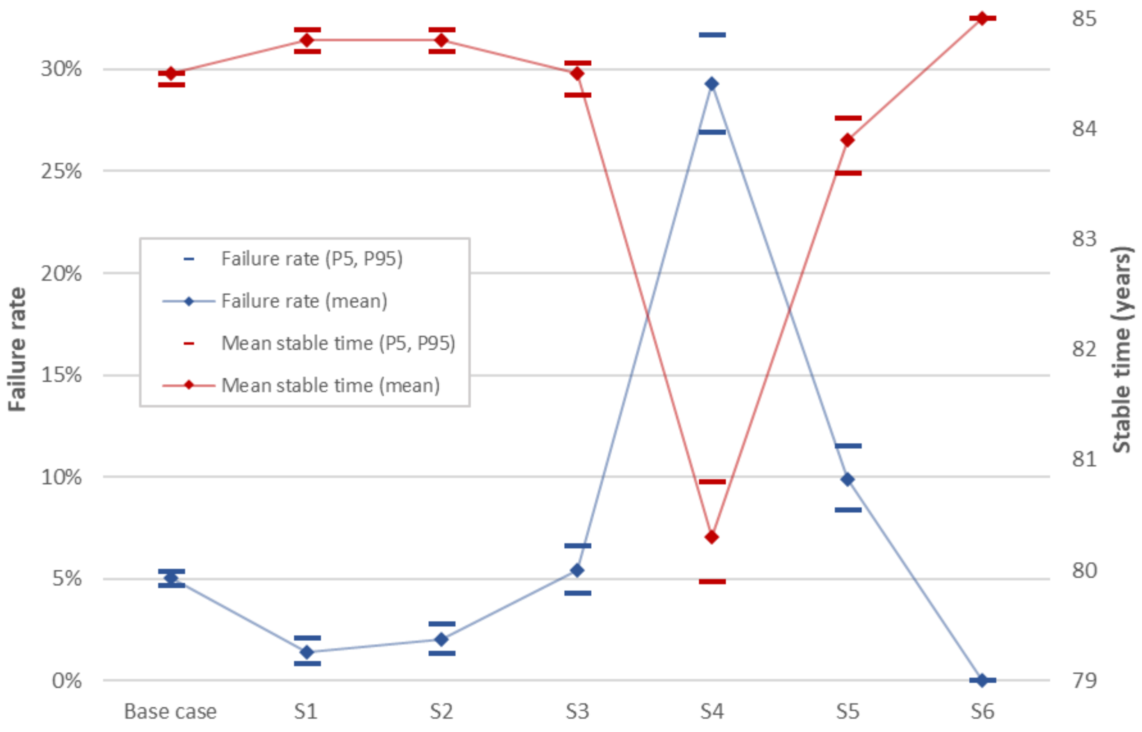

Figure 85: mean failure rate and stable time by scenario, including 90% confidence intervals

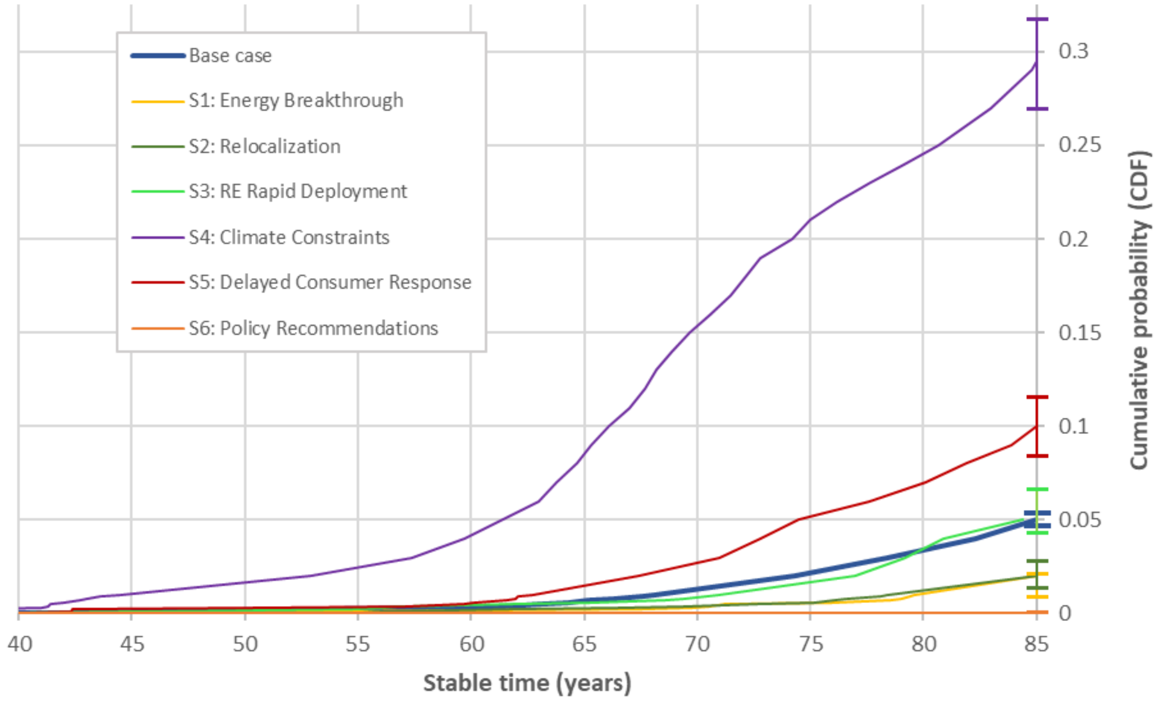

Figure 86: cumulative probability distributions for stable time by scenario, including 90% confidence intervals for failure rate

Cumulative probability distributions for stable time by scenario, shown in Figure 86, show improved system stability for scenarios 1, 2, and 6, and diminished system stability for scenarios 4 and 5. Scenarios 1 and 2 show very similar distributions, with overlapping 90%

confidence intervals. Scenario 6 exhibits a flat distribution, implying perfect system stability for the modelled ensemble. Scenario 5 entails a negative impact on system stability slightly greater in magnitude to the positive impact observed in scenarios 1 and 2. For scenario 4, system stability is severely impacted after 2055 with the majority of failures occurring between 2075 and 2090 (indicated by a steeper gradient between 60 to 75 years).

6.2.3 Supply

Mean TPES by scenario relative to the base case, shown in Figure 87, indicates increases in total energy requirements in scenarios 4 and 5, and decreases in scenarios 2 and 6. Scenarios 1 and 3 exhibit minor increases only and scenarios 4 and 5 are subject to distinct oscillations, before all four converge to approximately the same level as the base case by 2100. Scenarios 2 and 6 exhibit steady decreases in TPES relative to the base case, amounting to approximately 110 EJ/year and 360 EJ/year by 2100, respectively.

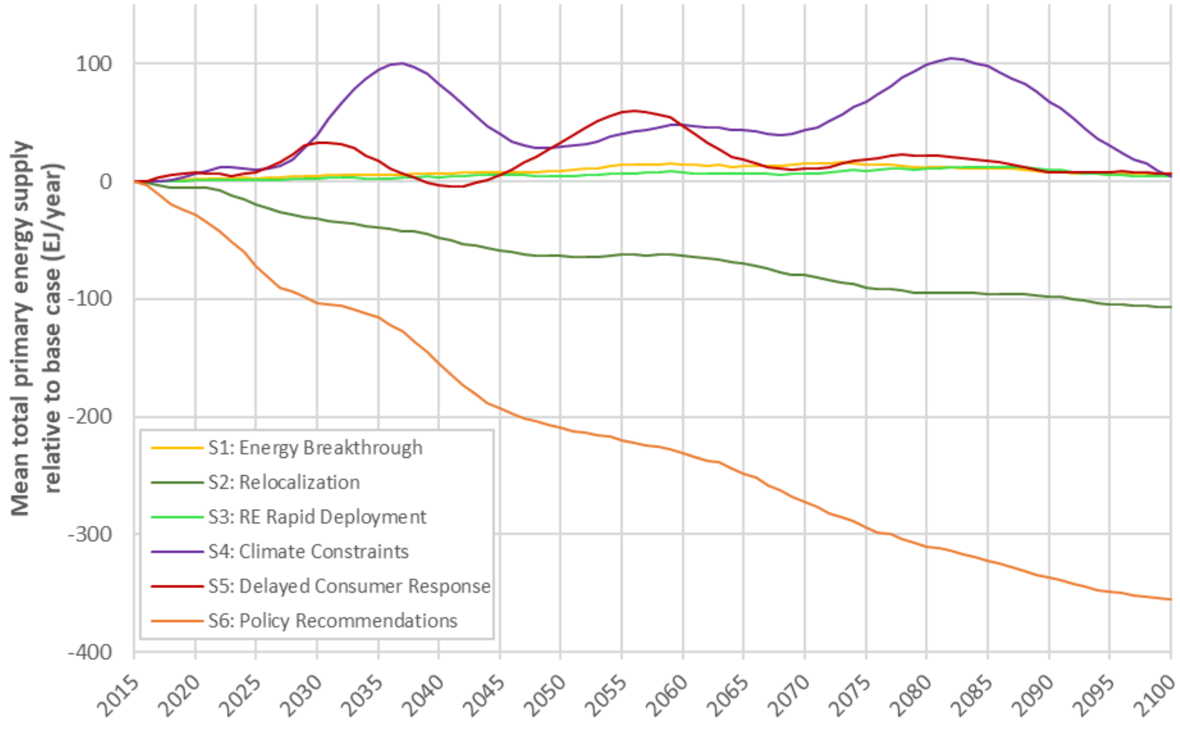

Figure 87: mean total primary energy supply (TPES) relative to the base case, by scenario

Figure 88 depicts mean primary energy supply by resource, by scenario, in 2025, 2050, 2075, and 2100. Mean TPES in 2100 is higher than in 2025 for all scenarios except scenario 6. Scenario 2 exhibits a marked decline in TPES from 2025 to 2050, before increasing slowly over the later simulation period to around 18% less than the base case by 2100. Until 2075, combined fossil fuel supply is lowest in scenario 6, followed by scenarios 4 and 2. However, by 2100 combined fossil fuel supply is still lowest in scenario 6, but followed by scenarios 2 and 1. Other RE supply is highest in scenario 1, but this appears to displace significantly more RE supply (largely wind, solar PV, biomass, and hydropower) than NRE supply. Note, quantities in Figure 88 are adjusted for primary equivalence to allow direct comparison.

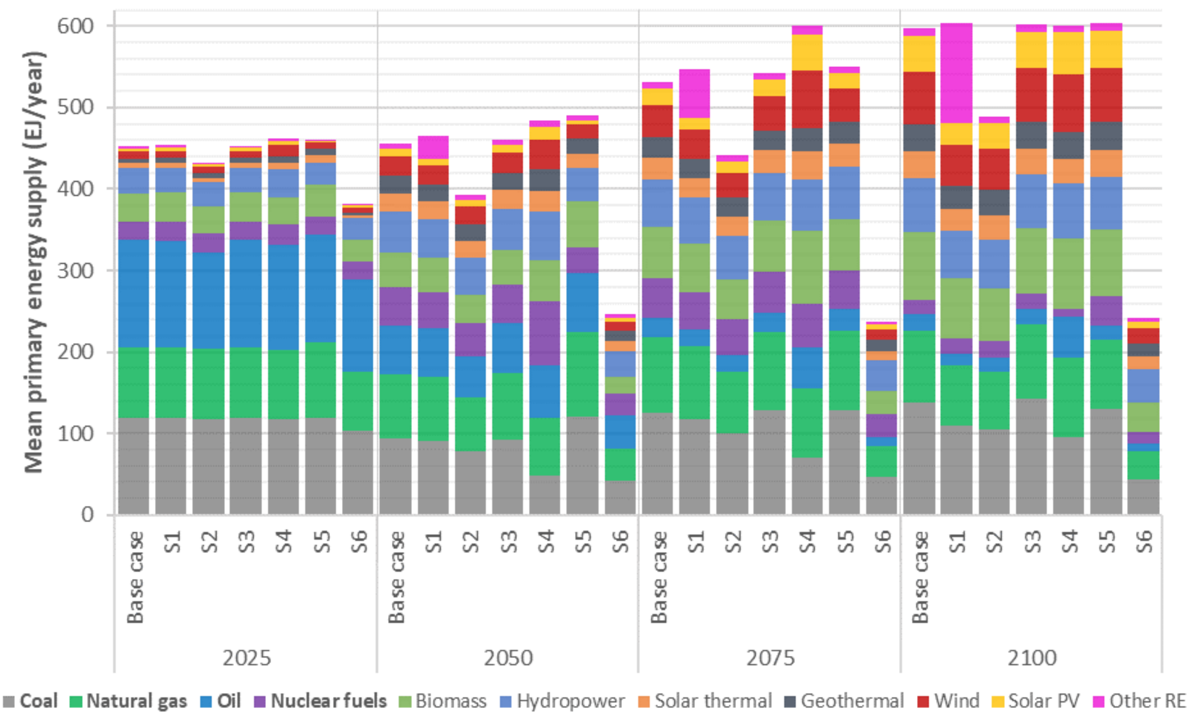

Figure 88: mean primary energy supply by resource, by scenario (NRE types in bold; adjusted for primary energy equivalence)

6.2.4 Demand

Mean final demand for ECs by scenario, relative to the base case, is shown in Figure 89, Figure 90, and Figure 91 for electricity, LaG fuels, and heat, respectively. Scenarios 1 and 4 see stronger electrification trends, with the rise in electricity consumption displacing mainly heat consumption, however, this is much more rapid and to a significantly greater degree in scenario 4. Scenario 2 shows reductions in final electricity and LaG fuel consumption relative to the base case (10 EJ/year and 27 EJ/year lower than the base case by 2100, respectively) but little change in final heat consumption. Scenario 3 shows a slight increase in the final consumption of all ECs. Scenario 5 sees strong increases in final LaG fuel and heat consumption relative to the base case (approximately 17 EJ/year higher by 2025 and 50 EJ/year higher by 2050, respectively) with substantially lower electrification in the early part of the simulated period, however, the final consumption of all ECs converges to the levels seen in the base case by 2100. Scenario 6 exhibits substantial steady declines in all three ECs relative to the base case, with combined consumption of ECs 130 EJ/year lower than the base case by 2100.

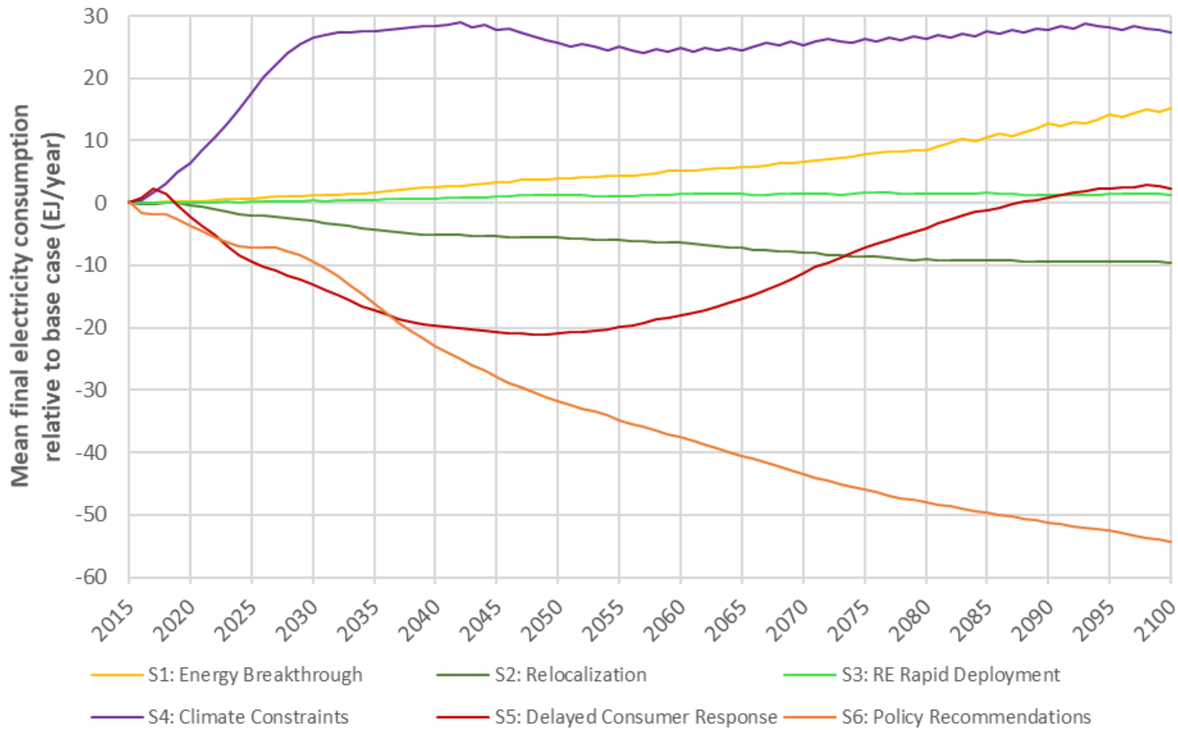

Figure 89: mean final (non-GES) electricity demand relative to the base case, by scenario

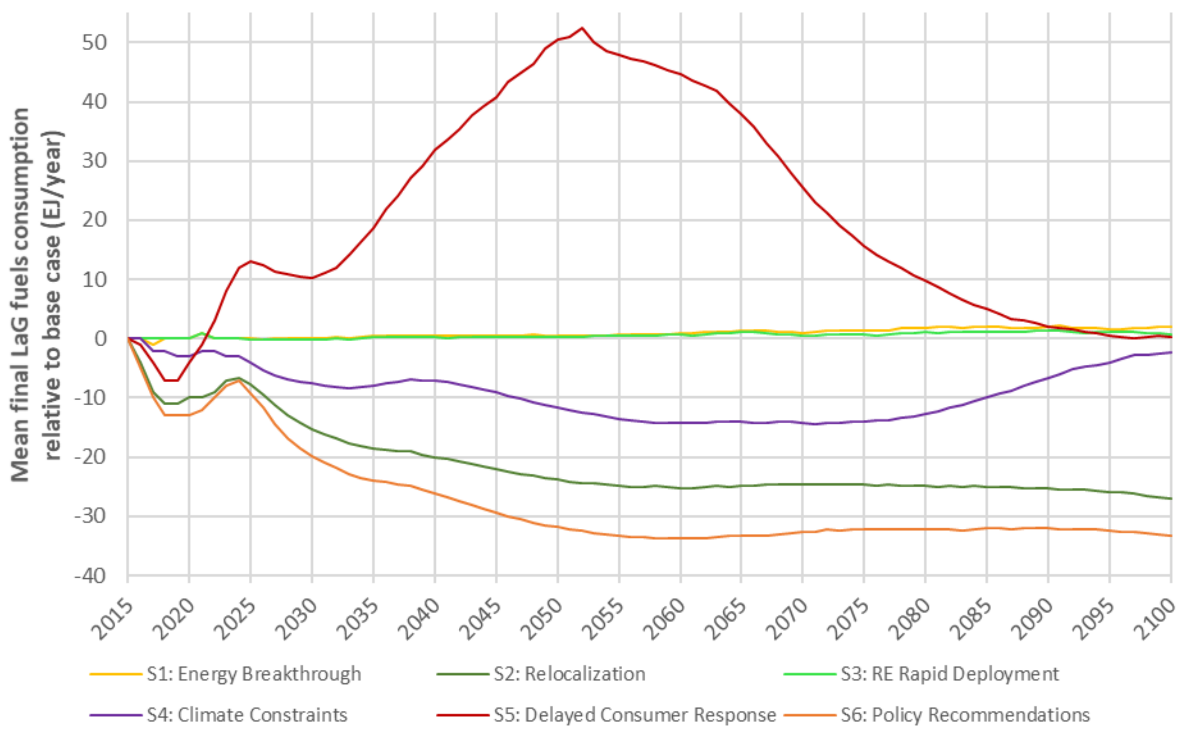

Figure 90: mean final (non-GES) LaG fuel demand relative to the base case, by scenario

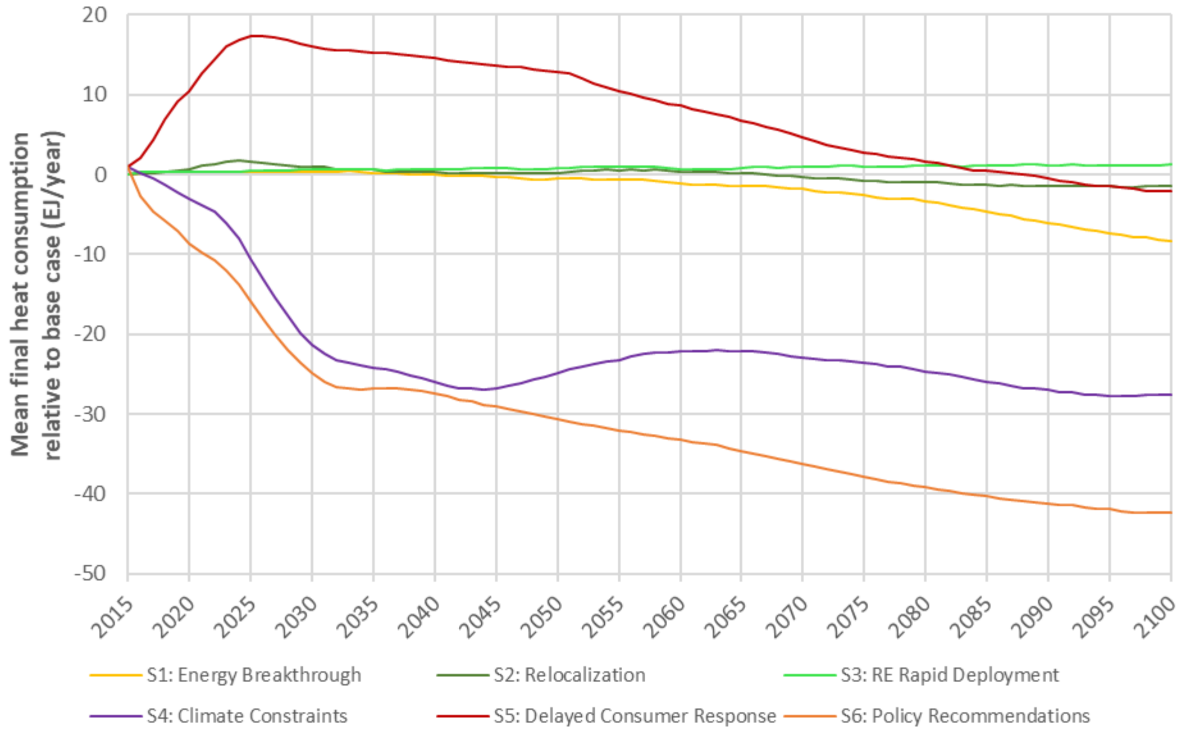

Figure 91: mean final (non-GES) heat demand relative to the base case, by scenario

Scenario specific differences in mean ES demands are given in section 10.3.

6.2.5 Primary resources

Figure 92 summarizes mean NRE depletion and RE exhaustion of primary energy resources by 2100 relative to the base case, by scenario. Scenario 1 shows minor (< 0.1) reductions in depletion or exhaustion for most primary energy resources except for slight increases (< 0.03) for oil and biomass, and a very large decrease in other RE exhaustion (resulting from treating this resource as effectively inexhaustible). Both scenarios 2 and 6 result in reduced depletion or exhaustion of all primary energy resources by 2100, however this is much more pronounced in scenario 6, particularly for nuclear fuels, hydropower, and biomass (0.38, 0.35, and 0.66 reductions in mean depletion or exhaustion relative to the base case, respectively). Scenario 3 exhibits slight changes only, except for biomass which sees a 0.1 increase in mean exhaustion relative to the base case. Scenario 4 increases depletion or exhaustion for most primary energy resources (particularly for nuclear fuels and biomass) except for natural gas and coal, which are reduced by 0.08 and 0.2, respectively). Scenario 5 sees few significant changes in depletion or exhaustion relative to the base case, except for a decrease in nuclear fuels depletion and an increase in biomass exhaustion, by 0.09 and 0.08, respectively.

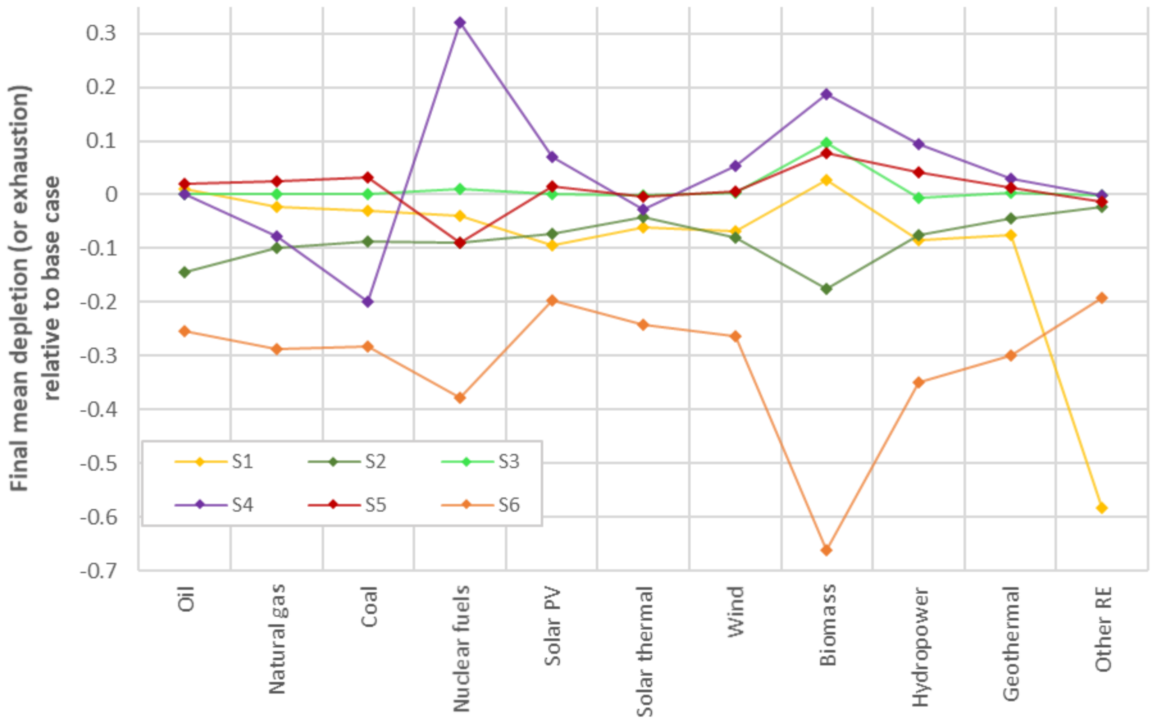

Figure 92: mean NRE depletion and RE exhaustion of primary energy resources in 2100 relative to the base case, by scenario

6.2.6 RE share of supply

Figure 93, showing mean RE shares of TPES in 2050 and 2100 by scenario, identifies few statistically significant differences due to wide and overlapping 90% confidence intervals. By 2050, the RE shares of TPES are largely in the 26-47% range, possibly higher in scenario 4 (32% to 49%) and possibly lower in scenario 5 (22% to 37%). By 2100, the typical range of RE shares of TPES has increased to 30-72% range, although possibly higher in scenario 1 (45% to 83%).

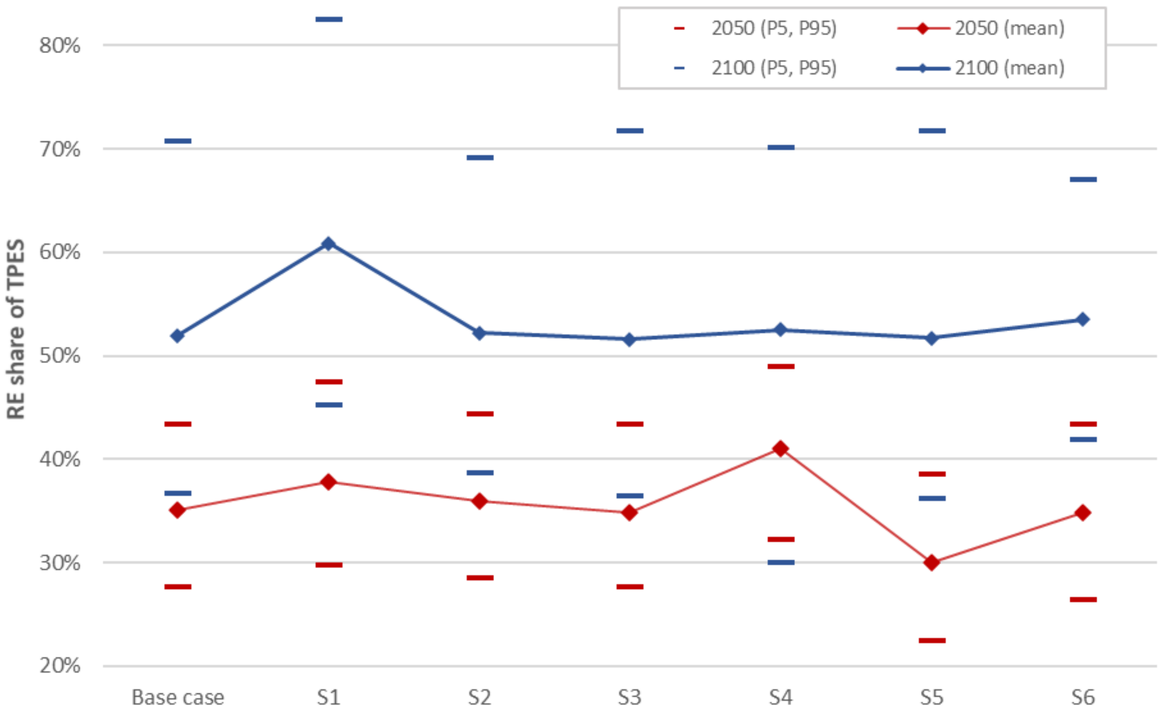

Figure 93: mean RE share of TPES in 2050 and 2100 by scenario, including 90% confidence intervals

6.2.7 EROI

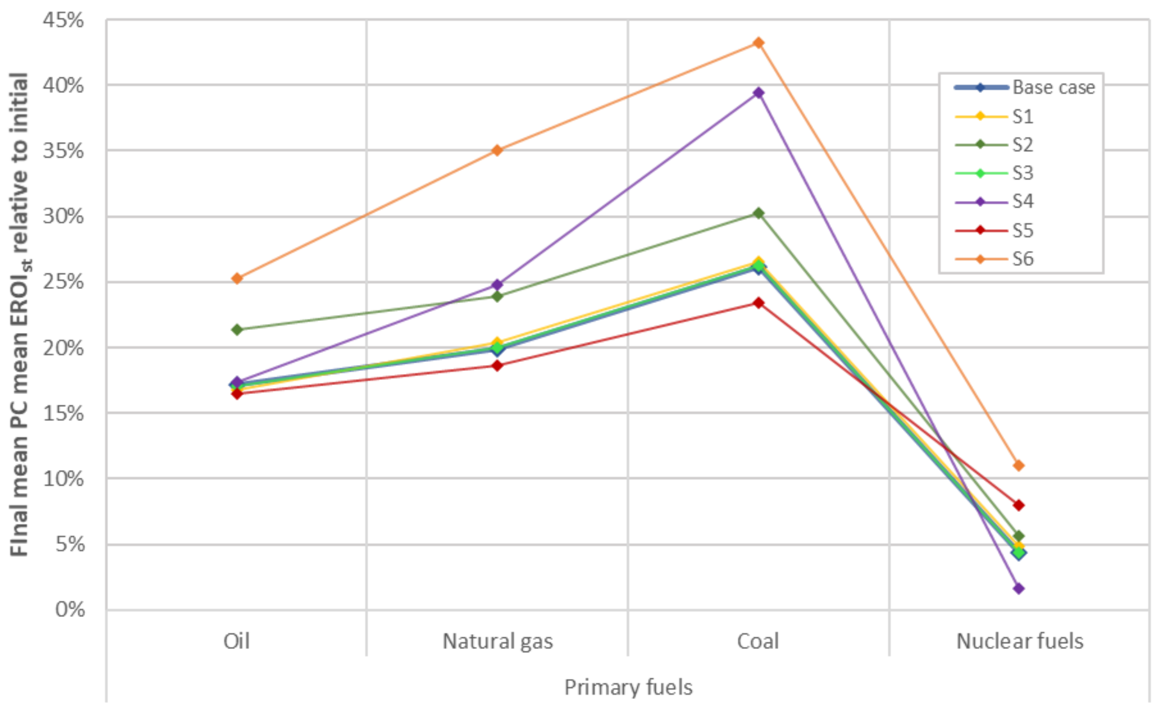

Figure 94: mean PC mean EROI in 2100 relative to 2015 by scenario (low)

Mean PC mean EROI for primary energy resources and mean point-of-use EROI for ECs in 2100 by scenario, relative to their initial values, are shown in Figure 94 and Figure 95. NRE resources exhibit major declines of 55% or more by 2100 due to depletion effects. Nuclear fuels experience the greatest mean EROI declines, by 89% or more. Mean EROI values for fossil fuels decline by 57-83%, with the largest declines typically occurring for oil, followed by natural gas and coal.

RE resources generally exhibit lesser declines in mean EROI by 2100, although several distinct groups are apparent, associated with the size of the absolute technical potential:

- Solar thermal, hydropower, geothermal, and other RE typically decline 40-60% (except in scenario 6).
- Wind and biomass typically decline 10-35% (except in scenario 6).
- Solar PV declines no more 12%.

Mean point-of-use EROI for ECs typically declines 30-50% by 2100 (except in scenario 6). Mean final EROI values are lowest in scenario 4 for all RE resources, nuclear fuels, and electricity, while mean final EROI is higher for natural gas and coal. Mean final EROI values are universally highest in scenario 6 (except for other RE in scenario 1, as an artefact of scenario implementation). Impacts on final EROI values are generally positive in scenarios 1 (weakly) and 2 (strongly), negative in scenario 5, and neutral in scenario 3.

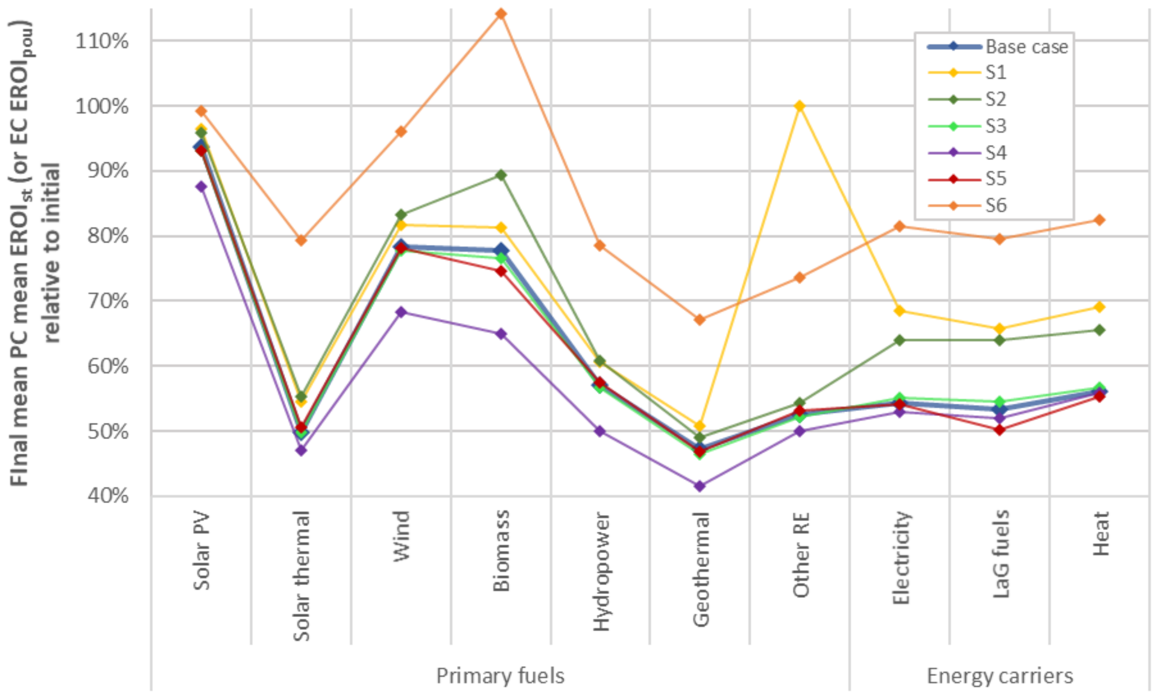

Figure 95: mean PC mean EROI and point-of-use EROI in 2100 relative to 2015 by scenario (high)

6.2.8 Penetration

6.2.8.1 Secondary

Mean secondary penetration by secondary PC type by scenario for electricity, shown in Figure 96, exhibits relatively minor differences between scenarios at each timestep, except for strong growth in other RE in scenario 1. Between 2025 and 2100, mean fossil fuel penetration in electricity production is lowest in scenarios 1, 4, and 6. However, by 2100 mean fossil fuel penetration is highest in scenario 4. Mean penetration appears relatively insensitive to the modelled scenarios for oil, geothermal, coal CHP, natural gas CHP, solar thermal, biomass, and biomass CHP, and other RE (with the exception of scenario 1). In contrast, hydropower, wind, solar PV, nuclear, natural gas, and coal penetration responds more strongly to modelled scenario conditions.

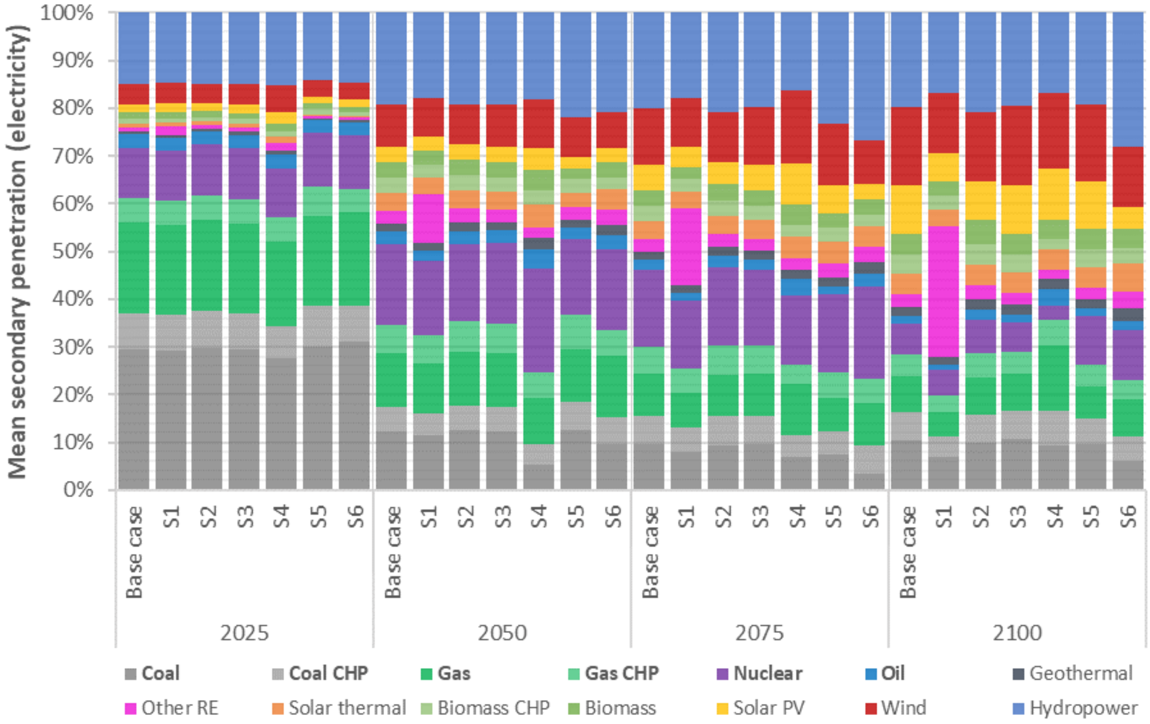

Figure 96: mean secondary penetration by secondary PC type by scenario for electricity

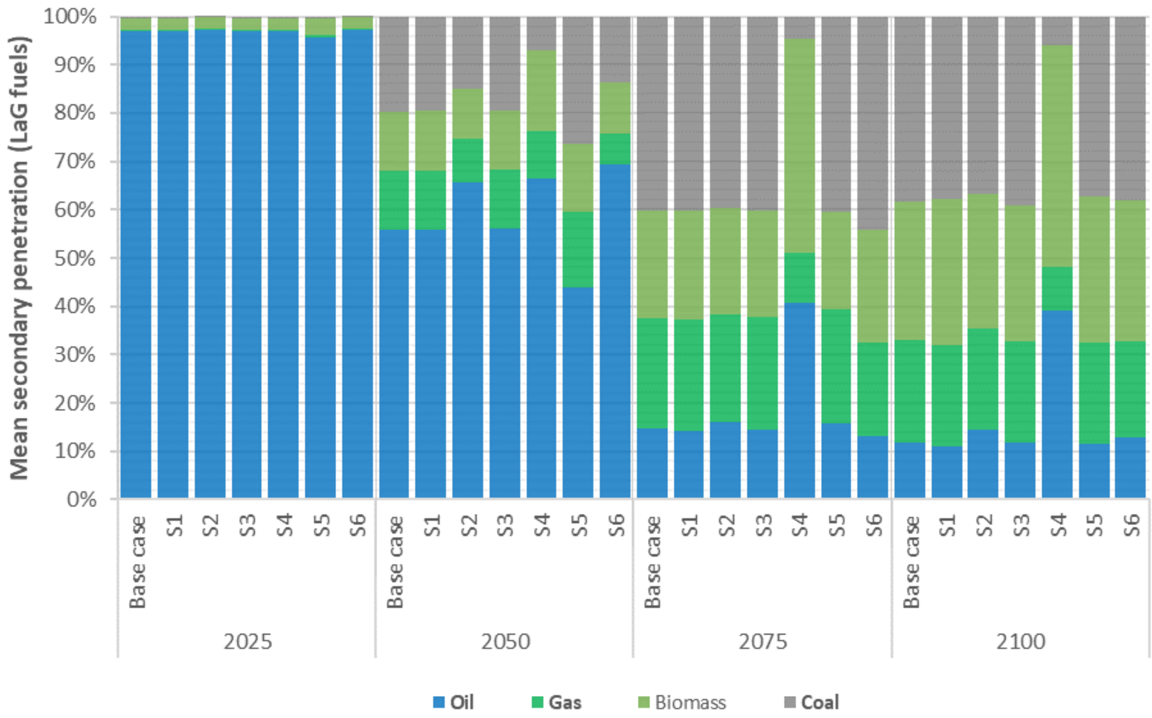

Figure 97: mean secondary penetration by secondary PC type by scenario for LaG fuels

Mean secondary penetration by secondary PC type by scenario for LaG fuels, shown in Figure 97, exhibits strong convergence after 2050 for all scenarios except scenario 4 (which sets reduced penetration limits for the conversion of coal and natural gas to LaG fuels). By the 2050 timestep, progress towards the final penetration levels has proceeded furthest in scenario 5 but is somewhat lagging in scenarios 2 and 6. In scenario 4, oil refining and the production of biofuels are consistently much higher than other scenarios after 2050.

Mean secondary penetration by secondary PC type by scenario for heat, shown in Figure 98, again exhibits relatively minor differences between scenarios at each timestep. Scenario 4 sees significantly greater penetration for CHP using natural gas, coal, and biomass, relative to other scenarios, primarily displacing the direct use of coal. Growth in solar thermal, geothermal, and oil penetration begins earlier in scenario 5, prior to 2025. By 2100, scenarios 1 and 6 see the lowest mean fossil fuel penetration in heat production, closely followed by scenario 2, although differences between all scenarios are minor.

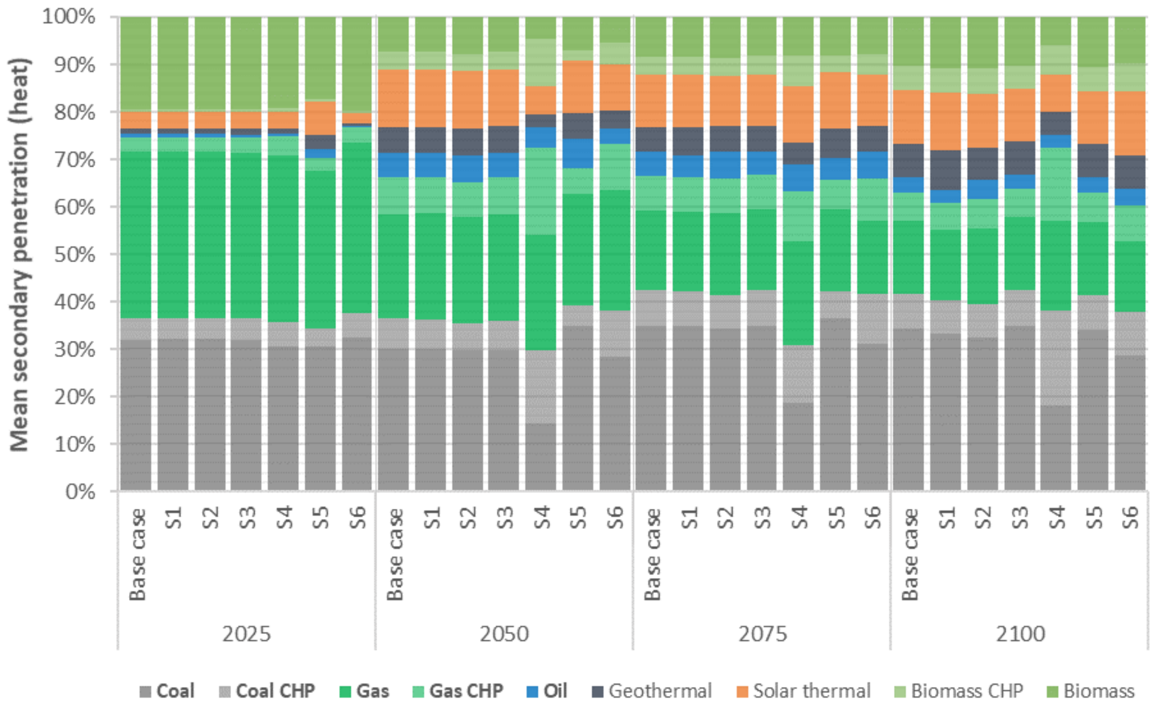

Figure 98: mean secondary penetration by secondary PC type by scenario for heat

6.2.8.2 End-use

Figure 99 shows mean EU penetration by EU PC type by scenario for the the provision of the regional passenger transportation ES. Scenarios 2 and 6 show consistently lower penetration levels for electric rail and electric vehicles, with correspondingly higher penetration in other EU PC types, particularly ICE rail, shipping, and aviation. Conversely, scenario 4 shows consistently higher penetration levels for electric rail and electric vehicles and lower penetration in other EU PC types, particularly ICE rail and light ICE vehicles. By 2075 rail (ICE and electric) has become the dominant mode for regional passenger transportation while the use of aviation and ICE vehicles is minor in all scenarios. Due to a delayed repsonse in downstream investment, scenario 5 exhibits fewer changes from initial penetration levels before 2050.

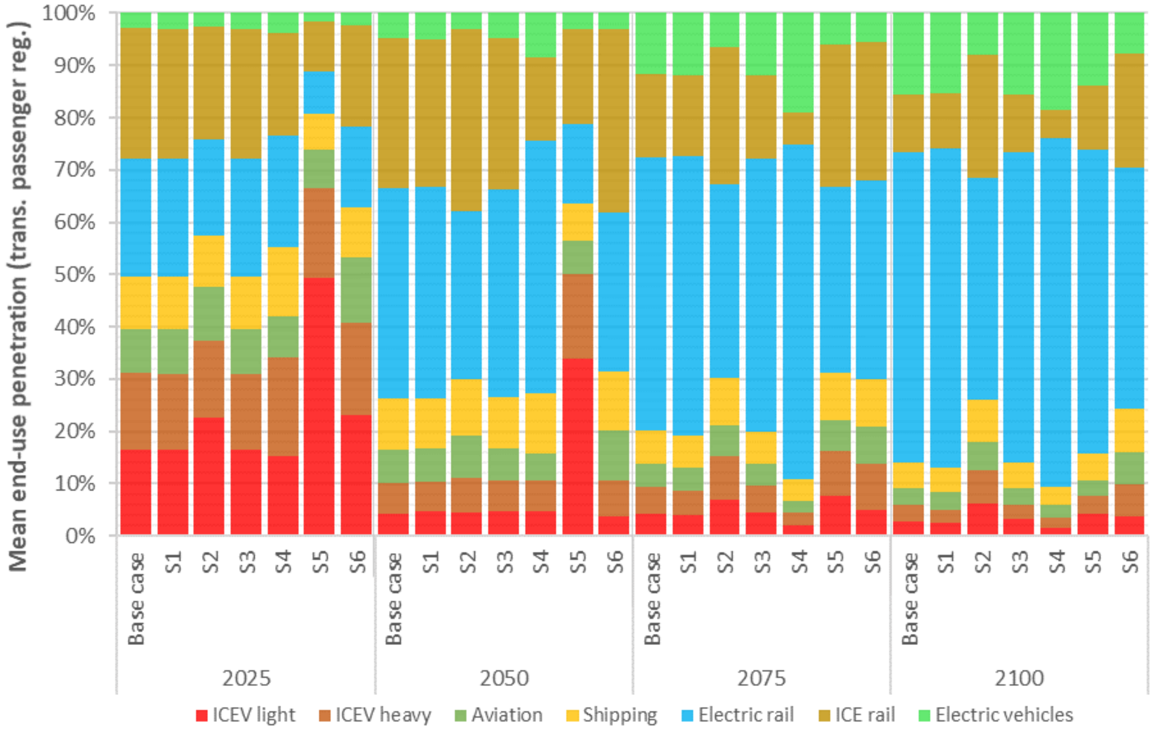

Figure 99: mean EU penetration by EU PC type by scenario for regional passenger transportation

Figure 100 shows mean EU penetration by EU PC type by scenario for the the provision of the regional freight transportation ES. Scenarios 2 and 6 show consistently lower penetration levels for electric rail, with correspondingly higher penetration in all other EU PC types except heavy ICE vehicles. Conversely, scenario 4 shows consistently higher penetration levels for electric rail and lower penetration in other EU PC types, particularly ICE rail. By 2075 rail (ICE and electric) has become the dominant mode for regional freight transportation while the use of aviation and heavy ICE vehicles is minor in all scenarios. As with passenger transportation, scenario 5 exhibits fewer changes from initial penetration levels before 2050.

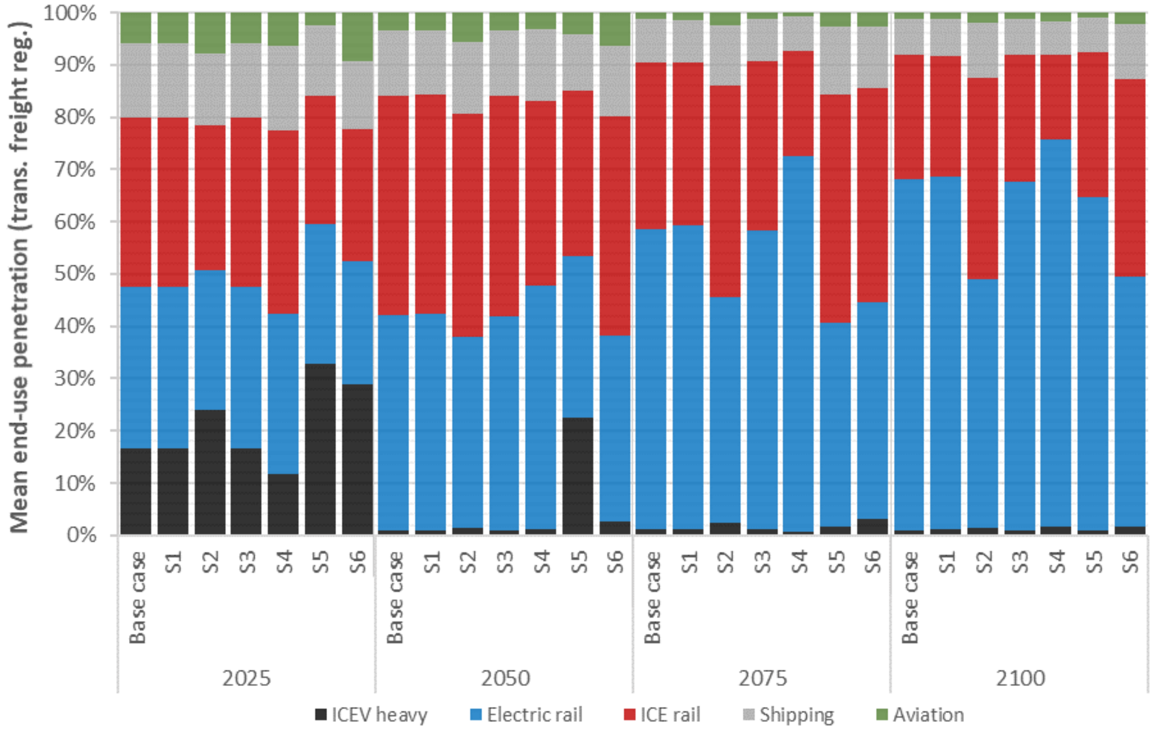

Figure 100: mean EU penetration by EU PC type by scenario for regional freight transportation

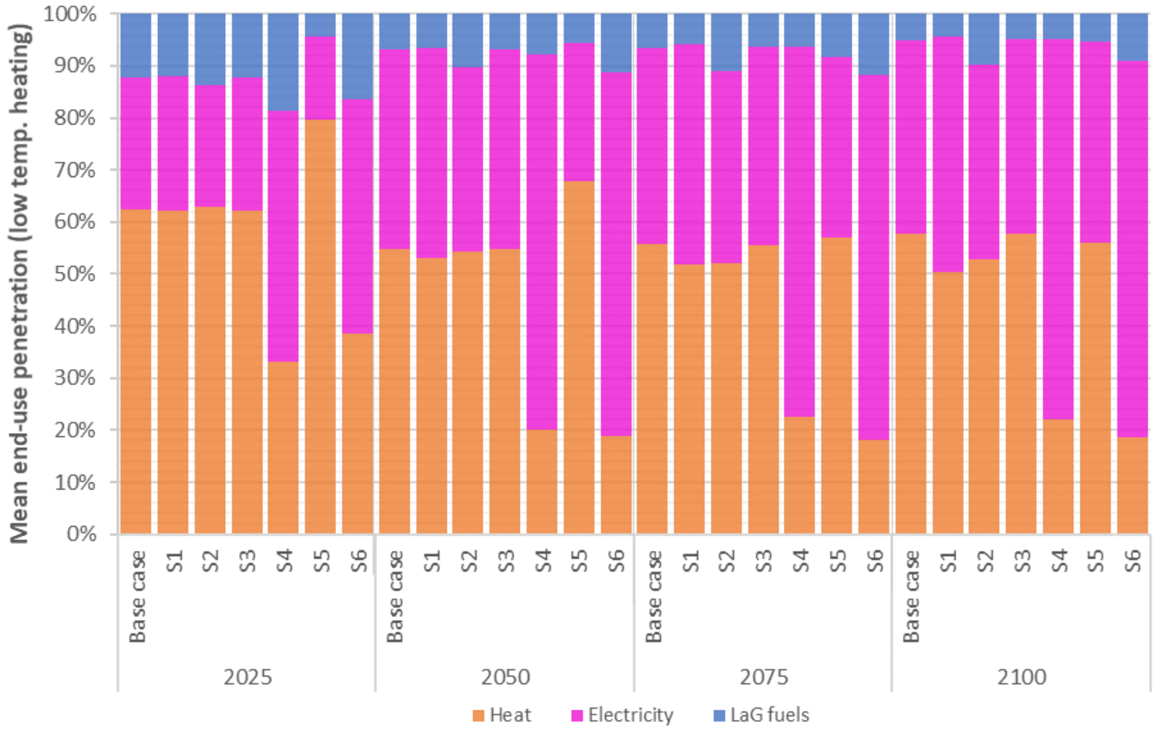

Figure 101: mean EU penetration by EU PC type by scenario for low temperature heating

Figure 101 shows mean EU penetration by EU PC type by scenario for the the provision of the low temperature heating ES. Higher electrification of low temperature heating is seen in scenarios 4 and 6, with correspondingly lower heat penetration. As with transportation, scenario 5 exhibits fewer changes from initial penetration levels before 2050.

Mean shares of IC passenger and freight transportation provided by aviation (as opposed to shipping), are shown in Figure 102. Rapid changes occur in the early simulation period for all scenarios, with aviation penetration decreasing from near 100% for passenger transportation and increasing from near 0% for freight transportation. These changes occur more slowly in scenario 5, with mean aviation shares converging to those observed in the base case between 2050 and 2100. Scenarios 1 and 3 show negligible differences from the base case. Scenario 2 exhibits moderate changes (by < 12%) relative to the base case, with lower mean aviation shares for IC passenger transportation and higher mean aviation shares for IC freight transportation. In scenario 4, mean aviation shares are significantly lower than the base case, particularly for IC passenger transportation (reaching almost 80% shipping by 2040). Scenario 6 exhibits somewhat lower (by < 10%) mean aviation penetration for IC passenger transportation and the lowest mean aviation penetration for freight (remaining below 17%).

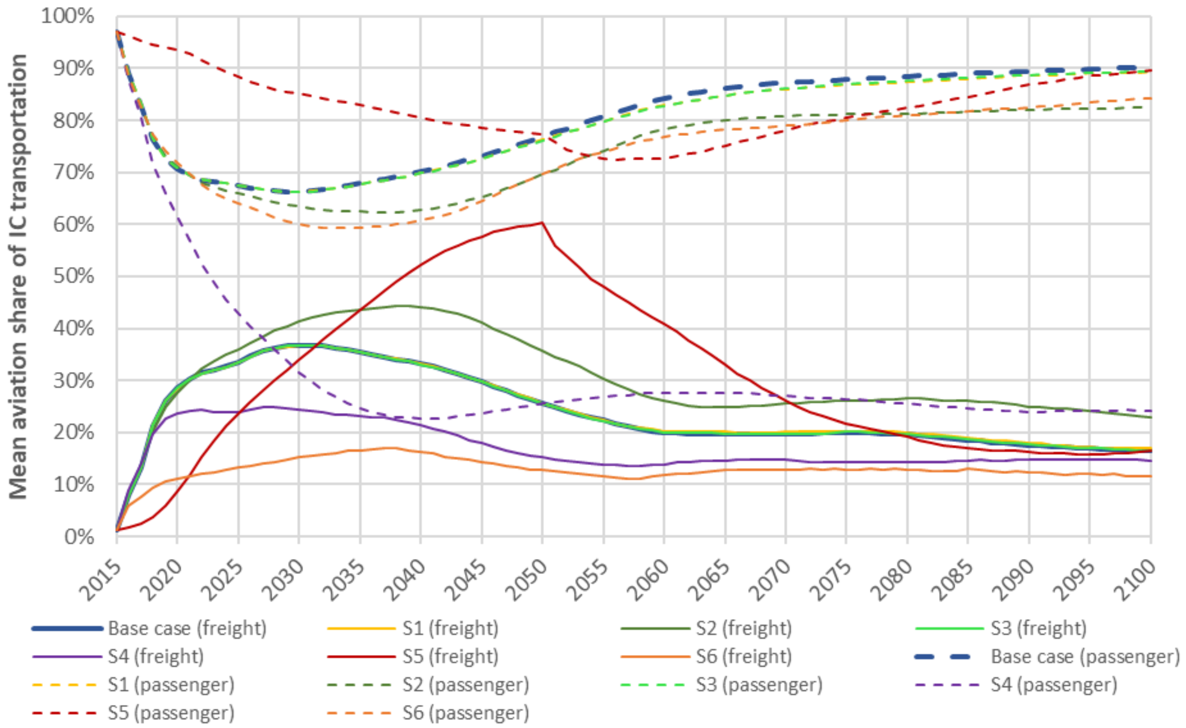

Figure 102: mean aviation shares of IC passenger and freight transportation by scenario

Mean shares of static mechanical work and high temperature process heat provided using electricity (as opposed to LaG fuels and heat, respectively) by scenario, are shown in Figure 103. In general, a process of electrification of these two ESs is observed. This is despite early declines in the mean electrified share of static mechanical work, between 10% and 15% from the 2015 level, in all scenarios except scenario 4 where a steady increase occurs. The mean electrified shares of static mechanical work exceed 80% by 2100 in all scenarios except 2 and 6, in which mean shares are essentially unchanged from their initial levels. Electrification of high temperature process heat is consistently higher in scenario 4 than in the base case (up to 30% higher mean). Scenarios 5 and 6 show lagging electrification of high temperature process heat relative to the base case, while scenario 1 sees a minor boost after 2050 (< 10%), and scenarios 2 and 3 exhibit little difference.

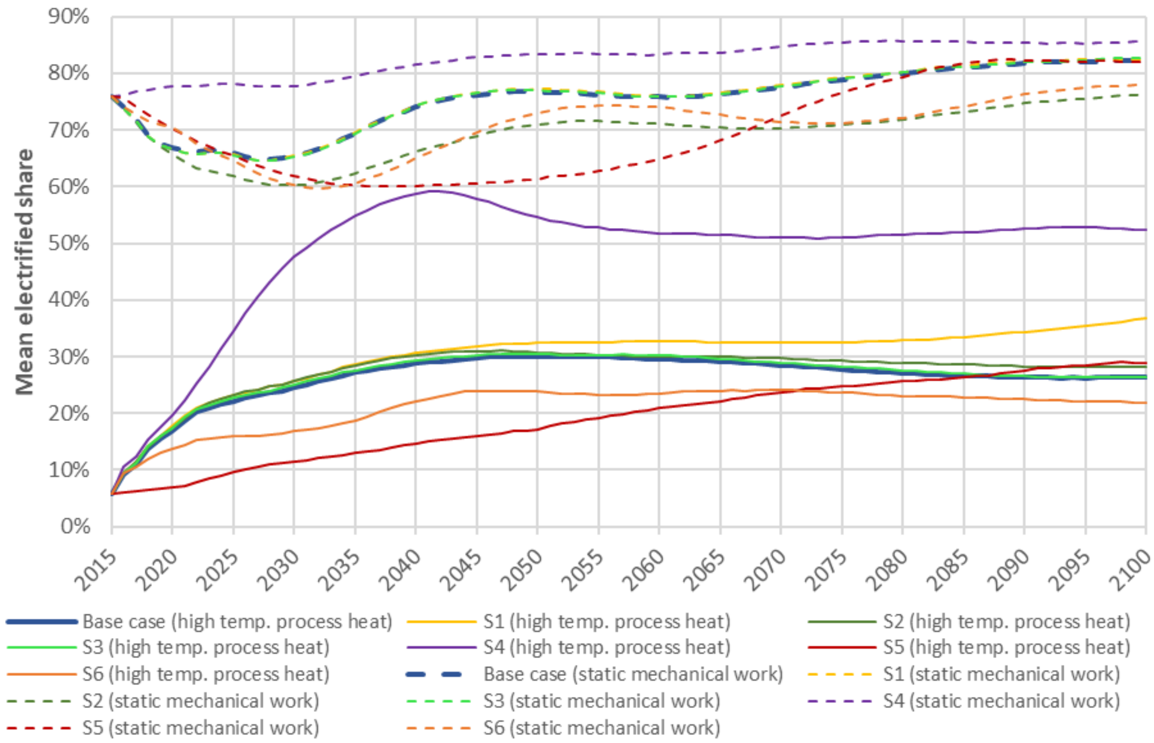

Figure 103: mean electrified shares of static mechanical work and high temperature process heat by scenario

6.2.9 GHG emissions

Figure 104 shows mean cumulative GHG emissions by scenario relative to the base case. Scenarios 1 and 3 see moderate decreases and increases (< 75 $GtCO_2e$) in mean cumulative GHG emissions relative to the base case, respectively, accruing primarily in the late simulation period. Scenarios 2 and 4 achieve significant reductions of similar magnitude in cumulative GHG emissions relative to the base case, reaching mean reductions of 312 $GtCO_2e$ and 206 $GtCO_2e$ by 2100, respectively. Scenario 5 exhibits significantly increased mean cumulative GHG emissions relative to the base case, peaking by 2080 before declining slightly to 150 $GtCO_2e$ by 2100. Scenario 6 achieves the lowest mean cumulative GHG emissions by a wide margin, with reductions steadily increasing over the simulated period to 832 $GtCO_2e$ less than the base case by 2100 (equivalent to approximately 26 years of 2015 global GHG emissions). Considering mean trends across the modelled scenarios, emissions budgets corresponding to 1.5°C and 2°C are depleted by 2036 and 2039 at the earliest (in scenario 5) and 2074 and 2081 at the latest (in scenario 6), respectively.

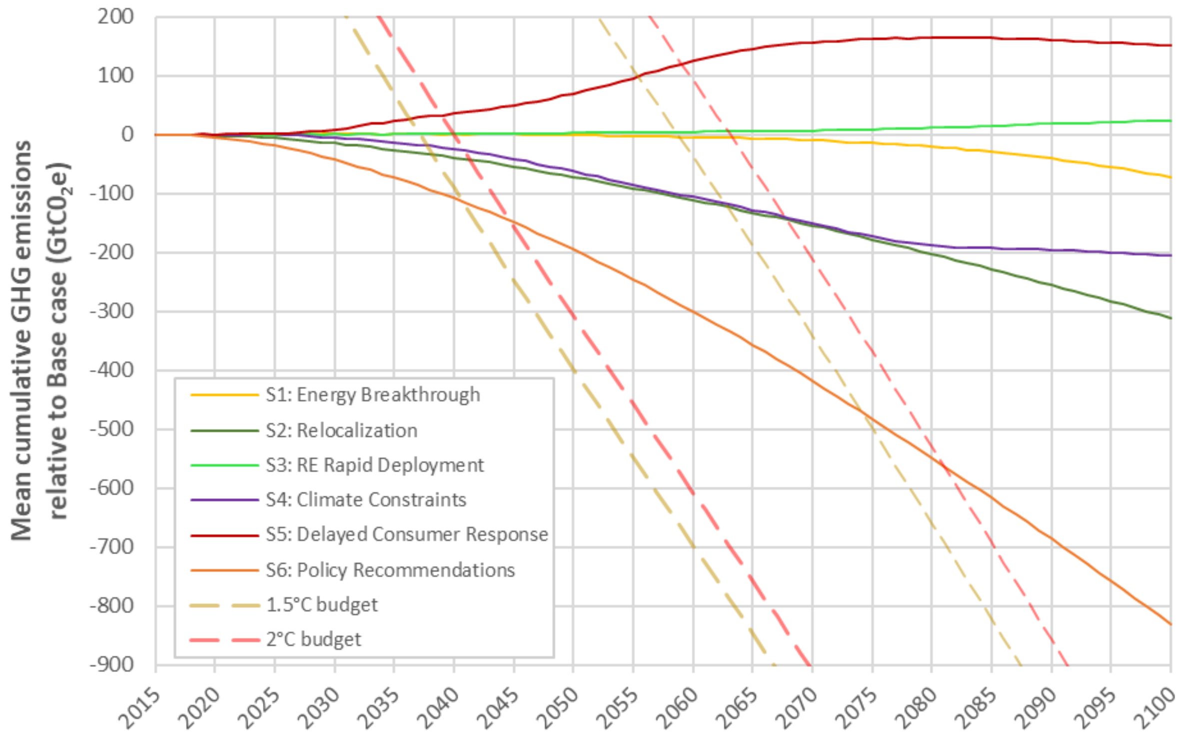

Figure 104: mean cumulative GHG emissions by scenario including emissions budget ranges, relative to the base case

Cumulative probability distributions for cumulative GHG emissions by scenario are shown in Figure 105 (for 2050) and Figure 106 (for 2100). The lower emissions budget range limits for 1.5°C and 2°C are both exceeded by distribution minima for all scenarios by 2050. The upper emissions budget range limit for 1.5°C is meaningfully exceeded only by scenario 5 by this time (with less than 10% likelihood). The upper emissions budget range limit for 2°C is exceeded by distribution minima for all scenarios by 2100. However, significant differences exist between scenarios, with median cumulative GHG emissions spanning a range of 975 $GtCO_2e$ and maxima spanning almost 2400 $GtCO_2e$ (between scenarios 5 and 6). These quantities amount to approximately 30 and 74 years of 2015 global GHG emissions, respectively, implying vastly different climate outcomes depending on policy choices. Scenario 4 exhibits a low distribution gradient above the 70th percentile in 2100, indicating that very high emissions outcomes are relatively more common in this scenario compared to those with a similar median effect (i.e., scenario 2). Notably, distribution minima coincide for all scenarios over time suggesting adverse circumstances affect the likelihood but not the potential magnitude of emission reductions.

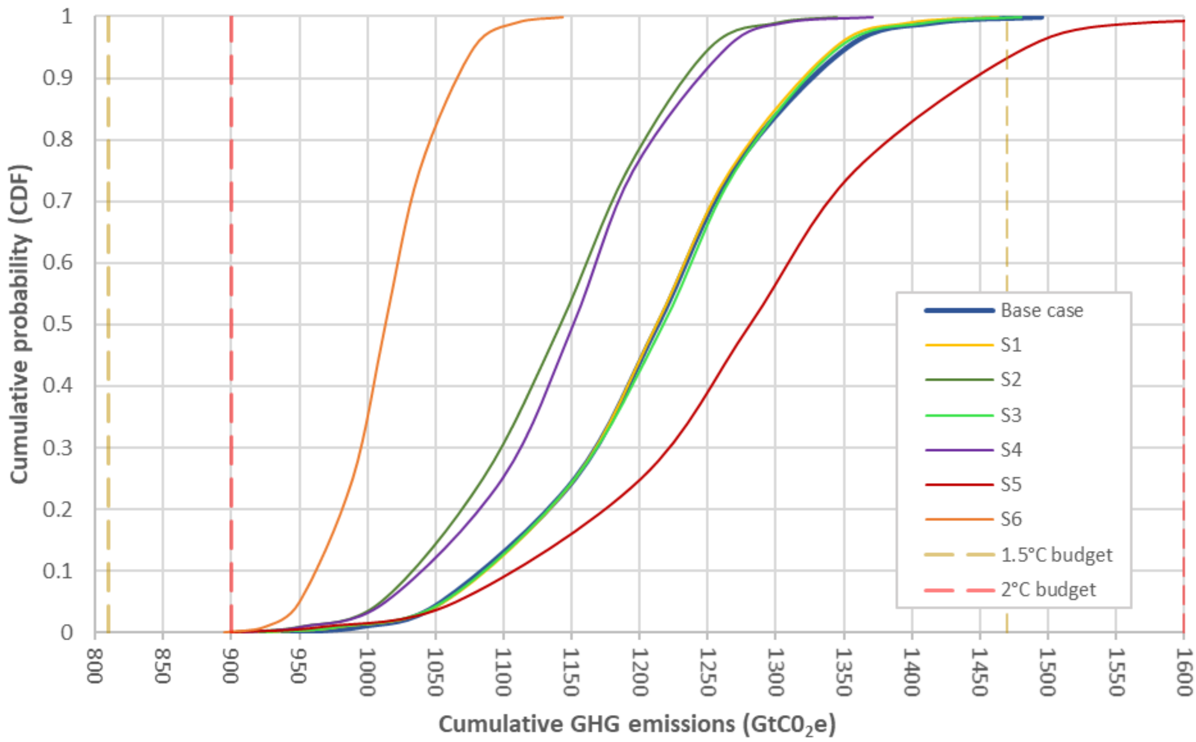

Figure 105: cumulative probability distributions for cumulative GHG emissions in 2050 by scenario including emissions budget ranges

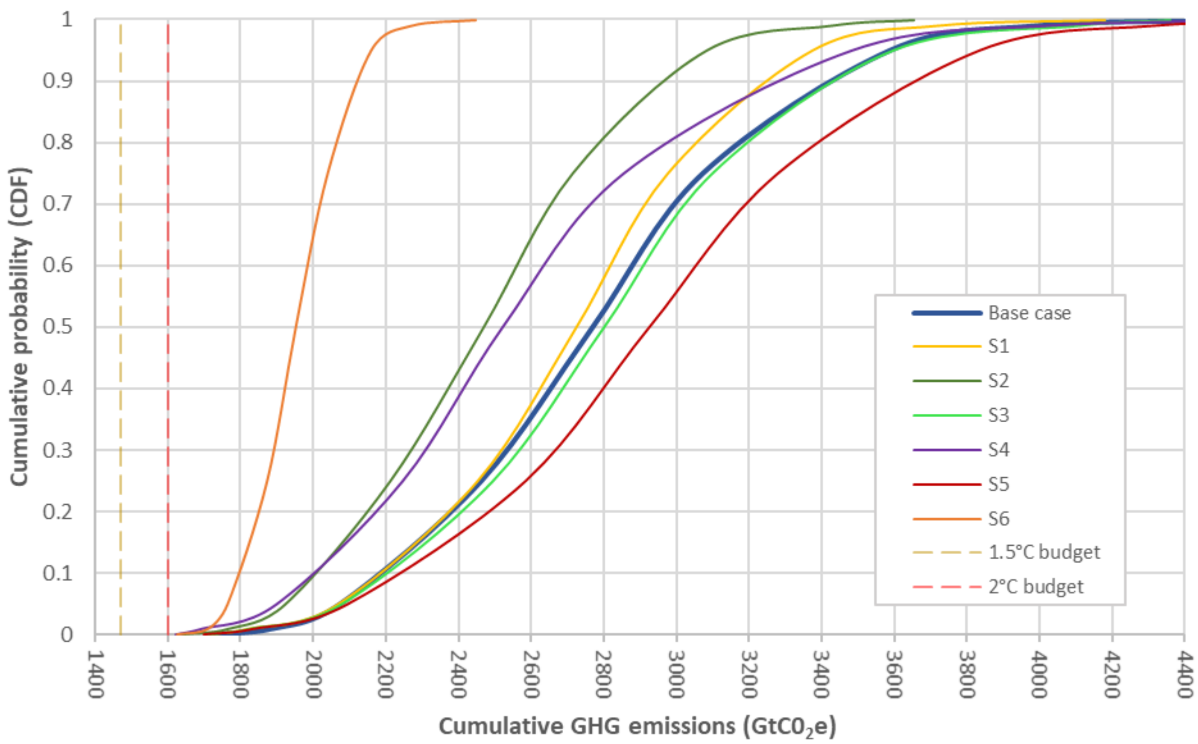

Figure 106: cumulative probability distributions for cumulative GHG emissions in 2100 by scenario including emissions budget upper limits

6.2.10 GES metabolism

Figure 107 shows mean ESMRs for each EC, by scenario, relative to the base case. Scenarios 1 and 2 appear to be similarly beneficial, with steadily increasing reductions in ESMRs relative to the base case (as much as 0.05), however, this benefit appears earlier but grows more slowly in scenario 2. Scenario 3 appears to be to be limited to a greater extent by the availability of electricity and heat. Scenario 3 exhibits minor differences only. Scenarios 4 and 5 appear to impose greater burdens on the global socio-economic system relative to the base case and appear to be limited to a greater extent by LaG fuel availability. Scenario 4 sees the greatest mean ESMR observed during the simulated period around 2075 (0.22), raising questions of feasibility. Scenario 6 exhibits the lowest ESMRs, between 0.06 and 0.08 lower than the base case by 2100.

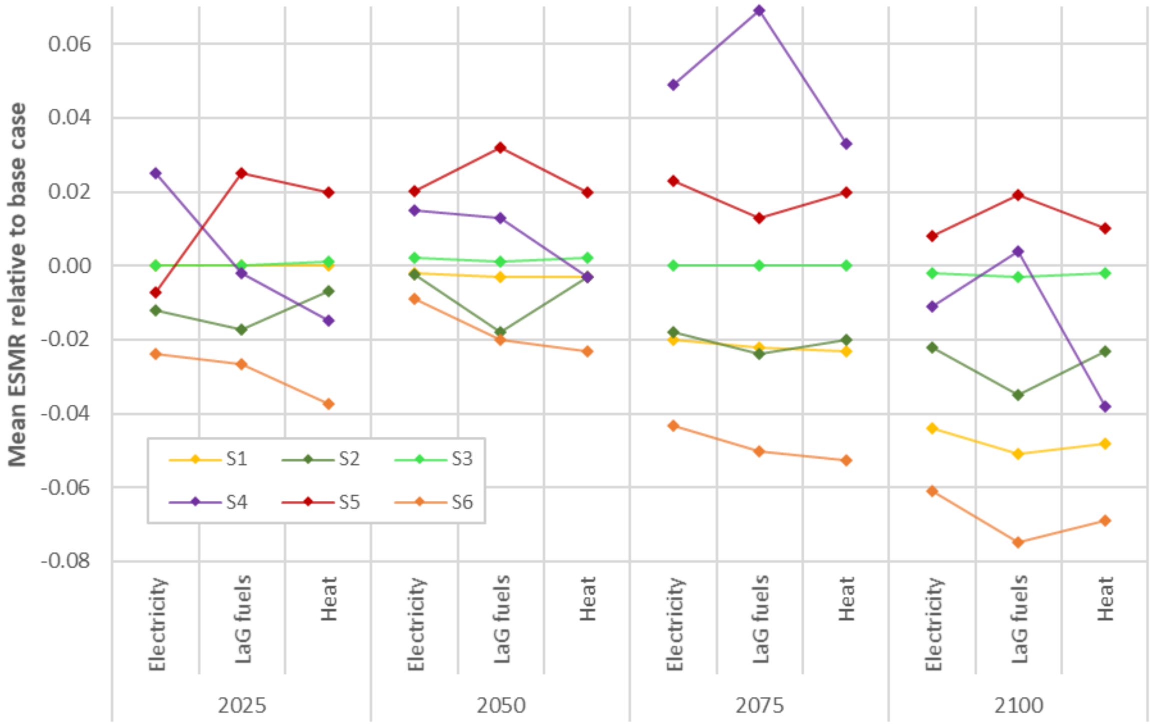

Figure 107: mean ESMRs by scenario relative to the base case

6.3 Sensitivity analysis

Refer to section 5.5.1 for sensitivity analysis details, including the calculation of the normalized sensitivity metric. Results here describe an ensemble of 10,000 realizations, with failed realizations included for stable time, but excluded for cumulative GHG emissions.

Figure 108 shows cumulative probability distributions for normalized sensitivity for both selected results, including upper and lower sensitivity thresholds. The sensitivity distribtution for cumulative GHG emissions exhibits lower mean and median sensitivity but is long-tailed, suggesting many input parameters have little impact but a small group have very high impact. Stable time is influenced by a wider range of input parameters. Sensitivity thresholds for stable time are 0.065 and 0.110. Sensitivity thresholds for cumulative GHG emissions are 0.063 and 0.117.

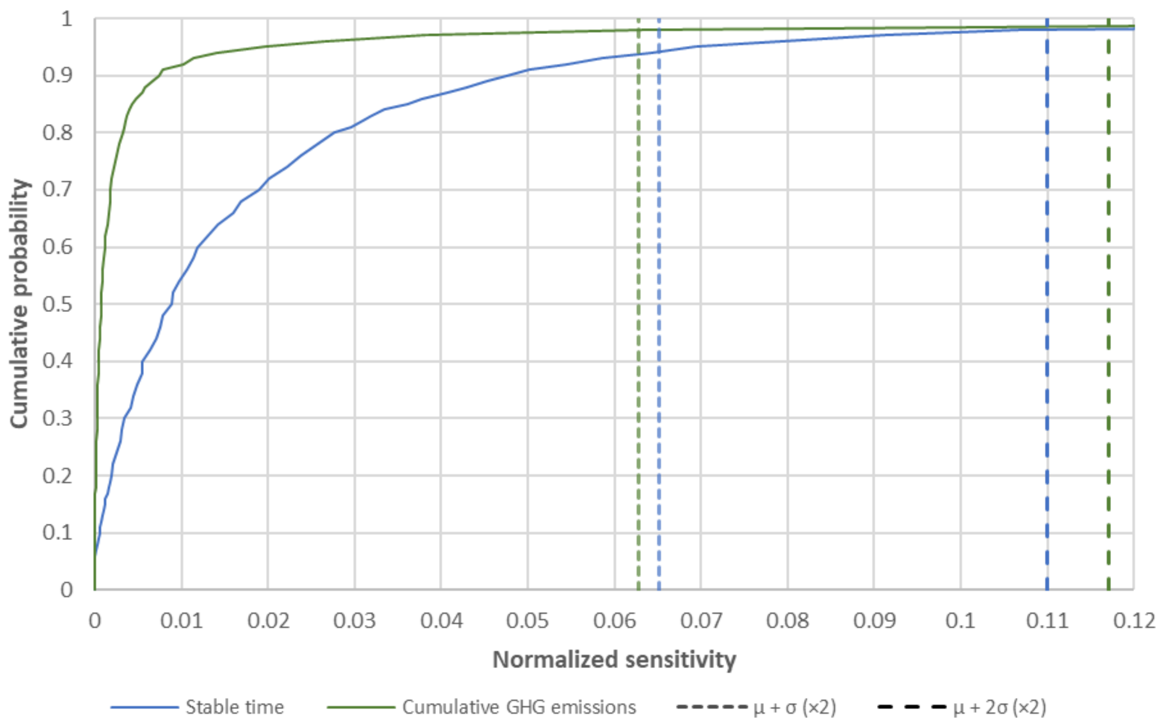

Figure 108: cumulative probability distributions for normalized sensitivity for selected results, including sensitivity thresholds

Charts in sections 6.3.1 and 6.3.2 include only input parameters with sensitivity values above one of the higher sensitivity thresholds or above both lower sensitivity thresholds. Note, contributions to sum normalized sensitivity are presented as negative where increases in the relevant input parameter are associated with undesirable outcomes (indicated by the sign of $SRC_{y,i}$). Additional sensitivity results for input parameters above lower sensitivity thresholds are given in section 10.5.

6.3.1 Non-decision input parameters

Sum normalized sensitivity values across both selected results for non-decision input parameters, ordered by absolute sum, are presented in Figure 109. These input parameters are therefore identified as those not considered amenable to human control having the greatest relative importance for GES transformation outcomes.

These results highlight the overwhelming importance of primary energy resource availability and quality for minimizing the risk of encountering net energy trap outcomes, particularly biomass potential (the single highest sensitivity input parameter relating to this outcome). Solar thermal, geothermal, and coal initial resource magnitudes are also crucial for system stability. Furthermore, EROI parameters characterizing resource quality for coal, oil, and natural gas exhibit high sensitivity. Together, these primary energy resource related input parameters represent the majority of absolute sum normalized sensitivity for stable time presented in Figure 109. Interestingly, higher initial EU to ES efficiencies for IC freight shipping, regional freight aviation, passenger electric rail, and electric mechanical systems, and the upper asymptote for the CF target for IPaC devices have significant negative impacts on system stability. Higher CapEx fractions for hydropower are also moderately negative for system stability.

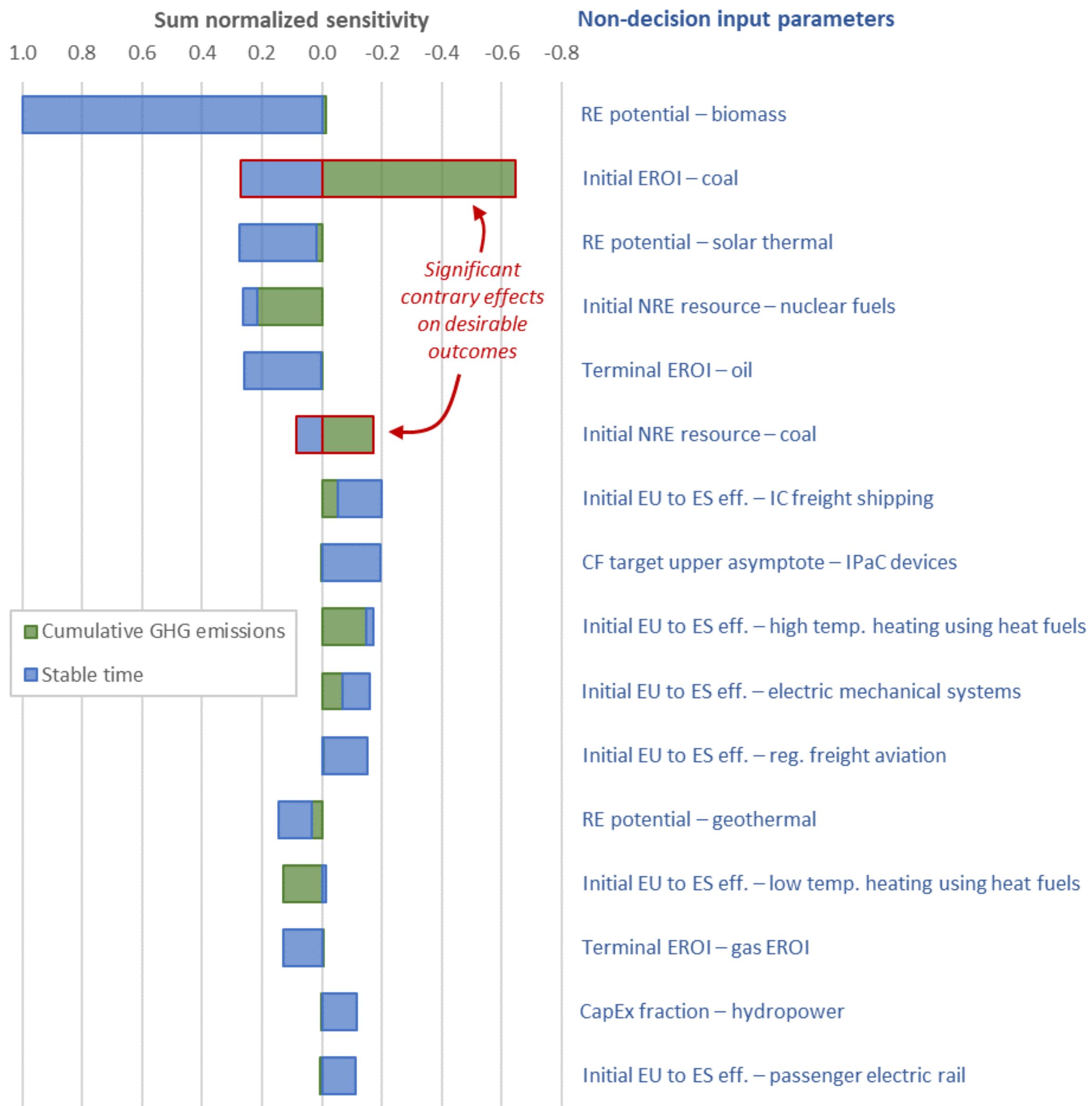

Figure 109: non-decision input parameters by sum normalized sensitivity across both selected results

Cumulative GHG emissions are also primarily affected by primary energy resource related input parameters. Higher nuclear fuel and geothermal initial resource magnitudes correspond to lower cumulative GHG emissions by the end of the simulated period, and *vice versa*. Cumulative GHG emissions are also moderately affected by initial EU to ES efficiencies for IC freight shipping, high temperature heating using heat fuels, and electric mechanical systems (negatively), and low temperature heating using heat fuels (positively).

Notably, coal initial resource and EROI contributions to sum normalized sensitivity are both significant (above respective lower sensitivity thresholds) and exhibit contrary effects on desirable outcomes (highlighted in Figure 109). This suggests greater coal availability and quality have significant positive implications for system stability, but strongly negative implications for cumulative GHG emissions by the end of the simulated period, and *vice versa*.

6.3.2 Policy recommendations

Sum normalized sensitivity values across both selected results for policy recommendations, ordered by sum, are presented in Figure 110. Results identify grouped input parameters aligned with policy actions having the greatest potential impacts on GES transformation outcomes, or system leverage points as described in section 5.5.1.

Reductions in ES demands represent the major leverage points for minimizing cumulative GHG emissions within the simulated period, particularly high temperature process heat and static mechanical work (representing the majority of absolute sum normalized sensitivity for cumulative GHG emissions presented in Figure 110). Low temperature heating, IPaC, and regional passenger and freight (regional and IC) transportation also offer significant contributions. These demand reductions generally have positive (or neutral) effects on system stability, particularly for high temperature process heat and static mechanical work. Note that policy recommendations for reducing demand include input parameters for both the initial rate of change and ultimate magnitude of demand.

Decreases in ECC via design improvements aimed at reducing PC lifecycle energy costs have significant positive effects on system stability, specifically for biofuel production, coal CHP, intermittent electricity AI, geothermal electricity generation, the conversion of coal to LaG fuels, and coal electricity generation. These reductions in ECC have minor mixed effects on cumulative GHG emissions, except for significant negative effects associated with the conversion of coal to LaG fuels and coal electricity generation (normalized sensitivity of 0.06

and 0.11, respectively; highlighted in Figure 110). ECC reductions in coal CHP have a minor negative impact on cumulative GHG emissions (normalized sensitivity ~0.03).

Finally, accelerated retirements (by reducing operational lifetimes) of electricity generation from coal and IC freight aviation are significantly positive for cumulative GHG emissions and system stability, respectively (normalized sensitivity > 0.1). Accelerated retirement of coal electricity generation has a minor impact on system stability (normalized sensitivity ~0.01).

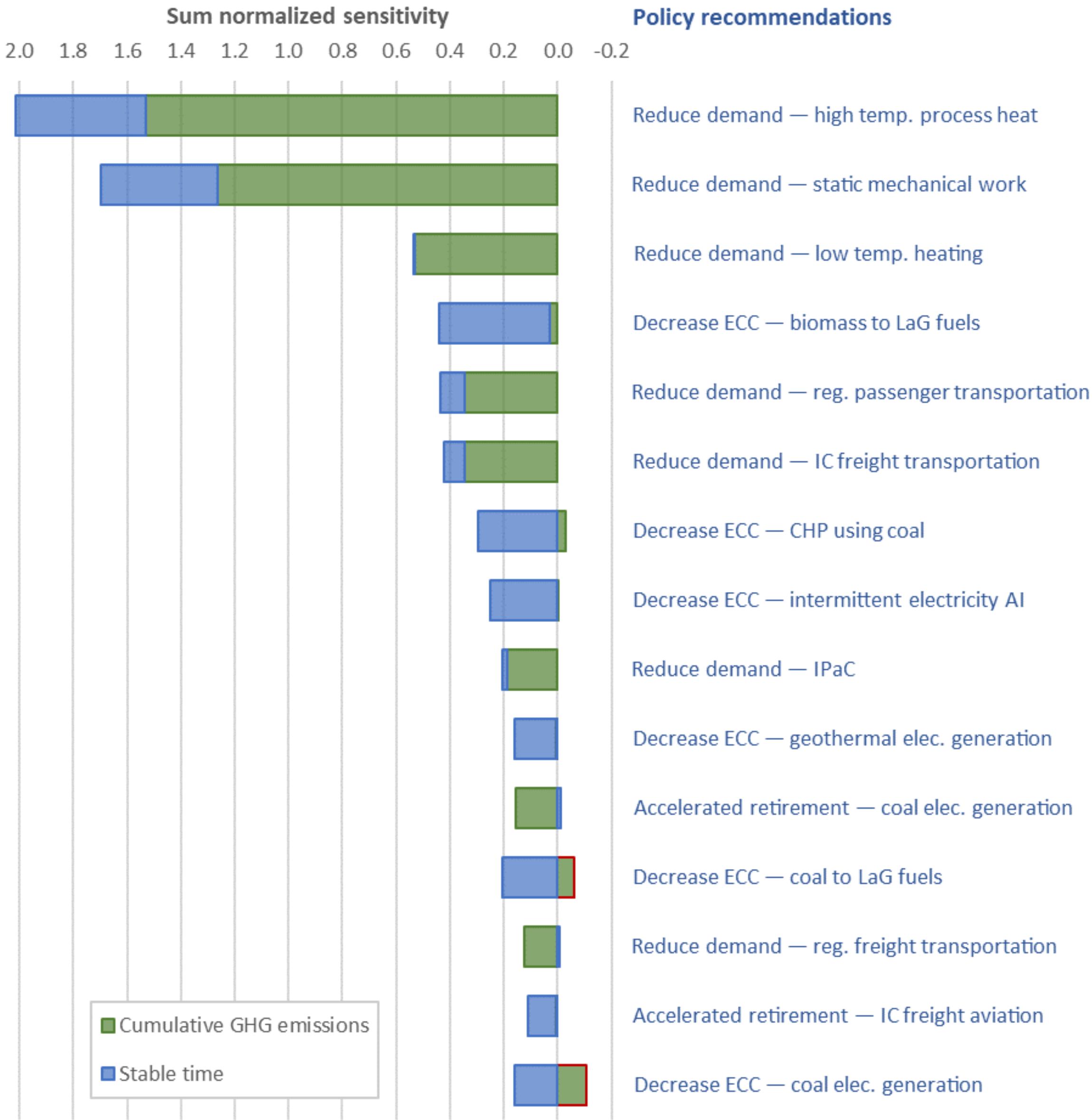

Figure 110: decision input parameters grouped by policy action by sum normalized sensitivity across both selected results

6.4 Diagnostic analysis

Refer to section 5.5.2 for diagnostic analysis details, including the definition of pedigree score.

6.4.1 Stable time

The diagnostic diagram for stable time, shown in Figure 111, shows few high-risk input parameters (9), but a relatively high number in the medium risk category (50). Pedigree scores are clustered due to the ordinal five-point grading scale used and averaging of component scores for the calculation of overall pedigree.

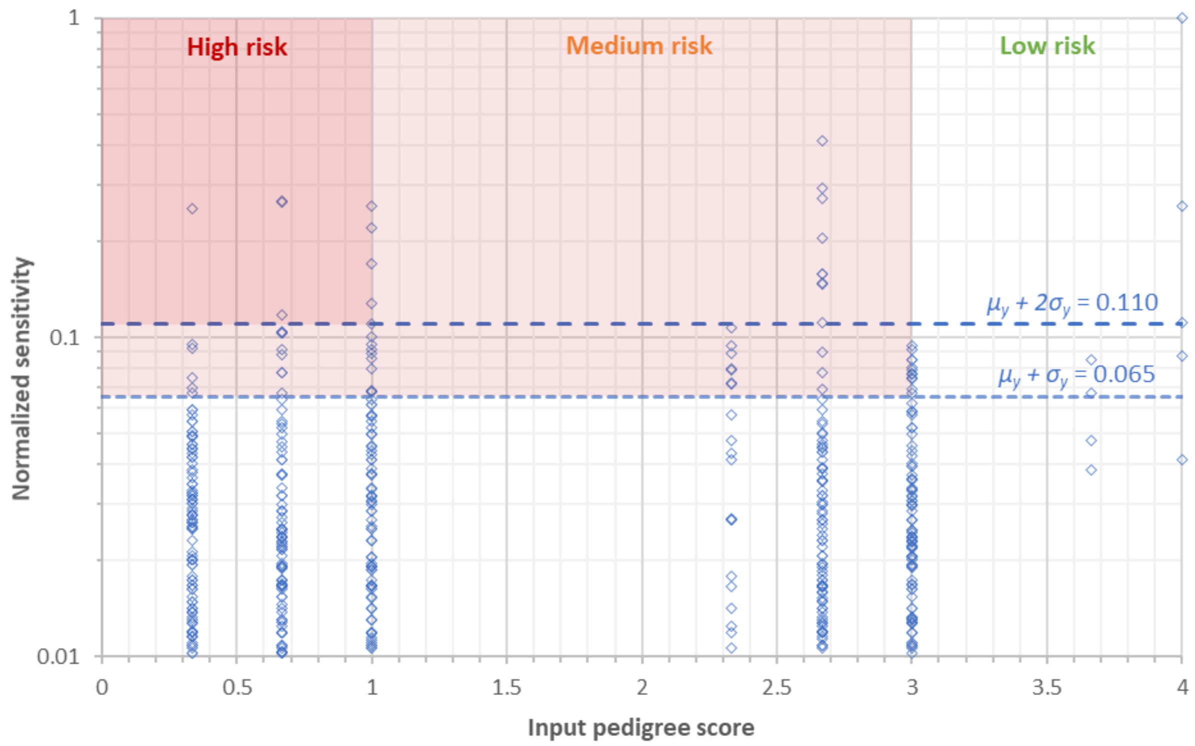

Figure 111: diagnostic diagram for stable time (semi-logarithmic)

High-risk input parameters for stable time are given in Table 9. The most notable group relate to ES demand (ES final demand multipliers and initial rates of change) for high temperature process heat and static mechanical work. These parameters have high normalized sensitivity values and low strength of knowledge as no suitable sources exist to independently project future ES demands as defined in the PRESS model, necessitating the use of own estimates subject to relatively weak assumptions (see section 9.8 for pedigree assessment component scores). Notably, ECC for intermittent electricity AI is subject to very low strength of knowledge as this input parameter is lacking suitable data sources and is defined using a cost proxy calculation and an order-of-magnitude range (see section 9.5.9.2 for details).

As discussed in section 5.5.2, particular attention must be given to input parameters categorized as high risk for both selected results. These are listed in bold red text in Table 9.

Table 9: high risk input parameters found via diagnostic analysis for stable time

Input parameter	Normalized sensitivity	Pedigree score
ES final demand multiplier – high temp. process heat	0.266	0.7
ES final demand multiplier – static mechanical work	0.264	0.7
Terminal EROI – oil	0.258	1.0
ECC – intermittent electricity AI	0.253	0.3
Initial ES demand rate of change – high temp. process heat	0.221	1.0
Initial ES demand rate of change – static mechanical work	0.171	1.0
Terminal EROI – natural gas	0.128	1.0
CapEx fraction – hydropower	0.117	0.7
PC lifetime – aviation freight IC	0.111	1.0

Medium risk results for stable time, given in section 10.6, exhibit two notable groups of input parameters: one with high normalized sensitivity (above the upper sensitivity threshold, 0.11) and moderate pedigree (2.7), and another with moderate normalized sensitivity (above the lower sensitivity threshold, 0.67) and very low pedigree (0.3). The first group includes ECC (for biofuel production, coal CHP, the conversion of coal to LaG fuels, coal electricity generation, and geothermal electricity generation), initial EROI for coal, and initial EU to ES efficiencies (for regional freight aviation, IC freight shipping, and passenger electric rail). The second group includes parameters for ECC (for passenger electric rail, LaG fuels AI, electrical AI, and regional passenger aviation) and the LaG fuel EC split factor for electric vehicles.

6.4.2 Cumulative GHG emissions

The diagnostic diagram for cumulative GHG emissions, shown in Figure 112, shows relatively few input parameters in the high and medium risk categories (11 in each), in line with the long-tailed distribtuion of normalized sensitivity shown in Figure 108.

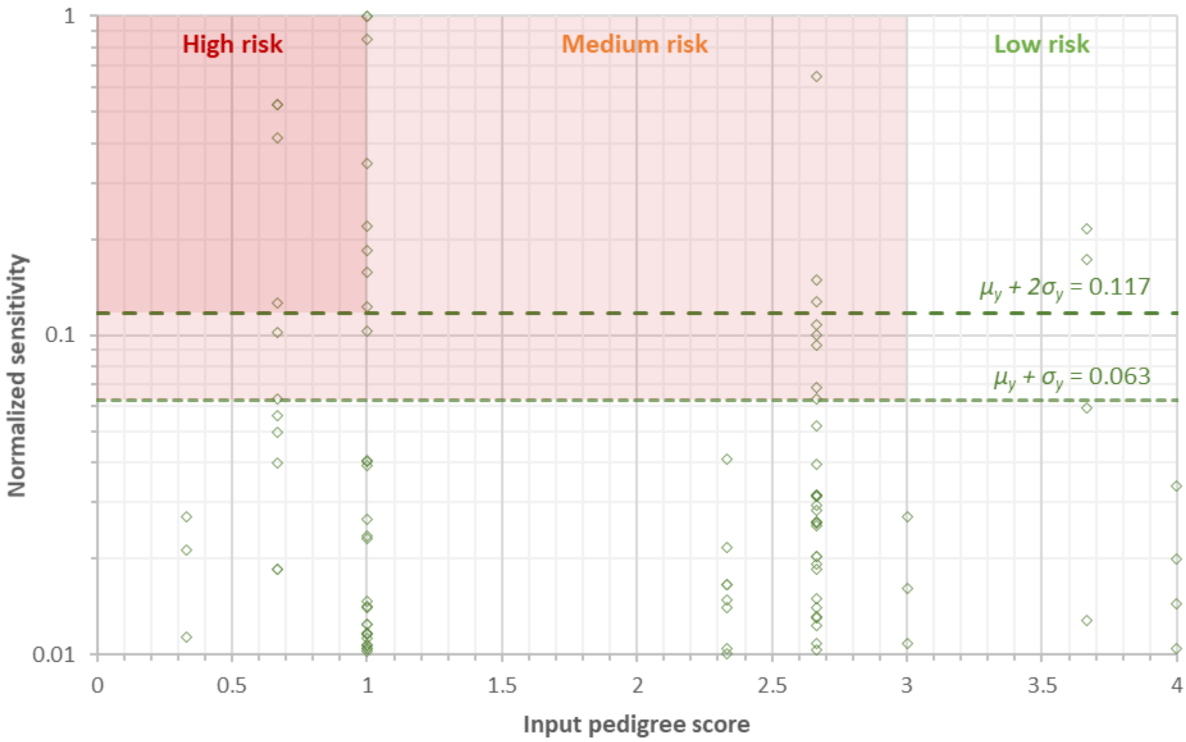

Figure 112: diagnostic diagram for cumulative GHG emissions (semi-logarithmic)

High-risk input parameters for cumulative GHG emissions are given in Table 10. Input parameters that appear in high or medium risk categories for both selected results are listed in bold text, with input parameters categorized as high risk for both selected results highlighted red. Input parameters relating to ES demand are again important, including high temperature process heat and static mechanical work (as in Table 9), but also ES final demand multipliers for low temperature heating and regional passenger transportation, and initial rates of change for all transportation ES. The ES final demand multiplier for low temperature heating merits particular attention due to the combination of high sensitivity and low pedigree.

Table 10: high risk input parameters found via diagnostic analysis for cumulative GHG emissions

Input parameter	Normalized sensitivity	Pedigree score
Initial ES demand rate of change – high temp. process heat	1.000	1.0
Initial ES demand rate of change – static mechanical work	0.845	1.0
ES final demand multiplier – low temp. heating	0.530	0.7
ES final demand multiplier – high temp. process heat	0.528	0.7
ES final demand multiplier – static mechanical work	0.417	0.7
Initial ES demand rate of change – transport freight IC	0.344	1.0
Initial ES demand rate of change – transport passenger regional	0.219	1.0

Input parameter	Normalized sensitivity	Pedigree score
Initial ES demand rate of change – IPaC	0.185	1.0
PC lifetime – coal generation	0.157	1.0
ES final demand multiplier – transport passenger regional	0.126	0.7
Initial ES demand rate of change – transport freight regional	0.123	1.0

Medium risk results for cumulative GHG emissions, given in section 10.6, exhibit two notable input parameters. The first is initial EROI for coal, with high normalized sensitivity (0.65, well above the upper sensitivity threshold) and moderate pedigree (2.7). The second is the ES final demand multiplier for IC freight transportation, with moderate normalized sensitivity (0.1, above the lower sensitivity threshold) and low pedigree (0.7).

7 Discussion

7.1 Proper interpretation of PRESS results

The solution space identified by the PRESS model is limited to the descriptive domain outlined in the pre-analytical framework presented in section 4.1. As such, the envelopes presented in chapter 6, represent the best outcomes (probabilistically defined) for GES transformation that can be expected from a biophysical, complex systems perspective, given the implied set of sociotechnical narratives represented in the relevant scenario (or base case). The use of least constraining defensible assumptions, initialization to the year 2015, and system control logic based on physically optimality contribute to a high degree of overall optimism. While real-world GES transformations cannot be predicted, outcomes more desirable than indicated by the solution space are revealed as highly improbable. However, emergent or exogenous changes capable of invalidating the basic model formulation will also invalidate the modelled solution space (as discussed in section 4.1.1).

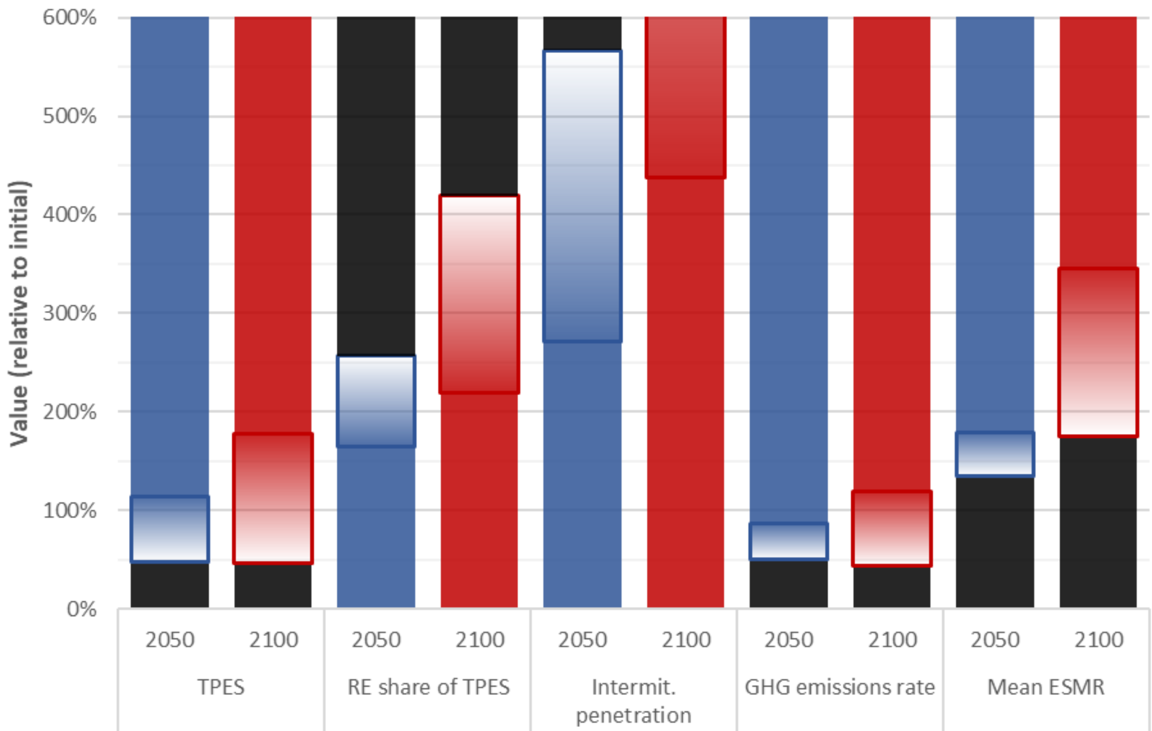

Figure 113: solution space visualization for the base case in 2050 and 2100

The solution space is highly multi-dimensional, encompassing all modelled output variables, but can be visualized for selected scenarios and dimensions (including time), as shown in

Figure 113. The bordered regions indicate modelled probabilistic envelopes presented in chapter 6, dark regions indicate physically implausible outcomes, and coloured bars show the possible range of less desirable outcomes (i.e., real-world outcomes are not limited in their degree of *undesirability*). For example, an energy transition scenario forecasting more than a 6-fold increase in global intermittent penetration in electricity supply by 2050, or more than a 50% decline in TPES by 2100, can be seen as implausible and should be treated with a high degree of scepticism.

As noted in chapter 5, the PRESS model features over 14,000 scalar and time series outputs. It is therefore not possible to comprehensively examine all observable changes, across all probabilistic levels. As such, results discussed in this chapter relate to a high-level summary of GES transformation outcomes, focussing on changes with the greatest relevance to achievable outcomes, system interactions, and various aspects of desirability. All results refer to the base case unless otherwise specified.

7.2 THE SOLUTION SPACE FOR GES TRANSFORMATION

Results in sections 6.1.4 and 6.1.5 show that substantial reorganizations of the GES are physically achievable. Notably, it is possible to greatly improve the provision of final ESs from the same or smaller TPES. TPES can drop by as much as half of its initial level, and in the most optimistic case can remain stable thereafter. However, the most drastic system-level improvements are generally seen before 2050 and improvements in both PC efficiencies and compositions are largely exhausted by this time. After 2035, mean TPES gradually returns towards its initial level driven by rising (mean) ES demands; although, this is subject to a broad range of possibilities (270-1000 EJ/year by 2100). This considerable range of outcomes is largely related to exogenous and probabilistic ES demands as the primary drivers of GES evolution (see ES demand envelopes in section 6.1.5), discussed further in section 7.3.

Modelled scenarios affect TPES materially. Scenarios 4 (Climate Constraints) and 5 (Delayed Consumer Response) show moderate increases in mean TPES over the simulated period while scenario 2 (Relocalization) shows moderate decreases. Notably, scenario 6 (Policy Recommendations) results in strong, consistent reductions in mean TPES of more than 50% relative to the base case by 2100. These results suggest ES demand reductions strongly affect the overall scale of the GES, as expected, while aggressive interventions and delays will largely result in scale increases.

7.2.1 The upstream sector

Figure 34 shows it is possible to rapidly reduce the production of fossil fuels, at least initially – results show mean production peaks for all fossil fuels coinciding with the beginning of the simulated period. These early declines are most notable for coal and oil, with gas production minimally affected. However, coal and gas production cannot be reduced to zero. In contrast, oil is heavily depleted by mid-century (depicted in Figure 44) with mean production remaining steady at around 20 EJ/yr – less than 15% of its 2015 production rate – and production rates of zero observed in some realizations after 2070. This persistence of fossil fuels occurs despite strong reductions applied to NRE utility values in the investment share calculation (as described in section 5.2.2). Also, rebounds are observed in both mean coal and gas production after 2050 contrary to widespread expectations. Fossil fuel persistence has strong implications for GHG emissions, outlined in section 7.2.7. The mean production of nuclear fuels approximately doubles towards mid-century before declining after 2075 due to depletion effects (as outlined in section 5.1, nuclear fuels modelled in PRESS refer to the fissile fuels used in current-generation reactors only).

Mean RE production grows significantly over the simulated period but is split more equally between the available RE resources than many conventional forecasts anticipate. In fact, primary RE production remains dominated by biomass and hydropower over the entire simulated period, although their mean contribution to total mean RE production falls from 90% in 2015 to approximately 50% by 2100. Wind and solar, the RE resources with the greatest technical potentials, play a moderate role only in most realizations, although both are subject to high degrees of uncertainty. As shown in Figure 46 and Figure 47, among all RE resources, by 2100 only biomass, solar, and wind have significant remaining room to grow in many realizations.

Consequently, the RE share of TPES will likely not exceed 45% by 2050, or 70% by 2100, and may be limited to as low as 37% by 2100 (as shown in Figure 49). These bounds are relatively insensitive across modelled scenarios, as depicted in Figure 93. Hence, while RE sources can assume a central role within the GES, a 100% RE basis does not appear possible during the

21st century. This is an important finding and raises serious doubts regarding many mainstream energy transition models and scenarios (such as those outlined in section 3.2.1). PRESS is not unique in this regard; the RE share of TPES projected by the MEDEAS model is slightly higher, but in the same approximate range [188]. IRENA [315] summarize energy transition scenarios in the literature, finding that a significant number project more than a 50% RE share of TPES by 2050 – PRESS results reveal these scenarios as highly implausible.

Strong electrification is foundational to achieving a successful energy transition, as discussed in section 2.2.2. PRESS results reflect this – Figure 38 and Figure 39 show significant shifts in the mean composition of EC supply and demand, respectively, from initial predominance of LaG fuels and heat towards electricity. Electricity shifts from the least to most important EC over the simulated period, with mean supply overtaking heat before 2030 and LaG fuels before 2050 (unadjusted for EC quality). However, this trend is subject to significant variability between realizations. Note that electrification is less apparent in the metabolic EC consumption of the GES itself, as shown in Figure 40, indicating a greater ongoing reliance on LaG fuels and heat relative to final consumption.

As shown in section 6.1.10.1, the mean penetration of fossil fuels in the production of all ECs declines over the simulated period – most significantly for electricity and LaG fuels. Notably, mean coal penetration in heat production remains steady and grows slightly after mid-century. The most significant shift is observed in LaG fuel production, with oil refining declining strongly (accounting for approximately half of production by 2050 and less than 15% by 2100) and the gap being filled by biofuels and the conversion of coal and gas to LaG fuels (i.e., via the Fischer-Tropsch process).

These trends largely account for the persistence of fossil fuels in primary supply, and rebounds in coal and gas production after 2050. It can be inferred that there is an enduring system requirement for these resources for the production of heat and LaG fuels as the GES reaches practical limits in the rate of electrification. This is particularly concerning given the high costs, significant environmental impacts, and low conversion efficiencies of Fisher-Tropsch conversion, as noted by Capellán-Pérez et al. [344]. Curtailment of this and other high emissions technologies is explored in Scenario 4, the implications of which are discussed in sections 7.2.5 and 7.2.7.

For biomass, the rise of biofuel production is initially offset by declines in biomass for heat production (largely traditional uses), causing mean biomass production to decline until around 2040, after which production grows strongly, surpassing 2015 levels. Critically, the global biomass technical potential is close to exhaustion by 2100 in some realizations. Such an outcome would risk of overexploitation of biomass beyond sustainable levels, potentially causing large-scale deforestation, biodiversity loss, impacts to hydrological cycles, and competition with agricultural land requirements [14, 23, 28, 33, 35, 36, 78, 151]. Notably, scenario 6 is strongly desirable regarding limiting the exhaustion of biomass resources, as depicted in Figure 84 and Figure 92.

7.2.2 The downstream sector

Penetration results in section 6.1.10.2 show strong and rapid changes in the composition of EU PC, most markedly for transportation. This is notable given that the transport sector is critical for all economic activity, as it underpins global supply chains, but remains highly dependent on affordable supplies of LaG fuels, as noted by Capellán-Pérez et al. [193] and Friedemann [205]. These rapid changes indicate that shifting away from the dominant modes of provisioning ESs, described below, represents one of the most immediate and effective ways to facilitate GES transformation.

Mean penetration results for regional passenger transportation show rapid shifts away from private vehicles and towards mass transit during the early years of the simulated period. Penetration growth is strongly concentrated in rail, with electric rail taking precedence after mid-century. Regional freight transportation sees a similar shift towards rail. This is consistent with the significantly greater efficiency and greater ease (and lower cost) of electrification of rail transportation relative to road-based modes noted by Grübler et al. [364] and Graus et al. [365]. However, the indicated scale of rail infrastructure buildout would entail considerable socio-economic consequences, as observed by Mediavilla et al. [366], “railways and changes in mobility patterns require more profound social transformations and costly infrastructures”. There is a clear need for further study in this area.

In contrast, penetration for electric vehicles (EVs) grows only slowly, reaching a mean penetration level of 15% by 2100 (although can rise as high as 40% in some realizations). These uncertain and likely modest prospects for EVs stands in stark contrast to expectations reflected in the vast majority of conventional energy transition studies described by Loftus et al. [223], but is in general agreement with MEDEAS model findings [193]. Shipping and aviation play relatively minor roles for both passenger and freight regional transportation after initial mean increases prior to 2050.

For IC transportation, initially rapid changes are seen in mean penetration (between shipping and aviation) for both passenger and freight transportation, after which means gradually return towards initial levels. However, envelope limits for IC passenger transportation penetration shift markedly towards shipping, indicating a significant number of realizations in which shipping becomes a major, or even dominant, mode for long-distance passenger travel. This may indicate potential for the return of mixed purpose (passenger and freight) long-distance shipping.

Outside of the transport sector, electrification is also observed in low temperature heating, high temperature process heat, and mechanical systems (as depicted in Figure 67 and Figure 69). However, these trends are much more modest, highly uncertain (particularly for low temperature heating, between electric and heat fuels), and are essentially exhausted by 2040, resulting in significant residual heat and LaG fuel demand.

Overall, scenarios have relatively muted effects on the downstream sector, except for scenario 5 prior to 2050 (as modelled) and scenario 4, which sees significantly higher electrification of all ESs and a steep reduction in IC passenger aviation (selecting shipping instead) relative to the base case. Scenario 6 also achieves substantially higher electrification of low temperature heating.

7.2.3 Efficiencies and PC utilization

Improvements in energy efficiency offer the simplest and cheapest path towards reducing GHG emissions and the overall scale of the GES, as described by GEA [49]. Endogenous efficiency improvements play a significant role in the PRESS model.

EU efficiency results presented in section 6.1.11.2 depict strong gains in EU to ES efficiencies, associated with the design of EU passive systems (described in sections 2.2.3 and 4.2.2.2). These gains are most significant for electric lighting, mechanical devices, light vehicles, freight rail, IC passenger aviation, low temperature heating, and high temperature process heating. As such, the GES transformation solution space as modelled is predicated on significant improvements in EU passive system design, with important implications for consumer expectations and behaviours. Most notably, regional transportation modes would quickly cease to resemble currently prevalent iterations, particularly for light vehicles – as noted by Paoli and Cullen [218], "passive system improvements or changes have a visible impact on the user. For example, to increase passive system efficiency in road transport, cars should be smaller and more streamlined".

Other efficiency gains shown in section 6.1.10.1 (EU conversion, and secondary conversion and reticulation), are comparatively minor. Note that in all cases, mean increases in efficiency (shown in Figure 70, Figure 71, and Figure 72) fall short of achievable maxima, although significant variability is seen over the ensemble. This stems from modelling choices representing both the design practicality of large efficiency gains and the power/efficiency trade-off, outlined in section 2.2.1 (modelling details in section 9.3.1.4.1).

Downstream sector CF results, given in section 6.1.9.2, show that the mean utilization of many EU PC types remains far below their respective EU CF targets over the simulated period, despite the increases in these targets assumed in PRESS (described in section 4.2.2.3). This CF suppression effect is likely driven by 1) the propagation of efficiency gains into aggregate stocks via investment in new PC (energetically favourable, despite diminished utilization), and 2) realization-level mode switching resulting from oscillations in the relative scarcity of ECs. It is unclear whether CF suppression is a real phenomenon manifesting at the system level or a modelling artefact, presenting another avenue for future research. Nevertheless, greater PC utilization, in part driven by increased use of social ES provisioning systems (such as *transit-as-a-service*, and a wider shift from private to public amenities) will continue to play an important role, as outlined by Grübler et al. [364] and Vogel et al. [128].

7.2.4 Electricity systems

The evolution of electricity systems is crucial given the marked trend towards electrification described in section 7.2.1. The main challenge to overcome is the integration of rising levels of intermittent, non-dispatchable supply, as described in section 4.2.5. As shown in section 6.1.13, global intermittent penetration in electricity systems unlikely to exceed 25% by 2050, or 50% by 2100, and may remain below 20% during the simulated period. This represents the possibility of strong growth in intermittent RE, but at much less optimistic rates than many mainstream energy transition scenarios suggest.

Depending on the intermittent penetration level and balance of mitigation options selected (i.e., PC overbuild mitigation vs. AI mitigation), intermittent RE types may see up to 25% reduction in CFs with commensurate reductions in baseload CFs – a substantial loss of potential power output. AI mitigation is favoured over PC overbuild mitigation on average, although subject to significant uncertainty spanning the entire possible range from 2035 onwards. Consequently, large stocks of intermittent electricity AI may be needed at higher intermittent penetration levels (up to 4,000 EJ/year by 2100), eclipsing TPES. An infrastructure buildout on this scale would represent a highly complex and socio-metabolically challenging global undertaking, deserving further research attention.

All modelled scenarios exhibit either unchanged or lower mean intermittent penetration levels relative to the base case by 2100 (depicted in section 10.4). This further supports measured expectations for the rapid deployment of intermittent RE, particularly solar and wind. Notably, scenarios 1 (Energy Breakthrough) and 6 result in significantly reduced mean requirements for intermittent electricity AI, up to 85% lower than the base by 2100, easing the associated socio-metabolic burden.

7.2.5 Socio-metabolic implications

Strong trends in declining primary energy resource quality are observed over the simulated period, as depicted in section 6.1.8. For NRE, all mean standard EROI ($EROI_{st}$) values exhibited by PC stocks fall below 20 by 2100, with oil, gas and nuclear fuels falling below 10. In some realizations, $EROI_{st}$ values for oil and nuclear fuels fall to very low levels, below 5, due to depletion effects. For RE, two groups are apparent:

- For solar PV, biomass, geothermal, and other RE, mean $EROI_{st}$ values converge to between 12 and 17 by 2100, and all fall below 10 in some realizations (most significantly for solar PV and other RE).
- For wind, hydropower, and solar thermal, mean $EROI_{st}$ values converge to between 38 and 62 by 2100, with values remaining above 10 in all realizations.

By 2100, only this second group of high-EROI RE resources exhibit the possibility for $EROI_{st}$ values above 40, across all primary energy resources. Despite significant uncertainty in $EROI_{st}$, particularly in initial values, narrowing distributions observed for all primary energy resources (except biomass) indicate convergence in these trends. Point-of-use EROI ($EROI_{pou}$) values for the production and delivery of electricity, LaG fuels, and heat show similar declines, as shown in Figure 54. Mean $EROI_{pou}$ values for all three fall below 10 by 2100 and can potentially drop below 3 (although subject to a wide range). As such, the declining quality of the primary energy gradients sustaining both the GES and HSES appears to represent a clear and unavoidable feature constraining future GES transformations.

This manifests in the rising relative socio-metabolic burden imposed by the hypercyclic component of the GES. As shown in Figure 40, mean GES metabolic EC consumption increases strongly from around 2060, at the latest, with an early shift from the capital hypercycle towards the autocatalytic loop. This is reflected in ESMR envelopes shown in Figure 78, extending noticeably into the region which may curtail reinvestment flows within the GES. However, significant uncertainties are present; by 2100, GES metabolic EC consumption may account for as little as 5% or as much as 45% of gross EC supply. Extended EROI ($EROI_{ext}$), corresponding to the inverse of ESMR, can fall as low as 2.3 by 2100 (with a mean of 5.7), indicating serious challenges to the socio-metabolic feasibility of GES transformation.

Notably, mean modelled initial ESMRs (6-7%) approximately align with the 2017 REN21 report [204], which notes that "The energy industry itself accounts for another 6% of TPES through its net demand for energy." Dupont et al. [177] estimates worldwide societal EROI in 2018 was between 9.4 and 8.5 – and although societal EROI does not correspond directly to $EROI_{ext}$ (the former being typically lower) – the implied ESMR range is 11-12%, coinciding with the initial upper limit of the envelope modelled in PRESS. These comparisons add strongly to confidence in the ESMR metric as an appropriate measure of the relative scale of the GES.

The observed EROI declines at all levels of the GES underscore the likelihood of serious impacts to economic prosperity and growth, and societal complexity, discussed in sections 2.1.1.4 and 3.1.3.4. Capellán-Pérez et al. [39] find approximately similar $EROI_{st}$ trajectories to the results discussed above, risking a decline into "dangerous territory" where the maintenance of complex, high-energy societies is no longer possible. As noted in section 2.1.1.4, estimates of minimum societal EROI in the literature range between 3 and 11, although values toward the lower end of this range would likely not account for the provision of essential social services. Hall and Klitgaard [184] note that historically, stable and prosperous societies have existed with EROI values as low as 4, but these were not industrialised. Brandt [51] estimates a minimum $EROI_{ext}$ for complex societies of around 2.25 (ESMR of 44%). Therefore, the range of $EROI_{ext}$ reductions implied by PRESS results – with corresponding societal EROI lower still – appears likely to seriously impact the basic socio-metabolic pattern of modern, high-energy societies.

Modelled scenarios significantly affect observed trends in $EROI_{st}$, $EROI_{pou}$, and ESMR, as depicted in sections 6.2.7 and 6.2.10. Overall, greater socio-metabolic impacts are implicated in scenarios 4 and 5, and reduced impacts in scenarios 1, 2, and 6, relative to the base case. These findings stress the negative consequences of both delays and aggressive interventions in the overall scale and burden of the GES (within the HSES), while highlighting the considerable benefits attainable through reductions in ES demands. Scenario 6 exhibits marked improvements in all metrics, with a mean reduction in ESMR approaching 10% relative to the base case – this emphasizes the value of utilizing identified leverage points in policy design. Scenario 4, while reducing $EROI_{st}$ declines in the NRE resources, sees the greatest ESMRs observed during the simulated period (with mean values over 20%) around 2075. This underscores the likely socio-metabolic infeasibility of major system interventions via 'forcing' policies consisting of inflexible constraints, formulated *a priori*, with insufficient understanding of system behaviour.

7.2.6 System stability

System stability, representing the ensemble incidence rate of net energy trap outcomes, is directly related to the ability of the GES to maintain approximate equivalence of supply and demand over the simulated period. Due to the significant and rapid changes observed in in both the upstream and downstream sectors (described in sections 7.2.1 and 7.2.2), early oscillations in the EC supply/demand balance are observed, as depicted in section 6.1.2. LaG fuels typically go into surplus during the early part of the simulation, prior to 2050, largely due to the general trend towards greater electrification of transportation described in section 7.2.2. However, after 2050, LaG fuels tend towards deficit more than heat or electricity, implying this EC is limiting factor for GES transformation. This result is supported by the MEDEAS model [188], which finds liquid fuel scarcity may become acute in the first half of the 21st century, driven by depletion dynamics.

Note that early simulation period model oscillations observed in EC supply/demand balance are also seen in GES metabolic EC consumption, ESMRs, $EROI_{pou}$, and CF maxima for intermittent PC. This behaviour is a modelling artefact resulting from representing supply/demand balance mathematically as an integral function (as described in section 4.2.9.1) and should not be interpreted literally. These model oscillations diminish quickly and are largely eliminated by 2040.

The base case probability distribution for stable time, depicted in Figure 32, shows reductions in system stability beginning around 2055 and accelerating after 2080. The indicated risk of a net energy trap before 2100 is 5%. However, estimates of system stability in PRESS reflect highly optimistic, best-case outcomes. The incidence of net energy trap outcomes depends strongly on the exogeneous interface between the GES and the HSES, which is represented in a simplified, high-level, and relatively non-constraining form, as described in section 4.2.4.5. As such, the real-world risk of net energy trap outcomes is likely substantially higher and may become a significant threat much earlier than indicated here.

Scenario results for system stability, given in section 6.2.2, show moderately positive effects in scenarios 1 and 2, and neutral to moderately negative impacts in scenarios 3 (RE Rapid Deployment) and 5. Notably, scenario 6 exhibits no net energy trap outcomes over all 1,000 modelled realizations. Scenario 4 shows strongly negative impacts on system stability, with the risk of a net energy trap rising more rapidly and to a much higher level – almost 30% by 2100. These results reinforce the strategic value of leverage points and the risks of major, ill-conceived system interventions. Interestingly, technological breakthroughs in new supply, such as next generation nuclear or OTEC, appear to have an underwhelming potential to avoid a net energy trap (as demonstrated by scenario 1). Note that early simulation period model oscillations, described above, are observed in TPES in scenarios 4 and 5.

7.2.7 GHG emissions

Results for GHG emissions, presented in section 6.1.12, show that the global emissions rate can drop significantly and rapidly, between 17% and 52% from 2015 levels by 2040, but cannot fall to zero due to the persistence of fossil fuels in the upstream sector described in section 7.2.1. By 2100, the emissions rate may exceed its initial level. Consequently, cumulative GHG emissions rise inexorably, surpassing the emissions budget corresponding to a 66% chance of remaining below 1.5°C by 2071, and the 2°C budget by 2077, at the latest. The very high degree of uncertainty evident here relates to the net effect of uncertainties in the GHG emissions rate and the probabilistic ranges corresponding to emissions budget estimates. The 2°C budget is potentially exceeded as early as 2038 in some realizations.

Modelled GHG emissions assume the global non-energy emissions rate is approximately static over the simulated period (as noted in section 4.2.9.3). Modelling non-energy emissions is not within scope and affects informational output metrics only, so can easily be adjusted analytically. Assuming instead that non-energy emissions decline linearly to zero by 2100 reduces total cumulative emissions by approximately 380 $GtCO_2e$. Similarly, assuming a decline to zero by 2050 reduces total cumulative emissions by 610 $GtCO_2e$. Applying the latter, more optimistic assumption, to modelled cumulative GHG emissions by 2100 indicates a very small (< 1%) probability of emissions below the 2°C budget. As such, is extremely unlikely that targets established under the Paris Agreement will be achieved without the large-scale deployment of CCS or other negative emissions technology.

The MEDEAS model [188] finds that the 1.5 and 2°C thresholds will likely passed before mid-century. Similarly, Stammer et al. [324] conclude that social constraints to energy transition imply that both deep decarbonization by 2050, and limiting warming below 1.7°C, are implausible. These findings are are broadly in line with PRESS results.

Newell et al. [62] and Keyßer and Lenzen [346] note that a significant number of global energy transition and decarbonization scenarios forecast global GHG emissions below 10 $GtCO_2e$/year by 2050. Many of these scenarios also project cumulative emissions between 2018 and 2100 of less than 600 $GtCO_2e$ [346]. In contrast, PRESS results suggest emissions rates below 22 $GtCO_2e$/year by 2050, and cumulative emissions below 1700 $GtCO_2e$ by 2100, are physically implausible. However, these scenarios typically rely heavily on large-sale CCS, so are not directly comparable to PRESS. Jenkins and Thernstrom [81] note that "Power sector CO2 emissions must fall nearly to zero by 2050 to achieve climate policy goals." PRESS results suggest this is not realistic, as depicted in Figure 62.

Cumulative GHG emissions scenario results, given in section 6.2.9, show all scenarios potentially exceeding both the 1.5°C and 2°C limits by 2050, and exceeding these limits by 2100. However, there are marked difference between scenarios, particularly apparent at higher percentiles. Scenarios 2 and 4 are both beneficial, exhibiting reductions in cumulative GHG emissions of similar magnitude relative to the base case. However, scenarios 2 achieves these reductions with far fewer adverse consequences for system stability and socio-metabolic burden (as discussed in sections 7.2.5 and 7.2.6, respectively). Scenario 6 see the best outcomes for cumulative emissions by a wide margin; reductions relative to the base case are approximately twice as large as those observed in scenarios 2 and 4.

Scenario 5 is the only scenario to substantially increase cumulative emissions relative to the base case, underscoring the negative consequences of delays or slow progress in necessary downstream, behavioural adaptations. The underwhelming system-level benefits of technological breakthroughs (scenario 1), noted in section 7.2.6, is also apparent in the reduction of cumulative GHG emissions. Scenario 3 has no significant impact on emissions, suggesting that policy approaches based simply on the promotion of RE (i.e., via subsidies or carbon pricing) will not be effective in achieving decarbonization at the system level.

Sgouridis and Csala [9] note a "safe emissions budget" of 1120 $GtCO_2e$ for the period of 2015 to 2100, corresponding approximately to the 1.5°C budget range mid-point. Of all modelled scenarios, only scenario 6 comes close – under very optimistic assumptions for non-energy emissions (a complete phase out by 2050) scenario 6 has an appreciable, albeit small, chance of remaining below this limit. Overall, scenario results suggest that it is highly unlikely eventual warming will remain below 2°C without relying on speculative and unproven large-scale CCS, regardless of selected policy interventions.

7.3 Sensitivity and leverage points

Sensitivity analysis reveals the potential impacts of estimation errors for each probabilistic input parameter on a selected model output, as described in section 3.3.2. These are the factors which most strongly influence desirable GES transformation outcomes. For non-decision parameters, not amenable to human control or modification, sensitive parameters also represent major systemic risk factors which are likely to strongly influence and constrain achievable outcomes. For decision parameters, sensitivity analysis can be used to identify system leverage points and formulate appropriate policy recommendations cognizant of system behaviour

Sensitivity analysis results for non-decision parameters, given in section 6.3.2, identify the critical importance of primary energy availability and quality. The highest positive sensitivity values for stable time (indicating system stability) are observed for biomass, solar thermal, and geothermal technical potentials, oil and gas terminal EROI, and coal initial RURR. These resources are all crucial for heat or LaG fuel production during the late simulation period. This further emphasizes the limits to electrification and the persistent need for non-electricity ECs within the metabolic pattern of the GES, described in sections 7.2.1 and 7.2.2. The technical potential of biomass available for energy production is the most important non-decision parameter affecting system stability, by a wide margin. Biomass is the only RE capable of conversion to both heat and LaG fuels. However, the true sustainable potential of biomass energy is both highly uncertain and contentious, as described in section 2.1. Large expansions of biomass harvesting for energy purposes entail significant environmental impacts, as discussed in section 7.2.1, and will likely represent a major future pressure point between the HSES and the wider biosphere. This centrality of primary energy gradients is understandable given their fundamental role as the ultimate source of all exosomatic energy flows, enabling the ongoing autopoiesis of both the GES and HSES, as discussed in section 3.1.

Primary energy resource parameters also exhibit high sensitivity for GHG emissions, particularly initial coal RURR and EROI. Greater availability and quality of coal results in significantly higher cumulative GHG emissions over the simulated period, and *vice versa*. These finding reveal a tension between the strong, contrary effects of coal on desirable outcomes in stable time and emissions. For example, a rebound in coal consumption may be required to avert a net energy trap – largely for LaG fuel production via the Fisher-Tropsch process (in light of likely LaG fuel scarcity noted in section 7.2.6) – but this will come with serious climate risks. GHG emissions are also substantially affected by nuclear fuel and geothermal resources, with higher resource magnitudes resulting in reduced emissions, and *vice versa*.

Several surprising and unintuitive sensitivity results are seen for non-decision parameters. Significant negative impacts on system stability are seen for higher initial EU to ES efficiencies for IC freight shipping, regional freight aviation, passenger electric rail, and electric mechanical systems. Moderate negative impacts on cumulative GHG emissions are seen for higher initial EU to ES efficiencies for IC freight shipping, high temperature heating using heat fuels, and electric mechanical systems. These results indicate that higher efficencies, particularly in EU passive systems, cannot be assumed to be universally beneficial or yield intuitive results at the system level. Reasons for these relationships are unclear as input parameter values will affect GES transformation via complex and path-dependent causal interactions. Further research is necessary to uncover specific dynamic processes involved.

Sensitivity analysis results for decision parameters, identifying system leverage points, are given in section 6.3.2. These results possess considerable practical value and deserve greater emphasis in strategies for facilitating energy transition and climate change mitigation.

The two most significant leverage points for the promotion of desirable GES transformation outcomes, by far, are the ES demands for high temperature process heat and static mechanical work. Reducing these demands greatly improves both system stability and GHG emissions over the simulated period. However, such reductions are limited in practice as they imply curtailment of the industrial sector (see Table 5), affecting economic output and the expression of required functions within the HSES. The strong association between these ES demands and the incidence of net energy trap outcomes indicates that demand levels at the upper end of the modelled ranges (maximum 5-fold increase between 2015 and 2100, for both) are likely unfeasible. Notably, high temperature process heat faces strong limits to electrification (as shown in Figure 69), contributing to the persistence of heat demand in the GES. ES demand reductions for regional passenger and IC freight transportation, and IPaC also have significant positive effects on both outcomes, but to a lesser degree.

Technology improvements for the reduction of lifecycle energy costs of capital (ECC) appear to be beneficial for system stability, specifically for biofuel production, coal CHP, intermittent electricity AI, geothermal electricity generation, the conversion of coal to LaG fuels, and coal electricity generation. This highlights the need for a lifecycle perspective in technological design, rather than purely cost or process efficiency.

Reducing ES demand for low temperature heating and regional freight transportation improves GHG emissions, with negligible effects on system stability. The accelerated retirement of PC (by reducing operational lifetime) can also yield positive effects; system stability is improved by the accelerated retirement of IC freight aviation PC, while GHG emissions are improved by the accelerated retirement of PC for electricity generation from coal. The reduction of ECC for the conversion of coal to LaG fuels and coal electricity generation, while beneficial for system stability as noted above, is moderately detrimental for GHG emissions. This indicates a trade-off between improving the lifecycle efficiency of coal conversion and discouraging the use of coal (reminiscent of the rebound effect).

Interestingly, improvements in demand flexibility and reductions in ES demand for IC passenger transportation, often the focus of decarbonization narratives, do not appear to have significant system-level impacts on either outcome.

7.4 EPISTEMIC RISKS

Diagnostic analysis results, given in section 6.4, identify absolute risks of estimation errors for each probabilistic input parameter on a selected model output, considering both impact and likelihood of estimation errors. As such, diagnostic result highlight epistemic risks, where the characterization of GES transformation is most constrained by insufficient strength of knowledge.

The greatest source of epistemic risk stem from input parameters appearing in high risk categories identified via diagnostic analysis for both stable time and cumulative GHG emissions (presented in Table 9 and Table 10). These include ES demand final levels and initial rates of change for high temperature process heat and static mechanical work. Input parameters appearing in high or medium risk categories for both selected results also present significant epistemic risk, including ES demand initial rates of change for regional passenger and IC freight transportation. These results suggest that improving the strength of knowledge regarding plausible future trajectories for exogenous ES demands, particularly in the industrial and transport sectors, would be highly beneficial for reducing epistemic risks. Other notable input parameters subject to high epistemic risk due to either very high normalized sensitivity (> 0.25) or very low pedigree (< 0.5) include terminal EROI for oil and ECC for intermittent electricity AI (affecting stable time), and the ES demand final level for low temperature heating (affecting GHG emissions).

All of the above parameters represent the best areas to focus additional data gathering and processing efforts to boost the associated strength of knowledge. This would substantially improve confidence in the solution space modelled in PRESS, expanding the descriptive domain while refining the represented set of socio-technical narratives.

8 SUMMARY AND CONCLUSIONS

> *"But the myth of the reductionist-scientific character of our studies of the future, and indeed of all complex systems, cannot hold. Only by being aware of our metaphors, and our ignorance, can we fashion the scientific tools we need for guiding our steps into the future, now appreciated as unknown and unknowable, but where our greatest challenge lies."*
>
> – Jerry Ravetz [281]

The GES is not simply a collection of technologies and resources within an unchanging environment, but rather, is fundamentally an example of a CAS. Its historical development and set of possible futures are shaped by its function within society, its essential biophysical dependencies, and the dynamic interactions and feedbacks which comprise its internal structures. As such, the complex, path-dependent process involved in its transformation from one energetic foundation to another cannot be properly understood or represented using conventional analytical methods based in reductionism.

The study of possible futures for the third energy transition, from fossil fuel dependence towards a re-established solar civilization, must depart from an appropriate conceptual vantage point. No definitive quantitative description is possible for complex systems, compelling a research orientation beginning from a position of epistemic humility. However, exploring dynamic pathways for GES transformation by considering the basic metabolic pattern arising from the autocatalytic production of exosomatic energy is a largely overlooked research avenue which can yield vital insights. This is carried out by developing a new methodology starting with an explicit pre-analytical framework, followed by the creation of the PRESS model designed to identify a solution space of energetically feasible and viable pathways for transformation of the GES from NRE dependence towards a RE basis, with explicit treatment of irreducible uncertainty.

8.1 KEY FINDINGS

The primary research objective and all secondary objectives stated in section 1.4 are successfully achieved through the identification of the GES transformation solution space and subsequent quantitative analysis, the results of which are summarized in this section.

Note that in accordance with the pre-analytical framework introduced in section 4.1, the research findings presented here assume ongoing efficiency improvements in existing technologies but do not include fundamentally new functional roles which have not yet been demonstrated at scale, have no epistemic basis for inclusion, and for which no meaningful parameter estimates can be given. The advent of such technologies will, of course, invalidate the findings of this research project but not its underlying methodological approach which can be updated with new modelled elements and input data, as required.

8.1.1 The centrality of primary energy and demand

The transformation of the GES is bound on two sides, by finite primary energy resources of variable and declining qualities and the requirements for the provision of vital energy services to society. Modelled results identify the critical importance of both to the evolution of new metabolic patterns and corresponding GES transformation pathways. Most notably, coal and biomass resources, and demands for high temperature process heat and static mechanical work are shown to be highly significant factors influencing transformation outcomes (see sections 6.3 and 7.3).

Technological change is intrinsic to this process but cannot obviate fundamental primary energy constraints or allow arbitrary increases in demand. Even speculative technological breakthroughs in new supply have a relatively muted impact, in contrast to widely held expectations. As primary energy resources are not within human control, the primary leverage points for promoting desirable transformation outcomes lie in demand reductions. This finding is reflected in a growing literature emphasizing the critical role of energy service demands in shaping possibilities for energy transition [14, 54, 232]. At a minimum, results suggest that aggregate global increases demand for high temperature process heat and static mechanical work approaching or exceeding 500% between 2015 and 2100 are physically implausible (see section 7.3), constraining the future growth of the industrial sector.

Future trajectories for energy service demand in the industrial and transport sectors also represent the primary area where insufficient strength of knowledge constrains the characterization of the solution space, as revealed by diagnostic analysis results (see section 7.4). As such, an improved understanding of the plausible ranges for these trajectories, and related socio-metabolic implications, is now vital.

8.1.2 The heat and liquid fuels problem

While there are no appreciable limits in total available primary energy gradients given the magnitude of direct solar irradiance reaching the surface of the Earth, constraints emerge instead from the specific profiles of non-fungible energy forms required within the metabolic pattern of the GES. For example, there is no immediate primary resource constraint to the production of electricity from intermittent RE sources such as solar and wind, but this form of energy cannot rise to arbitrary contributions to TPES due to the metabolic costs of system integration and residual demand for heat and liquid fuels (which cannot be driven to zero via electrification; see section 7.2.2). Consequently, the modelled solution space indicates a pronounced persistence of fossil fuels in primary supply, particularly for coal and natural gas (see Figure 34). Liquid fuel scarcity is a growing threat, especially after 2050, incentivizing the conversion of coal and natural gas to liquid fuels (see section 7.2.1), with highly adverse impacts for GHG emissions (see section 7.2.7).

8.1.3 Limits to achievable pace of change

The achievable pace of change is a primary consideration for energy transition as it has a direct bearing on the mitigation of climate change and other major societal challenges related to energy. Modelled results show that initially rapid changes are physically possible, driven primarily by downstream changes in the prevailing end-use modes for providing transportation energy services (including a marked shift from private vehicles towards efficient mass transit; see section 7.2.2). Substantial changes in the upstream production of energy carriers follow, but at a slower pace due to the extensive, long-lived infrastructures involved (see section 7.2.1). However, after this initial period of change, subsequent trends at the system level are gradual or may reverse direction due to negative (balancing) feedbacks. For example, the rising RE share of TPES slows considerably after mid-century, gradually approaching a mean value of 50% by 2100 (see Figure 49), while TPES itself falls initially before resuming a gradual growth trend after 2035 (see Figure 33). This behaviour may call into question the more extreme scenarios projecting continued rapid energy transitions toward expected targets (discussed in section 3.2.1).

8.1.4 The prospects for demand-led versus supply-led transitions

While most socio-technical narratives currently focus on supply-led energy transitions, demand-led transformations are likely more impactful, as noted by Grübler et al. [364]. This is reflected in PRESS model results indicating the limited benefits and potentially severe consequences of supply-side ‘forcing’ via the application of inflexible, top-down constraints on selected high emissions intensity technologies (exemplified by the Climate Constraints scenario). These unintended and unintuitive consequences arise from system feedbacks not captured by conventional analyses and tend to strongly aggravate both the risk of net energy trap outcomes and the relative socio-metabolic burdens imposed by the GES (see sections 7.2.5 and 7.2.6). Intended results can be partially achieved, but much less effectively overall than demand-side approaches (particularly compared to demand-side interventions based on identified leverage points; see section 7.3). Additionally, results suggest that supply-side technological breakthroughs or rapid deployment initiatives for RE typically fail to realize expected benefits due to pervasive system feedbacks (see section 7.2.7).

8.1.5 Societal complexity and growth

The modelled solution space indicates that the declining EROI of primary energy resources results in significant increases in the share of gross energy supply redirected back into the autocatalytic process of energy production, particularly after 2060 (see Figure 78). As discussed in section 3.1.3, this rising redirection of energy and other resources away from the dissipative component of society has strong implications for economic growth and sustainable levels of societal complexity. In this context, the prevailing socio-metabolic pattern of high-energy industrialized societies may be undermined. As noted by Glucina and Mayumi [73], “the real problem is a conflict between the physical impossibility of continual growth and the perceived political impossibility of limiting growth.”

These trends remain even in the presence of technological breakthroughs delivering abundant, high-EROI resources for electricity production (see section 7.2.5). The socio-metabolic feasibility of significant energy service demand reductions corresponding to identified leverage points, such as curtailing the industrial sector, are also called into question as these services are required for the expression of vital functions within society (see section 7.3).

8.1.6 Converging risks

Results suggest that GHG emissions reductions on the scale required to keep global mean temperature increases below 2°C are not physically plausible without the large-scale deployment of CCS or other negative emissions technologies (which remains fundamentally speculative). This conclusion is robust; it holds for all modelled scenarios and over all probabilistic levels (see Figure 105). The modelled option which comes closest to this goal is to implement system-cognizant interventions designed around identified leverage points (i.e., the Policy Recommendations scenario detailed in Table 6). The basic implausibility of achieving widely accepted climate goals identifies a major societal risk and a clear deficit in current energy transition planning.

The modelled risk of encountering a net energy trap during the 21st century is low but non-trivial at approximately 5% (see Figure 32). However, this is a very conservative estimate given the degree of optimism reflected in the solution space, implying that the real-world risk is likely substantially higher (and potentially arriving sooner). This risk is sensitive to socio-technical narratives and is strongly increased by delays in consumer behaviour change or even more so by major 'forcing' interventions intended to restrict GHG emissions (see Figure 85). These observations are in agreement with Capellán-Pérez et al. [50], who note "a significant systemic-energy scarcity risk exists: future global energy demand-driven transitions as performed in the past might be unfeasible." In contrast, the utilization of leverage points in policy design can largely eliminate the risk of a net energy trap.

Another major risk relates to the indicated expansions of both coal and biomass after 2050 (see Figure 35), potentially exacerbating both global and local environmental impacts related to their production and use. This risk is not widely perceived at present, as coal and biomass energy are not projected to grow strongly in most mainstream energy transition scenarios.

8.1.7 Synergies and trade-offs

The most significant interventions that have the potential to synergistically reduce both the risk of a net energy trap and GHG emissions are reductions in energy service demand for high temperature process heat and static mechanical work, as noted in section 8.1.1, and regional passenger transportation and IC freight transportation. The value of these synergies is exemplified by the strong improvements observed in the Policy Recommendations scenario relative to the base case, across all metrics.

As noted in section 7.2, there are opportunities in the expansion of transportation infrastructures which can provide combined passenger and freight transportation at scale, including rail and long-distance shipping. Notably, this trend would represent a largely unexpected return to transportation modes more common in the 20th century and earlier.

Notable trade-offs are also apparent in the modelled results. Firstly, there is a clear trade-off between delays in substantial demand-side adaptation and achievable outcomes for both net energy trap risk and GHG emissions (i.e., exhibited by the Delayed Consumer Response scenario; see Figure 86 and Figure 104). The time element is critical – GEA [49] stresses that an effective energy transition requires immediate action. Secondly, there is a trade-off between coal consumption required for averting a net energy trap and the serious associated climate risks (see Figure 109). This will likely bring coal back into focus as a high-profile and contentious policy issue in the coming decades, with various socio-technical perspectives either supporting or resisting its expansion.

8.2 REALIZING THE SOLUTION SPACE

The pervasive optimism reflected in the PRESS model formulation cannot be expected to reflect the real-world. However, to the extent this optimism can be translated into reality, vastly improved energy transition outcomes will be within reach.

The following are achievable improvements either implicitly included in, or indicated by, the identified solution space offering effective avenues to facilitate GES transformation and promote desirable outcomes:

- Shifting away from embedded, inefficient end-use modes for the provision of energy services is required, such as moving from private vehicles for short-distance transportation to a greater reliance on electric rail. At present, this necessary mode-switching is difficult to achieve due to upfront infrastructure costs and a high degree of change reticence among governments, institutions, and individuals.
- End-use modes must also undergo major redesigns in passive systems for the express purpose of much higher efficiencies in the final conversion of useful power to delivered energy services. This has strong implications for consumer expectations and behaviours, particularly for regional passenger transportation where new vehicles would necessarily be much smaller and lighter. New social norms, laws and regulations, markets, and supporting industries would be required.

- The implementation of these and other efficiency gains must actively control for rebound effects, preventing the redirection of efficiency improvements into scale and power increases, to deliver beneficial reductions in energy consumption.
- A general shift away from individualist models of energy service provision towards more efficient and integrated social provisioning is needed.
- Technological innovations in power capacity must focus on reducing full lifecycle energy costs rather than simply improving process-level efficiencies. This requires significantly wider use of detailed lifecycle assessment methods and a greater awareness of the importance of embodied energy.
- Decision making in all domains related to the energy transition must embrace an expanded scope through multi-criteria analysis, including a primary focus on biophysical criteria. Relatively less emphasis should be placed on narrow, economic measures such as cost-benefit analysis (as discussed in section 3.2.1.1).

8.3 Reframing GES transformation

A comprehensive transformation of the GES towards an RE basis will necessarily test the limits of modern societies to supply the required investments, adapt energy consumption behaviours, re-engineer production processes and infrastructures, and successfully integrate rising levels of intermittent RE supply. This must occur within the context of complex co-evolutionary processes, non-linear feedback, irreversibility, and emergent phenomena within the GES and HSES. For this reason, the GES cannot be designed *a priori.* Common narratives informed by experience to date have little guidance to offer for the future.

Unfortunately, prevailing narratives remain confined by technological optimism and, as such, will consistently underestimate both the difficulty of GES transformation and its broader implications for both society and the biosphere. As observed by Heuberger and Mac Dowell [367] and Loftus et al. [223], energy futures are often communicated to and understood by the general public without sufficient nuance or critical attention. This reflects the need for a deeper shift in scientific paradigm, from a mechanistic worldview to a complex systems perspective, both in the participatory generation of scientific knowledge and in popular understandings of this knowledge. Critically, complex problems cannot be compressed or diminished into simple narratives without losing important information, effectively ruling out definitive problem framings.

Societal problems over the modern era have typically been solved by the application of more technology and consequently more energy consumption, as described by Hall et al. [53] and Tainter [19]. This strategy is no longer feasible, presenting modern society with a serious dilemma. Solutions will instead have to come primarily from behavioural adaptation. Energy and society can no longer be understood as separate, with energy simply a product like any other – energy underpins the very existence of the complex systems of which we are a part. As our energy basis changes so too will the structure of society. Modern, high-energy societies, at least in their current forms, may soon be relegated to history – a grand energetic experiment never to be repeated.

Successful transformation of the GES is foundational to an acceptable future. We cannot remain on the same path, nor can we expect technology to solve the problem for us. Successfully navigating the challenges ahead will requiring a greater degree of technological realism and approaches to scientific problems rooted in epistemic humility and pluralism, such as Post-Normal Science. The solution space identified here can, among a plurality of system-cognizant approaches, provide essential tools for revealing the landscape ahead.

The third energy transition will be a multi-generational project. While it does not appear to be possible to 'solve' the twin threats of climate change and fossil fuel depletion, it is possible to buy significant time to allow deeper social and cultural transformations to unfold. These transformations will need to be guided by clear normative principles, including the preferential use of vital energy services for the protection of wellbeing rather than the growth of affluence. Ultimately, real, substantive solutions will need come from a profound shift in worldview and the discovery of complexity at the heart of the converging crises we face.

8.4 What can be done with this information?

As noted in section 1.2, the popularization of knowledge regarding what energy transition fundamentally is and what can be expected for the future is sorely needed. This research project is therefore of significant value to both researchers and policy makers seeking to understand *what can be achieved* in energy transitions, *how fast* these transitions can unfold, and *what they might mean* for society and the biosphere at large.

This research, consisting of the basic methodological approach, the PRESS model itself, and the modelled solution space for GES transformation, can serve five crucial purposes:

1) Enhancing realism and improving energy literacy in energy transition discourses by providing a biophysical, complex systems perspective which is currently underrepresented.
2) Contributing to best practices for complex energy systems modelling, including encouraging greater transparency and acknowledgment of epistemic uncertainty.
3) Adding to a necessary plurality of models offering contrasting perspectives on energy transition.
4) Utilizing the modelled solution space for the identification of physically implausible socio-technical narratives in energy transition studies and plans.
5) Applying the identified system leverage points to improve the overall efficacy and system-cognizance of policy design.

In simple terms, the research presented here can substantially improve the state of knowledge regarding possible energy transitions by:

- demonstrating the value of the biophysical, complex systems perspective,
- enabling the 'stress testing' of conventional scenarios and plans which do not embrace this perspective, and
- alerting policy makers to the presence of both beneficial and detrimental impacts associated with interventions in the GES.

As noted by Ruth [249], "For decisions to be viable, they must be acceptable under a wide range of assumptions about present and future system behaviour." Due to its probabilistic nature, this research adds significantly to the ability of researchers and policy makers to check their quantitative projections against an expanded set of behavioural assumptions for the GES.

8.5 AVENUES FOR FUTURE RESEARCH

Various areas have been identified during this project which would benefit from additional research. These include addressing the model limitations listed in section 5.4, to the extent possible, in addition to the following:

- More rigorous data gathering and processing efforts to improve the strength of knowledge – particularly for high-risk input parameters identified via diagnostic analysis (summarized in section 7.4) and stylized parameters such as ECC values.
- More realistic control systems, including exhaustive optimization in place of the heuristic method used for system control (i.e., allowing for replacement of control parameters with direct use of investment flows by time interval as decision variables; as an alternative approach).
- Endogenization of control variables where possible.
- Nesting regional and/or national PRESS-like (or other) models to better represent spatial and geographical dynamics and associated constraints.
- Investigation of the socio-economic implications and feasibility of rapid shifts in PC compositions, particularly where new, large-scale infrastructures are required – such as global expansions of rail or intermittent electricity AI.
- Aligning the probabilistic generation of logistic curves representing exogenous model interfaces with statistical analyses of available empirical data.
- Further disaggregation and dynamic representation of additional inputs, including ECC, CapEx fraction, decommissioning fraction, etc.
- Explicit modelling of the effect of cumulative output on RE EROI (i.e., including technological learning effects as many RE PC types are still relatively immature).
- Investigation of unexpected negative impacts on system stability and cumulative GHG emissions observed for higher initial passive system efficiencies, primarily in transportation and mechanical systems.
- Further disaggregation of spatial scales in transporation by introducing a local/regional transportation distinction and realistic logic for the allocation of available PC between these scales.

REFERENCES

1. Smil, V., *Energy at the crossroads: global perspectives and uncertainties*. 2003, Cambridge, MA: MIT Press.
2. Adams, R.N., *Paradoxical Harvest: Energy and Explanation in British History, 1870–1914*. 1982, Cambridge, UK: Cambridge University Press.
3. Prigogine, I. and I. Stengers, *Order out of chaos: man's new dialogue with nature*. 1984, Toronto, Canada: Bantam Books.
4. Taylor, T.G. and J.A. Tainter, *The Nexus of Population, Energy, Innovation, and Complexity.* American Journal of Economics and Sociology, 2016. **75**(4): p. 1005-1043.
5. White, L.A., *Energy and the evolution of culture.* American Anthropologist, 1943. **45**(3): p. 335-356.
6. Smil, V., *Energy in world history*. 1994, Boulder, CO: Westview Press.
7. Harris, M., *Cultural anthropology*. 1991, New York, NY: HarperCollins.
8. Tainter, J.A., et al., *Resource transitions and energy gain: contexts of organization.* Conservation Ecology, 2003. **7**(3): p. 4.
9. Sgouridis, S. and D. Csala, *A Framework for Defining Sustainable Energy Transitions: Principles, Dynamics, and Implications.* Sustainability, 2014. **6**(5): p. 2601.
10. Brown, J.H., et al., *Energetic Limits to Economic Growth.* BioScience, 2011. **61**(1): p. 19-26.
11. Brand-Correa, L.I. and J.K. Steinberger, *A Framework for Decoupling Human Need Satisfaction From Energy Use.* Ecological Economics, 2017. **141**(Supplement C): p. 43-52.
12. Cottrell, F., *Energy & society: the relation between energy, social change, and economic development*. 1970: McGraw-Hill Book Company.
13. Hall, C.A., C.J. Cleveland, and R.K. Kaufmann, *Energy and resource quality: the ecology of the economic process*. 1986, New York, NY: Wiley.
14. Smil, V., *Energy transitions: history, requirements, prospects*. 2010, Santa Barbara, CA: Praeger.
15. Palmer, G. and J. Floyd, *History as a Guide to Understanding the Future of Storage*, in *Energy storage and civilization a systems approach*. 2020, Springer: Cham. p. 1-28.
16. Court, V., *Energy Capture, Technological Change, and Economic Growth: An Evolutionary Perspective.* BioPhysical Economics and Resource Quality, 2018. **3**(3): p. 12.
17. Krausmann, F., et al., *The Global Sociometabolic Transition.* Journal of Industrial Ecology, 2008. **12**(5-6): p. 637-656.
18. Haberl, H., et al., *A socio-metabolic transition towards sustainability? Challenges for another Great Transformation.* Sustainable Development, 2011. **19**(1): p. 1-14.
19. Tainter, J.A., *Energy, complexity, and sustainability: A historical perspective.* Environmental Innovation and Societal Transitions, 2011. **1**(1): p. 89-95.
20. Foxon, T.J., *Energy and Economic Growth: Why we need a new pathway to prosperity*. 2017: Routledge.
21. Giampietro, M., K. Mayumi, and A.H. Sorman, *Energy analysis for a sustainable future: multi-scale integrated analysis of societal and ecosystem metabolism*. 2013, London, UK: Routledge.
22. Smil, V., *Fossil-Fueled Civilization*, in *Energy and civilization: a history*, V. Smil, Editor. 2017, The MIT Press: Cambridge, MA. p. 295-384.
23. Motesharrei, S., et al., *Modeling sustainability: population, inequality, consumption, and bidirectional coupling of the Earth and Human Systems.* National Science Review, 2016. **3**(4): p. 470-494.
24. Hubbert, M.K., *Energy from fossil fuels.* Science, 1949. **109**(2823): p. 103-109.
25. Tainter, J.A., T. Allen, and T.W. Hoekstra, *Energy transformations and post-normal science.* Energy, 2006. **31**(1): p. 44-58.

26. Georgescu-Roegen, N., *The entropy law and the economic process*. 1971, Harvard University Press: Cambridge, MA.
27. Sorman, A.H. and M. Giampietro, *The energetic metabolism of societies and the degrowth paradigm: analyzing biophysical constraints and realities.* Journal of Cleaner Production, 2013. **38**: p. 80-93.
28. Smil, V., *Examining energy transitions: A dozen insights based on performance.* Energy Research & Social Science, 2016. **22**: p. 194-197.
29. Nikiforuk, A., *The energy of slaves: Oil and the new servitude*. 2012: Greystone Books.
30. Bodger, P.S. and J.T. Baines, *Dynamics of an energy economic system subject to an energy substitution sequence.* Energy Systems and Policy, 1988. **12**: p. 167-178.
31. King, C.W., *The economic superorganism: beyond the competing narratives on energy, growth, and policy*. 2021, Springer: Cham, Switzerland.
32. Hagens, N.J., *Economics for the future – Beyond the superorganism.* Ecological Economics, 2020. **169**: p. 106520.
33. Abbasi, T. and S.A. Abbasi, *Biomass energy and the environmental impacts associated with its production and utilization.* Renewable and Sustainable Energy Reviews, 2010. **14**(3): p. 919-937.
34. Moriarty, P. and D. Honnery, *What is the global potential for renewable energy?* RSER Renewable and Sustainable Energy Reviews, 2012. **16**(1): p. 244-252.
35. Moriarty, P. and D. Honnery, *Can renewable energy power the future?* Energy Policy, 2016. **93**: p. 3-7.
36. Giampietro, M. and K. Mayumi, *The Biofuel Delusion: The Fallacy of Large Scale Agro-biofuels Production*. 2009, London, UK; Sterling, VA: Earthscan.
37. Murphy, D. and C.A. Hall, *Year in review—EROI or energy return on (energy) invested.* Annals of the New York Academy of Sciences, 2010. **1185**(1): p. 102-118.
38. Dale, M., S. Krumdieck, and P. Bodger, *A Dynamic Function for Energy Return on Investment.* Sustainability, 2011. **3**(10): p. 1972.
39. Capellán-Pérez, I., L. Miguel, and C. de Castro, *Dynamic Energy Return on Energy Investment (EROI) and material requirements in scenarios of global transition to renewable energies.* Energy Strategy Reviews, 2019. **26**: p. 100399.
40. BP, *BP Statistical Review of World Energy 2019*. 2019, BP. p. 64.
41. The Shift Project. *Historical Energy Production Statistics*. 2018 [cited 2018 7 April]; Available from: http://www.tsp-data-portal.org/Energy-Production-Statistics#tspQvChart.
42. Day, J.W., et al., *The Energy Pillars of Society: Perverse Interactions of Human Resource Use, the Economy, and Environmental Degradation.* BioPhysical Economics and Resource Quality, 2018. **3**(1): p. 2.
43. The Shift Project. *World Primary Energy Production*. 2019 [cited 2021 25 April]; Available from: https://theshiftdataportal.org/.
44. Edenhofer, O., et al., *On the economics of renewable energy sources.* Energy Economics, 2013. **40**: p. S12-S23.
45. Frankfurt School-UNEP Centre/BNEF, *Global Trends in Renewable Energy Investment 2018*, A. McCrone, et al., Editors. 2018, Frankfurt School – UNEP Collaborating Centre: Frankfurt, Germany. p. 86.
46. Sgouridis, S., D. Csala, and U. Bardi, *The sower's way: quantifying the narrowing net-energy pathways to a global energy transition.* Environmental Research Letters, 2016. **11**(9): p. 094009.
47. IPCC, *Climate Change 2014: Mitigation of Climate Change. Contribution of Working Group III to the Fifth Assessment Report of the Intergovernmental Panel on Climate Change*. 2014, Cambridge, United Kingdom and New York, NY, USA: Cambridge University Press. 1454.
48. Stern, N., et al., *Stern Review: The economics of climate change*. 2007, Cambridge, UK; New York, NY: Cambridge University Press. 692.

49. GEA, *Global Energy Assessment: Toward a Sustainable Future*, T.B. Johansson, et al., Editors. 2012, International Institute for Applied Systems Analysis: Cambridge, UK; New York, NY.
50. Capellán-Pérez, I., et al., *Fossil fuel depletion and socio-economic scenarios: An integrated approach.* Energy, 2014. **77**: p. 641-666.
51. Brandt, A.R., *How Does Energy Resource Depletion Affect Prosperity? Mathematics of a Minimum Energy Return on Investment (EROI).* BioPhysical Economics and Resource Quality, 2017. **2**(1): p. 2.
52. Murphy, D. and C.A.S. Hall, *Adjusting the economy to the new energy realities of the second half of the age of oil.* Ecological Modelling, 2011. **223**(1): p. 67-71.
53. Hall, C.A., J.G. Lambert, and S.B. Balogh, *EROI of different fuels and the implications for society.* Energy Policy, 2014. **64**: p. 141-152.
54. Floyd, J., et al., *Energy descent as a post-carbon transition scenario: How 'knowledge humility' reshapes energy futures for post-normal times.* Futures, 2020. **122**: p. 102565.
55. Heun, M.K. and M. de Wit, *Energy return on (energy) invested (EROI), oil prices, and energy transitions.* Energy Policy, 2012. **40**: p. 147-158.
56. Hall, C.A., *The History, Future, and Implications of EROI for Society*, in *Energy Return on Investment: A Unifying Principle for Biology, Economics, and Sustainability*, C.A. Hall, Editor. 2017, Springer International Publishing: Cham, Switzerland. p. 145-169.
57. UNDP. *Goal 7: AFFORDABLE AND CLEAN ENERGY*. 2020 [cited 2021 22 June]; Available from: https://www.undp.org/sustainable-development-goals#affordable-and-clean-energy.
58. IEA, *Energy for All: Financing access for the poor*. 2011, International Energy Agency: Oslo, Norway. p. 52.
59. Heard, B.P., et al., *Burden of proof: A comprehensive review of the feasibility of 100% renewable-electricity systems.* Renewable and Sustainable Energy Reviews, 2017. **76**: p. 1122-1133.
60. Martínez, D.M. and B.W. Ebenhack, *Understanding the role of energy consumption in human development through the use of saturation phenomena.* Energy Policy, 2008. **36**(4): p. 1430-1435.
61. IRENA, *Global Energy Transformation: A roadmap to 2050 (2019 edition)*. 2019, International Renewable Energy Agency: Abu Dhabi. p. 52.
62. Newell, R., et al., *Global Energy Outlook 2021: Pathways from Paris*. 2021, Resources for the Future (RFF). p. 46.
63. Kuhn, T.S., *The structure of scientific revolutions*. Second edition, enlarged. ed. International encyclopedia of unified science. Foundations of the unity of science, v. 2, no. 2. 1970, Chicago: University of Chicago Press.
64. Capra, F. and P.L. Luisi, *The systems view of life: a unifying vision*. 2014, Cambridge, UK: Cambridge University Press. 498.
65. Cleveland, C.J. and M. Ruth, *When, where, and by how much do biophysical limits constrain the economic process? A survey of Nicholas Georgescu-Roegen's contribution to ecological economics.* Ecological Economics, 1997. **22**: p. 203-223.
66. Odum, H.T., *Energy, Ecology, and Economics.* Ambio, 1973. **2**(6): p. 220-227.
67. Smil, V., *Moore's curse and the great energy delusion.* The American, 2008. **2**(6): p. 34-41.
68. Giampietro, M. and K. Mayumi, *Complex systems thinking and renewable energy systems*, in *Biofuels, Solar and Wind as Renewable Energy Systems*, D. Pimentel, Editor. 2008, Springer. p. 173-213.
69. Smil, V., *Energy in World History*, in *Energy and civilization: a history*, V. Smil, Editor. 2017, The MIT Press: Cambridge, MA. p. 385-442.
70. Winter, C.J., *Solar cities.* Renewable Energy, 1994. **4**(1): p. 15-26.
71. Odum, H.T. and E.C. Odum, *Energy basis for man and nature*. 1976: McGraw-Hill Book Company,New York. Medium: X; Size: Pages: 307.

72. Bardi, U., *What Future for the Anthropocene? A Biophysical Interpretation.* BioPhysical Economics and Resource Quality, 2016. **1**(1): p. 2.
73. Glucina, M.D. and K. Mayumi, *Connecting thermodynamics and economics.* Annals of the New York Academy of Sciences, 2010. **1185**(1): p. 11-29.
74. Spreng, D.T., *Net-energy analysis and the energy requirements of energy systems*. 1988, New York: Praeger.
75. Dale, M., S. Krumdieck, and P. Bodger, *Global energy modelling — A biophysical approach (GEMBA) Part 2: Methodology.* Ecological Economics, 2012. **73**: p. 158-167.
76. de Castro, C., et al., *Global wind power potential: Physical and technological limits.* Energy Policy, 2011. **39**(10): p. 6677-6682.
77. de Castro, C., et al., *Global solar electric potential: A review of their technical and sustainable limits.* Renewable and Sustainable Energy Reviews, 2013. **28**: p. 824-835.
78. de Castro, C., et al., *A top-down approach to assess physical and ecological limits of biofuels.* Energy, 2014. **64**: p. 506-512.
79. Scheidel, A. and A.H. Sorman, *Energy transitions and the global land rush: Ultimate drivers and persistent consequences.* Global Environmental Change, 2012. **22**(3): p. 588-595.
80. Kraxner, F., et al., *Global bioenergy scenarios–Future forest development, land-use implications, and trade-offs.* Biomass and Bioenergy, 2013. **57**: p. 86-96.
81. Jenkins, J.D. and S. Thernstrom, *Deep decarbonization of the electric power sector: Insights from recent literature*. 2017, Energy Innovation Reform Project: Arlington, VA. p. 10.
82. Heinberg, R. and D. Fridley, *Our Renewable Future*. Post Carbon Institute. 2016, Washington, DC: Island Press. 248.
83. Seibert, M.K. and W.E. Rees, *Through the Eye of a Needle: An Eco-Heterodox Perspective on the Renewable Energy Transition.* Energies, 2021. **14**(15): p. 4508.
84. Carbajales-Dale, M., C.J. Barnhart, and S.M. Benson, *Can we afford storage? A dynamic net energy analysis of renewable electricity generation supported by energy storage.* Energy & Environmental Science, 2014. **7**(5): p. 1538-1544.
85. Heptonstall, P., R. Gross, and F. Steiner, *The costs and impacts of intermittency – 2016 update*. 2017, Imperial College London: UK Energy Research Centre (UKERC). p. 72.
86. Brandt, A.R., M. Dale, and C.J. Barnhart, *Calculating systems-scale energy efficiency and net energy returns: A bottom-up matrix-based approach.* Energy, 2013. **62**: p. 235-247.
87. Trainer, T., *Can renewables etc. solve the greenhouse problem? The negative case.* Energy Policy, 2010. **38**(8): p. 4107-4114.
88. Trainer, T., *Estimating the EROI of whole systems for 100% renewable electricity supply capable of dealing with intermittency.* Energy Policy, 2018. **119**: p. 648-653.
89. York, R., *Do alternative energy sources displace fossil fuels?* Nature Climate Change, 2012. **2**(6): p. 441-443.
90. Farrell, A.E. and A.R. Brandt, *Risks of the oil transition.* Environmental Research Letters, 2006. **1**(1): p. 014004.
91. D'Alessandro, S., T. Luzzati, and M. Morroni, *Energy transition towards economic and environmental sustainability: feasible paths and policy implications.* Journal of Cleaner Production, 2010. **18**(6): p. 532-539.
92. Goldemberg, J. and L. Tadeo Prado, *The "decarbonization" of the world's energy matrix.* Energy Policy, 2010. **38**(7): p. 3274-3276.
93. Gazheli, A., J. van den Bergh, and M. Antal, *How realistic is green growth? Sectoral-level carbon intensity versus productivity.* Journal of Cleaner Production, 2016. **129**: p. 449-467.
94. Kallis, G., *Radical dematerialization and degrowth.* Philosophical transactions. Series A, Mathematical, physical, and engineering sciences, 2017. **375**(2095): p. 1-13.
95. Quilley, S., *De-Growth Is Not a Liberal Agenda: Relocalisation and the Limits to Low Energy Cosmopolitanism.* Environmental Values, 2013. **22**(2): p. 261-285.

96. Kish, K. and S. Quilley, *Wicked Dilemmas of Scale and Complexity in the Politics of Degrowth.* Ecological Economics, 2017. **142**: p. 306-317.
97. Heinberg, R. and T. Crownshaw, *Energy Decline and Authoritarianism.* BioPhysical Economics and Resource Quality, 2018. **3**(3): p. 8.
98. Ahmed, N.M., *Failing states, collapsing systems: biophysical triggers of political violence*. 2017, Cham, Switzerland: Springer.
99. Smil, V., *Energy in nature and society: general energetics of complex systems*. 2008, Cambridge, Mass.: MIT Press.
100. Tainter, J.A. and T.W. Patzek, *Our energy and complexity dilemma: prospects for the future*, in *Drilling Down*. 2012, Springer. p. 185-214.
101. Palmer, G. and J. Floyd, *Synthesis and Conclusions*, in *Energy storage and civilization a systems approach*. 2020, Springer: Cham. p. 139-156.
102. Catton, W.R., *Overshoot: The ecological basis of revolutionary change*. 1982: University of Illinois Press.
103. Wackernagel, M., et al., *Tracking the ecological overshoot of the human economy.* Proceedings of the National Academy of Sciences, 2002. **99**(14): p. 9266-9271.
104. Meadows, D., J. Randers, and D. Meadows, *Limits to growth: The 30-year update*. 2004: Chelsea Green Publishing.
105. Crownshaw, T., et al., *Over the horizon: Exploring the conditions of a post-growth world.* The Anthropocene Review, 2019. **6**(1-2): p. 117-141.
106. Crépin, A.-S. and C. Folke, *The economy, the biosphere and planetary boundaries: Towards biosphere economics.* International Review of Environmental and Resource Economics, 2015. **8**(1): p. 57-100.
107. Quilley, S., *Navigating the Anthropocene: environmental politics and complexity in an era of limits*, in *Handbook on Growth and Sustainability*. 2017, Edward Elgar Publishing.
108. Garrett, T.J., *Long-run evolution of the global economy: 1. Physical basis.* Earth's Future, 2014. **2**(3): p. 127-151.
109. Maturana, H.R. and F.J. Varela, *Autopoiesis and Cognition: the Realization of the Living*. 1980, Dordrecht, Holland; Boston, MA: D. Reidel Publishing Company.
110. Levin, S., et al., *Social-ecological systems as complex adaptive systems modeling and policy implications.* Environment and Development Economics, 2013. **18**(2): p. 111-132.
111. Von Bertalanffy, L., *General system theory: Foundations, development, applications*. 1969, New York, NY: George Braziller.
112. Forrester, J.W., *Industrial dynamics.* Journal of the Operational Research Society, 1997. **48**(10): p. 1037-1041.
113. Kay, J.J., *An introduction to systems thinking*, in *The ecosystem approach: Complexity, uncertainty, and managing for sustainability*, D. Waltner-Toews, J.J. Kay, and N.-M.E. Lister, Editors. 2008, Colombia University Press: New York, NY. p. 3-13.
114. Meadows, D., *Leverage points: Places to intervene in a system*. 1999, The Sustainability Institute: Hartland, VT. p. 19.
115. Odum, H.T., *Systems ecology; An introduction*. 1983, New York, NY: John Wiley and Sons. 644.
116. Giampietro, M. and S.G.F. Bukkens, *Analogy between Sudoku and the multi-scale integrated analysis of societal metabolism.* Ecological Informatics, 2015. **26**: p. 18-28.
117. de Castro, C. and I. Capellán-Pérez, *Standard, Point of Use, and Extended Energy Return on Energy Invested (EROI) from Comprehensive Material Requirements of Present Global Wind, Solar, and Hydro Power Technologies.* Energies, 2020. **13**(12): p. 3036.
118. Zencey, E., *Energy as Master Resource*, in *State of the World 2013: Is Sustainability Still Possible?* 2013, Island Press/Center for Resource Economics: Washington, DC. p. 73-83.
119. Neumeyer, C. and R. Goldston, *Dynamic EROI Assessment of the IPCC 21st Century Electricity Production Scenario.* Sustainability, 2016. **8**(5): p. 421.

120. Smil, V., *Science, energy, ethics, and civilization*, in *Visions of discovery: new light on physics, cosmology, and consciousness*, R.Y. Chiao, Editor. 2011, Cambridge University Press: Cambridge, UK. p. 709-729.
121. Davies, L.L., *Energy, Consumption, and the Amorality of Energy Law.* AJIL Unbound, 2017. **109**: p. 147-152.
122. Healy, N., J.C. Stephens, and S.A. Malin, *Embodied energy injustices: Unveiling and politicizing the transboundary harms of fossil fuel extractivism and fossil fuel supply chains.* Energy Research & Social Science, 2019. **48**: p. 219-234.
123. C2ES. *Global Emissions*. 2020 [cited 2020 7 July]; Available from: https://www.c2es.org/content/international-emissions/.
124. Sovacool, B.K. and F.W. Geels, *Further reflections on the temporality of energy transitions: A response to critics.* Energy Research & Social Science, 2016. **22**: p. 232-237.
125. Sovacool, B.K., et al., *New frontiers and conceptual frameworks for energy justice.* Energy Policy, 2017. **105**: p. 677-691.
126. Millward-Hopkins, J., et al., *Providing decent living with minimum energy: A global scenario.* Global Environmental Change, 2020. **65**: p. 102168.
127. Dholakia, R.R., N. Dholakia, and A.F. Firat, *From social psychology to political economy: A model of energy use behavior.* Journal of Economic Psychology, 1983. **3**(3): p. 231-247.
128. Vogel, J., et al., *Socio-economic conditions for satisfying human needs at low energy use: An international analysis of social provisioning.* Global Environmental Change, 2021: p. 102287.
129. O'Neill, D.W., et al., *A good life for all within planetary boundaries.* Nature Sustainability, 2018. **1**(2): p. 88-95.
130. Burke, M.J., *Energy-Sufficiency for a Just Transition: A Systematic Review.* Energies, 2020. **13**(10): p. 2444.
131. Dietz, R. and D.W. O'Neill, *Enough throughput*, in *Enough is enough: building a sustainable economy in a world of finite resources*. 2013, Berrett-Koehler Publishers: San Francisco.
132. Wenz, P., *Ethics, energy policy, and future generations.* Environmental ethics, 1983. **5**(3): p. 195-209.
133. Jamieson, D., *Energy, ethics and the transformation of nature*, in *The Ethics of Global Climate Change*, D.G. Arnold, Editor. 2011, Cambridge University Press. p. 16-37.
134. Elliot, H., *Ethics for a Finite World: An Essay Concerning a Sustainable Future*. 2005, Golden, CO: Fulcrum Publishing.
135. Brown, P. and G. Garver, *Right relationship: Building a whole earth economy*. 2009, San Francisco, CA: Berrett-Koehler Publishers.
136. Ehrlich, P.R., J.H. Lawton, and R.M. May, *Energy use and biodiversity loss.* Philosophical Transactions of the Royal Society of London. Series B: Biological Sciences, 1994. **344**(1307): p. 99-104.
137. Gasparatos, A., et al., *Renewable energy and biodiversity: Implications for transitioning to a Green Economy.* Renewable and Sustainable Energy Reviews, 2017. **70**: p. 161-184.
138. Poincaré, H. and G.B. Halsted, *The foundations of science; Science and hypothesis, the value of science, Science and method*. Science and education, by McKeen Cattell, vol. 1. 1913, New York, USA: The Science Press.
139. Funtowicz, S.O. and J.R. Ravetz, *Science for the post-normal age.* Futures, 1993. **25**(7): p. 739-755.
140. D'Alisa, G. and G. Kallis, *Post-normal science*, in *Degrowth: A Vocabulary for a New Era*, G. D'Alisa, F. Demaria, and G. Kallis, Editors. 2014, Taylor & Francis Group: London, UK.
141. Ayres, R.U. and B. Warr, *The economic growth engine: how energy and work drive material prosperity*. 2009, Cheltenham, UK; Northampton, MA: Edward Elgar.
142. Macknick, J., *Energy and CO2 emission data uncertainties.* Carbon Management, 2011. **2**(2): p. 189-205.

143. Newell, R., S. Iler, and D. Raimi, *Global Energy Outlooks Comparison Methods: 2018 Update*. 2018, Resources for the Future (RFF). p. 46.
144. Berner, C.L. and R. Flage, *Comparing and integrating the NUSAP notational scheme with an uncertainty based risk perspective.* Reliability Engineering & System Safety, 2016. **156**: p. 185-194.
145. Ruth, M. and B.M. Hannon, *Modeling dynamic economic systems.* 2012.
146. Gambhir, A., et al., *A Review of Criticisms of Integrated Assessment Models and Proposed Approaches to Address These, through the Lens of BECCS.* Energies, 2019. **12**(9): p. 1747.
147. Sousa, T., et al., *The Need for Robust, Consistent Methods in Societal Exergy Accounting.* Ecological Economics, 2017. **141**(Supplement C): p. 11-21.
148. Ayres, R.U., et al., *The underestimated contribution of energy to economic growth.* Structural Change and Economic Dynamics, 2013. **27**: p. 79-88.
149. Benes, J., et al., *The future of oil: Geology versus technology.* International Journal of Forecasting, 2015. **31**(1): p. 207-221.
150. Dale, M., *Meta-analysis of non-renewable energy resource estimates.* Energy Policy, 2012. **43**: p. 102-122.
151. DANIELSEN, F., et al., *Biofuel Plantations on Forested Lands: Double Jeopardy for Biodiversity and Climate.* Conservation Biology, 2009. **23**(2): p. 348-358.
152. Keith, D.W., et al., *The influence of large-scale wind power on global climate.* Proceedings of the National Academy of Sciences of the United States of America, 2004. **101**(46): p. 16115-16120.
153. Miller, L.M., F. Gans, and A. Kleidon, *Estimating maximum global land surface wind power extractability and associated climatic consequences.* Earth Syst. Dynam., 2011. **2**(1): p. 1-12.
154. Romero, J.C. and P. Linares, *Exergy as a global energy sustainability indicator. A review of the state of the art.* Renewable and Sustainable Energy Reviews, 2014. **33**: p. 427-442.
155. Whiting, K., L.G. Carmona, and T. Sousa, *A review of the use of exergy to evaluate the sustainability of fossil fuels and non-fuel mineral depletion.* Renewable and Sustainable Energy Reviews, 2017. **76**: p. 202-211.
156. Cleveland, C.J., R.K. Kaufmann, and D.I. Stern, *Aggregation and the role of energy in the economy.* Ecological Economics, 2000. **32**(2): p. 301-317.
157. Rye, C.D. and T. Jackson, *A review of EROEI-dynamics energy-transition models.* Energy Policy, 2018. **122**: p. 260-272.
158. Rocco, M.V., *Accounting for Energy-Resources use by Thermodynamics*, in *Primary Exergy Cost of Goods and Services: An Input – Output Approach*. 2016, Springer International Publishing: Cham. p. 43-60.
159. Keen, S., R.U. Ayres, and R. Standish, *A Note on the Role of Energy in Production.* Ecological Economics, 2019. **157**: p. 40-46.
160. Ayres, R.U. and B. Warr, *Accounting for growth: the role of physical work.* Structural Change and Economic Dynamics, 2005. **16**(2): p. 181-209.
161. Warr, B. and R.U. Ayres, *Useful work and information as drivers of economic growth.* Ecological Economics, 2012. **73**: p. 93-102.
162. Stern, D.I. and K. Enflo, *Causality between energy and output in the long-run.* Energy Economics, 2013. **39**: p. 135-146.
163. Santos, J., et al., *Useful Exergy Is Key in Obtaining Plausible Aggregate Production Functions and Recognizing the Role of Energy in Economic Growth: Portugal 1960–2009.* Ecological Economics, 2018. **148**: p. 103-120.
164. Ockwell, D.G., *Energy and economic growth: Grounding our understanding in physical reality.* Energy Policy, 2008. **36**(12): p. 4600-4604.
165. Murphy, D.J., *The implications of the declining energy return on investment of oil production.* Philosophical Transactions of the Royal Society of London A: Mathematical, Physical and Engineering Sciences, 2014. **372**(2006): p. 20130126.

166. Lambert, J.G., et al., *Energy, EROI and quality of life.* Energy Policy, 2014. **64**: p. 153-167.
167. Fagnart, J.-F. and M. Germain, *Net energy ratio, EROEI and the macroeconomy.* Structural Change and Economic Dynamics, 2016. **37**: p. 121-126.
168. Bhandari, K.P., et al., *Energy payback time (EPBT) and energy return on energy invested (EROI) of solar photovoltaic systems: A systematic review and meta-analysis.* Renewable and Sustainable Energy Reviews, 2015. **47**: p. 133-141.
169. Fagnart, J.-F. and M. Germain, *Energy, complexity and sustainable long-term growth.* Mathematical Social Sciences, 2015. **75**: p. 87-93.
170. Murphy, D., et al., *Order from Chaos: A Preliminary Protocol for Determining the EROI of Fuels.* Sustainability, 2011. **3**(10): p. 1888-1907.
171. Odum, H.T., *Environment, power, and society*. 1970, New York: Wiley-Interscience.
172. Boulding, K.E., *The Economics of Energy.* The ANNALS of the American Academy of Political and Social Science, 1973. **410**(1): p. 120-126.
173. Lotka, A.J., *Natural Selection as a Physical Principle.* Proceedings of the National Academy of Sciences, 1922. **8**(6): p. 151-154.
174. Fizaine, F. and V. Court, *Renewable electricity producing technologies and metal depletion: A sensitivity analysis using the EROI.* Ecological Economics, 2015. **110**: p. 106-118.
175. Diesendorf, M. and T. Wiedmann, *Implications of Trends in Energy Return on Energy Invested (EROI) for Transitioning to Renewable Electricity.* Ecological Economics, 2020. **176**: p. 106726.
176. Brand-Correa, L., et al., *Developing an Input-Output Based Method to Estimate a National-Level Energy Return on Investment (EROI).* Energies, 2017. **10**(4): p. 534.
177. Dupont, E., M. Germain, and H. Jeanmart, *Estimate of the Societal Energy Return on Investment (EROI).* Biophysical Economics and Sustainability, 2021. **6**(1): p. 2.
178. Fizaine, F. and V. Court, *Energy expenditure, economic growth, and the minimum EROI of society.* Energy Policy, 2016. **95**: p. 172-186.
179. Heinberg, R. *The Gross Society*. 2015 15 April [cited 2018 8 April]; Available from: http://www.postcarbon.org/the-gross-society/.
180. Hall, C.A., S. Balogh, and D.J. Murphy, *What is the minimum EROI that a sustainable society must have?* Energies, 2009. **2**(1): p. 25-47.
181. Court, V. and F. Fizaine, *Long-Term Estimates of the Energy-Return-on-Investment (EROI) of Coal, Oil, and Gas Global Productions.* Ecological Economics, 2017. **138**: p. 145-159.
182. Prieto, P.A., C.A.S. Hall, and R. Melgar, *Spain's Photovoltaic Revolution : the Energy Return on Investment*. 2011, Springer: Dordrecht.
183. Hall, C.A., *EROI and Industrial Economies*, in *Energy Return on Investment: A Unifying Principle for Biology, Economics, and Sustainability*, C.A. Hall, Editor. 2017, Springer International Publishing: Cham, Switzerland. p. 107-118.
184. Hall, C.A. and K.A. Klitgaard, *Peak Oil, EROI, Investments, and Our Financial Future*, in *Energy and the wealth of nations: understanding the biophysical economy*, C.A. Hall and K.A. Klitgaard, Editors. 2012, Springer: New York, NY. p. 5-8.
185. Verbruggen, A. and M. Al Marchohi, *Views on peak oil and its relation to climate change policy.* Energy Policy, 2010. **38**(10): p. 5572-5581.
186. Hall, C.A. and K.A. Klitgaard, *The Science Behind How Real Economies Work*, in *Energy and the wealth of nations: understanding the biophysical economy*, C.A. Hall and K.A. Klitgaard, Editors. 2012, Springer: New York, NY. p. 307-365.
187. Lenzen, M., *Current State of Development of Electricity-Generating Technologies: A Literature Review.* Energies, 2010. **3**(3): p. 462-591.
188. Capellán-Pérez, I., et al., *MEDEAS: a new modeling framework integrating global biophysical and socioeconomic constraints.* Energy & Environmental Science, 2020.
189. Sinn, H.-W., *Buffering volatility: A study on the limits of Germany's energy revolution.* European Economic Review, 2017. **99**: p. 130-150.

190. Palmer, G., *A Framework for Incorporating EROI into Electrical Storage.* BioPhysical Economics and Resource Quality, 2017. **2**(2): p. 6.
191. IEA, *Harnessing Variable Renewables*. 2011, International Energy Agency: Paris, France.
192. Trainer, T., *A critique of Jacobson and Delucchi's proposals for a world renewable energy supply.* Energy Policy, 2012. **44**: p. 476-481.
193. Capellán-Pérez, I., et al., *D4.1 (D13) Global Model: MEDEAS-World Model and IOA implementation at global geographical level*, in *EU Framework Program for Research and Innovation actions (H2020 LCE-21-2015)*. 2017, University of Valladolid. p. 253.
194. Denholm, P. and M. Hand, *Grid flexibility and storage required to achieve very high penetration of variable renewable electricity.* Energy Policy, 2011. **39**(3): p. 1817-1830.
195. Rugolo, J. and M.J. Aziz, *Electricity storage for intermittent renewable sources.* Energy & Environmental Science, 2012. **5**(5): p. 7151-7160.
196. IEA, *Empowering Variable Renewables: Options for Flexible Electricity Systems*. 2008, International Energy Agency: Paris, France.
197. Bird, L., M. Milligan, and D. Lew, *Integrating variable renewable energy: challenges and solutions*. 2013, National Renewable Energy Laboratory (NREL): Golden, CO.
198. Weitemeyer, S., et al., *Integration of Renewable Energy Sources in future power systems: The role of storage.* Renewable Energy, 2015. **75**: p. 14-20.
199. IRENA, *Renewable energy integration in power grids*. 2015, International Renewable Energy Agency.
200. Perez-Arriaga, I.J. *Managing large scale penetration of intermittent renewables*. in *MITEI Symposium on Managing Large-Scale Penetration of Intermittent Renewables*. 2011. Cambridge, MA: Massachusetts Institute of Technology.
201. Delarue, E. and J. Morris, *Renewables Intermittency: Operational Limits and Implications for Long-Term Energy System Models*, in *MIT Joint Program Report Series*. 2015, MIT Joint Program on the Science and Policy of Global Change.
202. Ferroni, F. and R.J. Hopkirk, *Energy Return on Energy Invested (ERoEI) for photovoltaic solar systems in regions of moderate insolation.* Energy Policy, 2016. **94**: p. 336-344.
203. Denholm, P. and R. Margolis, *Very Large-Scale Deployment of Grid-Connected Solar Photovoltaics in the United States: Challenges and Opportunities*, in *Solar 2006*. 2006, National Renewable Energy Lab. (NREL): Denver, Colorado. p. Medium: ED; Size: 8 pp.
204. REN21, *Renewables 2017 Global Status Report*. 2017, REN21 Secretariat: Paris, France.
205. Friedemann, A.J., *When Trucks Stop Running: Energy and the Future of Transportation*. 2016: Springer.
206. Brockway, P.E., et al., *Understanding China's past and future energy demand: An exergy efficiency and decomposition analysis.* Applied Energy, 2015. **155**: p. 892-903.
207. Jevons, W.S., *The Coal Question—An Inquiry Concerning the Progress of the Nation, and the Probable Exhaustion of our Coal-mines, M.A., ll.D*. 1865, New York, US (reprint in 1965): F.R.S. Augustus M. Kelley Publisher.
208. Rosen, M.A., *Second-law analysis: approaches and implications.* International Journal of Energy Research, 1999. **23**(5): p. 415-429.
209. Hall, C.A., *The Development of the Laws of Thermodynamics*, in *Energy Return on Investment: A Unifying Principle for Biology, Economics, and Sustainability*, C.A. Hall, Editor. 2017, Springer International Publishing: Cham, Switzerland. p. 7-20.
210. Ayres, R., *Energy, complexity and wealth maximization*. 2016, Cham, Switzerland: Springer. 593.
211. Ruzzenenti, F. and R. Basosi, *The role of the power/efficiency misconception in the rebound effect's size debate: Does efficiency actually lead to a power enhancement?* Energy Policy, 2008. **36**(9): p. 3626-3632.
212. Cullen, J.M., J.M. Allwood, and E.H. Borgstein, *Reducing Energy Demand: What Are the Practical Limits?* Environmental Science & Technology, 2011. **45**(4): p. 1711-1718.

213. Cullen, J.M. and J.M. Allwood, *Theoretical efficiency limits for energy conversion devices.* Energy, 2010. **35**(5): p. 2059-2069.
214. Nakićenović, N., P.V. Gilli, and R. Kurz, *Regional and global exergy and energy efficiencies.* Energy, 1996. **21**(3): p. 223-237.
215. Grübler, A., N. Nakićenović, and D.G. Victor, *Dynamics of energy technologies and global change.* Energy Policy, 1999. **27**(5): p. 247-280.
216. Nakićenović, N. and A. Grübler, *Energy conversion, conservation, and efficiency.* Energy, 1993. **18**(5): p. 421-435.
217. Patterson, M.G., *What is energy efficiency?: Concepts, indicators and methodological issues.* Energy Policy, 1996. **24**(5): p. 377-390.
218. Paoli, L. and J. Cullen, *Technical limits for energy conversion efficiency.* Energy, 2019: p. 116228.
219. Brockway, P.E., et al., *Energy efficiency and economy-wide rebound effects: A review of the evidence and its implications.* Renewable and Sustainable Energy Reviews, 2021: p. 110781.
220. Galeotti, M., *Environment and Economic Growth: Is Technical Change the Key to Decoupling?* , in *FEEM Working Papers*. 2003, Fondazione Eni Enrico Mattei (FEEM).
221. Arvesen, A., R.M. Bright, and E.G. Hertwich, *Considering only first-order effects? How simplifications lead to unrealistic technology optimism in climate change mitigation.* Energy Policy, 2011. **39**(11): p. 7448-7454.
222. Sakai, M., et al., *Thermodynamic Efficiency Gains and their Role as a Key 'Engine of Economic Growth'.* Energies, 2019. **12**(1): p. 110.
223. Loftus, P.J., et al., *A critical review of global decarbonization scenarios: what do they tell us about feasibility?* Wiley Interdisciplinary Reviews: Climate Change, 2015. **6**(1): p. 93-112.
224. Fell, M.J., *Energy services: A conceptual review.* Energy Research & Social Science, 2017. **27**: p. 129-140.
225. Cullen, J.M. and J.M. Allwood, *The efficient use of energy: Tracing the global flow of energy from fuel to service.* Energy Policy, 2010. **38**(1): p. 75-81.
226. Lovins, A.B., *Energy End-Use Efficiency*, in *Transitions to Sustainable Energy Systems*, I. Council, Editor. 2005, Rocky Mountain Institute: Snowmass, CO. p. 25.
227. Haas, R., et al., *Towards sustainability of energy systems: A primer on how to apply the concept of energy services to identify necessary trends and policies.* Energy Policy, 2008. **36**(11): p. 4012-4021.
228. Cook, E., *Man, energy, society*. 1976, San Francisco: W.H. Freeman.
229. Fouquet, R., *Historical energy transitions: Speed, prices and system transformation.* Energy Research & Social Science, 2016. **22**: p. 7-12.
230. Bonaiuti, M., *Are we entering the age of involuntary degrowth? Promethean technologies and declining returns of innovation.* Journal of Cleaner Production, 2018. **197**: p. 1800-1809.
231. Grübler, A., C. Wilson, and G. Nemet, *Apples, oranges, and consistent comparisons of the temporal dynamics of energy transitions.* Energy Research & Social Science, 2016. **22**: p. 18-25.
232. Grübler, A., *Energy transitions research: Insights and cautionary tales.* Energy Policy, 2012. **50**: p. 8-16.
233. Foxon, T.J., *Technological lock-in and the role of innovation*, in *Handbook of Sustainable Development*. 2014, Edward Elgar Publishing.
234. Meadows, D.H., et al., *The Limits to Growth: A Report for the Club of Rome's Project on the Predicament of Mankind*. 1972: Universe Books.
235. Turner, G.M., *A comparison of The Limits to Growth with 30 years of reality.* Global Environmental Change, 2008. **18**(3): p. 397-411.
236. Forrester, J.W., *World dynamics*. 1971: Wright-Allen Press.
237. Wiener, N., D. Hill, and S. Mitter, *Cybernetics : or, Control and communication in the animal and the machine*. 2019, MIT Press: Cambridge.

238. Von Bertalanffy, L., *An outline of general system theory.* British Journal for the Philosophy of Science, 1950.
239. Boulding, K.E., *General Systems Theory—The Skeleton of Science.* Management Science, 1956. **2**(3): p. 197-208.
240. Ziegler, H., *An introduction to thermomechanics*. 1983, North-Holland Pub. Co.: Amsterdam, New York.
241. Soddy, F., *Wealth, virtual wealth and debt: the solution of the economic paradox*. 1933, London, UK: George Allen and Unwin Ltd.
242. Boulding, K.E., *The economics of the coming spaceship earth.* Environmental Quality Issues in a Growing Economy, 1966.
243. Gilliland, M.W., *Energy Analysis and Public Policy.* Science, 1975. **189**(4208): p. 1051-1056.
244. Odum, E.P., *Fundamentals of ecology*. 1953, Philadelphia: Saunders.
245. Mandelbrot, B.B., *The fractal geometry of nature*. Updated and augmented. ed. 1983, New York: W.H. Freeman.
246. Gleick, J., *Chaos : making a new science*. 1988, New York, N.Y., U.S.A.: Penguin.
247. Holland, J.H., *Studying Complex Adaptive Systems.* Journal of Systems Science and Complexity, 2006. **19**(1): p. 1-8.
248. Chaisson, E.J., *Using complexity science to search for unity in the natural sciences.* Complexity and the Arrow of Time, 2013: p. 68-79.
249. Ruth, M., *Innovation, technology, and economic growth*, in *Handbook on Growth and Sustainability*, P.A. Victor and B. Dolter, Editors. 2017, Edward Elgar Publishing, Incorporated: Cheltenham, Gloucestershire, UNITED KINGDOM. p. 213-231.
250. Koestler, A., *Beyond atomism and holism – the concept of the Holon*, in *The ghost in the machine*. 1971, Henry Regnery: Chicago.
251. Eddy, B.G., et al., *An information ecology approach to science–policy integration in adaptive management of social-ecological systems.* Ecology and society, 2014. **19**(3).
252. Herbert, S., *The architecture of complexity.* Proceedings of the American Philosophical Society, 1962. **106**(6): p. 467-482.
253. Tainter, J.A., *The collapse of complex societies*. New studies in archaeology. 1988, Cambridge, UK; New York, NY: Cambridge University Press. 250.
254. Harris, M., *Cultural materialism: the struggle for a science of culture*. 1st ed. ed. 1979, New York: Random House.
255. Diaz-Maurin, F., *Power capacity: A key element in sustainability assessment.* Ecological Indicators, 2016. **66**: p. 467-480.
256. Wackernagel, M. and W. Rees, *Our ecological footprint: reducing human impact on the earth*. 1998, Gabriola Island, BC; Philadelphia, PA: New Society Publishers.
257. Smil, V., *Harvesting the biosphere: The human impact.* Population and development review, 2011. **37**(4): p. 613-636.
258. Kronenberg, T., *Finding common ground between ecological economics and post-Keynesian economics.* Ecological Economics, 2010. **69**(7): p. 1488-1494.
259. Fontana, G. and M. Sawyer, *Towards post-Keynesian ecological macroeconomics.* Ecological Economics, 2016. **121**: p. 186-195.
260. Ayres, R. and V. Voudouris, *The economic growth enigma: Capital, labour and useful energy?* Energy Policy, 2014. **64**: p. 16-28.
261. Ayres, R.U. and I. Nair, *Thermodynamics and economics.* Physics Today, 1984. **37**: p. 62-71.
262. Georgescu-Roegen, N., *The entropy law and the economic process in retrospect.* Eastern Economic Journal, 1986. **12**(1): p. 3-25.
263. Baumgärtner, S., *Thermodynamic models*, in *Modelling in Ecological Economics*, J. Proops and P. Safonov, Editors. 2004, Edward Elgar: Cheltenham, UK. p. 102-129.
264. Kümmel, R. and D. Lindenberger, *Energy in Growth Accounting and the Aggregation of Capital and Output.* Biophysical Economics and Sustainability, 2020. **5**(1): p. 5.

265. Smil, V., *Energy and Society*, in *Energy and civilization: a history*, V. Smil, Editor. 2017, The MIT Press: Cambridge, MA. p. 1-20.
266. Kleiber, M., *The Fire of Life: An Introduction to Animal Energetics*. 1961: Wiley.
267. Csereklyei, Z. and D.I. Stern, *Global energy use: Decoupling or convergence?* Energy Economics, 2015. **51**: p. 633-641.
268. UNEP, *Decoupling natural resource use and environmental impacts from economic growth. A Report of the Working Group on Decoupling to the International Resource Panel*, M. Fischer-Kowalski, et al., Editors. 2011, United Nations Environment Programme: Nairobi, Kenya. p. 174.
269. Krysiak, F.C., *Entropy, limits to growth, and the prospects for weak sustainability.* Ecological Economics, 2006. **58**(1): p. 182-191.
270. Kerschner, C., et al., *Economic vulnerability to peak oil.* Global environmental change, 2013. **23**(6): p. 1424-1433.
271. Bardi, U., S. Falsini, and I. Perissi, *Toward a General Theory of Societal Collapse: A Biophysical Examination of Tainter's Model of the Diminishing Returns of Complexity.* BioPhysical Economics and Resource Quality, 2019. **4**(1): p. 3.
272. Box, G.E.P., *Science and Statistics.* Journal of the American Statistical Association, 1976. **71**(356): p. 791-799.
273. Bernstein, P.L., *Against the gods: The remarkable story of risk*. 1996: Wiley New York.
274. Morton, T., *The ecological thought*. 2010, Harvard University Press: Cambridge, Mass.
275. Forrester, J.W., *System dynamics, systems thinking, and soft OR.* System dynamics review, 1994. **10**(2-3): p. 245-256.
276. Gödel, K., *Über formal unentscheidbare Sätze der Principia Mathematica und verwandter Systeme I.* Monatshefte für mathematik und physik, 1931. **38**(1): p. 173-198.
277. Popper, K.R., *Conjectures and refutations: the growth of scientific knowledge*. 3rd ed. (rev.). ed. 1969, London: Routledge & K. Paul.
278. Daly, H.E., *Economics in a full world.* Scientific American, 2005. **293**(3): p. 100-107.
279. Klitgaard, K.A. and L. Krall, *Ecological economics, degrowth, and institutional change.* Ecological Economics, 2012. **84**: p. 247-253.
280. Sterman, J.D., *System Dynamics Modeling: TOOLS FOR LEARNING IN A COMPLEX WORLD.* California Management Review, 2001. **43**(4): p. 8-25.
281. Ravetz, J.R., *Models as metaphors*, in *Public Participation in Sustainability Science A Handbook*, B. Kasemir, et al., Editors. 2003, Cambridge University Press: Cambridge, UK. p. 62-77.
282. Arrow, K., *"I Know a Hawk from a Handsaw"*, in *Eminent economists: their life philosophies*, M. Szenberg, Editor. 1992, Cambridge University Press: Cambridge, UK. p. 42-50.
283. Retortillo, P., et al. *An attempt to automate the analysis of complex system dynamics models: an example of WORLD 3*. in *26th International Conference of the System Dynamics Society*. 2008. Athens, Greece: Citeseer.
284. Saltelli, A., et al., *Five ways to ensure that models serve society: a manifesto.* Nature, 2020. **582**: p. 482-484.
285. Mooney, C.Z., *Monte Carlo Simulation*. 1997, Thousand Oaks, CA: Sage Publications.
286. Zio, E., *The Monte Carlo simulation method for system reliability and risk analysis*. 2012, Springer: London.
287. Thomopoulos, N.T., *Essentials of Monte Carlo simulation : statistical methods for building simulation models*. 2013, Springer: New York.
288. Rubinstein, R.Y. and D.P. Kroese, *Simulation and the Monte Carlo Method.* 2016.
289. Harrison, R.L., *Introduction to Monte Carlo Simulation.* AIP Conference Proceedings, 2010. **1204**(1): p. 17-21.
290. Bauer, N., et al., *Shared Socio-Economic Pathways of the Energy Sector – Quantifying the Narratives.* Global Environmental Change, 2017. **42**: p. 316-330.

291. DeCarolis, J.F., K. Hunter, and S. Sreepathi, *The case for repeatable analysis with energy economy optimization models.* Energy Economics, 2012. **34**(6): p. 1845-1853.
292. Stehfest, E., et al., *Integrated assessment of global environmental change with IMAGE 3.0: model description and policy applications*. 2014: Netherlands Environmental Assessment Agency (PBL).
293. Huppmann, D., et al., *The MESSAGEix Integrated Assessment Model and the ix modeling platform (ixmp): An open framework for integrated and cross-cutting analysis of energy, climate, the environment, and sustainable development.* Environmental Modelling & Software, 2019. **112**: p. 143-156.
294. Fujimori, S., T. Masui, and Y. Matsuoka, *AIM/CGE V2.0 Model Formula*, in *Post-2020 Climate Action: Global and Asian Perspectives*, S. Fujimori, M. Kainuma, and T. Masui, Editors. 2017, Springer Singapore: Singapore. p. 201-303.
295. Calvin, K., et al., *GCAM v5.1: representing the linkages between energy, water, land, climate, and economic systems.* Geosci. Model Dev., 2019. **12**(2): p. 677-698.
296. Luderer, G., et al., *Description of the REMIND model (Version 1.6)*. 2015.
297. IEA-ETSAP. *IEA-ETSAP*. 2021 [cited 2021 5 August]; Available from: https://iea-etsap.org/.
298. IEA, *World Energy Model*. 2020, International Energy Agency (IEA): Paris, France.
299. Climate Interactive. *En-ROADS: Climate Change Solutions Simulator*. 2021 [cited 2021 5 August]; Available from: https://www.climateinteractive.org/tools/en-roads/.
300. Mercure, J.-F., et al., *Environmental impact assessment for climate change policy with the simulation-based integrated assessment model E3ME-FTT-GENIE.* Energy Strategy Reviews, 2018. **20**: p. 195-208.
301. Pacala, S. and R. Socolow, *Stabilization Wedges: Solving the Climate Problem for the Next 50 Years with Current Technologies.* Science, 2004. **305**(5686): p. 968-972.
302. Barker, T. and S.Ş. Scrieciu, *Modeling Low Climate Stabilization with E3MG: Towards a 'New Economics' Approach to Simulating Energy-Environment-Economy System Dynamics.* The Energy Journal, 2010. **31**: p. 137-164.
303. Jacobson, M.Z. and M.A. Delucchi, *Providing all global energy with wind, water, and solar power, Part I: Technologies, energy resources, quantities and areas of infrastructure, and materials.* Energy Policy, 2011. **39**(3): p. 1154-1169.
304. Delucchi, M.A. and M.Z. Jacobson, *Providing all global energy with wind, water, and solar power, Part II: Reliability, system and transmission costs, and policies.* Energy Policy, 2011. **39**(3): p. 1170-1190.
305. Randers, J. and P. Gilding, *The one degree war plan.* Journal of Global Responsibility, 2010. **1**(1): p. 170-188.
306. Deep Decarbonization Pathways Project, *Pathways to deep decarbonization 2015 report*. 2015.
307. van Vuuren, D.P., et al., *Pathways to achieve a set of ambitious global sustainability objectives by 2050: Explorations using the IMAGE integrated assessment model.* Technological Forecasting and Social Change, 2015. **98**: p. 303-323.
308. van Vuuren, D.P., et al., *Carbon budgets and energy transition pathways.* Environmental Research Letters, 2016. **11**(7): p. 075002.
309. Edenhofer, O., et al., *Renewable energy sources and climate change mitigation: Special report of the intergovernmental panel on climate change*. 2011: Cambridge University Press.
310. Worldwatch Institute, *Renewable Revolution: Low-Carbon Energy by 2030*. 2009, Worldwatch Institute.
311. World Wildlife Fund, *Climate Solutions: WWF's Vision for 2050*. 2007, World Wildlife Fund: Gland, Switzerland.
312. IPCC, *Renewable energy sources and climate change mitigation—special report of the Intergovernmental Panel on Climate Change*, O. Edenhofer, R.P. Madruga, and Y. Sokona, Editors. 2012, Cambridge University Press: New York, NY.

313. Teske, S., et al., *Energy [R]evolution - A sustainable world energy outlook 2015*, S. Teske, S. Sawyer, and O. Schäfer, Editors. 2015, Greenpeace International.
314. Singer, S., J.-P. Denruyter, and D. Yener. *The Energy Report: 100% Renewable Energy by 2050*. 2017. Cham, Switzerland: Springer International Publishing.
315. IRENA, *World Energy Transitions Outlook: 1.5°C Pathway*. 2021, International Renewable Energy Agency: Abu Dhabi.
316. Ram, M., et al., *Global Energy System based on 100% Renewable Energy – Power, Heat, Transport and Desalination Sectors*. 2019, Lappeenranta University of Technology and Energy Watch Group: Lappeenranta, Finland.
317. IEA, *Net Zero by 2050*. 2021, International Energy Agency (IEA): Paris, France.
318. Magne, B., S. Kypreos, and H. Turton, *Technology options for low stabilization pathways with MERGE.* The Energy Journal, 2010. **31**(Special Issue).
319. Willson, P., et al., *Powering the Future: Mapping Out Low-carbon Path to 2050*, in *Parsons Brinckerhoff, Newcastle*. 2009, Parsons Brinckerhoff.
320. Söderholm, P., et al., *Governing the transition to low-carbon futures: A critical survey of energy scenarios for 2050.* Futures, 2011. **43**(10): p. 1105-1116.
321. Wilson, C., et al., *Evaluating Process-based integrated assessment models of climate change mitigation*. 2017: International Institute for Applied Systems Analysis (IIASA).
322. Wiseman, J., T. Edwards, and K. Luckins, *Post carbon pathways: A meta-analysis of 18 large-scale post carbon economy transition strategies.* Environmental Innovation and Societal Transitions, 2013. **8**: p. 76-93.
323. Kempener, R., et al., *A Global renewable energy roadmap: Comparing energy systems models with IRENA's remap 2030 project*, in *Informing Energy and Climate Policies Using Energy Systems Models*. 2015, Springer. p. 43-67.
324. Stammer, D., et al., *Hamburg Climate Futures Outlook 2021. Assessing the plausibility of deep decarbonization by 2050.*, in *Hamburg Climate Futures Outlook*. Cluster of Excellence Climate, Climatic Change, and Society (CLICCS): Hamburg, Germany.
325. Eggler, L., *D3.1 Review of information on IAMs*, in *LOCOMOTION*. 2020, University of Valladolid: Valladolid, Spain.
326. Saltelli, A., et al., *The technique is never neutral. How methodological choices condition the generation of narratives for sustainability.* Environmental Science & Policy, 2020. **106**: p. 87-98.
327. Nieto, J., et al., *Macroeconomic modelling under energy constraints: Global low carbon transition scenarios.* Energy Policy, 2020. **137**: p. 111090.
328. Sherwood, J., M. Carbajales-Dale, and B.R. Haney, *Putting the Biophysical (Back) in Economics: A Taxonomic Review of Modeling the Earth-Bound Economy.* Biophysical Economics and Sustainability, 2020. **5**(1): p. 4.
329. Fiddaman, T.S., *Exploring policy options with a behavioral climate–economy model.* System Dynamics Review, 2002. **18**(2): p. 243-267.
330. Solow, R.M., *A Contribution to the Theory of Economic Growth.* The Quarterly Journal of Economics, 1956. **70**(1): p. 65-94.
331. King, L.C. and J.C.J.M. van den Bergh, *Implications of net energy-return-on-investment for a low-carbon energy transition.* Nature Energy, 2018. **3**(4): p. 334-340.
332. Bardi, U. and S. Sgouridis, *In Support of a Physics-Based Energy Transition Planning: Sowing Our Future Energy Needs.* BioPhysical Economics and Resource Quality, 2017. **2**(4): p. 14.
333. Saltelli, A., et al., *Why so many published sensitivity analyses are false: A systematic review of sensitivity analysis practices.* Environmental Modelling & Software, 2019. **114**: p. 29-39.
334. Clack, C.T.M., et al., *Evaluation of a proposal for reliable low-cost grid power with 100% wind, water, and solar.* Proceedings of the National Academy of Sciences, 2017. **114**(26): p. 6722-6727.

335. Hounam, I., *STER - A Global Energy Supply Model*, in *Energy systems analysis: proceedings of the International Conference*. 1979: Dublin, Ireland.
336. Slesser, M., *ECCO User Manual Part 1. The Resource Use Institute.* Edinburgh, Scotland, 1992.
337. Sterman, J.D., *The energy transition and the economy: a system dynamics approach*. 1982, Massachusetts Institute of Technology: Boston, USA.
338. Bodger, P.S. and J.T. Baines, *Dynamics of an energy-economic system subject to an energy substitution sequence.* Energy systems and policy, 1988. **12**(3): p. 167-178.
339. Fiddaman, T. *A feedback-rich climate-economy model*. in *16th International Conference of the Systems Dynamics Society*. 1998. Quebec, Canada.
340. Hafner, S., et al., *Emergence of New Economics Energy Transition Models: A Review.* Ecological Economics, 2020. **177**: p. 106779.
341. Sers, M.R. and P.A. Victor, *The Energy-emissions Trap.* Ecological Economics, 2018. **151**: p. 10-21.
342. Dale, M.A.J., *GLOBAL ENERGY MODELLING: A BIOPHYSICAL APPROACH (GEMBA)*, in *Mechanical Engineering*. 2010, University of Canterbury: Christchurch, New Zealand. p. 441.
343. Dale, M., S. Krumdieck, and P. Bodger, *Global energy modelling — A biophysical approach (GEMBA) part 1: An overview of biophysical economics.* Ecological Economics, 2012. **73**: p. 152-157.
344. Capellán-Pérez, I., et al., *World Limits Model (WoLiM) 1.5 - Model Documentation. Technical Report*. 2017, Energy, Economy and System Dynamics Group of the University of Valladolid: Valladolid, Spain. p. 98.
345. Bardi, U., et al., *The Sower's Way: A Strategy to Attain the Energy Transition.* International Journal of Heat and Technology, 2016. **34**(2): p. 3.
346. Keyßer, L.T. and M. Lenzen, *1.5 °C degrowth scenarios suggest the need for new mitigation pathways.* Nature Communications, 2021. **12**(1): p. 2676.
347. Funtowicz, S.O. and J.R. Ravetz, *Science for the Post Normal Age*, in *Perspectives on Ecological Integrity*, L. Westra and J. Lemons, Editors. 1995, Springer: Dordrecht, Netherlands. p. 146-161.
348. Funtowicz, S. and J. Ravetz, *Post-normal science: a new science for new times.* Scientific European, 1990. **266**(10): p. 20-22.
349. Funtowicz, S.O. and J.R. Ravetz, *A New Scientific Methodology for Global Environmental Issues*, in *Ecological Economics: The Science and Management of Sustainability*, R. Costanza, Editor. 1991, Columbia University Press: New York, USA. p. 137-152.
350. Ravetz, I., *What is post-normal science.* Futures, 1999. **31**(7): p. 647-654.
351. Kay, J.J., et al., *An ecosystem approach for sustainability: addressing the challenge of complexity.* Futures, 1999. **31**(7): p. 721-742.
352. Van Der Sluijs, J.P., et al., *Combining Quantitative and Qualitative Measures of Uncertainty in Model-Based Environmental Assessment: The NUSAP System.* Risk Analysis, 2005. **25**(2): p. 481-492.
353. Saltelli, A., et al., *What do I make of your latinorum? Sensitivity auditing of mathematical modelling.* International Journal of Foresight and Innovation Policy, 2013. **9**(2-3-4): p. 213-234.
354. Saltelli, A., *Sensitivity Analysis for Importance Assessment.* Risk Analysis, 2002. **22**(3): p. 579-590.
355. Murphy, D.J., M. Carbajales-Dale, and D. Moeller, *Comparing Apples to Apples: Why the Net Energy Analysis Community Needs to Adopt the Life-Cycle Analysis Framework.* Energies, 2016. **9**(11): p. 917.
356. Lamont, A.D., *Assessing the long-term system value of intermittent electric generation technologies.* Energy Economics, 2008. **30**(3): p. 1208-1231.
357. Wang, Q.-G., et al., *Introduction*, in *PID Control for Multivariable Processes*, Q.-G. Wang, et al., Editors. 2008, Springer Berlin Heidelberg: Berlin, Heidelberg. p. 1-8.

358. Odhnoff, J., *On the Techniques of Optimizing and Satisficing.* The Swedish Journal of Economics, 1965. **67**(1): p. 24-39.
359. Wierzbicki, A.P., *A mathematical basis for satisficing decision making.* Mathematical Modelling, 1982. **3**(5): p. 391-405.
360. Goodrich, M.A., W.C. Stirling, and R.L. Frost, *A theory of satisficing decisions and control.* IEEE Transactions on Systems, Man, and Cybernetics - Part A: Systems and Humans, 1998. **28**(6): p. 763-779.
361. GoldSim Technology Group. *GoldSim User's Guide (Version 12.1)*. 2018 June; Available from: https://www.goldsim.com/Web/Customers/Education/Documentation/.
362. Millar, R.J., et al., *Emission budgets and pathways consistent with limiting warming to 1.5 °C.* Nature Geoscience, 2017. **10**(10): p. 741-747.
363. Friedlingstein, P., et al., *Persistent growth of CO2 emissions and implications for reaching climate targets.* Nature Geoscience, 2014. **7**(10): p. 709-715.
364. Grübler, A., et al., *A low energy demand scenario for meeting the 1.5 °C target and sustainable development goals without negative emission technologies.* Nature Energy, 2018. **3**(6): p. 515-527.
365. Graus, W., E. Blomen, and E. Worrell, *Global energy efficiency improvement in the long term: a demand- and supply-side perspective.* Energy Efficiency, 2011. **4**(3): p. 435-463.
366. Mediavilla, M., et al., *The transition towards renewable energies: Physical limits and temporal conditions.* Energy Policy, 2013. **52**: p. 297-311.
367. Heuberger, C.F. and N. Mac Dowell, *Real-World Challenges with a Rapid Transition to 100% Renewable Power Systems.* Joule, 2018. **2**(3): p. 367-370.
368. EIA. *Table 8.1. Average Operating Heat Rate for Selected Energy Sources*. 2019 [cited 2019 3 December]; Available from: https://www.eia.gov/electricity/annual/html/epa_08_01.html.
369. IEA, *Extended world energy balances*, in *IEA World Energy Statistics and Balances*. 2019, International Energy Agency.
370. Engineering ToolBox. *Fuels - Higher and Lower Calorific Values*. 2003 [cited 2019 3 December]; Available from: https://www.engineeringtoolbox.com/fuels-higher-calorific-values-d_169.html.
371. EIA, *International Energy Outlook 2019 (tables)*. 2019, U.S. Energy Information Administration.
372. Lisa Schwartz, M.W., William Morrow, Jeff Deason, Steven R. Schiller, Greg Leventis, Sarah Smith, Woei Ling Leow, Todd Levin, Steven Plotkin, Yan Zhou, Joseph Teng, *Electricity end uses, energy efficiency, and distributed energy resources baseline*. 2017, Lawrence Berkeley National Laboratory. p. 391.
373. Huang, W.-D. and Y.H.P. Zhang, *Energy Efficiency Analysis: Biomass-to-Wheel Efficiency Related with Biofuels Production, Fuel Distribution, and Powertrain Systems.* PLOS ONE, 2011. **6**(7): p. e22113.
374. Haberl, H., et al., *Bioenergy: how much can we expect for 2050?* Environmental Research Letters, 2013. **8**(3): p. 031004.
375. Creutzig, F., et al., *Bioenergy and climate change mitigation: an assessment.* GCB Bioenergy, 2015. **7**(5): p. 916-944.
376. Mohr, S., et al., *Projection of world fossil fuels by country.* Fuel, 2015. **141**: p. 120-135.
377. Maggio, G. and G. Cacciola, *When will oil, natural gas, and coal peak?* Fuel, 2012. **98**: p. 111-123.
378. Patzek, T.W. and G.D. Croft, *A global coal production forecast with multi-Hubbert cycle analysis.* Energy, 2010. **35**(8): p. 3109-3122.
379. World Nuclear Association. *Renewable Energy and Electricity*. 2020 [cited 2020 7 July]; Available from: https://www.world-nuclear.org/information-library/energy-and-the-environment/renewable-energy-and-electricity.aspx.
380. EIA. *Refinery Utilization and Capacity*. 2020 [cited 2020 7 July]; Available from: https://www.eia.gov/dnav/pet/pet_pnp_unc_dcu_nus_a.htm.

381. Natural Resources Canada. *Refinery Economics*. 2018 [cited 2020 7 July]; Available from: https://www.nrcan.gc.ca/energy/energy-sources-distribution/refinery-economics/4561.
382. Ramkumar, M. *Why Capacity and Utilization Are the Keys to Refining Revenue*. 2015 [cited 2020 7 July]; Available from: https://marketrealist.com/2015/12/capacity-utilization-keys-refining-revenue/#adnrb=900000.
383. Kucher, O. and J.J. Fletcher, *Economic Feasibility and Investment Decisions of Coal and Biomass to Liquids*. 2011, USAEE. p. 21.
384. Haq, Z., *Biomass for Electricity Generation*. 2011, U.S. Energy Information Administration. p. 18.
385. Lund, J.W., *Direct Utilization of Geothermal Energy.* Energies, 2010. **3**(8): p. 1443-1471.
386. EIA. *Monthly Biodiesel Production Report*. 2020 30 June 2020 [cited 2020 7 July]; Available from: https://www.eia.gov/biofuels/biodiesel/production/.
387. Logan, J., et al., *Electricity Generation Baseline Report*. 2017, National Energy Technology Laboratory (NREL). p. 261.
388. Jouhara, H., et al., *Waste heat recovery technologies and applications.* Thermal Science and Engineering Progress, 2018. **6**: p. 268-289.
389. GE, *GE Global Power Plant Efficiency Analysis*. 2015, GE. p. 4.
390. Wang, M., *Estimation of Energy Efficiencies of U.S. Petroleum Refineries*. 2008, Argonne National Laboratory. p. 10.
391. Höök, M. and K. Aleklett, *A review on coal-to-liquid fuels and its coal consumption.* International journal of energy research, 2010. **34**(10): p. 848-864.
392. Zhang, H.L., et al., *Concentrated solar power plants: Review and design methodology.* Renewable and Sustainable Energy Reviews, 2013. **22**: p. 466-481.
393. The World Bank. *Electric power transmission and distribution losses (% of output)*. 2018 [cited 2020 7 July]; Available from: https://data.worldbank.org/indicator/EG.ELC.LOSS.ZS.
394. Jackson, R., et al., *Opportunities for Energy Efficiency Improvements in the U.S. Electricity Transmission and Distribution System*. 2015, Oak Ridge National Laboratory: Oak Ridge, TN. p. 47.
395. ProCon.org. *Historical Timeline: History of Alternative Energy and Fossil Fuels*. 2019 24 September 2019 [cited 2020 17 January]; Available from: https://alternativeenergy.procon.org/view.timeline.php?timelineID=000015.
396. Powermag.com. *An Interactive TImeline: The History of Power*. 2014 [cited 2019 17 January]; Available from: https://www.powermag.com/an-interactive-timeline-the-history-of-power/.
397. Schulz, H., *Short history and present trends of Fischer–Tropsch synthesis.* Applied Catalysis A: General, 1999. **186**(1): p. 3-12.
398. Bell, T. *The History of Steel: From Iron Age to Electric Arc Furnaces*. 2019 27 August 2019 [cited 2020 18 January]; Available from: https://www.thebalance.com/steel-history-2340172.
399. Wikipedia. *Energy efficiency in transport*. 2020 2 July 2020 [cited 2020 7 July]; Available from: https://en.wikipedia.org/wiki/Energy_efficiency_in_transport.
400. Deutsche Bahn. *Energy efficiency increased*. 2016 Integrated Report 2016 [cited 2020 7 July]; Available from: https://ib.deutschebahn.com/ib2016/en/group-management-report/group-performance-environmental-dimension/progress-in-climate-protection/energy-efficiency-increased/.
401. Oak Ridge National Laboratory. *Transportation Energy Data Book: Edition 38.1*. 2020 30 April 2020 [cited 2020 7 July]; Available from: https://tedb.ornl.gov/data/.
402. Natural Resources Canada. *Transportation Sector – Energy Use Analysis*. National Energy Use Database 2020 [cited 2020 7 July]; Available from: https://oee.rncan.gc.ca/corporate/statistics/neud/dpa/showTable.cfm?type=AN&sector=tran&juris=00&rn=1&page=7.
403. IEA. *Tracking Transport 2020*. 2020 May 2020 [cited 2020 7 July]; Available from: https://www.iea.org/reports/tracking-transport-2020.

404. OpenEI. *Transparent Cost Database*. 2020 [cited 2020 7 July]; Available from: https://openei.org/apps/TCDB/#blank.
405. Dale, M., *A Comparative Analysis of Energy Costs of Photovoltaic, Solar Thermal, and Wind Electricity Generation Technologies.* Applied Sciences, 2013. **3**(2): p. 325-337.
406. Gagnon, N., C.A.S. Hall, and L. Brinker, *A Preliminary Investigation of Energy Return on Energy Investment for Global Oil and Gas Production.* Energies, 2009. **2**(3): p. 490-503.
407. Raugei, M. and E. Leccisi, *A comprehensive assessment of the energy performance of the full range of electricity generation technologies deployed in the United Kingdom.* Energy Policy, 2016. **90**: p. 46-59.
408. de Castro, C. and I. Capellán-Pérez, *Concentrated Solar Power: Actual Performance and Foreseeable Future in High Penetration Scenarios of Renewable Energies.* BioPhysical Economics and Resource Quality, 2018. **3**(3): p. 14.
409. Weißbach, D., et al., *Energy intensities, EROIs (energy returned on invested), and energy payback times of electricity generating power plants.* Energy, 2013. **52**: p. 210-221.
410. EPA, *Emission Factors for Greenhouse Gas Inventories*. 2014, U.S. Environmental Protection Agency. p. 5.
411. Quaschning, V. *Specific Carbon Dioxide Emissions of Various Fuels*. 2015 June 2015; Available from: https://www.volker-quaschning.de/datserv/CO2-spez/index_e.php.
412. Ritchie, H. and M. Roser. *CO_2 and Greenhouse Gas Emissions*. 2017 December 2019 [cited 2020 7 July]; Available from: https://ourworldindata.org/co2-and-other-greenhouse-gas-emissions.
413. EIA. *Annual Energy Outlook 2020: Table 8. Electricity Supply, Disposition, Prices, and Emissions*. 2020 [cited 2020 6 December]; Available from: https://www.eia.gov/outlooks/aeo/data/browser/#/?id=8-AEO2020&cases=ref2020&sourcekey=0.
414. Leiva, B., *Why Are Prices Proportional to Embodied Energies?* BioPhysical Economics and Resource Quality, 2019. **4**(3): p. 14.
415. EIA. *Rail continues to dominate coal shipments to the power sector*. 2016 24 February 2016 [cited 2020 6 December]; Available from: https://www.eia.gov/todayinenergy/detail.php?id=25092.
416. EIA. *Natural gas explained: Natural gas prices*. 2020 6 October 2020 [cited 2020 6 December]; Available from: https://www.eia.gov/energyexplained/natural-gas/prices.php.
417. Smil, V., *EMBODIED ENERGY: MOBILE DEVICES AND CARS*, in *IEEE Spectrum*. 2016, IEEE. p. 26.
418. Alstone, P., E. Mills, and A. Jacobson, *Embodied Energy and Off-Grid Lighting*, in *THE LUMINA PROJECT*. 2011, Office of Scientific and Technical Information. p. 30.

9 APPENDIX 1: PRESS MODEL DOCUMENTATION

Probabilistic Renewable Energy Solution Space Model version 1.3

9.1 VERSION HISTORY

Version	Date	Description
1.3	*31/01/2021*	Final stable model build including re-optimization of control parameters
1.2	*11/01/2021*	• Fixed ECC inputs following input data calculation error • Investment share calculations updated to correct for variable EC cost • Upstream CF curtailment for excessive surplus introduced
1.1	*13/07/2020*	• Fixed thermal equivalence weighting for EROI and ECC calculations (for electricity component) • Separated intermittent electricity AI as an independent secondary AI category, including updated modifiers • Simplified and condensed efficiency function input arrays • Changed efficiency calculations for oil heat and coal CHP • Various other fixes
1.0	*24/05/2020*	Initial stable model build

9.2 FEEDBACK LOOP DESCRIPTIONS

Feedback loops listed here relate to the causal loop diagrams in sections 4.2.6 and 5.2. Table 11 lists balancing (negative) feedback loops and Table 12 lists reinforcing (positive) feedback loops. Loops listed in blue text originate in system control.

Table 11: descriptions and associated phenomena for balancing feedback loops

Identifier	Description	Phenomena
B1	Increases in secondary reticulation efficiency cause greater EC production reducing EC deficit, which can lead to increased upstream curtailment, lower secondary CF, reduced secondary output, and slower subsequent gains in secondary reticulation efficiency.	*Diminishing efficiency gains*
B2	Increased production of ECs leads to reduced EC deficit which can increase upstream curtailment, reducing secondary CF and lowering production of ECs.	*Surplus avoidance via upstream curtailment*
B3	Increases in EU to ES efficiency reduce EU CF causing reduced EU output and slower subsequent gains in EU to ES efficiency.	Diminishing efficiency gains
B4	Increases in upstream investment increase GES metabolic consumption and ESMR, which can decrease investment.	*Metabolic limit to investment*
B5	Increases in upstream investment increase secondary AI, GES metabolic consumption, and ESMR, which can decrease investment.	*Metabolic limit to investment*
B6	Increases in upstream investment eventually increase upstream decommissioning, GES metabolic consumption and ESMR, which can decrease investment.	*Metabolic limit to investment*

Identifier	Description	Phenomena
B7	Increases in upstream investment increase secondary PC, GES metabolic consumption, and ESMR, which can decrease investment.	*Metabolic limit to investment*
B8	Increases in EC deficit increase upstream investment, secondary PC, and EC production, which reduces EC deficits.	*Supply-side deficit resolution*
B9	Increases in downstream investment increase GES metabolic consumption and ESMR, which can decrease investment.	*Metabolic limit to investment*
B10	Increases in downstream investment increase EU AI, GES metabolic consumption, and ESMR, which can decrease investment.	*Metabolic limit to investment*
B11	Increases in downstream investment eventually increase downstream decommissioning, GES metabolic consumption and ESMR, which can decrease investment.	*Metabolic limit to investment*
B12	Increases in downstream investment increase EU PC, GES metabolic consumption, and ESMR, which can decrease investment.	*Metabolic limit to investment*
B13	Increases in downstream investment increase EU PC, decreasing EU CF, which can decrease downstream investment.	*Upkeep of end-use capital*
B14	Increases in downstream investment increase EU PC, decreasing EU CF, final EC consumption, and EC deficit, which can decrease downstream investment.	*End-use power capacity utilization*
B15	Increases in downstream investment increase EU PC, decreasing EU CF and final EC consumption, increasing ESMR, which can decrease downstream investment.	*End-use power capacity utilization*
B16	Depletion of NRE resource decreases NRE EROI, increasing GES metabolic consumption, upstream investment, and eventually upstream decommissioning, reducing NRE PC slowing depletion of NRE resource.	*NRE resource quality decline*
B17	Exhaustion of RE potential decreases RE EROI, increasing GES metabolic consumption, upstream investment, and eventually upstream decommissioning, reducing RE PC slowing exhaustion of RE potential.	*RE resource quality decline*
B18	Depletion of NRE resource decreases NRE EROI, increasing GES metabolic consumption and ESMR, which can decrease investment and NRE power capacity, slowing depletion of NRE resource.	*NRE resource quality decline*
B19	Exhaustion of RE potential decreases RE EROI, increasing GES metabolic consumption and ESMR, which can decrease investment and RE power capacity, slowing exhaustion of RE potential.	*RE resource quality decline*
B20	Increases in upstream investment increase RE PC, which can increase intermittent penetration, secondary AI, GES metabolic consumption, and ESMR, which can decrease investment.	*Intermittent penetration feedback*
B21	Increases in upstream investment increase NRE PC, GES metabolic consumption, and ESMR, which can decrease investment.	*Metabolic limit to investment*
B22	Increases in upstream investment increase RE PC, GES metabolic consumption, and ESMR, which can decrease investment.	*Metabolic limit to investment*
B23	Decreases in RE EROI increases GES metabolic consumption, upstream investment, and eventually upstream decommissioning, slowing declines in RE EROI.	*RE resource redevelopment*
B24	Decreases in RE EROI increases GES metabolic consumption and ESMR, which can decrease upstream investment and eventually upstream decommissioning, reducing RE PC slowing exhaustion of RE potential which reduces declines in RE EROI.	*RE resource redevelopment*
B25	Increases in projected EC deficit increase investment magnitude and committed upstream investment, reducing projected EC deficit.	*Projected supply-side deficit resolution*
B26	Increases in projected EC deficit increase investment magnitude and committed targeted downstream investment, reducing projected EC deficit.	*Projected demand-side deficit resolution*
B27	Targeted increases in downstream investment increases EU PC avoiding consumption of ECs in deficit, which reduces EC deficits and downstream investment.	*Demand-side deficit resolution*

Table 12: descriptions and associated phenomena for reinforcing feedback loops

Identifier	Description	Phenomena
R1	Increases in upstream investment increase secondary PC and EC production, reducing ESMR, which can lead to higher upstream investment.	*Metabolic limit growth/decline*
R2	Increases in upstream investment eventually increase upstream decommissioning, decreasing secondary AI, GES metabolic consumption, and ESMR, which can increase investment.	*Decommissioning feedback*
R3	Increases in upstream investment eventually increase upstream decommissioning, decreasing secondary PC, GES metabolic consumption, and ESMR, which can increase investment.	*Decommissioning feedback*
R4	Increases in downstream investment increase EU PC and final EC consumption, reducing ESMR, which can increase investment.	*Metabolic limit growth/decline*
R5	Increases in downstream investment eventually increase downstream decommissioning, decreasing EU AI, GES metabolic consumption, and ESMR, which can increase investment.	*Decommissioning feedback*
R6	Increases in downstream investment eventually increase downstream decommissioning, decreasing EU PC, GES metabolic consumption, and ESMR, which can increase investment.	*Decommissioning feedback*
R7	Increases in downstream investment increase EU PC, final EC consumption, and EC deficit, which can increase downstream investment.	*Demand-side scale growth/decline*
R8	Increases in upstream investment increase GES metabolic consumption, EC deficit, and upstream investment.	*Commissioning feedback*
R9	Increases in downstream investment increase GES metabolic consumption, EC deficit, which can increase downstream investment.	*Commissioning feedback*
R10	Depletion of NRE resource decreases NRE EROI, increasing GES metabolic consumption, increasing upstream investment and NRE PC, which accelerates depletion of NRE resource.	*NRE resource quality decline*
R11	Exhaustion of RE potential decreases RE EROI, increasing GES metabolic consumption, increasing upstream investment and RE PC, which accelerates exhaustion of RE resource.	*RE resource quality decline*
R12	Decreases in NRE EROI increase EC deficit, projected EC deficit, investment magnitude, and upstream investment, decreasing NRE EROI.	*Projected NRE resource quality decline*
R13	Decreases in RE EROI increase EC deficit, projected EC deficit, investment magnitude, and upstream investment, decreasing RE EROI.	*Projected RE resource quality decline*

9.3 MODEL SECTORS

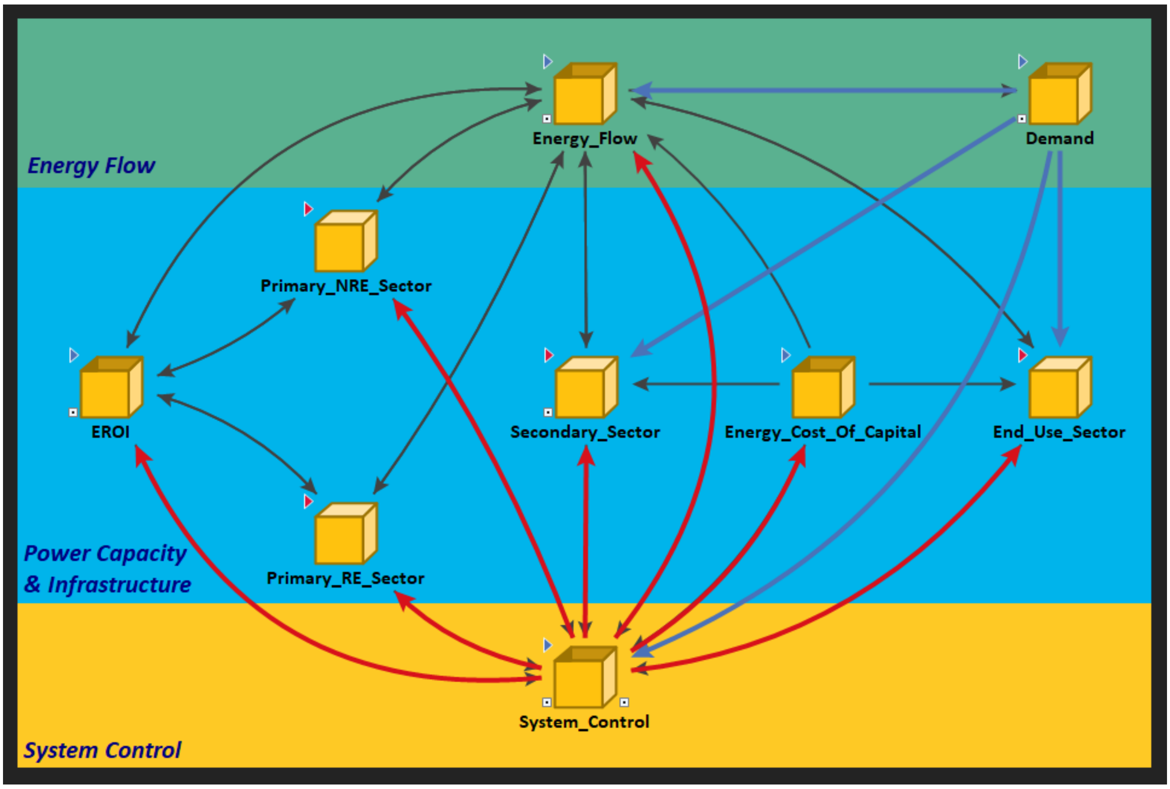

Figure 114: screenshot of the PRESS model within the GoldSim software UI

The PRESS model contains nine model sectors, five open and four localized, and 11 subsectors across three levels of containment. These sectors are arranged into three layers: energy flow, power capacity and infrastructure, and system control, as shown in Figure 114.

GoldSim software features and modelling conventions are detailed in GoldSim Technology Group [361]. The model is constructed to conform to a 500-element limit imposed on the academic GoldSim license used for this research.

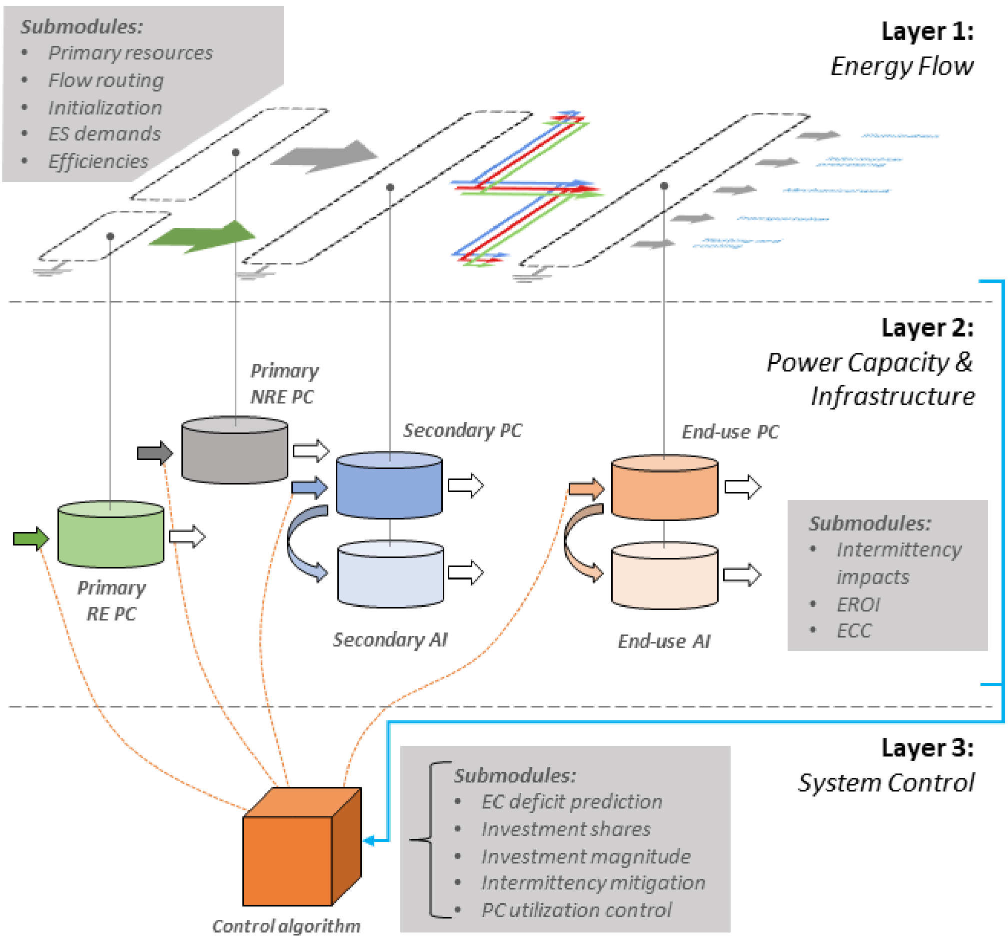

Figure 115: overview of the PRESS model and functional layers

The three functional layers within the PRESS model serve distinct purposes but exhibit mutual dependence, as depicted in Figure 115:

- Layer one contains primary NRE stocks, $\boldsymbol{\omega}$, all energy flows from primary energy resources to the provision of ES demands, $\boldsymbol{p}_x$, flow routing matrices, C_x, and corresponding utilization and efficiencies of PC, $\boldsymbol{u}_x$ and $\boldsymbol{e}_x$. Layer one also contains the static flow calculation and non-linear iterative solver required for model initialization.
- Layer two models PC and AI stocks constituting the GES and enabling the energy flows in layer one. These stocks progress through construction and operating lifecycle phases, $\boldsymbol{w}_x$ and $\boldsymbol{c}_x$, with associated EC input energy costs, $\boldsymbol{\lambda}_x$, $\boldsymbol{\xi}_x$, and $\boldsymbol{\pi}_x$, calculated from the energy cost metrics, EROI, $\boldsymbol{k}_x$, and ECC, $\boldsymbol{y}_x$, disaggregated into constituent ECs.
- Layer three contains the system control heuristic, taking in information regarding the evolving state of the GES from layers one and two and dynamically regulating PC investment flow and intermittency mitigation decision variables, $\boldsymbol{\hat{h}}_r$, $\boldsymbol{\hat{h}}_n$, $\boldsymbol{\hat{h}}_s$, $\boldsymbol{\hat{h}}_e$, and ψ, in response. These decision variables determine the evolution of stocks in layer two.

System control also dynamically adjusts PC utilization in layer one to maintain system stability.

9.3.1 Energy flow

The energy flow sector (shown in Figure 116) is part of layer one and is responsible for the calculation of EC inflows and outflows, $\boldsymbol{p_i}$ and $\boldsymbol{p_o}$, the cumulative supply/demand balance vector, $\boldsymbol{b}$, the final demand EC proportion vector, $\boldsymbol{\delta}$, the ESMR vector, $\boldsymbol{\kappa}$, and the summation of autocatalytic loop and capital hypercycle vectors, $\boldsymbol{p_a}$ and $\boldsymbol{p_c}$. Integrator elements are used for smoothing functions where required for promoting system stability. Various informational output metrics are also calculated here, including RE shares by EC type, system RE share, and point-of-use EROI by EC type.

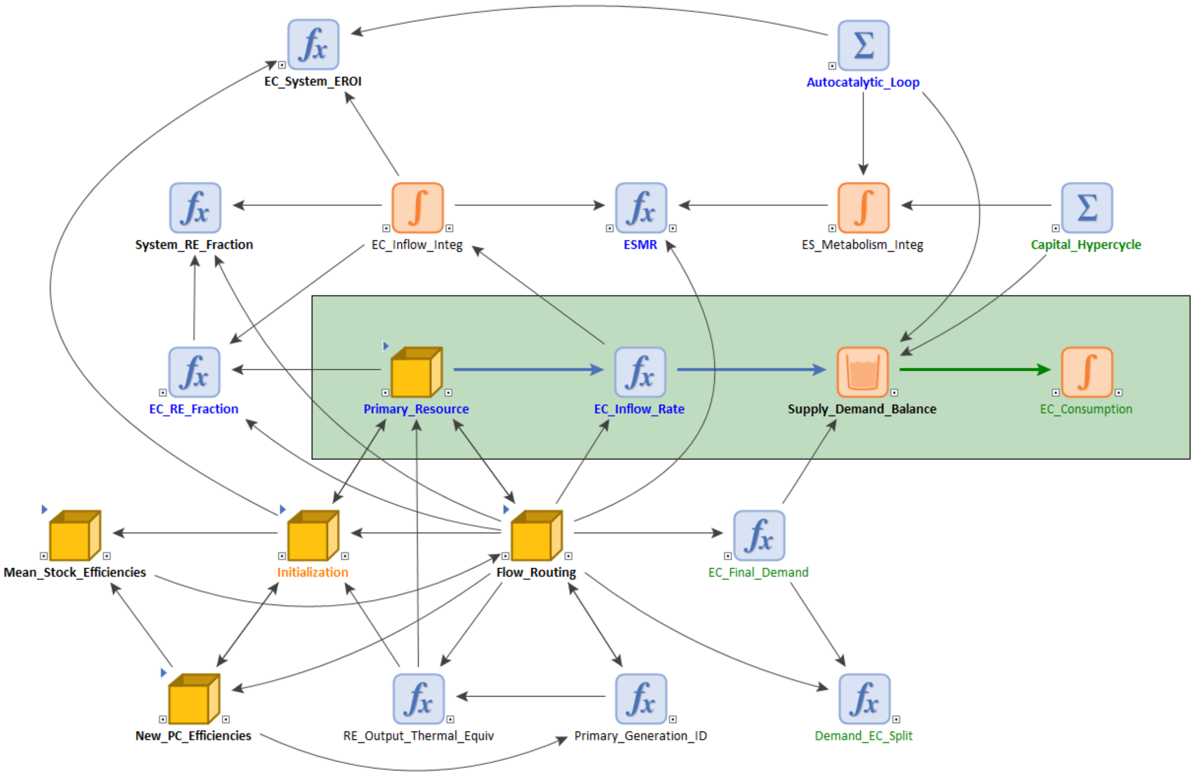

Figure 116: screenshot of the energy flow sector within the GoldSim software UI

9.3.1.1 Initialization

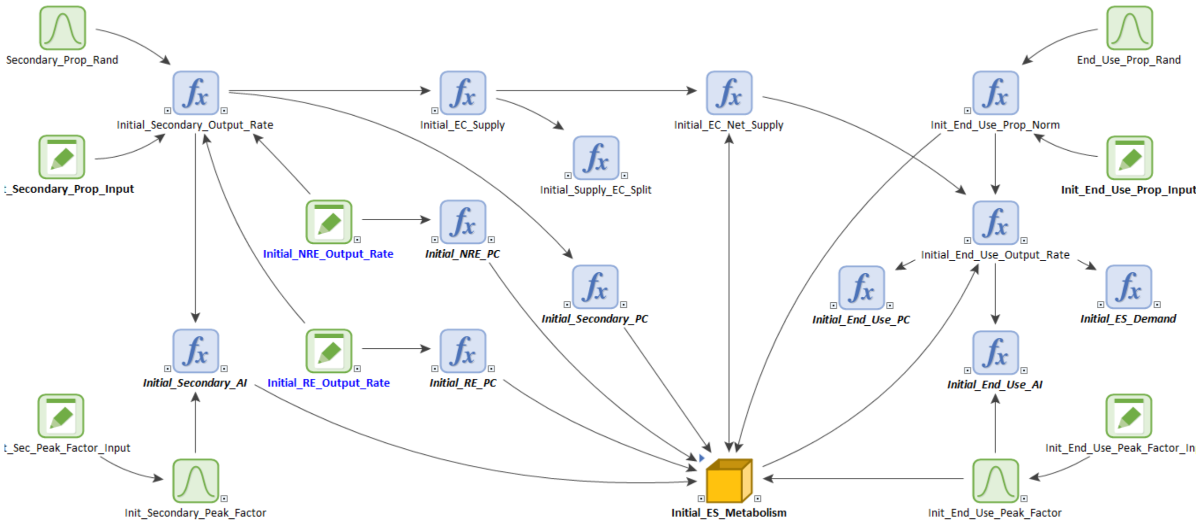

Figure 117: screenshot of the initialization subsector within the GoldSim software UI

The initialization subsector (shown in Figure 117) is responsible for the static flow calculation for model initialization as discussed in section 4.2.7.

Note that the normalized initial PC input proportion vectors, $\boldsymbol{s_s}$ and $\boldsymbol{s_e}$, are randomized with specified error fractions (see sections 9.5.3.1 and 9.5.3.2) and re-normalized such that the sum across each input type is equal to one.

9.3.1.1.1 Initial ES metabolism

The initial ES metabolism subsector (shown in Figure 118) is responsible for the calculation of initial autocatalytic loop consumption, and initial capital hypercycle consumption via a non-linear iterative solver, as discussed in section 4.2.7. The iterative solver script (the **Initial_Cap_HC_Solver** element in Figure 118) is given in section 9.4.5.2. A warning element is used to notify the user when the solver fails to converge to a suitable solution.

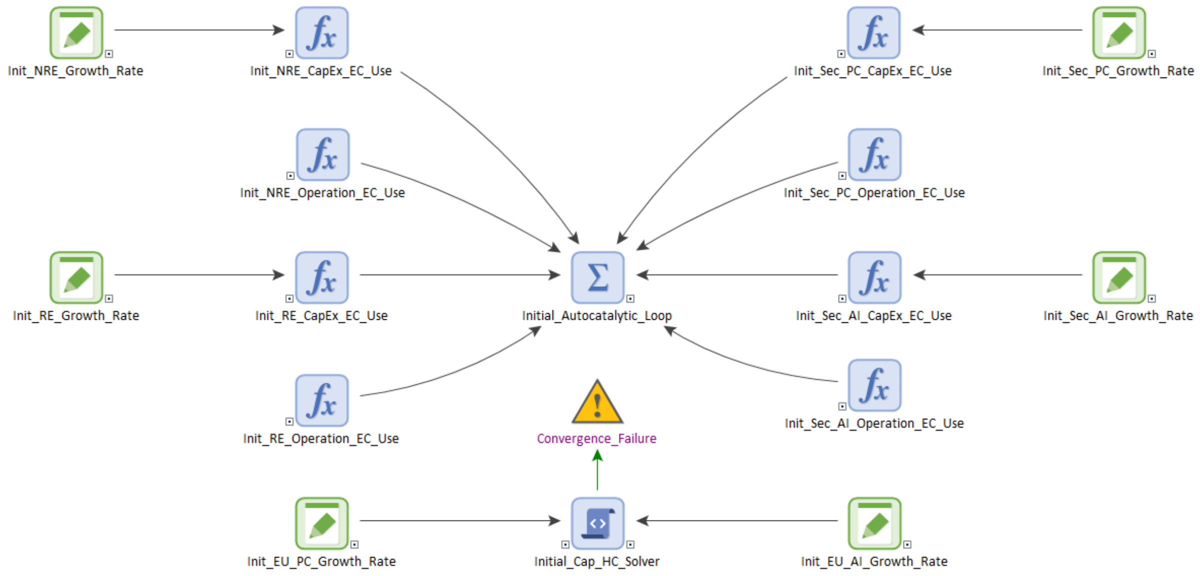

Figure 118: screenshot of the initial ES metabolism subsector within the GoldSim software UI

9.3.1.2 Primary resource

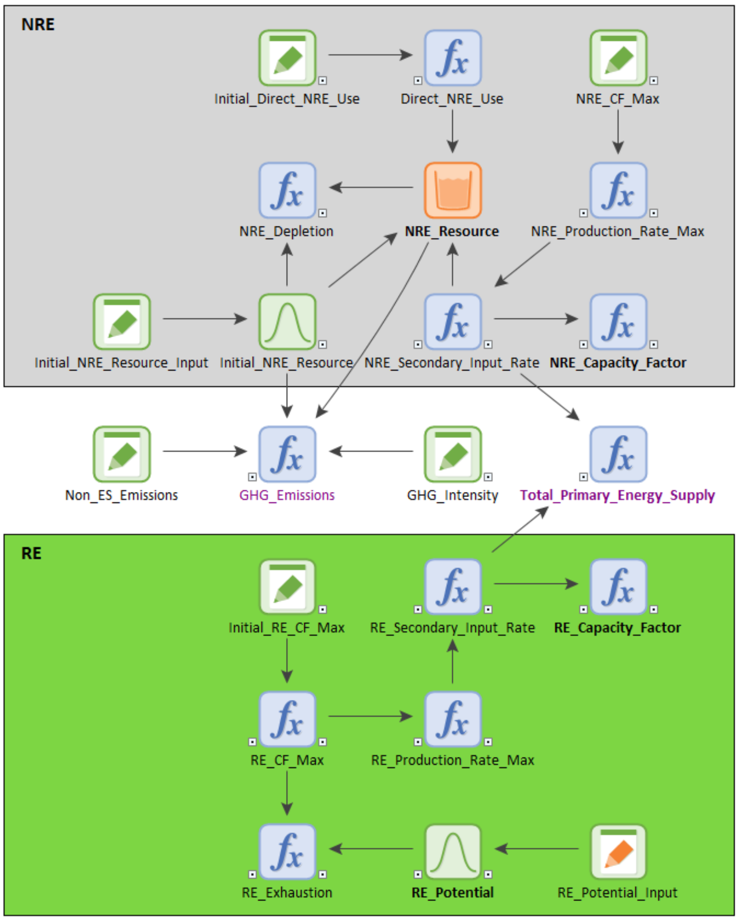

Figure 119: screenshot of the primary resource subsector within the GoldSim software UI

The primary resource subsector (shown in Figure 119) is responsible for the calculation of primary energy flows, $\boldsymbol{p_r}$ and $\boldsymbol{p_n}$, RE exhaustion, $\boldsymbol{x}$, and NRE depletion, $\boldsymbol{d}$. As described in section 4.2.3, primary energy flows are given by the lower of maximum primary PC outputs and corresponding aggregate secondary input capacities. The total primary energy supply (TPES) and cumulative global GHG emissions informational output metrics are also calculated here.

9.3.1.3 Flow routing

The flow routing subsector (shown in Figure 120) is responsible for the calculation of flow routing matrices, PC CFs, EU CF target trends (equations given in section 9.3.1.3.1), cumulative power outputs. Active upstream CF curtailment (section 5.2.5.3) is also implemented here.

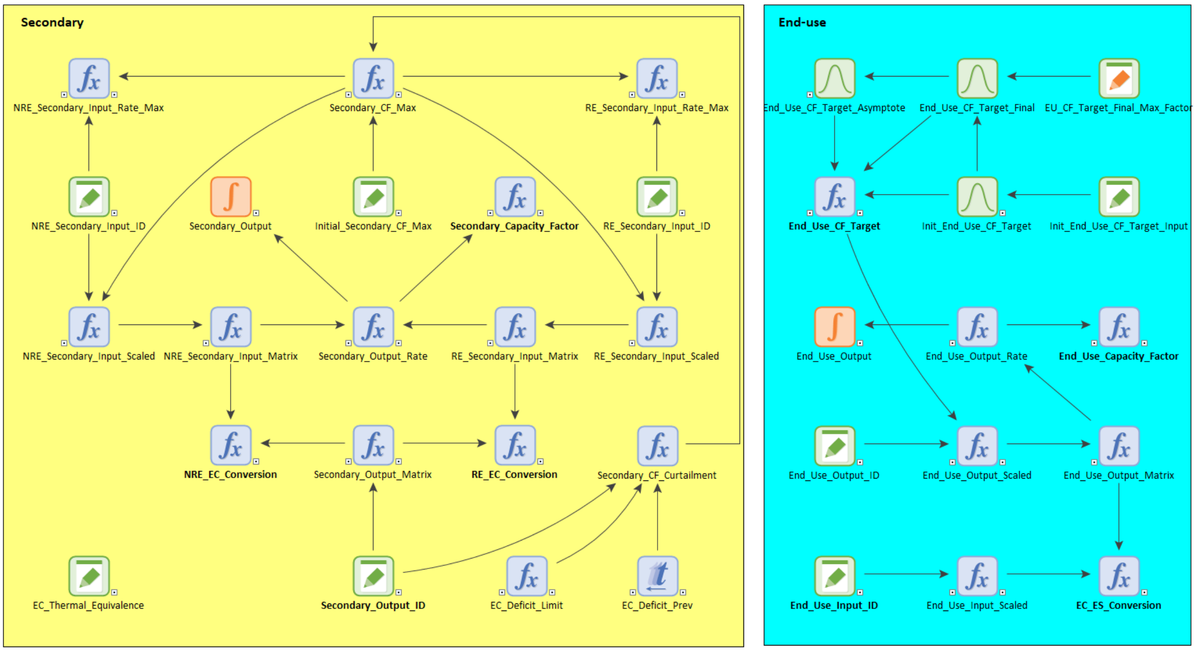

Figure 120: screenshot of the flow routing subsector within the GoldSim software UI

Figure 121 depicts flow mappings between PC types at the primary, secondary, and EU stages, and ES demands specified by the flow mapping identity matrices, I_{rsi}, I_{nsi}, I_{so}, I_{ei}, and I_{eo} introduced in section 4.2.3. NRE associated PC is listed in bold. Note that dotted lines indicate a partial return of input ECs due to cogeneration and waste heat recovery.

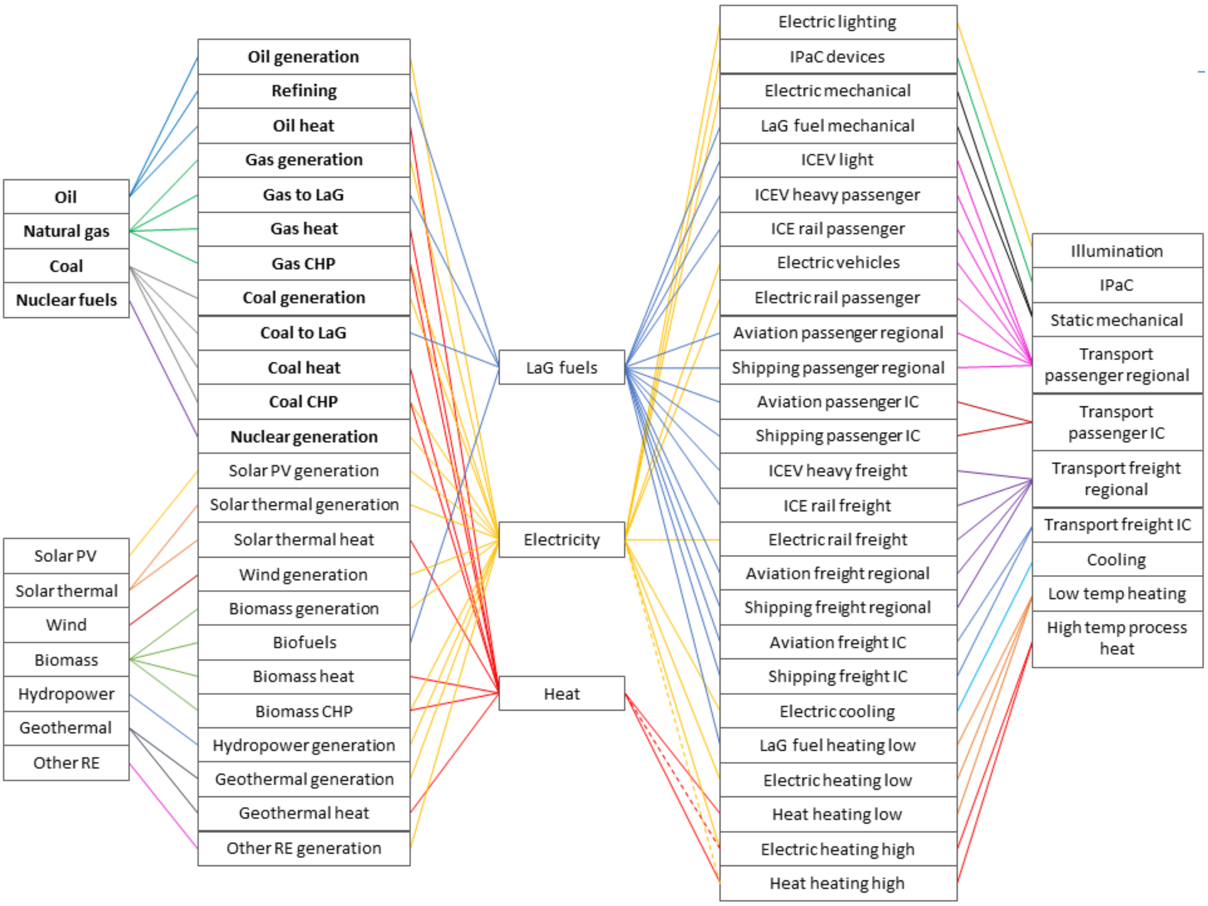

Figure 121: flow mappings between PC types at the primary, secondary, and EU stages, and ES demands

9.3.1.3.1 Logistic function for EU CF target trends

EU CF targets are expected to increase over time, from initial values to specified values after a defined simulation base period, ƫ (units of years):

$$\boldsymbol{u}_{et} = \boldsymbol{v}_{et} \oslash \left(\boldsymbol{j} + (\boldsymbol{v}_{et} \oslash \boldsymbol{u}_{et}(0) - \boldsymbol{j})^{\circ\left(1-\frac{t}{\text{ƫ}}\right)\boldsymbol{j}} \circ (\boldsymbol{v}_{et} \oslash \boldsymbol{u}_{et}(\text{ƫ}) - \boldsymbol{j})^{\circ\frac{t\boldsymbol{j}}{\text{ƫ}}}\right)$$

Where, $\boldsymbol{u}_{et}$ is the vector of EU CF targets (dimensionless),

$\boldsymbol{v}_{et}$ is the upper function asymptote vector (dimensionless),

$\boldsymbol{u}_{et}(0)$ is the vector of EU CF targets at $t = 0$, and

$\boldsymbol{u}_{et}(\text{ƫ})$ is the vector of EU CF targets at $t = \text{ƫ}$.

$\boldsymbol{v}_{et}$ is selected from Pareto distributions, as detailed in section 9.4.2.1, $\boldsymbol{u}_{et}(0)$ is selected from uniform distributions, and $\boldsymbol{u}_{et}(\text{ƫ})$ is selected from log-uniform distributions (lower magnitudes more likely due to practical considerations).

9.3.1.4 New PC efficiencies

The new PC efficiencies subsector (shown in Figure 122) is responsible for the calculation of secondary and EU conversion (PC input), and secondary reticulation and EU to ES (PC output) efficiencies for new PC, as cumulative secondary and EU PC power output increases. Equations are given in section 9.3.1.4.1.

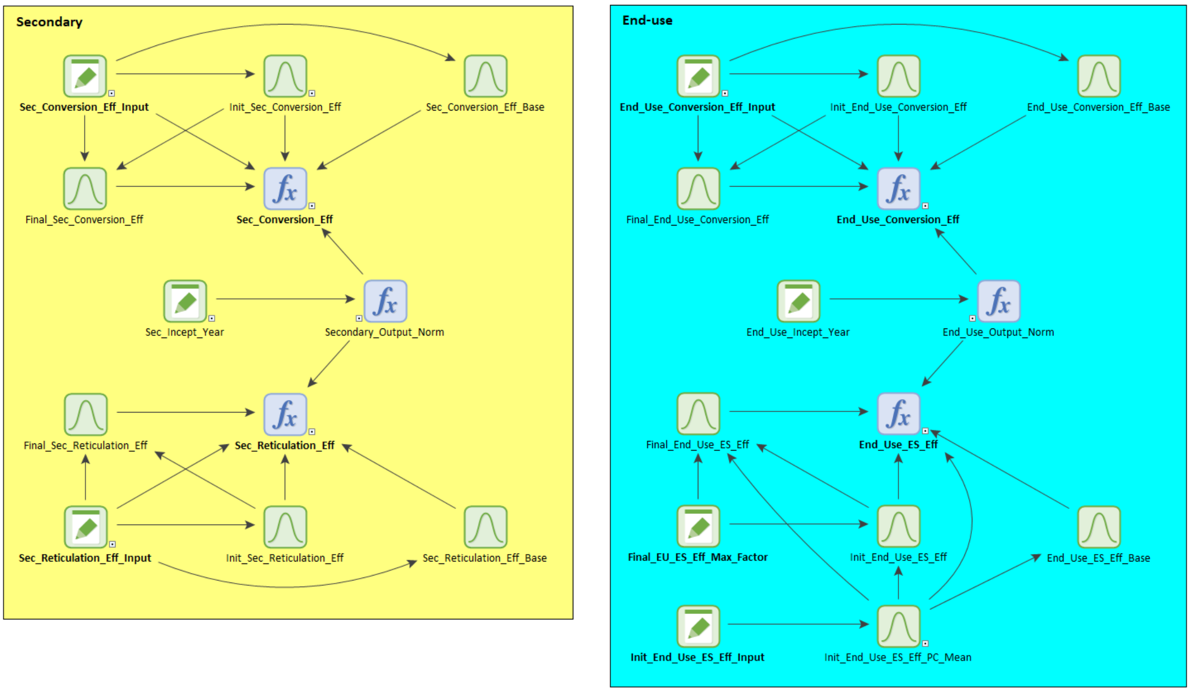

Figure 122: screenshot of the new PC efficiencies subsector within the GoldSim software UI

9.3.1.4.1 Logistic function for new PC efficiency trends

The effective efficiencies for new secondary or EU PC increases as functions of secondary or EU cumulative power output, due to technological learning effects. Ayres and Warr [141] conclude that the use of logistic curves to project future efficiency improvements, as functions of cumulative production, is justified. Cumulative power output from each PC type must be normalized by total pre-simulation cumulative power output to give the vector $\boldsymbol{\unicode{x1D7D}_x}$ (dimensionless):

$$\unicode{x1D7D}_x(t=\tau) = \int_0^{\tau} \boldsymbol{p_x}\,dt \oslash \int_{-\boldsymbol{n_x}}^{\boldsymbol{0}} \boldsymbol{p_x}\,dt \approx 2\int_0^{\tau} \boldsymbol{p_x}\,dt \oslash \left(\boldsymbol{n_x} \circ \boldsymbol{p_x}(0)\right)$$

Where, Subscript ***x*** is replaced with ***s*** and ***e*** to denote secondary and EU, respectively, and

$\boldsymbol{n_x}$ is a vector of technology ages (from technology inception to the start of the study period, in units of years).

Pre-simulation power output is assumed to take an approximately linear trend from technology inception to the start of the study period. Note that while using historical power output time series would be more accurate, and this linear approximation is likely to underestimate pre-simulation cumulative power output for mature technologies and overestimate it for new technologies, historical time series are not available for PC types as defined in the modelling formulation. Linear approximations are considered acceptable given other sources of stochasticity modelled in the generation of the logistic functions (see section 9.4.2).

Vectors of efficiencies for new PC additions, $\boldsymbol{\text{ə}}_{y}$, can then be given by,

$$\text{ə}_y = \boldsymbol{\alpha}_y + \left(\boldsymbol{\upsilon}_y - \boldsymbol{\alpha}_y\right) \oslash$$

$$\left(\boldsymbol{j} + \left(\left(\boldsymbol{\upsilon}_y - \text{ə}_y(\mathbf{0})\right) \oslash \left(\text{ə}_y(\mathbf{0})\right.\right.\right.$$

$$\left.\left.- \boldsymbol{\alpha}_y\right)\right)^{\circ(\boldsymbol{j} - \text{ꝑ}_x \oslash \text{ɑ}_x)} \circ \left(\boldsymbol{j} \oslash \left(\boldsymbol{j} \oslash \left(\boldsymbol{j} + \left(\boldsymbol{\upsilon}_y - \text{ə}_y(\mathbf{0})\right) \oslash \left(\text{ə}_y(\mathbf{0}) - \boldsymbol{\alpha}_y\right)\right.\right.\right.$$

$$\left.\left.\left.- \left(\text{ə}_y(\mathbf{0}) - \boldsymbol{e}_y(\mathbf{0})\right) \oslash \left(\boldsymbol{\upsilon}_y - \boldsymbol{\alpha}_y\right)\right) - \boldsymbol{j}\right)^{\circ(\text{ꝑ}_x \oslash \text{ɑ}_x)}\right)$$

Where, Subscript ***y*** is replaced with ***si*** and ***so*** (and the subscript ***x*** replaced by ***s***) to denote secondary conversion and reticulation efficiencies, and with ***ei*** and ***eo*** (and the subscript ***x*** replaced by ***e***) to denote EU conversion and EU to ES efficiencies, respectively,

$\boldsymbol{\text{ɑ}}_{x}$ is the normalized pre-simulation cumulative output from the PC stock in operation at the beginning of the study period (dimensionless),

$\boldsymbol{\text{ə}}_{x}(0)$ is the vector of initial new PC efficiency values at $\boldsymbol{\text{ꝑ}}_{x} = \mathbf{0}$ ($t = 0$),

$\boldsymbol{\upsilon}_{y}$ is the upper function asymptote vector (dimensionless), and

$\boldsymbol{\alpha}_{y}$ is the lower function asymptote vector (dimensionless).

The normalized pre-simulation cumulative output, $\boldsymbol{\text{ɑ}}_{x}$, is calculated over half of PC lifetime prior to the beginning of the study period, assuming a uniform PC age distribution and a linear pre-simulation trend in power output. The values are negative as they refer to points left of the origin on the x-axis. This vector allows the new PC efficiency curve to coincide with the specified PC stock mean efficiency, $\boldsymbol{e}_{x}(\mathbf{0})$:

$$\text{ɑ}_x = (\boldsymbol{l}_x \oslash \boldsymbol{n}_x) \circ (\boldsymbol{l}_x \oslash \mathbf{4}\boldsymbol{n}_x - \boldsymbol{j})$$

$$\therefore \text{ꝑ}_x \oslash \text{ɑ}_x = 2\int_0^{\tau} \boldsymbol{p}_x \, dt \oslash \left(\boldsymbol{l}_x \circ \boldsymbol{p}_x(\mathbf{0}) \circ (\boldsymbol{l}_x \oslash \mathbf{4}\boldsymbol{n}_x - \boldsymbol{j})\right)$$

$\boldsymbol{\text{ə}}_{x}(\mathbf{0})$ values are selected from triangular distributions spanning the initial mean PC stock efficiencies to the maximum final efficiencies, as initial new PC efficiencies are more likely closer to the initial mean PC stock efficiencies than the maximum theoretical efficiencies (probability maxima at initial mean PC stock efficiencies). $\boldsymbol{\upsilon_y}$ values are selected from uniform distributions spanning the initial new PC efficiencies to the maximum theoretical efficiencies. Initial mean PC stock EU to ES efficiencies, $\boldsymbol{e_{eo}(0)}$, are uncertain and are drawn from uniform distributions, spanning specified error ranges (see section 9.4 for details). $\boldsymbol{\alpha_y}$ values correspond to approximate efficiency values at the time of technology inception and are selected from distributions spanning zero to the initial mean PC stock efficiencies ($\boldsymbol{0} < \boldsymbol{\alpha_y} < \boldsymbol{e_y(0)}$):

- Triangular distributions are used for secondary and EU conversion efficiencies, with probability maxima at zero, as these efficiencies are more likely closer to zero than the average of existing PC at the time of technology inception (notes that for many energy conversion technologies, efficiencies started out much lower than their present day values [6, 141]).
- Uniform distributions are used for secondary reticulation and EU to ES efficiencies, as values at the time of technology inception are not biased to the lower ends of the distribution ranges.

9.3.1.5 Mean stock efficiencies

The mean stock efficiencies subsector (shown in Figure 123) is responsible for the calculation of secondary and EU conversion (PC input), and secondary reticulation and EU to ES (PC output) efficiencies for mean PC stocks, as the composition of PC stocks change. Equations are given in section 9.3.1.5.1. Function numerators are modelling using material delay elements in GoldSim.

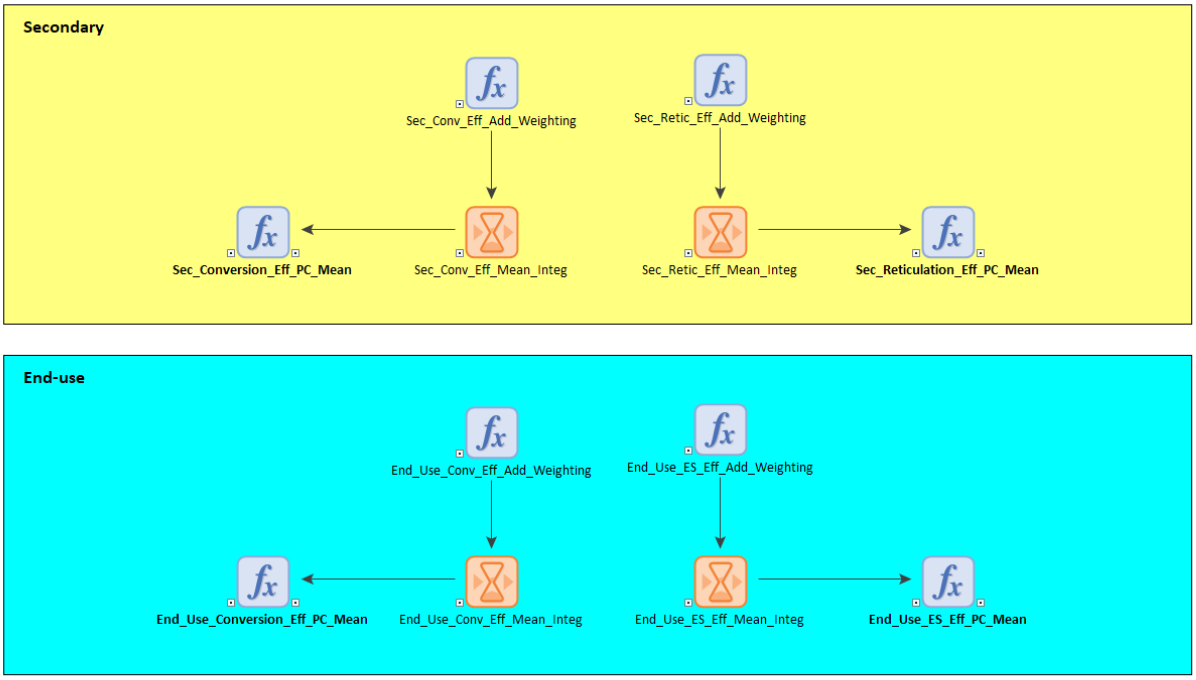

Figure 123: screenshot of the mean stock efficiencies subsector within the GoldSim software UI

9.3.1.5.1 Propagation of new PC efficiency values to mean PC stock values

Mean efficiency values for the extant PC stocks depend on the time-path of investment (the sequence of additions and subsequent decommissioning). Changes in new PC values propagate into mean PC stock values only to the extent that new investment occurs. Mean PC stock values also change as PC is removed at the end of life. These functions are implemented in GoldSim using material delay elements to represent the numerators.

$$\boldsymbol{e}_x(t=\tau) = \left(\boldsymbol{e}_x(\mathbf{0}) \circ \boldsymbol{c}_x(0) + \int_0^\tau \left(\text{ə}_x \circ \boldsymbol{h}_x - \text{ə}_x\left(\text{þ}_x(\tau\boldsymbol{j} - \boldsymbol{l}_x)\right) \circ \boldsymbol{h}_x(\tau\boldsymbol{j}-\boldsymbol{l}_x)\right) dt\right) \oslash \left(\boldsymbol{c}_x(0) + \int_0^\tau \left(\boldsymbol{h}_x - \boldsymbol{h}_x(\tau\boldsymbol{j}-\boldsymbol{l}_x)\right) dt\right)$$

Where, Subscript ***x*** is replaced with ***si***, ***so***, ***ei***, and ***eo*** to denote secondary conversion, secondary reticulation, EU conversion, and EU to ES efficiencies, respectively, and

For $\tau\boldsymbol{j} < \boldsymbol{l}_x$: $\text{ə}_x\left(\text{þ}_x(\tau\boldsymbol{j}-\boldsymbol{l}_x)\right) \approx \boldsymbol{e}_x(\mathbf{0})$.

The vectors $\boldsymbol{\text{ə}}_x$ are approximated as initial mean PC efficiency values for times prior to the start of the study period.

9.3.2 Demand

The demand sector (shown in Figure 124) is part of layer one and is responsible for the calculation of ES demand trends, $\boldsymbol{p_d}$, and demand flexibility, q, as functions of time. Equations are given in sections 9.3.2.1 and 9.3.2.2, respectively.

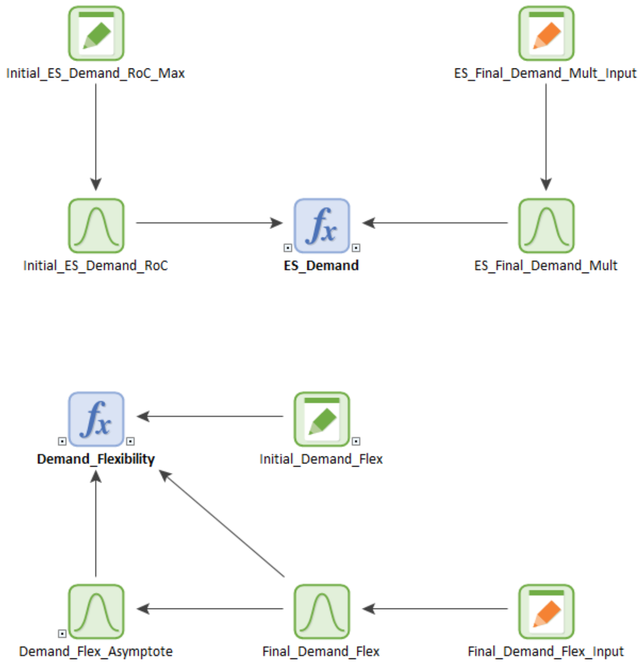

Figure 124: screenshot of the demand sector within the GoldSim software UI

9.3.2.1 Logistic function for ES demand trends

ES demands are widely expected to increase over time as more people gain access to modern energy services typical of lifesyles in the global North. However, as the primary exogenous variable tested by PRESS, a wide range of potential outcomes is included in the modelling formulation, including the possibility for declines in ES demands.

$$\boldsymbol{p_d} = \boldsymbol{p_d}(\infty) \oslash \left(\boldsymbol{j} + (\boldsymbol{p_d}(\infty) \oslash \boldsymbol{p_d}(0) - \boldsymbol{j}) \circ (e\boldsymbol{j})^{\circ\left(\frac{d\boldsymbol{p_d}(0)}{dt} t \oslash (\boldsymbol{p_d}(\infty) \oslash \boldsymbol{p_d}(0) - \boldsymbol{j})\right)}\right)$$

Where, $\boldsymbol{p_d}$ is the vector of ES demands (units of EJ/year),

$\boldsymbol{p_d}(0)$ is the vector of initial ES demands (units of EJ/year),

$\boldsymbol{p_d}(\infty)$ is the final function asymptote vector (units of EJ/year), and

$d\boldsymbol{p_d}(0)/dt$ is the vector of initial rates of change of ES demand (units of EJ/year^2).

$\boldsymbol{p_d}(\infty) \oslash \boldsymbol{p_d}(0)$ is specified directly as a vector of input multiples (eventual ES demand relative to initial), selected from specified uniform distributions, as $\boldsymbol{p_d}(0)$ is calculated as part of the initialization procedure. Input multiples, $\boldsymbol{p_d}(\infty) \oslash \boldsymbol{p_d}(0)$, can be less than one implying declining

ES demand over time, however, as there is a greater range for positive values, the likelihood of growth appropriately exceeds the likelihood of decline. It is assumed the lower function asymptote is zero (for $\boldsymbol{p}_d(\infty) \oslash \boldsymbol{p}_d(0) > \boldsymbol{j}$) for simplicity and to bound curves to realistic gradients. $d\boldsymbol{p}_d(0)/dt$ is negative for $\boldsymbol{p}_d(\infty) \oslash \boldsymbol{p}_d(0) < \boldsymbol{j}$, with values selected from uniform distributions.

9.3.2.2 Logistic function for demand flexibility trends

Demand flexibility is expected to increase over time, from intial values to specified values after a defined simulation base period, ƫ (units of years):

$$q = \frac{\upsilon_q}{1 + \left(\frac{\upsilon_q}{q(0)} - 1\right)^{1-\frac{t}{\text{ƫ}}} \left(\frac{\upsilon_q}{q(\text{ƫ})} - 1\right)^{\frac{t}{\text{ƫ}}}}$$

Where, q is demand flexibility (dimensionless),
υ_q is the upper function asymptote (dimensionless),
$q(0)$ is the demand flexibility value at $t = 0$, and
$q(\text{ƫ})$ is the demand flexibility values at $t = \text{ƫ}$, selected from a uniform distribution.

For intermittent electricity, demand flexibility has a double effect on the AI requirement: 1) reducing the need for mitigation infrastructure as intermittent penetration rises, and 2) reducing the intermittent electricity AI peak factor. These effects are assumed to be multiplicative for the dynamic intermittent electricity AI requirement, as the first relates to the temporal correlation of demand with intermittent supply and the second to correlation of demand with intermittent electricity AI capacity. This is optimistic, as these two responses are not independent. υ_q is the upper function asymptote (dimensionless), selected from a Pareto distribution as detailed in section 9.4.2.1. $q(\text{ƫ})$ is selected from a uniform distribution.

9.3.3 PC and AI sectors

9.3.3.1 Primary NRE and RE

The primary NRE and RE sectors (shown in Figure 125) are part of layer two and are responsible for the calculation of evolving primary NRE and RE PC stocks, from investment flows, $\hat{\boldsymbol{h}}_r$ and $\hat{\boldsymbol{h}}_n$, to ultimate decommissioning, via the construction and operating lifecycle phases (modelling using material delay elements in GoldSim). Primary NRE and RE EC input energy cost proportion matrices, S_x and S_n, are also calculated here, allowing the determination of dynamic EC input energy cost vectors for PC construction, operation, and decommissioning.

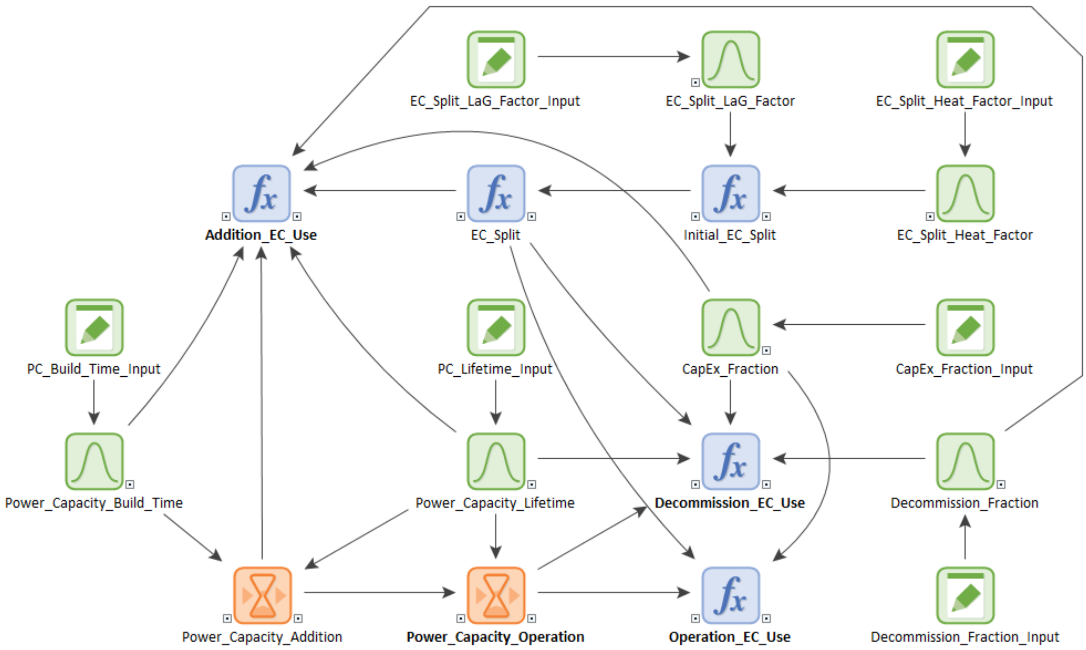

Figure 125: screenshot of the primary NRE and RE sectors (identical) within the GoldSim software UI

9.3.3.2 Secondary

The secondary sector (shown in Figure 127) is part of layer two and is responsible for the calculation of evolving secondary PC and AI stocks, from investment flows, $\hat{\boldsymbol{h}}_s$, to ultimate decommissioning, via the construction and operating lifecycle phases (modelling using material delay elements in GoldSim). The secondary EC input energy cost proportion matrix, S_s, is also calculated here, allowing the calculation of dynamic EC input energy cost vectors for PC construction, operation, and decommissioning. Additions to secondary AI stocks defined by the AI investment vector, $\hat{\boldsymbol{h}}_{sa}$, also requires the calculation of the corresponding peak factor vector, $\boldsymbol{v}_{sa}$, and AI requirement vector, $\boldsymbol{a}_{sa}$ (as described in section 4.2.2.4).

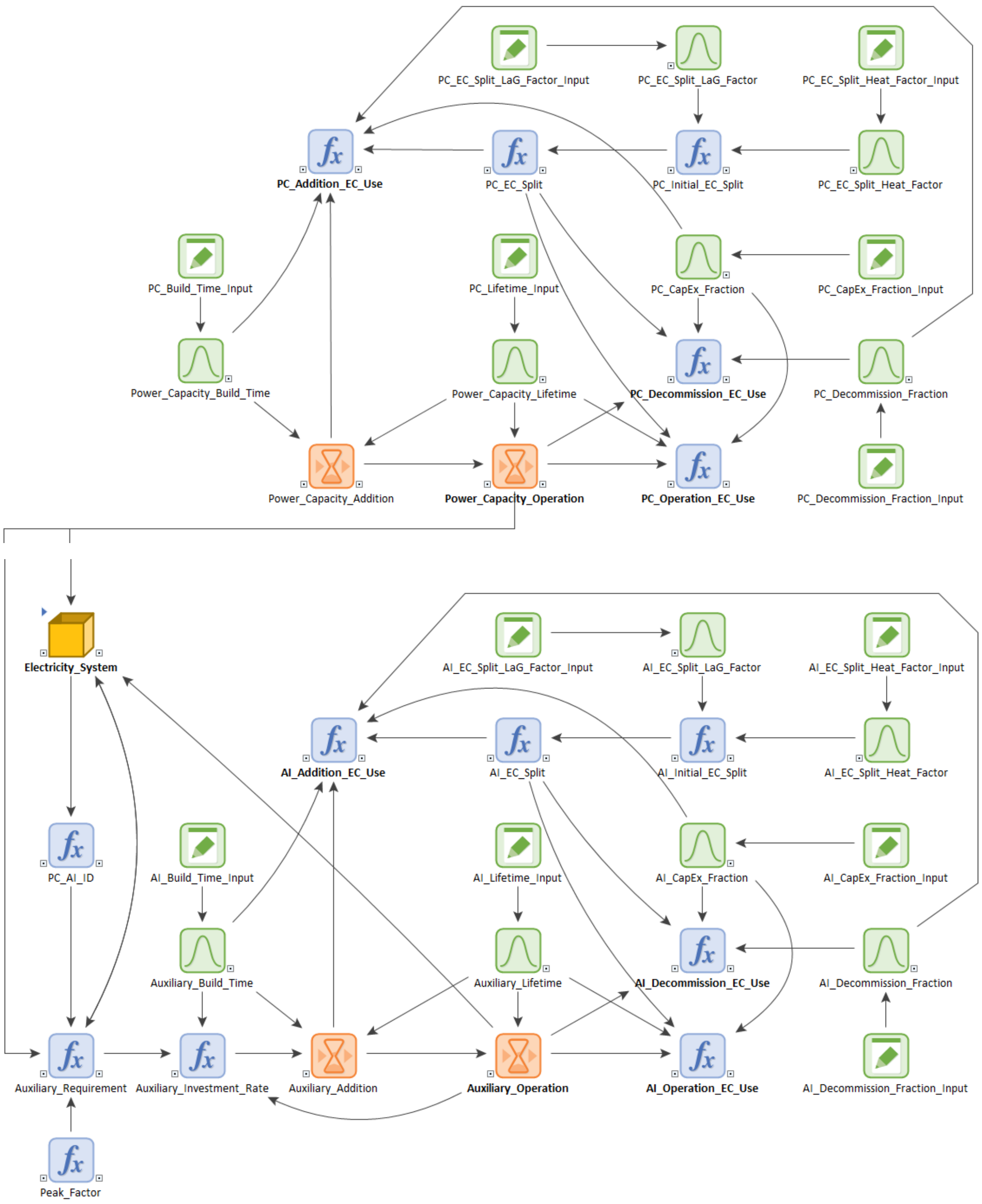

Figure 126: screenshot of the secondary sector within the GoldSim software UI

Figure 127 depicts requirement mappings between secondary PC types and secondary AI types specified by the AI requirement identity matrix, I_{sa}, introduced in section 4.2.2.4.

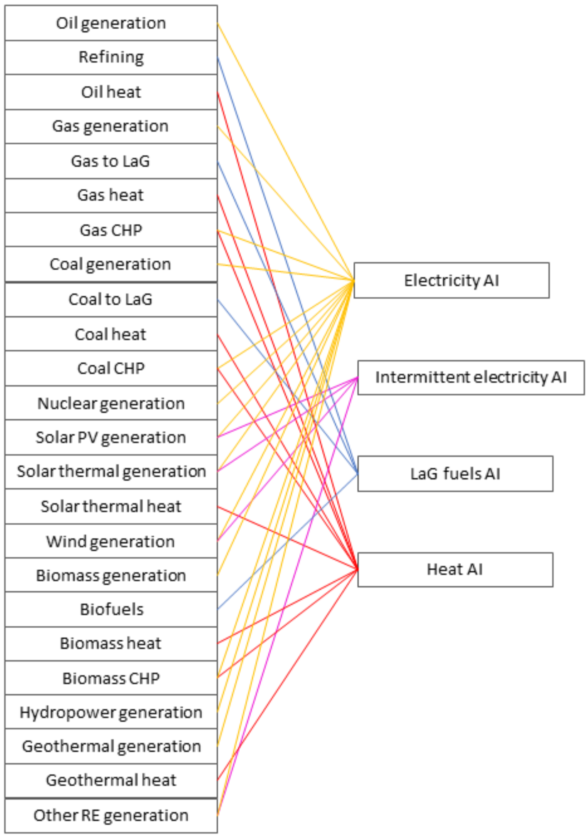

Figure 127: mapping diagram from secondary PC types to required secondary AI types

9.3.3.2.1 Electricity system

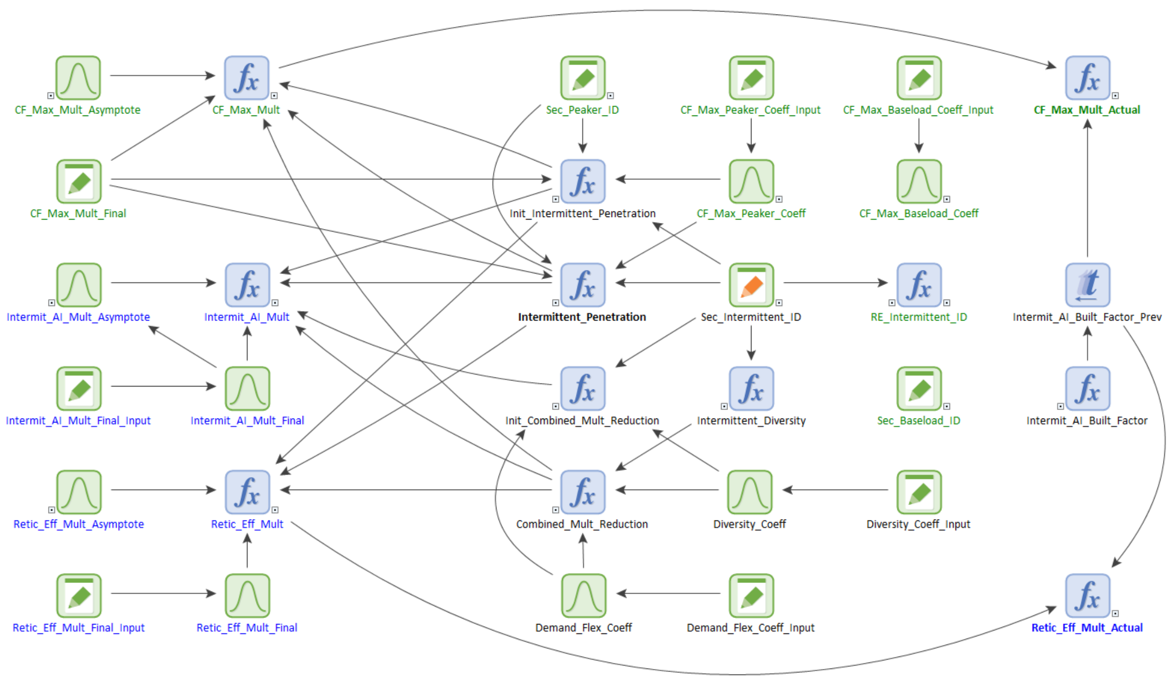

Figure 128: screenshot of the electricity system subsector within the GoldSim software UI

The electricity system subsector (shown in Figure 128) is responsible for the calculation of variables representing high-level dynamic interactions within electricity systems, including intermittent penetration, m, intermittent diversity, β, the combined intermittency mitigation reduction factor, r, and the built AI factor, $(\boldsymbol{c_{sa}})_d/(\boldsymbol{a_{sa}})_d$. These variables are used to calculate electricity system multipliers, χ_f, χ_g, and χ_h (equations given in section 9.3.3.2.1.1) for the dynamic modification of electricity system parameters via the decision variable for intermittency mitigation, ψ (determined by system control; see section 9.3.6). Generation type identity vectors, I_m, I_b, I_p, and I_k, intermittency mitigation reduction factor coefficients, ζ_β and ζ_q, and intermittent penetration generation response coefficients, ρ_b and ρ_p, are also defined here.

9.3.3.2.1.1 Logistic functions for electricity system multipliers

Multipliers representing dynamic interactions within the electricity system change as functions of intermittent penetration, m. Each is defined assuming full intermittency mitigation via the associated mitigation option (AI mitigation for χ_f and χ_g, and PC overbuild mitigation for χ_h) as the actual balance of mitigation is controlled by the decision variable ψ. All multipliers are scaled linearly by r, the combined intermittency mitigation reduction factor capturing the effects of intermittent diversity and demand flexibility.

$$\chi_f = \frac{r}{r(0)} \frac{\upsilon_f}{1 + (\upsilon_f - 1)^{\frac{1-m}{1-m(0)}} \left(\frac{\upsilon_f}{\chi_f(1)} - 1\right)^{\frac{m-m(0)}{1-m(0)}}}$$

Where, χ_f refers to the fractional modification of intermittent electricity AI required (dimensionless scalar; takes an initial value of 1),

$\chi_f(1)$ is the value of fractional modification of intermittent electricity AI required at 100% intermittent penetration, and

υ_f is the upper function asymptote (dimensionless scalar).

$$\chi_x = r\left(\frac{\upsilon_x}{1 + (\upsilon_x - 1)^{\frac{1-m}{1-m(0)}} \left(\frac{\upsilon_x}{\chi_x(1)} - 1\right)^{\frac{m-m(0)}{1-m(0)}}} - 1\right)$$

Where, Subscript x is replaced by g and h to refer to the fractional modification of intermittent electricity reticulation efficiencies and upstream CF maxima, respectively,

χ_g and χ_h (dimensionless scalars) take initial values of approximately zero,

$\chi_g(1)$ and $\chi_h(1)$ are the values of fractional modification of intermittent electricity reticulation efficiencies and upstream CF maxima at 100% intermittent penetration, respectively, and

υ_g and υ_h are the upper function asymptotes.

υ_f, υ_g, and υ_h are selected from Pareto distributions as detailed in section 9.4.2.1. $\chi_g(1)$ and $\chi_h(1)$ are selected from uniform distributions. Upper function asymptotes and function values at 100% intermittent penetration for χ_g and χ_h are specified assuming one as the initial function value, as these functions are specified at this level prior to being reduced by one for the application of these multipliers within the model formulation.

9.3.3.3 End-use

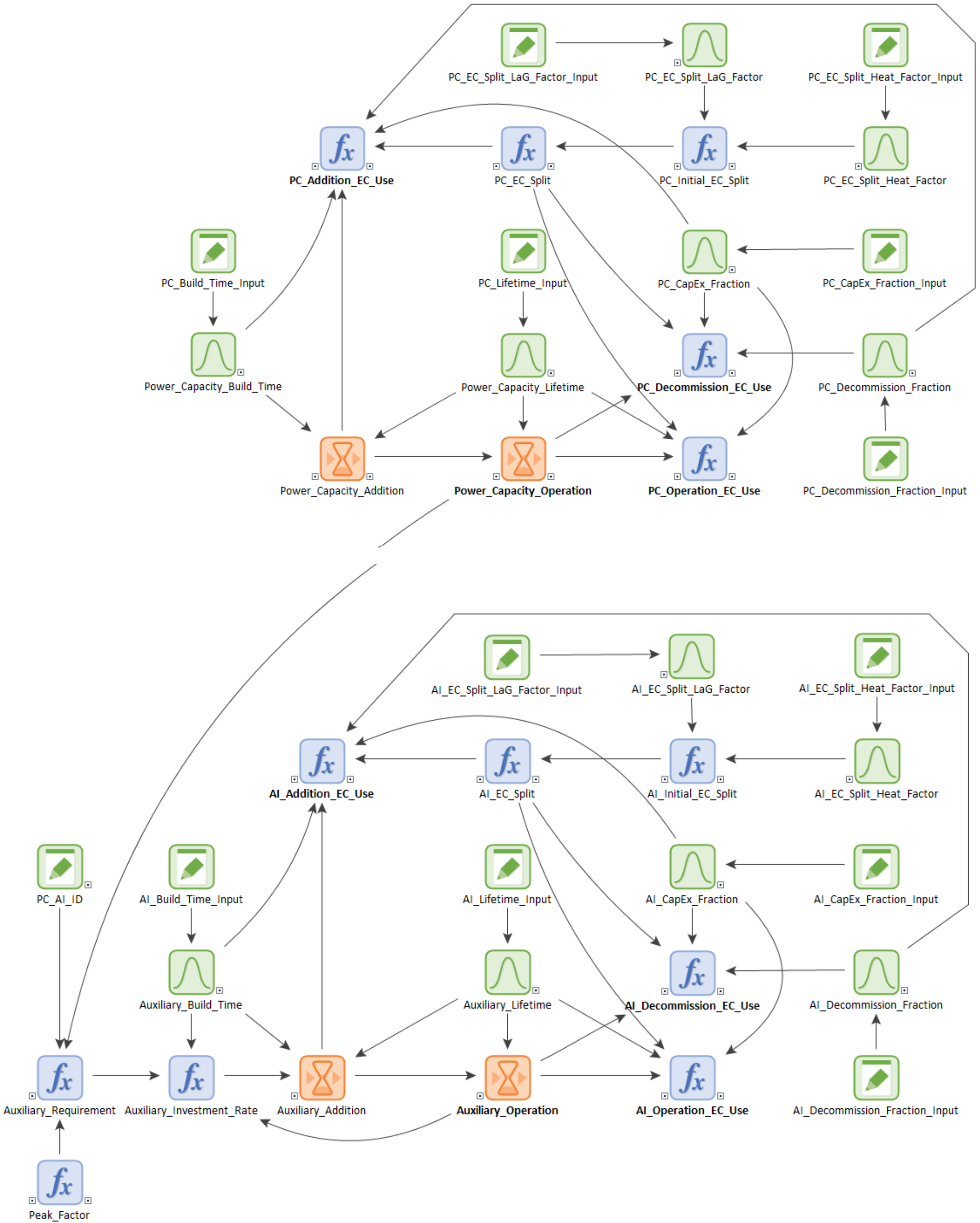

Figure 129: screenshot of the end-use sector within the GoldSim software UI

The end-use sector (shown in Figure 129) is part of layer two and is responsible for the calculation of evolving EU PC and AI stocks, from investment flows, $\boldsymbol{\hat{h}_e}$ (given by $\boldsymbol{\hat{h}_{es}} + \boldsymbol{\hat{h}_{et}}$), to ultimate decommissioning, via the construction and operating lifecycle phases (modelling using material delay elements in GoldSim). The EU EC input energy cost proportion matrix, S_e, is also calculated here, allowing the calculation of dynamic EC input energy cost vectors for PC construction, operation, and decommissioning. Additions to EU AI stocks defined by the AI investment vector, $\hat{\boldsymbol{h}}_{ea}$, also requires the calculation of the corresponding peak factor vector, $\boldsymbol{v}_{ea}$, and AI requirement vector, $\boldsymbol{a}_{ea}$ (as described in section 4.2.2.4).

Figure 130 depicts requirement mappings between EU PC types and EU AI types specified by the AI requirement identity matrix, I_{ea}, introduced in section 4.2.2.4.

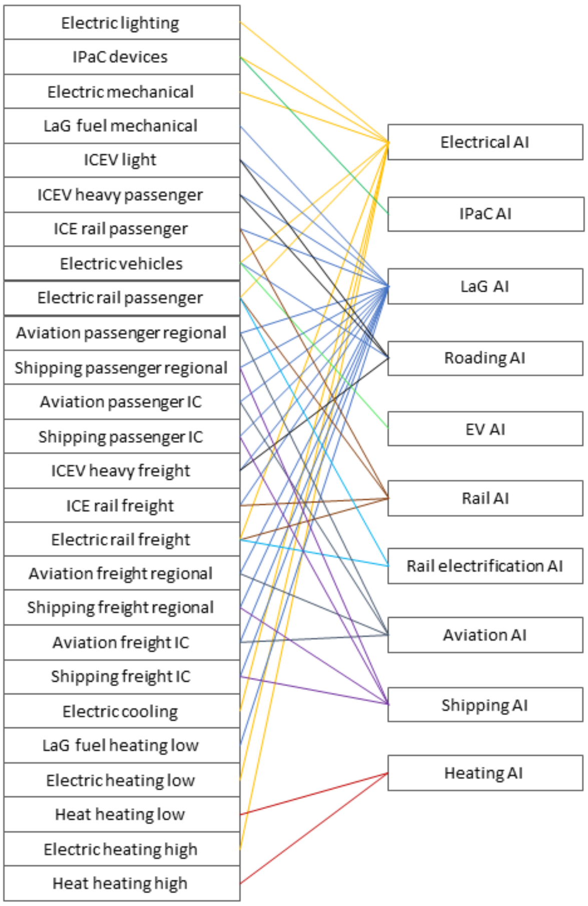

Figure 130: mapping diagram from EU PC types to required EU AI types

9.3.4 EROI

The EROI sector (shown in Figure 131) is part of layer two and is responsible for the calculation of RE and NRE EROI for mean PC stocks, as the composition of PC stocks change. Equations are given in section 9.3.4.1. Function numerators are modelling using material delay elements in GoldSim. Note that RE PC available for redevelopment can accumulate temporarily, modelled using a reservoir element.

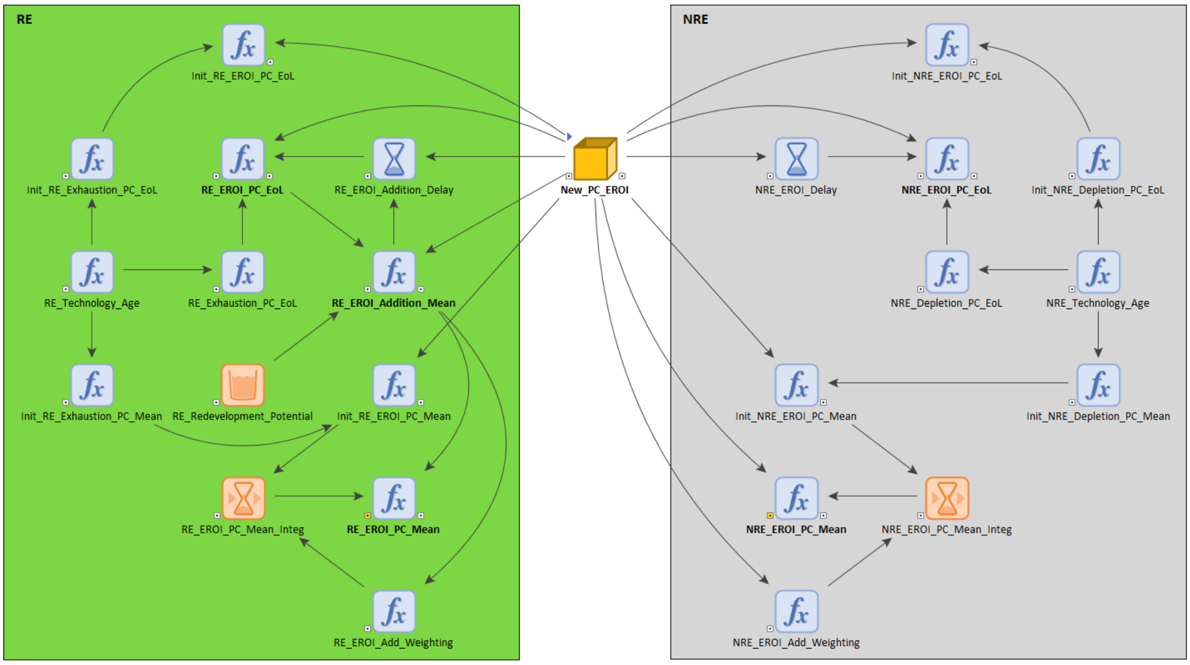

Figure 131: screenshot of the EROI sector within the GoldSim software UI

9.3.4.1 Propagation of new PC EROI values to mean PC stock values

Mean EROI values for the extant PC stocks depend on the time-path of investment (the sequence of additions and subsequent decommissioning). Changes in new PC values propagate into mean PC stock values only to the extent that new investment occurs. Mean PC stock values also change as PC is removed at the end of life. These functions are implemented in GoldSim using material delay elements to represent the numerators.

For RE EROI,

$$\boldsymbol{k_r}(t=\tau) = \left(\boldsymbol{k_r}(\boldsymbol{0}) \circ \boldsymbol{c_r}(0) + \int_0^{\tau} \left(\boldsymbol{ʎ_{rh}} \circ \boldsymbol{h_r} - \boldsymbol{ʎ_{rh}}\big(\boldsymbol{x}(\tau\boldsymbol{j} - \boldsymbol{l_x})\big) \circ \boldsymbol{h_r}(\tau\boldsymbol{j} - \boldsymbol{l_r})\right) dt\right) \oslash \left(\boldsymbol{c_r}(0) + \int_0^{\tau} \big(\boldsymbol{h_r} - \boldsymbol{h_r}(\tau\boldsymbol{j} - \boldsymbol{l_r})\big)\, dt\right)$$

Where, $\boldsymbol{k_r}(\boldsymbol{0}) = \boldsymbol{ʎ_r}\left(\boldsymbol{x} = -\boldsymbol{p_r}(0) \circ \boldsymbol{l_r} \oslash \left(2\boldsymbol{n_r} \circ \left(\boldsymbol{p_{rm}} - \boldsymbol{p_r}(0)\right)\right)\right)$,

For $\tau\boldsymbol{j} < \boldsymbol{l_r}$: $\boldsymbol{ʎ_{rh}}\big(\boldsymbol{x}(\tau\boldsymbol{j} - \boldsymbol{l_x})\big) \approx \boldsymbol{k_x}(\boldsymbol{0})$,

$\boldsymbol{ʎ_r}$ is the vector of EROI for new RE PC additions,

$\boldsymbol{ʎ_{rh}}$ is the vector of RE EROI for new PC additions adjusted for RE resource development, and

$\boldsymbol{n_r}$ is the vector of technology ages for RE PC (from technology inception to the start of the study period, in units of years).

Where RE PC decommissioning exceeds additions, higher than current EROI resources occupied by end-of-life PC can become available and be redeveloped:

$$\eta_{rh} = \begin{cases} \eta_r + (\boldsymbol{h}_r(\tau \boldsymbol{j} - \boldsymbol{l}_r) \oslash \boldsymbol{h}_r - \boldsymbol{j}) \circ \left(\eta_{rh}\left(\boldsymbol{x}(\tau \boldsymbol{j} - \boldsymbol{l}_r)\right) - \eta_r\right) \ where \ \boldsymbol{h}_r(\tau \boldsymbol{j} - \boldsymbol{l}_r) > \boldsymbol{h}_r \\ \eta_r \ where \ \boldsymbol{h}_r(\tau \boldsymbol{j} - \boldsymbol{l}_r) \leq \boldsymbol{h}_r \end{cases}$$

And for NRE EROI,

$$\boldsymbol{k}_n(t = \tau) = \left(\boldsymbol{k}_n(\boldsymbol{0}) \circ \boldsymbol{c}_n(0) + \int_0^{\tau} \left(\eta_n \circ \boldsymbol{h}_n - \eta_n\left(\boldsymbol{d}(\tau \boldsymbol{j} - \boldsymbol{l}_n)\right) \circ \boldsymbol{h}_n(\tau \boldsymbol{j} - \boldsymbol{l}_n)\right) dt\right) \oslash \left(\boldsymbol{c}_n(0) + \int_0^{\tau} \left(\boldsymbol{h}_n - \boldsymbol{h}_n(\tau \boldsymbol{j} - \boldsymbol{l}_n)\right) dt\right)$$

Where, $\boldsymbol{k}_n(\boldsymbol{0}) = \eta_n(\boldsymbol{d} = -\boldsymbol{p}_n \circ \boldsymbol{l}_n \circ (\boldsymbol{j} - \boldsymbol{l}_n \oslash 4\boldsymbol{n}_n) \oslash 2\boldsymbol{\omega})$,

For $\tau \boldsymbol{j} < \boldsymbol{l}_n$: $\eta_n\left(\boldsymbol{d}(\tau \boldsymbol{j} - \boldsymbol{l}_n)\right) \approx \boldsymbol{k}_n(\boldsymbol{0})$,

$\boldsymbol{\eta}_n$ is the vector of EROI for new NRE PC additions, and

$\boldsymbol{n}_n$ is the vector of technology ages for NRE PC (from technology inception to the start of the study period, in units of years).

The vectors $\boldsymbol{\eta}_{rh}$ and $\boldsymbol{\eta}_n$ are approximated as initial mean PC EROI values for times prior to the start of the study period. For the calculation of initial mean PC EROI values, power output is assumed to take an approximately linear trend from technology inception to the start of the study period:

- $\boldsymbol{k}_r(\boldsymbol{0})$ uses exhaustion calculated at the output power rate at time $-\boldsymbol{l}_r/2$ (assuming a uniform initial PC age distribution).
- $\boldsymbol{k}_n(\boldsymbol{0})$ uses depletion calculated via the time integral of output between $-\boldsymbol{l}_n/2$ and $\boldsymbol{0}$ (assuming a uniform initial PC age distribution).

9.3.4.2 New PC EROI

The new PC EROI subsector (shown in Figure 132) is responsible for the calculation of RE and NRE EROI for new PC, as RE exhaustion and NRE depletion increases. Equations are given in section 9.3.4.2.1. Function numerators are modelling using material delay elements in GoldSim.

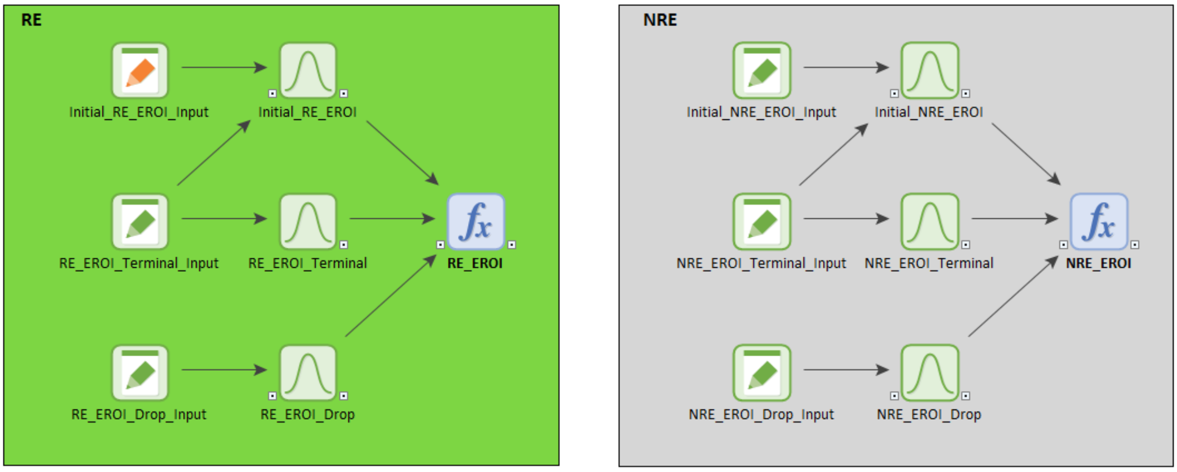

Figure 132: screenshot of the new PC EROI subsector within the GoldSim software UI

9.3.4.2.1 Logistic functions for new PC EROI trends

$$y_r = v_r \oslash \left(j + (v_r \oslash y_r(j) - j)^{\circ x} \circ \left(v_r \oslash \left(v_r - y_r(0)\right) - j\right)^{\circ(x-j)}\right)$$

$$y_n = v_n \oslash \left(j + (v_n \oslash y_n(j) - j)^{\circ d} \circ \left(v_n \oslash \left(v_n - y_n(0)\right) - j\right)^{\circ(d-j)}\right)$$

Where,

y_r and y_n are the vectors of EROI for new PC for RE and NRE, respectively,

$\boldsymbol{d}$ is the depletion vector (NRE) and $\boldsymbol{x}$ is the exhaustion vector (RE),

v_r and v_n are the upper function asymptote vectors,

$y_r(j)$ and $y_n(j)$ are the vectors of terminal EROI values, and

$y_r(0)$ and $y_n(0)$ are the vectors of initial EROI values.

v_r and v_n correspond to approximate pre-simulation peak EROI values and are specified via drop (pre-simulation decline) values, selected from uniform distributions, as the initial and pre-simulation peak distributions cannot be used directly due to distribution overlap. $y_r(j)$ and $y_n(j)$ correspond to full primary resource exploitation ($\boldsymbol{x} = \boldsymbol{j}$ and $\boldsymbol{d} = \boldsymbol{j}$), at which point new PC investment is prevented, although NRE PC can continue operating, bringing EROI below terminal values). These values are selected from uniform distributions. $y_r(0)$ and $y_n(0)$ are selected from truncated normal distributions with terminal EROI values representing lower bounds. Function lower asymptotes are assumed to be $\boldsymbol{0}$ for simplicity (EROI cannot go negative and at extreme depletion levels, energy is expended with negligible return).

9.3.5 Energy cost of capital

The energy cost of capital sector (shown in Figure 133) is part of layer two and is responsible for the calculation of ECC for secondary and EU PC and AI. As ECC values are modelled as static, this sector contains only elements for the sampling of probability distributions.

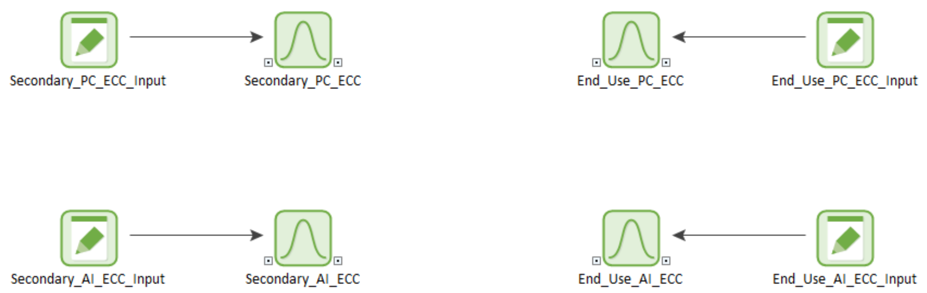

Figure 133: screenshot of the energy cost of capital sector within the GoldSim software UI

9.3.6 System control

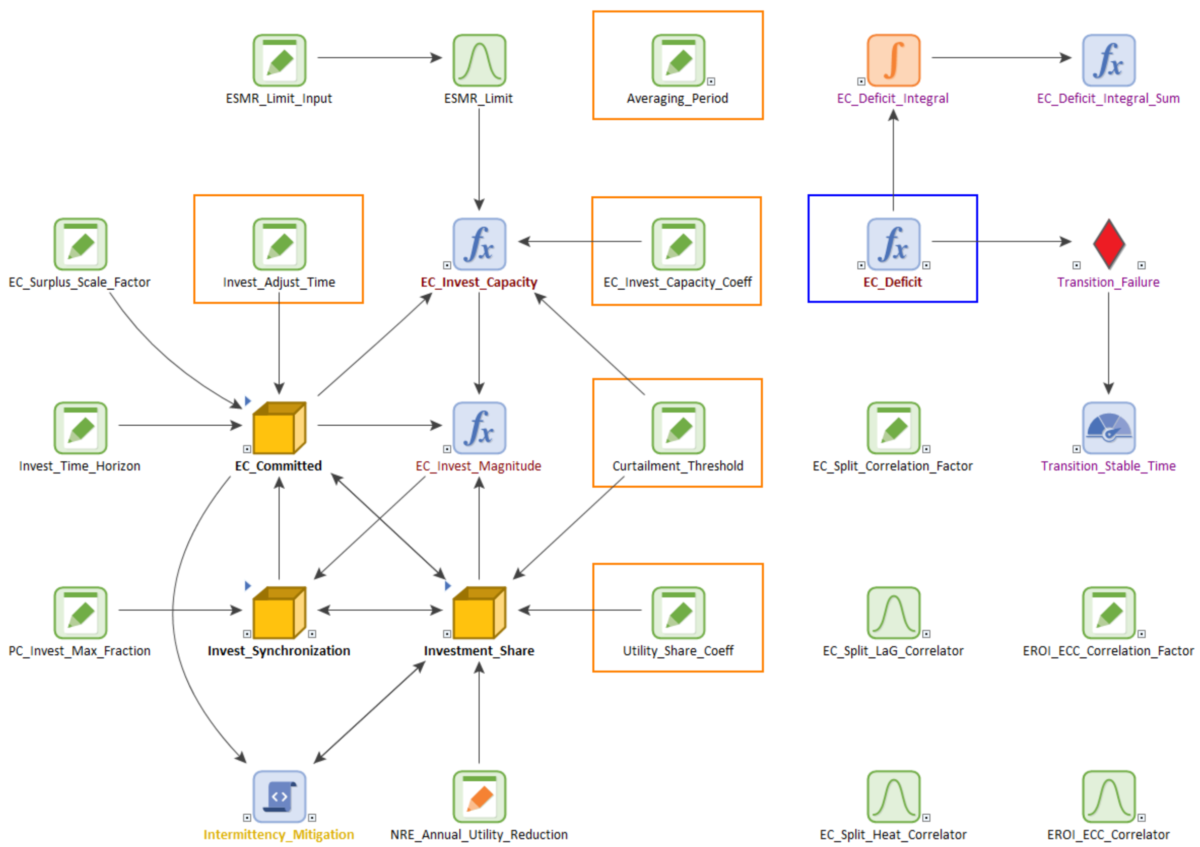

Figure 134: screenshot of the system control sector within the GoldSim software UI

The system control sector (shown in Figure 134) comprises layer three and is responsible for the calculation of time-dependent PC investment flow and intermittency mitigation decision variables, $\hat{h}_r$, $\hat{h}_n$, $\hat{h}_s$, $\hat{h}_e$, and ψ. This involves intermittency mitigation optimization (see script details in section 9.4.5.1), and the calculation of the EC deficit vector, investment magnitude, and the realization-level failure informational output metric (failure detection). Control parameters and input parameter correlation factors (see section 9.4.7) are specified here. This sector also contains the objective function, used only during the optimization and calibration process (see section for 9.6 details).

Note that it is possible that the initial ESMR ratio maxima is situated within the curtailment band the ESMR limit, depending on the optimized value of the curtailment threshold constant ($max(\boldsymbol{\kappa}(0))_i > ł(1 - \gamma_{ct})$). This is justified on the basis that investment within the GES could be considered to already be competing with other economic priorities. In the worst case, this corresponds to an initial minor curtailment of GES investment, not a hard limit.

9.3.6.1 EC committed

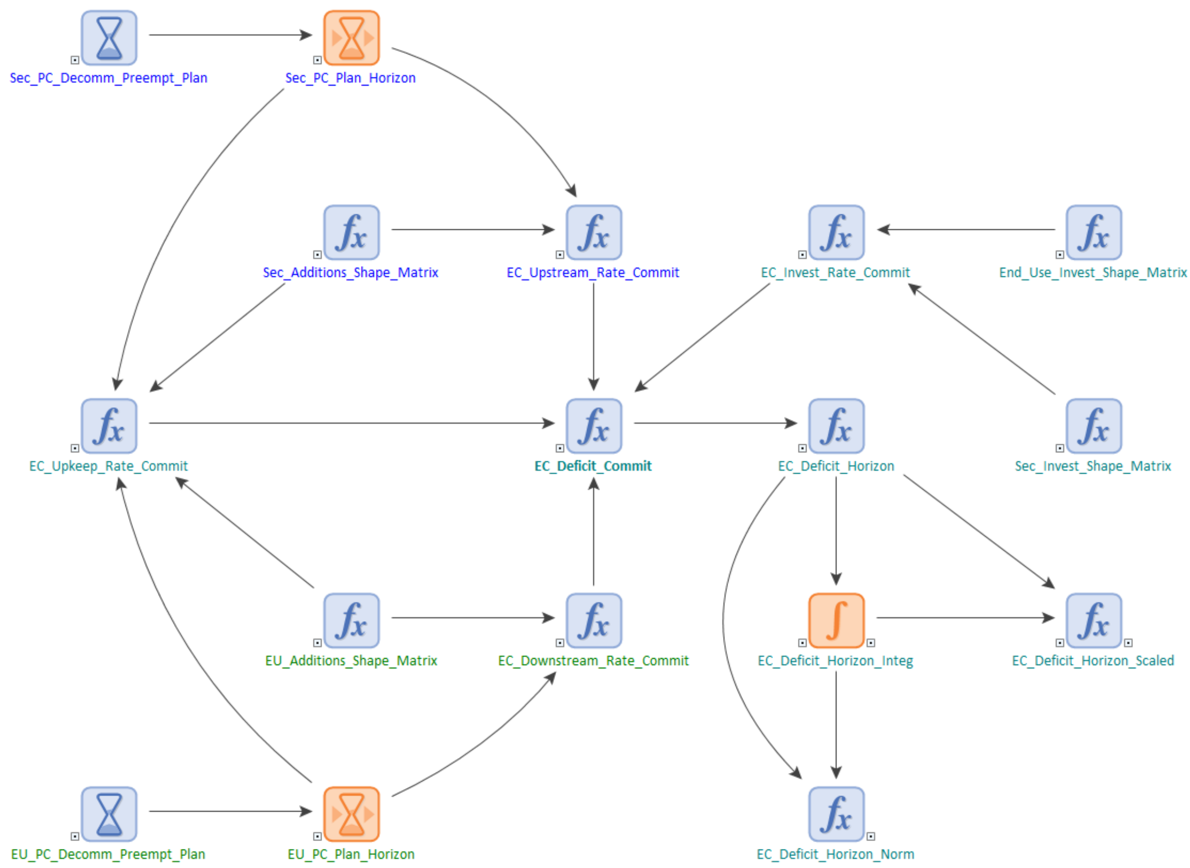

Figure 135: screenshot of the EC committed subsector within the GoldSim software UI

The EC committed subsector (shown in Figure 135) is responsible for the calculation of the projected EC deficit vector at the specified time horizon, ***d***. This involves the calculation of EC flow change projection matrices, U_i, U_o, and U_{κ}., using 'shape matrices' specifying normalized phase in and phase out patterns by PC type. The pre-emption of decommissioning flows is represented GoldSim using material delay elements. An integrator element is used for smoothing the projected EC deficit vector where rapid increases occur.

9.3.6.2 Investment share

The investment share subsector (shown in Figure 136) is responsible for the calculation of investment flow proportions directed towards each investment option (investment shares). This involves the calculation of yield matrices, Y_i, and Y_o, from upstream and downstream CFs and investment cost functions (from EROI and ECC, disaggregated by EC type). Yield is converted to corresponding utility matrices, W_i, and W_o, using projected EC deficit. Investment shares are then determined using logit choice functions, with proportions adjusted to an equivalent investment input basis using investment cost functions. Upstream and downstream curtailment functions are also applied to utility and investment shares based on penetration levels, preventing overinvestment into constrained investment options.

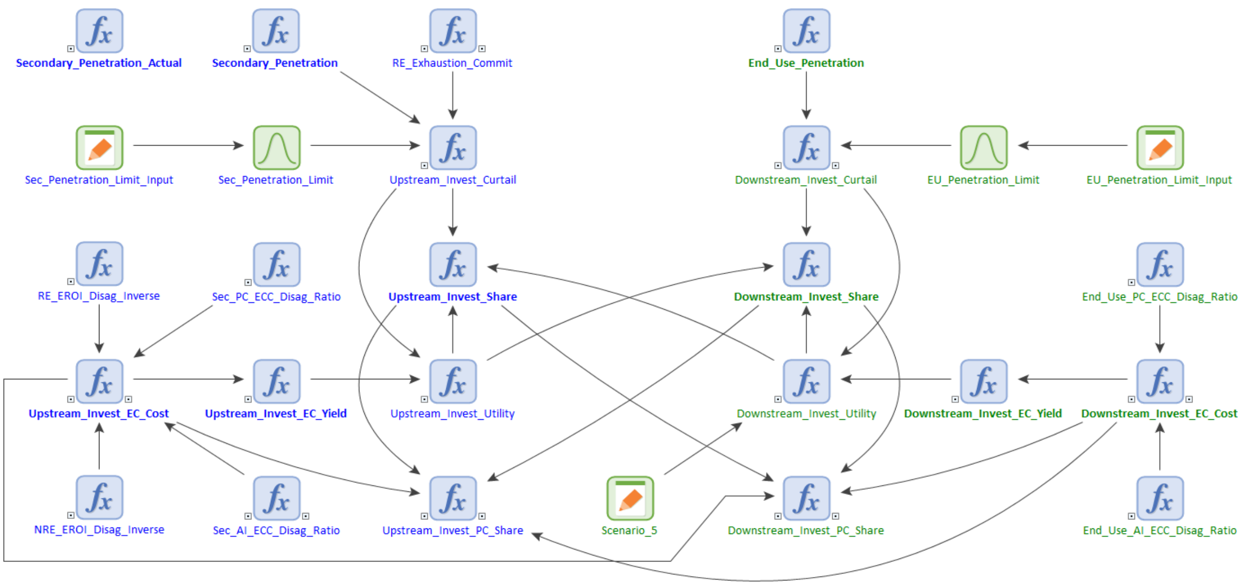

Figure 136: screenshot of the investment share subsector within the GoldSim software UI

Note that upstream yield and investment calculations:

- reference CF maxima as the synchronization of upstream additions (see section 9.3.6.3) minimizes capacity gaps between the primary and secondary stages causing upstream CFs to return to maxima over the long-term, and
- include the effects of the dynamic modification of electricity system parameters due to intermittent penetration (i.e., these effects are reflected in utility values).

Dynamic adjustments are made to curtailment function vectors and utility matrices:

- $\boldsymbol{ş}_i$ and $\boldsymbol{ş}_o$ are modified to account for primary resource availability and capacity utilization.
  - Values are reduced for very low PC utilization levels, curtailing further investment where a large surplus of PC already exists ($\boldsymbol{ş}_x \rightarrow \boldsymbol{0}$ as $\boldsymbol{u}_x \rightarrow \boldsymbol{0}$).
  - For upstream curtailment, values are reduced towards zero when primary energy resources enter advanced stages of depletion or exhaustion ($\boldsymbol{ş}_i \rightarrow \boldsymbol{0}$ as $\boldsymbol{d}, \boldsymbol{x} \rightarrow \boldsymbol{j}$).
- W_i and W_i are modified to account for fully curtailed and negative utility values, and reduced utility associated with the elimination of surplus:
  - Investment options at or above penetration limits ($\boldsymbol{ş}_x = \boldsymbol{0}$) or with negative sum rows (i.e., no net benefit) are removed by setting utility values to a very low number (-9).
  - The projected EC deficit vector, $\boldsymbol{d}$, has a scaling factor applied to negative values such that utility values associated with eliminating surplus is reduced relative to eliminating deficit. This asymmetric response is required as EC deficits are associated with net energy trap outcomes, so must be avoided more strongly than surpluses. However, negative values of $\boldsymbol{d}$ cannot be ignored entirely as excessive surplus can also cause system instability.
- See section 9.4.4 for full calculation details.

9.3.6.3 Invest synchronization

The invest synchronization subsector (shown in Figure 137) is responsible for the synchronization of upstream PC additions to minimize capacity gaps between the primary and secondary stages. Delays in upstream investment flows are modelled using material delay elements in GoldSim, with variable delay times driven by the magnitude of capacity gaps (to expedite the addition of PC in deficit). Note that further adjustments to investment flows are applied to correct for differences between the operational lifetimes of associated primary and secondary PC types (decommissioning flow pre-emption), using integrator elements as smoothing functions. The calculation of EU PC investment flows driven by EU PC utilization, denoted $\hat{\boldsymbol{h}}_{et}$, is also carried out here, with magnitude limits applied to prevent excessive swings in EU PC utilization.

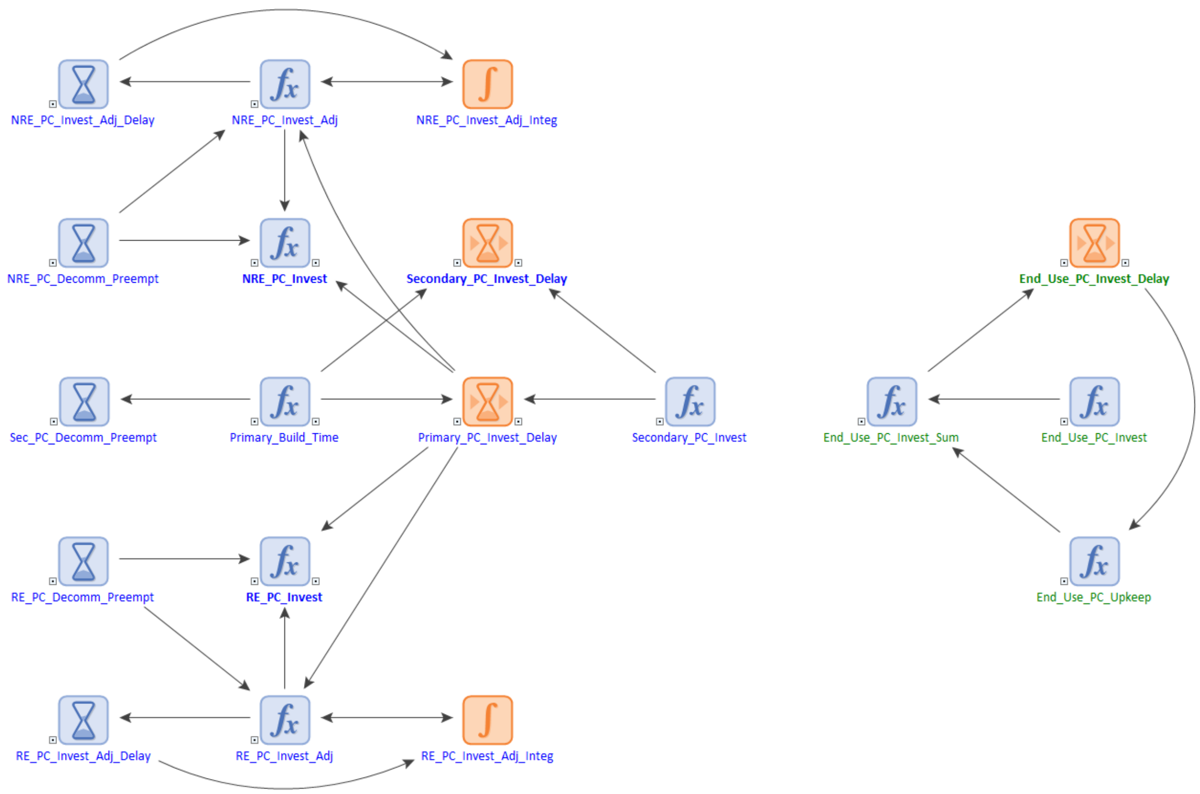

Figure 137: screenshot of the invest synchronization subsector within the GoldSim software UI

9.4 MODEL FUNCTIONS AND PARAMETERS

9.4.1 Global parameters

Name	Description	Unit	Value
EC_Invest_Capacity_Floor	Minimum value for scale factor for investment in response to sum forecast EC deficit (prevents total investment cessation)	EJ/yr^2	0.01
Asymptote_Max_Factor	Used in logistic functions: value of two implies that curves can range from being near the asymptote to being near the inflection point by end of the simulation (99% chance of inflection point prior to the end of the simulation)		2
Minimum_PC_Timeframe	Minimum time for upstream investment signal to lead to additions to PC in the build phase (non-zero minimum required for material delay elements)	yr	0.2
PC_Zero_Approx	Approximation used in place of zero to avoid divide by zero errors (mostly where denominator is a PC stock)	EJ/yr	0.001
Simulation_Base_Period	Base period used in time-dependent functions (sim. duration can be changed so should not be used)	yr	80
Utility_Remove	Discrete reduction applied to utility vector where specific PC investment should not take place (curtailment value reaches zero or Scenario 5 in effect)		-9
EC_Deficit_Limit_Base	Initial value for the allowable EC deficit limit (cumulative surplus before CF reductions occur)	yr	-2
EC_Deficit_Limit_Slope	Coefficient for change in the allowable EC deficit limit (linear function, base plus slope reached at sim. base period; cumulative surplus before CF reductions occur)	yr	-8

9.4.2 Stochastic inputs

Sector	Element name	Description	Unit	Array labels	Distribution	Minimum	Maximum	Most likely	Mean	Standard deviation	Input ref.
Demand	Demand_Flex_Asymptote	Sets the upper asymptote of the demand flexibility function (lower values more common)			Pareto	Final_Demand_Flex					n/a
Demand	ES_Final_Demand_Mult	Vector of the upper asymptotes of the ES demand function relative to initial ES demand (>0 for growth, <0 for decline)		ES_types	Uniform	ES_Final_Demand_Mult_Input[*, Min]	ES_Final_Demand_Mult_Input[*, Max]				5.1
Demand	Final_Demand_Flex	Sets the final value of the demand flexibility function (at sim. base period)			Uniform	Final_Demand_Flex_Input[Min]	Final_Demand_Flex_Input[Max]				5.4
Demand	Initial_ES_Demand_RoC	Vector of the initial annual rates of change of the ES demand function	1/yr	ES_types	Uniform	vector(0 1/yr)	vector(Initial_ES_Demand_RoC_Max)				5.2
End-use	AI_CapEx_Fraction	Vector of fractions of end-use auxiliary infrastructure investment energy devoted to capital (construction and decommissioning)		End_use_AI_types	Uniform	AI_CapEx_Fraction_Input[*, Min]	AI_CapEx_Fraction_Input[*, Max]				11.7
End-use	AI_Decommission_Fraction	Vector of fractions of end-use auxiliary infrastructure investment energy devoted to capital used in the decommissioning stage		End_use_AI_types	Uniform	AI_Decommission_Fraction_Input[*, Min]	AI_Decommission_Fraction_Input[*, Max]				11.8
End-use	AI_EC_Split_Heat_Factor	Vector of initial fractions of end-use auxiliary infrastructure input energy consisting of heat, divided by the heat share of initial EC supply		End_use_AI_types	Uniform	AI_EC_Split_Heat_Factor_Input[*, Min]	AI_EC_Split_Heat_Factor_Input[*, Max]				11.10
End-use	AI_EC_Split_LaG_Factor	Vector of initial fractions of end-use auxiliary infrastructure input energy consisting of liquid and gaseous fuels, divided by the LaG share of initial EC supply		End_use_AI_types	Uniform	AI_EC_Split_LaG_Factor_Input[*, Min]	AI_EC_Split_LaG_Factor_Input[*, Max]				11.9

Sector	Element name	Description	Unit	Array labels	Distribution	Minimum	Maximum	Most likely	Mean	Standard deviation	Input ref.
End-use	Auxiliary_Build_Time	Vector of values for end-use auxiliary infrastructure build time (investment decision to operation)	yr	End_use_AI_types	Uniform	AI_Build_Time_Input[*, Min]	AI_Build_Time_Input[*, Max]				11.11
End-use	Auxiliary_Lifetime	Vector of values for end-use auxiliary infrastructure lifetime (in operation)	yr	End_use_AI_types	Uniform	AI_Lifetime_Input[*, Min]	AI_Lifetime_Input[*, Max]				11.12
End-use	PC_CapEx_Fraction	Vector of fractions of end-use power capacity investment energy devoted to capital (construction and decommissioning)		End_use_PC_types	Uniform	PC_CapEx_Fraction_Input[*, Min]	PC_CapEx_Fraction_Input[*, Max]				11.1
End-use	PC_Decommission_Fraction	Vector of fractions of end-use power capacity investment energy devoted to capital used in the decommissioning stage		End_use_PC_types	Uniform	PC_Decommission_Fraction_Input[*, Min]	PC_Decommission_Fraction_Input[*, Max]				11.2
End-use	PC_EC_Split_Heat_Factor	Vector of initial fractions of end-use power capacity input energy consisting of heat, divided by the heat share of initial EC supply		End_use_PC_types	Uniform	PC_EC_Split_Heat_Factor_Input[*, Min]	PC_EC_Split_Heat_Factor_Input[*, Max]				11.4
End-use	PC_EC_Split_LaG_Factor	Vector of initial fractions of end-use power capacity input energy consisting of liquid and gaseous fuels, divided by the LaG share of initial EC supply		End_use_PC_types	Uniform	PC_EC_Split_LaG_Factor_Input[*, Min]	PC_EC_Split_LaG_Factor_Input[*, Max]				11.3
End-use	Power_Capacity_Build_Time	Vector of values for end-use power capacity build time (investment decision to operation)	yr	End_use_PC_types	Uniform	PC_Build_Time_Input[*, Min]	PC_Build_Time_Input[*, Max]				11.5
End-use	Power_Capacity_Lifetime	Vector of values for end-use power capacity lifetime (in operation)	yr	End_use_PC_types	Uniform	PC_Lifetime_Input[*, Min]	PC_Lifetime_Input[*, Max]				11.6

Sector	Element name	Description	Unit	Array labels	Distribution	Minimum	Maximum	Most likely	Mean	Standard deviation	Input ref.
Energy Cost Of Capital	End_Use_AI_ECC	Vector of ECC values for end-use auxiliary infrastructure (log-normal dist. as estimates vary by orders of magnitude)	yr	End_use_AI_types	Log-Normal				End_Use_AI_ECC_Input[*, Mean]	End_Use_AI_ECC_Input[*, SD]	7.4
Energy Cost Of Capital	End_Use_PC_ECC	Vector of ECC values for end-use power capacity (log-normal dist. as estimates vary by orders of magnitude)	yr	End_use_PC_types	Log-Normal				End_Use_PC_ECC_Input[*, Mean]	End_Use_PC_ECC_Input[*, SD]	7.3
Energy Cost Of Capital	Secondary_AI_ECC	Vector of ECC values for secondary auxiliary infrastructure (log-normal dist. as estimates vary by orders of magnitude)	yr	Secondary_AI_types	Log-Normal				Secondary_AI_ECC_Input[*, Mean]	Secondary_AI_ECC_Input[*, SD]	7.2
Energy Cost Of Capital	Secondary_PC_ECC	Vector of ECC values for secondary power capacity (log-normal dist. as estimates vary by orders of magnitude)	yr	Secondary_PC_types	Log-Normal				Secondary_PC_ECC_Input[*, Mean]	Secondary_PC_ECC_Input[*, SD]	7.1
Energy Flow/Flow Routing	End_Use_CF_Target_Asymptote	Vector of the upper asymptotes of the EU CF target function (lower values more common)		End_use_PC_types	Pareto	End_Use_CF_Target_Final					n/a
Energy Flow/Flow Routing	End_Use_CF_Target_Final	Vector of the final values of the EU CF target function (at sim. base period; log-uniform dist.)		End_use_PC_types	Log-Uniform	Init_End_Use_CF_Target	Init_End_Use_CF_Target * (vector(1) + EU_CF_Target_Final_Max_Factor)				3.3
Energy Flow/Flow Routing	Init_End_Use_CF_Target	Vector of the initial values of the EU CF target function		End_use_PC_types	Uniform	Init_End_Use_CF_Target_Input[*, Min]	Init_End_Use_CF_Target_Input[*, Max]				3.2

Sector	Element name	Description	Unit	Array labels	Distribution	Minimum	Maximum	Most likely	Mean	Standard deviation	Input ref.
Energy Flow/Initialization	End_Use_Prop_Rand	Random error vector for the initial proportions of energy carrier input flowing into each EU PC type (between -1 and 1)		End_use_PC_types	Uniform	vector(-1)	vector(1)				n/a
Energy Flow/Initialization	Init_End_Use_Peak_Factor	Vector of the initial values of peak factor for each EU AI type (defined assuming zero demand flexibility)		End_use_AI_types	Uniform	Init_End_Use_Peak_Factor_Input[*, Min]	Init_End_Use_Peak_Factor_Input[*, Max]				1.6
Energy Flow/Initialization	Init_Secondary_Peak_Factor	Vector of the initial values of peak factor for each secondary AI type (defined assuming zero demand flexibility)		Secondary_AI_types	Uniform	Init_Sec_Peak_Factor_Input[*, Min]	Init_Sec_Peak_Factor_Input[*, Max]				1.5
Energy Flow/Initialization	Secondary_Prop_Rand	Random error vector for the initial proportions of primary resource input flowing into each secondary PC type (between -1 and 1)		Secondary_PC_types	Uniform	vector(-1)	vector(1)				n/a
Energy Flow/New PC Efficiencies	End_Use_Conversion_Eff_Base	Vector of the lower asymptotes of the EU conversion efficiency function: between 0 and initial PC mean efficiency value (triangular dist. towards lower values)		End_use_PC_types	Triangular	vector(0)	End_Use_Conversion_Eff_Input[*, Min]	vector(0)			4.4
Energy Flow/New PC Efficiencies	End_Use_ES_Eff_Base	Vector of the lower asymptotes of the EU to ES efficiency function: between 0 and initial PC mean efficiency value		End_use_PC_types	Uniform	vector(0)	Init_End_Use_ES_Eff_PC_Mean				4.5
Energy Flow/New PC Efficiencies	Final_End_Use_Conversion_Eff	Vector of the upper asymptotes of the EU conversion efficiency function: between initial new PC value and maximum theoretical value		End_use_PC_types	Uniform	Init_End_Use_Conversion_Eff	End_Use_Conversion_Eff_Input[*, Max]				4.4

Sector	Element name	Description	Unit	Array labels	Distribution	Minimum	Maximum	Most likely	Mean	Standard deviation	Input ref.
Energy Flow/New PC Efficiencies	Final_End_Use_ES_Eff	Vector of the upper asymptotes of the EU to ES efficiency function: between initial new PC value and maximum theoretical value		End_use_PC_types	Uniform	Init_End_Use_ES_Eff	Init_End_Use_ES_Eff_PC_Mean * (vector(1) + Final_EU_ES_Eff_Max_Factor)				4.6
Energy Flow/New PC Efficiencies	Final_Sec_Conversion_Eff	Vector of the upper asymptotes of the secondary conversion efficiency function: between initial new PC value and maximum theoretical value		Secondary_PC_types	Uniform	Init_Sec_Conversion_Eff	Sec_Conversion_Eff_Input[*, Max]				4.1
Energy Flow/New PC Efficiencies	Final_Sec_Reticulation_Eff	Vector of the upper asymptotes of the secondary reticulation efficiency function: between initial new PC value and maximum theoretical value		Secondary_PC_types	Uniform	Init_Sec_Reticulation_Eff	Sec_Reticulation_Eff_Input[*, Max]				4.2
Energy Flow/New PC Efficiencies	Init_End_Use_Conversion_Eff	Vector of the initial values of the EU conversion efficiency function: between initial PC mean value and maximum theoretical value (triangular dist. towards lower values)		End_use_PC_types	Triangular	End_Use_Conversion_Eff_Input[*, Min]	End_Use_Conversion_Eff_Input[*, Max]	End_Use_Conversion_Eff_Input[*, Min]			4.1
Energy Flow/New PC Efficiencies	Init_End_Use_ES_Eff	Vector of the initial values of the EU to ES efficiency function: between initial PC mean value and maximum theoretical value (triangular dist. towards lower values)		End_use_PC_types	Triangular	Init_End_Use_ES_Eff_PC_Mean	Init_End_Use_ES_Eff_PC_Mean * (vector(1) + Final_EU_ES_Eff_Max_Factor)	Init_End_Use_ES_Eff_PC_Mean			4.5

Sector	Element name	Description	Unit	Array labels	Distribution	Minimum	Maximum	Most likely	Mean	Standard deviation	Input ref.
Energy Flow/New PC Efficiencies	Init_End_Use_ES_Eff_PC_Mean	Vector of the initial PC mean values for EU to ES efficiency: range given by estimates +/- assigned error value		End_use_PC_types	Uniform	Init_End_Use_ES_Eff_Input[*, Numeral]* (vector(1) - Init_End_Use_ES_Eff_Input[*, Error])	Init_End_Use_ES_Eff_Input[*, Numeral]* (vector(1) + Init_End_Use_ES_Eff_Input[*, Error])				4.5
Energy Flow/New PC Efficiencies	Init_Sec_Conversion_Eff	Vector of the initial values of the secondary conversion efficiency function: between initial PC mean value and maximum theoretical value (triangular dist. towards lower values)		Secondary_PC_types	Triangular	Sec_Conversion_Eff_Input [*, Min]	Sec_Conversion_Eff_Input [*, Max]	Sec_Conversion_Eff_Input [*, Min]			4.1
Energy Flow/New PC Efficiencies	Init_Sec_Reticulation_Eff	Vector of the initial values of the secondary reticulation efficiency function: between initial PC mean value and maximum theoretical value (triangular dist. towards lower values)		Secondary_PC_types	Triangular	Sec_Reticulation_Eff_Input[*, Min]	Sec_Reticulation_Eff_Input[*, Max]	Sec_Reticulation_Eff_Input[*, Min]			4.2
Energy Flow/New PC Efficiencies	Sec_Conversion_Eff_Base	Vector of the lower asymptotes of the secondary conversion efficiency function: between 0 and initial PC mean efficiency value (triangular dist. towards lower values)		Secondary_PC_types	Triangular	vector(0)	Sec_Conversion_Eff_Input[*, Min]	vector(0)			4.1
Energy Flow/New PC Efficiencies	Sec_Reticulation_Eff_Base	Vector of the lower asymptotes of the secondary reticulation efficiency function: between 0 and initial PC mean efficiency value		Secondary_PC_types	Uniform	vector(0)	Sec_Reticulation_Eff_Input[*, Min]				4.2
Energy Flow/Primary Resource	Initial_NRE_Resource	Vector of initial remaining non-renewable energy stocks by type, in terms of RURR (above terminal EROI; log-normal dist. as estimates vary by orders of magnitude)	EJ	NRE_types	Log-Normal				Initial_NRE_Resource_Input[*, Mean]	Initial_NRE_Resource_Input[*, SD]	2.1

Sector	Element name	Description	Unit	Array labels	Distribution	Minimum	Maximum	Most likely	Mean	Standard deviation	Input ref.
Energy Flow/Primary Resource	RE_Potential	Vector of initial remaining sustainably exploitable renewable energy flows by type (above terminal EROI; log-normal dist. as estimates vary by orders of magnitude)	EJ	RE_types	Log-Normal (truncated)	Initial_RE_Output_Rate	vector(99999 EJ/yr)		RE_Potential_Input[*, Mean]	RE_Potential_Input[*, SD]	2.2
EROI/New PC EROI	Initial_NRE_EROI	Vector of the initial values of the NRE EROI function for new PC (normal dist.)		NRE_types	Normal (truncated)	NRE_EROI_Terminal_Input[*, Max]	vector(999)		Initial_NRE_EROI_Input[*, Mean]	Initial_NRE_EROI_Input[*, SD]	6.4
EROI/New PC EROI	Initial_RE_EROI	Vector of the initial values of the RE EROI function for new PC (normal dist.)		RE_types	Normal (truncated)	RE_EROI_Terminal_Input[*, Max]	vector(999)		Initial_RE_EROI_Input[*, Mean]	Initial_RE_EROI_Input[*, SD]	6.1
EROI/New PC EROI	NRE_EROI_Drop	Vector of the differences between the upper asymptotes and initial values of the NRE EROI function		NRE_types	Uniform	NRE_EROI_Drop_Input[*, Min]	NRE_EROI_Drop_Input[*, Max]				6.6
EROI/New PC EROI	NRE_EROI_Terminal	Vector of the final values (depletion = 1) of the NRE EROI function (lowest acceptable EROI for a viable energy source)		NRE_types	Uniform	NRE_EROI_Terminal_Input[*, Min]	NRE_EROI_Terminal_Input[*, Max]				6.5
EROI/New PC EROI	RE_EROI_Drop	Vector of the differences between the upper asymptotes and initial values of the RE EROI function		RE_types	Uniform	RE_EROI_Drop_Input[*, Min]	RE_EROI_Drop_Input[*, Max]				6.3
EROI/New PC EROI	RE_EROI_Terminal	Vector of the final values (exhaustion = 1) of the RE EROI function (lowest acceptable EROI for a viable energy source)		RE_types	Uniform	RE_EROI_Terminal_Input[*, Min]	RE_EROI_Terminal_Input[*, Max]				6.2
Primary NRE	CapEx_Fraction	Vector of fractions of NRE investment energy devoted to capital (construction and decommissioning)		NRE_types	Uniform	CapEx_Fraction_Input[*, Min]	CapEx_Fraction_Input[*, Max]				8.1

Sector	Element name	Description	Unit	Array labels	Distribution	Minimum	Maximum	Most likely	Mean	Standard deviation	Input ref.
Primary NRE	Decommission_Fraction	Vector of fractions of NRE investment energy devoted to capital used in the decommissioning stage		NRE_types	Uniform	Decommission_Fraction_Input[*, Min]	Decommission_Fraction_Input[*, Max]				8.2
Primary NRE	EC_Split_Heat_Factor	Vector of initial fractions of NRE input energy consisting of heat, divided by the heat share of initial EC supply		NRE_types	Uniform	EC_Split_Heat_Factor_Input[*, Min]	EC_Split_Heat_Factor_Input[*, Max]				8.4
Primary NRE	EC_Split_LaG_Factor	Vector of initial fractions of NRE input energy consisting of liquid and gaseous fuels, divided by the LaG share of initial EC supply		NRE_types	Uniform	EC_Split_LaG_Factor_Input[*, Min]	EC_Split_LaG_Factor_Input[*, Max]				8.3
Primary NRE	Power_Capacity_Build_Time	Vector of values for NRE build time (investment decision to operation)	yr	NRE_types	Uniform	PC_Build_Time_Input[*, Min]	PC_Build_Time_Input[*, Max]				8.5
Primary NRE	Power_Capacity_Lifetime	Vector of values for NRE lifetime (in operation)	yr	NRE_types	Uniform	PC_Lifetime_Input[*, Min]	PC_Lifetime_Input[*, Max]				8.6
Primary RE	CapEx_Fraction	Vector of fractions of RE investment energy devoted to capital (construction and decommissioning)		RE_types	Uniform	CapEx_Fraction_Input[*, Min]	CapEx_Fraction_Input[*, Max]				9.1
Primary RE	Decommission_Fraction	Vector of fractions of RE investment energy devoted to capital used in the decommissioning stage		RE_types	Uniform	Decommission_Fraction_Input[*, Min]	Decommission_Fraction_Input[*, Max]				9.2
Primary RE	EC_Split_Heat_Factor	Vector of initial fractions of RE input energy consisting of heat, divided by the heat share of initial EC supply		RE_types	Uniform	EC_Split_Heat_Factor_Input[*, Min]	EC_Split_Heat_Factor_Input[*, Max]				9.4
Primary RE	EC_Split_LaG_Factor	Vector of initial fractions of RE input energy consisting of liquid and gaseous fuels, divided by the LaG share of initial EC supply		RE_types	Uniform	EC_Split_LaG_Factor_Input[*, Min]	EC_Split_LaG_Factor_Input[*, Max]				9.3

Sector	Element name	Description	Unit	Array labels	Distribution	Minimum	Maximum	Most likely	Mean	Standard deviation	Input ref.
Primary RE	Power_Capacity_Build_Time	Vector of values for RE build time (investment decision to operation)	yr	RE_types	Uniform	PC_Build_Time_Input[*, Min]	PC_Build_Time_Input[*, Max]				9.5
Primary RE	Power_Capacity_Lifetime	Vector of values for RE lifetime (in operation)	yr	RE_types	Uniform	PC_Lifetime_Input[*, Min]	PC_Lifetime_Input[*, Max]				9.6
Secondary/Electricity System	CF_Max_Baseload_Coeff	Sets the magnitude of the CF reduction response to intermittent penetration, relative to the intermittent generator response, for baseload generators			Uniform	CF_Max_Baseload_Coeff_Input[Min]	CF_Max_Baseload_Coeff_Input[Max]				10.19
Secondary/Electricity System	CF_Max_Mult_Asymptote	Sets the upper asymptote of the intermittent CF maximum multiplier (lower values more common)			Pareto	1					n/a
Secondary/Electricity System	CF_Max_Peaker_Coeff	Sets the magnitude of the CF reduction response to intermittent penetration, relative to the intermittent generator response, for peaking generators			Uniform	CF_Max_Peaker_Coeff_Input[Min]	CF_Max_Peaker_Coeff_Input[Max]				10.18
Secondary/Electricity System	Demand_Flex_Coeff	Sets the magnitude of the fractional reduction in intermittent response (CF, intermittent AI, reticulation efficiency) needed when demand flexibility is equal to 1			Uniform	Demand_Flex_Coeff_Input[Min]	Demand_Flex_Coeff_Input[Max]				10.17
Secondary/Electricity System	Diversity_Coeff	Sets the magnitude of the fractional reduction in intermittent response (CF, intermittent AI, reticulation efficiency) needed when intermittent diversity is equal to 1			Uniform	Diversity_Coeff_Input[Min]	Diversity_Coeff_Input[Max]				10.16

Sector	Element name	Description	Unit	Array labels	Distribution	Minimum	Maximum	Most likely	Mean	Standard deviation	Input ref.
Secondary/Electricity System	Intermit_AI_Mult_Asymptote	Sets the upper asymptote of the intermittent AI required multiplier (lower values more common)			Pareto	Intermit_AI_Mult_Final					n/a
Secondary/Electricity System	Intermit_AI_Mult_Final	Sets the final value (at intermittent penetration of 1) of the intermittent AI required multiplier			Uniform	Intermit_AI_Mult_Final_Input[Min]	Intermit_AI_Mult_Final_Input[Max]				10.13
Secondary/Electricity System	Retic_Eff_Mult_Asymptote	Sets the upper asymptote of the intermittent reticulation efficiency multiplier (lower values more common)			Pareto	1					n/a
Secondary/Electricity System	Retic_Eff_Mult_Final	Sets the final value (at intermittent penetration of 1) of the intermittent reticulation efficiency multiplier			Uniform	Retic_Eff_Mult_Final_Input[Min]	Retic_Eff_Mult_Final_Input[Max]				10.14
Secondary	AI_CapEx_Fraction	Vector of fractions of secondary auxiliary infrastructure investment energy devoted to capital (construction and decommissioning)		Secondary_AI_types	Uniform	AI_CapEx_Fraction_Input[*, Min]	AI_CapEx_Fraction_Input[*, Max]				10.7
Secondary	AI_Decommission_Fraction	Vector of fractions of secondary auxiliary infrastructure investment energy devoted to capital used in the decommissioning stage		Secondary_AI_types	Uniform	AI_Decommission_Fraction_Input[*, Min]	AI_Decommission_Fraction_Input[*, Max]				10.8
Secondary	AI_EC_Split_Heat_Factor	Vector of initial fractions of secondary auxiliary infrastructure input energy consisting of heat, divided by the heat share of initial EC supply		Secondary_AI_types	Uniform	AI_EC_Split_Heat_Factor_Input[*, Min]	AI_EC_Split_Heat_Factor_Input[*, Max]				10.10
Secondary	AI_EC_Split_LaG_Factor	Vector of initial fractions of secondary auxiliary infrastructure input energy consisting of liquid and gaseous fuels, divided by the LaG share of initial EC supply		Secondary_AI_types	Uniform	AI_EC_Split_LaG_Factor_Input[*, Min]	AI_EC_Split_LaG_Factor_Input[*, Max]				10.9

Sector	Element name	Description	Unit	Array labels	Distribution	Minimum	Maximum	Most likely	Mean	Standard deviation	Input ref.
Secondary	Auxiliary_Build_Time	Vector of values for secondary auxiliary infrastructure build time (investment decision to operation)	yr	Secondary_AI_types	Uniform	AI_Build_Time_Input[*, Min]	AI_Build_Time_Input[*, Max]				10.11
Secondary	Auxiliary_Lifetime	Vector of values for secondary auxiliary infrastructure lifetime (in operation)	yr	Secondary_AI_types	Uniform	AI_Lifetime_Input[*, Min]	AI_Lifetime_Input[*, Max]				10.12
Secondary	PC_CapEx_Fraction	Vector of fractions of secondary power capacity investment energy devoted to capital (construction and decommissioning)		Secondary_PC_types	Uniform	PC_CapEx_Fraction_Input[*, Min]	PC_CapEx_Fraction_Input[*, Max]				10.1
Secondary	PC_Decommission_Fraction	Vector of fractions of secondary power capacity investment energy devoted to capital used in the decommissioning stage		Secondary_PC_types	Uniform	PC_Decommission_Fraction_Input[*, Min]	PC_Decommission_Fraction_Input[*, Max]				10.2
Secondary	PC_EC_Split_Heat_Factor	Vector of initial fractions of secondary power capacity input energy consisting of heat, divided by the heat share of initial EC supply		Secondary_PC_types	Uniform	PC_EC_Split_Heat_Factor_Input[*, Min]	PC_EC_Split_Heat_Factor_Input[*, Max]				10.4
Secondary	PC_EC_Split_LaG_Factor	Vector of initial fractions of secondary power capacity input energy consisting of liquid and gaseous fuels, divided by the LaG share of initial EC supply		Secondary_PC_types	Uniform	PC_EC_Split_LaG_Factor_Input[*, Min]	PC_EC_Split_LaG_Factor_Input[*, Max]				10.3
Secondary	Power_Capacity_Build_Time	Vector of values for secondary power capacity build time (investment decision to operation)	yr	Secondary_PC_types	Uniform	PC_Build_Time_Input[*, Min]	PC_Build_Time_Input[*, Max]				10.5

Sector	Element name	Description	Unit	Array labels	Distribution	Minimum	Maximum	Most likely	Mean	Standard deviation	Input ref.
Secondary	Power_Capacity_Lifetime	Vector of values for secondary power capacity lifetime (in operation)	yr	Secondary_PC_types	Uniform	PC_Lifetime_Input[*, Min]	PC_Lifetime_Input[*, Max]				10.6
System Control/Invest Share	EU_Penetration_Limit	Vector of penetration limits for EU PC types (at this limit, no further investment can occur due to operational limitations)		End_use_PC_types	Uniform	EU_Penetration_Limit_Input[*, Min]	EU_Penetration_Limit_Input[*, Max]				12.3
System Control/Invest Share	Sec_Penetration_Limit	Vector of penetration limits for secondary PC types (at this limit, no further investment can occur due to operational limitations)		Secondary_PC_types	Uniform	Sec_Penetration_Limit_Input[*, Min]	Sec_Penetration_Limit_Input[*, Max]				12.2
System Control	EC_Split_Heat_Correlator	Random number between 0 and 1 used as an independent reference for correlating the initial fraction of PC and AI input energy consisting of heat relative to the heat share of initial EC supply			Uniform	0	1				12.9
System Control	EC_Split_LaG_Correlator	Random number between 0 and 1 used as an independent reference for correlating the initial fraction of PC and AI input energy consisting of LaG fuels relative to the LaG fuels share of initial EC supply			Uniform	0	1				12.9
System Control	EROI_ECC_Correlator	Random number between 0 and 1 used as an independent reference for correlating ECC estimates and the initial values of the EROI functions (in opposite directions)			Uniform	0	1				12.10

Sector	Element name	Description	Unit	Array labels	Distribution	Minimum	Maximum	Most likely	Mean	Standard deviation	Input ref.
System Control	ESMR_Limit	Sets the upper limit for the share of EC inflow that can be used within the GES metabolism (investment in new PC drops to zero at this limit)			Triangular	ESMR_Limit_Input[Min]	ESMR_Limit_Input[Max]	ESMR_Limit_Input[Min]			12.1

9.4.2.1 Shape factor for Pareto distributions

Logistic functions for demand flexibility and EU CF target as functions of time (see section 9.3.2), and electricity system multipliers as functions of intermittent penetration (see section 9.3.3.2.1.1), use upper function asymptotes as inputs to control the shape of the curves. These shapes are more sensitive to the choice of asymptote near the lower ends of the possible ranges. As such, these regions must be sampled more frequently to provide a greater representation of logistic function shapes:

- To achieve this, probability distributions specifying upper asymptotes for these functions use the Pareto distribution (Type I):
  - These distributions are specified such that cumulative probabilities of 0.99 occur between lower limits and twice the lower limit.
- The lower ends of these ranges correspond to the inflection point being at the middle of the *x* range (2055 for time dependent trends, 50% intermittent generation penetration for electricity system multipliers) while the upper extremes correspond to the inflection point at the extremes of the *x* range (2055 for time dependent trends, 50% intermittent generation penetration for electricity system multipliers), respectively. I.e., the function inflection point located at:
  - 2055 to 2100 for time dependent trends,
  - 50% to 100% intermittent generation penetration for the intermittent electricity AI required multiplier, and
  - 50% to 0% intermittent generation penetration for the intermittent electricity reticulation efficiency and upstream maximum CF multipliers.

- The Pareto distribution CDF expression can be rearranged to give the shape parameter: $ln(0.01)/ln(1/2)$, or the vectorized equivalent.
- This adjustment is used only where the upper asymptote parameter is not physically meaningful (unlike ES demand, EROI, and efficiency trends, where an upper asymptote value is specified).

9.4.3 Stocks

Sector	Element name	Type	Description	Unit	Array labels	Initial value/outflow	Rate of change/inputs (additions)	Rate of change (withdrawal requests)	Delay time
End-use	Auxiliary_Addition	Material Delay	Vector of stocks of end-use auxiliary infrastructure peak capacity in the build phase	EJ/yr	End_use_AI_types	(vector(1) + Init_EU_AI_Growth_Rate) * Initial_End_Use_AI / Auxiliary_Lifetime	Auxiliary_Investment_Rate		Auxiliary_Build_Time
End-use	Auxiliary_Operation	Material Delay	Vector of stocks of end-use auxiliary infrastructure peak capacity in the operating phase	EJ/yr	End_use_AI_types	Initial_End_Use_AI / Auxiliary_Lifetime	Auxiliary_Addition		Auxiliary_Lifetime
End-use	Power_Capacity_Addition	Material Delay	Vector of stocks of end-use nameplate EU power capacity in the build phase	EJ/yr	End_use_PC_types	(vector(1) + Init_EU_PC_Growth_Rate) * Initial_End_Use_PC / Power_Capacity_Lifetime	End_Use_PC_Invest_Delay		Power_Capacity_Build_Time
End-use	Power_Capacity_Operation	Material Delay	Vector of stocks of end-use nameplate EU power capacity in the operating phase	EJ/yr	End_use_PC_types	Initial_End_Use_PC / Power_Capacity_Lifetime	Power_Capacity_Addition		Power_Capacity_Lifetime
Energy Flow	EC_Consumption	Integrator	Vector of cumulative consumption by EC type (both final demand and ES metabolism); moving average of input used as smoothing function	EJ	EC_types	vector(0 EJ)	Supply_Demand_Balance.Withdrawal_Rate		
Energy Flow	EC_Inflow_Integ	Integrator	Vector of cumulative production by EC type; moving average of input used as smoothing function	EJ	EC_types	vector(0 EJ)	EC_Inflow_Rate		
Energy Flow	ES_Metabolism_Integ	Integrator	Vector of cumulative GES metabolic consumption by EC type; moving average of input used as smoothing function	EJ	EC_types	vector(0 EJ)	Autocatalytic_Loop + Capital_Hypercycle		

Sector	Element name	Type	Description	Unit	Array labels	Initial value/outflow	Rate of change/inputs (additions)	Rate of change (withdrawal requests)	Delay time
Energy Flow	Supply_Demand_Balance	Reservoir	Vector of cumulative production minus consumption by EC type (indicates cumulative supply/demand imbalances)	EJ	EC_types	vector(0 EJ)	EC_Inflow_Rate	EC_Final_Demand + Autocatalytic_Loop + Capital_Hypercycle	
Energy Flow/Flow Routing	End_Use_Output	Integrator	Vector of cumulative power output by EU PC type (drives EU efficiency improvements)	EJ	End_use_PC_types	vector(0 EJ)	End_Use_Output_Rate		
Energy Flow/Flow Routing	Secondary_Output	Integrator	Vector of cumulative power output by secondary PC type (drives secondary efficiency improvements)	EJ	Secondary_PC_types	vector(0 EJ)	Secondary_Output_Rate		
Energy Flow/Mean Stock Efficiencies	End_Use_Conv_Eff_Mean_Integ	Material Delay	Vector of cumulative new PC end-use conversion efficiency weighted by PC additions for PC in operation (for tracking mean efficiency of PC in operation)	EJ/yr	End_use_PC_types	End_Use_Conversion_Eff_Input[*, Min] * Initial_End_Use_PC / End_Use_Sector.Power_Capacity_Lifetime	End_Use_Conv_Eff_Add_Weighting		End_Use_Sector.Power_Capacity_Lifetime
Energy Flow/Mean Stock Efficiencies	End_Use_ES_Eff_Mean_Integ	Material Delay	Vector of cumulative new PC end-use to ES efficiency weighted by PC additions for PC in operation (for tracking mean efficiency of PC in operation)	EJ/yr	End_use_PC_types	Init_End_Use_ES_Eff_PC_Mean * Initial_End_Use_PC / End_Use_Sector.Power_Capacity_Lifetime	End_Use_ES_Eff_Add_Weighting		End_Use_Sector.Power_Capacity_Lifetime
Energy Flow/Mean Stock Efficiencies	Sec_Conv_Eff_Mean_Integ	Material Delay	Vector of cumulative new PC secondary conversion efficiency weighted by PC additions for PC in operation (for tracking mean efficiency of PC in operation)	EJ/yr	Secondary_PC_types	Sec_Conversion_Eff_Input[*, Min] * Initial_Secondary_PC / Secondary_Sector.Power_Capacity_Lifetime	Sec_Conv_Eff_Add_Weighting		Secondary_Sector.Power_Capacity_Lifetime

Sector	Element name	Type	Description	Unit	Array labels	Initial value/outflow	Rate of change/inputs (additions)	Rate of change (withdrawal requests)	Delay time
Energy Flow/Mean Stock Efficiencies	Sec_Retic_Eff_Mean_Integ	Material Delay	Vector of cumulative new PC secondary reticulation efficiency weighted by PC additions for PC in operation (for tracking mean efficiency of PC in operation)	EJ/yr	Secondary_PC_types	Sec_Reticulation_Eff_Input[*, Min] * Initial_Secondary_PC / Secondary_Sector.Power_Capacity_Lifetime	Sec_Retic_Eff_Add_Weighting		Secondary_Sector.Power_Capacity_Lifetime
Energy Flow/Primary Resource	NRE_Resource	Reservoir	Vector of remaining non-renewable energy stocks by type, in terms of RURR (above terminal EROI)	EJ	NRE_types	Initial_NRE_Resource	vector(0 EJ/yr)	NRE_Secondary_Input_Rate + Direct_NRE_Use	
EROI	NRE_EROI_PC_Mean_Integ	Material Delay	Vector of cumulative new NRE PC EROI weighted by PC additions for PC in operation (for tracking mean EROI of PC in operation)	EJ/yr	NRE_types	Init_NRE_EROI_PC_Mean* Initial_NRE_PC / Primary_NRE_Sector.Power_Capacity_Lifetime	NRE_EROI_Add_Weighting		Primary_NRE_Sector.Power_Capacity_Lifetime
EROI	RE_EROI_PC_Mean_Integ	Material Delay	Vector of cumulative new RE PC EROI weighted by PC additions for PC in operation (for tracking mean EROI of PC in operation)	EJ/yr	RE_types	Init_RE_EROI_PC_Mean * Initial_RE_PC / Primary_RE_Sector.Power_Capacity_Lifetime	RE_EROI_Add_Weighting		Primary_RE_Sector.Power_Capacity_Lifetime
EROI	RE_Redevelopment_Potential	Reservoir	Vector of cumulative unused RE potential available for redevelopment (post-decommissioning)	EJ/yr	RE_types	vector(0 EJ/yr)	max(Primary_RE_Sector.Power_Capacity_Operation - Primary_RE_Sector.Power_Capacity_Addition, vector(0 EJ/yr^2))	Primary_RE_Sector.Power_Capacity_Addition	
Primary NRE	Power_Capacity_Addition	Material Delay	Vector of stocks of NRE nameplate power capacity in the build phase	EJ/yr	NRE_types	(vector(1) + Init_NRE_Growth_Rate) * Initial_NRE_PC / Power_Capacity_Lifetime	NRE_PC_Invest		Power_Capacity_Build_Time
Primary NRE	Power_Capacity_Operation	Material Delay	Vector of stocks of NRE nameplate power capacity in the operating phase	EJ/yr	NRE_types	Initial_NRE_PC / Power_Capacity_Lifetime	Power_Capacity_Addition		Power_Capacity_Lifetime

Sector	Element name	Type	Description	Unit	Array labels	Initial value/outflow	Rate of change/inputs (additions)	Rate of change (withdrawal requests)	Delay time
Primary RE	Power_Capacity_Addition	Material Delay	Vector of stocks of RE nameplate power capacity in the build phase	EJ/yr	RE_types	(vector(1) + Init_RE_Growth_Rate) * Initial_RE_PC / Power_Capacity_Lifetime	RE_PC_Invest		Power_Capacity_Build_Time
Primary RE	Power_Capacity_Operation	Material Delay	Vector of stocks of RE nameplate power capacity in the operating phase	EJ/yr	RE_types	Initial_RE_PC / Power_Capacity_Lifetime	Power_Capacity_Addition		Power_Capacity_Lifetime
Secondary	Auxiliary_Addition	Material Delay	Vector of stocks of secondary auxiliary infrastructure peak capacity in the build phase	EJ/yr	Secondary_AI_types	(vector(1) + Init_Sec_AI_Growth_Rate) * Initial_Secondary_AI / Auxiliary_Lifetime	Auxiliary_Investment_Rate		Auxiliary_Build_Time
Secondary	Auxiliary_Operation	Material Delay	Vector of stocks of secondary auxiliary infrastructure peak capacity in the operating phase	EJ/yr	Secondary_AI_types	Initial_Secondary_AI / Auxiliary_Lifetime	Auxiliary_Addition		Auxiliary_Lifetime
Secondary	Power_Capacity_Addition	Material Delay	Vector of stocks of secondary nameplate power capacity in the build phase	EJ/yr	Secondary_PC_types	(vector(1) + Init_Sec_PC_Growth_Rate) * Initial_Secondary_PC / Power_Capacity_Lifetime	Secondary_PC_Invest_Delay		Power_Capacity_Build_Time
Secondary	Power_Capacity_Operation	Material Delay	Vector of stocks of secondary nameplate power capacity in the operating phase	EJ/yr	Secondary_PC_types	Initial_Secondary_PC / Power_Capacity_Lifetime	Power_Capacity_Addition		Power_Capacity_Lifetime
System Control/EC Committed	EC_Deficit_Horizon_Integ	Integrator	Vector of cumulative forecast EC deficit at the selected time horizon; moving average of input used as smoothing function	EJ-yr	EC_types	vector(0 EJ-yr)	EC_Deficit_Horizon		
System Control/EC Committed	EU_PC_Plan_Horizon	Material Delay	Vector of stocks of EU PC set to be decommissioned within the build time of the corresponding EU PC type	EJ/yr	End_use_PC_types	Initial_End_Use_PC / End_Use_Sector.Power_Capacity_Lifetime	EU_PC_Decomm_Preempt_Plan		End_Use_Sector.Power_Capacity_Build_Time

Sector	Element name	Type	Description	Unit	Array labels	Initial value/outflow	Rate of change/inputs (additions)	Rate of change (withdrawal requests)	Delay time
System Control/EC Committed	Sec_PC_Plan_Horizon	Material Delay	Vector of stocks of secondary PC set to be decommissioned within the composite build time of the corresponding secondary PC type and associated primary PC	EJ/yr	Secondary_PC_types	Initial_Secondary_PC / Secondary_Sector.Power_Capacity_Lifetime	Sec_PC_Decomm_Preempt_Plan		max(Primary_Build_Time, Secondary_Sector.Power_Capacity_Build_Time)
System Control/Invest Synchronization	End_Use_PC_Invest_Delay	Material Delay	Vector of stocks of EU PC committed to be built but within the minimum PC timeframe before being added to the build phase (required for synchronization)	EJ/yr	End_use_PC_types	vector(0 EJ/yr^2)	End_Use_PC_Invest_Sum		~Minimum_PC_Timeframe
System Control/Invest Synchronization	NRE_PC_Invest_Adj_Integ	Integrator	Vector of cumulative adjustments made to NRE PC investment for the purpose of balancing primary and secondary PC quantities, within the timeframe of primary PC build time	EJ/yr	NRE_types	vector(0 EJ/yr)	NRE_PC_Invest_Adj - NRE_PC_Invest_Adj_Delay		
System Control/Invest Synchronization	Primary_PC_Invest_Delay	Material Delay	Vector of stocks of secondary PC committed to investment, delayed by the difference between secondary and primary build times (where secondary is longer) linearly scaled by secondary CFs relative to their maxima	EJ/yr	Secondary_PC_types	vector(0 EJ/yr^2)	Secondary_PC_Invest		(Secondary_Capacity_Factor / Secondary_CF_Max) * max(vector(0 yr), Secondary_Sector.Power_Capacity_Build_Time - Primary_Build_Time) + vector(~Minimum_PC_Timeframe)

Sector	Element name	Type	Description	Unit	Array labels	Initial value/outflow	Rate of change/inputs (additions)	Rate of change (withdrawal requests)	Delay time
System Control/Invest Synchronization	RE_PC_Invest_Adj_Integ	Integrator	Vector of cumulative adjustments made to RE PC investment for the purpose of balancing primary and secondary PC quantities, within the timeframe of primary PC build time	EJ/yr	RE_types	vector(0 EJ/yr)	RE_PC_Invest_Adj - RE_PC_Invest_Adj_Delay		
System Control/Invest Synchronization	Secondary_PC_Invest_Delay	Material Delay	Vector of stocks of secondary PC committed to investment, delayed by the difference between primary and secondary build times (where primary is longer) linearly scaled by corresponding primary CFs relative to their maxima	EJ/yr	Secondary_PC_types	vector(0 EJ/yr^2)	Secondary_PC_Invest		(sumc(NRE_Capacity_Factor * NRE_Secondary_Input_ID / NRE_CF_Max) + sumc(RE_Capacity_Factor * RE_Secondary_Input_ID / RE_CF_Max)) * max(vector(0 yr), Primary_Build_Time - Secondary_Sector.Power_Capacity_Build_Time) + vector(~Minimum_PC_Timeframe)
System Control	EC_Deficit_Integral	Integrator	Vector of cumulative EC deficit (measured in years of consumption) above the EC deficit limit	yr^2	EC_types	vector(0 yr^2)	abs(max(vector(EC_Deficit_Limit), EC_Deficit))		

9.4.3.1 Additional parameters

A lower bound of **vector(0 EJ/yr)** is used for **RE_Redevelopment_Potential**, as usage of accumulated RE potential for redevelopment should be prevented when there is none available.

Moving averages are calculated for **EC_Consumption**, **EC_Inflow_Integ**, and **ES_Metabolism_Integ** (using **Averaging_Period**) and **EC_Deficit_Horizon_Integ** (using **Invest_Adjust_Time**). These smoothing functions minimize short-term variations in critical feedback loops for greater system stability.

9.4.4 Functions

9.4.4.1 Expression, summation, and conditional functions

Sector	**Element name**	**Type**	**Description**	**Unit**	**Array labels**	**Expression/condition/inputs**
Demand	Demand_Flexibility	Expression	The fraction of final demand responsive to short-term supply availability (follows logistic curve)			Demand_Flex_Asymptote / (1 + (((Demand_Flex_Asymptote / Initial_Demand_Flex) - 1)^(1 - (ETime / ~Simulation_Base_Period))) * (((Demand_Flex_Asymptote / Final_Demand_Flex) - 1)^(ETime / ~Simulation_Base_Period)))
Demand	ES_Demand	Expression	Vector of final ES demand by ES type (follows logistic curve; uses negative rate for declining curve)	EJ/yr	ES_types	if(ES_Final_Demand_Mult < vector(1), Initial_ES_Demand * (ES_Final_Demand_Mult / (vector(1) + (ES_Final_Demand_Mult - vector(1)) * exp(min(vector(700), Initial_ES_Demand_RoC * ETime / (vector(1) - (1 / ES_Final_Demand_Mult)))))), Initial_ES_Demand * (ES_Final_Demand_Mult / (vector(1) + (ES_Final_Demand_Mult - vector(1)) * exp(min(vector(700), - Initial_ES_Demand_RoC * ETime / (vector(1) - (1 / ES_Final_Demand_Mult))))))
End-use	AI_Addition_EC_Use	Expression	Vector of rates of energy carrier use for the purposes of adding new end-use auxiliary infrastructure	EJ/yr	EC_types	sumc((vector(End_use_AI_types, 1) - AI_Decommission_Fraction) * AI_CapEx_Fraction * (Auxiliary_Addition.Amount_in_Transit * End_Use_AI_ECC / Auxiliary_Build_Time) * AI_EC_Split)
End-use	AI_Decommission_EC_Use	Expression	Vector of rates of energy carrier use for the purposes of decommissioning end-of-life end-use auxiliary infrastructure	EJ/yr	EC_types	sumc(AI_Decommission_Fraction * AI_CapEx_Fraction * Auxiliary_Operation * End_Use_AI_ECC * AI_EC_Split)
End-use	AI_EC_Split	Expression	Matrix of the EC composition of end-use auxiliary infrastructure investment energy, adjusted for thermal energy equivalence		End_use_AI_types, EC_types	(Demand_EC_Split / Initial_Supply_EC_Split) * AI_Initial_EC_Split / sumr(EC_Thermal_Equivalence * (Demand_EC_Split / Initial_Supply_EC_Split) * AI_Initial_EC_Split)

Sector	Element name	Type	Description	Unit	Array labels	Expression/condition/inputs
End-use	AI_Initial_EC_Split	Expression	Initial shares of end-use auxiliary infrastructure input energy by EC type, adjusted for thermal energy		End_use_AI_types,	Initial_Supply_EC_Split * matrix(vector(1), AI_EC_Split_LaG_Factor, AI_EC_Split_Heat_Factor) / sumr(EC_Thermal_Equivalence * Initial_Supply_EC_Split * matrix(vector(1), AI_EC_Split_LaG_Factor, AI_EC_Split_Heat_Factor))
End-use	AI_Operation_EC_Use	Expression	Vector of rates of energy carrier use for the purposes of operating existing end-use auxiliary infrastructure	EJ/yr	EC_types	sumc((vector(End_use_AI_types, 1) - AI_CapEx_Fraction) * (Auxiliary_Operation.Amount_in_Transit * End_Use_AI_ECC / Auxiliary_Lifetime) * AI_EC_Split)
End-use	Auxiliary_Investment_Rate	Expression	Rate of investment in new end-use auxiliary infrastructure peak capacity	EJ/yr ^2	End_use_AI_types	max(Auxiliary_Requirement - Auxiliary_Operation.Amount_in_Transit, vector(0 EJ/yr)) / Auxiliary_Build_Time
End-use	Auxiliary_Requirement	Expression	Sum requirement for end-use auxiliary infrastructure peak capacity	EJ/yr	End_use_AI_types	sumc(Power_Capacity_Operation.Amount_in_Transit * End_Use_Capacity_Factor * PC_AI_ID) * Peak_Factor
End-use	PC_Addition_EC_Use	Expression	Vector of rates of energy carrier use for the purposes of adding new end-use power capacity	EJ/yr	EC_types	sumc((vector(End_use_PC_types, 1) - PC_Decommission_Fraction) * PC_CapEx_Fraction * (Power_Capacity_Addition.Amount_in_Transit * End_Use_PC_ECC / Power_Capacity_Build_Time) * PC_EC_Split)
End-use	PC_Decommission_EC_Use	Expression	Vector of rates of energy carrier use for the purposes of decommissioning end-of-life end-use power capacity	EJ/yr	EC_types	sumc(PC_Decommission_Fraction * PC_CapEx_Fraction * Power_Capacity_Operation * End_Use_PC_ECC * PC_EC_Split)
End-use	PC_EC_Split	Expression	Matrix of the EC composition of end-use power capacity investment energy, adjusted for thermal energy equivalence		End_use_PC_types, EC_types	(Demand_EC_Split / Initial_Supply_EC_Split) * PC_Initial_EC_Split / sumr(EC_Thermal_Equivalence * (Demand_EC_Split / Initial_Supply_EC_Split) * PC_Initial_EC_Split)
End-use	PC_Initial_EC_Split	Expression	Initial shares of end-use power capacity input energy by EC type, adjusted for thermal energy		End_use_PC_types, EC_types	Initial_Supply_EC_Split * matrix(vector(1), PC_EC_Split_LaG_Factor, PC_EC_Split_Heat_Factor) / sumr(EC_Thermal_Equivalence * Initial_Supply_EC_Split * matrix(vector(1), PC_EC_Split_LaG_Factor, PC_EC_Split_Heat_Factor))
End-use	PC_Operation_EC_Use	Expression	Vector of rates of energy carrier use for the purposes of operating existing end-use power capacity	EJ/yr	EC_types	sumc((vector(End_use_PC_types, 1) - PC_CapEx_Fraction) * (End_Use_Capacity_Factor / Init_End_Use_CF_Target) * (Power_Capacity_Operation.Amount_in_Transit * End_Use_PC_ECC / Power_Capacity_Lifetime) * PC_EC_Split)
End-use	Peak_Factor	Expression	Vector of ratios of peak to average power output by EU AI type (reduced linearly by increasing demand flexibility)		End_use_AI_types	(Init_End_Use_Peak_Factor - vector(1)) * vector(1 - Demand_Flexibility) + vector(1)

Sector	Element name	Type	Description	Unit	Array labels	Expression/condition/inputs
Energy Flow	Autocatalytic_Loop	Sum	Sum of EC flows for construction, operation, and decommissioning of primary and secondary PC and AI	EJ/yr	EC_types	Primary_NRE_Sector.Addition_EC_Use, Primary_NRE_Sector.Operation_EC_Use, Primary_NRE_Sector.Decommission_EC_Use, Primary_RE_Sector.Addition_EC_Use, Primary_RE_Sector.Operation_EC_Use, Primary_RE_Sector.Decommission_EC_Use, Secondary_Sector.PC_Operation_EC_Use, Secondary_Sector.PC_Addition_EC_Use, Secondary_Sector.PC_Decommission_EC_Use, Secondary_Sector.AI_Operation_EC_Use, Secondary_Sector.AI_Addition_EC_Use, Secondary_Sector.AI_Decommission_EC_Use
Energy Flow	Capital_Hyper cycle	Sum	Sum of EC flows for construction, operation, and decommissioning of end-use PC and AI	EJ/yr	EC_types	End_Use_Sector.AI_Decommission_EC_Use, End_Use_Sector.AI_Operation_EC_Use, End_Use_Sector.PC_Addition_EC_Use, End_Use_Sector.PC_Decommission_EC_Use, End_Use_Sector.PC_Operation_EC_Use, End_Use_Sector.AI_Addition_EC_Use
Energy Flow	Demand_EC_ Split	Expression	Vector of fractional shares of final demand by EC, adjusted for thermal equivalence (does not sum to one)		EC_types	EC_Final_Demand / sumv(EC_Thermal_Equivalence * EC_Final_Demand)
Energy Flow	EC_Final_ Demand	Expression	Vector of final demand by EC (given by ES demand and EU PC composition)	EJ/yr	EC_types	max(sumc(ES_Demand * EC_ES_Conversion), ~PC_Zero_Approx)
Energy Flow	EC_Inflow_Ra te	Expression	Vector of energy production (inflow) by EC (given by available primary and secondary PC)	EJ/yr	EC_types	(sumc(NRE_Secondary_Input_Rate * NRE_EC_Conversion) + sumc(RE_Secondary_Input_Rate * RE_EC_Conversion))
Energy Flow	EC_RE_Fra ction	Expression	Vector of fractional shares of energy production from RE sources by EC		EC_types	min(vector(1), sumc(RE_Secondary_Input_Rate * RE_EC_Conversion) / max(vector(~PC_Zero_Approx), EC_Inflow_Integ.Moving_Average))
Energy Flow	EC_System_E ROI	Expression	Vector of system EROI by EC (EC inflow divided by upstream EC requirements; EC specific point-of-use EROI)		EC_types	EC_Inflow_Integ.Moving_Average / if(ETime = 0 yr, Initial_Autocatalytic_Loop, max(vector(~PC_Zero_Approx), Autocatalytic_Loop))
Energy Flow	ESMR	Expression	Vector of GES internal metabolic use relative to gross energy production by EC (represents 'cost' of the GES; corrected for secondary curtailment)		EC_types	ES_Metabolism_Integ.Moving_Average / (max(vector(~PC_Zero_Approx), EC_Inflow_Integ.Moving_Average) / max(vector(0.01), if(EC_Deficit_Prev > vector(EC_types, 0 yr), vector(EC_types, 1), if(EC_Deficit_Prev < vector(EC_types, EC_Deficit_Limit), vector(EC_types, 0), vector(EC_types, 1) - (EC_Deficit_Prev / EC_Deficit_Limit)))))
Energy Flow	Primary_Generatio n_ID	Expression	Vector of primary PC electricity generation identity by secondary PC type (value of 1 indicates that the production of electricity is considered primary)		Secondary_PC_type s	if(Secondary_Output_ID[*, Electricity] = vector(1) AND Init_Sec_Conversion_Eff = vector(1), 1, 0)

Sector	Element name	Type	Description	Unit	Array labels	Expression/condition/inputs
Energy Flow	RE_Output_Thermal_Equiv	Expression	Vector of output thermal equivalence weighting by RE type		RE_types	vector(1) + sumr(Primary_Generation_ID * RE_Secondary_Input_ID * getcolumn(Secondary_Output_ID, 1)) * (EC_Thermal_Equivalence[Electricity] - 1)
Energy Flow	System_RE_Fraction	Expression	Fractional share of total energy production from RE sources, adjusted for thermal equivalence			sumv(EC_RE_Fraction * (EC_Thermal_Equivalence * EC_Inflow_Integ.Moving_Average / sumv(EC_Thermal_Equivalence * EC_Inflow_Integ.Moving_Average)))
Energy Flow/Flow Routing	EC_Deficit_Limit	Expression	Lower allowable limit for EC deficit (upper limit for surplus; at this limit, corresponding secondary PC CF is reduced by 99%)	yr		~EC_Deficit_Limit_Base + (ETime/~Simulation_Base_Period) * ~EC_Deficit_Limit_Slope
Energy Flow/Flow Routing	EC_ES_Conversion	Expression	Matrix of the conversion of energy service demand to input ECs (refers to reverse direction)		EC_types, ES_types	mult(End_Use_Output_Matrix, End_Use_Input_Scaled)
Energy Flow/Flow Routing	End_Use_Capacity_Factor	Expression	Vector of capacity factors by end-use PC type		End_use_PC_types	End_Use_Output_Rate / max(vector(~PC_Zero_Approx), End_Use_Sector.Amount_in_Transit)
Energy Flow/Flow Routing	End_Use_CF_Target	Expression	Vector of target capacity factors by end-use PC type (above target value, upkeep investment is triggered; follows logistic curve)		End_use_PC_types	End_Use_CF_Target_Asymptote / (vector(1) + (((End_Use_CF_Target_Asymptote / Init_End_Use_CF_Target) - vector(1))^(1 - (ETime / ~Simulation_Base_Period))) * (((End_Use_CF_Target_Asymptote / End_Use_CF_Target_Final) - vector(1))^(ETime / ~Simulation_Base_Period)))
Energy Flow/Flow Routing	End_Use_Input_Scaled	Expression	Matrix of conversion of end-use power output to input ECs (refers to reverse direction)		End_use_PC_types, EC_types	trans(End_Use_Input_ID / End_Use_Conversion_Eff_PC_Mean)
Energy Flow/Flow Routing	End_Use_Output_Matrix	Expression	Matrix of conversion of energy service demand to end-use power output (refers to reverse direction)		ES_types, End_use_PC_types	End_Use_Output_Scaled / End_Use_ES_Eff_PC_Mean
Energy Flow/Flow Routing	End_Use_Output_Rate	Expression	Vector of power output by end-use PC type	EJ/yr	End_use_PC_types	sumc(ES_Demand * End_Use_Output_Matrix)
Energy Flow/Flow Routing	End_Use_Output_Scaled	Expression	Matrix of normalized energy service provision by end-use PC type		ES_types, End_use_PC_types	trans((End_Use_Output_ID * End_Use_Sector.Amount_in_Transit * End_Use_CF_Target * End_Use_ES_Eff_PC_Mean) / sumc(End_Use_Output_ID * End_Use_Sector.Amount_in_Transit * End_Use_CF_Target * End_Use_ES_Eff_PC_Mean))

Sector	Element name	Type	Description	Unit	Array labels	Expression/condition/inputs
Energy Flow/Flow Routing	NRE_EC_Conversion	Expression	Matrix of conversion of NRE input to EC output		NRE_types, EC_types	mult(NRE_Secondary_Input_Matrix, Secondary_Output_Matrix)
Energy Flow/Flow Routing	NRE_Secondary_Input_Matrix	Expression	Matrix of conversion of NRE input to secondary power output		NRE_types, Secondary_PC_types	Sec_Conversion_Eff_PC_Mean * NRE_Secondary_Input_Scaled
Energy Flow/Flow Routing	NRE_Secondary_Input_Rate_Max	Expression	Vector of maximum secondary capacity to process primary NRE input by NRE type	EJ/yr	NRE_types	sumr(NRE_Secondary_Input_ID * Secondary_Sector.Amount_in_Transit * Secondary_CF_Max / Sec_Conversion_Eff_PC_Mean)
Energy Flow/Flow Routing	NRE_Secondary_Input_Scaled	Expression	Matrix of normalized capacity to process primary NRE input by secondary PC type		NRE_types, Secondary_PC_types	(NRE_Secondary_Input_ID * Secondary_Sector.Amount_in_Transit * Secondary_CF_Max / Sec_Conversion_Eff_PC_Mean) / sumr(NRE_Secondary_Input_ID * Secondary_Sector.Amount_in_Transit * Secondary_CF_Max / Sec_Conversion_Eff_PC_Mean)
Energy Flow/Flow Routing	RE_EC_Conversion	Expression	Matrix of conversion of RE input to EC output		RE_types, EC_types	mult(RE_Secondary_Input_Matrix, Secondary_Output_Matrix)
Energy Flow/Flow Routing	RE_Secondary_Input_Matrix	Expression	Matrix of conversion of RE input to secondary power output		RE_types, Secondary_PC_types	Sec_Conversion_Eff_PC_Mean * RE_Secondary_Input_Scaled
Energy Flow/Flow Routing	RE_Secondary_Input_Rate_Max	Expression	Vector of maximum secondary capacity to process primary RE input by RE type	EJ/yr	RE_types	sumr(RE_Secondary_Input_ID * Secondary_Sector.Amount_in_Transit * Secondary_CF_Max / Sec_Conversion_Eff_PC_Mean)
Energy Flow/Flow Routing	RE_Secondary_Input_Scaled	Expression	Matrix of normalized capacity to process primary RE input by secondary PC type		RE_types, Secondary_PC_types	(RE_Secondary_Input_ID * Secondary_Sector.Amount_in_Transit * Secondary_CF_Max / Sec_Conversion_Eff_PC_Mean) / sumr(RE_Secondary_Input_ID * Secondary_Sector.Amount_in_Transit * Secondary_CF_Max / Sec_Conversion_Eff_PC_Mean)
Energy Flow/Flow Routing	Secondary_Capacity_Factor	Expression	Vector of capacity factors by secondary PC type		Secondary_PC_types	Secondary_Output_Rate / max(vector(~PC_Zero_Approx), Secondary_Sector.Amount_in_Transit)

Sector	Element name	Type	Description	Unit	Array labels	Expression/condition/inputs
Energy Flow/Flow Routing	Secondary_CF_Curtailment	Expression	Linearly curtails secondary PC CF when EC deficit of the relevant EC type goes negative, up to a maximum of 99% at the surplus limit		Secondary_PC_types	max(vector(0.01), sumr(if(EC_Deficit_Prev > vector(EC_types, 0 yr), vector(EC_types, 1), if(EC_Deficit_Prev < vector(EC_types, EC_Deficit_Limit), vector(EC_types, 0), vector(EC_types, 1) - (EC_Deficit_Prev / EC_Deficit_Limit))) * Secondary_Output_ID))
Energy Flow/Flow Routing	Secondary_CF_Max	Expression	Vector of maximum capacity factors by secondary PC type (reduced by increased intermittent penetration and curtailment due to oversupply)		Secondary_PC_types	Initial_Secondary_CF_Max * max(vector(0), vector(1) + ((vector(1) - Primary_Generation_ID) * Secondary_Sector.Sec_Intermittent_ID + Secondary_Sector.Sec_Peaker_ID * Secondary_Sector.CF_Max_Peaker_Coeff + Secondary_Sector.Sec_Baseload_ID * Secondary_Sector.CF_Max_Baseload_Coeff) * Secondary_Sector.CF_Max_Mult_Actual) * Secondary_CF_Curtailment
Energy Flow/Flow Routing	Secondary_Output_Matrix	Expression	Matrix of conversion of secondary power output to delivered ECs (reduced by increased intermittent penetration)		Secondary_PC_types,	Secondary_Output_ID * Sec_Reticulation_Eff_PC_Mean * (vector(1) + Secondary_Sector.Sec_Intermittent_ID * Secondary_Sector.Retic_Eff_Mult_Actual)
Energy Flow/Flow Routing	Secondary_Output_Rate	Expression	Vector of power output by secondary PC type	EJ/yr	Secondary_PC_types	sumc(NRE_Secondary_Input_Rate * NRE_Secondary_Input_Matrix) + sumc(RE_Secondary_Input_Rate * RE_Secondary_Input_Matrix)
Energy Flow/Initialization/Initial ES Metabolism	Convergence_Failure	Interrupt	Skips realization and proceeds to the next when initialization fails to converge to a viable solution			On False: Initial_Cap_HC_Solver.Converged
Energy Flow/Initialization/Initial ES Metabolism	Init_NRE_CapEx_EC_Use	Expression	Vector of initial rates of energy carrier use for the purposes of adding new NRE PC and decommissioning end-of-life NRE PC	EJ/yr	EC_types	sumc((vector(NRE_types, 1) - Primary_NRE_Sector.Decommission_Fraction) * NRE_CF_Max * Primary_NRE_Sector.CapEx_Fraction * ((vector(NRE_types, 1) + Init_NRE_Growth_Rate) * (Initial_NRE_PC / Initial_NRE_EROI) * Primary_NRE_Sector.Initial_EC_Split)) + sumc(Primary_NRE_Sector.Decommission_Fraction * Primary_NRE_Sector.CapEx_Fraction * NRE_CF_Max * (Initial_NRE_PC / Init_NRE_EROI_PC_EoL) * Primary_NRE_Sector.Initial_EC_Split)
Energy Flow/Initialization/Initial ES Metabolism	Init_NRE_Operation_EC_Use	Expression	Vector of initial rates of energy carrier use for the purposes of operating existing NRE power capacity	EJ/yr	EC_types	sumc((vector(NRE_types, 1) - Primary_NRE_Sector.CapEx_Fraction) * NRE_CF_Max * (Initial_NRE_PC / Init_NRE_EROI_PC_Mean) * Primary_NRE_Sector.Initial_EC_Split)

Sector	Element name	Type	Description	Unit	Array labels	Expression/condition/inputs
Energy Flow/Initialization/Initial ES Metabolism	Init_RE_CapEx_EC_Use	Expression	Vector of initial rates of energy carrier use for the purposes of adding new RE PC and decommissioning end-of-life RE PC	EJ/yr	EC_types	sumc(RE_Output_Thermal_Equiv * (vector(RE_types, 1) - Primary_RE_Sector.Decommission_Fraction) * Initial_RE_CF_Max * Primary_RE_Sector.CapEx_Fraction * ((vector(RE_types, 1) + Init_RE_Growth_Rate) * (Initial_RE_PC / Initial_RE_EROI) * Primary_RE_Sector.Initial_EC_Split)) + sumc(RE_Output_Thermal_Equiv * Primary_RE_Sector.Decommission_Fraction * Primary_RE_Sector.CapEx_Fraction * Initial_RE_CF_Max * (Initial_RE_PC / Init_RE_EROI_PC_EoL) * Primary_RE_Sector.Initial_EC_Split)
Energy Flow/Initialization/Initial ES Metabolism	Init_RE_Operation_EC_Use	Expression	Vector of initial rates of energy carrier use for the purposes of operating existing RE power capacity	EJ/yr	EC_types	sumc(RE_Output_Thermal_Equiv * (vector(RE_types, 1) - Primary_RE_Sector.CapEx_Fraction) * Initial_RE_CF_Max * (Initial_RE_PC / Init_RE_EROI_PC_Mean) * Primary_RE_Sector.Initial_EC_Split)
Energy Flow/Initialization/Initial ES Metabolism	Init_Sec_AI_CapEx_EC_Use	Expression	Vector of initial rates of energy carrier use for the purposes of adding new secondary AI and decommissioning end-of-life secondary AI	EJ/yr	EC_types	sumc((vector(Secondary_AI_types, 1) - Secondary_Sector.AI_Decommission_Fraction) * Secondary_Sector.AI_CapEx_Fraction * ((vector(Secondary_AI_types, 1) + Init_Sec_AI_Growth_Rate) * Initial_Secondary_AI * Secondary_AI_ECC / Secondary_Sector.Auxiliary_Lifetime) * Secondary_Sector.AI_Initial_EC_Split) + sumc(Secondary_Sector.AI_Decommission_Fraction * Secondary_Sector.AI_CapEx_Fraction * (Initial_Secondary_AI / Secondary_Sector.Auxiliary_Lifetime) * Secondary_AI_ECC * Secondary_Sector.AI_Initial_EC_Split)
Energy Flow/Initialization/Initial ES Metabolism	Init_Sec_AI_Operation_EC_Use	Expression	Vector of initial rates of energy carrier use for the purposes of operating existing secondary auxiliary infrastructure	EJ/yr	EC_types	sumc((vector(Secondary_AI_types, 1) - Secondary_Sector.AI_CapEx_Fraction) * (Initial_Secondary_AI * Secondary_AI_ECC / Secondary_Sector.Auxiliary_Lifetime) * Secondary_Sector.AI_Initial_EC_Split)
Energy Flow/Initialization/Initial ES Metabolism	Init_Sec_PC_CapEx_EC_Use	Expression	Vector of initial rates of energy carrier use for the purposes of adding new secondary PC and decommissioning end-of-life secondary PC	EJ/yr	EC_types	sumc((vector(Secondary_PC_types, 1) - Secondary_Sector.PC_Decommission_Fraction) * Secondary_Sector.PC_CapEx_Fraction * ((vector(Secondary_PC_types, 1) + Init_Sec_PC_Growth_Rate) * Initial_Secondary_PC * Secondary_PC_ECC / Secondary_Sector.Power_Capacity_Lifetime) * Secondary_Sector.PC_Initial_EC_Split) + sumc(Secondary_Sector.PC_Decommission_Fraction * Secondary_Sector.PC_CapEx_Fraction * (Initial_Secondary_PC / Secondary_Sector.Power_Capacity_Lifetime) * Secondary_PC_ECC * Secondary_Sector.PC_Initial_EC_Split)
Energy Flow/Initialization/Initial ES Metabolism	Init_Sec_PC_Operation_EC_Use	Expression	Vector of initial rates of energy carrier use for the purposes of operating exisiting secondary power capacity	EJ/yr	EC_types	sumc((vector(Secondary_PC_types, 1) - Secondary_Sector.PC_CapEx_Fraction) * (Initial_Secondary_PC * Secondary_PC_ECC / Secondary_Sector.Power_Capacity_Lifetime) * Secondary_Sector.PC_Initial_EC_Split)

Sector	Element name	Type	Description	Unit	Array labels	Expression/condition/inputs
Energy Flow/Initialization/Initial ES Metabolism	Initial_Autocatalytic_Loop	Sum	Sum of initial EC flows for construction, operation, and decommissioning of primary and secondary PC and AI	EJ/yr	EC_types	Init_NRE_CapEx_EC_Use, Init_NRE_Operation_EC_Use, Init_RE_CapEx_EC_Use, Init_RE_Operation_EC_Use, Init_Sec_AI_Operation_EC_Use, Init_Sec_AI_CapEx_EC_Use, Init_Sec_PC_CapEx_EC_Use, Init_Sec_PC_Operation_EC_Use
Energy Flow/Initialization	Init_End_Use_Prop_Norm	Expression	Matrix of normalized initial flow of ECs to end-use PC types		EC_types, End_use_PC_t	Init_End_Use_Prop_Input[*, Numeral] * (vector(End_use_PC_types, 1) + End_Use_Prop_Rand * Init_End_Use_Prop_Input[*, Error]) * End_Use_Input_ID / sumr(Init_End_Use_Prop_Input[*, Numeral] * (vector(End_use_PC_types, 1) + End_Use_Prop_Rand * Init_End_Use_Prop_Input[*, Error]) * End_Use_Input_ID)
Energy Flow/Initialization	Initial_EC_Net_Supply	Expression	Vector of initial net EC supply (minus initial autocatalytic loop value)	EJ/yr	EC_types	Initial_EC_Supply - Initial_Autocatalytic_Loop
Energy Flow/Initialization	Initial_EC_Supply	Expression	Vector of initial gross EC supply	EJ/yr	EC_types	sumc(Initial_Secondary_Output_Rate * Sec_Reticulation_Eff_Input[*, Min] * Secondary_Output_ID)
Energy Flow/Initialization	Initial_End_Use_AI	Expression	Vector of initial end-use AI stocks (in operation)	EJ/yr	End_use_AI_types	sumc(Initial_End_Use_Output_Rate * End_Use_Sector.PC_AI_ID) * ((Init_End_Use_Peak_Factor - vector(1)) * vector(1 - Initial_Demand_Flex) + vector(1))
Energy Flow/Initialization	Initial_End_Use_Output_Rate	Expression	Vector of initial end-use power output	EJ/yr	End_use_PC_types	End_Use_Conversion_Eff_Input[*, Min] * sumc((Initial_EC_Net_Supply - Initial_Cap_HC_Solver) * Init_End_Use_Prop_Norm)
Energy Flow/Initialization	Initial_End_Use_PC	Expression	Vector of initial end-use PC stocks (in operation)	EJ/yr	End_use_PC_types	Initial_End_Use_Output_Rate / Init_End_Use_CF_Target
Energy Flow/Initialization	Initial_ES_Demand	Expression	Vector of initial energy services delivered	EJ/yr	ES_types	sumc(Initial_End_Use_Output_Rate * End_Use_Output_ID * Init_End_Use_ES_Eff_PC_Mean)
Energy Flow/Initialization	Initial_NRE_PC	Expression	Vector of initial NRE PC stocks (in operation)	EJ/yr	NRE_types	(Initial_NRE_Output_Rate - Initial_Direct_NRE_Use) / NRE_CF_Max
Energy Flow/Initialization	Initial_RE_PC	Expression	Vector of initial RE PC stocks (in operation)	EJ/yr	RE_types	Initial_RE_Output_Rate / Initial_RE_CF_Max
Energy Flow/Initialization	Initial_Secondary_AI	Expression	Vector of initial secondary AI stocks (in operation)	EJ/yr	Secondary_AI_types	sumc(Initial_Secondary_Output_Rate * Secondary_Sector.PC_AI_ID) * ((Init_Secondary_Peak_Factor - vector(1)) * vector(1 - Initial_Demand_Flex) + vector(1))

Sector	Element name	Type	Description	Unit	Array labels	Expression/condition/inputs
Energy Flow/Initialization	Initial_Secondary_Output_Rate	Expression	Vector of initial secondary power output	EJ/yr	Secondary_PC_types	Sec_Conversion_Eff_Input[*, Min] * (sumc((Initial_NRE_Output_Rate - Initial_Direct_NRE_Use) * (Init_Secondary_Prop_Input[*, Numeral] * (vector(1) + Secondary_Prop_Rand * Init_Secondary_Prop_Input[*, Error]) * NRE_Secondary_Input_ID / sumr(Init_Secondary_Prop_Input[*, Numeral] * (vector(1) + Secondary_Prop_Rand * Init_Secondary_Prop_Input[*, Error]) * NRE_Secondary_Input_ID))) + sumc(Initial_RE_Output_Rate * (Init_Secondary_Prop_Input[*, Numeral] * (vector(1) + Secondary_Prop_Rand * Init_Secondary_Prop_Input[*, Error]) * RE_Secondary_Input_ID / sumr(Init_Secondary_Prop_Input[*, Numeral] * (vector(1) + Secondary_Prop_Rand * Init_Secondary_Prop_Input[*, Error]) * RE_Secondary_Input_ID))))
Energy Flow/Initialization	Initial_Secondary_PC	Expression	Vector of initial secondary PC stocks (in operation)	EJ/yr	Secondary_PC_types	Initial_Secondary_Output_Rate / Initial_Secondary_CF_Max
Energy Flow/Initialization	Initial_Supply_EC_Split	Expression	Vector of fractional shares of initial supply by EC, adjusted for thermal equivalence (does not sum to one)		EC_types	Initial_EC_Supply / sumv(EC_Thermal_Equivalence * Initial_EC_Supply)
Energy Flow/Mean Stock Efficiencies	End_Use_Conv_Eff_Add_Weighting	Expression	Vector of new PC end-use conversion efficiency weighted by PC additions	EJ/yr^2	End_use_PC_types	End_Use_Sector.Power_Capacity_Addition * End_Use_Conversion_Eff
Energy Flow/Mean Stock Efficiencies	End_Use_Conversion_Eff_PC_Mean	Expression	Vector of mean end-use conversion efficiency for PC in operation		End_use_PC_types	if(End_Use_Sector.Amount_in_Transit < vector(~PC_Zero_Approx), End_Use_Conversion_Eff, End_Use_Conv_Eff_Mean_Integ.Amount_in_Transit / max(End_Use_Sector.Amount_in_Transit, ~PC_Zero_Approx))
Energy Flow/Mean Stock Efficiencies	End_Use_ES_Eff_Add_Weighting	Expression	Vector of new PC end-use to ES efficiency weighted by PC additions	EJ/yr^2	End_use_PC_types	End_Use_Sector.Power_Capacity_Addition * End_Use_ES_Eff
Energy Flow/Mean Stock Efficiencies	End_Use_ES_Eff_PC_Mean	Expression	Vector of mean end-use to ES efficiency for PC in operation		End_use_PC_types	if(End_Use_Sector.Amount_in_Transit < vector(~PC_Zero_Approx), End_Use_ES_Eff, End_Use_ES_Eff_Mean_Integ.Amount_in_Transit / max(End_Use_Sector.Amount_in_Transit, ~PC_Zero_Approx))

Sector	Element name	Type	Description	Unit	Array labels	Expression/condition/inputs
Energy Flow/Mean Stock Efficiencies	Sec_Conv_Eff_Add_Weighting	Expression	Vector of new PC secondary conversion efficiency weighted by PC additions	EJ/yr^2	Secondary_PC_types	Secondary_Sector.Power_Capacity_Addition * Sec_Conversion_Eff
Energy Flow/Mean Stock Efficiencies	Sec_Conversion_Eff_PC_Mean	Expression	Vector of mean secondary conversion efficiency for PC in operation		Secondary_PC_types	if(Secondary_Sector.Amount_in_Transit < vector(~PC_Zero_Approx), Sec_Conversion_Eff, Sec_Conv_Eff_Mean_Integ.Amount_in_Transit / max(Secondary_Sector.Amount_in_Transit, vector(~PC_Zero_Approx)))
Energy Flow/Mean Stock Efficiencies	Sec_Retic_Eff_Add_Weighting	Expression	Vector of new PC secondary reticulation efficiency weighted by PC additions	EJ/yr^2	Secondary_PC_types	Secondary_Sector.Power_Capacity_Addition * Sec_Reticulation_Eff
Energy Flow/Mean Stock Efficiencies	Sec_Reticulation_Eff_PC_Mean	Expression	Vector of mean secondary reticulation efficiency for PC in operation		Secondary_PC_types	if(Secondary_Sector.Amount_in_Transit < vector(~PC_Zero_Approx), Sec_Reticulation_Eff, Sec_Retic_Eff_Mean_Integ.Amount_in_Transit / max(Secondary_Sector.Amount_in_Transit, vector(~PC_Zero_Approx)))
Energy Flow/New PC Efficiencies	End_Use_Conversion_Eff	Expression	Vector of new PC end-use conversion efficiency (follows logistic curve; function of cumulative end-use power output)		End_use_PC_types	((Final_End_Use_Conversion_Eff - End_Use_Conversion_Eff_Base) / (vector(1) + (((Final_End_Use_Conversion_Eff - Init_End_Use_Conversion_Eff) / (Init_End_Use_Conversion_Eff - End_Use_Conversion_Eff_Base))^(vector(1) - End_Use_Output_Norm)) * ((((vector(1) + ((Final_End_Use_Conversion_Eff - Init_End_Use_Conversion_Eff) / (Init_End_Use_Conversion_Eff - End_Use_Conversion_Eff_Base)))^vector(-1) - ((Init_End_Use_Conversion_Eff - End_Use_Conversion_Eff_Input[*, Min]) / (Final_End_Use_Conversion_Eff - End_Use_Conversion_Eff_Base)))^vector(-1) - vector(1))^End_Use_Output_Norm))) + End_Use_Conversion_Eff_Base
Energy Flow/New PC Efficiencies	End_Use_ES_Eff	Expression	Vector of new PC end-use to ES efficiency (follows logistic curve; function of cumulative end-use power output)		End_use_PC_types	((Final_End_Use_ES_Eff - End_Use_ES_Eff_Base) / (vector(1) + (((Final_End_Use_ES_Eff - Init_End_Use_ES_Eff) / (Init_End_Use_ES_Eff - End_Use_ES_Eff_Base))^(vector(1) - End_Use_Output_Norm)) * ((((vector(1) + ((Final_End_Use_ES_Eff - Init_End_Use_ES_Eff) / (Init_End_Use_ES_Eff - End_Use_ES_Eff_Base)))^vector(-1) - ((Init_End_Use_ES_Eff - Init_End_Use_ES_Eff_PC_Mean) / (Final_End_Use_ES_Eff - End_Use_ES_Eff_Base)))^vector(-1) - vector(1))^End_Use_Output_Norm))) + End_Use_ES_Eff_Base

Sector	Element name	Type	Description	Unit	Array labels	Expression/condition/inputs
Energy Flow/New PC Efficiencies	End_Use_Output_Norm	Expression	Vector of normalized end-use output power (1 between incept date and sim. beginning) divided by normalized mean PC output power value (negative), assuming linear output trend since incept		End_use_PC_types	max(vector(-49), 2 * End_Use_Output / (Initial_End_Use_Output_Rate * End_Use_Sector.Power_Capacity_Lifetime * ((End_Use_Sector.Power_Capacity_Lifetime / (4 * (vector(StartTime + 1900 yr) - End_Use_Incept_Year))) - vector(1))))
Energy Flow/New PC Efficiencies	Sec_Conversion_Eff	Expression	Vector of new PC secondary conversion efficiency (follows logistic curve; function of cumulative secondary power output)		Secondary_PC_types	((Final_Sec_Conversion_Eff - Sec_Conversion_Eff_Base) / (vector(1) + (((Final_Sec_Conversion_Eff - Init_Sec_Conversion_Eff) / (Init_Sec_Conversion_Eff - Sec_Conversion_Eff_Base))^(vector(1) - Secondary_Output_Norm)) * ((((vector(1) + ((Final_Sec_Conversion_Eff - Init_Sec_Conversion_Eff) / (Init_Sec_Conversion_Eff - Sec_Conversion_Eff_Base)))^vector(-1) - ((Init_Sec_Conversion_Eff - Sec_Conversion_Eff_Input[*, Min]) / (Final_Sec_Conversion_Eff - Sec_Conversion_Eff_Base)))^vector(-1) - vector(1))^Secondary_Output_Norm))) + Sec_Conversion_Eff_Base
Energy Flow/New PC Efficiencies	Sec_Reticulation_Eff	Expression	Vector of new PC secondary reticulation efficiency (follows logistic curve; function of cumulative secondary power output)		Secondary_PC_types	((Final_Sec_Reticulation_Eff - Sec_Reticulation_Eff_Base) / (vector(1) + (((Final_Sec_Reticulation_Eff - Init_Sec_Reticulation_Eff) / (Init_Sec_Reticulation_Eff - Sec_Reticulation_Eff_Base))^(vector(1) - Secondary_Output_Norm)) * ((((vector(1) + ((Final_Sec_Reticulation_Eff - Init_Sec_Reticulation_Eff) / (Init_Sec_Reticulation_Eff - Sec_Reticulation_Eff_Base)))^vector(-1) - ((Init_Sec_Reticulation_Eff - Sec_Reticulation_Eff_Input[*, Min]) / (Final_Sec_Reticulation_Eff - Sec_Reticulation_Eff_Base)))^vector(-1) - vector(1))^Secondary_Output_Norm))) + Sec_Reticulation_Eff_Base
Energy Flow/New PC Efficiencies	Secondary_Output_Norm	Expression	Vector of normalized secondary output power (1 between incept date and sim. beginning) divided by normalized mean PC output power value (negative), assuming linear output trend since incept		Secondary_PC_types	max(vector(-49), 2 * Secondary_Output / (Initial_Secondary_Output_Rate * Secondary_Sector.Power_Capacity_Lifetime * ((Secondary_Sector.Power_Capacity_Lifetime / (4 * (vector(StartTime + 1900 yr) - Sec_Incept_Year))) - vector(1))))
Energy Flow/Primary Resource	Direct_NRE_Use	Expression	Vector of direct (non-energy) use of primary resource by NRE type (initial values scale with the mean of final ES demand relative to initial ES demand)	EJ/yr	NRE_types	Initial_Direct_NRE_Use * meanv(ES_Demand / Initial_ES_Demand)
Energy Flow/Primary Resource	GHG_Emissions	Expression	Cumulative GHG emissions based on primary energy GHG intensity values (includes constant estimate for agriculture and land use emissions)			sumv((Initial_NRE_Resource - NRE_Resource) * GHG_Intensity) + Non_ES_Emissions * ETime

Sector	Element name	Type	Description	Unit	Array labels	Expression/condition/inputs
Energy Flow/Primary Resource	NRE_Capacity_Factor	Expression	Vector of capacity factors by NRE type		NRE_types	NRE_Secondary_Input_Rate / max(vector(~PC_Zero_Approx), Primary_NRE_Sector.Amount_in_Transit)
Energy Flow/Primary Resource	NRE_Depletion	Expression	Vector of normalized resource depletion by NRE type (0 at sim. beginning, 1 when terminal EROI is reached)		NRE_types	(Initial_NRE_Resource - NRE_Resource) / Initial_NRE_Resource
Energy Flow/Primary Resource	NRE_Production_Rate_Max	Expression	Vector of maximum primary NRE capacity to produce output by NRE type	EJ/yr	NRE_types	Primary_NRE_Sector.Amount_in_Transit * NRE_CF_Max
Energy Flow/Primary Resource	NRE_Secondary_Input_Rate	Expression	Vector of actual primary NRE output by NRE type (minimum of primary and secondary capacities)	EJ/yr	NRE_types	min(NRE_Production_Rate_Max, NRE_Secondary_Input_Rate_Max)
Energy Flow/Primary Resource	RE_Capacity_Factor	Expression	Vector of capacity factors by RE type		RE_types	RE_Secondary_Input_Rate / max(vector(~PC_Zero_Approx), Primary_RE_Sector.Amount_in_Transit)
Energy Flow/Primary Resource	RE_CF_Max	Expression	Vector of maximum capacity factors by RE type (reduced by increased intermittent penetration)		RE_types	Initial_RE_CF_Max * (vector(1) + Secondary_Sector.RE_Intermittent_ID * Secondary_Sector.CF_Max_Mult_Actual)
Energy Flow/Primary Resource	RE_Exhaustion	Expression	Vector of normalized resource exhaustion by RE type (0 at sim. beginning, 1 when terminal EROI is reached)		RE_types	min(vector(99), (Primary_RE_Sector.Amount_in_Transit * RE_CF_Max - Initial_RE_Output_Rate) / (RE_Potential - Initial_RE_Output_Rate))
Energy Flow/Primary Resource	RE_Production_Rate_Max	Expression	Vector of maximum primary RE capacity to produce output by RE type	EJ/yr	RE_types	Primary_RE_Sector.Amount_in_Transit * RE_CF_Max
Energy Flow/Primary Resource	RE_Secondary_Input_Rate	Expression	Vector of actual primary RE output by RE type (minimum of primary and secondary capacities)	EJ/yr	RE_types	min(RE_Production_Rate_Max, RE_Secondary_Input_Rate_Max)
Energy Flow/Primary Resource	Total_Primary_Energy_Supply	Expression	Sum of primary energy production (excluding direct), adjusted for thermal equivalence	EJ/yr	RE_types	sumv(NRE_Secondary_Input_Rate) + sumv(RE_Secondary_Input_Rate * RE_Output_Thermal_Equiv)

Sector	Element name	Type	Description	Unit	Array labels	Expression/condition/inputs
EROI/New PC EROI	NRE_EROI	Expression	Vector of new PC EROI by NRE type (follows logistic curve; function of NRE depletion; EROI does not consider penetration effects as these are modelled explicitly, i.e. reflects resource quality only)		NRE_types	max(vector(0.01), (NRE_EROI_Drop + Initial_NRE_EROI) / (vector(1) + ((((NRE_EROI_Drop + Initial_NRE_EROI) / NRE_EROI_Terminal) - vector(1))^NRE_Depletion) * ((((NRE_EROI_Drop + Initial_NRE_EROI) / NRE_EROI_Drop) - vector(1))^(NRE_Depletion - vector(1)))))
EROI/New PC EROI	RE_EROI	Expression	Vector of new PC EROI by RE type (follows logistic curve; function of RE exhaustion; EROI does not consider penetration effects as these are modelled explicitly, i.e. reflects resource quality only)		RE_types	max(vector(0.01), (RE_EROI_Drop + Initial_RE_EROI) / (vector(1) + ((((RE_EROI_Drop + Initial_RE_EROI) / RE_EROI_Terminal) - vector(1))^RE_Exhaustion) * (((((RE_EROI_Drop + Initial_RE_EROI) / RE_EROI_Drop) - vector(1))^(RE_Exhaustion - vector(1))))))
EROI	Init_NRE_Depletion_PC_EoL	Expression	Vector of initial NRE depletion for end-of-life PC (negative), assuming linear output trend since incept		NRE_types	- ((Initial_NRE_Output_Rate - Initial_Direct_NRE_Use) / Initial_NRE_Resource) * Primary_NRE_Sector.Power_Capacity_Lifetime * (vector(1) - ((Primary_NRE_Sector.Power_Capacity_Lifetime) / (2 * NRE_Technology_Age)))
EROI	Init_NRE_Depletion_PC_Mean	Expression	Vector of initial mean PC NRE depletion (negative), assuming linear output trend since incept		NRE_types	((Initial_NRE_Output_Rate - Initial_Direct_NRE_Use) * Primary_NRE_Sector.Power_Capacity_Lifetime / (2 * Initial_NRE_Resource)) * ((Primary_NRE_Sector.Power_Capacity_Lifetime / (4 * NRE_Technology_Age)) - vector(1))
EROI	Init_NRE_EROI_PC_EoL	Expression	Vector of initial EROI for end-of-life NRE PC, assuming linear output trend since incept		NRE_types	(NRE_EROI_Drop + Initial_NRE_EROI) / (vector(1) + ((((NRE_EROI_Drop + Initial_NRE_EROI) / NRE_EROI_Terminal) - vector(1))^Init_NRE_Depletion_PC_EoL) * ((((NRE_EROI_Drop + Initial_NRE_EROI) / NRE_EROI_Drop) - vector(1))^(Init_NRE_Depletion_PC_EoL - vector(1))))
EROI	Init_NRE_EROI_PC_Mean	Expression	Vector of initial NRE PC mean EROI, assuming linear output trend since incept		NRE_types	(NRE_EROI_Drop + Initial_NRE_EROI) / (vector(1) + ((((NRE_EROI_Drop + Initial_NRE_EROI) / NRE_EROI_Terminal) - vector(1))^Init_NRE_Depletion_PC_Mean) * ((((NRE_EROI_Drop + Initial_NRE_EROI) / NRE_EROI_Drop) - vector(1))^(Init_NRE_Depletion_PC_Mean - vector(1))))
EROI	Init_RE_EROI_PC_EoL	Expression	Vector of initial EROI for end-of-life RE PC, assuming linear output trend since incept		RE_types	(RE_EROI_Drop + Initial_RE_EROI) / (vector(1) + ((((RE_EROI_Drop + Initial_RE_EROI) / RE_EROI_Terminal) - vector(1))^Init_RE_Exhaustion_PC_EoL) * (((((RE_EROI_Drop + Initial_RE_EROI) / RE_EROI_Drop) - vector(1))^(Init_RE_Exhaustion_PC_EoL - vector(1)))))
EROI	Init_RE_EROI_PC_Mean	Expression	Vector of initial RE PC mean EROI, assuming linear output trend since incept		RE_types	(RE_EROI_Drop + Initial_RE_EROI) / (vector(1) + ((((RE_EROI_Drop + Initial_RE_EROI) / RE_EROI_Terminal) - vector(1))^Init_RE_Exhaustion_PC_Mean) * (((((RE_EROI_Drop + Initial_RE_EROI) / RE_EROI_Drop) - vector(1))^(Init_RE_Exhaustion_PC_Mean - vector(1)))))

Sector	Element name	Type	Description	Unit	Array labels	Expression/condition/inputs
EROI	Init_RE_Exhaustion_PC_EoL	Expression	Vector of initial RE exhaustion for end-of-life PC (negative), assuming linear output trend since incept		RE_types	- Initial_RE_Output_Rate * (Primary_RE_Sector.Power_Capacity_Lifetime / RE_Technology_Age) / (RE_Potential - Initial_RE_Output_Rate)
EROI	Init_RE_Exhaustion_PC_Mean	Expression	Vector of initial mean PC RE exhaustion (negative), assuming linear output trend since incept		RE_types	- Initial_RE_Output_Rate * (Primary_RE_Sector.Power_Capacity_Lifetime / (2 * RE_Technology_Age)) / (RE_Potential - Initial_RE_Output_Rate)
EROI	NRE_Depletion_PC_EoL	Expression	Vector of NRE depletion for end-of-life PC		NRE_types	min(vector(0), ((Initial_NRE_Output_Rate - Initial_Direct_NRE_Use) / Initial_NRE_Resource) * (vector(ETime) - Primary_NRE_Sector.Power_Capacity_Lifetime) * (vector(1) + ((vector(ETime) - Primary_NRE_Sector.Power_Capacity_Lifetime) / (2 * NRE_Technology_Age))))
EROI	NRE_EROI_Add_Weighting	Expression	Vector of new NRE PC EROI weighted by PC additions	EJ/yr^2	NRE_types	Primary_NRE_Sector.Power_Capacity_Addition * NRE_EROI
EROI	NRE_EROI_PC_EoL	Expression	Vector of EROI for end-of-life NRE PC (uses delayed value after one lifetime elapsed)		NRE_types	if(ETime < Primary_NRE_Sector.Power_Capacity_Lifetime, (NRE_EROI_Drop + Initial_NRE_EROI) / (vector(1) + ((((NRE_EROI_Drop + Initial_NRE_EROI) / NRE_EROI_Terminal) - vector(1))^NRE_Depletion_PC_EoL) * ((((NRE_EROI_Drop + Initial_NRE_EROI) / NRE_EROI_Drop) - vector(1))^(NRE_Depletion_PC_EoL - vector(1)))), NRE_EROI_Delay)
EROI	NRE_EROI_PC_Mean	Expression	Vector of NRE PC mean EROI		NRE_types	max(vector(0.01), if(Primary_NRE_Sector.Amount_in_Transit < vector(2 * ~PC_Zero_Approx), NRE_EROI, NRE_EROI_PC_Mean_Integ.Amount_in_Transit / max(Primary_NRE_Sector.Amount_in_Transit, vector(~PC_Zero_Approx))))
EROI	NRE_Technology_Age	Expression	Vector of maximum technology age by NRE type (calculated from corresponding secondary incept years)	yr	NRE_types	maxr((vector(Secondary_PC_types, StartTime + 1900 yr) - Sec_Incept_Year) * NRE_Secondary_Input_ID)
EROI	RE_EROI_Add_Weighting	Expression	Vector of new RE PC EROI weighted by PC additions	EJ/yr^2	RE_types	Primary_RE_Sector.Power_Capacity_Addition * RE_EROI_Addition_Mean
EROI	RE_EROI_Addition_Mean	Expression	Vector of effective EROI for PC additions by RE type (assumes any unused RE potential available is preferentially redeveloped due to greater resource quality)		RE_types	max((RE_Redevelopment_Potential.Withdrawal_Rate / Primary_RE_Sector.Power_Capacity_Addition) * (max(RE_EROI_PC_EoL, RE_EROI) - RE_EROI) + RE_EROI, RE_EROI_Terminal)

Sector	Element name	Type	Description	Unit	Array labels	Expression/condition/inputs
EROI	RE_EROI_PC_EoL	Expression	Vector of EROI for end-of-life RE PC (uses delayed value after one lifetime elapsed)		RE_types	if(ETime < Primary_RE_Sector.Power_Capacity_Lifetime, (RE_EROI_Drop + Initial_RE_EROI) / (vector(1) + ((((RE_EROI_Drop + Initial_RE_EROI) / RE_EROI_Terminal) - vector(1))^RE_Exhaustion_PC_EoL) * (((((RE_EROI_Drop + Initial_RE_EROI) / RE_EROI_Drop) - vector(1))^(RE_Exhaustion_PC_EoL - vector(1))))), RE_EROI_Addition_Delay)
EROI	RE_EROI_PC_Mean	Expression	Vector of RE PC mean EROI		RE_types	max(vector(0.01), if(Primary_RE_Sector.Amount_in_Transit < vector(2 * ~PC_Zero_Approx), RE_EROI_Addition_Mean, RE_EROI_PC_Mean_Integ.Amount_in_Transit / max(Primary_RE_Sector.Amount_in_Transit, vector(~PC_Zero_Approx))))
EROI	RE_Exhaustion_PC_EoL	Expression	Vector of RE exhaustion for end-of-life PC		RE_types	min(vector(0), Initial_RE_Output_Rate * ((vector(ETime) - Primary_RE_Sector.Power_Capacity_Lifetime) / RE_Technology_Age) / (RE_Potential - Initial_RE_Output_Rate))
EROI	RE_Technology_Age	Expression	Vector of maximum technology age by RE type (calculated from corresponding secondary incept years)	yr	RE_types	maxr((vector(Secondary_PC_types, StartTime + 1900 yr) - Sec_Incept_Year) * RE_Secondary_Input_ID)
Primary NRE	Addition_EC_Use	Expression	Vector of rates of energy carrier use for the purposes of adding new NRE power capacity	EJ/yr	EC_types	sumc((vector(NRE_types, 1) - Decommission_Fraction) * (Power_Capacity_Lifetime / Power_Capacity_Build_Time) * NRE_CF_Max * CapEx_Fraction * (Power_Capacity_Addition.Amount_in_Transit / NRE_EROI) * EC_Split)
Primary NRE	Decommission_EC_Use	Expression	Vector of rates of energy carrier use for the purposes of decommissioning NRE power capacity	EJ/yr	EC_types	sumc(Decommission_Fraction * CapEx_Fraction * NRE_CF_Max * Power_Capacity_Lifetime * (Power_Capacity_Operation / NRE_EROI_PC_EoL) * EC_Split)
Primary NRE	EC_Split	Expression	Matrix of the EC composition of NRE investment energy, adjusted for thermal energy equivalence		NRE_types, EC_types	(Demand_EC_Split / Initial_Supply_EC_Split) * Initial_EC_Split / sumr(EC_Thermal_Equivalence * (Demand_EC_Split / Initial_Supply_EC_Split) * Initial_EC_Split)
Primary NRE	Initial_EC_Split	Expression	Initial shares of NRE input energy by EC type, adjusted for thermal energy		NRE_types, EC_types	Initial_Supply_EC_Split * matrix(vector(1), EC_Split_LaG_Factor, EC_Split_Heat_Factor) / sumr(EC_Thermal_Equivalence * Initial_Supply_EC_Split * matrix(vector(1), EC_Split_LaG_Factor, EC_Split_Heat_Factor))
Primary NRE	Operation_EC_Use	Expression	Vector of rates of energy carrier use for the purposes of operating existing NRE power capacity	EJ/yr	EC_types	sumc((vector(NRE_types, 1) - CapEx_Fraction) * NRE_Capacity_Factor * (Power_Capacity_Operation.Amount_in_Transit / NRE_EROI_PC_Mean) * EC_Split)
Primary RE	Addition_EC_Use	Expression	Vector of rates of energy carrier use for the purposes of adding new RE power capacity (adjusted for thermal equivalence of primary electricity output)	EJ/yr	EC_types	sumc(RE_Output_Thermal_Equiv * (vector(RE_types, 1) - Decommission_Fraction) * (Power_Capacity_Lifetime / Power_Capacity_Build_Time) * Initial_RE_CF_Max * CapEx_Fraction * (Power_Capacity_Addition.Amount_in_Transit / RE_EROI_Addition_Mean) * EC_Split)

Sector	Element name	Type	Description	Unit	Array labels	Expression/condition/inputs
Primary RE	Decommission_EC_Use	Expression	Vector of rates of energy carrier use for the purposes of decommissioning RE power capacity (adjusted for thermal equivalence of primary electricity output)	EJ/yr	EC_types	sumc(RE_Output_Thermal_Equiv * Decommission_Fraction * CapEx_Fraction * Initial_RE_CF_Max * Power_Capacity_Lifetime * (Power_Capacity_Operation / RE_EROI_PC_EoL) * EC_Split)
Primary RE	EC_Split	Expression	Matrix of the EC composition of RE investment energy (adjusted for thermal equivalence of primary electricity output)		RE_types, EC_types	(Demand_EC_Split / Initial_Supply_EC_Split) * Initial_EC_Split / sumr(EC_Thermal_Equivalence * (Demand_EC_Split / Initial_Supply_EC_Split) * Initial_EC_Split)
Primary RE	Initial_EC_Split	Expression	Initial shares of RE input energy by EC type (adjusted for thermal equivalence of primary electricity output)		RE_types, EC_types	Initial_Supply_EC_Split * matrix(vector(1), EC_Split_LaG_Factor, EC_Split_Heat_Factor) / sumr(EC_Thermal_Equivalence * Initial_Supply_EC_Split * matrix(vector(1), EC_Split_LaG_Factor, EC_Split_Heat_Factor))
Primary RE	Operation_EC_Use	Expression	Vector of rates of energy carrier use for the purposes of operating existing RE power capacity (adjusted for thermal equivalence of primary electricity output)	EJ/yr	EC_types	sumc(RE_Output_Thermal_Equiv * (vector(RE_types, 1) - CapEx_Fraction) * RE_Capacity_Factor * (Power_Capacity_Operation.Amount_in_Transit / RE_EROI_PC_Mean) * EC_Split)
Secondary/Electricity System	CF_Max_Mult	Expression	Fractional reduction in maximum CF for intermittent generation (plus baseload and peaking generation via respective coefficients) in the absence of alternative mitigation (follows logistic curve; function of intermittent penetration, reduced by increases in intermittent diversity and demand flexibility)			((CF_Max_Mult_Asymptote / (1+ ((CF_Max_Mult_Asymptote - 1)^((1 - Intermittent_Penetration) / (1 - Init_Intermittent_Penetration))) * (((CF_Max_Mult_Asymptote / CF_Max_Mult_Final) - 1)^((Intermittent_Penetration - Init_Intermittent_Penetration) / (1 - Init_Intermittent_Penetration))))) - 1) * Combined_Mult_Reduction
Secondary/Electricity System	CF_Max_Mult_Actual	Expression	Effective fractional reduction in maximum CF for intermittent generation (plus baseload and peaking generation via respective coefficients) given the level of built intermittent AI mitigation			CF_Max_Mult * (1 - Intermit_AI_Built_Factor_Prev)

Sector	Element name	Type	Description	Unit	Array labels	Expression/condition/inputs
Secondary/Electricity System	Combined_Mult_Reduction	Expression	Combined fractional reduction in modification of maximum CF, reticulation efficiency and intermittent AI required as a function of intermittent diversity and demand flexibility			(1 - Intermittent_Diversity * Diversity_Coeff) * (1 - Demand_Flexibility * Demand_Flex_Coeff)
Secondary/Electricity System	Init_Combined_Mult_Reduction	Expression	Initial combined fractional reduction in modification of maximum CF, reticulation efficiency and intermittent AI required as a function of intermittent diversity and demand flexibility			(1 - ((((sumv(Initial_Secondary_PC * Initial_Secondary_CF_Max * Sec_Intermittent_ID) / sumv(Sec_Intermittent_ID)) / maxv(Initial_Secondary_PC * Initial_Secondary_CF_Max * Sec_Intermittent_ID)) / (1 - 1 / sumv(Sec_Intermittent_ID))) - 1 / sumv(Sec_Intermittent_ID)) * Diversity_Coeff) * (1 - Initial_Demand_Flex * Demand_Flex_Coeff)
Secondary/Electricity System	Init_Intermittent_Penetration	Expression	Initial fractional share of total electricity generation from intermittent sources (defined in terms of generation potential prior to transmission and distribution, i.e. peakers at maximum technical CF)			sumv(Initial_Secondary_PC * if(Sec_Peaker_ID = vector(Secondary_PC_types, 1), (1 + CF_Max_Peaker_Coeff * (CF_Max_Mult_Final - 1)) * Initial_Secondary_CF_Max, Initial_Secondary_CF_Max) * Sec_Intermittent_ID) / sumv(Initial_Secondary_PC * if(Sec_Peaker_ID = vector(Secondary_PC_types, 1), (1 + CF_Max_Peaker_Coeff * (CF_Max_Mult_Final - 1)) * Initial_Secondary_CF_Max, Initial_Secondary_CF_Max) * Secondary_Output_ID[*, Electricity])
Secondary/Electricity System	Intermit_AI_Built_Factor	Expression	Normalized level of intermittent AI in operation relative to the total required for full mitigation via AI			min(1, Auxiliary_Operation.Amount_in_Transit[2] / max(~PC_Zero_Approx, Auxiliary_Requirement[2]))
Secondary/Electricity System	Intermit_AI_Mult	Expression	Fractional increase in intermittent AI required in the absence of alternative mitigation (follows logistic curve; function of intermittent penetration, reduced by increases in intermittent diversity and demand flexibility)			(Combined_Mult_Reduction / Init_Combined_Mult_Reduction) * (Intermit_AI_Mult_Asymptote / (1+ ((Intermit_AI_Mult_Asymptote - 1)^((1 - Intermittent_Penetration) / (1 - Init_Intermittent_Penetration))) * (((Intermit_AI_Mult_Asymptote / Intermit_AI_Mult_Final) - 1)^((Intermittent_Penetration - Init_Intermittent_Penetration) / (1 - Init_Intermittent_Penetration)))))
Secondary/Electricity System	Intermittent_Diversity	Expression	Ratio of mean intermittent generation potential to maximum intermittent generation potential (1 when all equal, << 1 when one dominates)			(((sumv(Power_Capacity_Operation.Amount_in_Transit * Initial_Secondary_CF_Max * Sec_Intermittent_ID) / sumv(Sec_Intermittent_ID)) / maxv(Power_Capacity_Operation.Amount_in_Transit * Initial_Secondary_CF_Max * Sec_Intermittent_ID)) / (1 - 1 / sumv(Sec_Intermittent_ID))) - 1 / sumv(Sec_Intermittent_ID)
Secondary/Electricity System	Intermittent_Penetration	Expression	Fractional share of total electricity generation from intermittent sources (defined in terms of generation potential prior to transmission and distribution, i.e. peakers at maximum technical CF)			sumv(Power_Capacity_Operation.Amount_in_Transit * if(Sec_Peaker_ID = vector(Secondary_PC_types, 1), (1 + CF_Max_Peaker_Coeff * (CF_Max_Mult_Final - 1)) * Initial_Secondary_CF_Max, Initial_Secondary_CF_Max) * Sec_Intermittent_ID) / sumv(Power_Capacity_Operation.Amount_in_Transit * if(Sec_Peaker_ID = vector(Secondary_PC_types, 1), (1 + CF_Max_Peaker_Coeff * (CF_Max_Mult_Final - 1)) * Initial_Secondary_CF_Max, Initial_Secondary_CF_Max) * Secondary_Output_ID[*, Electricity])

Sector	Element name	Type	Description	Unit	Array labels	Expression/condition/inputs
Secondary/Electricity System	RE_Intermittent_ID	Expression	Vector of intermittent generation by RE type (value of 1 indicates that electricity production is considered intermittent)		RE_types	sumr(Sec_Intermittent_ID * Primary_Generation_ID * RE_Secondary_Input_ID)
Secondary/Electricity System	Retic_Eff_Mult	Expression	Fractional reduction in secondary reticulation efficiency for intermittent generation in the absence of alternative mitigation (follows logistic curve; function of intermittent penetration, reduced by increases in intermittent diversity and demand flexibility)			((Retic_Eff_Mult_Asymptote / (1+ ((Retic_Eff_Mult_Asymptote - 1)^((1 - Intermittent_Penetration) / (1 - Init_Intermittent_Penetration))) * (((Retic_Eff_Mult_Asymptote / Retic_Eff_Mult_Final) - 1)^((Intermittent_Penetration - Init_Intermittent_Penetration) / (1 - Init_Intermittent_Penetration))))) - 1) * Combined_Mult_Reduction
Secondary/Electricity System	Retic_Eff_Mult_Actual	Expression	Fractional reduction in secondary reticulation efficiency for intermittent generation given the level of built intermittent AI mitigation			Retic_Eff_Mult * Intermit_AI_Built_Factor_Prev
Secondary	AI_Addition_EC_Use	Expression	Vector of rates of energy carrier use for the purposes of adding new secondary auxiliary infrastructure	EJ/yr	EC_types	sumc((vector(Secondary_AI_types, 1) - AI_Decommission_Fraction) * AI_CapEx_Fraction * (Auxiliary_Addition.Amount_in_Transit * Secondary_AI_ECC / Auxiliary_Build_Time) * AI_EC_Split)
Secondary	AI_Decommission_EC_Use	Expression	Vector of rates of energy carrier use for the purposes of decommissioning end-of-life secondary auxiliary infrastructure	EJ/yr	EC_types	sumc(AI_Decommission_Fraction * AI_CapEx_Fraction * Auxiliary_Operation * Secondary_AI_ECC * AI_EC_Split)
Secondary	AI_EC_Split	Expression	Matrix of the EC composition of secondary auxiliary infrastructure investment energy, adjusted for thermal energy equivalence		Secondary_AI_types, EC_types	(Demand_EC_Split / Initial_Supply_EC_Split) * AI_Initial_EC_Split / sumr(EC_Thermal_Equivalence * (Demand_EC_Split / Initial_Supply_EC_Split) * AI_Initial_EC_Split)
Secondary	AI_Initial_EC_Split	Expression	Initial shares of secondary auxiliary infrastructure input energy by EC type, adjusted for thermal energy		Secondary_AI_types, EC_types	Initial_Supply_EC_Split * matrix(vector(1), AI_EC_Split_LaG_Factor, AI_EC_Split_Heat_Factor) / sumr(EC_Thermal_Equivalence * Initial_Supply_EC_Split * matrix(vector(1), AI_EC_Split_LaG_Factor, AI_EC_Split_Heat_Factor))
Secondary	AI_Operation_EC_Use	Expression	Vector of rates of energy carrier use for the purposes of operating existing secondary auxiliary infrastructure	EJ/yr	EC_types	sumc((vector(Secondary_AI_types, 1) - AI_CapEx_Fraction) * (Auxiliary_Operation.Amount_in_Transit * Secondary_AI_ECC / Auxiliary_Lifetime) * AI_EC_Split)
Secondary	Auxiliary_Investment_Rate	Expression	Rate of investment in new secondary auxiliary infrastructure peak capacity	EJ/yr^2	Secondary_AI_types	vector(1, Intermittency_Mitigation, 1, 1) * max(vector(0 EJ/yr), Auxiliary_Requirement - Auxiliary_Operation.Amount_in_Transit) / Auxiliary_Build_Time

Sector	Element name	Type	Description	Unit	Array labels	Expression/condition/inputs
Secondary	Auxiliary_Requirement	Expression	Sum requirement for secondary auxiliary infrastructure peak capacity	EJ/yr	Secondary_AI_types	sumc(Power_Capacity_Operation.Amount_in_Transit * Secondary_Capacity_Factor * PC_AI_ID) * Peak_Factor * vector(1, Intermit_AI_Mult, 1, 1)
Secondary	PC_Addition_EC_Use	Expression	Vector of rates of energy carrier use for the purposes of adding new secondary power capacity	EJ/yr	EC_types	sumc((vector(Secondary_PC_types, 1) - PC_Decommission_Fraction) * PC_CapEx_Fraction * (Power_Capacity_Addition.Amount_in_Transit * Secondary_PC_ECC / Power_Capacity_Build_Time) * PC_EC_Split)
Secondary	PC_AI_ID	Expression	Matrix of secondary AI requirement identities by secondary PC type		Secondary_PC_types, Secondary_AI_types	matrix(Secondary_Output_ID[*, 1], Sec_Intermittent_ID, Secondary_Output_ID[*, 2], Secondary_Output_ID[*, 3])
Secondary	PC_Decommission_EC_Use	Expression	Vector of rates of energy carrier use for the purposes of decommissioning end-of-life secondary power capacity	EJ/yr	EC_types	sumc(PC_Decommission_Fraction * PC_CapEx_Fraction * Power_Capacity_Operation * Secondary_PC_ECC * PC_EC_Split)
Secondary	PC_EC_Split	Expression	Matrix of the EC composition of secondary power capacity investment energy, adjusted for thermal energy equivalence		Secondary_PC_types, EC_types	(Demand_EC_Split / Initial_Supply_EC_Split) * PC_Initial_EC_Split / sumr(EC_Thermal_Equivalence * (Demand_EC_Split / Initial_Supply_EC_Split) * PC_Initial_EC_Split)
Secondary	PC_Initial_EC_Split	Expression	Initial shares of secondary power capacity input energy by EC type, adjusted for thermal energy		Secondary_PC_types, EC_types	Initial_Supply_EC_Split * matrix(vector(1), PC_EC_Split_LaG_Factor, PC_EC_Split_Heat_Factor) / sumr(EC_Thermal_Equivalence * Initial_Supply_EC_Split * matrix(vector(1), PC_EC_Split_LaG_Factor, PC_EC_Split_Heat_Factor))
Secondary	PC_Operation_EC_Use	Expression	Vector of rates of energy carrier use for the purposes of operating existing secondary power capacity	EJ/yr	EC_types	sumc((vector(Secondary_PC_types, 1) - PC_CapEx_Fraction) * (Secondary_Capacity_Factor / Initial_Secondary_CF_Max) * (Power_Capacity_Operation.Amount_in_Transit * Secondary_PC_ECC / Power_Capacity_Lifetime) * PC_EC_Split)
Secondary	Peak_Factor	Expression	Vector of ratios of peak to average power output by secondary AI type (reduced linearly by increasing demand flexibility)		Secondary_AI_types	(Init_Secondary_Peak_Factor - vector(1)) * vector(1 - Demand_Flexibility) + vector(1)
System Control/EC Committed	EC_Deficit_Commit	Expression	Matrix of forecast EC supply/demand balance (EC deficit, measured in EJ) by time elapsed from the current timestep (each row represents 0.5 year increment)	EJ	Plan_horizon, EC_types	- (matrix(1) * Supply_Demand_Balance + mult(matrix(Plan_horizon, Plan_horizon, if(row >= col, 0.5 yr, 0 yr)), matrix(1) * (EC_Inflow_Integ.Moving_Average - EC_Consumption.Moving_Average) + EC_Upstream_Rate_Commit + EC_Downstream_Rate_Commit - EC_Invest_Rate_Commit - EC_Upkeep_Rate_Commit))

Sector	Element name	Type	Description	Unit	Array labels	Expression/condition/inputs
System Control/EC Committed	EC_Deficit_Horizon	Expression	Vector of forecast EC supply/demand balance (EC deficit, measured in EJ) at the selected time horizon	EJ	EC_types	vector(vinterp(EC_Deficit_Commit[*, 1], Invest_Time_Horizon / 0.5 yr), vinterp(EC_Deficit_Commit[*, 2], Invest_Time_Horizon / 0.5 yr), vinterp(EC_Deficit_Commit[*, 3], Invest_Time_Horizon / 0.5 yr))
System Control/EC Committed	EC_Deficit_Horizon_Norm	Expression	Vector of normalized forecast EC supply/demand balance (EC deficit, measured in EJ) at the selected time horizon (uses lower of moving average and actual, minimum set to zero with vector sum of 1; represents relative priority of ECs)		EC_types	(min(EC_Deficit_Horizon, EC_Deficit_Horizon_Integ.Moving_Average) - vector(EC_types, minv(min(EC_Deficit_Horizon, EC_Deficit_Horizon_Integ.Moving_Average)))) / sumv(min(EC_Deficit_Horizon, EC_Deficit_Horizon_Integ.Moving_Average) - vector(EC_types, minv(min(EC_Deficit_Horizon, EC_Deficit_Horizon_Integ.Moving_Average))))
System Control/EC Committed	EC_Deficit_Horizon_Scaled	Expression	Vector of forecast EC supply/demand balance (EC deficit, measured in EJ) at the selected time horizon, with negatives values reduced in magnitude (uses lower of moving average and actual)	EJ	EC_types	if(min(EC_Deficit_Horizon, EC_Deficit_Horizon_Integ.Moving_Average) < vector(0 EJ), EC_Surplus_Scale_Factor * min(EC_Deficit_Horizon, EC_Deficit_Horizon_Integ.Moving_Average), min(EC_Deficit_Horizon, EC_Deficit_Horizon_Integ.Moving_Average))
System Control/EC Committed	EC_Downstream_Rate_Commit	Expression	Matrix of net change to EC outflows due to forecast changes in EU PC stocks by time elapsed from the current timestep (each row represents 0.5 year increment)	EJ/yr	Plan_horizon, EC_types	mult(EU_Additions_Shape_Matrix, End_Use_Capacity_Factor * (End_Use_Sector.Amount_in_Transit_2 * (mult(End_Use_Output_ID * End_Use_ES_Eff, EC_ES_Conversion) - End_Use_Input_Scaled) - EU_PC_Plan_Horizon.Amount_in_Transit * (mult(End_Use_Output_ID * End_Use_ES_Eff_PC_Mean, EC_ES_Conversion) - End_Use_Input_Scaled)))
System Control/EC Committed	EC_Invest_Rate_Commit	Expression	Matrix of net change to EC outflows due to investments in new PC and AI by time elapsed from the current timestep (each row represents 0.5 year increment)	EJ/yr	Plan_horizon, EC_types	mult(Sec_Invest_Shape_Matrix, (Secondary_Sector.Amount_in_Transit_2 + Secondary_PC_Invest_Delay.Amount_in_Transit) * ((Secondary_Sector.Power_Capacity_Lifetime + max(Primary_Build_Time, Secondary_Sector.Power_Capacity_Build_Time)) * Secondary_Sector.PC_CapEx_Fraction / max(Primary_Build_Time, Secondary_Sector.Power_Capacity_Build_Time)) * Upstream_Invest_EC_Cost) + mult(End_Use_Invest_Shape_Matrix, End_Use_Sector.Amount_in_Transit_2 * ((End_Use_Sector.Power_Capacity_Lifetime + End_Use_Sector.Power_Capacity_Build_Time) * End_Use_Sector.PC_CapEx_Fraction / End_Use_Sector.Power_Capacity_Build_Time) * Downstream_Invest_EC_Cost)

Sector	Element name	Type	Description	Unit	Array labels	Expression/condition/inputs
System Control/EC Committed	EC_Upkeep_Rate_Commit	Expression	Matrix of net change to EC outflows due to forecast changes in upkeep requirements for PC and AI in operation by time elapsed from the current timestep (each row represents 0.5 year increment)	EJ/yr	Plan_horizon, EC_types	mult((Secondary_CF_Max / Initial_Secondary_CF_Max) * Sec_Additions_Shape_Matrix * (Secondary_Sector.Amount_in_Transit_2 + Secondary_PC_Invest_Delay.Amount_in_Transit - Sec_PC_Plan_Horizon.Amount_in_Transit), ((Secondary_Sector.Power_Capacity_Lifetime + max(Primary_Build_Time, Secondary_Sector.Power_Capacity_Build_Time)) * (Secondary_Sector.PC_CapEx_Fraction - vector(Secondary_PC_types, 1)) / Secondary_Sector.Power_Capacity_Lifetime) * Upstream_Invest_EC_Cost) + mult((End_Use_Capacity_Factor / End_Use_CF_Target) * EU_Additions_Shape_Matrix * (End_Use_Sector.Amount_in_Transit_2 - EU_PC_Plan_Horizon.Amount_in_Transit), ((End_Use_Sector.Power_Capacity_Lifetime + End_Use_Sector.Power_Capacity_Build_Time) * (End_Use_Sector.PC_CapEx_Fraction - vector(End_use_PC_types, 1)) / End_Use_Sector.Power_Capacity_Lifetime) * Downstream_Invest_EC_Cost)
System Control/EC Committed	EC_Upstream_Rate_Commit	Expression	Matrix of net change to EC inflows due to forecast changes in secondary PC stocks by time elapsed from the current timestep (each row represents 0.5 year increment)	EJ/yr	Plan_horizon, EC_types	mult(Sec_Additions_Shape_Matrix, ((Secondary_Sector.Amount_in_Transit_2 + Secondary_PC_Invest_Delay.Amount_in_Transit) * Sec_Reticulation_Eff - Sec_PC_Plan_Horizon.Amount_in_Transit * Sec_Reticulation_Eff_PC_Mean) * (vector(Secondary_PC_types, 1) + Secondary_Sector.Sec_Intermittent_ID * Secondary_Sector.Retic_Eff_Mult_Actual) * Secondary_CF_Max * Secondary_Output_ID)
System Control/EC Committed	End_Use_Invest_Shape_Matrix	Expression	Matrix of normalized EU investment flows by time elapsed from the current timestep (each row represents 0.5 year increment)		Plan_horizon, End_use_PC_types	matrix(Plan_horizon, End_use_PC_types, if(getitem(End_Use_Sector.Power_Capacity_Build_Time, col) > 0.5 * row yr, 1 - (0.5 * row yr / getitem(End_Use_Sector.Power_Capacity_Build_Time, col)), 0)) * if(End_Use_Sector.Power_Capacity_Build_Time < 0.5 yr, End_Use_Sector.Power_Capacity_Build_Time / 0.5 yr, vector(End_use_PC_types, 1))
System Control/EC Committed	EU_Additions_Shape_Matrix	Expression	Matrix of normalized EU EC intake flows by time elapsed from the current timestep (each row represents 0.5 year increment)		Plan_horizon, End_use_PC_types	matrix(Plan_horizon, End_use_PC_types, if(getitem(End_Use_Sector.Power_Capacity_Build_Time, col) <= 0.5 * row yr, 1, 0.5 * row yr / getitem(End_Use_Sector.Power_Capacity_Build_Time, col)))
System Control/EC Committed	Sec_Additions_Shape_Matrix	Expression	Matrix of normalized secondary EC output flows by time elapsed from the current timestep (each row represents 0.5 year increment)		Plan_horizon, Secondary_PC_types	matrix(Plan_horizon, Secondary_PC_types, if(getitem(max(Primary_Build_Time, Secondary_Sector.Power_Capacity_Build_Time), col) <= 0.5 * row yr, 1, 0.5 * row yr / getitem(max(Primary_Build_Time, Secondary_Sector.Power_Capacity_Build_Time), col)))

Sector	Element name	Type	Description	Unit	Array labels	Expression/condition/inputs
System Control/EC Committed	Sec_Invest_Shape_Matrix	Expression	Matrix of normalized secondary investment flows by time elapsed from the current timestep (each row represents 0.5 year increment)		Plan_horizon, Secondary_PC_types	matrix(Plan_horizon, Secondary_PC_types, if(getitem(max(Primary_Build_Time, Secondary_Sector.Power_Capacity_Build_Time), col) > 0.5 * row yr, 1 - (0.5 * row yr / getitem(max(Primary_Build_Time, Secondary_Sector.Power_Capacity_Build_Time), col)), 0))
System Control/Invest Synchronization	End_Use_PC_Invest	Expression	Vector of investment flows for EU (downstream) PC given by invest share and invest magnitude calculations (investment signal for system transformation)	EJ/yr^2	End_use_PC_types	if(ETime = 0 yr, vector(0), vector(1)) * max(vector(0 EJ/yr^2), Downstream_Invest_PC_Share * EC_Invest_Magnitude)
System Control/Invest Synchronization	End_Use_PC_Invest_Sum	Expression	Vector of sum investment flows for EU (downstream) PC including investment signal and upkeep function (capped by maximum turnover factor)	EJ/yr^2	End_use_PC_types	if(ETime = 0 yr, vector(0), vector(1)) * min((sumr(ES_Demand * End_Use_Output_ID) / (End_Use_CF_Target * End_Use_ES_Eff * End_Use_Sector.Power_Capacity_Lifetime)) * PC_Invest_Max_Fraction, End_Use_PC_Invest + End_Use_PC_Upkeep)
System Control/Invest Synchronization	End_Use_PC_Upkeep	Expression	Vector of investment flows for EU (downstream) PC given by upkeep requirements (returns CF to CF target based on prevailing PC composition)	EJ/yr^2	End_use_PC_types	max(vector(0 EJ/yr^2), sumc(max(vector(ES_types, 0 EJ/yr), ES_Demand - sumc(End_Use_Output_ID * End_Use_Sector.Amount_in_Transit * End_Use_CF_Target * End_Use_ES_Eff_PC_Mean) - sumc(End_Use_Output_ID * (End_Use_Sector.Amount_in_Transit_2 + End_Use_PC_Invest_Delay.Amount_in_Transit) * End_Use_CF_Target * End_Use_ES_Eff)) * End_Use_Output_Scaled * Downstream_Invest_Curtail / sumr(End_Use_Output_Scaled * Downstream_Invest_Curtail)) / (End_Use_CF_Target * End_Use_ES_Eff * End_Use_Sector.Power_Capacity_Build_Time))
System Control/Invest Synchronization	NRE_PC_Invest	Expression	Vector of investment flows for primary NRE PC synchronized with corresponding secondary PC investment (includes invest signal, stock replacement, and primary/secondary capacity adjustment)	EJ/yr^2	NRE_types	if(NRE_Depletion >= vector(1), vector(0), vector(1)) * max(vector(0 EJ/yr^2), sumr(Secondary_CF_Max * (Primary_PC_Invest_Delay / Sec_Conversion_Eff) * NRE_Secondary_Input_ID / NRE_CF_Max) + NRE_PC_Invest_Adj + if(ETime < Primary_NRE_Sector.Power_Capacity_Build_Time, vector(0 EJ/yr^2), NRE_PC_Decomm_Preempt))
System Control/Invest Synchronization	NRE_PC_Invest_Adj	Expression	Vector of adjustments to NRE PC investment for the purpose of balancing primary and secondary PC quantities	EJ/yr^2	NRE_types	if(NRE_Depletion >= vector(1), vector(0), vector(1)) * max(- sumr(Secondary_CF_Max * (Primary_PC_Invest_Delay / Sec_Conversion_Eff) * NRE_Secondary_Input_ID / NRE_CF_Max) - if(ETime < Primary_NRE_Sector.Power_Capacity_Build_Time, vector(0 EJ/yr^2), NRE_PC_Decomm_Preempt), ((NRE_Secondary_Input_Rate_Max - NRE_Production_Rate_Max) / NRE_CF_Max - NRE_PC_Invest_Adj_Integ) / ~Minimum_PC_Timeframe)
System Control/Invest	Primary_Build_Time	Expression	Vector of corresponding primary PC build times by secondary PC type	yr	Secondary_PC_types	sumc(Primary_NRE_Sector.Power_Capacity_Build_Time * NRE_Secondary_Input_ID) + sumc(Primary_RE_Sector.Power_Capacity_Build_Time * RE_Secondary_Input_ID)

Sector	Element name	Type	Description	Unit	Array labels	Expression/condition/inputs
System Control/Invest Synchronization	RE_PC_Invest	Expression	Vector of investment flows for primary RE PC synchronized with corresponding secondary PC investment (includes invest signal, stock replacement, and primary/secondary capacity adjustment)	EJ/yr ^2	RE_types	if(RE_Exhaustion_Commit > vector(1), vector(0), vector(1)) * max(vector(0 EJ/yr^2), sumr(Secondary_CF_Max * (Primary_PC_Invest_Delay / Sec_Conversion_Eff) * RE_Secondary_Input_ID / RE_CF_Max) + RE_PC_Invest_Adj + if(ETime < Primary_RE_Sector.Power_Capacity_Build_Time, vector(0 EJ/yr^2), RE_PC_Decomm_Preempt))
System Control/Invest Synchronization	RE_PC_Invest_Adj	Expression	Vector of adjustments to RE PC investment for the purpose of balancing primary and secondary PC quantities	EJ/yr ^2	RE_types	if(RE_Exhaustion_Commit > vector(1), vector(0), vector(1)) * max(- sumr(Secondary_CF_Max * (Primary_PC_Invest_Delay / Sec_Conversion_Eff) * RE_Secondary_Input_ID / RE_CF_Max) - if(ETime < Primary_RE_Sector.Power_Capacity_Build_Time, vector(0 EJ/yr^2), RE_PC_Decomm_Preempt), ((RE_Secondary_Input_Rate_Max - RE_Production_Rate_Max) / RE_CF_Max - RE_PC_Invest_Adj_Integ) / ~Minimum_PC_Timeframe)
System Control/Invest Synchronization	Secondary_PC_Invest	Expression	Vector of investment flows for primary and secondary (upstream) PC given by invest share and invest magnitude calculations (investment signal for system transformation; capped by maximum turnover factor)	EJ/yr ^2	Secondary_PC_types	if(ETime = 0 yr, vector(0), vector(1)) * min((sumr(max(vector(EC_types,0 EJ/yr), EC_Inflow_Integ.Moving_Average) * Secondary_Output_ID) / (Initial_Secondary_CF_Max * Sec_Reticulation_Eff * Secondary_Sector.Power_Capacity_Lifetime)) * PC_Invest_Max_Fraction, max(vector(0 EJ/yr^2), Upstream_Invest_PC_Share * EC_Invest_Magnitude))
System Control/Invest Share	Downstream_Invest_Curtail	Expression	Vector of curtailment coefficients for EU PC (downstream) investment (takes into account penetration level relative to limit and capacity factor relative to CF maxima)		End_use_PC_types	if((End_Use_Penetration / EU_Penetration_Limit) < vector(1 - Curtailment_Threshold), vector(1), if(End_Use_Penetration >= EU_Penetration_Limit, vector(0), (vector(1) - (End_Use_Penetration / EU_Penetration_Limit)) / Curtailment_Threshold)) * min(vector(1), End_Use_Capacity_Factor / End_Use_CF_Target) * if((End_Use_Capacity_Factor / End_Use_CF_Target) < vector(1 - Curtailment_Threshold), vector(0), if((End_Use_Capacity_Factor / End_Use_CF_Target) > vector(1), vector(1), ((End_Use_Capacity_Factor / End_Use_CF_Target) - vector(1 - Curtailment_Threshold)) / Curtailment_Threshold))
System Control/Invest Share	Downstream_Invest_EC_Cost	Expression	Matrix of normalized (per unit PC, per year) lifetime downstream EC cost by EU PC type (construction, operation, and decommissioning; expressed as uniform flow)		End_use_PC_types, EC_types	End_Use_PC_ECC_Disag_Ratio + End_Use_CF_Target * mult(End_Use_Sector.PC_AI_ID * End_Use_Sector.Peak_Factor, End_Use_AI_ECC_Disag_Ratio)
System Control/Invest Share	Downstream_Invest_EC_Yield	Expression	Matrix of ratios of net downstream EC saved per unit EC invested by EU PC type		End_use_PC_types, EC_types	End_Use_Capacity_Factor * (mult(End_Use_Output_ID * End_Use_ES_Eff, EC_ES_Conversion) - End_Use_Input_Scaled) / Downstream_Invest_EC_Cost - matrix(1)

Sector	Element name	Type	Description	Unit	Array labels	Expression/condition/inputs
System Control/Invest Share	Downstream_Invest_PC_Share	Expression	Vector of fractional shares of downstream investment by EU PC type translated to PC quantities (inversely scaled by PC cost and normalized, weighted by relative EC importance)		End_use_PC_types	sumr((Downstream_Invest_Share * (matrix(End_use_PC_types, EC_types, 1) / Downstream_Invest_EC_Cost) / (sumc(Upstream_Invest_Share * (matrix(Secondary_PC_types, EC_types, 1) / Upstream_Invest_EC_Cost)) + sumc(Downstream_Invest_Share * (matrix(End_use_PC_types, EC_types, 1) / Downstream_Invest_EC_Cost)))) * EC_Deficit_Horizon_Norm)
System Control/Invest Share	Downstream_Invest_Share	Expression	Vector of fractional shares of downstream investment by EU PC type (given by logit function of utility; without curtailment upstream plus downstream sums to 1)		End_use_PC_types	Downstream_Invest_Curtail * exp(Downstream_Invest_Utility) / (sumv(exp(Upstream_Invest_Utility)) + sumv(exp(Downstream_Invest_Utility)))
System Control/Invest Share	Downstream_Invest_Utility	Expression	Vector of downstream utility values by EU PC type (sum product of yield and scaled forecast supply/demand balance by EC type, multiplied by specified utility coefficient)		End_use_PC_types	min(vector(700), if(Downstream_Invest_Curtail = vector(0) OR sumr(Downstream_Invest_EC_Yield * EC_Deficit_Horizon_Scaled) < vector(0 EJ) OR (Scenario_5 = 1 AND ETime < 35 yr), vector(~Utility_Remove), Utility_Share_Coeff * sumr(Downstream_Invest_EC_Yield * EC_Deficit_Horizon_Scaled)))
System Control/Invest Share	End_Use_AI_EC C_Disag_Ratio	Expression	Matrix of EU AI ECC values split by EC type divided by sum lifecycle time (EC input per unit, per year)		End_use_AI_types, EC_types	End_Use_AI_ECC * End_Use_Sector.AI_EC_Split / (End_Use_Sector.Auxiliary_Lifetime + End_Use_Sector.Auxiliary_Build_Time)
System Control/Invest Share	End_Use_PC_E CC_Disag_Ratio	Expression	Matrix of EU PC ECC values split by EC type divided by sum lifecycle time (EC input per unit, per year)		End_use_PC_types, EC_types	End_Use_PC_ECC * End_Use_Sector.PC_EC_Split * (End_Use_Sector.PC_CapEx_Fraction + (vector(1) - End_Use_Sector.PC_CapEx_Fraction) * (End_Use_Capacity_Factor / Init_End_Use_CF_Target)) / (End_Use_Sector.Power_Capacity_Lifetime + End_Use_Sector.Power_Capacity_Build_Time)
System Control/Invest Share	End_Use_Penetration	Expression	Vector of fractional shares of energy service provision by EU PC type (includes committed PC investments)		End_use_PC_types	maxr((End_Use_Sector.Amount_in_Transit + End_Use_Sector.Amount_in_Transit_2 + End_Use_PC_Invest_Delay.Amount_in_Transit) * End_Use_Capacity_Factor * End_Use_ES_Eff_PC_Mean * End_Use_Output_ID / sumc((End_Use_Sector.Amount_in_Transit + End_Use_Sector.Amount_in_Transit_2 + End_Use_PC_Invest_Delay.Amount_in_Transit) * End_Use_Capacity_Factor * End_Use_ES_Eff_PC_Mean * End_Use_Output_ID))
System Control/Invest Share	NRE_EROI_Disag_Inverse	Expression	Matrix of inverse NRE EROI values split by EC type divided by sum lifecycle time (EC input per unit, per year)		NRE_types, EC_types	Primary_NRE_Sector.EC_Split / NRE_EROI

Sector	Element name	Type	Description	Unit	Array labels	Expression/condition/inputs
System Control/Invest Share	RE_EROI_Disag_Invers e	Expression	Matrix of inverse RE EROI values split by EC type divided by sum lifecycle time (EC input per unit, per year; adjusted for thermal equivalence of primary electricity output)		RE_types, EC_types	RE_Output_Thermal_Equiv * (Primary_RE_Sector.EC_Split * (Primary_RE_Sector.CapEx_Fraction + (vector(1) - Primary_RE_Sector.CapEx_Fraction) * (RE_CF_Max / Initial_RE_CF_Max)) / RE_EROI_Addition_Mean)
System Control/Invest Share	RE_Exhaustion_Com mit	Expression	Vector of RE exhaustion values to be reached when all committed RE PC comes online		RE_types	((Primary_RE_Sector.Amount_in_Transit + Primary_RE_Sector.Amount_in_Transit_2 + sumr((Initial_Secondary_CF_Max / Sec_Conversion_Eff_PC_Mean) * Primary_PC_Invest_Delay.Amount_in_Transit * RE_Secondary_Input_ID / RE_CF_Max)) * Initial_RE_CF_Max - Initial_RE_Output_Rate) / (RE_Potential - Initial_RE_Output_Rate)
System Control/Invest Share	Sec_AI_ECC_Disag_Ratio	Expression	Matrix of secondary AI ECC values split by EC type divided by sum lifecycle time (EC input per unit, per year)		Secondary_AI_types, EC_types	Secondary_AI_ECC * Secondary_Sector.AI_EC_Split / (Secondary_Sector.Auxiliary_Lifetime + Secondary_Sector.Auxiliary_Build_Time)
System Control/Invest Share	Sec_PC_ECC_Dis ag_Ratio	Expression	Matrix of secondary PC ECC values split by EC type divided by sum lifecycle time (EC input per unit, per year)		Secondary_PC_t ypes, EC_types	Secondary_PC_ECC * Secondary_Sector.PC_EC_Split * (Secondary_Sector.PC_CapEx_Fraction + (vector(1) - Secondary_Sector.PC_CapEx_Fraction) * (Secondary_CF_Max / Initial_Secondary_CF_Max)) / (Secondary_Sector.Power_Capacity_Lifetime + Secondary_Sector.Power_Capacity_Build_Time)
System Control/Invest Share	Secondary_Penetration	Expression	Vector of fractional shares of gross EC production by secondary PC type (prior to transmission and distribution; includes committed PC investments; note: for CHP, the result is the maximum of heat and electricity penetration values)		Secondary_PC_types	maxr((Secondary_Sector.Amount_in_Transit + Secondary_Sector.Amount_in_Transit_2 + Secondary_PC_Invest_Delay.Amount_in_Transit) * Secondary_CF_Max * Secondary_Output_Matrix / sumc((Secondary_Sector.Amount_in_Transit + Secondary_Sector.Amount_in_Transit_2 + Secondary_PC_Invest_Delay.Amount_in_Transit) * Secondary_CF_Max * Secondary_Output_Matrix))
System Control/Invest Share	Secondary_Penetration_Actu al	Expression	Vector of actual fractional shares of gross EC production by secondary PC type (prior to transmission and distribution; note: for CHP, the result is the maximum of heat and electricity penetration values)		Secondary_PC_types	sumr(Secondary_Output_Rate * Secondary_Output_Matrix / sumc(Secondary_Output_Rate * Secondary_Output_Matrix))

Sector	Element name	Type	Description	Unit	Array labels	Expression/condition/inputs
System Control/Invest Share	Upstream_Invest_Curtail	Expression	Vector of curtailment coefficients for primary and secondary PC (upstream) investment (takes into account penetration level relative to limit, NRE depletion, committed RE exhaustion, and capacity factor relative to CF maxima)		Secondary_PC_types	if((Secondary_Penetration / Sec_Penetration_Limit) < vector(1 - Curtailment_Threshold), vector(1), if(Secondary_Penetration >= Sec_Penetration_Limit, vector(0), (vector(1) - (Secondary_Penetration / Sec_Penetration_Limit)) / Curtailment_Threshold)) * (sumc(RE_Secondary_Input_ID) + sumc(if(NRE_Depletion < vector(NRE_types, 1 - Curtailment_Threshold), vector(NRE_types, 1), if(NRE_Depletion > vector(NRE_types, 1), vector(NRE_types, 0), (vector(NRE_types, 1) - NRE_Depletion) / Curtailment_Threshold)) * NRE_Secondary_Input_ID)) * (sumc(NRE_Secondary_Input_ID) + sumc(if(RE_Exhaustion_Commit < vector(RE_types, 1 - Curtailment_Threshold), vector(RE_types, 1), if(RE_Exhaustion_Commit > vector(RE_types, 1), vector(RE_types, 0), (vector(RE_types, 1) - RE_Exhaustion_Commit) / Curtailment_Threshold)) * RE_Secondary_Input_ID)) * if((Secondary_Capacity_Factor / Secondary_CF_Max) < vector(1 - Curtailment_Threshold), vector(0), ((Secondary_Capacity_Factor / Secondary_CF_Max) - vector(1 - Curtailment_Threshold)) / Curtailment_Threshold)
System Control/Invest Share	Upstream_Invest_EC_Cost	Expression	Matrix of normalized (per unit PC, per year) lifetime upstream EC cost by secondary PC type (construction, operation, and decommissioning; expressed as uniform flow)		Secondary_PC_types, EC_types	Sec_PC_ECC_Disag_Ratio + Secondary_CF_Max * (mult(Secondary_Sector.PC_AI_ID * Secondary_Sector.Peak_Factor * vector(Secondary_AI_types, 1, Secondary_Sector.Intermit_AI_Mult * Intermittency_Mitigation, 1, 1), Sec_AI_ECC_Disag_Ratio) + mult(trans((NRE_Capacity_Factor / NRE_CF_Max) * NRE_Secondary_Input_ID / Sec_Conversion_Eff), NRE_EROI_Disag_Inverse) + mult(trans((RE_Capacity_Factor / RE_CF_Max) * RE_Secondary_Input_ID / Sec_Conversion_Eff), RE_EROI_Disag_Inverse))
System Control/Invest Share	Upstream_Invest_EC_Yield	Expression	Matrix of ratios of net upstream EC produced per unit EC invested by EU PC type		Secondary_PC_types, EC_types	Secondary_CF_Max * Secondary_Output_ID * Sec_Reticulation_Eff * (vector(1) + Intermittency_Mitigation * Secondary_Sector.Sec_Intermittent_ID * Secondary_Sector.Retic_Eff_Mult_Actual) / Upstream_Invest_EC_Cost - matrix(1)
System Control/Invest Share	Upstream_Invest_PC_Share	Expression	Vector of fractional shares of upstream investment by secondary PC type translated to PC quantities (inversely scaled by PC cost and normalized, weighted by relative EC importance)		Secondary_PC_types	sumr((Upstream_Invest_Share * (matrix(Secondary_PC_types, EC_types, 1) / Upstream_Invest_EC_Cost) / (sumc(Upstream_Invest_Share * (matrix(Secondary_PC_types, EC_types, 1) / Upstream_Invest_EC_Cost)) + sumc(Downstream_Invest_Share * (matrix(End_use_PC_types, EC_types, 1) / Downstream_Invest_EC_Cost)))) * EC_Deficit_Horizon_Norm)
System Control/Invest Share	Upstream_Invest_Share	Expression	Vector of fractional shares of upstream investment by secondary PC type (given by logit function of utility; without curtailment upstream plus downstream sums to 1)		Secondary_PC_types	Upstream_Invest_Curtail * exp(Upstream_Invest_Utility) / (sumv(exp(Upstream_Invest_Utility)) + sumv(exp(Downstream_Invest_Utility)))

Sector	Element name	Type	Description	Unit	Array labels	Expression/condition/inputs
System Control/Invest Share	Upstream_Invest_Utility	Expression	Vector of upstream utility values by secondary PC type (sum product of yield and scaled forecast supply/demand balance by EC type, multiplied by specified utility coefficient)		Secondary_PC_types	min(vector(700), if(Upstream_Invest_Curtail = vector(0) OR sumr(Upstream_Invest_EC_Yield * EC_Deficit_Horizon_Scaled) < vector(0 EJ), vector(~Utility_Remove), Utility_Share_Coeff * sumr(Upstream_Invest_EC_Yield * EC_Deficit_Horizon_Scaled) * (sumc(RE_Secondary_Input_ID) + sumc(NRE_Secondary_Input_ID * (vector(NRE_types, 1) - NRE_Annual_Utility_Reduction * GHG_Intensity / meanv(GHG_Intensity))^(ETime / 1 yr)))))
System Control	EC_Deficit	Expression	Cumulative EC deficit (measured in years of current consumption) by EC type (positive values indicate surplus; can be considered a proxy for EC price)	yr	EC_types	if(EC_Consumption.Moving_Average <= 2 * ~PC_Zero_Approx, vector(0 yr), -(Supply_Demand_Balance / EC_Consumption.Moving_Average))
System Control	EC_Deficit_Integral_Sum	Expression	Vector sum of cumulative EC deficit (measured in years of current consumption) above the EC deficit limit	yr^2		sumv(EC_Deficit_Integral)
System Control	EC_Invest_Capacity	Expression	Scale factor for investment in response to sum forecast EC deficit (corresponds to additional commitment to sum lifecycle EC expenditure per year; linear function given by specified capacity coefficient; reduced when any ESMR approaches ESMR limit; minimum given by specified capacity floor)	EJ/yr^2		max(~EC_Invest_Capacity_Floor, EC_Invest_Capacity_Coeff * sumv(max(vector(EC_types, 0 EJ), EC_Deficit_Horizon_Integ.Moving_Average)) * if(maxv(ESMR) <= ESMR_Limit * (1 - Curtailment_Threshold), 1, (ESMR_Limit - maxv(ESMR)) / Curtailment_Threshold))
System Control	EC_Invest_Magnitude	Expression	Invest capacity scale factor translated to applicable multiple given EC cost associated with invest PC share vectors	EJ/yr^2		sumv(EC_Deficit_Horizon_Norm * ((EC_Inflow_Integ.Moving_Average / sumv(EC_Inflow_Integ.Moving_Average)) * EC_Invest_Capacity) / max(vector(EC_types, 0.001), sumc(Upstream_Invest_PC_Share * Upstream_Invest_EC_Cost) + sumc(Downstream_Invest_PC_Share * Downstream_Invest_EC_Cost)))
System Control	Transition_Failure	Milestone	Condition trigger to detect when EC deficit magnitude or rate of change is no longer consistent with a feasible transition pathway			On True: meanv(EC_Deficit) > 3 yr; On True: maxv(EC_Deficit) > 5 yr; On True: meanv(EC_Consumption.Moving_Average / max(vector(EC_types, ~PC_Zero_Approx), EC_Inflow_Integ.Moving_Average)) > 2
System Control	Transition_Stable_Time	Selector	Returns time elapsed prior to transition failure (successful transition return sim. duration)	yr		If: Transition_Failure.ETime > 0 yr, Then: Transition_Failure.Etime, Else: ETime

9.4.4.2 Previous value and information delay functions

Sector	Element name	Type	Description	Unit	Array labels	Reference	Initial value	Delay time
Energy Flow/Flow Routing	EC_Deficit_Prev	Previous value	Vector of values of EC_Deficit calculated in the previous timestep	yr		EC_Deficit	vector(0 yr)	
EROI	NRE_EROI_Delay	Information Delay	Vector of new PC EROI by NRE type, delayed by PC lifetime (for end-of-life PC)		NRE_types	NRE_EROI	Initial_NRE_EROI	Primary_NRE_Sector.Power_Capacity_Lifetime
EROI	RE_EROI_Addition_Delay	Information Delay	Vector of new PC EROI by RE type, delayed by PC lifetime (for end-of-life PC)		RE_types	RE_EROI_Addition_Mean	Initial_RE_EROI	Primary_RE_Sector.Power_Capacity_Lifetime
Secondary/Electricity System	Intermit_AI_Built_Factor_Prev	Previous value	Normalized level of intermittent AI in operation relative to the total required for full mitigation via AI, calculated in the previous timestep			Intermit_AI_Built_Factor	0	
System Control/EC Committed	EU_PC_Decomm_Preempt_Plan	Information Delay	Vector of EU PC additions delayed by lifetime minus build time (PC flow to be decommissioned at the end of the planning horizon)	EJ/yr^2	End_use_PC_types	End_Use_Sector.Power_Capacity_Addition	Initial_End_Use_PC / End_Use_Sector.Power_Capacity_Lifetime	End_Use_Sector.Power_Capacity_Lifetime - End_Use_Sector.Power_Capacity_Build_Time
System Control/EC Committed	Sec_PC_Decomm_Preempt_Plan	Information Delay	Vector of secondary PC additions delayed by secondary lifetime minus composite build time of the corresponding secondary PC type and associated primary PC (PC flow to be decommissioned at the end of the planning horizon)	EJ/yr^2	Secondary_PC_types	Secondary_Sector.Power_Capacity_Addition	Initial_Secondary_PC / Secondary_Sector.Power_Capacity_Lifetime	Secondary_Sector.Power_Capacity_Lifetime - max(Primary_Build_Time, Secondary_Sector.Power_Capacity_Build_Time)
System Control/Invest Synchronization	NRE_PC_Decomm_Preempt	Information Delay	Vector of NRE PC additions delayed by lifetime minus build time (PC flow to be decommissioned at the end of the planning horizon)	EJ/yr^2	NRE_types	Primary_NRE_Sector.Power_Capacity_Addition	Initial_NRE_PC / Primary_NRE_Sector.Power_Capacity_Lifetime	Primary_NRE_Sector.Power_Capacity_Lifetime - Primary_NRE_Sector.Power_Capacity_Build_Time
System Control/Invest Synchronization	NRE_PC_Invest_Adj_Delay	Information Delay	Vector of adjustments to NRE PC investment for the purpose of balancing primary and secondary PC quantities, delayed by NRE PC build time	EJ/yr^2	NRE_types	NRE_PC_Invest_Adj	vector(0 EJ/yr^2)	Primary_NRE_Sector.Power_Capacity_Build_Time

System Control/Invest Synchronization	RE_PC_Decomm_Preempt	Information Delay	Vector of RE PC additions delayed by lifetime minus build time (PC flow to be decommissioned at the end of the planning horizon)	EJ/yr^2	RE_types	Primary_RE_Sector.Power_Capacity_Addition	Initial_RE_PC / Primary_RE_Sector.Power_Capacity_Lifetime	Primary_RE_Sector.Power_Capacity_Lifetime - Primary_RE_Sector.Power_Capacity_Build_Time
System Control/Invest Synchronization	RE_PC_Invest_Adj_Delay	Information Delay	Vector of adjustments to RE PC investment for the purpose of balancing primary and secondary PC quantities, delayed by RE PC build time	EJ/yr^2	RE_types	RE_PC_Invest_Adj	vector(0 EJ/yr^2)	Primary_RE_Sector.Power_Capacity_Build_Time
System Control/Invest Synchronization	Sec_PC_Decomm_Preempt	Information Delay	Vector of secondary PC additions delayed by secondary lifetime minus the corresponding primary PC build time (PC flow to be decommissioned at the end of the planning horizon)	EJ/yr^2	Secondary_PC_types	Secondary_Sector.Power_Capacity_Addition	Initial_Secondary_PC / Secondary_Sector.Power_Capacity_Lifetime	Secondary_Sector.Power_Capacity_Lifetime - Primary_Build_Time

9.4.5 Scripts

Model scripts are created using GoldSim's inbuilt scripting functionality. This tool is based on the C++ scripting language.

9.4.5.1 Intermittency mitigation optimization

Sector	System Control
Element name	Intermittency_Mitigation
Description	Weighting function to find the optimal balance of mitigation for electricity generation intermittency based on mitigation costs and relative EC importance (0 corresponds to CF reductions only, 1 to mitigation using AI only)
Unit	
Array labels	
Initial value	0

Script Code:

```
-----------------
// Implicit variable defining the result of the script.
VALUE Result
Script:
-------
VALUE<Vector[EC_types]>[EJ/yr] CF_Reduction_EC_Cost = - sumc(Primary_RE_Sector.Amount_in_Transit *
Initial_RE_CF_Max * Secondary_Sector.RE_Intermittent_ID * Secondary_Sector.CF_Max_Mult * RE_EC_Conversion) -
sumc(Secondary_Sector.Amount_in_Transit * Initial_Secondary_CF_Max * Secondary_Sector.Sec_Intermittent_ID *
(vector(Secondary_PC_types, 1) - Primary_Generation_ID) * Secondary_Sector.CF_Max_Mult * Secondary_Output_Matrix)
VALUE<Vector[EC_types]>[EJ/yr] Intermit_AI_EC_Cost = mult(Secondary_Sector.Auxiliary_Requirement *
vector(Secondary_AI_types, 0, 1, 0, 0), Sec_AI_ECC_Disag_Ratio) - sumc(Secondary_Output_Rate * Secondary_Output_ID *
Sec_Reticulation_Eff_PC_Mean * Secondary_Sector.Sec_Intermittent_ID * Secondary_Sector.Retic_Eff_Mult)
```

```
Result = sumv(if(~Intermit_AI_EC_Cost > ~CF_Reduction_EC_Cost, vector(EC_types, 0), vector(EC_types, 1)) *
max(vector(EC_types, 0), EC_Deficit_Horizon_Norm))
```

9.4.5.2 Initial capital hypercycle solver

Sector	Energy Flow/Initialization/Initial ES Metabolism
Element name	Initial_Cap_HC_Solver
Description	Iterative solver to find the sum of initial EC flows for construction, operation, and decommissioning of end-use PC and AI consistent with initial net EC supply
Unit	EJ/yr
Array labels	EC_types
Initial value	0.22 * Initial_EC_Net_Supply

Script Code:

```
-----------------
// Implicit variable defining the result of the script.
VALUE<Vector[EC_types]>[EJ/yr] Result
Script:
-------
VALUE Solve_Limit = 99
VALUE[EJ^2/yr^2] MSE_Threshold = 0.001 EJ^2/yr^2
VALUE Initial_Band_Size = 0.75
VALUE Band_Scaling_Factor = 0.75
VALUE[EJ/yr] Min_Band = 0.005 EJ/yr
VALUE<Vector[EC_types]>[EJ/yr] Cap_HC_0 = 0.22 * Initial_EC_Net_Supply
VALUE<Vector[EC_types]>[EJ/yr] Cap_HC_1 = vector(0 EJ/yr)
VALUE<Matrix[EC_types,Pos]>[EJ/yr] Cap_HC_Mat = matrix(0 EJ/yr)
VALUE<Vector[EC_types]>[EJ/yr] Band = ~Cap_HC_0 * ~Initial_Band_Size
VALUE<Vector[End_use_PC_types]>[EJ/yr] Output = vector(0 EJ/yr)
VALUE<Vector[End_use_PC_types]>[EJ/yr] PC = vector(0 EJ/yr)
VALUE<Vector[End_use_AI_types]>[EJ/yr] AI = vector(0 EJ/yr)
VALUE<Vector[EC_types]>[EJ/yr] PC_Addition = vector(0 EJ/yr)
VALUE<Vector[EC_types]>[EJ/yr] PC_Decomm = vector(0 EJ/yr)
VALUE<Vector[EC_types]>[EJ/yr] PC_Operation = vector(0 EJ/yr)
VALUE<Vector[EC_types]>[EJ/yr] AI_Addition = vector(0 EJ/yr)
VALUE<Vector[EC_types]>[EJ/yr] AI_Decomm = vector(0 EJ/yr)
VALUE<Vector[EC_types]>[EJ/yr] AI_Operation = vector(0 EJ/yr)
VALUE<Vector[Pos]>[EJ^2/yr^2] MSE_Pos = vector(99999 EJ^2/yr^2)
CONDITION Converged (variable exposed) = false
VALUE Solve_Count (variable exposed) = 0
REPEAT
FOR (EC = 1; ~EC <= GetRowCount(~Cap_HC_0); EC = ~EC + 1)
Cap_HC_Mat[*,*] = matrix(~Cap_HC_0, ~Cap_HC_0, ~Cap_HC_0)
Cap_HC_Mat[~EC,1] = max(0 EJ/yr, ~Cap_HC_0[~EC] - ~Band[~EC])
Cap_HC_Mat[~EC,3] = min(Initial_EC_Net_Supply[~EC], ~Cap_HC_0[~EC] + ~Band[~EC])
FOR (Pos = 1; ~Pos <= GetColumnCount(~Cap_HC_Mat); Pos = ~Pos + 1)
```

```
Cap_HC_1[*] = ~Cap_HC_Mat[*, ~Pos]
Output[*] = End_Use_Conversion_Eff_Input[*, Min] * sumc((Initial_EC_Net_Supply - ~Cap_HC_1) *
Init_End_Use_Prop_Norm)
PC[*] = ~Output / Init_End_Use_CF_Target
AI[*] = sumc(~Output * End_Use_Sector.PC_AI_ID) * ((Init_End_Use_Peak_Factor - vector(1)) * vector(1 -
Initial_Demand_Flex) + vector(1))
PC_Addition[*] = sumc((vector(End_use_PC_types, 1) - End_Use_Sector.PC_Decommission_Fraction) *
End_Use_Sector.PC_CapEx_Fraction * ((vector(End_use_PC_types, 1) + Init_EU_PC_Growth_Rate) * ~PC * End_Use_PC_ECC
/ End_Use_Sector.Power_Capacity_Lifetime) * End_Use_Sector.PC_Initial_EC_Split)
PC_Decomm[*] = sumc(End_Use_Sector.PC_Decommission_Fraction * End_Use_Sector.PC_CapEx_Fraction * (~PC /
End_Use_Sector.Power_Capacity_Lifetime) * End_Use_PC_ECC * End_Use_Sector.PC_Initial_EC_Split)
PC_Operation[*] = sumc((vector(End_use_PC_types, 1) - End_Use_Sector.PC_CapEx_Fraction) * (~PC * End_Use_PC_ECC /
End_Use_Sector.Power_Capacity_Lifetime) * End_Use_Sector.PC_Initial_EC_Split)
AI_Addition[*] = sumc((vector(End_use_AI_types, 1) - End_Use_Sector.AI_Decommission_Fraction) *
End_Use_Sector.AI_CapEx_Fraction * ((vector(End_use_AI_types, 1) + Init_EU_AI_Growth_Rate) * ~AI * End_Use_AI_ECC /
End_Use_Sector.Auxiliary_Lifetime) * End_Use_Sector.AI_Initial_EC_Split)
AI_Decomm[*] = sumc(End_Use_Sector.AI_Decommission_Fraction * End_Use_Sector.AI_CapEx_Fraction * (~AI /
End_Use_Sector.Auxiliary_Lifetime) * End_Use_AI_ECC * End_Use_Sector.AI_Initial_EC_Split)
AI_Operation[*] = sumc((vector(End_use_AI_types, 1) - End_Use_Sector.AI_CapEx_Fraction) * (~AI * End_Use_AI_ECC /
End_Use_Sector.Auxiliary_Lifetime) * End_Use_Sector.AI_Initial_EC_Split)
MSE_Pos[~Pos] = meanv((~Cap_HC_1 - (~PC_Addition + ~PC_Decomm + ~PC_Operation + ~AI_Addition + ~AI_Decomm +
~AI_Operation))^2)
END FOR // Pos
Cap_HC_0[~EC] = ~Cap_HC_Mat[~EC, vIndex(~MSE_Pos, minv(~MSE_Pos))]
Band[~EC] = max(~Min_Band, ~Band[~EC] * ~Band_Scaling_Factor)
END FOR // EC
Solve_Count = ~Solve_Count + 1
Converged = meanv(~MSE_Pos) < ~MSE_Threshold
UNTIL (~Converged OR ~Solve_Count = ~Solve_Limit)
Result[*] = ~Cap_HC_0
```

9.4.6 Miscellaneous array label sets

Index	**Normal_dist_inputs**	**Uniform_dist_inputs**	**Range_inputs**	**Trend_points**
1	Mean	Max	Numeral	Initial
2	SD	Min	Error	Final

In addition, two ordinal label sets are used:

- **Plan_horizon** (0 to 20; representing the planning timeframe)
- **Pos** (1 to 3; for search intervals within the **Initial_Cap_HC_Solver** script)

9.4.7 Input parameter correlations

GoldSim offers input stochastic element correlation functionality which can be used to simulate interdependency between input parameters.

9.4.7.1 ES final demand

All entries of the ES final demand multiplier vector (**ES_Final_Demand_Mult**) are correlated to each other using a correlation matrix with a base correlation factor of 0.5 (still significant randomness) as increases in demand for one ES is more likely to occur with increases in other ESs, and vice versa. Sub-groups are assumed to be more highly correlated (correlation factor 0.8) due to sectoral similarity in patterns of consumption:

- Illumination, IPaC, cooling, and low-temp heating (household/commercial)
- Static mechanical and high temp process heat (industrial)
- Regional and IC passenger transportation (movement of people)
- Regional and IC freight transportation (movement of goods)

9.4.7.2 EC split factors for heat and LaG fuels

All LaG fuel EC split factor vectors for PC and AI (**EC_Split_LaG_Factor** for RE primary and NRE primary sectors, **PC_EC_Split_LaG_Factor** and **AI_EC_Split_LaG_Factor** for secondary and end-use sectors) are correlated to a uniformly distributed, unitary, scalar stochastic element (**EC_Split_LaG_Correlator**). Similarly, all heat EC split factor vectors for PC and AI (**EC_Split_Heat_Factor** for RE primary and NRE primary sectors, **PC_EC_Split_Heat_Factor** and **AI_EC_Split_Heat_Factor** for secondary and end-use sectors) are correlated to another uniformly distributed, unitary, scalar stochastic element (**EC_Split_Heat_Correlator**). The correlation factor used for both is 0.8.

The LaG factor represents geographical remoteness and the need for transportation and servicing that will be difficult to electrify, while the heat factor represents the degree of heavy industry required for manufacturing and maintenance. Bias in consumption of ECs for particular PC and AI types within the autocatalytic loop and capital hypercycle (GES metabolism) relative to final consumption is likely to relate to that seen in similar PC and AI types (as defined in sections 9.5.10, 9.5.11, 9.5.12, and 9.5.13). This correlation reflects alignment in the epistemically uncertain degree of structural dependence on particular ECs for upkeep and transformation of the GES over time.

9.4.7.3 EROI and ECC

All vectors for EROI (**Initial_NRE_EROI** and **Initial_RE_EROI**) and ECC (**Secondary_PC_ECC**, **Secondary _AI_ECC**, **End_Use_PC_ECC**, and **End_Use_AI_ECC**), including pre-simulation EROI declines (**NRE_EROI_Drop** and **RE_EROI_Drop**), are correlated to a uniformly distributed, unitary, scalar stochastic element (**EROI_ECC_Correlator**). The correlation factor used is 0.5 (still significant randomness) and is applied with a negative sign for ECC as these values are negatively proportional to EROI as boundary definitions change.

Studies estimating EROI (and by extension, ECC) use pre-analytic boundary definitions that can be more or less comprehensive regarding various production activities and second- or third-order dependencies. The 'true' boundary from a functional perspective extent is epistemically uncertain, but values will tend to rise or fall together when similar boundaries are implicitly assumed. For EROI, this correlation extends to drop (pre-simulation decline) values as both are subject to the same boundary assumption effect.

9.4.7.4 Initial NRE resource

All entries of the initial NRE resource vector (**Initial_NRE_Resource**) are correlated to each other using a correlation matrix with a correlation factor of 0.5 (still significant randomness). Actual resource quantities accessible above terminal EROI (larger than 'reserves', which depend on economic viability) are epistemically uncertain. Optimism or pessimism in resource estimates is likely to affect other estimates similarly when using consistent assumptions and methodologies, although not with a high degree of correlation due to differences in geology, technologies, geopolitical factors, resource distribution, etc.

9.4.7.5 Efficiencies

Subgroups of efficiency estimates are subject to correlation effects due to underlying technological and design similarities. This affects estimates for initial, final, base (observed at the time of technology inception), and PC mean (for EU to ES only) efficiencies. Correlation matrices are used with a base correlation factor of 0, as most pairs of vector entries are not expected to be correlated.

9.4.7.5.1 Secondary conversion

The following technology subgroups are correlated with a 0.5 correlation factor:

- Primary fuels to heat conversion (burners, furnaces, boilers, etc.) – oil, gas, coal, and biomass heat
- Synthetic fuels (Fischer-Tropsch synthesis) – gas to LaG and coal to LaG
- Combined heat and power (CHP) – gas, coal, and biomass
- Heat cycle electricity generation – coal, nuclear, solar thermal, biomass, and geothermal generation

The resulting correlation matrix is applied to the **Init_Sec_Conversion_Eff**, **Final_Sec_Conversion_Eff**, and **Sec_Conversion_Eff_Base** vectors.

9.4.7.5.2 Reticulation systems

The following technology subgroups are correlated with a 0.8 correlation factor due to a high degree of technological similarity:

- Electricity reticulation (electricity transmission and distribution)
- Heat reticulation (steam systems, direct heating, heating elements, etc.)

LaG fuel reticulation correlations are not needed as reticulation is assumed to be perfectly efficient (no uncertainty). Combined heat and power (CHP) using gas, coal and biomass are each correlated to both of the above subgroups with a factor of 0.5. The resulting correlation matrix is applied to the **Init_Sec_Reticulation_Eff**, **Final_Sec_Reticulation_Eff**, and **Sec_Reticulation_Eff_Base** vectors.

9.4.7.5.3 End-use conversion

The following technology subgroups are correlated with a 0.5 correlation factor:

- Electric motors – electric mechanical, electric vehicles, and electric rail (passenger and freight)
- Internal combustion engines – LaG fuel mechanical, all ICEV, all ICE rail, and all shipping

In addition, jet engines (all aviation) are correlated with a 0.8 correlation factor due to a high degree of technological similarity. Heat conversion correlations are not needed as conversion is assumed to be perfectly efficient (no uncertainty; conversion losses modelled at secondary stage). The resulting correlation matrix is applied to the **Init_End_Use_Conversion_Eff**, **Final_End_Use_Conversion_Eff**, and **End_Use_Conversion_Eff_Base** vectors.

9.4.7.5.4 End-use passive systems

The following technology subgroups are correlated with a 0.5 correlation factor due to passive system design similarities (innovations in one can generally be applied to others in the same category):

- Mechanical systems – electric and LaG mechanical
- Light vehicles – ICEV light and electric vehicles
- Heavy vehicles – ICEV heavy (passenger and freight)
- Rail – all rail
- Aircraft – all aviation
- Ships – all shipping

- Low temperature heating – LaG fuels, heat, and electric heating low
- High temperature heating – heat and electric heating high

The resulting correlation matrix is applied to the **Init_End_Use_ES_Eff**, **Final_End_Use_ES_Eff**, **End_Use_ES_Eff_Base**, and **Init_End_Use_ES_Eff_PC_Mean** vectors.

9.5 INPUT PARAMETER CALCULATIONS AND ASSUMPTIONS

9.5.1 Data sources

	Title	**Citation**	**Used for input reference:**
1	*BP Statistical Review of World Energy 2019*	[40]	1.1, 1.3, 1.4, 1.7, 1.8, 1.9, 1.10, 1.12, 2.1, 2.4
2	*EIA - Table 8.1. Average Operating Heat Rate for Selected Energy Sources*	[368]	4.1
3	*IEA Extended World Energy Balances*	[369]	1.1, 1.2, 1.3, 1.4, 1.7, 1.8, 1.9, 1.10, 1.12, 1.11, 2.1, 2.5, 2.6, 3.4, 4.1, 4.2
4	*Fuels - Higher and Lower Calorific Values*	[370]	2.1
5	*EIA International Energy Outlook 2019*	[371]	1.1, 1.2, 1.3, 1.7, 1.8, 1.9, 1.10, 1.11, 1.12, 2.4, 3.1, 4.5
6	*Electricity End Uses, Energy Efficiency, and Distributed Energy Resources baseline*	[372]	1.2, 1.11
7	*Energy Efficiency Analysis: Biomass-to-Wheel Efficiency Related with Biofuels Production, Fuel Distribution, and Powertrain Systems*	[373]	1.1, 4.1
8	*IIASA Global Energy Assessment*	[49]	1.2, 2.1, 2.2, 4.4, 4.5, 4.6
9	*The Shift Project - Historical Energy Production Statistics*	[41]	2.1
10	*World Limits Model (WoLiM) 1.5 Model Documentation*	[344]	2.1, 2.2, 2.4, 7.2, 10.6, 10.13, 10.14
11	*Global energy modelling: a biophysical approach (GEMBA)*	[342]	2.2, 4.3, 6.1, 6.4, 6.6, 7.1
12	*Meta-analysis of non-renewable energy resource estimates*	[150]	2.1
13	*Bioenergy: how much can we expect for 2050?*	[374]	2.2
14	*Bioenergy and climate change mitigation: an assessment*	[375]	2.2
15	*Projection of world fossil fuels by country*	[376]	2.1
16	*When will oil, natural gas, and coal peak?*	[377]	2.1
17	*A global coal production forecast with multi-Hubbert cycle analysis*	[378]	2.1
18	*What is the global potential for renewable energy?*	[34]	2.2
19	*Renewable Energy and Electricity*	[379]	2.4
20	*Refinery Utilization and Capacity*	[380]	3.1
21	*Refinery Economics*	[381]	3.1
22	*Why Capacity and Utilization Are the Keys to Refining Revenue*	[382]	3.1
23	*Economic Feasibility and Investment Decisions of Coal and Biomass to Liquids*	[383]	3.1
24	*Biomass for Electricity Generation*	[384]	3.1
25	*Direct Utilization of Geothermal Energy*	[385]	3.1
26	*Monthly Biodiesel Production Report*	[386]	3.1
27	*Electricity Generation Baseline Report*	[387]	2.4, 3.1
28	*Waste heat recovery technologies and applications*	[388]	3.4, 3.5
29	*GE Global Power Plant Efficiency Analysis*	[389]	4.1

	Title	Citation	Used for input reference:
30	*Estimation of Energy Efficiencies of U.S. Petroleum Refineries*	[390]	4.1
31	*A review on coal-to-liquid fuels and its coal consumption*	[391]	4.1
32	*Concentrated solar power plants: Review and design methodology*	[392]	4.1
33	*Global energy efficiency improvement in the long term: a demand- and supply-side perspective*	[365]	4.1, 4.2, 4.4, 4.5, 4.6
34	*Electric power transmission and distribution losses (% of output)*	[393]	4.2
35	*Opportunities for Energy Efficiency Improvements in the U.S. Electricity Transmission and Distribution System*	[394]	4.2
36	*Energy in world history*	[6]	4.3, 4.7
37	*Historical Timeline: History of Alternative Energy and Fossil Fuels*	[395]	4.3, 4.7
38	*An Interactive Timeline: The History of Power*	[396]	4.3
39	*Short history and present trends of Fischer–Tropsch synthesis*	[397]	4.3
40	*The History of Steel: From Iron Age to Electric Arc Furnaces*	[398]	4.7
41	*Technical limits for energy conversion efficiency*	[218]	4.4
42	*Theoretical efficiency limits for energy conversion devices*	[213]	4.1, 4.4
43	*Reducing Energy Demand: What Are the Practical Limits?*	[212]	1.2, 4.4, 4.6
44	*Energy efficiency in transport*	[399]	4.5
45	*Energy efficiency increased*	[400]	4.5
46	*Transportation Energy Data Book*	[401]	4.5
47	*Transportation Sector – Energy Use Analysis*	[402]	4.5
48	*Energy in nature and society: general energetics of complex systems*	[99]	4.3
49	*Tracking Transport*	[403]	4.5
50	*Transparent Cost Database*	[404]	2.4, 3.1
51	*A Comparative Analysis of Energy Costs of Photovoltaic, Solar Thermal, and Wind Electricity Generation Technologies*	[405]	6.1, 7.1
52	*Dynamic Energy Return on Energy Investment (EROI) and material requirements in scenarios of global transition to renewable energies*	[39]	6.1, 7.1
53	*Order from Chaos: A Preliminary Protocol for Determining the EROI of Fuels*	[170]	3.6
54	*Dynamic EROI Assessment of the IPCC 21st Century Electricity Production Scenario*	[119]	2.4, 3.1, 6.1, 6.4, 7.1, 9.1, 9.2, 9.5, 9.6, 10.1, 10.2, 10.5, 10.6
55	*A Preliminary Investigation of Energy Return on Energy Investment for Global Oil and Gas Production*	[406]	6.4, 6.6
56	*Long-Term Estimates of the Energy-Return-on-Investment (EROI) of Coal, Oil, and Gas Global Productions*	[181]	6.4, 6.6
57	*The implications of the declining energy return on investment of oil production*	[165]	6.4, 6.6
58	*A comprehensive assessment of the energy performance of the full range of electricity generation technologies deployed in the United Kingdom*	[407]	6.1, 7.1
59	*Concentrated Solar Power: Actual Performance and Foreseeable Future in High Penetration Scenarios of Renewable Energies*	[408]	3.1, 7.1
60	*Energy intensities, EROIs (energy returned on invested), and energy payback times of electricity generating power plants*	[409]	6.1, 7.1, 10.13
61	*EROI of different fuels and the implications for society*	[53]	6.1, 6.4, 6.6, 7.1
62	*Can we afford storage? A dynamic net energy analysis of renewable electricity generation supported by energy storage*	[84]	10.13
63	*A Framework for Incorporating EROI into Electrical Storage*	[190]	10.13
64	*The costs and impacts of intermittency – 2016 update*	[85]	10.13
65	*Electricity storage for intermittent renewable sources*	[195]	10.14

	Title	Citation	Used for input reference:
66	*Emission Factors for Greenhouse Gas Inventories*	[410]	2.6
67	*Statistics - Specific Carbon Dioxide Emissions of Various Fuels*	[411]	2.6
68	*Global Emissions*	[123]	2.7
69	*How have global CO2 emissions changed over time?*	[412]	2.7

9.5.2 Preliminary data processing

Three sources contained large data sets that required processing to render data in a form suitable for PRESS. In most cases, this is due to the need for different levels of aggregation and disaggregation corresponding to the PRESS model formulation. The following sections list data processing steps taken prior to utilization of these sources for specific input arrays.

9.5.2.1 BP Statistical Review of World Energy [40]

- Values are converted to common units of EJ (energy) and EJ/yr (power) using the provided conversion table.
- Primary energy quantities are adjusted for nuclear, hydropower, and renewables to reverse the thermal equivalence method used by BP and align with the PRESS model treatment of primary energy sources.
- Biofuels production is removed from oil consumption as it is modelled explicitly in PRESS.
- Where possible, 2013-2018 values are averaged to give indicative values approximately aligned with 2015:
    - o Where only 2017 and 2018 data are available, these are averaged and assumed to provide a suitable indication for ~2015 (insufficient information to do otherwise).
    - o Where only 2018 is available, the values are used as given.

9.5.2.2 IEA Extended World Balances [369]

9.5.2.2.1 Notes

- IEA uses the “primary energy equivalent” convention for electricity and heat produced from non-combustible sources (nuclear, geothermal, solar, hydropower, wind):
    - o “The principle adopted by the IEA is that the primary energy form is *the first energy form downstream in the production process for which multiple energy uses are practical*.”
    - o The production of electricity is considered to be primary for hydropower, wind, tide/wave/ocean, and solar photovoltaic.
    - o Heat is considered primary for direct uses and the by-product of electricity generation for nuclear, geothermal and solar thermal.
    - o For downstream transformations, the IEA adopts the “physical energy content” method.
    - o This aligns with the PRESS model formulation.
- The IEA assumes an average gross calorific value of 38 TJ/million m^3 for natural gas.
- The IEA notes significance variation in data quality by region:

Region	Main source of data	Data quality	Exogenous variables
Africa	FAO database and AfDB	low	population growth rate
Non-OECD Americas	national and OLADE	high	none
Asia	surveys	high to low	population growth rate
Non-OECD Europe and Eurasia	questionnaires and FAO	high to medium	none
Middle East	FAO	medium to low	none

- Primary conversion efficiencies are assumed based on surveyed average values:
  - 10% for geothermal electricity
  - 50% for geothermal heat
  - 33% for solar thermal electricity and nuclear electricity
  - 100% for solar thermal heat
- No final non-energy consumption is reported for biomass (biomass considered by the IEA is the component used for energy purposes only).

9.5.2.2.2 Data processing

- Where data is not available, refinery own use is estimated to be 5% of refinery throughput,
  split between refinery gas and fuel oil.
- Data for latest 5-year period (2013 to 2017) is exported (2018 data not available at time of analysis) and averaged to give indicative values approximately aligned with 2015.
- Electricity output values are converted from GWh to EJ.
- Product categories with (5-year average) values less than 0.1 EJ are disregarded as insignificant:
  - Gas coke
  - Aviation gasoline
  - Gasoline type jet fuel
  - Paraffin waxes
  - Bio jet kerosene
- Primary energy sources are aggregated as follows:

Oil	Coal	Solar	Biomass
• Crude oil • Natural gas liquids • Other hydrocarbons (includes oil shale and oil sands)	• Anthracite • Coking coal • Other bituminous coal • Sub-bituminous coal • Lignite	• Solar photovoltaics • Solar thermal	• Primary solid biofuels • Biogases • Biogasoline • Biodiesels • Other liquid biofuels • Charcoal

- Energy carriers are aggregated as follows:

Liquid and gaseous (LaG) fuels	Heat
• Motor gasoline excl. biofuels • Kerosene type jet fuel excl. biofuels	• Heat (traded)

• Other kerosene • Gas/diesel oil excl. biofuels • Fuel oil • Biogasoline • Biodiesels • Other liquid biofuels	• Heat (final consumption; estimation described below)

- Non-traded heat final consumption is assumed to be represented by the total final consumption (excluding non-energy use) of the following products, with a representative 50% conversion efficiency (aligns with IEA convention but does not match modelled secondary conversion efficiencies in 9.5.6.1 perfectly, however this difference is insignificant for the calculation of normalized end-use input proportion values):
    - Coal (aggregated)
    - Natural gas (aggregated)
    - Petroleum coke
    - Coke oven coke
    - Coke oven gas
    - Blast furnace gas
- Heat output flows are calculated as totals (traded and non-traded) for heat plants (main activity and CHP).
- Waste flows are insignificant (<1% TPES) and do not fit either the definition of NRE as a stock or RE as a flow, so are ignored:
    - Practically, these flows will always be limited to a small fraction of the total and depend on the availability of concentrated combustible or convertible wastes.
    - Insufficient information is available to separate these flows from main primary flows (additional assumptions do not add clarity and provide little functional difference).
- The primary energy equivalent of final non-energy consumption is calculated as the final non-energy consumption plus the sum of transformed (secondary) flows, multiplied by the fraction of non-energy to total final consumption over all derivative products.

9.5.2.3 Dynamic EROI Assessment of the IPCC 21st Century Electricity Production Scenario [119]

- Total lifecycle energy inputs are calculated by summing construction, decommissioning, and operations (after converting to a total per peak capacity). Fuel processing is excluded as this either covers primary activities (nuclear) or represents a loss of fuel (e.g., gas flaring) that should be reflected by the relevant conversion efficiency.
- For RE, EROI values are used and the CapEx fraction, decommissioning fraction, build time, and lifetime are assumed to refer to primary PC.
- For NRE, EROI values are used to calculate corresponding ECC values for secondary PC (see 9.5.9.1).
- For nuclear, the fuel processing cost is assumed to refer to primary activities and is converted to a primary-level EROI value (using thermal equivalent for electricity).
- As stated, gas refers to CCGT and hydro to run-of-river (assumed to be representative of aggregate PC as modelled in PRESS).

- EROI estimates for solar PV span a wide range, but the report assumes a trend towards higher values. A representative value is taken for initial RE EROI.

9.5.3 Initialization

9.5.3.1 Init_Secondary_Prop_Input

<table>
<tr><td>Input reference:</td><td>1.1</td></tr>
<tr><td>Description:</td><td>Matrix of normalized estimates of initial flow of primary energy to secondary PC types and associated maximum fractional error</td></tr>
<tr><td>Sources:</td><td>1, 3, 5, 7</td></tr>
<tr><th colspan="2">General calculations and assumptions</th></tr>
<tr><td colspan="2">• Raw primary inputs to secondary conversion are converted to an input vector normalized by primary input type (values for each primary input type sum to one)
• A standard error of ±0.1 (as a fraction of the normalized estimate; uniform) is assumed for all primary inputs, except biofuels:
o Data is aggregated from many national sources, of varying quality.
o Availability of secondary data sources ensure major errors are minimized.
o Misreporting and unreported energy transactions, and approximations and assumptions used in data collation can create systematic errors, particularly for minor energy sources and biomass.
o Random error means normalization is violated – this is corrected by renormalizing the resulting vector after assigning errors in each model realization (see expression for Initial_Secondary_Output_Rate in section 9.4.4).</td></tr>
<tr><th colspan="2">Source-specific calculations and assumptions</th></tr>
<tr><td>Sources 1 & 5</td><td>2013-2018 average values for electricity generation are converted back to primary equivalents using secondary conversion efficiency values from 9.5.6.1</td></tr>
<tr><td>Source 3</td><td>• Raw values for electricity generation inputs are given by the sums of primary inflows to main and autoproducer electricity plants, by primary fuel type.
• Oil heat is given by the sum of primary oil inflows to main and autoproducer heat plants (likely an underestimate, but value insignificant).
• Gas and coal CHP values are given by the respective sums of primary inflows to main and autoproducer CHP plants.
• Where required, primary heat values are calculated as the difference between TPES for the relevant fuel type, excluding primary equivalent non-energy use, and use categories associated with other energy carriers.
• Refinery input includes quantities for non-energy products – energy-only refinery input is estimated as total refinery input multiplied by the ratio of TPES excluding non-energy to total TPES.
• IEA data reports output energy from biofuel production at the primary level, not calorific value of biomass input, however the PRESS model treats biofuel production as a secondary process so needs total biomass input:
o IEA has a mismatch in semantic definition of biomass primary energy (non-equivalent categories aggregated).
o Assume cellulosic wastes are recovered from biofuel production and used for electricity and heat.
o Source 7 [373] gives biomass to fuel efficiencies around 50% for most biofuel production methods – primary value reported by IEA is divided by 0.5 to give primary biomass input.
o Due to increased uncertainty associated with this adjustment, biofuels have a higher error factor (±0.2).</td></tr>
</table>

9.5.3.2 Init_End_Use_Prop_Input

Input reference:	1.2

<table>
<tr><td>Description:</td><td>Matrix of normalized estimates of initial flow of ECs to end-use PC types and associated maximum fractional error</td></tr>
<tr><td>Sources:</td><td>3, 5, 6, 8, 43</td></tr>
<tr><td colspan="2">General calculations and assumptions</td></tr>
<tr><td colspan="2">

- Refers to EC flows for final consumption (non-energy system) purposes only, as GES requirements are represented explicitly via the autocatalytic loop and capital hypercycle (modelled end-use PC is the component used for final consumption purposes only).
- Raw EC inputs to end-use PC are converted to an input vector normalized by EC type (values for each EC sum to one).
- This vector is populated using proportions of total EC consumption (including GES requirements); therefore, it is assumed that the normalized flow proportions between the GES requirements and final consumption are approximately equivalent.
- For simplicity, electricity production at the final consumption stage using LaG fuels (onsite, typically small-scale) can be subsumed into the LaG fuel mechanical category as it is functionally equivalent and will remain a small proportion of the total.
- Air travel can be split into freight and passenger assuming 10% freight (approximate value based on an informal search) at both the regional and intercontinental levels.
- Likewise, shipping can be split into freight and passenger assuming 50% freight at the regional level (passenger cruises significant at this range) and 95% freight at the intercontinental level (primarily large tankers and cargo ships, very little passenger transportation).
- Error factor of ±0.2 is used for all PC types:
  - This is higher error than for 9.5.3.1, due to paucity, incompleteness, and lower quality of data.
  - In addition, more approximations and assumptions are required to disaggregate available data sources to the required categories.
  - Random error means normalization is violated – this is corrected by renormalizing the resulting vector after assigning errors in each model realization (see expression for **Init_End_Use_Prop_Norm** in section 9.4.4).

</td></tr>
<tr><td colspan="2">Source-specific calculations and assumptions</td></tr>
<tr><td>Source 3</td><td>

- Raw transport EC inputs (aggregated) are given by the relevant inputs to transportation final consumption categories: World aviation bunkers, Domestic aviation, Road, Rail, World marine bunkers, and Domestic navigation:
  - Further disaggregation is needed to define passenger/freight shares.
  - The IEA's international/domestic distinction does not exactly correspond to the modelled regional/IC distinction (a component of international will also be regional), so this could be refined using other data sources.
- The difference between total final LaG fuel consumption, excluding non-energy consumption, and the LaG fuel consumption in the transportation sector is assumed to represent the sum of LaG fuel mechanical plus LaG fuel heating (by definition, due to exhaustive categories):
  - LaG fuel mechanical includes electricity generation from LaG fuel (small generators).
  - This split is approximated as 90% mechanical and 10% heat (mechanical uses deemed order of magnitude more common than heat; high uncertainty).
- Heat fuel heating high and low are estimated by summing calculated heat final consumption by sector and an evaluation of the likely end uses based on the nature of the relevant sector:
  - High heat - Mining and quarrying, Construction, Iron and steel, Chemical and petrochemical, Non-ferrous metals, Non-metallic minerals, Transport equipment, and Machinery
  - Low heat - Food and tobacco, "Paper, pulp and printing", Wood and wood products, Textile and leather, Industry not elsewhere specified, Residential, Commercial and public services, Agriculture/forestry, Fishing, and Final consumption not elsewhere specified
  - This split is approximate at best and therefore, entails high uncertainty.
- For electrified rail, 28% is assumed for passenger services and 72% for freight, as per source 43.

</td></tr>
<tr><td>Source 5</td><td>

Data for transport proportions used in place of that available from source 6 below as it applies to the global level:

- Primary energy supply values for oil, coal and natural gas are converted from quad BTU to EJ.
- ICEV light and ICEV heavy passenger/freight total matches IEA total very closely.

</td></tr>
</table>

	• EIA data indicates more energy usage in rail, for both passenger and freight – likely due to treatment of electricity and thermal equivalent at primary level – insufficient information given to resolve, also indicated ratios are similar, so no changes made. • Totals for passenger aviation and marine transport are very similar between IEA and EIA so no changes are made.

Source 6	Data from figures 1.7, 1.9, & 4.7:
	• For residential and commercial, Other Uses (undefined MELs) and Cooking & Cleaning Appliances are both assumed to be approximately 50% heating and 50% mechanical load (approximate; high uncertainty).
	• Manufacturing electricity end-use, depicted in figure 4.7, is assumed to be typical of industrial electricity use:
	  o Motors, HVAC, and other process are assigned to electric mechanical.
	  o Electro-chemical, and conventional boiler are assigned to electric heating low.
	  o Process cooling and refrigeration is assigned to electric cooling.
	  o Process heating is assigned to electric heating high.
	  o Other is assigned to IPaC.
	• As this data refers to the US, global proportions of electricity consumption within each sector (residential, commercial, industrial) are assumed to be similar (high uncertainty).
	• The sectoral proportions are weighted by total sectoral electricity consumption from source 3 (IEA) to give representative global system electricity proportions.
	• The high heat estimate is particularly uncertain as only one aggregate industrial sector is represented.
	
	Figure 5.7 can be used to establish splits between passenger and freight EC consumption, and also for ICEV light and heavy for ~2015 (read graphically to give approximate proportions):
	• The chart indicates primary energy, so it is necessary to assume similar split for LaG use (transformations/losses for all transport types using the same EC are similar).
	• Passenger rail – 0.2
	• Air (domestic) – 6
	• Shipping (domestic) – 2
	• Freight rail – 1
	• It is necessary to assume that global transport proportions for the categories above are similar to the US (high uncertainty).

Source 8	• Estimated motorized passenger travel shares by mode given in figure 9.7 on page 586 (chapter 9) – world chart. • The indicated data source is the IEA, but this appears to be no longer available directly. • Data pertains to 2005 – assume travel mode shares are similar in 2015 • Values are converted to LaG fuel input proportions by dividing by composite end-use efficiencies (from inputs 4.4 and 4.5) for each PC type. • Results are then scaled to absolute equivalents by multiplying by the sum of equivalent categories from source 5. • Final calculated estimates using source 3 values use the average of the above and alternative estimates. • Insufficient information is available to resolve air travel into regional and IC (unclear whether international is reported).

9.5.3.3 Initial_NRE_Output_Rate

Input reference:	1.3
Description:	Vector of estimates for the initial rates of primary NRE power output, including direct use
Sources:	1, 3, 5
General calculations and assumptions	
For all sources, available data between 2013 and 2018 are averaged to give approximate values aligned with 2015	
Source-specific calculations and assumptions	

Source 1	• Production figures are used for Oil, Natural Gas and Coal. • Consumption figures are used for Nuclear.
Source 5	• Primary energy supply values for oil, coal and natural gas are converted from quad BTU to EJ. • The assumed conversion factor for nuclear is not stated (likely higher factor due to lower primary energy value relative to other sources).

9.5.3.4 Initial_RE_Output_Rate

Input reference:	1.4
Description:	Vector of estimates for the initial rates of primary RE power output
Sources:	1, 3
General calculations and assumptions	
• For all sources, available data between 2013 and 2018 are averaged to give approximate values aligned with 2015. • Biomass output value is adjusted to account for biofuel primary input, as detailed in 9.5.3.1.	
Source-specific calculations and assumptions	
Source 3	IEA reports total biomass output including low temperature heat uses (traditional biomass), unlike other major sources such as EIA and BP.

9.5.3.5 Init_Sec_Peak_Factor_Input

Input reference:	1.5
Description:	Matrix of maximum and minimum estimates for peak factor for each secondary AI type (defined assuming zero demand flexibility)
Sources:	(Own estimate)
General calculations and assumptions	
• Peak factor is a measure of AI utilization and refers to the average ratio of peak flow rate to average throughput, observed at the network scale. • No suitable data available – this information is not widely reported. • High resolution EC production data could be analysed, but this data is regionally specific and unlikely to be representative of global infrastructure utilization. • EC transportation will always be subject to varying demand (temporally heterogeneous flow rates), hence peak factor is > 1. • Electricity AI has a higher peak factor than LaG fuels AI due to presence of strong diurnal and seasonal patterns – assume peak factor between 1.3 and 2 (medium temporal heterogeneity; an informal search revealed values from US, Ireland, South Africa, and Australia to span this range, with some outliers over 2). • Intermittent electricity AI is characterized by a high peak factor due to short charge/discharge and/or peak transmission windows (not directly affected by intermittent RE diversity as infrastructure is typically geographically dispersed and built to serve concentrations of particular RE sources) – assume peak factor between 2 and 5 (high temporal heterogeneity). • Peak factors for LaG fuels AI and heat AI are lower as both are subject to diurnal and seasonal patterns, but have an ability to store energy as fuel and hold local reserves – assume peak factor between 1.1 and 1.3 (low temporal heterogeneity).	

9.5.3.6 Init_End_Use_Peak_Factor_Input

Input reference:	1.6
Description:	Matrix of maximum and minimum estimates for peak factor for each EU AI type (defined assuming zero demand flexibility)
Sources:	(Own estimate)
General calculations and assumptions	
• Peak factor is a measure of AI utilization and refers to the average ratio of peak flow rate to average throughput, observed at the network scale. • No suitable data available – this information is not widely reported. • It is unclear how these values could be calculated directly, as the AI they relate to is not concretely defined (by design) and it is left semantically open due to functional uncertainty.	

• End-use AI can be broadly categorised into medium and high temporal heterogeneity based on an assessment of the nature of demand for corresponding energy services: ○ End-use AI tends to face lower average utilization rates and more prominent usage peaks than secondary infrastructure. ○ AI associated with transportation and logistics is assumed to be subject to medium temporal heterogeneity (between 1.3 and 2) as utilization is typically optimized for operational efficiency to some degree – LaG, roading, rail, rail electrification, aviation, shipping. ○ AI associated primarily with residential and commercial energy services is assumed to be subject to high temporal heterogeneity (range 2 to 4) as optimizing utilization is not a primary operational consideration – electrical, IPaC, EV, heating.

9.5.3.7 *Init_NRE_Growth_Rate*

Input reference:	1.7
Description:	Vector of estimates for the initial annual growth rates of primary NRE PC
Sources:	1, 3, 5
General calculations and assumptions	
Assume growth rate in output or throughput is equivalent to the growth rate in underlying PC (no change to capacity factors)	
Source-specific calculations and assumptions	
Source 1	Annual growth rates between 2013 and 2018 are averaged for all NRE primary sources (production data for oil, natural gas and coal, consumption data for nuclear).
Source 3	Growth rate in production values between 2013 and 2017 are averaged.
Source 5	Annual growth rates between 2013 and 2018 are averaged for all NRE primary sources.

9.5.3.8 *Init_RE_Growth_Rate*

Input reference:	1.8
Description:	Vector of estimates for the initial annual growth rates of primary RE PC
Sources:	1, 3, 5
General calculations and assumptions	
Assume growth rate in output or throughput is equivalent to the growth rate in underlying PC (no change to capacity factors)	
Source-specific calculations and assumptions	
Source 1	Annual growth rates between 2013 and 2018 are averaged for all RE primary sources (electricity generation data for hydropower, generation capacity for solar PV, wind, geothermal).
Source 3	Growth rate in production values are averaged between 2013 and 2017.
Source 5	Annual growth rates between 2013 and 2018 are averaged for installed generating capacity.

9.5.3.9 *Init_Sec_PC_Growth_Rate*

Input reference:	1.9
Description:	Vector of estimates for the initial annual growth rates of secondary PC
Sources:	1, 3, 5
General calculations and assumptions	
Assume growth rate in output or throughput is equivalent to the growth rate in underlying PC (no change to capacity factors)	
Source-specific calculations and assumptions	
Source 1	• Annual growth rates between 2013 and 2018 are averaged. • Electricity generation data used for: ○ Oil generation ○ Gas generation ○ Coal generation ○ Nuclear generation ○ Hydropower ○ Solar PV

	◦ Wind • Production data is used for biofuels. • Assume that secondary PC growth rates equivalent to that indicated at the primary level for: ◦ Geothermal generation ◦ Refining (Oil)
Source 3	• Annual growth rates between 2013 and 2017 are averaged. • For each secondary PC type, the most appropriate categories as reported by the IEA are identified, normally corresponding to the process input flow. • The same flow aggregations are used as elsewhere for IEA data.
Source 5	• Where capacity data is not directly available, assume that secondary PC growth rates are equivalent to that indicated at the primary level where there is a direct correspondence between primary and secondary: ◦ Wind ◦ Solar PV ◦ Refining (Oil) ◦ Geothermal generation (Geothermal) ◦ Hydropower ◦ Other renewable

9.5.3.10 Init_Sec_AI_Growth_Rate

Input reference:	1.10
Description:	Vector of estimates for the initial annual growth rates of secondary AI
Sources:	1, 3, 5
General calculations and assumptions	
• AI growth rates are derived from estimates in 9.5.3.9. • The growth rate for electricity AI assumed to be average of growth rates for gas, coal, nuclear and hydropower generation (dominant forms of electricity generation as of 2015). • The growth rate for intermittent electricity AI assumed to be average of growth rates for solar PV and wind generation (dominant forms of intermittent electricity generation as of 2015). • The growth rate for LaG AI assumed to be same as growth rate for refining (dominant form of LaG fuel production as of 2015). • The growth rate for heat AI assumed to be average of growth rates for gas and coal heat (dominant forms of heat production as of 2015).	

9.5.3.11 Init_EU_PC_Growth_Rate

Input reference:	1.11
Description:	Vector of estimates for the initial annual growth rates of EU PC
Sources:	3, 5, 6
General calculations and assumptions	
Assume growth rate in output or throughput is equivalent to the growth rate in underlying PC (no change to capacity factors)	
Source-specific calculations and assumptions	
Source 3	General end-use categories can be identified from IEA dataset using similar designations as used in 9.5.3.2: • Misc. electrical (indicated by final electricity consumption for residential and commercial sectors; used for lighting, IPaC, electric mechanical, electric cooling, electric heating low/high) • Misc. LaG fuel (indicated by final LaG demand excl. non-energy and transportation consumption; used for LaG mechanical and heating) • ICEVs (indicated by road LaG consumption; used for ICEV light/heavy passenger and heavy freight) • ICE rail (indicated by rail LaG consumption; used for ICE rail passenger/freight) • EVs (indicated by road electricity consumption; used for electric vehicles) • Electric rail (indicated by rail electricity consumption; used for electric rail passenger/freight)

	• Aviation regional (indicated by domestic aviation LaG consumption; used for aviation regional passenger/freight) • Shipping regional (indicated by domestic navigation LaG consumption; used for shipping regional passenger/freight) • Aviation IC (indicated by world aviation bunkers; used for aviation IC passenger/freight) • Shipping IC (indicated by world marine bunkers; used for shipping IC passenger/freight) • Heat low (indicated by coal and natural gas low heat industrial grouping (described in 9.5.3.2); used for heat fuel heating low) • Heat high (indicated by coal and natural gas high heat industrial grouping (described in 9.5.3.2); used for heat fuel heating high)

Source 6	• Transport end-use PC growth rates are calculated from direct ES provision where available and fuel consumption otherwise:
	    ○ Total seat miles used for aviation passenger, not revenue seat miles
	    ○ Light-duty vehicles used for ICEV light
	    ○ Buses used for ICEV passenger heavy
	    ○ Passenger rail used for ICE rail passenger and electric rail passenger
	    ○ Heavy-duty trucks used for ICEV heavy freight
	    ○ Freight rail used for ICE rail freight and electric rail freight
	    ○ Marine vessels used for shipping freight regional and IC
	• An estimate for combined low temperature heat is given by coal and natural gas consumption in the residential and commercial sectors.
	• An estimate for combined high temperature process heat is given by coal and natural gas consumption in the industrial sector.

9.5.3.12 Init_EU_AI_Growth_Rate

Input reference:	1.12
Description:	Vector of estimates for the initial annual growth rates of EU AI
Sources:	1, 3, 5
General calculations and assumptions	
• AI growth rates are derived from estimates in 9.5.3.11. • The growth rates for electrical AI and IPaC AI are assumed to be same as growth rate for general electrical end uses (uniform growth rate). • The growth rate for LaG AI is assumed to be average of growth rates for ICEV light & heavy freight, aviation, and shipping (dominant forms of LaG fuel usage as of 2015). • The growth rate for roading AI is assumed to be average of growth rates for ICEV light & heavy (dominant forms of road usage as of 2015). • The growth rate for EV AI is assumed to be same as growth rate for EV PC. • The growth rate for rail AI is assumed to be average of growth rates for all rail types. • The growth rate for rail electrification AI is assumed to be average of growth rates for electric rail. • The growth rate for aviation AI is assumed to be average of growth rates for all aviation. • The growth rate for shipping AI is assumed to be average of growth rates for all shipping. • The growth rate for heating AI is assumed to be average of growth rates for heat fuel heating high and low.	

9.5.4 Primary resource

9.5.4.1 Initial_NRE_Resource_Input

Input reference:	2.1
Description:	Matrix of mean and standard deviation estimates for initial remaining non-renewable energy stocks by type, in terms of remaining URR (above terminal EROI)
Sources:	1, 3, 4, 8, 9, 10, 12, 15, 16, 17
General calculations and assumptions	
NRE resource estimates are assumed to be log-normally distributed: • Estimates vary by orders of magnitude.	

• Medians are less than means (distributions skew to the low side). • Distributions have high kurtosis (long tail on the high side). • Distributions have zero probability density bordering 0 EJ.	
Source-specific calculations and assumptions	
Source 1	For coal proved reserves, values are converted to EJ using calorific values from source 4, assuming 30.5 MJ/kg for anthracite and bituminous (weighted towards bituminous as it is more common) and 22 MJ/kg for sub-bituminous and lignite (weighted towards sub-bituminous as it is more common).
Source 8	• Values from table 7.1, conventional are added to unconventional where appropriate. • Reserve values are used over resource values as resource estimates are highly uncertain and speculative, also significant proportions will be unattainable due to negative net energy. • High estimate for unconventional are gas not used as this is highly speculative and is an outlier relative to other estimates – includes significant contribution from gas hydrates (unproven and non-commercial). • The unconventional uranium estimate is not used as it is not counted as reserves – highly speculative and production to date is insignificant.
Source 9	• Cumulative extraction is calculated by summing all values (in EJ) back to the beginning of the dataset (1900) for each resource. These values are used to calculate RURR as of 2015 from URR values from other sources. • This may underestimate coal extraction to date somewhat, as production in the 19th century was significant, so a linear production trend is assumed for global coal production between 1800 and 1900 (calculated cumulative production 1900-2014 + 50 × 1900 production).

Source 10	• NRE URR values as reported in table 2 are converted to 2015 RURR by subtracting 2014 cumulative extraction values from source 9:
	  o Including low, medium, and high cases where given.
	  o Conventional and unconventional are added where appropriate.
	• Values from sources 15 and 16 are ignored as these are surveyed separately.

Source 12	• As the distributions of estimates contain erroneously high and outdated estimates (particularly for coal, nuclear and oil) percentile outputs are chosen to construct low, medium and high cases uninfluenced by the high tail-end of the distributions.
	• Due to high spread exhibited and given that the listed distributions for each resource were not designed with physical modelling in mind, the given distribution parameters are not used:
	  o The normal distributions have significant probability density bordering URR = 0 EJ, which is physically implausible.
	  o The alternative distributions (GEV, log-logistic, Frechet, Cauchy, and fatigue life) tend to exhibit excessively long tails to the high end to represent erroneously high and outdated estimates.
	  o For conventional gas, where higher estimates are more recent, the distribution is more symmetrical than for other NRE so using the 75th percentile is appropriate.
	  o For conventional oil, there were early erroneously low estimates for URR prior to 1960 – to correct for this, the median, 75th and 90th percentiles are used for the low, medium and high cases, respectively (still avoids tail region containing outdated overestimates).
	• The low case is constructed from the 25th percentile for each resource (table 2; median for conventional oil). The low case for nuclear fuel is ignored, as the 25th percentile value only just exceeds cumulative extraction to date, which is physically implausible.
	• The medium case is constructed from the median for each resource (table 2; 75th percentile for conventional oil) plus the low estimate for total unconventional gas (Laherrere).
	• The low and medium cases include the low estimate for total unconventional gas (Laherrere) and the low estimate for unconventional oil (1000 EJ tar sands plus 1000 EJ shale oil – approximate GEV distribution PDF maxima, read from figures A6 and A8).
	• The high case is constructed from the 75th percentile for each resource (table 2; 90th percentile for conventional oil), adding the high estimate for total unconventional gas (Edmonds and Reilly for coal seam plus Bentley for tight gas) and the high estimate for unconventional oil (2100 EJ

	tar sands and 4500 EJ shale oil – approximate normal distribution PDF maxima, read from figures A5 and A7).
Source 15	• URR values are taken from table 1 (low, BG, and high). • High values for gas and oil are ignored as these contain large contributions from hydrates and kerogen respectively (unproven and non-commercial; the authors note these values should be used with caution).
Source 16	U_{tot} (URR) values from tables 1, 2 & 3 are converted to EJ using standard conversion factors (listed in the 'Conversion factors' sheet).

9.5.4.2 RE_Potential_Input

Input reference:	2.2
Description:	Matrix of mean and standard deviation estimates for initial remaining sustainably exploitable renewable energy flows by type (above terminal EROI)
Sources:	8, 10, 11, 13, 14, 18
General calculations and assumptions	

• Technical potential estimates exceeding 500 EJ are ignored as these generally pay little attention to various pertinent constraints which reduce net energy to non-viable levels (see source 18 [34]):
  o They also entail an unacceptable level of ambiguity and uncertainty given that they exceed current TPES.
  o Where distinctions are made between technical potential and 'realizable' or 'economic' potential (typically much lower) the latter are used as the modelled potential is that which is assumed to exceed the terminal EROI value.
• High estimates are ignored where unrealistic assumptions are apparent (not taking into account supporting infrastructures, transmission requirements, spacing and servicing issues, etc. – as noted by source 10 [344]).
• The distributions are truncated on the low side by initial RE output rates (this assumes present day RE output rates are sustainable and provide demonstrated minima to distributions of potential resource).	

Source-specific calculations and assumptions	
Source 8	• Technical potential estimates are taken from table 7.2. • Only biomass and hydropower estimates are used as others appear to be largely speculative and use unrealistic assumptions.

Source 10	• Biomass total potential is taken from table 3 (NPP harvestable corresponds to biomass total primary flow).
	• Solar thermal is given in table 4 (0.7 TW_{th}).
	• Geothermal (electricity plus heat) primary potential is given on page 36 (0.6 TW_{th}).
	• TWe values from table 5 are converted to EJ/yr:
	  o The wind estimate includes onshore and offshore.
	  o The sum of biomass, waste & MSW and oceanic, as reported in table 5, is used for Other RE.

Source 11	Percentile outputs are chosen to construct low, medium and high cases, similarly to source 12 for 9.5.4.1:
	• The low case for each resource uses the 25^{th} percentile, the medium case uses the median, and the high case uses the 75^{th} percentile:
	  o For solar (PV and thermal), the 10^{th} and 25^{th} (and median for solar thermal) are used due to the very high estimate range stemming from unrealistic assumptions.
	  o Median values are still very high, to the point of being effectively unlimited relative to today's TPES (1330 EJ/yr for PV and 186 EJ/yr for thermal), which introduces heavy kurtosis to the relevant distributions.
	• The 75^{th} percentile for geothermal is not used, as all estimates exceeding 1000 EJ/yr assume the availability of 'hot-dry rock' technology which is still in early development and unproven on a large scale.
	• The sum of tidal and wave is used for Other RE:
	  o OTEC is ignored as it remains speculative.
	  o Wave is used in place of 'all ocean' as the latter includes deployment of speculative technologies at scale.

Source 18	• For Hafele (1981), 'realizable' potential values are used. • For Lightfoot/Green (2002), the maxima and minima are taken as discrete estimates. • For Klimenko et al. (2009), 'economic' potential values are used. • Geothermal electricity values are divided by 0.1 to represent primary heat equivalent (IEA standard conversion factor for geothermal generation), which is then added to the geothermal heat value.

9.5.4.3 NRE_CF_Max

Input reference:	2.3
Description:	Vector of estimates for the maximum capacity factors of primary NRE PC
Sources:	(own estimate)
General calculations and assumptions	
• No data available for NRE capacity utilization at the global level, however, this tends to be high as strong economic incentives exist to avoid excess capacity. • Oil and gas wells are typically kept at high levels of utilization after commissioning, with only infrequent shut ins for maintenance, well testing, and operational reasons – an approximate capacity factor of 95% is assumed. • Coal and nuclear fuel production both depend on expansive mining operations which can be closed for various reasons including maintenance, weather, labour, and economic issues – a lower figure for capacity factor of 85% is assumed.	

9.5.4.4 Initial_RE_CF_Max

Input reference:	2.4
Description:	Vector of estimates for the initial maximum capacity factors of primary RE PC
Sources:	1, 5, 10, 19, 27, 50, 54
General calculations and assumptions	
• Assume present day capacity factors are indicative of practical maxima. Currently intermittent generation penetration is low, so minimal curtailment is occurring. • Where electricity generation is considered secondary, the capacity factor is assumed to be the same as the primary level (conversion equipment is typically sized the same or slightly higher power capacity than primary supply). • Assume biomass capacity factor is 75%. Use of available productive capacity will tend to be maximized, but as an agricultural system, losses, crop failures and climatic variations will limit this to a lower practical maximum.	
Source-specific calculations and assumptions	
Source 1	Solar PV and wind generation output values are averaged over the 2013-2018 period and divided by installed capacity over the same period to give capacity factors.

Source 5	• Primary energy supply values for oil, coal and natural gas are converted from quad BTU to EJ.
	• For sources where electricity generation is considered primary, generation output values are averaged over the 2013-2018 period and divided by installed capacity over the same period to give capacity factors:
	    o Average must be used as capacity factor is largely determined by resource availability.
	    o Generation output in terms of billion kWh is converted to GW to align with installed capacity.
	• Reported capacity values from EIA are not applicable as they are seasonally adjusted, which does not align with PRESS model formulation.

Source 10	• Values are taken from table 5. • The midpoint of 0.6 is used for hydro. • 0.22 is chosen for wind (weighted towards onshore, as this is more common).
Source 19	• This source does not report seasonally or intermittency adjusted values – appropriate for PRESS model formulation. • Projected or expected figures are ignored, as are those for specific installations. • Where a range is given, the mid-point is used.
Source 50	• Averages are calculated over each broad category corresponding to RE PC types. • Ocean energy assumed to represent RE Other.

9.5.4.5 *Initial_Direct_NRE_Use*

Input reference:	2.5
Description:	Vector of estimates for the direct (non-energy) consumption flows of NRE
Sources:	3
General calculations and assumptions	
Non-energy flows are used, as calculated in source 3 data processing described in section 9.5.2.2.	

9.5.4.6 *GHG_Intensity*

Input reference:	2.6
Description:	Vector of estimates for the emissions intensity of primary NRE production (in terms of $GtCO_2e$ per EJ)
Sources:	66, 67
Source-specific calculations and assumptions	
Source 67	• The sub-bituminous coal value is used for Coal (common coal types are in the middle of the GHG intensity range). • The value is converted to $GtCO_2e/EJ$.
Source 68	• The hard coal value is used for Coal (conservative, as GHG intensity is lower than for soft or brown coals) • The value is converted to $GtCO_2e/EJ$.

9.5.4.7 *Non_ES_Emissions*

Input reference:	2.7
Description:	Vector of estimates for the rate of non-energy emissions (exogenous to the GES, but contributes to cumulative emissions)
Sources:	68, 69
General calculations and assumptions	
Non-energy emissions are assumed remain constant over time: • This effectively assumes any increases in agriculture, forestry, and other land use activities, which are likely due to a growing global population, are balanced by reductions in emissions intensity in the relevant sectors (optimistic). • Modelling of uncertainty in non-energy emissions is beyond scope.	
Source-specific calculations and assumptions	
Source 69	The sum of non-energy sectors for 2013 is used (26%, not including bunker fuels).
Source 70	The global total for 2015 is used.

9.5.5 Flow routing

9.5.5.1 *Initial_Secondary_CF_Max*

Input reference:	3.1
Description:	Vector of estimates for the initial maximum capacity factors of secondary PC (lower than technical maxima for peaking generators)
Sources:	5, 20, 21, 22, 23, 24, 25, 26, 27, 50, 54, 59
General calculations and assumptions	

• Where electricity generation is considered primary, the same capacity factor as at the secondary level is assumed (conversion equipment typically sized the same or slightly higher power capacity than primary supply).
• Oil heating is typically used residentially on a seasonal basis and operates below maximum power output most of the time – assume capacity factor of 0.2 (40% of year, 50% average loading).
• As no readily available data exists for Gas-to-Liquids utilization rates, its capacity factor is assumed to be the same as refining (similar large-scale industrial petrochemical processing, with strong incentives to maximize utilization).
• Gas, coal, and biomass heating are used for both industrial and residential/commercial uses:
  o Industrial uses of gas (high utilization rate) are larger than residential (low utilization rate) and much larger than commercial.
  o Coal use is dominated by heavy industry.	

- Biomass availability is more variable and includes significant component of traditional usage (typically for cooking in temperate developing countries), implying much lower utilization of PC on average.
  - A capacity factor of 0.7 is assumed for gas heating, 0.2 for biomass, and 0.8 for coal heating.
  - These values are uncertain, but not particularly important given the low capital requirements for heat PC at the secondary level.
- Coal, gas, and biomass CHP serve both industrial and residential purposes (often district heating):
  - Heating needs are seasonal, but CHP output will often be sized to provide for base needs, not peak.
  - Gas CHP unit require less maintenance downtime; coal and biomass require more due to the use of solid fuels.
  - Coal CHP is more common for industrial purposes.
  - Biomass availability is variable.
  - Capacity factors of 0.8 for gas, 0.7 for coal, and 0.6 for biomass are assumed.

Source-specific calculations and assumptions	

Source 5	• Primary energy supply values for oil, coal and natural gas are converted from quad BTU to EJ.
	• For sources where electricity generation is considered secondary, annual generation output values are divided by installed capacity over the 2013-2018 period and the resulting maxima are taken to give capacity factors.
	  o Maxima are used as these represent the highest practical level of utilization (not determined by resource availability).
	  o Generation output in terms of billion kWh is converted to GW to align with installed capacity.
	• These figures are 'real world' capacity factor maxima, not technical maxima – must take account of typical grid balancing conditions and operational constraints.
	• Reported capacity values from EIA are not applicable as they are seasonally adjusted, which does not align with PRESS model formulation.

Source 20	• The maximum of 'operable utilization rate' for the period of 2013-2018 is used for refining. • Global refining utilization is assumed to be similar to the US.
Source 23	Reported 'operating capacity' is used.
Source 24	Biomass conversion capacity factors are calculated from values given in tables 9 and 10 – dedicated biomass corresponds to biomass generation and industrial cogeneration to biomass CHP.
Source 25	The global geothermal capacity factor from table 1 is used.
Source 26	• The maximum of the annual averages of output divided by capacity is calculated and used for biofuel production capacity factor. Only 8 months are available for 2019 – annual capacity is adjusted pro rata. • This report details biodiesel in the US only – global biofuel production is assumed to have similar capacity factor.

Source 27	• For coal generation, the maxima from figure 5-2 is used, given that recent market conditions have suppressed coal generation utilization rates and it is unclear such market conditions will continue indefinitely.
	• As noted on page 89, open-cycle and closed-cycle gas-fired generators have different capacity factors – the latter tend to act as baseload supply and the former as peaking plant:
	  o Baseload generation is in some cases becoming uneconomic due to the rising penetration of intermittent generation (even at still low levels) and greater peaking requirements. As such, the estimate should be weighted towards the lower open-cycle figure.
	  o Figure 6-3 shows a maximum for open-cycle gas generation of approximately 15% since 2011.
	  o A base capacity factor maximum of 25% is assumed for gas generation as a whole.
	  o This represents a balance between the average of the open-cycle and closed-cycle values (in order to establish initial PC quantity more accurately) and the maximum open-cycle value representing the longer-term realistic maximum capacity factor (not including the explicitly modelled change in gas generation capacity factor due to intermittent penetration, which potentially has a dominant effect).

	• For biomass generation, a maximum value of 70% is chosen – assumes LFG/MSW dominates other biomass generation. • Solar is ignored as only utility scale installation is discussed here, which has higher capacity values, but global solar is dominated by small-scale. • For oil generation, the maximum value for steam turbines (15%) is chosen as they are common and assumed to be representative (optimistic).
Source 50	• Averages are calculated from the available data for each broad category corresponding to modelled RE PC types. • Estimates are assumed to reflect approximate proportions of the various sub-categories presented here.
Source 59	Assume representative value for solar CSP of 0.25 (based on range given in table 2).

9.5.5.2 Init_End_Use_CF_Target_Input

Input reference:	3.2
Description:	Matrix of maximum and minimum estimates for the initial target capacity factors of EU PC (level above which replacement investment is initiated)
Sources:	(Own estimate)

General calculations and assumptions

- Initial capacity factors are assumed based on assessment of the nature of each end-use PC type and its typically patterns of use.
- Light vehicles:
  - Using an informal search for average household vehicle utilization (kilometres per year), and assuming full utilization is roughly equivalent to continuous 150 km/hr, initial capacity factor for ICEV light is approximately 1% (high uncertainty).
  - Alternatively, Smil notes that average light vehicle fuel consumption is 50 GJ/yr:
    - This corresponds to around 15 GJ/yr output power (30% conversion efficiency).
    - The average light vehicle has a power rating of approximately 100 kW (3200 GJ per year).
    - This implies a CF value of 0.005, or 0.5%.
  - Assume similar average patterns of use between vehicle types in this category: 2-wheelers, 3-wheelers, light duty vehicles, etc.
- End-use PC types associated primarily with household use (ICEV light, EVs, low temperature heating) have the lowest utilization, followed by commercial (freight, lighting, cooling), and industrial (mechanical, high temperature process heat).
- Vehicles typically have low capacity factors as they are normally used intermittently and, when used, are operated near their maximum power output levels for short periods only:
  - For freight transportation, significant downtime is required for loading, unloading, fuelling, and coordination of freight volumes with available capacity and routes.
  - Household vehicles operate only sporadically, as required by owners (parked for much of the time).
  - Rated vehicle power output is for maximum acceleration requirements, not cruising.
  - Aviation, rail, heavy freight, and shipping are typically operated at higher capacity factors as they represent large amounts of capital and are typically operated by commercial enterprises seeking to maximize utilization.
  - Intercontinental transportation capacity factors are higher than regional as trips are longer and, as such, loading, unloading, and fuelling are less frequent.
- Much of low temperature heating and cooling demand is seasonal (aside from cooking and general appliance usage) – this means capacity is not used for the much of the year. Low temperature heating and cooling PC is typically operated at maximum rated output for only short periods.
- Lighting and IPaC have higher capacity factors as they are used on a semi-consistent basis and power output is approximately constant.

9.5.5.3 EU_CF_Target_Final_Max_Factor

Input reference:	3.3
Description:	Vector of estimates for the maximum fractional increase in target capacity factors of EU PC (value at sim. base period relative to initial)

Sources:	(Own estimate)

General calculations and assumptions

- Maximum possible fractional increases from the initial capacity factor target are assumed based on the nature of each end-use PC type and its potential for further optimization and shared usage. Increases in the capacity factor target would stem largely from greater time utilization of existing end-use PC, not operating at higher levels relative to nameplate power rating (which sets a practical upper limit for final capacity factor target <<1, with the exception of IPaC PC which typically operates near its rated power).
- PC types are grouped into four tiers representing remaining potential for increased utilization:
    - Very low (assume up to 20% increase):
        - High temperature process heat (heat fuels and electric)
        - These represent intensive industrial applications that are already highly optimized in terms of utilization.
    - Low (assume up to 50% increase):
        - Lighting, IPaC, mechanical (LaG and electric), shipping, aviation, heavy freight, and freight rail
        - These are already largely optimised in terms of utilization, but further improvements are possible through shared utilization and more advanced logistics optimization.
    - Medium (assume up to 100% increase):
        - ICEV heavy, passenger rail (LaG and electric), cooling, and low temperature heating
        - Significant capacity factor increases possible through shared utilization of heating and cooling, and efficiencies of scale in mass transit.
    - High (assume up to 300% increase):
        - ICEV light
        - Light private vehicles could be subject to strong increases in capacity factor as Transport as a Service (TaaS) models become more common and private ownership of vehicles ceases to be the dominant mode of private mobility.

9.5.5.4 Secondary_Output_ID

Input reference:	3.4
Description:	Matrix of EC output identity by secondary PC type (split across electricity and heat for CHP)
Sources:	3

General calculations and assumptions

This input matrix consists of identities only, except for the energy carrier output split (heat and electricity) for the three CHP types (gas, coal, and biomass).

Source-specific calculations and assumptions

Source 3	• Main activity and autoproducer CHP outputs of heat and electricity are summed for coal and natural gas CHP. • Main activity only is used for biomass as autoproducer CHP does not report any heat output. • Fractions (summing to one) are calculated for each. • This assumes the split between main activity and autoproducer CHP remains roughly constant over time (almost equal for coal). • Also assumes this split is relatively inflexible and cannot be easily modified.

9.5.5.5 End_Use_Input_ID

Input reference:	3.5
Description:	Matrix of EC input identity by EU PC type (includes cogeneration and heat recovery for high temp. process heat)
Sources:	28

General calculations and assumptions

- This input matrix consists of identities only, except for cogeneration and waste heat recovery factors.
- Source 28 reviews various waste heat recovery technologies, for both electricity production and heat recovery – most can recover <10% of input energy. There are operational limitations to heat recovery, which “largely depends on key factors such as the quality, quantity and the nature of heat source in terms of suitability and effectiveness.”

• Heat recovery via heat exchangers is more common than cogeneration (high temperature waste heat required for cogeneration as the process is limited by Carnot efficiency). • In many cases, operational, design, or economic factors will limit cogeneration and waste heat recovery. • Therefore, assume 2% of aggregate input energy to high temperature processes is recovered as electricity, and 5% as low temperature heat. • It is assumed these factors are static and unresponsive to technological improvements.

9.5.5.6 EC_Thermal_Equivalence

Input reference:	3.6
Description:	Vector of thermal equivalence factors by EC type (electricity has greater thermal equivalent energy value than heat and LaG fuels)
Sources:	53
Source-specific calculations and assumptions	
Source 53	At a minimum, electricity inputs and outputs must be converted to primary energy equivalent (using 2.6 as the conversion factor).

9.5.5.7 NRE_Secondary_Input_ID

Input reference:	3.7
Description:	Matrix of NRE input identities by secondary PC type
Sources:	
General calculations and assumptions	
Values are equal to one where a given secondary PC type utilizes a primary energy type and zero otherwise.	

9.5.5.8 RE_Secondary_Input_ID

Input reference:	3.8
Description:	Matrix of RE input identities by secondary PC type
Sources:	
General calculations and assumptions	
Values are equal to one where a given secondary PC type utilizes a primary energy type and zero otherwise.	

9.5.5.9 End_Use_Output_ID

Input reference:	3.9
Description:	Matrix of energy service output identities by EU PC type
Sources:	
General calculations and assumptions	
Values are equal to one where a given end-use PC type provides an ES type and zero otherwise.	

9.5.6 PC efficiencies

9.5.6.1 Sec_Conversion_Eff_Input

Input reference:	4.1
Description:	Matrix of ranges for secondary conversion efficiency (min. corresponds to the initial PC mean value and max. corresponds to the maximum theoretical value; a value of 1 indicates that no secondary conversion occurs)
Sources:	2, 3, 7, 29, 30, 31, 32, 33, 42
General calculations and assumptions	
Values for biomass heat are optimistic given the predominance of traditional uses of biomass for cooking which are highly inefficient: • Corrections to account for this are infeasible due to lack of data and may introduce unacceptable ambiguities. • These uses do not rely on significant PC investment and global data on fuel collection is incomplete, so may lie at least partially outside the GES as modelled.	

Maxima: There is limited room for growth in secondary conversion efficiency (diminishing returns on investment, most technologies are mature, and many are limited by low Carnot efficiency). Where required (used alongside available estimates), the assumed approximate magnitude for increases is based on comparison to available values and an assessment of technological maturity and potential. Estimates are calculated based on percentage increases from initial values: • No increase (where secondary conversion does not occur; value static at 1) • Low increase (5%) – refining (cannot exceed 1) • Medium increase (15%) – heat (oil, gas, coal, biomass, and geothermal) • High increase (25%) – CHP (gas, coal, and biomass), coal to LaG, gas to LaG, solar thermal generation, biomass generation, biofuels, and geothermal heat (all are immature or currently minor sources and significant further improvements can be expected)	
Source-specific calculations and assumptions	
Source 2	**Minima:** • Values are converted to percentage by dividing BTUs per kWh by heat rates. • 2013-2018 averages (~2015) are calculated for oil, gas, nuclear, and coal generation.
Source 3	**Minima:** 2013-2018 average (~2015) sum output is divided by sum input to estimate conversion efficiency by fuel type for the following categories: • Generation – electricity plants (main activity and autoproducer) • Heat – heat plants (main activity and autoproducer) • Refining – oil refineries (including feedstocks) • CHP – heat plus electricity output from main activity and autoproducer CHP plants
Source 7	**Minima:** • For biofuels production, a representative biomass-to-fuel efficiency value of 45% is taken from the technology-specific ranges given in figure 4 (assumes the contribution of ester diesel is minimal). • For biomass generation, current biomass-to-fuel efficiency of 32% is used (discussed in the results section). **Maxima:** • For biofuels production, a representative maximum potential biomass-to-fuel efficiency value of 60% is taken from the technology-specific ranges given in figure 4 (assumes minor technological progress beyond that stated). • For biomass generation, potential biomass-to-fuel efficiency of 43% is used (as discussed in the results section).
Source 31	**Minima:** A representative figure from the range given of 65% is assumed (this assumes more DCL than ICL).
Source 32	**Minima:** An approximate value for ~2015 for solar CSP efficiency is taken from table 8 (17%).
Source 33	**Maxima:** • Stated assumed technical potential efficiency values in transformation sector section are used. • As noted, authors assume single digit efficiency improvements in transformation sector for technologies beyond those directly considered.
Source 42	**Minima:** • Values are taken from table 1. • Value for renewables is ignored as it appears ambiguous and insufficient information is given.

9.5.6.2 Sec_Reticulation_Eff_Input

Input reference:	4.2
Description:	Matrix of ranges for secondary reticulation efficiency (min. corresponds to the initial PC mean value and max. corresponds to the maximum theoretical value; a value of 1 indicates that no reticulation losses occur)
Sources:	3, 34, 35

General calculations and assumptions

Assume reticulation efficiency for LaG fuels is 1 (lossless). There would in fact be small losses due to spill and fuel requirements of transportation, but due to lack of data and for simplicity these are assumed to be zero.
 	
Minima:
Assume all reticulation efficiencies by EC type are identical, except:
• Reticulation efficiencies for geographically dispersed RE generation (solar PV, solar thermal, wind, hydropower, and other RE) are assumed to be is less than the average base value (95%) due to higher transmission requirements (a larger proportion will not be collocated with population centres).
• CHP efficiencies are assumed to be averages of electricity and heat reticulation efficiencies weighted by CHP split factors from 9.5.5.4.
 	
Maxima:
• Electricity:
  o Best practice values for electricity transmission and distribution losses are not suitable due to geographic/climate differences.
  o Source 33 notes the potential for 6% improvement in distribution efficiency.
  o Source 35 details several options for reducing losses in transmission (table 1) and distribution (table 2) in the US power system:
    ▪ Most involve economic or operational trade-offs so cannot be exploited to their full technical potential.
    ▪ A plausible representative maximum reduction in aggregate losses of 50% is assumed, through a portfolio of technological options.
    ▪ 50% reduction in losses corresponds to approximately 8% increase in assumed base reticulation (transmission and distribution) efficiency.
    ▪ This value refers to low intermittent penetration (the effect of AI built for intermittency mitigation, dynamically reducing reticulation efficiency for intermittent generation, is explicitly modelled).
• No improvement occurs for LaG fuels, as reticulation efficiency is assumed to be lossless.
• Maximum potential reticulation efficiency for heat is assumed to be 15% (final reticulation efficiency of 95%). Further improvements are unlikely due to diminishing returns and unavoidable losses.
• For CHP, the electricity and heat fractional improvements are weighted by CHP split factors from 9.5.5.4 to give applicable maximum final reticulation efficiencies.

Source-specific calculations and assumptions	
Source 3	• Calculated 2013-2017 averages are used (~2015). • For both electricity and LaG fuels, final consumption is divided by total output from transformation processes to give reticulation efficiency. 17% losses for global electricity likely includes significant electricity theft as technical losses do not typically exceed 13%. • For heat, only the traded quantity can be analysed – traded heat final consumption is divided by total heat plant output. Traded heat reticulation efficiency is assumed to be typical of all heat reticulation.
Source 34	The 2014 value is used.
Source 35	Approximate value for ~2015 of 8% is taken from figure 1.

9.5.6.3 Sec_Incept_Year

Input reference:	4.3
Description:	Vector of approximate incept years by secondary PC (year functional category became widely available)
Sources:	11, 36, 37, 38, 39, 48
General calculations and assumptions	
• Assume oil-fired generation was available approximately 10 years after the first coal-fired power plants (oil-fired generation was briefly competitive at this time).	

• Assume solar thermal heat dates to the first commercial solar thermal water heaters, available just before 1900. This is earlier than advanced thermosiphon systems and concentrated solar power, but much later than many preindustrial passive solar food processing and building techniques.	
Source-specific calculations and assumptions	
Source 11	Incept years before calibration (table 7-1) are used for each relevant PC type. Where multiple options exist, they are assumed to be for heat (typically this is the earliest use for each fuel): • OTEC is ignored (speculative and unproven). • Values for gas heat and solar PV are ignored (questionable; estimates derived from source 36 are more reliable).
Source 36	Approximate (decadal) incept years are taken from the text. Where multiple options exist, dates corresponding to technological innovations marking the beginning of current types of PC are used (i.e. obsolete precursors not functionally interchangeable with current technologies are ignored): • Oil – first commercial wells and early refining of finished products • Gas – first gas networks and early gas turbines (heat slightly earlier than turbines) • Coal – first coal electricity generating plants • Nuclear – first commercial reactors • Solar PV – first uses of monocrystalline panels • Wind – first commercial wind turbines for rural electricity generation
Source 37	First instances of each type of PC are located on the timeline and the approximate (decadal) incept years are taken: • Oil – first commercial oil well drilled in Pennsylvania • Biofuels – first diesel engines to run on vegetable oil, ethanol as a fuel already well established • Solar PV – first silicon solar cell developed at Bell Laboratories • Nuclear – first nuclear power reactor to generate electricity built in Idaho • Geothermal – first commercial scale geothermal electric plants built in California • Solar thermal generation – first large scale solar-thermal power plant begins operation in California
Source 38	First instances of each type of PC are located on the timeline and the approximate (decadal) incept years are taken: • Gas generation – first gas turbines • Wind – first large-scale wind farm • Biomass generation – first wood-fired power plant • Other generation – first tidal power project (other RE encompasses more than tidal, but the total remains insignificant and this approximate date indicates these technologies are relatively new)
Source 48	Smil notes that CHP did not enter widespread use until the 1970s (for gas and coal; biomass CHP comes at the same time as biomass generation).

9.5.6.4 End_Use_Conversion_Eff_Input

Input reference:	4.4
Description:	Matrix of ranges for EU conversion efficiency (min. corresponds to the initial PC mean value and max. corresponds to the maximum theoretical value; a value of 1 indicates that no EU conversion occurs)
Sources:	8, 33, 41, 42
General calculations and assumptions	

• This efficiency refers to EC input converted to applied output power, at the physical boundary of the device.
• Assumes the use of heat pumps remains minor as maximum potential end-use conversion efficiency for electric heating low is less than 1 (can be 3-4 for ground source heat pumps):
    o This assumes the share of ES demand for low temperature heating which can be met by heat pumps (primarily space heating) remains low compared with cooking, water heating, and others.
    o This assumption is justified on the grounds that large increases in end-use to ES efficiency for low temperature heating (up to a factor of 2.7) and/or stable or declining final demand would be consistent with a shift towards passive design that significantly reduces the need for continuous space heating.	

o PRESS version 1.1 tested with 2.5 as the maximum value for electric heating low end-use conversion efficiency. Little impact on the primary transition metrics is observed (transition failure rate increases by 0.001, mean cumulative GHG emissions by 2100 decreases by <50 $GtCO_2e$, RE fraction for heat increases by ~10%).	
Source-specific calculations and assumptions	

Source 8	• Motor efficiencies taken from figure 8.20. Assumed values are used for electrical mechanical and electric vehicles.
	• Virtualization of computer servers has potential energy savings of 70% (section 10.4.3.10):
	    o Assume comparable savings are achievable for other IPaC devices.
	    o The average minimum conversion efficiency is increased accordingly.
	• Research and development in LED lighting is expected to eventually lead to lamps reaching 200 lm/W (section 10.4.3.8):
	    o This gives a maximum conversion efficiency of 0.3, relative to a theoretical maximum of ~650 lm/W
	    o This approximate theoretical maximum is based on black-body radiation in the visible spectrum, emitting uniformly in all directions, assuming no adjustment for preferred wavelengths.
	• Section 10.4.3.8 notes that older heating equipment in buildings is 60-70% efficient, whereas new equipment can be up to 95% efficient:
	    o The minima and maxima are used for LaG fuels and electric heating, respectively.
	    o This does not apply to heat, as conversion occurs at the secondary stage.

Source 33	Global average technical potential for improvement in luminous efficacy (equivalent to end-use conversion efficiency) is given in table 8 (60%). The minimum value is increased by this factor to give the maximum.
Source 41	• Values are taken from table 2. • Representative values are taken from the ranges given for the most appropriate device or devices for each end-use category (for both current and TEL – minima and maxima, respectively). • For the electric lighting maximum, a multiplier of 5 is selected, representing the approximate difference between current and TEL ranges. • Where the end-use PC uses a heat cycle, the indicated efficiencies are impratical as they correspond to the Carnot efficiency (zero power output). As per source 43, an approximation factor of 0.5 is used.
Source 42	• Values are taken from table 3. • Only electric lighting, IPaC, electric heating (low and high temperature), and LaG fuel heating values are used as others relate to the conversion of ECs to motion (extends beyond the end-use to ES efficiency definition) or conversion of primary energy to ECs (secondary stage). • For LaG fuel heating, a representative value of 0.62 is chosen (oil & gas burners).

9.5.6.5 Init_End_Use_ES_Eff_Input

Input reference:	4.5
Description:	Matrix of estimates of initial PC mean values for EU to ES efficiency and associated maximum fractional error
Sources:	5, 8, 33, 44, 45, 46, 47, 49
General calculations and assumptions	
• This efficiency refers to applied output power, at the physical boundary of the device, converted to useful energy services, defined relative to selected reference modes representing ideal service provision. • A rough approximation is used for the potential increase of end-use to ES efficiency of passenger shipping in input 4.6, so the initial values are treated with higher uncertainty (0.5). • Other transport modes are assessed based on observed variation in reported values and assigned an error factor (0.2 or 0.5): o The baseline level of uncertainty regarding end-use to ES efficiencies for transportation modes at the global level is high, due to geographic heterogeneity and a lack of comprehensive data, therefore, a minimum error factor of 0.2 is assumed.	

- Significant variation in the energy intensity of freight aviation is seen between sources 45 and 47, so the corresponding values are treated with higher uncertainty (0.5).
- Passenger shipping and ICEV heavy passenger also exhibit larger differences in reported efficiencies between sources, so the corresponding values are treated with higher uncertainty (0.5).

Reference modes:

- Where multiple modes exist for a given ES, each type of passive system is assessed via the available literature the mode with the highest potential final efficiency (utilizing maxima from 9.5.6.6) representing the reference mode:
    - Equivalent passive systems are assumed to be mechanical (electric and LaG fuel), light vehicles (ICE and electric), passenger rail (ICE and electric), passenger aviation (regional and IC), passenger shipping (regional and IC), freight rail (ICE and electric), freight aviation (regional and IC), freight shipping (regional and IC), low temperature heating (LaG fuels, electric, and heat), and high temperature heating (electric and heat).
    - While this assumption is not strictly accurate for non-transport PC due to the significant diversity of passive systems associated with different PC types, insufficient information exists to resolve these differences.
    - Mechanical and high temperature heating passive systems entail greater differences in passive systems (e.g., electric motor vs. internal combustion drivetrains, blast vs. arc furnaces), therefore, are modelled with greater uncertainty (0.2).
    - This alignment of passive systems fits with the assumption that each mode is structurally interchangeable regarding the satisfaction of ES demand, often using equivalent AI.
- As a validation check on calculated reference mode efficiencies, the efficiency for travel by bicycle on a flat surface is approximately 14 kJ/p-km for 60W applied power (not total metabolic power) by a 70 kg cyclist. Therefore, it is assumed that the passive systems of transport modes using exosomatic energy might, at best, use approximately four times more applied energy per passenger-kilometre than bicycles under ideal conditions. This greater use of applied energy is justified due to a significantly higher power level (see section 2.2.1), luggage capacity, and the greater structural protection and weatherization required for general purpose vehicles relative to bicycles.

Source-specific calculations and assumptions	
Source 5	For passenger aviation, seat-miles per gallon values from the aircraft efficiency dataset (averaged 2013-2018 for ~2015) are converted to end-use to ES efficiency by first converting to MJ/p-km (using 142.2 MJ/gal for aviation fuel) then taking the inverse, multiplying by the corresponding minima from 9.5.6.4 (to decompose to end-use to ES efficiency), then dividing the reference mode end-use to ES efficiency value by the result: • Regional jets stock value used for regional. • Average aircraft stock value used for IC.
Source 8	Values are read from figure 9.12, pg. 589, chapter 9 (Energy intensity of domestic transport system in Japan): • Car value used for ICEV light (2.2 MJ/p-km). • Bus value used for ICEV heavy passenger (0.8 MJ/p-km). • Rail passenger value used for electric rail passenger (0.15 MJ/p-km). • Air value used for aviation passenger regional (1.7 MJ/p-km). • Rail freight value used for electric rail freight (0.2 MJ/t-km). • Truck value used for ICEV heavy freight (3.8 MJ/t-km). • Shipping value used for shipping freight regional (0.6 MJ/t-km). • Data is from 2008, assumed similar in 2015 (time series not provided). • The rail values are appropriate for electric rail as the Japanese rail system is largely electrified. • Values are not used for IC as data refers to domestic (regional) transportation.

Source 33	Composite MJ/p-km and MJ/t-km values from table 3 are converted to end-use to ES efficiency by taking the inverse, multiplying by the corresponding minima from 9.5.6.4 (to decompose to end-use to ES efficiency), then dividing the reference mode end-use to ES efficiency value by the result:
	• For light vehicles:
	  o Assume an average of 1.5 occupants per vehicle.
	  o Assume initially 90% LDV, 8% two-wheel, and 2% three-wheel.
	  o Use volumetric energy density of gasoline of 34 MJ/L.
	• For ICEV heavy freight, assume 25% medium freight and 75% heavy freight.

	• Due to similarity in passive systems, end-use to ES efficiency values for passenger rail and freight rail are aligned by decomposing using the average of current end-use conversion efficiency across ICE and electric modes:
	  o This is an approximation, assuming approximately equal initial proportions of ICE and electric modes (supported by 9.5.3.2).
	  o The approximation entails higher uncertainty (0.2).
	• Data is from 2005, assumed similar in 2015 (time series not provided).

Source 44	• Representative values are taken from Land Passenger Transport means table, estimated by comparing examples given to average global fleet composition:
	  o 2 MJ/p-km for ICEV light
	  o 0.6 MJ/p-km for ICEV heavy passenger
	  o 0.5 MJ/p-km for electric vehicles
	  o 0.25 MJ/p-km for rail passenger (ICE and electric)
	  o 1.74 MJ/p-km for passenger aviation (approximate value for the Boeing 747-400, using 45 MJ/L for aviation fuel, assuming 80% average occupancy)
	  o 5.7 MJ/p-km for the *MS Oasis of the Seas*, assuming full occupancy and 35 MJ/L for diesel fuel:
	    ▪ This compares to 0.72 MJ/p-km reported for German passenger ship transport.
	    ▪ The latter value is assumed for shipping passenger regional.
	    ▪ For shipping passenger IC, cruise ships are not designed primarily for transportation efficiency and significantly more efficient designs are likely achievable with current technology should mass ocean transit return at scale, however, energy requirements are likely higher than short-distance ferries due to longer trips, greater supply and amenity requirements, and higher speeds – to represent this balance, the average of the two values is taken to give a representative value.
	    ▪ For passenger shipping, the potential increase factor (in 9.5.6.6) is doubled to account for significant design changes that would occur between current ocean cruise ships (representing the base value but not designed for efficient transportation) and re-emergent ocean-based mass transit.
	    ▪ This is a rough approximation so shipping passenger IC is treated with higher uncertainty in (0.2).
	• The Freight table value for rail freight in the UK (0.41 MJ/t-km) is used for ICE rail freight. This value refers to primary energy input so is used for ICE mode and the resulting end-use to ES efficiency is assumed for electric rail freight due to similarity in passive systems.

Source 45	• Approximate values are taken directly from table, between 2015 and 2016. • As values relate to primary energy, rail passenger and freight values are used for ICE modes and the resulting end-use to ES efficiencies are assumed for electric rail due to similarity in passive systems. • For passenger rail, a value midway between regional and long-distance is assumed (0.7 MJ/p-km).

Source 46	• Representative values chosen from the 2015 row in tables 2.14, 2.15 and 2.16:
	  o 4000 BTU/p-mile for ICEV light (in between car and light truck, assuming closer to the car value)
	  o 4000 BTU/p-mile for ICEV heavy passenger (high, due to low mass transit occupancy in the US)
	  o 2500 BTU/p-mile for aviation passenger regional
	  o 1600 BTU/p-mile for ICE rail passenger (intercity and commuter)
	  o 800 BTU/p-mile for electric rail passenger (rail)
	  o 300 BTU/ton-mile for ICE rail freight
	  o 214 BTU/ton-mile for shipping freight regional (2014 value for waterborne commerce)
	  o Trucking is ignored as values are not per transported payload weight.

	• Values are converted using 1 BTU = 947.8 MJ and 1 ton = 0.907 tonnes.
Source 47	• 2015 values are used. • Light vehicles are used for ICEV light. • Passenger rail are used for ICE rail passenger (mainly diesel for rail in Canada). • Freight rail are used for ICE rail freight (mainly diesel for rail in Canada). • The same passive system equivalences are used as with other sources.
Source 49	Values are read from the Energy intensity of passenger transport modes section (2018 chart): • Assume values are appropriate for 2015. • The cars value is used for ICEV light (2.8 MJ/p-km). Assume weighting from large cars and 2/3-wheelers cancel. • The buses and minibuses value is used for ICEV heavy passenger (0.7 MJ/p-km). • Assume rail refers to electric rail as the value is too low for ICE rail (0.2 MJ/p-km). • The aviation value is used for aviation passenger regional and IC (2.8 MJ/p-km).

9.5.6.6 Final_EU_ES_Eff_Max_Factor

Input reference:	4.6
Description:	Vector of the maximum fractional increase from initial PC mean EU to ES efficiency to the upper asymptotes of the EU to ES efficiency function
Sources:	8, 33, 43
General calculations and assumptions	
• This factor sets the upper end of the possible range for increases in end-use to ES efficiency, in terms of a multiple of the initial value (higher values indicate greater potential for increased efficiency of passive systems). • Given that the potential increase for electric lighting from source 43 is very optimistic and relies on ideal but unrealistic conditions, an estimate of 2 (a doubling of end-use to ES efficiency) is included.	
Source-specific calculations and assumptions	

Source 8	• The passive system changes detailed are discussed in isolation, therefore, these directly correspond to end-use to ES efficiency and do not need to be decomposed.
	• Most of the technological options discussed are mutually exclusive and therefore, are not cumulative. In addition, most are applicable under particular conditions only, and some refer to the replacement of obsolete, less efficient technology that does not represent average PC.
	• Percent savings for electrical mechanical is taken from table 8.19 (Total Cost-effective Saving from Electricity use in Pump, Compressed Air, and Fan Systems). The same factor is assumed for LaG mechanical due to similar passive systems.
	• Percent savings for low temperature heating is taken from section 8.4.3 (Steam and Process Heating Systems) and section 10.4.3 (Options Related to Building-Scale Energy Systems and to Energy Using Devices):
	  ○ Steam systems do not encompass all low temperature heating (residential and commercial space heating, cooking, etc.) but do comprise a significant proportion – these can achieve savings of around 20%.
	  ○ Steam systems also include some high temperature heating but this represents a lower proportion so is not used for that estimate.
	  ○ Space heating requirements in temperate climates can be reduced by up to 67%.
	  ○ Better insulation can reduce heating requirements in cold climates by 75-90%.
	  ○ DCV can save 20–30% of the combined ventilation, heating, and cooling energy use in commercial buildings.
	  ○ 50% of the heat in hot wastewater can be captured and used to preheat cold incoming water or air.
	  ○ Heat pumps using CO_2 as a working fluid enable about 30% energy savings compared to conventional water heaters.
	  ○ Taking account of the above, a representative maximum potential value of 60% aggregate savings in low temperature heating is assumed (optimistic).
	• Percent savings for electric cooling is taken from section 10.4.3 (Options Related to Building-Scale Energy Systems and to Energy Using Devices):

	○ District cooling schemes can reduce cooling requirements by 45%. ○ Air conditioning savings can be up to 60% in some cases. ○ Integrating more vegetation into buildings can reduce cooling by 10-30% in some cases. ○ Better insulation can reduce heating requirements in cold climates by 75-90%. ○ Natural ventilation in temperate climates can reduce cooling requirements by 30-40%. ○ Evaporative cooling in arid regions can reduce cooling requirements by 92-95% (but depends on water availability). ○ Underground earth pipe cooling can reduce summer cooling loads by 65%. ○ Solid desiccant systems can reduce overall energy use for cooling and dehumidification by 50%. ○ Savings in combined cooling and ventilation energy use of 30–60% can be achieved through a combination of DV and CC cooling. ○ DCV can save 20–30% of the combined ventilation, heating, and cooling energy use in commercial buildings. ○ New efficient refrigerators use 30% less energy than the maximum allowed under regulations. ○ Taking account of the above, a representative maximum potential value of 75% aggregate savings in electric cooling is assumed (optimistic). • Percent savings for electric lighting taken from section 10.4.3.8: ○ Retrofits of fluorescent lighting can typically achieve 30–50% lighting electricity savings. ○ New construction can reach 75% savings for electric lighting compared to current standards. ○ Annual savings of 30–80% from daylighting of perimeter offices in commercial buildings are achievable. ○ Taking account of the above, a representative maximum potential value of 75% aggregate savings in electric lighting is assumed (optimistic). ○ Percent savings for IPaC devices taken from section 10.4.3.10: ○ Energy savings of 50–70% are possible from active power management. ○ A representative maximum potential value of 60% aggregate savings in IPaC devices is assumed (optimistic).
Source 33	• Indicated improvements are mostly in terms of composite conversion and end-use to ES efficiency (efficiency improvements are not separated by conversion and end-use stages). • World average values are taken from table 3 – the 2005 value is divided by the 2050 technical potential to give the multiplier factor for composite conversion and end-use to ES efficiency: ○ This assumes the 2050 technical potentials correspond to the long-term end-use to ES efficiency function asymptotes (no improvement beyond this). ○ This is optimistic, as the baseline is 2005, not 2015 (arbitrary adjustments would be needed to correct for this). • To decompose these to end-use to ES efficiency alone, values are divided by the corresponding end-use conversion efficiency multipliers from 9.5.6.4: ○ For ICEV light, LDV values are used. This is optimistic as largest light vehicle efficiency improvement is indicated for LDV. ○ For ICEV heavy freight, the average of medium and heavy freight is used, assuming approximately equal fleet composition. ○ Where there is overall design similarity in passive systems (drivetrain and chassis), estimates are aligned: ▪ ICEV light and electric vehicles ▪ Passenger aviation and freight aviation (internal layouts already largely optimized, improvements to come from engine and aerodynamics) ▪ National marine factor is used for all shipping types.

	▪ For rail, potential end-use to ES efficiency increases are calculated using average end-use conversion efficiency multipliers from 9.5.6.4, across ICE and electric modes. ▪ For high and low temperature heating, potential end-use to ES efficiency increases are calculated using average end-use conversion efficiency multipliers from 9.5.6.4, across electric and heat, and electric, heat, and LaG fuels respectively. • For high temperature heating (heat and electric), minimal detail is given, but a representative value of 30% energy (input) saving is chosen based on potential process improvements surveyed in the Industry section. • For low temperate heating (LaG fuels, heat, and electric), a representative value of 50% efficiency improvement is chosen based on estimates given in table 7. Only space heating is discussed here – this is assumed to be a reasonable approximation given that space heating currently dominates low temperate heating demand. • For electric cooling (cold appliances and air conditioning) and IPaC devices (other appliances), the stated potential savings of 60% and 65% (average), respectively, are converted to composite efficiency improvements and decomposed to end-use to ES efficiency improvement alone. This assumes similar savings are possible for non-residential PC. • Insufficient information is given to provide estimates for static mechanical or lighting (the stated luminous efficacy corresponds to conversion efficiency, not end-use to ES efficiency).
Source 43	• Values from table 1: o Appliance, driven system, and train o From tables S.8, S.15 & S.21 • Maximum end-use to ES efficiency increase factors are calculated from F, the fraction of current energy use that could be saved, by the expression $1/(1-0.01F)$. • Where an end-use category corresponds to more than one system type given in table 1, a weighted average is calculated, with energy supplied to the system as the weighting factor. • Authors conclude there are “no practical energy savings available in the passive systems of consumer electronics” (refers a large component of IPaC devices). • Driven systems (excluding refrigeration) are assumed to represent LaG fuel static mechanical. • Driven systems (excluding refrigeration), washing machine, dishwasher and other appliance (weighted by electricity component) are assumed to represent electric static mechanical. • Truck is used for ICEV heavy passenger and freight (definition includes buses, but passive systems are similar). • Freight train (table S.21) is used for ICE and electric rail freight. • Passenger train (table S.21) is used for ICE and electric rail passenger. • Increases in efficiency for transportation modes do not include increased occupancy. Adjustments are not made as estimates for modes where occupancy can be substantially increased (cars, buses, passenger rail) are already highly optimistic and, in some cases, this may compete with the assumed changes in design parameters (particularly weight reductions). • Refrigerator/freezer (appliances) refrigeration and cooled space are assumed to represent electric cooling. • For low temperature and high temperature heating, respectively, passive systems are assumed to be identical for all ECs as different weightings produce significant discrepancies in the maximum increase factors that inappropriately favour some PC types over others: o This is necessary to align with underlying assumption that low temperature and high temperature heating ES demands are each homogeneous. o Heated space (weighted by half the total energy consumption for this system: 36 EJ), cooker (weighted by total energy consumption), clothes dryer, and hot water systems are assumed to represent all forms of low temperature heating. o Furnace and steam systems are assumed to represent both forms of high temperature heating.

9.5.6.7 End_Use_Incept_Year

Input reference:	4.7
Description:	Vector of approximate incept years by EU PC (year functional category became widely available)
Sources:	36, 37, 40
Source-specific calculations and assumptions	
Source 36	Approximate (decadal) incept years taken from the text. Where multiple options exist, dates corresponding to technological innovations marking the beginning of current types of PC are used (i.e. obsolete precursors not functionally interchangeable with current technologies are ignored): • Aviation – first turbojet aircraft • Electric cooling – widespread diffusion of refrigeration • Electric heating low temperature – first large-scale electrification of cities • Shipping – first marine diesel engines • IPaC – first integrated circuits • ICEV heavy – beginning of trucking industry and bus services • ICE rail – earliest replacement of locomotive steam engines with diesel and diesel-electric
Source 37	First instances of each type of PC are located on the timeline and the approximate (decadal) incept years are taken: • ICEV light – Model T goes into mass production • Electric vehicles – GM's EV1 electric car is made available to the public
Source 40	• The year the world's first commercial electric arc furnace came into operation is used for electric heating high temperature. • This estimate entails high uncertainty, due to the wide variety of technologies used in high temperature electric heating, including heating elements, electric arcs, steam systems, and others. • Electric arc furnaces are selected as a representative technology they are a major case where the use of electricity can compete with heat fuels in industrial processes (the production of metal alloys).

9.5.7 Demand

9.5.7.1 ES_Final_Demand_Mult_Input

Input reference:	5.1
Description:	Matrix of maximum and minimum estimates for the fractional increase from initial ES demand to the upper asymptotes of the ES demand function
Sources:	(Own estimate)
General calculations and assumptions	

The ESs are grouped and approximate potential ranges relative to today's consumption levels based on their general characteristics and outlook:
• Future demand scenarios are not known:
    o Aggregate declines are possible, but generally not expected.
    o Increases are more likely and easier to reconcile with a stable global socio-economic context (not assumed, but the global system will seek to achieve this outcome).
• Uniform distributions are assumed:
    o Future ES demand scenarios cannot be known with enough specificity to justify the choice of a more complex distribution.
    o As the primary set of independent parameters to be tested by PRESS, these should be as free of arbitrary assumptions as possible.
• The developed world (OECD) population is approximately 20% of the world total and the developing world per capita consumption of many energy services is significantly lower. Therefore, the world population (allowing for population growth) consuming at the current developed world level corresponds to a multiple of approximately 5.
• A core group of ESs constitutes illumination, static mechanical, transport passenger regional, transport freight regional, cooling, and high temperature process heat:	

○ This group is primarily residential, commercial, and industrial ES demand, and the regional movement of people and goods, except for IPaC and low temperature heating, which are special cases. ○ For this group, a final demand multiplier range of 0.5 to 5 is assumed. ○ This range gives an order of magnitude difference, approximately spanning world average consumption dropping to current developing world levels, to world average consumption rising to current developed world levels. ○ Growth is more likely than decline due to the uniform distribution (mean is >1). ○ These energy services are general in nature, not subject to unusual pressures for growth or high dependence on geopolitical factors. • IPaC ○ A final demand multiplier range of 0.8 to 10 is assumed. ○ Due to the relative immaturity, at the global level, of IPaC infrastructure, and the high social utility of IPaC services, this ES is considered to have stronger growth imperatives and to be more resistant to declines. ○ Significant growth may continue in developed countries, with the developing world seeking to catch up. ○ Aggregate declines are possible, but very unlikely. • Intercontinental movement of goods and people: ○ This group is comprised of transport passenger IC and transport freight IC. ○ A final demand multiplier range of 0.2 to 8 is assumed. ○ This range represents higher uncertainty, as these energy services are less intrinsically necessary, strongly dependent on economic and geopolitical conditions, and could fall substantially but are also generally expected to continue a strong growth trajectory. • Low temperature heating: ○ A final demand multiplier range of 0.2 to 2 is assumed. ○ Strong increases are less likely as space heating in cold and temperate climates is already relatively ubiquitous, while cooking and other non-discretionary uses of low temperature heat do not grow rapidly. ○ Warmer climates have little to no requirement for space heating. ○ Climate change may further limit the scope for increases in demand for low temperature heating. ○ Strong declines are possible through building redesigns and shifting attitudes changing the nature of heat provision (heating people directly and smaller spaces rather than entire buildings, etc.).

9.5.7.2 Initial_ES_Demand_RoC_Max

Input reference:	5.2
Description:	Estimate for the initial maximum annual rate of change of the ES demand function
Sources:	(Own estimate)
General calculations and assumptions	
A maximum initial rate of change of 5% per year is assumed: • Population growth and increasing per capita consumption are unlikely to exceed this rate of change at the global level. • This rate of change is applied symmetrically to growing and declining ES demand trends (positive and negative, respectively).	

9.5.7.3 Initial_Demand_Flex

Input reference:	5.3
Description:	Estimate for the initial value of the demand flexibility function (initial fraction of final demand responsive to short-term supply availability)
Sources:	(Own estimate)
General calculations and assumptions	
Assume a small but non-negligible initial proportion of demand is flexible and responsive to price signals (5%).	

9.5.7.4 Final_Demand_Flex_Input

Input reference:	5.4
Description:	Vector of maximum and minimum estimates for the final value of the demand flexibility function (at sim. base period)

Sources:	(Own estimate)
General calculations and assumptions	
The proportion of flexible, price-responsive demand reached at the simulation base period (80 years, or 2095) is assumed to be uniformly distributed, ranging from 10% to 50%: • 10% represents an approximate doubling from current levels and is considered entirely possible and likely, particularly given policy efforts directed at achieving this. • 50% is considered an upper limit, beyond which ES demand is largely inflexible and non-discretionary due to operational and temporal limitations (cannot follow supply on the timescales required).	

9.5.8 EROI

9.5.8.1 Initial_RE_EROI_Input

Input reference:	6.1
Description:	Matrix of mean and standard deviation estimates for initial new PC EROI by RE type
Sources:	11, 51, 52, 54, 58, 60, 61
General calculations and assumptions	

• Data is not available for EROI at the primary level for solar thermal and geothermal (EC production modelled as secondary in PRESS):
    o The maximum estimate for secondary EROI (from 9.5.9.1) is taken as a practical lower bound, as primary EROI cannot be lower than secondary.
    o A practical maximum of 100 is assumed for solar thermal and 50 for geothermal at the primary level (similar to other high-EROI primary resources, such as hydropower or offshore wind).
• A truncated normal distribution is assumed:
    o There is a central tendency in EROI estimates, with possibility of significant deviation.
    o Distributions are truncated to the maxima of terminal EROI ranges, as initial EROI values lower than this are highly unlikely and could lead to improperly generated logistic curves for EROI as a function of resource exhaustion.	

Source-specific calculations and assumptions	
Source 11	Mean and median values are taken from table 6-2 for RE sources where electricity production is considered primary, plus biomass.
Source 51	25^{th} and 75^{th} percentile values for wind all and PV all are taken from figure 3 then inverted to give upper and lower EROI estimates.
Source 52	• Initial $EROI_{st}$ values for dispatchable RE electricity generation are taken from table 1. • Oceanic is assumed to represent other RE.
Source 58	EROI estimates for RE sources where electricity production is considered primary are taken from figure 4.
Source 60	• EROI values are taken from figure 2 for RE sources where electricity production is considered primary. • 'EMROI' is used as this uses primary energy equivalence, in line with PRESS modelling formulation.
Source 61	As values in section 3.3 are given by PV technology, not as global installed averages, a representative range for solar PV is selected from within the values given (10 to 30).
Source 62	• Approximate EROI values for sources where electricity production is considered primary are taken from figure 3. • A range is taken from table 1 for solar PV (6 to 12).

9.5.8.2 RE_EROI_Terminal_Input

Input reference:	6.2
Description:	Matrix of maximum and minimum estimates for the final values (exhaustion = 1) of the RE EROI function (lowest acceptable EROI for a viable energy source)
Sources:	(Own estimate)
General calculations and assumptions	

- For most RE sources, the minimum acceptable EROI is assumed to range between 1 (absolute minimum, where input equals output) and 5 (low EROI that may challenge economic viability).
- Exceptions are biomass and RE other, where the upper limit for terminal EROI is 2:
    - Biomass terminal EROI is lower due to lower EROI for traditional modes of harvesting requiring only simple inputs and also the ability to produce more desirable ECs via biomass, namely LaG fuels, which may justify operating at lower EROI values.
    - RE other terminal EROI is lower due to its lower bound for initial EROI.

9.5.8.3 RE_EROI_Drop_Input

Input reference:	6.3
Description:	Matrix of maximum and minimum estimates for the pre-simulation decline in the RE EROI function (between upper asymptote and initial value)
Sources:	(Own estimate)
General calculations and assumptions	
• Declines should refer to the period after technology incept years, from technological maturity to ~2015. • Scarce timeseries data for the EROI of RE sources is available as most are currently producing at negligible rates compared with technical potential, with minor EROI declines observed to date. • Consequently, little information can be discerned regarding the characteristics of the associated resource quality distributions. • Therefore, the minimum drop value for most RE sources is assumed to be 0 (no change between original and current new EROI). Hydropower, geothermal, and biomass are exceptions to this, as these occupy a significant share of their technical potentials – as such, their minimum drop values are assumed to be 10% of the means of current EROI estimates from 9.5.8.1. • The maximum conceivable drop value for all RE sources is assumed to be 100% of the means of current EROI estimates for technologies that occupy a significant share of their technical potentials (hydropower, geothermal, and biomass), and 10% for all others. • This provides ranges that are an order of magnitude apart for significantly exhausted versus non-exhausted RE sources, relative to mean EROI estimates.	

9.5.8.4 Initial_NRE_EROI_Input

Input reference:	6.4
Description:	Matrix of mean and standard deviation estimates for initial new PC EROI by NRE type
Sources:	11, 54, 55, 56, 57, 61
General calculations and assumptions	

• EROI estimates are assumed to include exploration activities required to locate and prove reserves.
• As only one estimate was found for nuclear fuels, upper and lower bounds are assumed to be ±25% of this estimate.
• Truncated normal distributions are assumed:
  o There is a central tendency in EROI estimates, with possibility of significant deviation.
  o Distributions are truncated to the maxima of terminal EROI ranges, as initial EROI values lower than this are unlikely and could lead to improperly generated logistic curves for EROI as a function of resource depletion.	

Source-specific calculations and assumptions	
Source 11	Mean and median values are taken from table 6-2.
Source 54	See section 9.5.2.3.
Source 55	• The best guess linear extrapolation given in figure 2 is used – approximately 14 for ~2015. • This value is assumed for both gas and oil.
Source 56	Values are read from figure 9, taking the new model and price-based method as separate estimates.
Source 57	The indicated approximate global oil EROI value of 17 used (page 5).
Source 62	• An approximate range for oil is taken from figure 9 (10 to 40; 2010 values assumed equivalent to ~2015). This is optimistic as gas EROI normally reported as higher than oil EROI. • An approximate range for gas is taken from figure 10. • An approximate range for coal is taken from figure 11.

9.5.8.5 *NRE_EROI_Terminal_Input*

Input reference:	6.5
Description:	Matrix of maximum and minimum estimates for the final values (depletion = 1) of the NRE EROI function (lowest acceptable EROI for a viable energy source)
Sources:	(Own estimate)
General calculations and assumptions	
For all NRE sources, the minimum acceptable EROI is assumed to range between 1 (absolute minimum, where sum of input flows equals output flow) and 5 (low EROI that may begin to challenge economic viability).	

9.5.8.6 *NRE_EROI_Drop_Input*

Input reference:	6.6
Description:	Matrix of maximum and minimum estimates for the pre-simulation decline in the NRE EROI function (between upper asymptote and initial value)
Sources:	11, 55, 56, 57, 61
General calculations and assumptions	
Declines should refer to the period after technology incept years, from technological maturity to ~2015. Peak observed EROI values from all sources converted to a uniform distribution of drop (delta) values: • The maxima are formed by subtracting the initial EROI estimate minima from the corresponding peak EROI estimate maxima. • The minima are formed by subtracting the initial EROI estimate means from the corresponding peak EROI estimate means.	
Source-specific calculations and assumptions	
Source 11	• Coal maximum and minimum peak values are taken from figure 6-2. • Oil maximum and minimum peak values are taken from figure 6-4. • Gas maximum and minimum peak values are taken from figure 6-7.
Source 55	Approximate peak value is taken from figure 1.
Source 56	• Values are read from figure 9 and table 4, taking the new model and price-based method as separate estimates. • As these peaks occur significantly after technology incept years, it is assumed they still offer a suitable upper asymptote) for EROI functions, which are normalized to prior production assuming a linear increase.
Source 57	The indicated approximate global oil peak EROI value of 30 I used (page 5).
Source 62	• The range for oil peak values is taken from figure 9. • The range for oil peak values is taken from figure 10. • The range for coal peak values is taken from figure 11.

9.5.9 Energy Cost of Capital

9.5.9.1 *Secondary_PC_ECC_Input*

Input reference:	7.1
Description:	Matrix of mean and standard deviation estimates for energy cost of capital by secondary PC type (defined relative to initial CF)
Sources:	11, 51, 52, 54, 58, 59, 60, 61
General calculations and assumptions	
• Where EROI estimates at the primary and secondary stages are available, these are converted to ECC as detailed in section 4.2.4.2. • High, low, and best guess ECC estimates are calculated from minimum, maximum, and mean secondary EROI using maximum, minimum, and mean primary EROI and PC lifetime, respectively. • These estimates form indicative ranges which are then grouped and approximated, with secondary PC lacking associated EROI estimates assigned to groups based on similar levels of technological and capital complexity. • Log-normal distributions are used as ECC estimates can be expected to vary by orders of magnitude.	

- Standard deviation is assumed to be the same as the mean, as this allows for a distribution where the 50th percentile is not significantly less than the mean, but a wide range over an order of magnitude in either direction is still possible (more than 99.9% of the distribution lies between 0.1σ and 10σ). - Best guess ECC estimates for geothermal generation and oil generation are not useful but grouping is still possible by inspection of high estimates, and assessment of capital similarity: - Oil generation has only one associated secondary EROI estimate (likely low). - Geothermal generation low and best guess ECC estimates are less than zero which is not physically meaningful but implies low secondary PC ECC. - Four tiers are identified for ECC: - High cost (2.5 years) – biofuels and biomass generation (large energy inputs required for feedstock preparation and process requirements, i.e., mainly operational energy costs) - Medium cost (1.5 years) – coal and nuclear generation (applied to other PC considered to be in a similar cost: oil generation, refining, coal and gas to LaG, refining, coal and biomass CHP, and geothermal generation) - Low cost (0.5 years) – gas generation and solar thermal generation (applied to gas CHP, and geothermal generation) - Minimal cost (0.05 years) – all other, including secondary PC for heat and processes where EC production is considered primary (an order of magnitude lower than the other tiers, but a significant range is still possible)	
Source-specific calculations and assumptions	
Source 11	Mean and median values are taken from table 6-2 for sources where EC production is considered secondary (excluding outliers). Bio-diesel and bio-ethanol are considered together for biofuels.
Source 51	25th and 75th percentile values for CSP are read from figure 3 then inverted to give upper and lower EROI estimates.
Source 52	Initial primary EROI value for biomass generation is taken from table 1.
Source 54	See section 9.5.2.3.
Source 58	EROI estimates (for secondary electricity production) are taken from figure 4.
Source 59	A representative value for primary EROI is taken from table 8 (present system, scenario 1; this input does not include penetration level effects in PRESS as these are modelled explicitly).
Source 60	- Values are taken from figure 2 for generation types where electricity production is considered secondary. 'EMROI' is used as this uses primary energy equivalence, in line with PRESS modelling formulation.
Source 62	Approximate values for RE sources where electricity production is considered secondary are taken from figure 3.

9.5.9.2 Secondary_AI_ECC_Input

Input reference:	7.2
Description:	Matrix of mean and standard deviation estimates for energy cost of capital by secondary AI type
Sources:	10
General calculations and assumptions	
- Transmission and distribution costs typically make up a significant proportion of final cost of electricity, but less than the cost of generation [413]. Assuming a consistent embodied energy of prices [414], and taking into account the peak factor for electricity AI, this indicates an **ECC for electricity AI of approximately 0.2 years**. - While the transportation and distribution of LaG fuels and heating fuels is less capital intensive than electricity, costs are significant, approaching or exceeding the commodity cost [415, 416]. As such, ECC for LaG fuels AI and heat AI is conservatively estimated at 0.1 years (by comparison to electricity AI). - Log-normal distributions are used as ECC estimates can be expected to vary by orders of magnitude. - Standard deviation is assumed to be the same as the mean, as this allows for a distribution where the 50th percentile is not significantly less than the mean, but a wide range over an order of magnitude in either direction is still possible (more than 99.9% of the distribution lies between 0.1σ and 10σ).	
Source-specific calculations and assumptions	

Source 10	• Table 6 shows balancing costs initially around \$3.50 2011 USD/MWh, rising to \$7 2011 US/MWh for intermittent penetration > 50%.
	• This compares levelized cost of energy between \$10 and \$20 USD/MWh for most sources.
	• Hence, assuming a consistent embodied energy of costs [414], and taking into account the peak factor for intermittent electricity AI and CFs of secondary generation, the (initial, low intermittent penetration) **ECC of intermittent electricity AI can be conservatively estimated at 0.1 years**:
	  o Initially less than, but comparable to, electricity AI (assuming balancing costs represents full effective mitigation of intermittency).
	  o This ECC is subject to a higher initial average peak factor.
	  o The effective ECC will increase with higher intermittent penetration and decrease with higher intermittent diversity and demand flexibility.

9.5.9.3 End_Use_PC_ECC_Input

Input reference:	7.3
Description:	Matrix of mean and standard deviation estimates for energy cost of capital by EU PC type (defined relative to initial CF)
Sources:	(Own estimate)

General calculations and assumptions

- A cursory calculation can be performed for light vehicles (ICEV light):
  - An average power light vehicle is rated for 100 kW output power, which represents power capacity of 3200 GJ per year.
  - Smil [417] notes that the average light vehicle requires approximately 100 GJ for its manufacture (optimistic, as some estimates are a factor of 2 or 3 higher than this).
  - This does not include energy required for upkeep (servicing and replacement parts), so this value is increased by 50% (approximate adjustment).
  - This implies an ECC of $150\ GJ/3200\ GJ/yr = 0.05$ years.
  - The embodied energy of electric vehicles is higher, so assuming similar driving habits and a similar proportion of energy required for upkeep, the corresponding ECC value is estimated at 0.1 years.
- For electric lighting, a typical (~10W) LED bulb, representing 315 MJ/yr power capacity, requires approximately 50 MJ in its manufacture [418]:
  - This corresponds to an ECC value of 0.15 years.
  - While LED is now the dominant lighting technology, this figure is reduced to 0.1 years as a conservative estimate, as embodied energy relative to power capacity is much higher for LED than for other lighting technologies.
- As very little data exists for the embodied energy of end-use PC, as defined in PRESS, similarity in ECC values among end-use PC types is assumed (lifetime input energy relative to nameplate capacity is relatively uniform, dependent on few factors). Effectively, this means shorter-lived PC is more energy intensive per output power than long-lived PC.
- Log-normal distributions are used as ECC estimates can be expected to vary by orders of magnitude.
- Standard deviation is assumed to be the same as the mean, as this allows for a distribution where the 50th percentile is not significantly less than the mean, but a wide range over an order of magnitude in either direction is still possible (more than 99.9% of the distribution lies between 0.1σ and 10σ).
- CF, representing average to peak power ratio, must also be considered as embodied energy relative to power capacity for PC with very low CF is unlikely to be as high (this category of PC requires short bursts of power that are not sustained for long so do not require the same level of sustained structural support, e.g., vehicles are not designed to operate continuously at peak acceleration).
- End-use PC types are split into three tiers based on capital complexity (indicated by cost) and CF (low average to peak power ratio) with ECC values set by comparison with estimates above:
  - High cost (0.2 years) – IPaC devices, shipping (all), and high temperature heating (electric and heat fuels)
  - Medium cost (0.1 years) – electric vehicles, mechanical (electric and LaG fuels), rail (all), aviation (all)
  - Low cost (0.05 years) – all other

9.5.9.4 End_Use_AI_ECC_Input

Input reference:	7.4
Description:	Matrix of mean and standard deviation estimates for energy cost of capital by EU AI type
Sources:	(Own estimate)
General calculations and assumptions	

- For end-use AI, costs per unit delivered power are typically minor but not negligible.
- Higher associated peak factors mean more AI will be required per unit delivered power.
- Log-normal distributions are used as ECC estimates can be expected to vary by orders of magnitude.
- Standard deviation is assumed to be the same as the mean, as this allows for a distribution where the 50th percentile is not significantly less than the mean, but a wide range over an order of magnitude in either direction is still possible (more than 99.9% of the distribution lies between 0.1σ and 10σ)
- End-use AI types are split into two tiers based on capital complexity (indicated by cost), with estimated ECC values set by comparison with secondary PC and AI and end-use PC:
    - High cost (0.1 years) – IPaC, roading, rail, aviation, and shipping
    - Low cost (0.05 years) – all other

9.5.10 Primary NRE sector

9.5.10.1 CapEx_Fraction_Input

Input reference:	8.1
Description:	Matrix of maximum and minimum possible values for the fraction of NRE investment energy devoted to capital (construction and decommissioning)
Sources:	(Own estimate)
General calculations and assumptions	

Two tiers are identified based on the relative magnitude of ongoing operation and maintenance energy costs:

- Low cost (assume CapEx fraction between 75% and 90%) – oil and natural gas (resources are fluids; activities include pumping, well logging, inspections, running production equipment)
- High cost (assume CapEx fraction between 50% and 75%) – coal and nuclear fuels (resources are solids; activities include operating heavy mining equipment, bulk material processing, earthworks, and demolition)

9.5.10.2 Decommission_Fraction_Input

Input reference:	8.2
Description:	Matrix of maximum and minimum possible values for the fraction of NRE investment energy devoted to capital used in the decommissioning stage
Sources:	(Own estimate)
General calculations and assumptions	

Two tiers are identified based on complexity and cost of site decommissioning and restoration:

- Low cost (assume decommissioning fraction between 0% and 5%) – oil and natural gas (site remediation involves shutting in and cementing wells, removing production equipment and sometimes site clean-up)
- High cost (assume decommissioning fraction between 10% and 20%) – coal and nuclear fuels (site remediation often involves closing open mining pits, removing large amounts of production equipment, decommissioning bulk handling facilities, removing hazardous tailings, and ongoing site containment measures)

9.5.10.3 EC_Split_LaG_Factor_Input

Input reference:	8.3
Description:	Matrix of maximum and minimum possible values for the initial fraction of NRE input energy consisting of liquid and gaseous fuels, divided by the LaG share of initial EC supply
Sources:	(Own estimate)
General calculations and assumptions	

This is a measure of geographical remoteness. Remaining NRE energy resources tend to be increasingly remote, therefore, the LaG factor can be assumed to be above one (range 1 to 1.4).

9.5.10.4 *EC_Split_Heat_Factor_Input*

Input reference:	8.4
Description:	Matrix of maximum and minimum possible values for the initial fraction of NRE input energy consisting of heat, divided by the heat share of initial EC supply
Sources:	(Own estimate)
General calculations and assumptions	
This is a measure of the degree of heavy industry as well as direct process heat requirements. NRE energy resources require significant heavy capital equipment and, in many cases, supplementary process heat, therefore, the heat factor can be assumed to be above one (range 1 to 1.4).	

9.5.10.5 *PC_Build_Time_Input*

Input reference:	8.5
Description:	Matrix of maximum and minimum possible values for NRE power capacity build time (investment decision to operation)
Sources:	(Own estimate)
General calculations and assumptions	

• Assume exploration activities precede PC investment and cause no additional delays beyond that modelled for NRE PC.
• All primary NRE infrastructure requires significant time to build, rarely shorter than several years.
• Two tiers are identified based on complexity and cost of planning, permitting, and construction:
    o Short (assume average build times between 2 and 5 years) – oil and natural gas
    o Long (assume average build times between 5 and 10 years) – coal and nuclear fuels	

9.5.10.6 *PC_Lifetime_Input*

Input reference:	8.6
Description:	Matrix of maximum and minimum possible values for NRE power capacity lifetime (in operation)
Sources:	(Own estimate)
General calculations and assumptions	

• All primary NRE infrastructures have lifetimes in the decades, but rarely beyond 40 years due to depletion of the in-situ resource.
• Two tiers are identified based on typical resource production profiles:
    o Short (assume average lifetimes between 10 and 25 years) – oil and natural gas
    o Long (assume average build times between 15 and 40 years) – coal and nuclear fuels	

9.5.11 Primary RE sector

9.5.11.1 *CapEx_Fraction_Input*

Input reference:	9.1
Description:	Matrix of maximum and minimum possible values for the fraction of RE investment energy devoted to capital (construction and decommissioning)
Sources:	54
General calculations and assumptions	
Three tiers are identified based on relative magnitude of ongoing operation and maintenance energy costs (with reference to estimates from source 54; see 9.5.2.3): • Low cost (assume CapEx fraction between 90% and 100%) – solar PV, wind, and hydropower (basic turbine/panel and structural maintenance only) • Medium cost (assume CapEx fraction between 75% and 90%) – solar thermal, geothermal, and other RE (more extensive maintenance of working fluid and generation systems) • High cost (assume CapEx fraction between 25% and 75%) – biomass (large energy inputs required for feedstock preparation and process requirements; this encompasses both modern and traditional biomass energy – operation and maintenance costs are assumed to be high relative to capital for both)	

9.5.11.2 Decommission_Fraction_Input

Input reference:	9.2
Description:	Matrix of maximum and minimum possible values for the fraction of RE investment energy devoted to capital used in the decommissioning stage
Sources:	54
General calculations and assumptions	
Based on complexity and cost of site decommissioning and restoration (with reference to estimates from source 54), assume decommissioning fraction between 0% and 5% for all RE types (RE installations typically do not have major decommissioning and site remediation costs).	

9.5.11.3 EC_Split_LaG_Factor_Input

Input reference:	9.3
Description:	Matrix of maximum and minimum possible values for the initial fraction of RE input energy consisting of liquid and gaseous fuels, divided by the LaG share of initial EC supply
Sources:	(Own estimate)
General calculations and assumptions	
This is a measure of geographical remoteness – two tiers are identified: • Most RE energy resources tend to be geographically remote and the best sites are relatively concentrated (solar thermal, wind, hydropower, geothermal, and other RE), or require significant mechanization to cover large fuel collection areas (biomass), therefore, the heat factor can be assumed to be above one (range 1 to 1.4). • Solar PV is not generally remote in most regions and suitable sites are more accessible, therefore, the heat factor can be assumed to be around one (range 0.8 to 1.2).	

9.5.11.4 EC_Split_Heat_Factor_Input

Input reference:	9.4
Description:	Matrix of maximum and minimum possible values for the initial fraction of RE input energy consisting of heat, divided by the heat share of initial EC supply
Sources:	(Own estimate)
General calculations and assumptions	
This is a measure of the degree of heavy industry required as well as direct process heat requirements: • Most RE energy resources tend to require significant heavy capital equipment, concrete, steel and high-temperature manufacturing processes (all except biomass), therefore, the heat factor can be assumed to be above one (range 1 to 1.4). • Biomass does not necessarily require significant heavy capital equipment, concrete, steel or high-temperature manufacturing processes (particularly for local, small-scale and traditional biomass), but does often require heat for feedstock preparation and process requirements, therefore, the heat factor can also be assumed to be above one (range 1 to 1.4).	

9.5.11.5 PC_Build_Time_Input

Input reference:	9.5
Description:	Matrix of maximum and minimum possible values for RE power capacity build time (investment decision to operation)
Sources:	54
General calculations and assumptions	

• Primary RE infrastructure generally requires less time to build than NRE.
• Three tiers are identified based on complexity and cost of planning, permitting, and construction (with reference to estimates from source 54):
  o Short (assume average build times between 1 and 3 years) – solar PV
  o Long (assume average build times between 4 and 8 years) – hydropower
  o Medium (assume average build times between 2 and 5 years) – all other	

9.5.11.6 PC_Lifetime_Input

Input reference:	9.6

Description:	Matrix of maximum and minimum possible values for RE power capacity lifetime (in operation)
Sources:	54

General calculations and assumptions

- Primary RE infrastructure generally has longer lifetimes than NRE as depletion of the resource does not occur, but with significant variation.
- Three tiers are identified based on typical useful lifetimes of capital equipment (with reference to estimates from source 54):
  - Medium (assume average lifetimes between 30 and 50 years) – biomass and geothermal
  - Long (assume average lifetimes between 50 and 100 years) – hydropower (dams may last longer but generating equipment must be replaced)
  - Short (assume average lifetimes between 20 and 30 years) – all other

9.5.12 Secondary sector

9.5.12.1 PC_CapEx_Fraction_Input

Input reference:	10.1
Description:	Matrix of maximum and minimum possible values for the fraction of secondary power capacity investment energy devoted to capital (construction and decommissioning)
Sources:	54

General calculations and assumptions

- Secondary PC generally has higher ongoing operation and maintenance energy costs than primary PC as conversion processes are typically energy intensive.
- Three tiers are identified based on relative magnitude of ongoing operation and maintenance energy costs (with reference to estimates from source 54; see 9.5.2.3):
  - Low cost (assume CapEx fraction between 90% and 100%) – oil and gas heat, and all secondary PC where electricity generation is considered primary
  - High cost (assume CapEx fraction between 25% and 75%) – refining, coal generation, coal to LaG, coal CHP, nuclear generation, and all biomass (all require large energy inputs for fuel processing and ancillary operational needs)
  - Medium cost (assume CapEx fraction between 50% and 75%) – all other

9.5.12.2 PC_Decommission_Fraction_Input

Input reference:	10.2
Description:	Matrix of maximum and minimum possible values for the fraction of secondary power capacity investment energy devoted to capital used in the decommissioning stage
Sources:	54

General calculations and assumptions

Three tiers are identified based on complexity and cost of site decommissioning and restoration (with reference to estimates from source 54; see 9.5.2.3):

- Low cost (assume decommissioning fraction between 0% and 5%) – oil and gas generation, oil and gas heat, solar PV (equipment is relatively easy to remove, sites do not need extensive remediation efforts)
- High cost (assume decommissioning fraction between 10% and 30%) – nuclear generation (site remediation often involves extensive decontamination and radioactive waste removal, followed by ongoing site monitoring and containment measures)
- Medium cost (assume decommissioning fraction between 5% and 10%) – all other

9.5.12.3 PC_EC_Split_LaG_Factor_Input

Input reference:	10.3
Description:	Matrix of maximum and minimum possible values for the initial fraction of secondary power capacity input energy consisting of liquid and gaseous fuels, divided by the LaG share of initial EC supply
Sources:	(Own estimate)

General calculations and assumptions

This is a measure of geographical remoteness – two tiers are identified:

• Some secondary PC types tend to be co-located with remote RE energy resources (solar PV, solar thermal generation, wind, hydropower, geothermal heat and generation, and other RE), therefore, the LaG factor can be assumed to be above one (range 1 to 1.4). • Most secondary PC types are not particularly remote and tend to be located closer to demand centres (all other), therefore, the LaG factor can be assumed to be around one (range 0.8 to 1.2).

9.5.12.4 PC_EC_Split_Heat_Factor_Input

Input reference:	10.4
Description:	Matrix of maximum and minimum possible values for the initial fraction of secondary power capacity input energy consisting of heat, divided by the heat share of initial EC supply
Sources:	(Own estimate)
General calculations and assumptions	
This is a measure of the degree of heavy industry required as well as direct process heat requirements. Secondary PC (energy conversion and fuel upgrading) requires significant heavy capital equipment and in many cases supplementary process heat, therefore, the heat factor can be assumed to be above one (range 1 to 1.4).	

9.5.12.5 PC_Build_Time_Input

Input reference:	10.5
Description:	Matrix of maximum and minimum possible values for secondary power capacity build time (investment decision to operation)
Sources:	54
General calculations and assumptions	
Three tiers are identified based on complexity and cost of planning, permitting, and construction (with reference to estimates from source 54): • Short (assume average build times between 0.5 and 1 years) – all heat and RE sources where electricity generation is considered primary • Long (assume average build times between 5 and 10 years) – refining, coal and gas to LaG, and nuclear generation • Medium (assume average build times between 3 and 6 years) – all other	

9.5.12.6 PC_Lifetime_Input

Input reference:	10.6
Description:	Matrix of maximum and minimum possible values for secondary power capacity lifetime (in operation)
Sources:	10, 54
General calculations and assumptions	

• Secondary PC generally has long lifetimes, higher for more complex and costly PC types.
• Three tiers are identified based on typical useful lifetimes of capital equipment (with reference to sources 10 and 54):
  o Medium (assume average lifetimes between 30 and 50 years) – all NRE associated PC except nuclear, biofuels, hydropower, and geothermal heat and generation
  o Long (assume average lifetimes between 40 and 60 years) – nuclear generation
  o Short (assume average lifetimes between 20 and 30 years) – all other	

9.5.12.7 AI_CapEx_Fraction_Input

Input reference:	10.7
Description:	Matrix of maximum and minimum possible values for the fraction of secondary auxiliary infrastructure investment energy devoted to capital (construction and decommissioning)
Sources:	(Own estimate)
General calculations and assumptions	
Two tiers are identified based on relative magnitude of ongoing operation and maintenance energy costs: • Low cost (assume CapEx fraction between 90% and 100%) – heat and LaG AI • High cost (assume CapEx fraction between 50% and 75%) – electricity and intermittent electricity AI (more complex infrastructure requiring more maintenance, replacement parts, and operational energy requirements)	

9.5.12.8 AI_Decommission_Fraction_Input

Input reference:	10.8
Description:	Matrix of maximum and minimum possible values for the fraction of secondary auxiliary infrastructure investment energy devoted to capital used in the decommissioning stage
Sources:	(Own estimate)
General calculations and assumptions	
Based on complexity and cost of site decommissioning, assume decommissioning fraction between 0% and 5% for all secondary AI types.	

9.5.12.9 AI_EC_Split_LaG_Factor_Input

Input reference:	10.9
Description:	Matrix of maximum and minimum possible values for the initial fraction of secondary auxiliary infrastructure input energy consisting of liquid and gaseous fuels, divided by the LaG share of initial EC supply
Sources:	(Own estimate)
General calculations and assumptions	
This is a measure of geographical remoteness – two tiers are identified: • Some secondary AI types tend to span vast distances (electricity and intermittent electricity), therefore, the LaG factor can be assumed to be above one (range 1 to 1.4). • Other secondary AI types are not particularly remote and tend to be primarily concentrated closer to demand centres (heat and LaG), therefore, the LaG factor can be assumed to be around one (range 0.8 to 1.2).	

9.5.12.10 AI_EC_Split_Heat_Factor_Input

Input reference:	10.10
Description:	Matrix of maximum and minimum possible values for the initial fraction of secondary auxiliary infrastructure input energy consisting of heat, divided by the heat share of initial EC supply
Sources:	(Own estimate)
General calculations and assumptions	
This is a measure of the degree of heavy industry required as well as direct process heat requirements. Secondary AI (EC transmission, transport, and distribution) requires significant heavy capital equipment and in some cases supplementary process heat, therefore, the heat factor can be assumed to be above one (range 1 to 1.4).	

9.5.12.11 AI_Build_Time_Input

Input reference:	10.11
Description:	Matrix of maximum and minimum possible values for secondary auxiliary infrastructure build time (investment decision to operation)
Sources:	(Own estimate)
General calculations and assumptions	
Two tiers are identified based on complexity and cost of planning, permitting, and construction: • Short (assume average build times between 0.5 and 1 years) – intermittent electricity and heat (simple and/or often built within an existing infrastructure footprint) • Long (assume average build times between 3 and 6 years) – electricity and LaG (more complex infrastructure typically involving greenfield development)	

9.5.12.12 AI_Lifetime_Input

Input reference:	10.12
Description:	Matrix of maximum and minimum possible values for secondary auxiliary infrastructure lifetime (in operation)
Sources:	(Own estimate)
General calculations and assumptions	
• Secondary AI generally has long lifetimes (transmission and distribution networks, pipelines, trucking, rail and shipping, terminals, etc.) except for intermittent electricity AI involving electrochemical storage.	

• Two tiers are identified based on typical useful lifetimes of capital equipment:
  ◦ Short (assume average lifetimes between 15 and 25 years) – intermittent electricity (will be shorter if dominated by electrochemical storage, longer if dominated by grid overbuild and other measures; this is not explicitly modelled)
  ◦ Long (assume average lifetimes between 30 and 60 years) – all other

9.5.12.13 Intermit_AI_Mult_Final_Input

Input reference:	10.13
Description:	Vector of maximum and minimum estimates for the final value (at intermittent penetration of 1) of the intermittent AI required multiplier (defined in the absence of alternative mitigation)
Sources:	10, 60, 62, 63, 64
General calculations and assumptions	

• This input refers to the final (100% intermittent generation) multiplier for the quantity of AI required (per unit of intermittent generation output) for intermittency mitigation, in the limiting case where no alternative mitigation measures occur (e.g., increased demand flexibility, CF curtailment for intermittent generation).
• Considering estimates given in the studies reviewed:
  ◦ These studies typically consider either intermittent generation penetration levels much lower than 100%, inadequate levels of intermittency mitigation (e.g., low storage capacity ignoring inter-seasonal requirements), or a combination of mitigation measures beyond infrastructure, therefore, will tend to underestimate in the quantity of AI required in the limiting case.
  ◦ Following consideration of these limitations in the studies below, an increase in the quantity of AI required for intermittent generation (energy cost per unit of delivered intermittent electricity) of one to two orders of magnitude is assumed (final multiplier of 10 to 100).
  ◦ This order of magnitude range broadly spans the available estimates, without unwarranted precision given underlying uncertainties.
  ◦ This range assumes no optimization of mitigation approaches beyond storage technology selection and identification of the optimal storage versus transmission overbuild balance (composition of intermittent electricity AI).	

Source-specific calculations and assumptions	
Source 10	• Table 6 shows balancing costs initially around \$3.50 2011 USD/MWh, rising to \$7 2011 US/MWh for intermittent penetration > 50%. • Balancing costs are estimated only up to 50% penetration. • A doubling of the aggregate quantity of intermittent electricity AI required at 100% penetration, from the 50% level, can be expected at a minimum (assuming at least a linear increase with intermittent penetration) • This corresponds to an approximate multiplier of 4.
Source 60	Comparing reported buffered and unbuffered EROI values indicates buffering infrastructure to cost approximately 1.5 to 4 times as much as the underlying generation output in energy terms: • Considering ECC estimates for secondary PC and corresponding primary EROI, this would imply final effective ECC for intermittency buffering to be in the approximate range of 2 to 15 years. • Given the range of possible values for peak factor for intermittent electricity AI, this implies an increase in the quantity of AI required in the range of 5 to 100. • This assumes this level of buffering (10 days storage) is sufficient for 100% penetration (highly optimistic).
Source 62	• Figure 4 shows increases in combined EPBT for wind & solar for 72 hrs storage of approximately 0.8 to 1 years (ignoring geologic storage only). • This is highly optimistic, as seasonal storage requirements much longer than 72 hours are not considered. • This translates to an increase in the energy intensity of intermittent electricity AI by an approximate factor of 2 to 5, given the range of possible values for peak factor for intermittent electricity AI.
Source 63	• Table 3 indicates that the embodied energy of storage is 4 (wind) to 113 (solar PV) times more than that of generation capacity over the same timeframe (50 years), depending on the choice of storage technology (PHS is much lower, but is geographically limited).

	• This translates to an increase in the energy intensity of intermittent electricity AI of approximately 30 to 300, taking into average peak factors for intermittent electricity AI. • The high end of this range should be disregarded, as it corresponds to using only electrochemical storage (without transmission overbuild) combined with solar PV, alongside very low levels of demand flexibility.
Source 64	• This review suggests integration costs of £15 to £45/MWh for 50% penetration (~$20 to $65 USD/MWh). • The upper end of this range, corresponding to relatively inflexible systems where few other mitigation measures are taken, should be used. • This is roughly equivalent to higher LCOE values, implying an increase in the energy intensity of intermittent electricity AI of approximately 10 (an order of magnitude increase). • This figure is highly optimistic, given that it relates to 50% penetration, so a doubling of the aggregate quantity of intermittent electricity AI required at 100% penetration, from the 50% level, can be expected at a minimum (assuming at least a linear increase with intermittent penetration).

9.5.12.14 Retic_Eff_Mult_Final_Input

Input reference:	10.14
Description:	Vector of maximum and minimum estimates for the final value (at intermittent penetration of 1) of the intermittent reticulation efficiency multiplier (defined in the absence of alternative mitigation)
Sources:	65
General calculations and assumptions	
Assume upper and lower limits for the intermittent RE reticulation efficiency multiplier at 100% intermittent penetration, in the limiting case where no alternative mitigation measures occur (e.g., increased demand flexibility, CF curtailment for intermittent generation, etc.): • The upper limit (80%) corresponds approximately to a combination of long-distance transmission efficiency and round-trip storage efficiency, weighted towards transmission. • The lower limit (60%) corresponds approximately to a combination of long-distance transmission efficiency and round-trip storage efficiency, weighted towards storage.	
Source-specific calculations and assumptions	
Source 65	• Local efficiencies for intermittent generation plus storage are found to be in the range of 70% to 90%. • Adding the effect of typical transmission efficiency to this to give a system-level figure gives approximately 60% to 80%.

9.5.12.15 CF_Max_Mult_Final

Input reference:	10.15
Description:	Estimate for the final value (at intermittent penetration of 1) of the CF reduction multiplier (defined in the absence of alternative mitigation; approximates 0 by definition)
Sources:	10
General calculations and assumptions	
It is assumed intermittent RE PC behaves similarly to baseload PC near the lower CF asymptote (with different slope).	
Source-specific calculations and assumptions	
Source 10	• As shown in figure 22 on page 41, NREL assumes the CF of baseload generation converges to zero as intermittent penetration rises to 100%. • The logistic function cannot accept zero as a lower asymptote, so 0.01 is used as an approximation.

9.5.12.16 Diversity_Coeff_Input

Input reference:	10.16
Description:	Vector of maximum and minimum estimates for the magnitude of the fractional reduction in intermittent response (CF reduction, intermittent AI increase, reticulation efficiency reduction) needed when intermittent diversity is equal to 1

Sources:	(Own estimate)
General calculations and assumptions	

- A higher diversity of intermittent RE sources that are not correlated to each other in output will lessen the need for intermittency mitigation measures to some degree.
- Assume a fractional reduction in need for mitigation measures when intermittent diversity is equal to one is between 0.1 and 0.25 (perfect diversity of intermittent RE sources requires 10-25% less mitigation effort).
- This is significant, but relatively minor, as even with high diversity periods where all intermittent RE output is near zero in any region will still occur.

9.5.12.17 Demand_Flex_Coeff_Input

Input reference:	10.17
Description:	Vector of maximum and minimum estimates for the magnitude of the fractional reduction in intermittent response (CF reduction, intermittent AI increase, reticulation efficiency reduction) needed when demand flexibility is equal to 1
Sources:	(Own estimate)
General calculations and assumptions	

It is assumed the fractional reduction in need for mitigation measures when demand flexibility is equal to one is between 0.25 and 0.75 (perfect flexibility of demand requires 25-75% less mitigation effort):

- This is potentially highly significant, as demand-side adaptation to align with intermittent supply can greatly reduce the need for mitigation measures.
- Note that even with perfect demand flexibility, high intermittent penetration still requires mitigation measures as demand cannot always conform perfectly to intermittent RE output due to operational and temporal limiations (e.g., industrial process demand).

9.5.12.18 CF_Max_Peaker_Coeff_Input

Input reference:	10.18
Description:	Vector of maximum and minimum estimates for the magnitude of the CF reduction response to intermittent penetration, relative to the intermittent generator response, for peaking generators
Sources:	(Own estimate)
General calculations and assumptions	

- Peaker CF moves in the opposite direction to intermittent RE and baseload CF as intermittent penetration increases:
    - Higher intermittent output increases the need for fast peaking generation to fill gaps between supply and demand.
    - Note that this does not necessarily increase the quantity of peaking generation capacity in the system (although this can happen indirectly due to higher CF affecting yield calculations), only its utilization.
- Gas and oil generation PC does not consist entirely of peaking plant, as closed-cycle turbines will also be present, although these could become less common in the future electricity system as the need for slow-ramping baseload generation declines.
- A lower limit is given by the final practical level that peaker CF could conceivably reach while still being classified as peaking plant – a final CF of 0.7 for gas generation corresponds to a peaker coefficient of approximately -0.7.
- An upper limit of -0.5 is assumed (peaker CF to converge to at least 150% of its original value as intermittent penetration approaches 100%).

9.5.12.19 CF_Max_Baseload_Coeff_Input

Input reference:	10.19
Description:	Vector of maximum and minimum estimates for the magnitude of the CF reduction response to intermittent penetration, relative to the intermittent generator response, for baseload generators
Sources:	(Own estimate)
General calculations and assumptions	

- Baseload CF moves in the same direction as intermittent RE CF. Baseload utilization is reduced as intermittent penetration increases, due to operational limitations and the costs of more frequent start-up and shutdown procedures.
- Assume baseload exhibits between 50% and 150% of the CF response of intermittent RE:

◦ The relative response compared with that of intermittent RE at high intermittent generation penetration levels is uncertain. ◦ Both curves converge to the same lower asymptote of CF = 0.01 near 100% intermittent generation penetration.

9.5.12.20 Sec_Intermittent_ID

Input reference:	10.20
Description:	Vector of intermittent generation identities by secondary PC type
Sources:	(Own estimate)

General calculations and assumptions

- Assume intermittent generation includes:
    - Solar PV
    - Solar thermal generation
    - Wind
    - Other RE
- These RE sources are not intermittent to the same degree, e.g., solar thermal generation is typically sited in places where sunshine is much more consistent than typical small-scale solar PV.
- Other RE is currently very minor but consists mostly of wave and tidal energy, which are intermittent.
- Hydropower is not counted as intermittent – although run-of-river hydropower can be intermittent it is a small component of overall hydropower globally.
- Other RE is considered non-intermittent (dispatchable) in scenario 1 (Energy breakthrough).

9.5.12.21 Sec_Baseload_ID

Input reference:	10.21
Description:	Vector of baseload generation identities by secondary PC type
Sources:	

General calculations and assumptions

Values are equal to one for electricity generator types considered to be baseload (dispatchable) and zero otherwise

9.5.12.22 Sec_Peaker_ID

Input reference:	10.22
Description:	Vector of peaking generation identities by secondary PC type
Sources:	

General calculations and assumptions

Values are equal to one for electricity generator types considered to be peaking plant (dispatchable and rapidly ramping, designed to respond to short-term demand variations) and zero otherwise.

9.5.13 End-use sector

9.5.13.1 PC_CapEx_Fraction_Input

Input reference:	11.1
Description:	Matrix of maximum and minimum possible values for the fraction of end-use power capacity investment energy devoted to capital (construction and decommissioning)
Sources:	(Own estimate)

General calculations and assumptions

- End-use PC generally has lower relative ongoing operation and maintenance energy costs than primary or secondary PC, as these are typically devices and vehicles designed to convert ECs to energy services (simpler and more standardized than primary or secondary PC), requiring only basic maintenance.
- Two tiers are identified based on relative magnitude of ongoing operation and maintenance energy costs:
    - Low cost (assume CapEx fraction between 90% and 100%) – all electricity consuming end-use PC except EVs and electric heating high
    - High cost (assume CapEx fraction between 75% and 90%) – all other (greater upkeep requirements due to mechanical and high temperature processes)

• EVs have a lower CapEx fraction because battery replacement must occur mid-life to enable full vehicle lifetime.

9.5.13.2 PC_Decommission_Fraction_Input

Input reference:	11.2
Description:	Matrix of maximum and minimum possible values for the fraction of end-use power capacity investment energy devoted to capital used in the decommissioning stage
Sources:	(Own estimate)
General calculations and assumptions	
Two tiers are identified based on complexity and cost of PC decommissioning and disposal/recycling: • High cost (assume decommissioning fraction between 5% and 10%) – IPaC, electric vehicles, all rail, shipping and aviation, all high temperature heating • Low cost – all other – assume decommissioning fraction between 0% and 5%	

9.5.13.3 PC_EC_Split_LaG_Factor_Input

Input reference:	11.3
Description:	Matrix of maximum and minimum possible values for the initial fraction of end-use power capacity input energy consisting of liquid and gaseous fuels, divided by the LaG share of initial EC supply
Sources:	(Own estimate)
General calculations and assumptions	
This is a measure of geographical remoteness. End-use PC is not typically geographically remote and tends to be located closer to demand centres, the LaG factor for all end-use PC types can be assumed to be around one (range 0.8 to 1.2).	

9.5.13.4 PC_EC_Split_Heat_Factor_Input

Input reference:	11.4
Description:	Matrix of maximum and minimum possible values for the initial fraction of end-use power capacity input energy consisting of heat, divided by the heat share of initial EC supply
Sources:	(Own estimate)
General calculations and assumptions	
This is a measure of the degree of heavy manufacturing required as well as embodied energy – two tiers are identified: • Some end-use PC types require significant heavy industry to produce and contain large quantities of high-embodied energy materials and components (IPaC, heavy vehicles, all rail, shipping and aviation, all high temperature heating), therefore, the heat factor can be assumed to be above one (range 1 to 1.4). • Most end-use PC types require only standard manufacturing processes (all other), therefore, the heat factor can be assumed to be around one (range 0.8 to 1.2).	

9.5.13.5 PC_Build_Time_Input

Input reference:	11.5
Description:	Matrix of maximum and minimum possible values for end-use power capacity build time (investment decision to operation)
Sources:	(Own estimate)
General calculations and assumptions	
Three tiers are identified based on complexity and cost of manufacturing and lead times involved: • Long (assume average build times between 1 and 3 years) – all rail, shipping, aviation, and all high temperature heating • Medium (assume average build times between 0.5 and 1 years) – light and heavy vehicles • Short (assume average build times between 0.2 and 0.5 years) – all other	

9.5.13.6 PC_Lifetime_Input

Input reference:	11.6
Description:	Matrix of maximum and minimum possible values for end-use power capacity lifetime (in operation)
Sources:	(Own estimate)
General calculations and assumptions	

• As end-use PC types are mostly vehicles or consumer goods, lifetimes are typically much shorter than primary or secondary PC, rarely beyond 30 years.
• Three tiers are identified based on typical useful lifetimes:
  o Short (assume average lifetimes between 5 and 10 years) – electric lighting and IPaC
  o Medium (assume average lifetimes between 10 and 20 years) – LaG fuel mechanical, light and heavy vehicles, electric cooling, all heating low
  o Long (assume average lifetimes between 20 and 40 years) – all other

9.5.13.7 AI_CapEx_Fraction_Input

Input reference:	11.7
Description:	Matrix of maximum and minimum possible values for the fraction of end-use auxiliary infrastructure investment energy devoted to capital (construction and decommissioning)
Sources:	(Own estimate)
General calculations and assumptions	
Two tiers are identified based on relative magnitude of ongoing operation and maintenance energy costs: • High cost (assume CapEx fraction between 75% and 90%) – IPaC, roading, rail, aviation, and shipping • Low cost (assume CapEx fraction between 90% and 100%) – all other	

9.5.13.8 AI_Decommission_Fraction_Input

Input reference:	11.8
Description:	Matrix of maximum and minimum possible values for the fraction of end-use auxiliary infrastructure investment energy devoted to capital used in the decommissioning stage
Sources:	(Own estimate)
General calculations and assumptions	
Two tiers are identified based on complexity and cost of end-use AI decommissioning and site restoration: • High cost (assume decommissioning fraction between 5% and 10%) – roading, rail, aviation, and shipping • Low cost (assume decommissioning fraction between 0% and 5%) – all other	

9.5.13.9 AI_EC_Split_LaG_Factor_Input

Input reference:	11.9
Description:	Matrix of maximum and minimum possible values for the initial fraction of end-use auxiliary infrastructure input energy consisting of liquid and gaseous fuels, divided by the LaG share of initial EC supply
Sources:	(Own estimate)
General calculations and assumptions	
This is a measure of geographical remoteness – two tiers are identified: • Some end-use AI types tend to be distributed along transit corridors (LaG, roading, EV, rail, and rail electrification), therefore, the LaG factor can be assumed to be above one (range 1 to 1.4). • Other end-use AI types are not particularly remote and tend to be primarily concentrated closer to demand centres (all other), therefore, the LaG factor can be assumed to be around one (range 0.8 to 1.2).	

9.5.13.10 AI_EC_Split_Heat_Factor_Input

Input reference:	11.10
Description:	Matrix of maximum and minimum possible values for the initial fraction of end-use auxiliary infrastructure input energy consisting of heat, divided by the heat share of initial EC supply
Sources:	(Own estimate)
General calculations and assumptions	
This is a measure of the degree of heavy industry required as well as embodied energy – two tiers are identified: • Some end-use AI types require significant heavy industry to produce and contain large quantities of high-embodied energy materials such as concrete and steel (IPaC, roading, rail, shipping, and aviation), therefore, the heat factor can be assumed to be above one (range 1 to 1.4). • Other end-use AI types require only standard construction and installation processes (all other), therefore, the heat factor can be assumed to be around one (range 0.8 to 1.2).	

9.5.13.11 AI_Build_Time_Input

Input reference:	11.11
Description:	Matrix of maximum and minimum possible values for end-use auxiliary infrastructure build time (investment decision to operation)
Sources:	(Own estimate)
General calculations and assumptions	
Two tiers are identified based on complexity and cost of planning, permitting, and construction: • Long (assume average build times between 3 and 6 years) – roading, rail, shipping, and aviation (more complex infrastructure often involving greenfield development) • Short (assume average build times between 0.5 and 1 years) – all other (simple or often built within existing infrastructure footprint)	

9.5.13.12 AI_Lifetime_Input

Input reference:	11.12
Description:	Matrix of maximum and minimum possible values for end-use auxiliary infrastructure lifetime (in operation)
Sources:	(Own estimate)
General calculations and assumptions	
• End-use AI generally has long lifetimes, except for IPaC and EV AI due to rapid obsolescence of technology. • Two tiers are identified based on typical useful lifetimes of capital equipment: o Short (assume average lifetimes between 5 and 15 years) – IPaC and EV o Long (assume average lifetimes between 25 and 50 years) – all other	

9.5.13.13 PC_AI_ID

Input reference:	11.13
Description:	Matrix of EU AI requirement identities by EU PC type
Sources:	
General calculations and assumptions	
Values are equal to one where a given EU PC type requires associated AI and zero otherwise: • EU PC types that consume electricity, LaG fuels, and heat are assumed to require electrical AI, LaG AI and heating AI, respectively. • All road vehicles are assumed to require roading AI. • All rail types are assumed to require rail AI. • All aviation types are assumed to require aviation AI. • All shipping types are assumed to require shipping AI. • IPaC, EVs, and electrified rail are assumed to require additional AI specific to their type.	

9.5.14 System control

9.5.14.1 ESMR_Limit_Input

Input reference:	12.1
Description:	Vector of maximum and minimum estimates for the upper limit for the share of EC inflow that can be used within the GES metabolism (investment in new PC drops to zero at this limit)
Sources:	(Own estimate)
General calculations and assumptions	
• The ESMR refers to the upper limit for the share of EC inflow that can be used within the GES metabolism, rather than for final consumption (investment in new PC drops to zero at this limit). • This limit must be somewhere between the initial maximum ESMR and one (where all inflow for a particular EC is being consumed within the GES metabolism). • The lower bound established by comparison to the initial maximum ESMR, allowing for the curtailment threshold (optimistically assuming that investment flows are not initially constrained due to the ESMR)	

◦ Running 200 model realizations reveals that the initial maximum ESMR can be expected to fall within 0.03 to 0.12 (P5 to P95), with a mean of approximately 0.07 (initial maximum is for heat ESMR in all cases, but values are similar for LaG fuels and electricity) ◦ To be initially unconstrained for most realizations (beginning of the curtailment range starting at 0.1) with a curtailment threshold value of 0.8 implies a lower bound for the ESMR limit of 0.5 • Lower values are more likely than higher as values close to one would be much more likely to imply an unmanageable diversion of energy from final consumption, hence a triangular distribution is used (with probability maximum at the lower bound and zero at the upper bound). ◦ The cumulative probability of exceeding falls as the value rises. ◦ Little else is known about the shape of the distribution, so a linear PDF is appropriate. • This means the investment curtailment range starts at a minimum of 0.1 and a maximum of 0.2 (where full investment is still possible; corresponds to ESMR limits of 0.5 and 1 respectively) up to the actual ESMR limit (where investment is completely curtailed due to excessive ESMR).

9.5.14.2 Sec_Penetration_Limit_Input

Input reference:	12.2
Description:	Vector of maximum and minimum estimates for the penetration limits for secondary PC types (at this limit, no further investment can occur due to operational limitations)
Sources:	(Own estimate)
General calculations and assumptions	
Assume penetration limits for secondary PC types (upstream) based on the characteristics of the PC in relation to EC demand: • Constrained to low penetration (can only feasibly provide a minor contribution to EC supply; assume penetration limit between 10% and 30%) – oil heat, all CHP, and all RE heat (all suitable for niche uses only due to technical limitations or required co-location of demand; RE sources cannot supply heat levels required for some industrial processes) • Constrained to less than full penetration (can provide most, but not all, EC supply; assume penetration limit between 75% and 100%) – gas and coal to LaG and biofuels (limited fuel hydrocarbon fractions can be produced), gas heat (coal required for some industrial processes), and coal, geothermal and nuclear generation (baseload plant unable to meet all electricity demand due to ramping limitations) • Unconstrained – all other	

9.5.14.3 EU_Penetration_Limit_Input

Input reference:	12.3
Description:	Vector of maximum and minimum estimates for the penetration limits for EU PC types (at this limit, no further investment can occur due to operational limitations)
Sources:	(Own estimate)
General calculations and assumptions	
Assume penetration limits for end-use PC types (downstream) based on the characteristics of the PC in relation to ES demand: • Constrained to low penetration (can only feasibly provide a minor contribution to ES due to practicality issues; assume penetration limit between 10% and 30%) – regional shipping (geographic constraints), regional aviation (suitable only for longer distances), and LaG heating (air quality issues and suitable only for residential usage in cold climates) • Constrained to less than full penetration (can provide most, but not all, of a particular ES; assume penetration limit between 75% and 100%) – electrical mechanical (some mechanical energy is required far from electricity supply), LaG fuel mechanical (noise and air quality issues), rail (some proportion of transportation demand will always be to/from locations far from rail networks), electric vehicles (some proportion of transportation demand will always be beyond electric vehicle range limitations, outside regions with charging infrastructure), IC shipping (geographic constraints), and high temperature electric heating (heating using electricity unsuitable for some high temperature industrial processes) • Unconstrained – all other	

9.5.14.4 NRE_Annual_Utility_Reduction

Input reference:	12.4
Description:	Assumed baseline annual rate of reduction in upstream utility values linked to NRE sources (actual rate weighted by emissions intensities; required to represent policy efforts directed to transitioning away from NRE towards RE)
Sources:	(Own estimate)
General calculations and assumptions	
2.5%/yr is used as the base annual reduction in upstream utility for NRE sources: • This gives a utility halving time of approximately 28 years (a reduction in utility of ~90% occurs over the simulated period). • This base rate is weighted by NRE emissions intensity (GtCO2e/EJ) of each fuel relative to the average across all NRE.	

9.5.14.5 Scenario_5

Input reference:	12.5
Description:	Scenario 5 identity
Sources:	(Own estimate)
General calculations and assumptions	
This value is equal to 1 when scenario 5 is active and 0 otherwise. This acts as a switch to block any downstream investment based on utility (upkeep only) until 35 years have elapsed (2050).	

9.5.14.6 EC_Surplus_Scale_Factor

Input reference:	12.6
Description:	Scaling factor applied to negative values of forecast EC supply/demand balance (EC deficit, measured in EJ) at the selected time horizon (used for utility calculation; represents balance between stability and efficiency in share calculation)
Sources:	(Own estimate)
General calculations and assumptions	
• A scaling factor is applied to negative values of forecast EC supply/demand balance (EC deficit, measured in EJ) at the selected time horizon. • Negative values (surplus) should not be acted on as strongly as positive values (deficit). • This affects the upstream and downstream utility calculations and is tuned to balance stability and efficiency in the investment share calculation. • 0.1 was used after testing various values.	

9.5.14.7 Invest_Time_Horizon

Input reference:	12.7
Description:	Selected time horizon for calculating forecast EC supply/demand balance
Sources:	(Own estimate)
General calculations and assumptions	
• This is the selected time horizon for calculating forecast EC supply/demand balance. • A higher value will optimize for long-term outcomes at the cost of larger short-term variations in the supply/demand balance. • 10 years was selected after testing various values.	

9.5.14.8 PC_Invest_Max_Fraction

Input reference:	12.8
Description:	Maximum ratio between actual investment flow for any secondary/EU PC type and the investment flow which would be required if all EC production/ES provision was provided by that PC type
Sources:	(Own estimate)
General calculations and assumptions	
• This is a maximum allowable ratio between actual investment flow for any secondary or end-use PC type and the investment flow which would be required if all EC production or ES provision was provided by that PC type.	

• This limit is required to prevent overinvestment in PC due to temporary spikes in investment signals. • A factor of 10 was selected after testing various values.

9.5.14.9 EC_Split_Correlation_Factor

Input reference:	12.9
Description:	Estimate for correlation factor used in the generation of EC split heat and LaG factors
Sources:	(Own estimate)
General calculations and assumptions	
• This is the correlation factor used in the stochastic generation of EC split heat and LaG factors. • This is needed as EC split heat and LaG factors are not independent, i.e., higher values in one will tend to occur with higher values in others. • As the strength of this relationship is expected to be relatively high, a correlation factor of 0.8 is used.	

9.5.14.10 EROI_ECC_Correlation_Factor

Input reference:	12.10
Description:	Estimate for correlation factor used in the generation of EROI and ECC values
Sources:	(Own estimate)
General calculations and assumptions	
• This is the correlation factor used in the stochastic generation of EROI and ECC values. • This is needed as EROI and ECC values are not independent, i.e., higher values in one will tend to occur with higher values in others. • As the strength of this relationship is expected to be moderate, a correlation factor of 0.5 is used.	

9.5.15 Final input arrays

The arrays are displayed in landscape, grouped by the primary (higher order) label set. All arrays except those in red text have been transposed for display purposes.

9.5.15.1 NRE types

Input ref.	**Secondary labels**	*Oil*	*Natural_gas*	*Coal*	*Nuclear_fuels*
1.3		181.6	126.1	160.9	27.0
1.7		0.016	0.022	-0.010	0.019
2.1	*Mean*	10115	14103	17886	2824
	SD	3787	6817	6688	845
2.3		0.95	0.95	0.85	0.85
2.5		22.9	7.0	2.2	0.0
2.6		0.072	0.053	0.093	0.000
6.4	*Mean*	18.9	34.9	52.7	185.0
	SD	9.1	25.0	25.4	37.8
6.5	*Max*	5	5	5	5
	Min	1	1	1	1
6.6	*Max*	90	200	79	185
	Min	30	57	19	19
8.1	*Max*	0.9	0.9	0.75	0.75

Input ref.	**Secondary labels**	*Oil*	*Natural_gas*	*Coal*	*Nuclear_fuels*
	Min	0.75	0.75	0.5	0.5
8.2	*Max*	0.05	0.05	0.2	0.2
	Min	0	0	0.1	0.1
8.3	*Max*	1.4	1.4	1.4	1.4
	Min	1	1	1	1
8.4	*Max*	1.4	1.4	1.4	1.4
	Min	1	1	1	1
8.5	*Max*	5	5	10	10
	Min	2	2	5	5
8.6	*Max*	25	25	40	40
	Min	10	10	15	15

9.5.15.2 RE types

Input reference	**Secondary labels**	*Solar_PV*	*Solar_thermal*	*Wind*	*Biomass*	*Hydropower*	*Geothermal*	*Other*
1.4		1.08	1.35	3.21	55.29	14.26	2.59	0.02
1.8		0.308	0.055	0.138	0.010	0.023	0.044	0.147
2.2	*Mean*	101.5	79.5	106.2	176.1	47.8	72.4	7.4
	SD	54.8	70.2	100.2	104.3	20.8	59.9	4.4
2.4		0.14	0.33	0.26	0.75	0.43	0.84	0.35
6.1	*Mean*	12.2	75.5	45.9	18.0	87.0	31.0	20.1
	SD	7.3	24.5	23.9	2.0	38.6	19.0	15.2
6.2	*Max*	5	5	5	2	5	5	2
	Min	1	1	1	1	1	1	1
6.3	*Max*	1.2	7.6	4.6	18.0	87.0	31.0	2.0
	Min	0	0	0	1.8	8.7	3.1	0
9.1	*Max*	1	0.9	1	0.75	1	0.9	0.9
	Min	0.9	0.75	0.9	0.25	0.9	0.75	0.75
9.2	*Max*	0.05	0.05	0.05	0.05	0.05	0.05	0.05
	Min	0	0	0	0	0	0	0
9.3	*Max*	1.2	1.4	1.4	1.4	1.4	1.4	1.4
	Min	0.8	1	1	1	1	1	1
9.4	*Max*	1.4	1.4	1.4	1.4	1.4	1.4	1.4
	Min	1	1	1	1	1	1	1
9.5	*Max*	3	5	5	5	8	5	5
	Min	1	2	2	2	4	2	2
9.6	*Max*	30	30	30	50	100	50	30

Input reference	Secondary labels	*Solar_PV*	*Solar_thermal*	*Wind*	*Biomass*	*Hydropower*	*Geothermal*	*Other*
	Min	20	20	20	30	50	30	20

9.5.15.3 Secondary PC types

9.5.15.3.1 Label index 1-12

Input reference	Secondary labels	*Oil_generation*	*Refining*	*Oil_heat*	*Gas_generation*	*Gas_to_LaG*	*Gas_heat*	*Gas_CHP*	*Coal_generation*	*Coal_to_LaG*	*Coal_heat*	*Coal_CHP*	*Nuclear_generation*
1.1	*Numeral*	0.0467	0.9532	0.0002	0.3432	0.0054	0.5447	0.1067	0.5056	0.0023	0.3482	0.1439	1.0000
	Error	0.1	0.1	0.1	0.1	0.1	0.1	0.1	0.1	0.1	0.1	0.1	0.1
1.9		-0.012	0.016	-0.083	0.035	-0.011	0.011	-0.012	0.013	0.149	-0.033	-0.004	0.009
3.1		0.26	0.93	0.20	0.42	0.93	0.70	0.80	0.67	0.89	0.80	0.70	0.89
3.4	*Electricity*	1	0	0	1	0	0	0.54	1	0	0	0.63	1
	LaG_fuels	0	1	0	0	1	0	0	0	1	0	0	0
	Heat	0	0	1	0	0	1	0.46	0	0	1	0.37	0
3.7	*Oil*	1	1	1	0	0	0	0	0	0	0	0	0
	Natural_gas	0	0	0	1	1	1	1	0	0	0	0	0
	Coal	0	0	0	0	0	0	0	1	1	1	1	0
	Nuclear_fuels	0	0	0	0	0	0	0	0	0	0	0	1
3.8	*Solar_PV*	0	0	0	0	0	0	0	0	0	0	0	0
	Solar_thermal	0	0	0	0	0	0	0	0	0	0	0	0
	Wind	0	0	0	0	0	0	0	0	0	0	0	0
	Biomass	0	0	0	0	0	0	0	0	0	0	0	0
	Hydropower	0	0	0	0	0	0	0	0	0	0	0	0
	Geothermal	0	0	0	0	0	0	0	0	0	0	0	0
	Other	0	0	0	0	0	0	0	0	0	0	0	0
4.1	*Max*	0.50	0.98	0.79	0.52	0.55	0.89	0.74	0.44	0.85	0.94	0.66	0.39
	Min	0.32	0.94	0.69	0.42	0.44	0.78	0.59	0.34	0.68	0.81	0.53	0.33
4.2	*Max*	0.96	1.00	0.95	0.96	1.00	0.95	0.96	0.96	1.00	0.95	0.96	0.96
	Min	0.89	1.00	0.83	0.89	1.00	0.83	0.86	0.89	1.00	0.83	0.87	0.89
4.3		1890	1870	1870	1940	1930	1930	1970	1883	1930	1800	1970	1956
7.1	*Mean*	1.5	1.5	0.05	0.5	1.5	0.05	0.5	1.5	1.5	0.05	1.5	1.5
	SD	1.5	1.5	0.05	0.5	1.5	0.05	0.5	1.5	1.5	0.05	1.5	1.5
10.1	*Max*	0.75	0.5	1	0.75	0.75	1	0.75	0.5	0.5	0.75	0.5	0.5
	Min	0.5	0.25	0.9	0.5	0.5	0.9	0.5	0.25	0.25	0.5	0.25	0.25
10.2	*Max*	0.05	0.1	0.05	0.05	0.1	0.05	0.1	0.1	0.1	0.1	0.1	0.3
	Min	0	0.05	0	0	0.05	0	0.05	0.05	0.05	0.05	0.05	0.1

Input reference	Secondary labels	Oil_generation	Refining	Oil_heat	Gas_generation	Gas_to_LaG	Gas_heat	Gas_CHP	Coal_generation	Coal_to_LaG	Coal_heat	Coal_CHP	Nuclear_generation
10.3	*Max*	1.2	1.2	1.2	1.2	1.2	1.2	1.2	1.2	1.2	1.2	1.2	1.2
	Min	0.8	0.8	0.8	0.8	0.8	0.8	0.8	0.8	0.8	0.8	0.8	0.8
10.4	*Max*	1.4	1.4	1.4	1.4	1.4	1.4	1.4	1.4	1.4	1.4	1.4	1.4
	Min	1	1	1	1	1	1	1	1	1	1	1	1
10.5	*Max*	6	10	1	6	10	1	6	6	10	1	6	10
	Min	3	5	0.5	3	5	0.5	3	3	5	0.5	3	5
10.6	*Max*	50	50	50	50	50	50	50	50	50	50	50	60
	Min	30	30	30	30	30	30	30	30	30	30	30	40
10.20		0	0	0	0	0	0	0	0	0	0	0	0
10.21		0	0	0	0	0	0	0	1	0	0	0	1
10.22		1	0	0	1	0	0	0	0	0	0	0	0
12.2	*Max*	999	999	0.3	999	1	1	0.3	1	1	999	0.3	1
	Min	999	999	0.1	999	0.75	0.75	0.1	0.75	0.75	999	0.1	0.75

9.5.15.3.2 Label index 13-24

Input reference	Secondary labels	Solar_PV_generation	Solar_thermal_generation	Solar_thermal_heat	Wind_generation	Biomass_generation	Biofuels	Biomass_heat	Biomass_CHP	Hydropower_generation	Geothermal_generation	Geothermal_heat	Other_generation
1.1	*Numeral*	1.0000	0.0903	0.9097	1.0000	0.0616	0.1237	0.7818	0.0329	1.0000	0.8053	0.1947	1.0000
	Error	0.1	0.1	0.1	0.1	0.1	0.2	0.1	0.1	0.1	0.1	0.1	0.1
1.9		0.325	0.132	0.049	0.142	0.122	0.051	-0.001	0.034	0.023	0.043	0.105	0.104
3.1		0.14	0.33	0.33	0.26	0.73	0.74	0.20	0.63	0.40	0.77	0.28	0.35
3.4	*Electricity*	1	1	0	1	1	0	0	0.45	1	1	0	1
	LaG_fuels	0	0	0	0	0	1	0	0	0	0	0	0
	Heat	0	0	1	0	0	0	1	0.55	0	0	1	0
3.7	*Oil*	0	0	0	0	0	0	0	0	0	0	0	0
	Natural_gas	0	0	0	0	0	0	0	0	0	0	0	0
	Coal	0	0	0	0	0	0	0	0	0	0	0	0
	Nuclear_fuels	0	0	0	0	0	0	0	0	0	0	0	0
3.8	*Solar_PV*	1	0	0	0	0	0	0	0	0	0	0	0
	Solar_thermal	0	1	1	0	0	0	0	0	0	0	0	0
	Wind	0	0	0	1	0	0	0	0	0	0	0	0
	Biomass	0	0	0	0	1	1	1	1	0	0	0	0
	Hydropower	0	0	0	0	0	0	0	0	1	0	0	0
	Geothermal	0	0	0	0	0	0	0	0	0	1	1	0

Input reference	Secondary labels	Solar_PV_generation	Solar_thermal_generation	Solar_thermal_heat	Wind_generation	Biomass_generation	Biofuels	Biomass_heat	Biomass_CHP	Hydropower_generation	Geothermal_generation	Geothermal_heat	Other_generation
	Other	0	0	0	0	0	0	0	0	0	0	0	1
4.1	*Max*	1.00	0.27	1.00	1.00	0.39	0.60	0.91	0.69	1.00	0.12	0.63	1.00
	Min	1.00	0.22	1.00	1.00	0.27	0.48	0.79	0.55	1.00	0.10	0.50	1.00
4.2	*Max*	0.91	0.91	0.95	0.91	0.96	1.00	0.95	0.96	0.91	0.96	0.95	0.91
	Min	0.84	0.84	0.83	0.84	0.89	1.00	0.83	0.86	0.84	0.89	0.83	0.84
4.3		1965	1980	1900	1960	1980	1900	1800	1980	1888	1960	1900	1970
7.1	*Mean*	0.05	0.5	0.05	0.05	2.5	2.5	0.05	1.5	0.05	0.5	0.05	0.05
	SD	0.05	0.5	0.05	0.05	2.5	2.5	0.05	1.5	0.05	0.5	0.05	0.05
10.1	*Max*	1	0.75	0.75	1	0.5	0.5	0.5	0.5	1	0.75	0.75	1
	Min	0.9	0.5	0.5	0.9	0.25	0.25	0.25	0.25	0.9	0.5	0.5	0.9
10.2	*Max*	0.05	0.1	0.1	0.1	0.1	0.1	0.1	0.1	0.1	0.1	0.1	0.1
	Min	0	0.05	0.05	0.05	0.05	0.05	0.05	0.05	0.05	0.05	0.05	0.05
10.3	*Max*	1.4	1.4	1.2	1.4	1.2	1.2	1.2	1.2	1.4	1.4	1.4	1.4
	Min	1	1	0.8	1	0.8	0.8	0.8	0.8	1	1	1	1
10.4	*Max*	1.4	1.4	1.4	1.4	1.4	1.4	1.4	1.4	1.4	1.4	1.4	1.4
	Min	1	1	1	1	1	1	1	1	1	1	1	1
10.5	*Max*	1	6	6	1	6	6	1	6	1	6	1	1
	Min	0.5	3	3	0.5	3	3	0.5	3	0.5	3	0.5	0.5
10.6	*Max*	30	30	30	30	30	50	30	30	50	50	30	30
	Min	20	20	20	20	20	30	20	20	30	30	20	20
10.20		1	1	0	1	0	0	0	0	0	0	0	1
10.21		0	0	0	0	1	0	0	0	0	1	0	0
10.22		0	0	0	0	0	0	0	0	0	0	0	0
12.2	*Max*	999	999	0.3	999	999	1	0.3	0.3	999	1	0.3	999
	Min	999	999	0.1	999	999	0.75	0.1	0.1	999	0.75	0.1	999

9.5.15.4 End-use PC types

9.5.15.4.1 Label index 1-13

Input reference	Secondary labels	Electric_lighting	IPaC_devices	Electric_mechanical	LaG_fuel_mechanical	ICEV_light	ICEV_heavy_passenger	ICE_rail_passenger	Electric_vehicles	Electric_rail_passenger	Aviation_passenger_regional	Shipping_passenger_regional	Aviation_passenger_IC	Shipping_passenger_IC
1.2	*Numeral*	0.105	0.121	0.382	0.135	0.373	0.053	0.004	0.002	0.003	0.034	0.009	0.054	0.003

Input reference	Secondary labels	Electric_lighting	IPaC_devices	Electric_mechanical	LaG_fuel_mechanical	ICEV_light	ICEV_heavy_passenger	ICE_rail_passenger	Electric_vehicles	Electric_rail_passenger	Aviation_passenger_regional	Shipping_passenger_regional	Aviation_passenger_IC	Shipping_passenger_IC
	Error	0.2	0.2	0.2	0.2	0.2	0.2	0.2	0.2	0.2	0.2	0.2	0.2	0.2
1.11		0.020	0.020	0.020	-0.010	0.023	0.024	0.042	0.147	0.057	0.052	0.013	0.049	0.033
3.2	*Max*	0.4	0.6	0.4	0.2	0.015	0.05	0.2	0.015	0.2	0.2	0.2	0.2	0.3
	Min	0.2	0.2	0.2	0.1	0.005	0.02	0.1	0.005	0.1	0.1	0.1	0.1	0.2
3.3		0.5	0.5	0.5	0.5	3	1	1	3	1	0.5	0.5	0.5	0.5
3.5	*Electricity*	1	1	1	0	0	0	0	1	1	0	0	0	0
	LaG_fuels	0	0	0	1	1	1	1	0	0	1	1	1	1
	Heat	0	0	0	0	0	0	0	0	0	0	0	0	0
3.9	*Illumination*	1	0	0	0	0	0	0	0	0	0	0	0	0
	IPaC	0	1	0	0	0	0	0	0	0	0	0	0	0
	Static_mechanical	0	0	1	1	0	0	0	0	0	0	0	0	0
	Transport_passenger_regional	0	0	0	0	1	1	1	1	1	1	1	0	0
	Transport_passenger_IC	0	0	0	0	0	0	0	0	0	0	0	1	1
	Transport_freight_regional	0	0	0	0	0	0	0	0	0	0	0	0	0
	Transport_freight_IC	0	0	0	0	0	0	0	0	0	0	0	0	0
	Cooling	0	0	0	0	0	0	0	0	0	0	0	0	0
	Low_temp_heating	0	0	0	0	0	0	0	0	0	0	0	0	0
	High_temp_process_heat	0	0	0	0	0	0	0	0	0	0	0	0	0
4.4	*Max*	0.39	0.58	0.95	0.52	0.38	0.42	0.49	0.97	0.98	0.46	0.52	0.46	0.52
	Min	0.13	0.20	0.89	0.42	0.18	0.25	0.35	0.90	0.94	0.35	0.42	0.35	0.42
4.5	*Numeral*	0.10	0.59	0.43	0.43	0.13	0.25	0.23	0.13	0.22	0.08	0.17	0.41	0.19
	Error	0.1	0.1	0.2	0.2	0.2	0.5	0.2	0.2	0.2	0.2	0.5	0.2	0.5
4.6		7.67	0.55	0.93	0.83	5.44	0.84	0.47	5.44	0.47	1.04	1.06	1.04	1.06
4.7		1880	1960	1880	1890	1890	1920	1920	2000	1900	1950	1890	1950	1890
7.3	*Mean*	0.1	0.2	0.1	0.1	0.05	0.05	0.1	0.1	0.1	0.1	0.2	0.1	0.2
	SD	0.1	0.2	0.1	0.1	0.05	0.05	0.1	0.1	0.1	0.1	0.2	0.1	0.2
11.1	*Max*	1	1	1	0.9	0.9	0.9	0.9	0.9	1	0.9	0.9	0.9	0.9
	Min	0.9	0.9	0.9	0.75	0.75	0.75	0.75	0.75	0.9	0.75	0.75	0.75	0.75
11.2	*Max*	0.05	0.1	0.05	0.05	0.05	0.05	0.1	0.1	0.1	0.1	0.1	0.1	0.1
	Min	0	0.05	0	0	0	0	0.05	0.05	0.05	0.05	0.05	0.05	0.05
11.3	*Max*	1.2	1.2	1.2	1.2	1.2	1.2	1.2	1.2	1.2	1.2	1.2	1.2	1.2
	Min	0.8	0.8	0.8	0.8	0.8	0.8	0.8	0.8	0.8	0.8	0.8	0.8	0.8
11.4	*Max*	1.2	1.4	1.2	1.2	1.2	1.4	1.4	1.2	1.4	1.4	1.4	1.4	1.4
	Min	0.8	1	0.8	0.8	0.8	1	1	0.8	1	1	1	1	1
11.5	*Max*	0.5	0.5	0.5	0.5	1	1	3	1	3	3	3	3	3

Input reference	Secondary labels	Electric_lighting	IPaC_devices	Electric_mechanical	LaG_fuel_mechanical	ICEV_light	ICEV_heavy_passenger	ICE_rail_passenger	Electric_vehicles	Electric_rail_passenger	Aviation_passenger_regional	Shipping_passenger_regional	Aviation_passenger_IC	Shipping_passenger_IC
	Min	0.2	0.2	0.2	0.2	0.5	0.5	1	0.5	1	1	1	1	1
11.6	*Max*	10	10	40	20	20	20	40	20	40	40	40	40	40
	Min	5	5	20	10	10	10	20	10	20	20	20	20	20
11.13	*Electrical_AI*	1	1	1	0	0	0	0	1	1	0	0	0	0
	IPaC_AI	0	1	0	0	0	0	0	0	0	0	0	0	0
	LaG_AI	0	0	0	1	1	1	1	0	0	1	1	1	1
	Roading_AI	0	0	0	0	1	1	0	1	0	0	0	0	0
	EV_AI	0	0	0	0	0	0	0	1	0	0	0	0	0
	Rail_AI	0	0	0	0	0	0	1	0	1	0	0	0	0
	Rail_electrification_AI	0	0	0	0	0	0	0	0	1	0	0	0	0
	Aviation_AI	0	0	0	0	0	0	0	0	0	1	0	1	0
	Shipping_AI	0	0	0	0	0	0	0	0	0	0	1	0	1
	Heating_AI	0	0	0	0	0	0	0	0	0	0	0	0	0
12.3	*Max*	999	999	1	1	999	999	1	1	1	0.3	0.3	999	1
	Min	999	999	0.75	0.75	999	999	0.75	0.75	0.75	0.1	0.1	999	0.75

9.5.15.4.2 Label index 13-26

Input reference	Secondary labels	ICEV_heavy_freight	ICE_rail_freight	Electric_rail_freight	Aviation_freight_regional	Shipping_freight_regional	Aviation_freight_IC	Shipping_freight_IC	Electric_cooling	LaG_fuel_heating_low	Electric_heating_low	Heat_heating_low	Electric_heating_high	Heat_heating_high
1.2	*Numeral*	0.227	0.008	0.008	0.004	0.009	0.006	0.065	0.139	0.015	0.188	0.571	0.050	0.429
	Error	0.2	0.2	0.2	0.2	0.2	0.2	0.2	0.2	0.2	0.2	0.2	0.2	0.2
1.11		0.019	0.000	0.015	0.042	0.020	0.039	0.031	0.020	-0.010	0.020	-0.004	0.020	-0.004
3.2	*Max*	0.15	0.2	0.2	0.2	0.3	0.3	0.4	0.15	0.15	0.15	0.15	0.75	0.75
	Min	0.05	0.1	0.1	0.1	0.2	0.2	0.2	0.05	0.05	0.05	0.05	0.5	0.5
3.3		0.5	0.5	0.5	0.5	0.5	0.5	0.5	1	1	1	1	0.2	0.2
3.5	*Electricity*	0	0	1	0	0	0	0	1	0	1	0	0.98	-0.02
	LaG_fuels	1	1	0	1	1	1	1	0	1	0	0	0	0
	Heat	0	0	0	0	0	0	0	0	0	0	1	-0.05	0.95
3.9	*Illumination*	0	0	0	0	0	0	0	0	0	0	0	0	0
	IPaC	0	0	0	0	0	0	0	0	0	0	0	0	0

Input reference	Secondary labels	ICEV_heavy_freight	ICE_rail_freight	Electric_rail_freight	Aviation_freight_regional	Shipping_freight_regional	Aviation_freight_IC	Shipping_freight_IC	Electric_cooling	LaG_fuel_heating_low	Electric_heating_low	Heat_heating_low	Electric_heating_high	Heat_heating_high
	Static_mechanical	0	0	0	0	0	0	0	0	0	0	0	0	0
	Transport_passenger_regional	0	0	0	0	0	0	0	0	0	0	0	0	0
	Transport_passenger_IC	0	0	0	0	0	0	0	0	0	0	0	0	0
	Transport_freight_regional	1	1	1	1	1	0	0	0	0	0	0	0	0
	Transport_freight_IC	0	0	0	0	0	1	1	0	0	0	0	0	0
	Cooling	0	0	0	0	0	0	0	1	0	0	0	0	0
	Low_temp_heating	0	0	0	0	0	0	0	0	1	1	1	0	0
	High_temp_process_heat	0	0	0	0	0	0	0	0	0	0	0	1	1
4.4	Max	0.42	0.49	0.98	0.46	0.52	0.46	0.52	6.50	0.94	0.95	1.00	0.95	1.00
	Min	0.25	0.35	0.94	0.35	0.42	0.35	0.42	5.00	0.71	0.73	1.00	0.80	1.00
4.5	Numeral	0.07	0.39	0.39	0.03	0.28	0.05	0.32	0.13	0.25	0.25	0.25	0.41	0.41
	Error	0.2	0.2	0.2	0.5	0.2	0.5	0.5	0.1	0.1	0.1	0.1	0.2	0.2
4.6		1.14	1.14	1.14	1.04	1.06	1.04	1.06	5.89	2.71	2.71	2.71	1.01	1.01
4.7		1920	1920	1900	1950	1890	1950	1890	1920	1880	1900	1800	1910	1800
7.3	Mean	0.05	0.1	0.1	0.1	0.2	0.1	0.2	0.05	0.05	0.05	0.05	0.2	0.2
	SD	0.05	0.1	0.1	0.1	0.2	0.1	0.2	0.05	0.05	0.05	0.05	0.2	0.2
11.1	Max	0.9	0.9	1	0.9	0.9	0.9	0.9	1	0.9	1	0.9	0.9	0.9
	Min	0.75	0.75	0.9	0.75	0.75	0.75	0.75	0.9	0.75	0.9	0.75	0.75	0.75
11.2	Max	0.05	0.1	0.1	0.1	0.1	0.1	0.1	0.05	0.05	0.05	0.05	0.1	0.1
	Min	0	0.05	0.05	0.05	0.05	0.05	0.05	0	0	0	0	0.05	0.05
11.3	Max	1.2	1.2	1.2	1.2	1.2	1.2	1.2	1.2	1.2	1.2	1.2	1.2	1.2
	Min	0.8	0.8	0.8	0.8	0.8	0.8	0.8	0.8	0.8	0.8	0.8	0.8	0.8
11.4	Max	1.4	1.4	1.4	1.4	1.4	1.4	1.4	1.2	1.2	1.2	1.2	1.4	1.4
	Min	1	1	1	1	1	1	1	0.8	0.8	0.8	0.8	1	1
11.5	Max	1	3	3	3	3	3	3	0.5	0.5	0.5	0.5	3	3
	Min	0.5	1	1	1	1	1	1	0.2	0.2	0.2	0.2	1	1
11.6	Max	20	40	40	40	40	40	40	20	20	20	20	40	40
	Min	10	20	20	20	20	20	20	10	10	10	10	20	20
11.13	Electrical_AI	0	0	1	0	0	0	0	1	0	1	0	1	0
	IPaC_AI	0	0	0	0	0	0	0	0	0	0	0	0	0
	LaG_AI	1	1	0	1	1	1	1	0	1	0	0	0	0
	Roading_AI	1	0	0	0	0	0	0	0	0	0	0	0	0
	EV_AI	0	0	0	0	0	0	0	0	0	0	0	0	0
	Rail_AI	0	1	1	0	0	0	0	0	0	0	0	0	0
	Rail_electrification_AI	0	0	1	0	0	0	0	0	0	0	0	0	0

Input reference	Secondary labels	*ICEV_heavy_freight*	*ICE_rail_freight*	*Electric_rail_freight*	*Aviation_freight_regional*	*Shipping_freight_regional*	*Aviation_freight_IC*	*Shipping_freight_IC*	*Electric_cooling*	*LaG_fuel_heating_low*	*Electric_heating_low*	*Heat_heating_low*	*Electric_heating_high*	*Heat_heating_high*
	Aviation_AI	0	0	0	1	0	1	0	0	0	0	0	0	0
	Shipping_AI	0	0	0	0	1	0	1	0	0	0	0	0	0
	Heating_AI	0	0	0	0	0	0	0	0	0	0	1	0	1
12.3	*Max*	999	1	1	0.3	0.3	999	1	999	0.3	999	999	1	999
	Min	999	0.75	0.75	0.1	0.1	999	0.75	999	0.1	999	999	0.75	999

9.5.15.5 EC types

Input reference	*Electricity*	*LaG_fuels*	*Heat*
3.6	2.6	1	1

9.5.15.6 Secondary AI types

Input reference	Secondary labels	*Electricity_AI*	*Intermittent_electricity_AI*	*LaG_fuels_AI*	*Heat_AI*
1.5	*Max*	2	5	1.3	1.3
	Min	1.3	2	1.1	1.1
1.10		0.020	0.233	0.016	-0.011
7.2	*Mean*	0.2	0.1	0.1	0.1
	SD	0.2	0.1	0.1	0.1
10.7	*Max*	0.75	0.75	1	1
	Min	0.5	0.5	0.9	0.9
10.8	*Max*	0.05	0.05	0.05	0.05
	Min	0	0	0	0
10.9	*Max*	1.4	1.4	1.2	1.2
	Min	1	1	0.8	0.8
10.10	*Max*	1.4	1.4	1.4	1.4
	Min	1	1	1	1
10.11	*Max*	6	1	6	1
	Min	3	0.5	3	0.5
10.12	*Max*	60	25	60	60

Input reference	Secondary labels	Electricity_AI	Intermittent_electricity_AI	LaG_fuels_AI	Heat_AI
	Min	30	15	30	30

9.5.15.7 End-use AI types

Input reference	Secondary labels	Electrical_AI	IPaC_AI	LaG_AI	Roading_AI	EV_AI	Rail_AI	Rail_electrification_AI	Aviation_AI	Shipping_AI	Heating_AI
1.6	*Max*	4	4	2	2	4	2	2	2	2	4
	Min	2	2	1.3	1.3	2	1.3	1.3	1.3	1.3	2
1.12		0.020	0.020	0.032	0.022	0.147	0.029	0.036	0.046	0.024	-0.004
7.4	*Mean*	0.05	0.1	0.05	0.1	0.05	0.1	0.05	0.1	0.1	0.05
	SD	0.05	0.1	0.05	0.1	0.05	0.1	0.05	0.1	0.1	0.05
11.7	*Max*	1	0.9	1	0.9	1	0.9	1	0.9	0.9	1
	Min	0.9	0.75	0.9	0.75	0.9	0.75	0.9	0.75	0.75	0.9
11.8	*Max*	0.05	0.05	0.1	0.2	0.1	0.1	0.1	0.2	0.2	0.05
	Min	0	0	0.05	0.1	0.05	0.05	0.05	0.1	0.1	0
11.9	*Max*	1.2	1.2	1.4	1.4	1.4	1.4	1.4	1.2	1.2	1.2
	Min	0.8	0.8	1	1	1	1	1	0.8	0.8	0.8
11.10	*Max*	1.2	1.4	1.2	1.4	1.2	1.4	1.2	1.4	1.4	1.2
	Min	0.8	1	0.8	1	0.8	1	0.8	1	1	0.8
11.11	*Max*	1	1	1	6	1	6	1	6	6	1
	Min	0.5	0.5	0.5	3	0.5	3	0.5	3	3	0.5
11.12	*Max*	50	15	50	50	15	50	50	50	50	50
	Min	25	5	25	25	5	25	25	25	25	25

9.5.15.8 ES types

Input reference	Secondary labels	Illumination	IPaC	Static_mechanical	Transport_passenger_regional	Transport_passenger_IC	Transport_freight_regional	Transport_freight_IC	Cooling	Low_temp_heating	High_temp_process_heat
5.1	*Max*	5	10	5	5	8	5	8	5	2	5
	Min	0.5	0.8	0.5	0.5	0.2	0.5	0.2	0.5	0.2	0.5

9.5.15.9 Uniform dist. inputs

Input reference	*Max*	*Min*
5.4	0.5	0.1
10.13	100	10
10.14	0.8	0.6
10.16	0.25	0.1
10.17	0.75	0.25
10.18	-0.5	-0.7
10.19	1.5	-0.5
12.1	1	0.5

9.5.15.10 Scalar inputs

Input reference	**2.7**	**5.2**	**5.3**	**10.15**	**12.4**	**12.5**	**12.6**	**12.7**	**12.8**	**12.9**	**12.10**
Value	9	0.05	0.05	0.01	0.025	0	0.1	10	10	0.8	0.5

9.6 OPTIMIZATION AND CALIBRATION

The PRESS model optimization procedure is carried out using GoldSim's inbuilt optimization functionality. The selected objective function to be minimized for the optimization is the time integral of the absolute EC supply/demand imbalance (in units of years) summed across all EC types (**EC_Deficit_Integral_Sum**). This measures the total amount of deviation from perfect supply/demand balance over the simulation period. The optimization is subject to the required condition that all realizations in the optimization sequence are successful (**Transition_Failure.Completion_Status = false**). For the definition of transition failure, as discussed in section 4.2.9.3, selected thresholds are: *a* > 5 years, *b* > 3 years, and *d* > 1 (deficit growing faster than elapsed time). Note that parameter *c* is not defined.

The directly optimized control parameters are listed in Table 13 along with other deterministic input parameters which are manually tested and selected for optimal system control.

Table 13: summary of control parameters used in the PRESS model

Optimized control parameters	**Ancillary control parameters**	
• **EC_Invest_Capacity_Coeff** (Υ_{mc}) • **Averaging_Period** • **Curtailment_Threshold** (Υ_{ct}) • **Invest_Adjust_Time** • **Utility_Share_Coeff** (Υ_{sh})	• **Invest_Time_Horizon** (Υ_{th}) • **EC_Invest_Capacity_Floor** • **Asymptote_Max_Factor** • **Minimum_PC_Timeframe** • **PC_Zero_Approx** • **Simulation_Base_Period**	• **PC_Invest_Max_Fraction** • **Utility_Remove** • **NRE_Annual_Utility_Reduction** (Υ_{nr}) • **EC_Surplus_Scale_Factor** • **EC_Deficit_Limit_Base** • **EC_Deficit_Limit_Slope**

The optimization is repeated for a sequence of selected (deterministic) input sets to find optimized control parameter values that are stable over a wide range of model realizations. The optimization is first carried out at specified input distribution quantiles, beginning at the 0.5 quantile (median), then alternated up and down by increments of 0.1 (0.4, 0.6, 0.3, 0.7, etc.). The optimization is then carried out for the global mean input set.

Due to the high degree of non-linearity present in PRESS, appropriate exploration of the input space and avoidance of local optima is required. For better exploration, randomized optimization sequences are used. To avoid local optima, objective function and control parameter values are averaged across the best 5 realizations, excluding those where a significant jump in objective value occurs. Where an optimal value converges on its defined boundary during the optimization process, the boundary is relaxed and the optimization for that realization is restarted.

9.6.1 Global ensemble optimality check and manual adjustment

Optimization based on specified (deterministic) realizations suffers from over-tuning. Control parameter values can be found that minimize the objective function as far as possible for a given realization, but do not do the same globally for a large ensemble of stochastically generated realizations. This is particularly apparent where linear dependence between an optimized control parameter and input quantile has been observed.

With the control parameter values found via realization-level optimization as a starting point, global ensemble-level optimality can be checked by comparing result distributions for the objective function and associated outputs. This global check is carried out by running an ensemble of 100 realizations (using Latin hypercube sampling strata mid-points) using the scenario manager tool within GoldSim. The five main optimized control parameters and selected ancillary control parameters below are tested via this method:

- **Invest_Time_Horizon**
- **PC_Invest_Max_Fraction**
- **NRE_Annual_Utility_Reduction**
- **EC_Surplus_Scale_Factor**
- ***Plan_horizon*** length
- Transition failure criteria (*a*, *b*, *c*, and *d*)

Discrete test increments are used simultaneously for each input being tested with successive iterations using smaller increments (5 steps compared initially, reduced to 3 steps as adjustments become smaller). The following outputs are compared, in order of importance: transition failure rate, the objective function distribution, and transition stable time distribution. The transition failure status by realization is also checked to ensure adjustments do not create new realization-level failures.

9.6.2 Optimization and calibration results

9.6.2.1 Final values

Name	Description	Unit	Value
Averaging_Period	Time period used for moving averages of EC inflow, EC outflow, and GES metabolism	Years	**0.5**
Curtailment_Threshold (γ_{ct})	Fractional band over which curtailment occurs for investment share (in response to penetration levels, NRE depletion, and RE exhaustion) and investment capacity (in response to ESMR relative to the ESMR limit)		**0.8**
EC_Invest_Capacity_Coeff (γ_{mc})	Coefficient used to control the magnitude of the investment response to sum forecast EC deficit	1/year^2	**0.016**
Invest_Adjust_Time	Time period used for moving average of cumulative forecast EC deficit at the selected time horizon	Years	**1.75**
Utility_Share_Coeff (γ_{sh})	Coefficient used to control the distribution of investment to available upstream and downstream options (secondary and EU PC) via the invest share logit function	1/EJ	**0.00002**

9.6.2.2 Optimization sequence

Table 14 summarizes the steps of the optimization procedure and final adjustments to control parameter values. Green values below are the calculated means across the best five realizations (with lowest objective function values) produced by the optimization process, excluding those exhibiting a discontinuity in objective function value.

Table 14: PRESS model optimization sequence results and finalized control parameter values

Control parameter		**Averaging_Period**	**Curtailment_Threshold** (γ_{ct})	**EC_Invest_Capacity_Coeff** (γ_{mc})	**Invest_Adjust_Time**	**Utility_Share_Coeff** (γ_{sh})	***Objective function value***
Unit		Years		1/year^2	Years	1/EJ	**Years^2**
Starting value		0.75	0.75	0.03	1.5	0.0002	
Limits	**Upper**	*3*	*1*	*0.05*	*5*	*0.001*	

	Lower	*0.1*	*0.25*	*0.005*	*0.25*	*5E-06*	
Input quantile	**0.5**	1.28	0.83	0.031	2.01	0.00023	**76.3**
	0.4	0.79	0.67	0.032	2.17	0.00028	**81.9**
	0.6	1.14	0.85	0.033	2.12	0.00036	**79.0**
	0.3	0.91	0.81	0.035	1.73	0.00016	**79.9**
	0.7	0.50	0.78	0.024	1.02	0.00048	**80.3**
	0.2	0.56	0.67	0.024	1.20	0.00033	**177.7**
	0.8	0.19	0.72	0.019	0.64	0.00007	**79.1**
	0.15	2.18	0.81	0.036	0.47	0.00030	**267.8**
	0.85	0.12	0.91	0.040	2.08	0.00095	**64.4**
Global mean input		1.20	0.71	0.028	1.89	0.00037	**82.3**
Summary statistics	*Mean*	0.89	0.78	0.030	1.53	0.00035	**106.9**
	Median	**0.85**	**0.79**	**0.032**	**1.81**	**0.00032**	**80.1**
	Minima	0.12	0.67	0.019	0.47	0.00007	**64.4**
	Maxima	2.18	0.91	0.040	2.17	0.00095	**267.8**
Selected		0.85	**0.8**	0.030	**1.75**	0.00035	
Global ensemble optimality adjustment		**0.5**	**n/a**	**0.016**	**n/a**	**0.00002**	

The mean, median, maximum, and minimum values for all control parameter values are reviewed and appropriate global optima values are selected. Global ensemble-level optimality adjustments are then applied where significant improvements are possible. The 0.1 quantile was found to be unable to produce a successful realization, so this was changed to 0.15 (and 0.9 to 0.85 for symmetry).

Linear dependence between optimized control parameter values and input quantile is also checked. An R^2 of 0.46 was observed for **Averaging_Period** (higher input quantiles tend to have shorter optimal averaging periods). Further testing revealed a minimal impact from this dependence on the objective function and system stability, and this is confirmed via the global ensemble optimality check and adjustment for this variable. R^2 is less than 0.2 for all other optimized control parameters indicating minimal dependence on the input quantile.

Systematic checks during the optimization sequence confirmed that reductions in the objective function (implying greater system stability) via the modification of control parameters do not appear to come at the expense of other key metrics of energy transition success, including cumulative GHG emissions, $EROI_{pou}$, and the RE share of TPES. This implies that the choice of objective function is appropriate. Furthermore, the incidence of realization failures is stable as control parameters approach their final, globally adjusted values.

Therefore, the system control heuristic can be considered stable and reliable as a means of producing best-case GES transformation pathways.

9.7 Scenario implementation

Scenarios are implemented in PRESS using the scenario manager functionality in Goldsim. Relevant input arrays are designated as scenario inputs able to accept specified parameter modifications for each scenario, as described in Table 15.

Table 15: implementation details for scenarios in the PRESS model

Scenario	**Name**	**Implementation in the PRESS model**
1	*Energy Breakthrough*	• The new technology is assumed to have an EROI of 50, at a similar level to other high-EROI energy production such at hydropower or coal. • This new generation type is assumed to be non-baseload, non-intermittent, and with maximum CF unaffected by intermittent penetration (similarly to hydropower). **Implementation:** • ***Mean*** entry for ***Other*** in **RE_Potential_Input** (input ref. 2.2) set to 9999 EJ/yr and ***SD*** set to 1 EJ/yr • ***Mean*** entry for ***Other*** in **Initial_RE_EROI_Input** (input ref. 6.1) set to 50 and ***SD*** set to 0 • ***Other*** entry in **Sec_Intermittent_ID** (input ref. 10.20) set to 0
2	*Relocalization*	• Aggregate personal mobility is curtailed but less so than the flow of goods (personal mobility prioritized over long economic supply chains). • IC transportation is assumed to decline more on average than regional, for both people and goods, as IC transportation has a greater discretionary component. • For freight, greater declines can occur than considered in the base case. **Implementation:** **ES_Final_Demand_Mult_Input** (input ref. 2.2) modified: • ***Max*** entry for ***Transport_passenger_regional*** set to 1 • ***Max*** entry for ***Transport_passenger_IC*** set to 0.8 • ***Max*** entry for ***Transport_freight_regional*** set to 0.6 and ***Min*** set to 0.2 • ***Max*** entry for ***Transport_freight_IC*** set to 0.4 and ***Min*** set to 0.1
3	*RE Rapid Deployment*	The mean NRE annual utility reduction rate applied in the base case, γ_{nr}, is quadrupled to apply a greater system forcing over time. **Implementation:** **NRE_Annual_Utility_Reduction** (input ref. 12.4) set to 0.1

Scenario	Name	Implementation in the PRESS model

4	*Climate Constraints*	High GHG emissions intensity technologies are subject to much lower penetration limits than in the base case, beyond which no further investment will occur.
		
		Implementation:
		Max and ***Min*** entries modified to the same value (uniform distribution becomes deterministic):
		• In **Sec_Penetration_limit_Input** (input ref. 12.2):
		  ○ ***Gas_generation*** set to 0.25
		  ○ ***Gas_to_LaG*** set to 0.1
		  ○ ***Coal_generation*** set to 0.1
		  ○ ***Coal_to_LaG*** set to 0.05
		  ○ ***Coal_heat*** set to 0.25
		• In **EU_Penetration_limit_Input** (input ref. 12.3):
		  ○ ***LaG_fuel_mechanical*** set to 0.25
		  ○ ***ICEV_light*** set to 0.25
		  ○ ***ICEV_heavy_passenger*** set to 0.5
		  ○ ***ICE_rail_passenger*** set to 0.25
		  ○ ***Aviation_passenger_regional*** set to 0.1
		  ○ ***Aviation_passenger_IC*** set to 0.25
		  ○ ***ICEV_heavy_freight*** set to 0.25
		  ○ ***ICE_rail_freight*** set to 0.5
		  ○ ***Aviation_freight_regional*** set to 0.1
		  ○ ***Aviation_freight_IC*** set to 0.25
		  ○ ***Heat_heating_low*** set to 0.25
		  ○ ***Heat_heating_high*** set to 0.5

5	*Delayed Consumer Response*	Investments maintain changes in end-use capital composition approximately in line with trends observed at the beginning of the simulation period. **Implementation:** **Scenario_5** (input ref. 12.5) set to 1. This sets values calculated by the **Downstream_Invest_Utility** function to the value of **Utility_Remove** prior to an elapsed simulation time of 35 yr (see section 9.4.4).

Scenario	Name	Implementation in the PRESS model

6	*Policy Recommendations*	Changes are enacted in the model in accordance with the composite sensitivity score (changes in higher scoring input parameters prioritized) to a level degree considered ambitious but plausible.
		
		Implementation:
		• ***Max*** entries in **ES_Final_Demand_Mult_Input** (input ref. 2.2) are modified:
		  ○ ***Static_mechanical*** and ***High_temp_process_heat*** are set to 0.75 (at least 25% aggregate reductions from present day levels by 2100)
		  ○ ***IPaC***, ***Transport_passenger_regional***, ***Transport_freight_regional***, ***Transport_freight_IC***, and ***Low_temp_heating*** are set to 1 (no aggregate increases beyond present day levels)
		• ***Max*** and ***Min*** entries set to 0.1 (uniform distribution becomes deterministic):
		  ○ ***Coal_generation*** in **Sec_Penetration_limit_Input** (input ref. 12.2)
		  ○ ***Aviation_freight_IC*** in **EU_Penetration_limit_Input** (input ref. 12.3)
		• ***Mean*** and ***SD*** entries in **Secondary_PC_ECC_Input** (input ref. 7.1) and **Secondary_AI_ECC_Input** (input ref. 7.2) are reduced by 50%:
		  ○ ***Coal_generation*** (to 0.75 yr)
		  ○ ***Coal_to_LaG*** (to 0.75 yr)
		  ○ ***Coal_CHP*** (to 0.75 yr)
		  ○ ***Biofuels*** (to 1.25 yr)
		  ○ ***Geothermal_generation*** (to 0.25 yr)
		  ○ ***Intermittent_electricity_AI*** (to 0.05 yr)

9.8 Pedigree Assessment

Pedigree assessment is carried out for probabilistic inputs arrays only, as deterministic inputs are not included in sensitivity or diagnostic analysis. Each input array is assessed based on the three criteria summarized in Table 8, and a composite mean score is calculated representing the relative strength of knowledge for the input array. Results are presented in Table 16 below. Input arrays considered to contain decision parameters (at least partially subject to control via policy) are also indicated.

Table 16: pedigree assessment results and decision variable status by input array

Input reference	Input array name	Number of sources	Limiting quality of sources	Strength of assumptions	Mean score	*Decision parameter?*
1.1	Init_Secondary_Prop_Input	*3*	*4*	*1*	2.67	No
1.2	Init_End_Use_Prop_Input	*5*	*2*	*1*	2.67	No
1.5	Init_Sec_Peak_Factor_Input	*0*	*1*	*1*	0.67	No
1.6	Init_End_Use_Peak_Factor_Input	*0*	*1*	*1*	0.67	No
2.1	Initial_NRE_Resource_Input	*5*	*3*	*3*	3.67	No
2.2	RE_Potential_Input	*5*	*3*	*4*	4.00	No
3.2	Init_End_Use_CF_Target_Input	*0*	*0*	*2*	0.67	No
3.3	EU_CF_Target_Final_Max_Factor	*0*	*1*	*2*	1.00	***Yes***
4.1	Sec_Conversion_Eff_Input	*5*	*2*	*2*	3.00	***Yes***

Input reference	Input array name	Number of sources	Limiting quality of sources	Strength of assumptions	Mean score	*Decision parameter?*
4.2	Sec_Reticulation_Eff_Input	*3*	*4*	*2*	3.00	***Yes***
4.4	End_Use_Conversion_Eff_Input	*4*	*3*	*2*	3.00	***Yes***
4.5	Init_End_Use_ES_Eff_Input	*5*	*2*	*1*	2.67	No
4.6	Final_EU_ES_Eff_Max_Factor	*3*	*3*	*1*	2.33	***Yes***
5.1	ES_Final_Demand_Mult_Input	*0*	*1*	*1*	0.67	***Yes***
5.2	Initial_ES_Demand_RoC_Max	*0*	*1*	*2*	1.00	***Yes***
5.4	Final_Demand_Flex_Input	*0*	*0*	*1*	0.33	***Yes***
6.1	Initial_RE_EROI_Input	*5*	*2*	*1*	2.67	No
6.2	RE_EROI_Terminal_Input	*0*	*1*	*2*	1.00	No
6.3	RE_EROI_Drop_Input	*0*	*1*	*1*	0.67	No
6.4	Initial_NRE_EROI_Input	*5*	*2*	*1*	2.67	No
6.5	NRE_EROI_Terminal_Input	*0*	*1*	*2*	1.00	No
6.6	NRE_EROI_Drop_Input	*5*	*2*	*1*	2.67	No
7.1	Secondary_PC_ECC_Input	*5*	*2*	*1*	2.67	***Yes***
7.2	Secondary_AI_ECC_Input	*0*	*1*	*0*	0.33	***Yes***
7.3	End_Use_PC_ECC_Input	*0*	*1*	*0*	0.33	***Yes***
7.4	End_Use_AI_ECC_Input	*0*	*1*	*0*	0.33	***Yes***
8.1	CapEx_Fraction_Input	*0*	*1*	*1*	0.67	No
8.2	Decommission_Fraction_Input	*0*	*1*	*1*	0.67	No
8.3	EC_Split_LaG_Factor_Input	*0*	*1*	*0*	0.33	No
8.4	EC_Split_Heat_Factor_Input	*0*	*1*	*0*	0.33	No
8.5	PC_Build_Time_Input	*0*	*1*	*2*	1.00	No
8.6	PC_Lifetime_Input	*0*	*1*	*2*	1.00	***Yes***
9.1	CapEx_Fraction_Input	*0*	*1*	*1*	0.67	No
9.2	Decommission_Fraction_Input	*0*	*1*	*1*	0.67	No
9.3	EC_Split_LaG_Factor_Input	*0*	*1*	*0*	0.33	No
9.4	EC_Split_Heat_Factor_Input	*0*	*1*	*0*	0.33	No
9.5	PC_Build_Time_Input	*0*	*1*	*2*	1.00	No
9.6	PC_Lifetime_Input	*0*	*1*	*2*	1.00	***Yes***
10.1	PC_CapEx_Fraction_Input	*0*	*1*	*1*	0.67	No
10.2	PC_Decommission_Fraction_Input	*0*	*1*	*1*	0.67	No
10.3	PC_EC_Split_LaG_Factor_Input	*0*	*1*	*0*	0.33	No
10.4	PC_EC_Split_Heat_Factor_Input	*0*	*1*	*0*	0.33	No
10.5	PC_Build_Time_Input	*0*	*1*	*2*	1.00	No
10.6	PC_Lifetime_Input	*0*	*1*	*2*	1.00	***Yes***
10.7	AI_CapEx_Fraction_Input	*0*	*1*	*1*	0.67	No
10.8	AI_Decommission_Fraction_Input	*0*	*1*	*1*	0.67	No
10.9	AI_EC_Split_LaG_Factor_Input	*0*	*1*	*0*	0.33	No
10.10	AI_EC_Split_Heat_Factor_Input	*0*	*1*	*0*	0.33	No
10.11	AI_Build_Time_Input	*0*	*1*	*2*	1.00	No
10.12	AI_Lifetime_Input	*0*	*1*	*2*	1.00	***Yes***

Input reference	Input array name	Number of sources	Limiting quality of sources	Strength of assumptions	Mean score	*Decision parameter?*
10.13	Intermit_AI_Mult_Final_Input	*5*	*2*	*0*	2.33	No
10.14	Retic_Eff_Mult_Final_Input	*0*	*1*	*2*	1.00	No
10.16	Diversity_Coeff_Input	*0*	*1*	*1*	0.67	No
10.17	Demand_Flex_Coeff_Input	*0*	*1*	*1*	0.67	No
10.18	CF_Max_Peaker_Coeff_Input	*0*	*1*	*1*	0.67	No
10.19	CF_Max_Baseload_Coeff_Input	*0*	*1*	*1*	0.67	No
11.1	PC_CapEx_Fraction_Input	*0*	*1*	*1*	0.67	No
11.2	PC_Decommission_Fraction_Input	*0*	*1*	*1*	0.67	No
11.3	PC_EC_Split_LaG_Factor_Input	*0*	*1*	*0*	0.33	No
11.4	PC_EC_Split_Heat_Factor_Input	*0*	*1*	*0*	0.33	No
11.5	PC_Build_Time_Input	*0*	*1*	*2*	1.00	No
11.6	PC_Lifetime_Input	*0*	*1*	*2*	1.00	***Yes***
11.7	AI_CapEx_Fraction_Input	*0*	*1*	*1*	0.67	No
11.8	AI_Decommission_Fraction_Input	*0*	*1*	*1*	0.67	No
11.9	AI_EC_Split_LaG_Factor_Input	*0*	*1*	*0*	0.33	No
11.10	AI_EC_Split_Heat_Factor_Input	*0*	*1*	*0*	0.33	No
11.11	AI_Build_Time_Input	*0*	*1*	*2*	1.00	No
11.12	AI_Lifetime_Input	*0*	*1*	*2*	1.00	***Yes***
12.1	ESMR_Limit_Input	*0*	*1*	*2*	1.00	***Yes***
12.2	Sec_Penetration_Limit_Input	*0*	*1*	*1*	0.67	***Yes***
12.3	EU_Penetration_Limit_Input	*0*	*1*	*1*	0.67	***Yes***

10 APPENDIX 2: ADDITIONAL RESULTS

Supplementary results referred to in chapter 6 are presented here.

10.1 PENETRATION

Range magnitudes are given by the difference between envelope upper and lower limits (5th and 95th percentiles) and act as a indicators for uncertainty over time in the respective output variable.

10.1.1 Secondary

Secondary penetration range magnitudes for secondary PC, depicted in Figure 138 and Figure 139, show generally increasing ranges, and therefore uncertainties, for all PC types. For the majority of PC types, range magnitudes increase relatively steadily with decreasing gradients after mid-century, reaching less than 20% by 2100. These PC types see minor variations only in penetration between realizations. The greatest range magnitudes by 2100 (> 25%), and highest associated uncertainties in ultimate penetration, primarily relate to alternative modes for LaG fuel and heat production, specifically oil refining, the conversion of coal and natural gas to LaG fuels, biofuels production, and coal and natural gas heat. Oil refining, the conversion of coal to LaG fuels, gas heat, biomass heat, and solar thermal heat all exhibit early peaks, between 2035 and 2060, before declining then increasing again. This indicates greater transitory variations in penetration between realizations during the early simulation period. Oil heat and nuclear generation exhibit late peaks, between 2070 and 2090, before declining. Wind and solar PV exhibit increasing gradients after mid-century, implying growing variations in penetration between realizations over the late simulation period

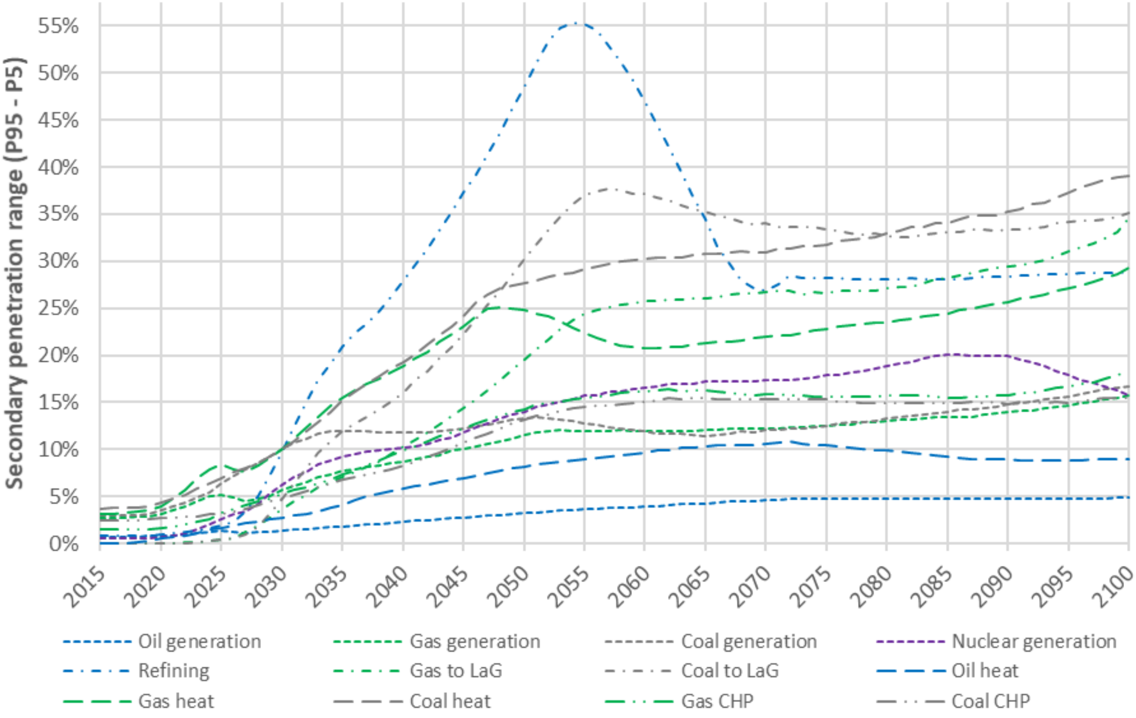

Figure 138: secondary penetration range magnitudes for secondary NRE PC

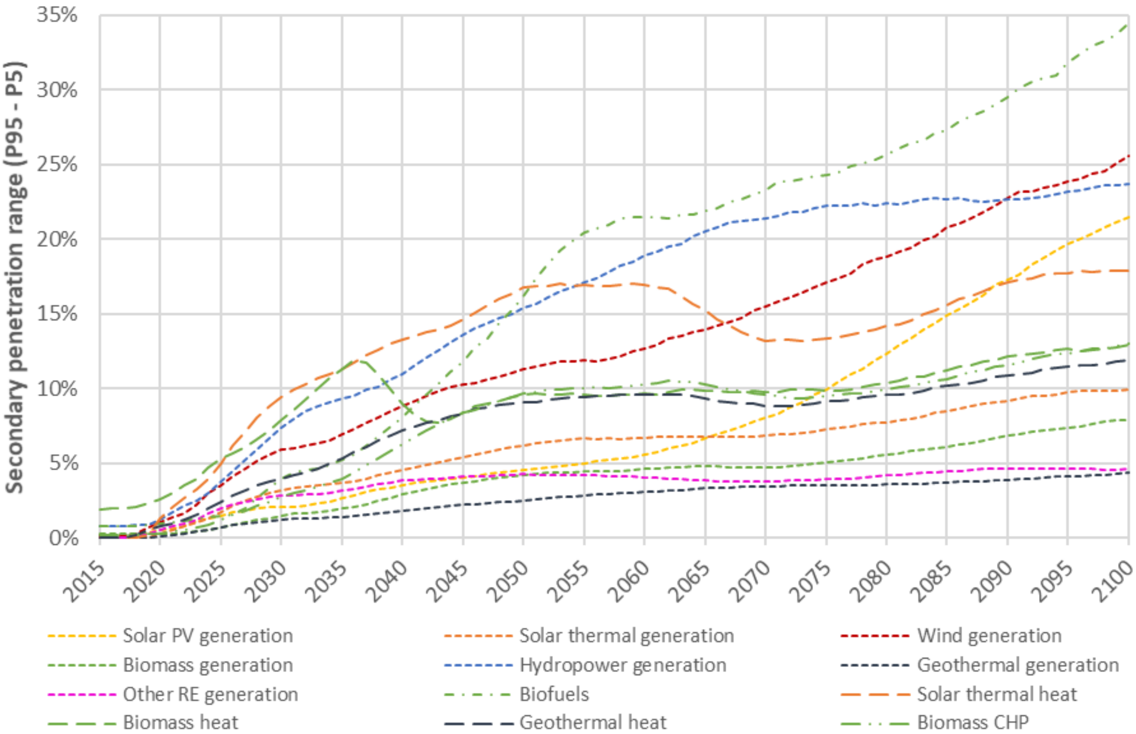

Figure 139: secondary penetration range magnitudes for secondary RE PC

10.1.2 End-use

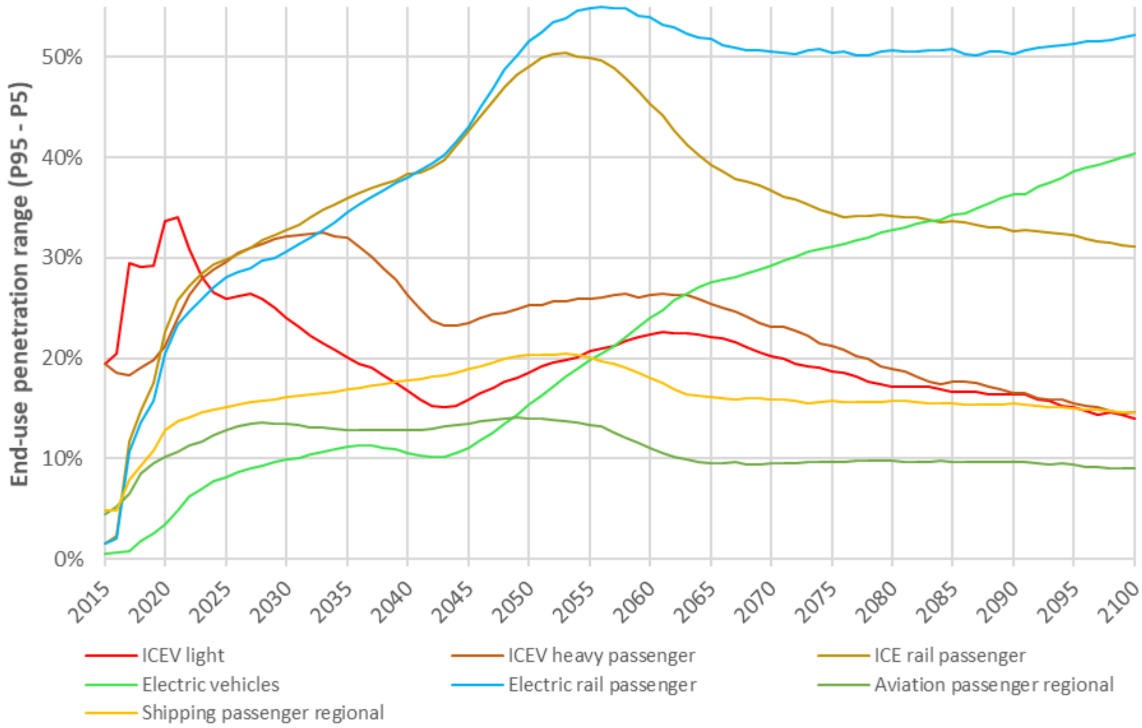

Figure 140: EU penetration range magnitudes for passenger transportation PC

EU penetration range magnitudes for EU PC are depicted in Figure 140, Figure 141, and Figure 142. This excludes mechanical systems, high temperature process heating, and IC transportation (ranges for these PC types are given in section 6.1.10.2). Range magnitude trends can be seperated into two general groups. The first group sees strong increases in range magnitudes, reaching 25% or more by 2100, implying major variations in penetration between these modes. This group include all rail types (electric and ICE, passenger and freight), electric vehicles, electric and heat low temperature heating. Note that ICE passenger rail reaches a peak by 2050 before declining by approximately 20% from 2055 to 2100. Range magnitude trends for all other PC types are under 20% by 2100 following initial increases or transitory oscillations, indicating minor variations only in penetration between realizations. Notably, this group includes all ICE vehicles (light and heavy, passenger and freight), and regional aviation and shipping (passenger and freight).

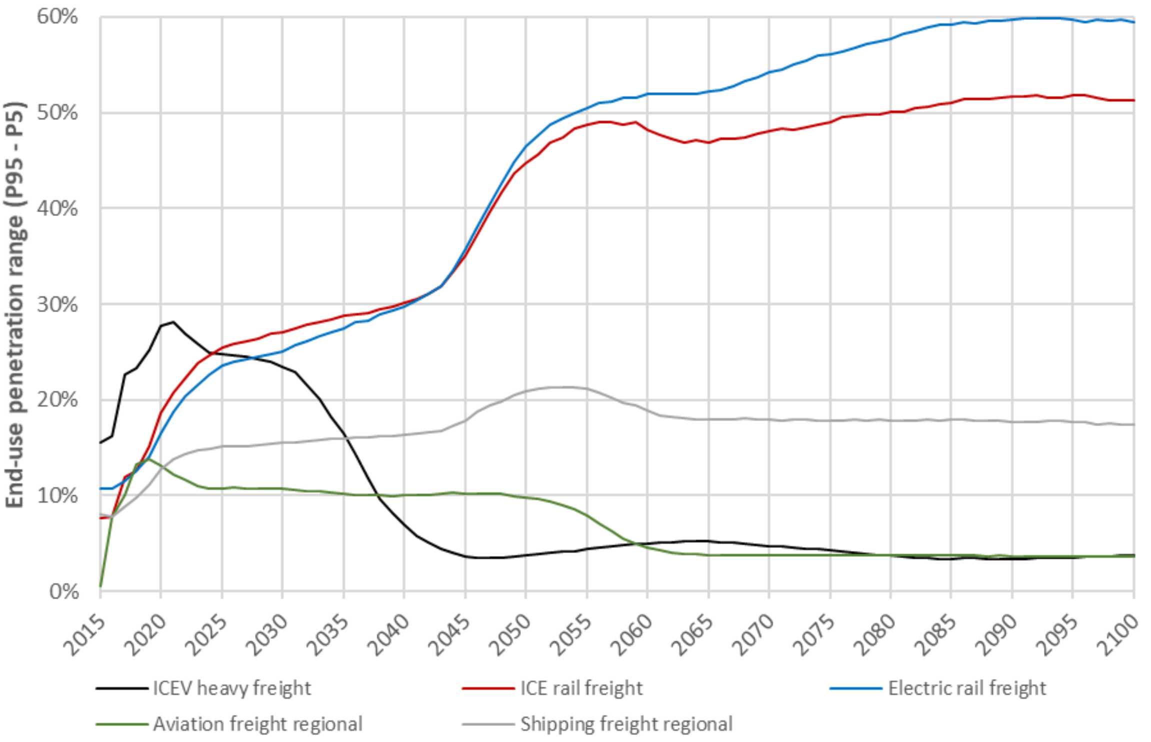

Figure 141: EU penetration range magnitudes for freight transportation PC

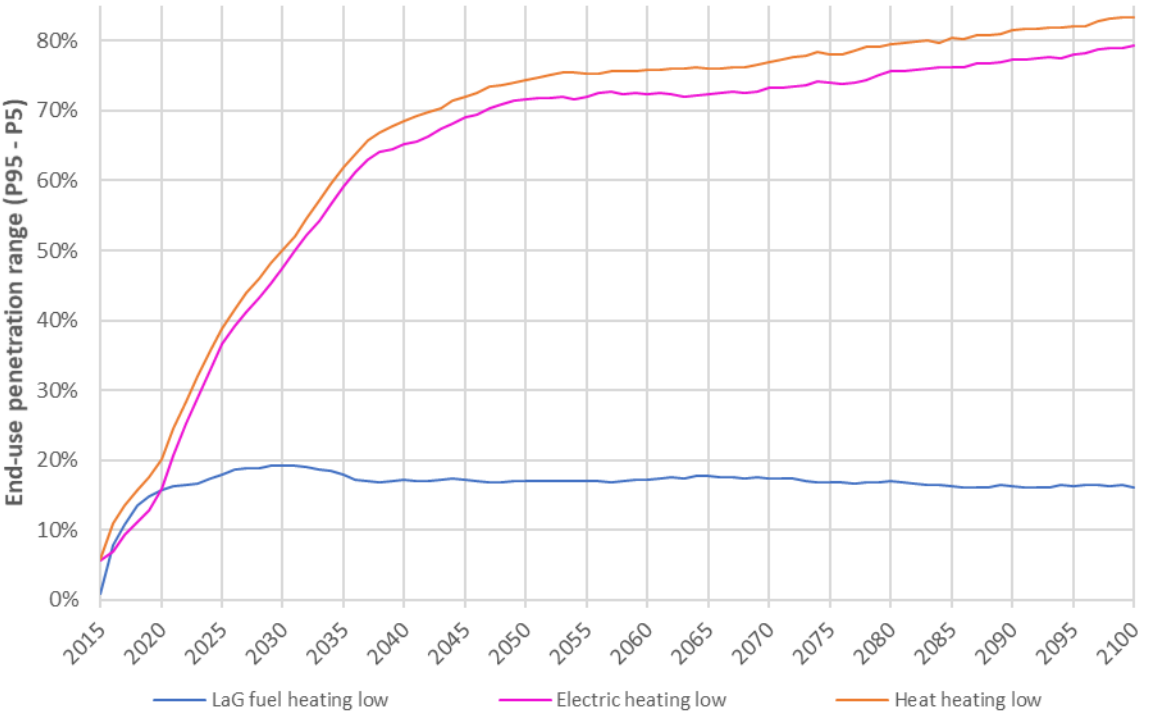

Figure 142: EU penetration range magnitudes for low temperature heating PC

10.2 EFFICIENCIES

Figure 143 shows the progression in EU conversion and EU to ES efficiencies (indicated by 5-year increment markers linked by a line) for electric cooling towards the achievable maxima (indicated by a bold marker). Efficiency gains accelerate in the first three 5-year periods, before slowing as efficiencies get closer to their achievable maxima. Note that EU conversion efficiency for electric cooling is substantially above one as useful delivered power output is greater than electric power input, due to the nature of the heat cycle used for cooling and refrigeration.

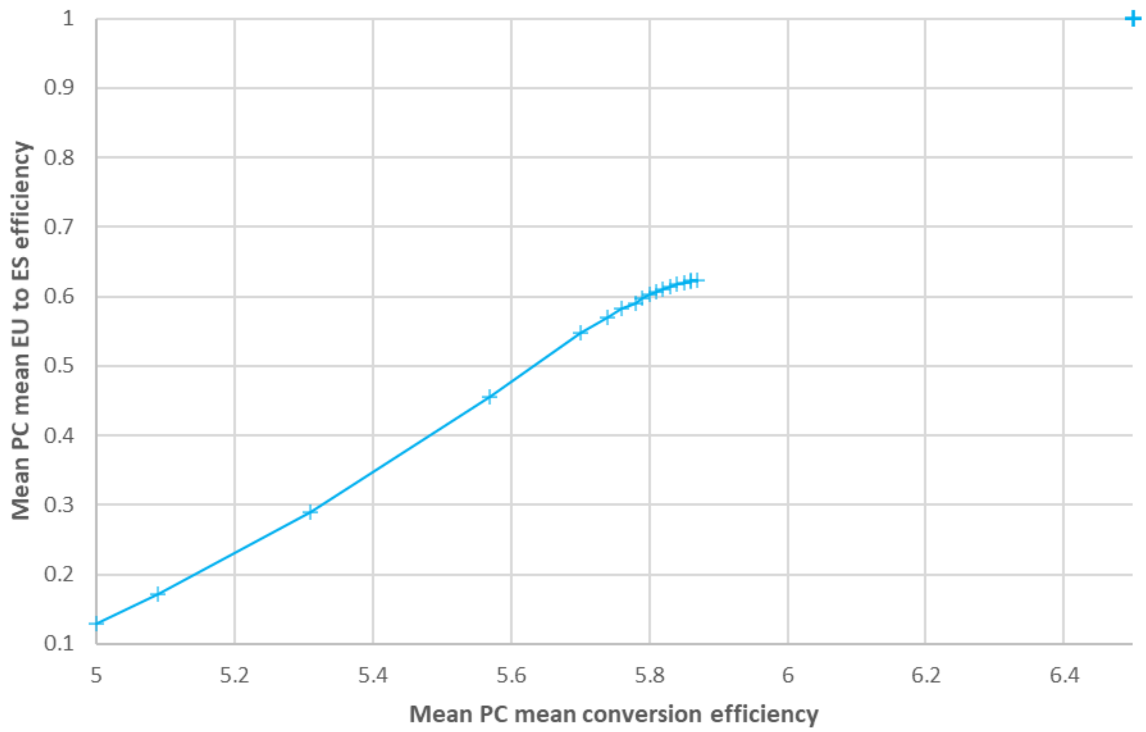

Figure 143: EU PC mean efficiency trend and achievable maxima for electric cooling (markers at 5-year increments)

10.3 ES DEMAND

Modelled scenarios 2 and 6 (Relocalization and Policy Recommendation) entail modification to base case ES demands, as described in section 5.3. The resulting changes in mean ES demands are depicted in Figure 145 for scenario 2, and Figure 144 and Figure 146 for scenario 6.

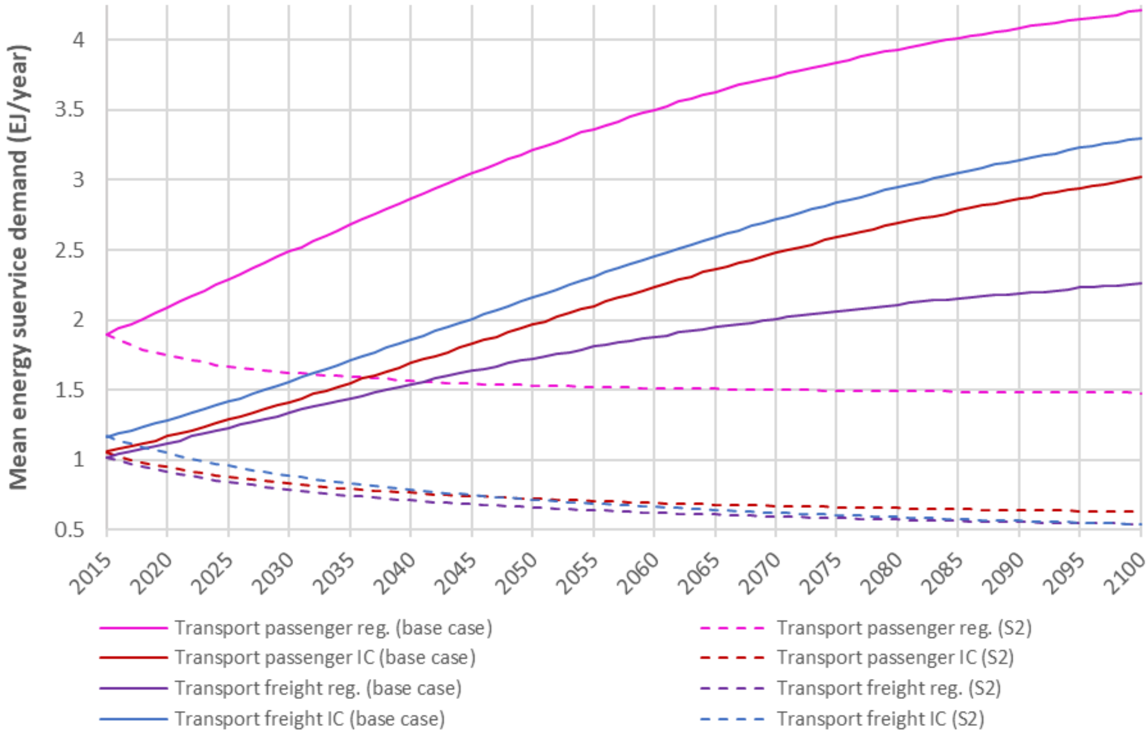

Figure 144: scenario differences in mean ES demands (S2)

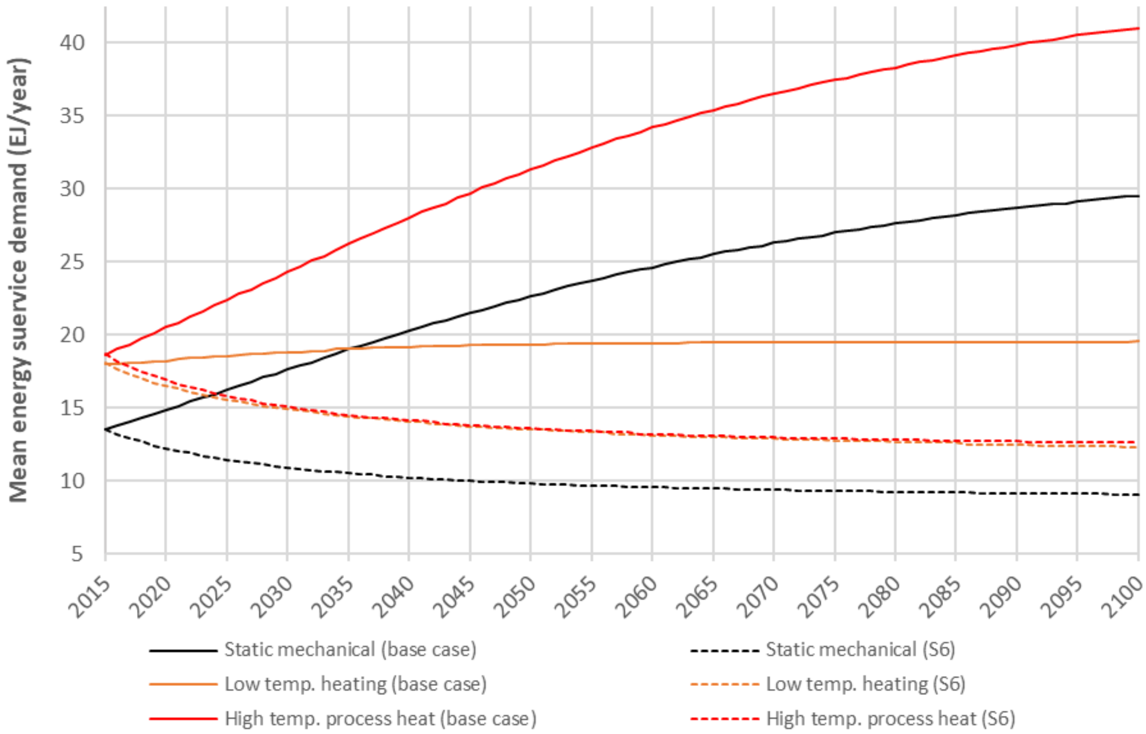

Figure 145: scenario differences in mean ES demands (S6; major)

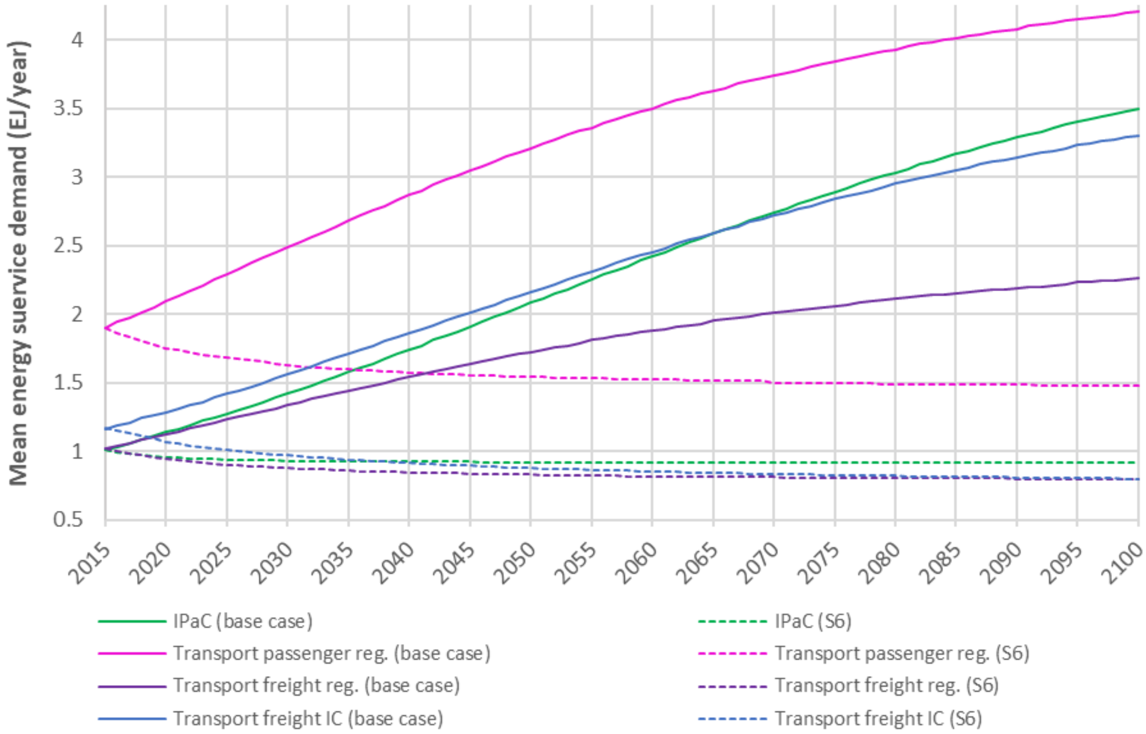

Figure 146: scenario differences in mean ES demands (S6; moderate and minor)

10.4 INTERMITTENCY IMPACTS IN ELECTRICITY SYSTEMS

Figure 147 summarizes mean output variables describing intermittency impacts and mitigation in electricity systems by scenario, relative to the base case, in 2050 and 2100. Mean intermittent penetration is increased only in scenario 4 in 2050, by 16%, but is reduced or unchanged in all other scenarios and times, by up to 34% (scenario 1 in 2100). Mean intermittent diversity is reduced only in scenario 5 in 2050, by 6%, but is increased or unchanged in all other scenarios and times, by up to 36% (scenario 1 in 2100). Relative to the base case (in which AI mitigation is generally favoured), a greater tendency towards AI mitigation is seen only in scenario 2, while greater tendencies towards PC overbuild mitigation is seen in most other scenarios, particularly scenarios 1, 4, and 5. Mean absolute quantities of intermittent electricity AI are increased only in scenario 4 in 2050, by 72%, but are reduced or unchanged in all other scenarios and times, by up to 85% (scenario 6 in 2100). Scenarios 1 and 6 exhibit consistently lower mean intermittent penetration and quantities of intermittent electricity AI, and higher intermittent diversity and intermittent reticulation efficiencies. Scenario 2 sees consistently low quantities of intermittent electricity AI and the smallest reductions in intermittent CF maxima of all scenarios. Scenario 3 shows minor differences from the bae case only. By 2100, scenario 4 sees the greatest reductions in intermittent CF maxima of all scenarios. Scenario 5 exhibits major differences from the base case in 2050, driven by a preference for PC overbuild mitigation leading to larger reductions in intermittent CF maxima but higher intermittent reticulation efficiencies. However, by 2100 scenario 5 has largely converged with the base case.

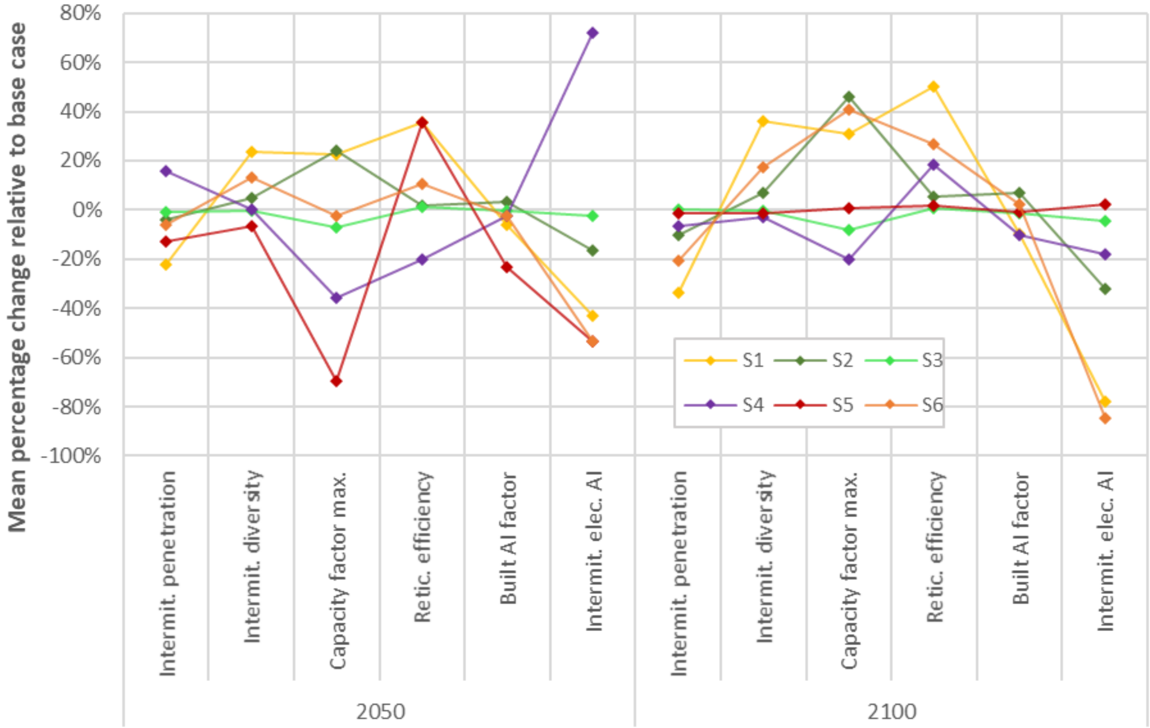

Figure 147: mean electricity system intermittency mitigation variables relative to the base case in 2050 and 2100

10.5 Sensitivity analysis

Sensitivity analysis results beyond those presented in section 6.3 (input parameters with normalized sensitivity values between upper and lower sensitivity thresholds excluding results above lower thresholds for both selected results), are presented in Table 17 and Table 18 for non-decision and decision input parameters, respectively. Note, in response to increases in input parameter values, negative cumulative GHG emissions $SRC_{y,i}$ values and positive stable time $SRC_{y,i}$ values are associated with desirable outcomes.

Table 17: additional sensitivity results for non-decision input parameters above lower sensitivity thresholds

Input parameter	Selected result	$SRC_{y,i}$	Normalized sensitivity
Decommissioning fraction – electric mechanical systems	Stable time	-0.03	0.104
EC split LaG factor – electric vehicles		0.037	0.095
Intermittent electricity AI required multiplier (at 100% penetration)		-0.036	0.089
Terminal EROI – coal		0.028	0.089

Input parameter	Selected result	$SRC_{y,i}$	Normalized sensitivity
CapEx fraction – oil heat		0.027	0.088
RE potential – hydropower		0.021	0.087
EU to ES efficiency at technology inception – IPaC devices		-0.026	0.077
Initial EU to ES efficiency – shipping passenger regional		-0.041	0.069
Pre-simulation EROI decline – wind		-0.026	0.067
Initial NRE resource – oil		0.015	0.067
Initial EU to ES efficiency – electric mechanical	Cumulative GHG emissions	-0.047	0.101
Initial EU to ES efficiency – high temp. heating using heat fuels		-0.045	0.093

Table 18: additional sensitivity results for decision input parameters above lower sensitivity thresholds

Input parameter	Selected result	$SRC_{y,i}$	Normalized sensitivity
Final EU to ES efficiency – electric rail passenger	Stable time	0.047	0.107
Penetration limit – solar thermal heat		0.026	0.103
Final CF target – IPaC devices		0.046	0.100
AI lifetime – heating AI		0.026	0.095
Final EU to ES efficiency – low temp. heating using heat fuels		0.034	0.094
Final secondary reticulation efficiency – gas CHP		-0.038	0.094
ECC – electric rail passenger		-0.03	0.092
Penetration limit – biomass heat		0.029	0.092
Final secondary reticulation efficiency – biomass heat		0.042	0.092
ESMR limit		0.028	0.086
Final secondary reticulation efficiency – oil generation		-0.041	0.085
Final secondary conversion efficiency – biofuels		0.029	0.080
Final EU to ES efficiency – ICE rail freight		-0.035	0.080
Initial EU conversion efficiency – electric mechanical systems		0.032	0.079
Final EU to ES efficiency – electric mechanical systems		0.032	0.079
Penetration limit – shipping freight IC		0.026	0.077
Secondary reticulation efficiency at technology inception – solar thermal heat		0.037	0.077
Final EU conversion efficiency – electric mechanical systems		-0.031	0.077
ECC – LaG fuels AI		0.027	0.075
EU conversion efficiency at technology inception – electric rail passenger		-0.029	0.075
Initial secondary reticulation efficiency – coal CHP		-0.034	0.074
Final EU to ES efficiency – electric rail freight		0.033	0.072
Final EU to ES efficiency – shipping passenger regional		0.045	0.071
ECC – electrical AI		-0.026	0.070
Initial secondary conversion efficiency – biomass heat		0.021	0.069
PC lifetime – coal to LaG		0.016	0.068
Final CF target – high temp. electric heating		0.038	0.068
Final CF target – high temp. heating using heat fuels		-0.038	0.068
Initial EU conversion efficiency – electric lighting		0.026	0.067

Input parameter	Selected result	$SRC_{y,i}$	Normalized sensitivity
ECC – aviation passenger regional		0.026	0.067
Initial ES demand rate of change – transport passenger IC	Cumulative GHG emissions	0.037	0.104
ES final demand multiplier – transport freight IC		0.049	0.102
ES final demand multiplier – transport freight regional		0.038	0.063

10.6 DIAGNOSTIC ANALYSIS

Medium risk input parameters found via diagnostic analysis are presented in Table 19 and Table 20, for the stable time and cumulative GHG emissions selected results, respectively.

Table 19: medium risk input parameters found via diagnostic analysis for stable time

Input parameter	Normalized sensitivity	Pedigree score
ECC – biofuels	0.411	2.7
ECC – coal CHP	0.294	2.7
Initial EROI – coal	0.273	2.7
ECC – coal to LaG fuels	0.205	2.7
ECC – coal generation	0.158	2.7
ECC – geothermal generation	0.158	2.7
Initial EU to ES efficiency – aviation freight regional	0.149	2.7
Initial EU to ES efficiency – shipping freight IC	0.147	2.7
Initial EU to ES PC mean efficiency – electric rail passenger	0.112	2.7
Final EU to ES efficiency – electric rail passenger	0.107	2.3
Decommissioning fraction – electric mechanical	0.104	0.7
Penetration limit – solar thermal heat	0.103	0.7
Final CF target – IPaC devices	0.100	1.0
AI lifetime – heating AI	0.095	1.0
EC split LaG factor – electric vehicles	0.095	0.3
Final EU to ES efficiency – low temp. heating using heat fuels	0.094	2.3
Final secondary reticulation efficiency – gas CHP	0.094	3.0
ECC – electric rail passenger	0.092	0.3
Penetration limit – biomass heat	0.092	0.7
Final secondary reticulation efficiency – biomass heat	0.092	3.0
Initial ES demand rate of change – transport passenger regional	0.092	1.0
Initial EU to ES PC mean efficiency – electric mechanical	0.090	2.7
Intermittent electricity AI required multiplier (at 100% penetration)	0.089	2.3
Terminal EROI – coal	0.089	1.0
CapEx fraction – oil heat	0.088	0.7
ESMR limit	0.086	1.0
Final secondary reticulation efficiency – oil generation	0.085	3.0
Final secondary conversion efficiency – biofuels	0.080	3.0

Input parameter	Normalized sensitivity	Pedigree score
Initial ES demand rate of change – transport freight IC	0.080	1.0
Final EU to ES efficiency – ICE rail freight	0.080	2.3
Initial EU conversion efficiency – electric mechanical systems	0.079	3.0
Final EU to ES efficiency – electric mechanical systems	0.079	2.3
Penetration limit – shipping freight IC	0.077	0.7
EU to ES efficiency at technology inception – IPaC devices	0.077	2.7
Secondary reticulation efficiency at technology inception – solar thermal heat	0.077	3.0
Final EU conversion efficiency – electric mechanical systems	0.077	3.0
ECC – LaG fuels AI	0.075	0.3
EU conversion efficiency at technology inception – electric rail passenger	0.075	3.0
Initial secondary reticulation efficiency – coal CHP	0.074	3.0
Final EU to ES efficiency – electric rail freight	0.072	2.3
Final EU to ES efficiency – shipping passenger regional	0.071	2.3
ECC – electrical AI	0.070	0.3
Initial EU to ES efficiency – shipping passenger regional	0.069	2.7
Initial secondary conversion efficiency – biomass heat	0.069	3.0
PC lifetime – coal to LaG	0.068	1.0
Final CF target – high temp. electric heating	0.068	1.0
Final CF target – high temp. heating using heat fuels	0.068	1.0
Pre-simulation EROI decline – wind	0.067	0.7
Initial EU conversion efficiency – electric lighting	0.067	3.0
ECC – aviation passenger regional	0.067	0.3

Table 20: medium risk input parameters found via diagnostic analysis for cumulative GHG emissions

Input parameter	Normalized sensitivity	Pedigree score
Initial EROI – coal	0.647	2.7
Initial EU to ES PC mean efficiency – high temp. heating using heat fuels	0.149	2.7
Initial EU to ES efficiency – low temp. heating using heat fuels	0.128	2.7
ECC – coal generation	0.108	2.7
Initial ES demand rate of change – transport passenger IC	0.104	1.0
ES final demand multiplier – transport freight IC	0.102	0.7
Initial EU to ES efficiency – electric mechanical	0.101	2.7
Initial EU to ES efficiency – heat heating high	0.093	2.7
Initial EU to ES PC mean efficiency – electric mechanical	0.069	2.7
ES final demand multiplier – transport freight regional	0.063	0.7
ECC – coal to LaG fuels	0.063	2.7